# Spatial Ecology of Arctic Grayling in the Parsnip Core Area

Fish and Wildlife Compensation Program
Peace Project No. PEA-F21-F-3178

**Prepared for:**

Fish and Wildlife Compensation Program – Peace
3333 22nd Ave
Prince George, BC
V2N 1B4

**Prepared by:**

Eduardo Martins, Bryce O'Connor, Joseph Bottoms, Ian Clevenger, Marie Auger-Methé, Michael Power, David Patterson, Mark Shrimpton and Steven Cooke

University of Northern British Columbia
3333 University Way
Prince George, BC
V2N 4Z9

Prepared with financial support of the Fish and Wildlife Compensation Program on behalf of its program partners BC Hydro, the Province of BC, Fisheries and Oceans Canada, First Nations and Public Stakeholders.

31-March-2021

## Executive Summary

Flooding of the Upper Peace after construction of the W.A.C. Bennett Dam in 1967 resulted in a considerable loss of riverine habitat to Arctic grayling (*Thymallus arcticus*). The decrease in available habitat, alteration of natural hydrology and evidence of drastic reductions in population size caused great concern for the sustainability of Arctic grayling populations in the Williston Reservoir Watershed. The recent review by Stamford et al. (2017) and monitoring framework by Hagen and Stamford (2017) highlighted a number of critical information gaps related to the spatial ecology of Arctic grayling such as: (1) the unknown distribution of Arctic grayling within the streams of the different core areas (*sensu* Stamford et al. 2017); and (2) the lack of understanding of Arctic grayling migrations. Furthermore, it is unknown whether populations of bull trout (*Salvelinus confluentus*) are limiting the abundance of Arctic grayling and their spatial distribution.

The goal of this project is to investigate the spatial ecology of sub-adult and adult Arctic grayling and their interactions with bull trout in the Parsnip River mainstem and tributaries, a core area of Arctic grayling populations in the Williston Reservoir Watershed.

The information gathered in this study will fill in data gaps that were identified as moderate and high immediacy for the Parsnip core area (data gaps 5.1.3a-i in Table 6 of Stamford et al. 2017) and will also be relevant to other core areas in the Williston Reservoir Watershed (2.3.1b-c and 2.3.5 in Table 1 of Stamford et al. 2017). Therefore, the outcomes of this study will primarily address the priority action # 9 (PEA.RLR.S03.RI.09) of the *Peace Region Rivers, Lakes, and Reservoirs Action Plan* (FWCP 2020). However, given that the study will collect data on bull trout, it will also contribute information to address priority # 13 (PEA.RLR.S04.RI.13) of the *Peace Region Rivers, Lakes, and Reservoirs Action Plan* (FWCP 2020), particularly by filling in high immediacy data gaps 5.1a and 5.1b outlined in Table 5.1c in Hagen and Webber (2019).

This report focuses on project activities in Year 3 of 4 but results integrate data collected since Year 1. The methods used to address the study objectives include: acoustic telemetry, capture-recapture, temperature data logging, stable isotope analysis and spatial modeling.

In 2020, a total of 69 fish (44 Arctic grayling and 25 bull trout) were tagged in the Parsnip watershed, increasing the project total to 157 grayling and 63 bull trout tagged since 2018. Due to a high and sustained spring freshet, 21 acoustic receivers were lost, while 49 receivers were successfully downloaded. After adjusting for receiver losses and replacements, Arctic grayling and bull trout tagged for this study are being continuously monitored by an array of 61 receivers, with plans for early-season deployments in place

for 2021. Coarse telemetry analyses showed that Arctic grayling on average moved 4.3 ± 6.3 km per movement event lasting less than 24 hours, while bull trout moved 12.3 ± 8.3 km per event over the course of this study. Telemetry data show a seasonal pattern of both species using the Parsnip mainstem as overwintering habitat and making use of the tributaries in the open-water season.

In 2020, eight new water temperature logging stations were deployed in the Parsnip watershed. Three of these new water temperature logging sites received associated air temperature loggers. In the fall of 2020, data from 65 water temperature loggers and 40 air temperature loggers were downloaded. The mean 2020 summer water temperature in the Parsnip River was 9.47$^{o}$C (± 2.37$^{o}$C). The mean 2020 summer air temperature was 11.20$^{o}$C (± 3.13$^{o}$C). The 2020 mean summer detection temperatures of Arctic grayling and bull trout were 9.62$^{o}$C (± 1.94$^{o}$C) and 10.26$^{o}$C (± 2.12$^{o}$C) respectively. Spatial stream network (SSN) models were fit for the averaged 2019 and 2020 summer thermal riverscape in the Parsnip River watershed. The SSN models were used to predict continuous temperatures for the entire watershed and visualize trends in average temperature and temperature variability.

During previous field seasons, a total of 235 biological samples comprised of adipose fin, fish muscle, invertebrate, plant, particulate organic matter, were obtained for stable isotope analysis. In the summer of 2020, the sample size was expanded by collecting an additional 167 samples. This larger sample size has allowed us to build on preliminary analyses done in 2019. Carbon ($\delta^{13}C$) and nitrogen ($\delta^{15}N$) isotope concentrations in the samples were analyzed in order to understand trophic positions and trends between bull trout and Arctic grayling, as well as look into dietary preferences by size. Bull trout were found to occupy a larger dietary niche and higher trophic position than Arctic grayling. Arctic grayling exhibited no relationship between $\delta^{15}N$ and fork length, whereas bull trout $\delta^{15}N$ was positively related to fork length.

The project successfully completed objectives for the 2020 field season including expansion of the temperature monitoring array, increasing the sample size for tagged Arctic grayling and bull trout and stable isotope analyses. In 2021 four key objectives will be focused on:

- Deploy up to 10 acoustic receivers in key sites where they were lost in 2020. This will be done as soon as flow decrease to levels that allow for safe working conditions (<400 $m^3$/sec measured at the Water Survey of Canada hydrometric station in the lower Parsnip River).

- Deploy 33 acoustic transmitters left over from last year in Arctic grayling and as sentinel tags for detection efficiency monitoring.

- Download existing temperature data loggers and take down the temperature monitoring network.

- Download existing acoustic receivers and take down the acoustic monitoring network.

We have engaged in eight outreach activities presenting project objectives and preliminary results to a diverse audience and featuring in an episode of an angling show (Reelistic Outdoors) that highlighted the project objectives and approaches.

# Table of Contents

## List of Tables



## List of Figures

# 1. Introduction

The construction of the 183-m high W.A.C. Bennett Dam in 1967, forming the Williston Reservoir flooded roughly 350 km of the Peace, Finlay, and Parsnip River valleys (Hagen and Stamford 2017). Arctic grayling (*Thymallus arcticus*) in the Upper Peace watershed show a fluvial life history form (Clarke *et al*. 2007). Therefore, flooding of the Upper Peace resulted in a considerable loss of riverine habitat. Prior to impoundment, Arctic grayling were widespread and abundant in tributary streams of the Upper Peace. However, presently Arctic grayling are restricted to just eight of the larger watersheds in the Williston Reservoir watershed (Hagen and Stamford 2017). The decrease in available habitat, alteration of natural hydrology (change from large flowing rivers to reservoir) and evidence of drastic reductions in population size cause great uncertainty about the sustainability of Arctic grayling populations in the Williston Reservoir Watershed (Stamford and Taylor 2005). The recent review by Stamford et al. (2017) and monitoring framework by Hagen and Stamford (2017) highlighted a number of critical information gaps related to the spatial ecology – the causes and consequences of a species distribution over time and space (Hastings *et al*. 2011) – of Arctic grayling. For example, two important spatial ecology data gaps identified in the review are: (1) the unknown distribution of Arctic grayling within the streams of the different core areas (*sensu* Stamford *et al*. 2017); and (2) the lack of understanding of Arctic grayling migrations.

Knowledge of a species' spatial ecology is fundamental to the effective development and implementation of enhancement and conservation programs (Allen and Singh 2016, Ogburn *et al*. 2017). To identify critical habitats and potential limiting factors (e.g. habitat conditions, human impacts, interspecific interactions), these programs often require detailed information derived from spatial ecology studies describing where, when and why individuals move and are distributed in space (Cooke *et al*. 2016). Although the description of distribution and migrations is a necessary step in understanding the spatial ecology of Arctic grayling, it is not sufficient to determine its drivers. Both abiotic and biotic factors play an important role in influencing the spatial ecology of species (Royle *et al.* 2017). Among abiotic factors, the spatio-temporal availability of thermal habitats is one of the most important drivers of fish distribution and migrations in freshwater environments (Lucas and Baras 2001, Isaak *et al*. 2010). Despite the general perception that the thermal environment in running freshwater is homogeneous, streams actually exhibit substantial thermal variability at small (10 to 100 m) and large (> 1,000 m) spatial scales due, for example, to the variability in elevation, riparian vegetation shade and groundwater input along their extension (Kurylyk *et al*. 2015). Temperature has a strong potential to limit Arctic grayling populations, as highlighted by Stamford *et al*. (2017), and it is known that the occurrence of Arctic grayling and bull trout is negatively related to water temperature (Hawkshaw *et al*. 2014, Isaak *et al*. 2010). Therefore, a full description of the distribution and migrations of Arctic grayling in the Williston Reservoir Watershed requires a detailed characterization of the distribution of thermal habitats. Spatial stream network modeling (SSNM) provides high resolution predictions of temperature patterns

over large spatial extents and their application to animal occurrence data has become more widespread (Isaak *et al*. 2014). A novel combination of telemetry detection data and spatial modeling will provide a detailed characterization of Arctic grayling thermal ecology and available thermal habitat as well as interactions with bull trout (see below).

Understanding diets and dietary relationships of coexisting species is important to determine resource partitioning (Wrona et al. 1981) as overlap in dietary resource use is thought to influence spatial ecology and population trends of coexisting fish (Stamford et al. 2017). Coexisting species often exploit different resource niches, resulting in reduced competition between the species (Millinsky 1982). Further, competition influences diet selection, in which competitive individuals select for higher nutrition food sources resulting in others adopting a generalist diet pattern (Milinsky 1982). Interspecific competition has been defined as "the demand of more than one organism for the same resource of the environment in excess of immediate supply" (Larkin 1956). Therefore, dietary trends can be a viewed as the result of single or compounding factors such as habitat availability, stream productivity, spatial distribution and interspecific competition (Evangelista et al. 2014, Magnan and Fitzgerald 1984). Intraspecific competition can also drive diet preference as larger, dominant individuals establish feeding hierarchies within a species (Hughes 1992). Feeding hierarchies have been observed within freshwater fish populations where larger fish tend to outcompete other individuals for optimal feeding positions (Hughes 1992). In the Williston Reservoir Watershed, Arctic grayling co-occur with bull trout (*Salvelinus confluentus*) in streams of several core areas, and there is a strong potential for size-dependent overlap in resource use. For example, as juveniles, both species prey heavily on terrestrial drift, aquatic insects and other invertebrate prey and individuals larger than 150 mm will increasingly include fish as prey (Stewart *et al*. 2007a,b). Arctic grayling feeding behavior also appears to be related to the degree of competition for prey resources (Stewart *et al*. 2007b). Overlap in resource use and/or risks of predation by larger bull trout on smaller Arctic grayling, may significantly influence the spatial ecology of Arctic grayling in ways that limit the potential growth of its populations (Stamford *et al*. 2017). Therefore, examining trophic positions of multiple species, trends in dietary niche between bull trout and Arctic grayling, as well as dietary breadths of both species is necessary to characterize the trophic relationships at the community, interspecific and intraspecific levels.

## 2. Objectives and Linkage to FWCP Action Plans and Priority Actions

The goal of this project is to investigate the spatial ecology of sub-adult and adult Arctic grayling and their interactions with bull trout in the Parsnip mainstem and tributaries, a core area of Arctic grayling populations in the Williston Reservoir Watershed. Specifically, the objectives are to:

i. Investigate the migrations of sub-adult and adult Arctic grayling among the Parsnip mainstem, tributaries and a nearby watershed (Pack River);

ii. Describe and define the distribution and thermal habitat use of sub-adult and adult Arctic grayling;
iii. Determine the overlap in distribution patterns of sub-adult and adult Arctic grayling and bull trout;
iv. Determine the patterns of resource use and the resulting trophic relationship between Arctic grayling and bull trout.

The information gathered in this study will fill in data gaps that were identified as moderate and high immediacy for the Parsnip core area (data gaps 5.1.3a-i in Table 6 of Stamford et al. 2017) and will also be relevant to other core areas in the Williston Reservoir Watershed (2.3.1b-c and 2.3.5 in Table 1 of Stamford et al. 2017). Therefore, the outcomes of this study will primarily address the priority action # 9 (PEA.RLR.S03.RI.09) of the *Peace Region Rivers, Lakes, and Reservoirs Action Plan* (FWCP 2020). However, given that the study will collect data on bull trout, it will also contribute information to address priority # 13 (PEA.RLR.S04.RI.13) of the *Peace Region Rivers, Lakes, and Reservoirs Action Plan* (FWCP 2020), particularly by filling in high immediacy data gaps 5.1a and 5.1b outlined in Table 5.1c in Hagen and Webber (2019).

## 3. Study Area

The project was conducted in the Parsnip River core area (watershed), with a focus on five streams in 2020: Parsnip River, Anzac River, Table River, Hominka River, and Missinka River. The Parsnip River watershed lies within the territory of the Tse'khene First Nation.

### 3.1. Parsnip River

The Parsnip River (54.769403°, −122.501018°) has a watershed area of 5,612 km$^2$ (Hagen *et al*. 2015). Total river length is 175 km, and the majority of this is low gradient. The river has a wide channel with many meanders, large gravel bars and clay banks. Substrate is a mix of cobble, gravel and fines. The Parsnip River and its major tributaries drain a mountainous area in the Hart Ranges of the Rocky Mountains, which lies east of the Rocky Mountain Trench. The Parsnip has turbid water as a result, and high peak flows from late-May to early June. Substantial glacial influence occurs in the Upper Parsnip River. However, in late summer downstream of the Missinka River (54.578597°, -122.034947°), turbidity improves (Hagen et al. 2015). The highest flows occur in late May, and the lowest flows occur during the period from September to March (Blackman 2002a). Discharge and temperature data are available from a Hydrometric Data gauge located above the confluence with the Misinchinka River (Station 07EE007, Water Survey of Canada).

### 3.2. Anzac River

The Anzac River (54.902632°, −122.280257°) drains a 939 km$^2$ watershed and is 78 km in length with an average gradient of 0.7% (Blackman 2002a). The stream drains a mountainous region of the Hart Ranges in the Rocky Mountains, on the East side of the Parsnip mainstem. Watershed elevation ranges from 730 m at the confluence with the Parsnip River to 2,495 m in the headwaters (Beaudry et al. 2000). The upper river is characterized by bedrock canyons with a moderate gradient (1-2%). The lower river lies in a wide unconfined valley. As the river nears the Parsnip River confluence it creates large meanders, many oxbows and has a low gradient (<0.5%) (Blackman 2002a). Snowmelt causes high river turbidity and flows in the spring months. However, the Anzac is low and clear in the late summer months and fall. Substrate is mainly composed of clean cobble and gravel. No hydrometric data are available for the Anzac River.

### 3.3. Table River

The Table River (54.755545°, −122.090737°) drains a 506 km$^2$ watershed and is 56 km in length with an average gradient of 0.7% (Blackman 2002a). The stream drains a mountainous region of the Hart Ranges in the Rocky Mountains, on the East side of the Parsnip mainstem. Watershed elevation ranges from 725 m at the confluence with the Parsnip River to 2500 m in the headwaters (Beaudry et al. 2000). The upper river has a moderate gradient (1-2%). The lower river has a low gradient (<0.5%) and contains many oxbows, side channels and abandoned channels (Blackman 2002a). No hydrometric data are available for the Table River.

### 3.4. Hominka River

The Hominka River (54.696944°, -121.837500°) drains a 433 km$^2$ watershed (Hagen et al. 2015). The stream drains a mountainous region of the Hart Ranges in the Rocky Mountains, on the East side of the Parsnip mainstem. Watershed elevation ranges from 669 m at the confluence with the Parsnip River to 2,100 m in the headwaters. The upper watershed is confined by steep slopes which quickly ascend to alpine terrain, and the river has a moderate gradient (3-5%). The lower river is sinuous, low gradient (<0.5%) and drains many adjoining marsh wetlands (Beaudry et al. 2000). No hydrometric data are available for the Hominka River.

### 3.5. Missinka River

The Missinka River (54.596666°, -121.737500°) drains a 434 km$^2$ watershed (Hagen et al. 2015). The stream drains a mountainous region of the Hart Ranges in the Rocky

Mountains, on the East side of the Parsnip mainstem. Watershed elevation ranges from 740 m at the confluence with the Parsnip River to 2,346 m in the headwaters. The upper river is entrenched, confined by steep valley walls, and the river has a moderate gradient (1-3%). The lower river is sinuous, low gradient (<0.5%) with a wide alluvial floodplain (Beaudry et al. 2000). No hydrometric data are available for the Missinka River.

## 4. Methods

The methods used to address the study objectives include: acoustic telemetry, capture-recapture, temperature data logging, stable isotope analysis and spatial stream network modeling. Arctic grayling and bull trout were captured by angling. Captured fish were tagged (acoustic transmitters, and/or PIT [Passive Integrated Transponder] and anchor tags), sampled for muscle and adipose fin tissue (use in stable isotope analyses), and released. Fish tagged with acoustic transmitters have been continuously monitored by an array of acoustic receivers deployed throughout the Parsnip River watershed and in the Pack River. A small subset of potential prey for Arctic grayling and bull trout were caught by angling, kick-netting and electrofishing, were sacrificed for stable isotope analysis (to fully characterize the food webs where Arctic grayling and bull trout are located). Separate data loggers were deployed to monitor both air and water temperature throughout the Parsnip watershed.

### 4.1. Fish Capture and Tagging

Arctic grayling and bull trout were captured by angling at various sites in the Anzac, Table, Hominka, Missinka and Parsnip rivers (Figure 1). Captured Arctic grayling and bull trout > 230 g were surgically tagged with acoustic transmitters. For surgical tag implantation, the fish were sedated by electro-anaesthesia (Ward et al. 2017, Abrams et al. 2018) using electric gloves attached to a Transcutaneous Nerve Stimulation (TENS) 3000 unit (Koalaty Products Inc., Tampa, USA), while kept in a V-shaped trough filled with ambient water. A small incision (20-30 mm) was made on the ventral midline 30-50 mm posterior to the pectoral fins and an acoustic tag (V9, Vemco, Bedford, Canada) and a PIT tag (12mm HDX, Oregon RFID) were inserted into the peritoneal cavity. The incision was closed with 3-4 simple interrupted sutures (Wagner et al. 2011). The tags as well as the tagging instruments were all disinfected in a bath of Virkon (Lanxess, Germany) for 10 minutes and rinsed with distilled water. The fish were also externally tagged with an anchor tag (below the dorsal fin), measured (fork length), weighed and sampled for muscle and adipose fin tissue. After processing, the fish were placed into a recovery bag filled with ambient water and released at the capture site after regaining equilibrium and responding vigorously when grabbed by the tail.

To augment spatial information on Arctic grayling and bull trout, additional fish were captured and tagged with anchor and/or PIT (8mm FDX or 12mm HDX) tags, including fish < 230 g. The captured fish were immobilized by electro-anaesthesia (see above) and

quickly handled in a V-shaped trough filled with ambient water, where they were externally tagged with an anchor tag (below the dorsal fin) and PIT tag (injected into the abdominal cavity), measured (fork length), weighed, and sampled for muscle tissue and adipose fin tissue. The location of capture or recapture of tagged fish was recorded with a GPS. In an effort to increase the number of recaptures, local First Nations and recreational anglers have been asked to report the capture of any tagged fish as well as the date/time and spatial coordinates of capture. We have been working with the Angler's Atlas to use their MyCatch app and their capacity to reach out to thousands of anglers in BC to request that any tagged fish caught by anglers be reported along with the relevant information (date/time, location, and tag number).

Fish handling and tagging protocols were approved by the UNBC Animal Care and Use Committee (Protocol number: 2018-06). Permits to capture and tagging fish in this study were issued by the BC Ministry of Forests, Lands, Natural Resource Operations and Rural Development (Fish Collection Permit numbers: PG18-356580, PG19-523435, and PG20-606121).

## 4.2 Monitoring of Fish with Acoustic Telemetry

### *4.2.1 Field Data Collection*

Acoustic receivers (VR2W, Vemco, Bedford, Canada) were deployed widely across the watershed in clusters of 2-4 receivers spaced 0.5-2 km from one another (Royle et al. 2014). Receivers were moored hydrophone-up on the streambed using a system of concrete blocks, steel cable, and duckbill earth anchors. Given the narrow width of the streams (10-60m) in the study area and the typically high detection efficiency of acoustic receivers at short distances (< 50m), only one receiver was deployed at each point location at 5-20m from the banks. Data download windows are typically constrained to late summer and early fall by seasonally high water and difficult site access. As such, data collected by acoustic receivers from 2018-2019 were downloaded in 2019, data collected in 2019-2020 were downloaded in 2020, and data collected from 2020-2021 will be downloaded in 2021.

### *4.2.2 Receiver Array Maintenance*

The original acoustic array used in this study was installed in 2018 and consisted of 55 acoustic receivers deployed in the Parsnip River watershed and one receiver deployed in the Pack River watershed. The array grew in 2019, with an additional 26 acoustic receivers (including two replacements) deployed in the Parsnip River watershed and an additional two receivers in the lower Pack River (Figure 2). Between 2018 and 2019, eight acoustic receivers were lost; seven to shifting sediment burying the receiver or exposing the anchor (Table River – 4; Anzac River - 2; Parsnip River – 1*)* and one was lost due to vandalism. The vandalized receiver was sent to Vemco for repair and was not replaced, while two of the seven sites where receivers were lost to natural disturbance were

deemed feasible for replacement (one in the lower Table River; one in the upper Anzac River). Deployment methods were adjusted after the 2018-2019 losses, with focus shifting from pool habitats (which were associated with sediment deposition and small, mobile sediments) to slow, deep run/glide habitats (which were associated with better receiver retention and larger, more stable cobble substrates). Between 2019 and 2020, 21 additional acoustic receivers were lost due to an unusually high and sustained spring freshet which impacted the riverine environment to the point that some sites were no longer recognizable from the year before (Table River – 7; Parsnip River – 5; Anzac River – 4; Hominka River – 3; Missinka River – 2; Misinchinka River – 1). Due to the clustered deployment strategy and large spatial extent of the receiver array, these losses, while unfortunate due to data loss, will not affect our ability to carry out the project objectives. After accounting for replaced and unreplaced losses, Arctic grayling and bull trout tagged pursuant to this study are being continuously monitored by an array of 61 receivers. Evaluation of array detection efficiency is ongoing with specific testing goals in place for the 2021 field season to evaluate our preliminary observations about the influences of flow and river morphology on detection efficiency.

*4.2.3 Data Preparation and Analyses*

Pre-processing and analyses of telemetry data were conducted in R Statistical Software (R Core Development Team 2020). Data was reproducibly pre-processed following the protocols outlined in the package *actel* (Flavio and Baktoft 2020). Exploratory analyses of the telemetry data were conducted using the packages *actel*, *RSP* (Niella et al. 2020), and *overlap* (Ridout and Linkie 2009). For the 2018 – 2020 seasons, telemetry data has been analyzed in a coarse exploratory framework. Once collection of the telemetry data is completed in the fall of 2021, analyses will be extended to include both fine-scale analyses of movements and migrations as well as quantitative metrics of home range size and activity center using spatial capture-recapture models (Royle et al. 2014). Coarse exploratory analyses included plotting individual fish detection histories to estimate residency histories across the duration of the monitoring period. Using package *RSP*, individual movement patterns are visualized by 'tracks', defined as individual movement events occurring in less than a 24-hour period. Population-level metrics were estimated for both Arctic grayling and bull trout. Arrival and departure times to and from the Parsnip mainstem and each tributary were plotted by species using package *actel* and used for coarse estimates of migration timing. Spatio-temporal overlap between Arctic grayling and bull trout was visualized monthly from January to August 2020 using dynamic Brownian Bridge Movement Models (dBBMM) as a way to gain coarse insights into the migration behaviors of these species.

Arctic grayling spawning migrations are characterized in part by the early arrival of males to the spawning grounds (Lashmar and Ptolemy 2002), so receiver sites in the middle-to-upper reaches of the tributaries were explored for sexual differences in order-

of-arrival times using package *overlap* (Ridout and Linkie 2009). This package fits kernel density functions to two datasets and analyzes them for periods of temporal overlap and in this analysis was applied to Arctic grayling detection data subset by sex. Analyses done in packages *actel* and *RSP* required a shapefile of the study area. Polygons of each river were downloaded from the Freshwater Rivers Atlas of BC (GeoBC) and merged in QGIS (v 3.14.16). Rivers were buffered by 200 m to ensure they would be detected by the pixel size of the import function and their extent traced by a polygon. The difference between the river shapefiles and the extent polygon was taken to create one rectangular polygon with "empty" space depicting water.

## 4.3. Temperature Monitoring

### *4.3.1 Field Data Collection*

Air and water temperature data loggers (DS1921Z, Maxim Integrated, San Jose, USA; MX2203 and MX2201, Onset, Bourne, USA) were deployed throughout the study area in the 2018, 2019 and 2020 field seasons. Water temperature loggers were attached to acoustic receiver moorings or boulders in the stream following methods outlined by Isaak *et al*. (2013). Air temperature loggers were installed 2 m off the ground on stable vegetation 0 m and 10 m from the stream. Inferences made from predicted temperatures can be greatly affected by the spatial relationships of sampled sites (Som et al. 2014). Spatial Stream Network Models use universal kriging, a geospatial technique for spatial data interpolation. Optimal network design for the estimation of semivariance is critical for gaining accurate and insightful conclusions from spatial data (Dale and Fortin 2014, Cressie et al. 2006). To accurately describe semivariance, a measure of spatial autocorrelation, it is suggested to include areas of high leverage in spatial trends (Zimmerman 2006). For a dendritic river network, such as the Parsnip watershed, we spread temperature loggers over an elevational gradient and clustered loggers around confluences (Figure 2). Temperature data was downloaded at the same time as the acoustic receivers in September and October of 2020.

### *4.3.2 Data Cleaning and Imputation*

Data collection and cleaning was conducted according to methods outlined by Sowder and Steel (2012). Some temperature records were incomplete for a variety of reasons including battery failure, exposure to air and logger malfunctions. Time series with greater than 30% record completion during a temporal window of interest were imputed using a regularized iterative Principal Component Analysis algorithm implemented in the *missMDA* package in R Statistical Software (Josse and Husson 2016, R Core Development Team 2020). This data imputation technique creates a complete time series of daily mean air and water temperatures for each location. The algorithm implemented in the *missMDA* package minimizes and provides the mean square error of prediction (MSEP) for imputation using leave-one-out cross validation. The data loggers recorded a

variety of sub-daily measurements, so data was aggregated into daily values for imputation. This technique of data imputation has a demonstrated history for temperature records and SSNM's (Isaak et al. 2018).

*4.3.3 Hydrological Layer Pre-processing*

Spatial statistical models such as the SSNM require valid autocovariance functions to account for large error variance cause by spatial autocorrelation among measurement locations. Due to the branching structure of river networks and the influence of downstream flow and tributary confluences, autocovariance functions need to be based on network distance, as patterns in spatial autocorrelation are not adequately described by euclidean distance (Isaak et al. 2014). Specialized toolsets are required to fit spatial models to stream networks, which calculate a variety of watershed attributes including stream network distance, flow direction and landscape contributing areas. Before watershed attributes can be gathered, water temperature data was prepared in a points shapefile holding information on aggregated temperature metrics and data logging site locations. A gridded air temperature raster layer at 1km resolution was created with Universal Kriging in SAGA GIS (Conrad et al. 2015). Both air and water temperature data were aggregated across a relevant time window of July 1$^{st}$ to September 15$^{th}$ of 2019 and 2020. This time window represents the "trophic feeding" window of Arctic grayling seasonal migrations. This temporal window was chosen based on historical movement studies as well as preliminary analysis of acoustic telemetry data using the *actel* package in R Statistical Software (Blackman 2002b, Flavio and Baktoft 2020, R Core Development Team 2020). The openSTARS package in R Statistical Software was used to produce a pre-processed stream layer (SSN object) (Kattwinkel and Szöcs 2018, R Core Development Team 2020). The openSTARS package uses R and GrassGIS (Neteler et al. 2012) to derive watershed physical components from a digital elevation model (DEM). Additional landscape covariates created by the openSTARS package include upstream contributing area (H2OAreaA), elevation and slope (Table 1).

*4.3.4 Spatial Stream Network Model Selection*

Following creation of the SSN object, the *SSN* package in R Statistical Software was used to generate and evaluate spatial statistical models which predict temperature metrics across the entire watershed (Ver Hoef et al. 2014, R Core Development Team 2020). Model selection was based on a multi-stage process following methods outlined in Peterson and Ver Hoef (2010) and Marsha et al. (2021). First covariates were selected using a threshold of inclusion, where evidence of a weak relationship with the response metric resulted in removal of the covariate ($p > 0.15$ for a two-sided *t-test* under a null hypothesis of zero slope). Then the covariates which passed the threshold test were evaluated for multi-collinearity and where covariates had correlation coefficients $>|0.8|$ only a single covariate was retained. The third stage involved the selection of covariance parameters used to describe spatial autocorrelation among network connected, un-connected and euclidean distances. A matrix was created with all possible combinations of covariance parameters in the *SSN* package. The combination of covariance parameters which yielded

the lowest AIC score were selected and used for prediction of water temperature across the Parsnip watershed.

## 4.4. Stable Isotope Analysis

### *4.4.1 Stable Isotope Sample Collection*

Sampling for stable isotope analysis (SIA) occurred at eight sites stratified across the upper and lower reaches of the Anzac, Hominka, Table rivers, as well as the lower Missinka river (Figure 1). All sites were angled for a total of 2 person-hours (=2 anglers x 1hr effort) to target large, mature fish. White muscle tissue and adipose fin samples were also provided by collecting samples during acoustic implantation surgery. Sampling of aquatic macro-invertebrates, other fish, periphyton and terrestrial vegetation, was conducted at the same eight sites. Benthic macro-invertebrates were sampled by conducting three rounds of 30 second kicknets in shallow riffles. Collected macro-invertebrates were then identified and stored for lab processing by genera. Potential prey fish such as slimy sculpin (*Cottus cognatus*), juvenile burbot (*Lota lota*) and mountain whitefish (*Prosopium williamsoni*) were captured during kick netting or via electrofishing, using a backpack electrofisher (LR-24, Smith-Root, Vancouver, WA, USA). Sampling was conducted along stream margins, beginning with conservative settings (100v, 40Hz, 10% duty cycle), then adjusted for optimal capture. Particulate organic matter was collected via scrubbing 5 large rocks in 3L of stream water for 30 seconds. Terrestrial vegetation was sampled via collecting the five most abundant riparian species.

A large variety of samples is important to reduce uncertainty in dietary sources as well as provide insight into food web structure as small sample sizes can skew results of metrics (Layman et al. 2007). Further, having samples representative of many different food sources will help generate a larger, more holistic food web characterization by the end of the project. Preliminary analyses on differences in summer diets of bull trout and Arctic grayling highlighted previously low sample sizes. In 2020 there was a significant effort to increase both bull trout and Arctic grayling sample sizes as well as obtain a larger variety of size classes represented in our data.

### *4.4.2 Stable Isotope Sample Preparation and Analysis*

In the laboratory, all collected material was kept in a –30°C freezer until processing for stable isotope analysis. Periphyton samples were filtered using a vacuum filtration system fitted with a fibreglass filter. All samples were dried in a standard laboratory convection oven set at 50°C for a minimum of 48 hours and then ground to a powder using a mortar and pestle. Measurements of $\delta^{13}C$ and $\delta^{15}N$ isotope from ground samples was done with a Delta Plus Continuous Flow Stable Isotope Ratio Mass Spectrometer (Thermo Finnigan, Bremen, Germany) coupled to a Carlo Erba elemental analyzer (CHNS-O EA1108, Carlo Erba, Milan, Italy) at the Environmental Isotope Laboratory, University of Waterloo (Waterloo, ON).

*4.4.3 Stable Isotope Data Analysis*

SIA is a common method used to investigate ecosystem food webs, determine trophic interactions between species and diet analysis, all done by looking at $\delta^{13}C$ and $\delta^{15}N$ ratios (e.g. Harrison et al. 2017, Estrada et al. 2003). R Statistical Software packages such as *SIBER* (Stable Isotope Bayesian Ellipses in R) have been developed to estimate dietary breadth and dietary overlap from stable isotope data (Jackson et al. 2011, Layman et al. 2007). *SIBER* is considered a powerful tool and accurate method of understanding trophic relations and niches, as isotope enrichment in tissues increases with trophic level (Jackson et al. 2011, France 1995). SIA using ellipses creates an accurate analysis of consumer diet with resulting ellipse variance representing among individual variation in diet (Harrison et al. 2017, Semmens et al. 2009). Ellipses are chosen as they can be used to determine niche similarity among species or communities (Jackson et al. 2011, Layman et al. 2007).

Results of samples collected in 2020 were received in January of 2021. Basic isoplots fitted with 95% confidence ellipses were plotted and a set of comparative metrics such as total ellipse area and standard ellipse area corrected for small sample sizes (Layman et al. 2007) were calculated for both Arctic grayling and bull trout, as well as with invertebrates and prey fish. Total ellipse area (TA) and standard ellipse area corrected for a small sample size ($SEA_c$), were calculated to provide insight on trophic positioning between species and at a larger scale (Jackson et al. 2011, Layman et al. 2007). An unequal variances *t*-test was used for determining differences in levels of carbon and nitrogen between bull trout and Arctic grayling. Residuals were assessed for normality using Q-Q plots. Homogeneity of variance was assessed using Levene's test. Ultimately, all data tested met the assumptions of the tests applied. A general linear model was fitted to the fork length, C isotope and N isotope data to determine patterns of dietary preferences among size classes in a species. These varied analyses enabled us to investigate differences not only between species but also among varying size classes within species. All analyses were done using R Statistical Software (R Core Development Team 2020).

# 5. Results and Outcomes

5.1. Fish Capture, Tagging and Recaptures in 2020

A total of 69 fish (44 Arctic grayling and 25 bull trout) were tagged in 2020, (13 Arctic grayling and three bull trout in the Hominka River, three and two in the Missinka River, 12 and eight in the Table River, 15 and six in the Anzac River, zero and one at Colbourne Creek, one and three in the Parsnip River, and zero and two in the Pack River) (Figure 2). All fish were tagged with acoustic transmitters, PIT tags and anchor tags. To date, a total of 220 fish have been tagged across the watershed.

Among tagged Arctic grayling, 16 were identified as females (mean ±1 SD: 481.6 ± 151.0 g for weight; 33.4 ± 3.0 cm for fork length), 12 were identified as males (mean ±1 SD: 598.8 ± 134.3 g for weight; 39.3 ± 9.5 cm for fork length), and 16 could not have the sex determined (mean ± 1 SD: 407.1± 209.2 g for weight; 30.4 ±6.1 cm for fork length).

Among tagged bull trout, six were identified as females (mean ± 1 SD: 2,391.7 ± 759.0 g for weight; 58.3 ± 7.1 cm for fork length), 11 were identified as males (mean ± 1 SD: 2,320.6 ± 975.0 g for weight; 63.4 ± 14.8 cm for fork length), and eight ± 1 SD: 867.3 ± 1,040.6 g for weight; 39.3 ± 15.5 cm for fork length).

Seven fish were recaptured in 2020. Project staff recaptured three Arctic grayling in the month of September; one each in the Anzac, Table, and Hominka Rivers. An angler recaptured one grayling and one bull trout from the Anzac River during the month of July and one bull trout from the Anzac River in August. Another angler recaptured one bull trout from the Anzac River in August.

5.2. Acoustic Telemetry Monitoring

5.2 Telemetry results

Exploratory analyses of individual detection histories (Appendix A.1) showed that migratory populations of Arctic grayling and bull trout in the Parsnip core region show relatively high tributary fidelity during their spring and summer migrations. Of the fish that have been monitored long enough to have multiple seasons of track histories, the majority showed a residency period in the Parsnip mainstem over the winter months and a circular migration to the same tributary as they spent time in during the previous summer. Only eleven fish were detected having visited multiple tributaries in addition to the Parsnip mainstem, and only one of these (bull trout 24384) showed any pattern of spending sustained time in more than one tributary; each summer saw this individual spend about a month each in the Anzac and Table Rivers. Of the remaining multi-tributary users, Hominka/Anzac River splits were the most commonly observed. Individual detection histories were both analyzed and visualized using package RSP 'tracks'. RSP tracks are single movement 'events' (a series of detections spanning two or more receivers and lasting less than 24 hours), and they revealed that bull trout on average moved farther per event (12.3 ± 8.3 km per event) than Arctic grayling (4.3 ± 6.3 km)(Appendix A.2). There was no significant difference ($t = 0.08$, $P = 0.93$) in the number of movement events between Arctic grayling (13.6 ± 9.6 events per individual over the duration of the study) and bull trout (13.3 ± 15.2), though the mean total distance moved was slightly lower in the tagged Arctic grayling (38.3 ± 40.4 km) than in the tagged bull trout (50.0 ± 45.2 km). Bull trout that showed large-scale movement events commonly showed track histories that left the detection range of the telemetry array downstream of the Misinchinka River, likely continuing on towards the Williston Reservoir (Appendix

A.3). In contrast, only one tagged Arctic grayling showed a movement history that extended downstream of the Misinchinka River (Arctic grayling 19305).

Dynamic Brownian Bridge Movement Models (dBBMM) were used to visualize the distribution of both species and were plotted by month from January – August 2020 (Appendix A.4)(Niella et al 2020). From the monthly observations, overwintering habitat use was concentrated at the confluences of the Anzac and Hominka Rivers with the Parsnip mainstem. Some movement around the mainstem was common over the winter months, with some brief periods of activity in the lowest reaches of the Anzac and Hominka Rivers. Grayling were not observed in the tributaries during the winter months, but the middle reach of the Table River saw bull trout activity in the months of January – April. In May, all detected bull trout and some Arctic grayling began to enter the tributaries, with much of the Parsnip mainstem occupied by Arctic grayling. By June, Arctic grayling have committed to the tributaries, and even the highest reaches in the array detect movement of both species. In July, the spatial extent of bull trout spread back to include the Parsnip mainstem, while Arctic grayling distribution largely remained in the tributaries and the Parsnip mainstem between the Table and Hominka Rivers. Interestingly, the Parsnip mainstem downstream of the Anzac River saw widespread Arctic grayling movements during the month of August when detection in the tributaries was still significant. These movement patterns can be seen in the arrival time plots generated by the package *actel*, with June and July showing peaks in the arrival data for the tributaries, and September and October showing peaks in arrival times back into the Parsnip mainstem (Appendix A.5). As was seen with the distribution plots, the data display a clear periodicity in the tributaries with little to no activity occurring in the winter months. The arrival of Arctic grayling to spawning grounds is characterized in part by an early arrival of males. Overlap analyses were performed at each receiver site in the middle-to-upper tributaries that returned at least 3 detections of both male and female Arctic grayling occurring at any time during the year (Appendix A.6). Two sites in the Anzac River (ANZR08, ANZR37) and three sites in the Table River (TBLR09, TBLR15, TBLR35) showed evidence of early male arrival.

## 5.3. Temperature Monitoring

### *5.3.1 Field Data Collection*

In 2020, eight new water temperature logging stations were deployed in the Parsnip watershed. Three of these new water temperature logging locations received associated air temperature loggers. New deployments were targeted in previously unsampled portions of the watershed which do not hold populations of Arctic grayling but contribute to the downstream thermal riverscape. In the fall of 2020, data from 65 water temperature loggers and 40 air temperature loggers were downloaded.

### *5.3.2 Temperature Data Imputation and Summary Metrics*

Data were available from 39 logger locations in 2018 for late summer (August 1-September 15) revealing a mean temperature of 11.90°C (± 2.98°C). The mean water temperatures for the trophic feeding window (July 1 – September 15) in 2019 and 2020 were 10.60°C (± 1.66°C) and 9.47°C (± 2.37°C) respectively. These summary metrics and the SSNM's were derived from 57 complete water temperature times series in 2019 and 51 in 2020. The corresponding mean air temperatures in 2019 and 2020 were 11.90°C (± 2.35°C) and 11.20°C (± 3.13°C) respectively. These summary metrics and air temperature covariates in the SSNM's were derived from 21 useable air temperature times series in 2019 and 17 in 2020. The MSEP for imputation of water temperature was 0.1960°C for 2018, 0.1670°C for 2019 and 0.1941°C for 2020. The MSEP for data imputation of air temperature was 0.6522°C and 0.8150°C for 2019 and 2020, respectively. Box and whisker plots were used to visualize detection temperatures for Arctic grayling (Figure 3) and bull trout (Figure 4) during the late summer in 2018 and the trophic feeding window in 2019 and 2020. For these visualizations, only a subset of acoustic receivers with attached temperature loggers could be used (2018 n=15, 2019 n=40, 2020 n=25). Mean Arctic grayling detection temperature was 10.29°C (± 2.47°C) in 2018, 10.62°C (± 1.35°C) in 2019 and 9.62°C (± 1.94°C) in 2020. Mean bull trout detection temperature was 8.91°C (± 1.70°C) in 2018, 10.52°C (± 1.52°C) in 2019 and 10.26°C (± 2.12°C) in 2020. Comparing results between 2018 and 2019/2020 should be done with caution because the 2018 data covers a shorter temporal scale and a significantly reduced telemetry and temperature logging array.

*5.3.3 Spatial Stream Network Model*

Spatial Stream Network Models were fit for the trophic feeding window (July 1st – September 15th) average weekly average temperature (AWAT) and average weekly coefficient of variation (AWCoefVar) in 2019 and 2020 (see temperature data logging sites and AWAT metrics in Figures 5 and 6). No single mix of covariance parameters could most accurately predict the two response metrics in each year. This speaks to variability in temperature data across metrics and years. The two covariates representing air temperature (AvTmpA) and reach contributing area (H2OAreaA) passed the model covariate selection process. Covariates describing average elevation and slope were too highly correlated to air temperature and reach contributing area so were discarded from the analysis. The final covariates, covariance parameters and the root mean squared prediction error (RMSPE) of the models can be seen in Table 1. Two trends are apparent in the SSNM predictions. The first is that elevational gradients dominate the averaged thermal landscape (Figures 7 and 9). The second is that variability (AWCoefVar) was not homogenous across the thermal landscape but varied across sites and years.

5.4. Stable Isotope Analysis

Since 2018, a total of 401 biological samples have been collected for isotopic analysis of carbon ($\delta^{13}C$) and nitrogen ($\delta^{15}N$) (Table 2). Samples included adipose fin tissue (n = 118),

muscle tissue (n = 126), prey fish (n = 41), invertebrates (n = 30), terrestrial vegetation (n = 70) and aquatic vegetation or periphyton (n = 16).

Stable isotope biplots fitted with 95% ellipses were used to determine breadth size of Arctic grayling and bull trout diets as well as infer trends about resource use and overlap (Figure 11). When comparing bull trout and Arctic grayling dietary breath (TA), bull trout were found to occupy a larger dietary niche in comparison to Arctic grayling ($TA_{bull}$ = 67.8, $TA_{grayling}$= 17.7). $SEA_c$ also confirmed this relationship ($SEA_{c\ bull}$ = 17.4, $SEA_{c\ grayling}$ = 2.8). These data indicate that bull trout are consuming a diverse selection of dietary items while Arctic grayling exhibit more homogeneous dietary preferences between individuals (Figure 11). A stable isotope biplot was also used to investigate food web positioning of Arctic grayling and bull trout (Figure 12). Bull trout were found to occupy the top trophic position with Arctic grayling being the next highest. Prey fish diets registered slightly below Arctic grayling.

Significant differences in mean isotopic carbon ($t$ = 5.18, df = 124, P < 0.001) and nitrogen ($t$ = -9,83, df = 41, P < 0.001) between Arctic grayling and bull trout were identified (Figures 13, 14). Mean $\delta^{15}N$ levels were measured at 7.28‰ for Arctic grayling and 10.87‰ for bull trout (Figure. 13). Mean $\delta^{13}C$ levels in arctic grayling were calculated at –28.12‰ and bull trout were measured at –30.01‰ (Figure 14). A linear regression revealed no relationship between Arctic grayling $\delta^{15}N$ and fork length (F = 1.54, df = 84, P = 0.21) (Figure 15), but a positive relationship between $\delta^{15}N$ and fork length in bull trout ($\beta$ = 0.098, 95% CI [0.007, 0.013], $t$ = 6.99, P<0.001, $R^2$ = 0.58, Figure 16).

5.5. Community Outreach

We have engaged in eight outreach activities in 2020:

i. Online Undergrad thesis presentation: Online presentations of 2019/2020 NREM 430 studies, April 23rd 2020. Undergraduate student Ian Clevenger presented a summary of the project along with preliminary findings of analyses done on stable isotope data. The presentation lasted 15 minutes and was attended by a mixed group of peers, professors, local FLNRORD staff and the general public.
ii. Instagram post by the project lead (Eduardo Martins) on August 6 briefly describing the project goal and highlighting the FWCP support. Audience reached: 74 direct followers.
iii. During the field season, the team was approached by a local filmmaker who wanted to incorporate the study into the narrative of his episode on the Table River for the Reelistic Outdoors show. Joe Bottoms and Ian Clevenger were included in a 5-minute segment of the episode, catching and tagging fish as well as Joe gave an overview of the project scope as well as the importance of furthering the understanding of Arctic grayling in the Parsnip watershed. The episode aired on 8 December, 2020 on the Sportsman Channel.

iv. Presentation of the spatial stream network model and thermal habitat use by Arctic grayling at the Canadian Conference for Fisheries Research in the Telemetry Symposium by Bryce O'Connor February 15-19, 2021.
v. Presentation of the spatial stream network model and thermal habitat use by Arctic grayling at the Washington-British Columbia Chapter of the American Fisheries Society Annual Meeting by Bryce O'Connor March 1-3, 2021.
vi. Presentation of the spatial stream network model and thermal habitat use by Arctic grayling at UNBC Research Week by Bryce O'Connor March 3, 2021.
vii. Presentation of project overview and thermal habitat use by Arctic grayling to UNBC Student Chapter of The Wildlife Society by Bryce O'Connor March 25, 2021.
viii. Discussion of preliminary results and progress update to Ministry of FLNRORD fisheries branch staff by Dr. Eduardo Martins, Joseph Bottoms, Ian Clevenger and Bryce O'Connor March 31, 2021.

# 6. Discussion

## 6.1. Acoustic Telemetry Monitoring

### *6.1.1 Movement Patterns*

Analyses of 2020 data were limited by the loss of 21 acoustic receivers during prolonged springtime flood conditions. Despite these losses, the ability of the packages *actel* and *RSP* to handle discontinuous spatial and temporal data still allowed for insights into the coarse scale patterns of Arctic grayling movements in the Parsnip watershed. As salmonids, high fidelity to a certain tributary is perhaps unsurprising. An analysis of the data using spatial capture-recapture will refine these results to include descriptions of where individual fish home range centers are distributed across the watershed during different migratory life phases.

Of the eleven fish that produced detection histories that include more than one tributary, many of these showed straying into nearby rivers in the later summer, suggesting that these were more related to feeding movements than spawning migrations. Concentrations of fish overwintering near the confluences of the Anzac and Hominka Rivers as well as in the Parsnip mainstem between the Anzac and Table Rivers suggest that these are important areas for overwinter survival of these populations.

Mid-tributary use of the Table River by bull trout, while present in the data for January – March 2020, ceases in May concurrent with ice-out. Whether these data represent a bull trout that was trapped by ice formation in the fall, an area of groundwater upwelling providing limited overwintering habitat, or if it is simply an error in the data resulting from a fish dying near the receiver will become clear in 2021 data download season. Detection history in this region can be traced to one bull trout that was tagged in July of

2019. It moved between TBLR24 and TBLR23 over the winter of 2019-2020 and it was not detected again after 27 April. Notable in the data is that only one tagged grayling was detected downstream of the mouth of the Misinchinka River while seven bull trout showed evidence of moving downstream of the Misinchinka confluence and presumably toward the Williston reservoir. This could explain the longer distance-per-event and mean total distances observed in the bull trout movement data, as fluvial Arctic grayling populations remained more widespread in the Parsnip core region during their detection histories than bull trout, which contain both fluvial and adfluvial individuals.

Spring spawning migrations of Arctic grayling appear to start in early May after ice-out with Arctic grayling starting to enter the tributaries alongside the spring migrations of bull trout. By June, Arctic grayling are found into the middle and upper reaches of the tributaries. Over the duration of the study, males were observed arriving first at Anzac River sites 8 and 27 and at Table River sites 9, 15, and 35. Anzac River site 8 reversed this pattern in 2020, suggesting that it is less central to spawning behavior and is rather a stopover along the migration route. While these analyses are coarse, this supports that the first migration of the spring may be linked to spawning in these populations.

After spawning, Arctic grayling showed a more decentralized distribution in 2020. Still present in the tributaries, Arctic grayling were also observed using the Parsnip mainstem downstream of the Anzac River during the month of August. This reach of the Parsnip River is low gradient, braiding, and largely absent of any major tributary inputs until the Colbourne Creek inlet near the northern extent of the receiver array. While this is not a description of typical Arctic grayling habitat, the timeframe of this activity suggests that this area of the Parsnip River may be important feeding habitat for Arctic grayling.

### *6.1.2 Next Steps in 2021*

During the 2021 field season, early-season efforts will be made to replace some of the freshet-lost acoustic receivers at critical junctions throughout the watershed. Candidate sites will be identified in the Anzac and Table Rivers with the goal of better understanding the timing and spatial use of Arctic grayling spawning migrations. Sampling efforts will resume in the early summer in a final deployment of our remaining acoustic transmitters. Analyses of telemetry data will be expanded following the 2021 fall data download season by the inclusion of spatial capture-recapture analyses.

## 6.2. Temperature Monitoring

### *6.2.1 Field Data Collection*

Temperature loggers deployed in 2020 bolstered the existing sampling design in the Anzac, Table, Parsnip, Hominka, Missinka, Misinkchinka, Reynolds, Colbourne, Wichcika, Bills, Firth and other smaller (unnamed) watersheds. Including smaller streams and new deployments along elevation gradients increased the predictive power

of the current dataset. Temperature monitoring array expansion and maintenance is a necessary step to create an accurate autocovariance function required to build the SSNM's (Som et al. 2014). The drawbacks of this spatial model's large minimum sample size are greatly outweighed by the benefits of the temperature map and associated predictions which can supply the information needed to support regionally significant resource conservation decisions (Isaak et al. 2014). In order to enhance the SSNM's predictive ability, maintenance of the temperature monitoring array will continue in 2021. The current model leans heavily on the spatial pattern among monitored sites to create accurate predictions. Of particular concern is the loss of temperature logging sites in the upper Table and middle Anzac Rivers. Work to replace these deployments will be required early in the 2021 field season to capture as much of the summer thermal profiles as possible for each site. Summer 2020 was highlighted by flood events and dramatic shifts in substrate structure. This extreme year puts into perspective how dynamic this watershed is and these types of extreme events should be kept in mind for future deployments.

*6.2.2 Temperature Data Imputation and Summary Metrics*

Data imputation using the *missMDA* R package continues to be an effective method to complete time series of temperature data when technological failure occurs due to logger issues or natural events. Data inadequacies often inhibit complete dataset analysis and the low MSEP of the imputation is a positive indication of its utility (Isaak et al. 2018). Preliminary data summaries suggest that although a temperature gradient was present in the Parsnip River, it did not hold thermally stressful temperatures in Arctic grayling critical habitats. The observed mean water temperatures (11.09$^{o}$C, 10.76$^{o}$C, 9.47$^{o}$C in 2018, 2019 and 2020) were consistent with reported thermal occurrence of adult Arctic grayling in the Williston watershed (Ballard and Shrimpton 2009). Additionally, maximum grayling detection temperature (a daily average) was 15.2$^{o}$C in 2020. In Williston Reservoir tributaries, the previously reported Arctic grayling upper occurrence was 14.5$^{o}$C (Ballard and Shrimpton 2009). The widespread availability of coldwater habitat (< 14.5$^{o}$C) in the watershed is a possible cause for the wide-ranging Arctic grayling distribution revealed by preliminary analysis of telemetry data (Figures 1, 2, Appendix A.1). This observation is contrary to past reporting and professional opinion which states that Arctic grayling occupy habitat in the upper tributaries of the Parsnip River during the summer feeding season (Blackman 2002b). While past beliefs about movement behaviour are generally true, our research has highlighted that Arctic grayling movement is variable and especially so in mild summers when preferred thermal habitat is widely available. Conversely, even in these mild years, Arctic grayling were detected at temperatures at and above 14.5$^{o}$C (Figure 3). This would suggest that Parsnip River Arctic grayling are vulnerable to predicted increases in mean temperature that are likely in all climate change scenarios (IPCC 2014). Detection temperatures of Arctic grayling in late summer 2018 revealed a wider spread in detection temperatures versus available temperatures. This disparity may be indicative of thermal habitat occupancy under

warmer conditions. This could either indicate selection of warm water temperatures to maximize growth, or a limitation in available cold-water habitat (CWH) pushing Arctic grayling into unfavourable conditions. Given the limitations of data from 2018 including a small sample size, and skewed temporal scale towards August, this observation should be interpreted with caution.

In other regions, it has been shown that bull trout occupy colder water temperatures and will experience different repercussions to changes in available CWH than species at lower trophic levels with wider thermal niches (Isaak et al. 2015). Our data from 2019 and 2020 suggest thermal occupancy between the two species differed by <1°C. A conservative comparison to detection temperatures in 2018 shows a more likely disparity (> 1°C) in thermal occupancy under more extreme climatic conditions. Extreme climatic conditions could decrease thermal habitat overlap between the two species. While this disparity may seem small, it must be considered that the compared metrics are means aggregated across a large spatial scale and that the real disparity is likely to be larger when variation around these mean temperature metrics is considered. It appears that across all three years the mean temperature metrics created by combining individual observation sites across the watershed does not cause concerns of thermal habitat limitation for either species (Figures 5 and 6). Arctic grayling in the Big Hole River in Montana have a much broader thermal niche than reported here, occupying water at temperatures as high as 26°C (Byorth et al. 1996). Other literature suggests a more intermediary upper avoidance temperature of 18°C (Coutant 1977). Past studies from the Williston Reservoir and our data however suggest Arctic grayling are rarely found at temperatures above 14.5°C (Ballard and Shrimpton 2009).

*6.2.3 Spatial Stream Network Model*

The temperature prediction plots created by the SSNMs can be seen in Figures 7-10. Two interesting spatial trends are depicted in these temperature maps. The first is that elevational gradients dominate the averaged thermal landscape in the Parsnip watershed (Figures 7 and 9). Streams draining the high elevation Hart Ranges on the northeast side of the watershed are providing significant cold-water input to downstream habitats. Lower elevation tributary streams on the southwest side of the watershed are warmer and provide an average thermal regime which is unfavourable for Arctic grayling and bull trout. The second, unforeseen result is the great disparity in variation relative to the mean (AWCoefVar) between the two years (Figures 8 and 10). In 2019, variation followed an expected trend with smaller tributaries being more variable than the larger mainstem. This is because smaller streams are more susceptible to changes in air temperature than larger water bodies with greater thermal inertia (Fullerton et al. 2015). A second interesting observation in 2019 is that while AWCoefVar was highest (0.06-0.08) in small high elevation streams in the Hart Ranges (Upper Anzac, Table, Hominka, Missinka Rivers etc.), small low elevation streams on the southwest side of the Parsnip mainstem

(Firth, Bills, Wichcika Creeks etc.) were predicted with lower variation around the mean (0.04-0.06). The presumed cause of this difference is that unique topography and elevational gradients in the Hart Ranges increase variation by creating microclimates which counteract the effects of heightened air temperature (Kurylyk et al. 2015, Woods et al. 2015). The small low elevation streams lack these strong microclimates and therefore have lower variation around their mean. In 2020, the AWCoefVar across the entire watershed was high at all prediction sites. This generally agrees with our exploration of Arctic grayling and bull trout detection temperatures seen in Figures 3 and 4 where 2020 was colder but had more variability in the thermal landscape. This heightened variation is not a concern because the mean temperatures reported from observed sites and SSNM predictions indicate no risk of incipient temperature thresholds for Arctic grayling or bull trout. The homogeneity of high AWCoefVar in 2020 compared to 2019 is interesting. Thermal habitat variation in addition to mean temperatures should begin to be considered in management decisions. It is well documented that high variation at temperatures near upper thermal preferences can have negative effects on species which will differentially impact various life stages and life history tactics (Morash et al. 2021). Monitoring water temperature and calculation of variability in addition to average metrics should continue in order to advise landscape management decisions which impact aquatic thermal habitat. Landscape management decisions in areas of inconstant thermal habitats should consider the downstream implications of possible disturbances such as forest canopy removal, which has a demonstrated history of increasing stream temperatures (Caissie 2006).

### *6.2.4 Next Steps in Analysis of Thermal Habitat Use*

Critical next steps in the analysis of temperature data include the collection of additional covariates which aid the prediction of water temperature. We are exploring the possibility of remotely sensed discharge data. The single Water Survey Canada discharge gauge on the Parsnip River is not sufficient to describe our observation sites which cover the entire spatial extent of the watershed. Currently the development of a site-occupancy model to describe thermal occupancy is ongoing. This modelling approach explicitly includes variations in detection efficiency to account for the imperfect observation process of acoustic telemetry (Kéry and Schaub 2012). At times of increased discharge or when a receiver mooring is damaged, a single telemetry receiver may be performing sub-optimally. If this is not corrected for in the analysis of telemetry data, false-negatives may bias our analysis and skew our understanding of thermal habitat use. Following the development of thermal occupancy curves using the site-occupancy model, a probability threshold for thermal occupancy will be established and applied to the SSNM prediction maps (>0.7; Isaak et al. 2017, Heinle et al. 2021). This will provide a powerful visualization of available thermal habitat and habitat use as well as allow us to quantify general metrics of thermal habitat use that can be quickly applied to landscape level management decisions (ie. Environmental Stewardship Initiatives).

## 6.3. Stable Isotope Analysis

### *6.3.1 Comparison of Bull Trout and Arctic Grayling Dietary Isotopes*

It has been well established that $\delta^{15}N$ changes at a consistent rate between trophic positions (Adams and Sterner 2000, France 1995). Most studies account for a 3.4‰ change in $\delta^{15}N$ positions (France 1995), though there is debate as to how this value changes between species and communities (Adams and Sterner 2000). We found significant differences in $\delta^{15}N$ concentrations between Arctic grayling and bull trout, indicating both species rely on different dietary inputs (Figure 13). Prey sources at the same trophic level as Arctic grayling appear to contribute to bull trout diet as their $\delta^{13}C$ levels align (Figure 11, 14). Additionally, mean $\delta^{15}N$ for bull trout is around 3.5‰ more enriched than grayling (10.87‰ vs 7.28‰). Bull trout and Arctic grayling diets differ in source when considering terrestrial vs aquatic derived inputs (Figure 14). When considering both species diets, the findings of statistically significant differences in $\delta^{13}C$ and $\delta^{15}N$ concentrations mean that adult bull trout and Arctic grayling have distinct diets. Arctic grayling likely contribute to bull trout diet in part with other potential prey fish. This is consistent with previous studies that have noted bull trout preying on Arctic grayling and other similar prey fish, especially as bull trout grow larger in length (McPhail and Baxter 1996).

### *6.3.2 Dietary Analyses Based on Fork Length*

Our results confirm that length and life history are likely main drivers in individual dietary patterns of both Arctic grayling and bull trout as seen in other studies on the species (Moore and Kenagy 2004, McPhail and Baxter 1996). Juvenile or smaller bull trout are likely feeding on lower trophic levels being primarily insectivorous before switching to larger prey such as whitefish, sculpin and Arctic grayling (Figure 16). This is thought to happen at around 110 mm in fork length (McPhail and Baxter 1996, Guy et al. 2011). Stream resident bull trout are also hypothesized to be primarily insectivorous (McPhail and Baxter 1996), while fluvial and adfluvial individuals consume high protein diets, composed primarily of fish that may be up to 50% of their body length (Beauchamp and Tassell 2001). These high energy requirements are likely due to the increased energetic costs of high movement and or the need to acclimate to variable stream temperatures. Differences in life history and body size explain the large dietary variation shown by bull trout in our study (Figure 15, 16). Bull trout that are isotopically similar to Arctic grayling may be resident or smaller individuals, consuming benthic invertebrates as they cannot outcompete fluvial and adfluvial fish for larger prey items. Additionally, the bull trout at the higher end of the $\delta^{15}N$ spectrum may be preying upon resident or juvenile bull trout, Arctic grayling, or whitefish, given their substantially higher $\delta^{15}N$ levels. Having a large sample or population primarily composed of fluvial bull trout would explain the large variation in individual diets (Figure 11) as their foraging tendencies are regarded as

primarily opportunistic, switching between prey fish and invertebrates depending on abundance and competition (McPhail and Baxter 1996). Adfluvial bull trout that feed in the reservoir likely explain the two individuals that are outside of the calculated breadth as they appear to consume higher amounts of lacustrine derived nutrients (lower $\delta^{13}C$) than the sample mean (Figure 13).

Arctic grayling are regarded as primarily insectivorous foragers with terrestrial invertebrates being important dietary items both seasonally and as fish grow larger (Zuev et al. 2016, Stewart et al. 2007a). Juvenile diets primarily consist of zooplankton and small invertebrates (Schmidt and O'Brien 1981, Stewart et al. 2007a). As individuals grow larger, they rely on seasonally available invertebrates found in summer feeding tributaries (Stewart et al. 2007a). Aquatic larvae and pupae are regarded as important year-round prey while other dietary items that belong to the Orders Diptera and Ephemeroptera are seasonally important (Zuev et al. 2016). Competition between bull trout and Arctic grayling is thought to primarily occur when juvenile bull trout adopt an insectivorous diet similar to that of Arctic grayling (Hagen and Stamford 2017, Northcote 1993). This is apparent in figure 15 and 16 where we can see bull trout at the smaller end of the size range exhibiting similar $\delta^{15}N$ concentrations as adult grayling. This is supported by Larkin (1956), who reasoned that species may have similar diets but feed at different sites. Bull trout and grayling likely have reduced interspecific competition through use of different habitats and also may be separated by differing thermal preferences similar to what has been noted in other bull trout populations (Heinle et al. 2021). Crock et al. (2003) found that when Arctic grayling move into summer feeding areas, they exhibit site fidelity, staying within 300 m of their feeding territory. Bull trout however, are known to undergo extensive migrations from winter feeding areas to cold spawning habitat (McPhail and Baxter 1996, Mulfeld and Marotz, 2004). Temporal differences may also be influencing dietary competition, as Arctic grayling and bull trout life histories are extremely diverse in the system, resulting in times of increased and decreased co-occupancy of streams. This further supports the idea that bull trout and Arctic grayling exhibit patterns of sympatric resource partitioning, though there are almost certainly times of increased competition, such as periods of low resource availability (Lakse et al. 2018).

### *6.3.3 Foodweb Level Analysis*

Prey fish and Arctic grayling have an area of overlap in terms of dietary items, which has been noted in the literature as both grayling and prey fish, such as mountain whitefish, consume aquatic benthic organisms such as invertebrate larvae (Whiteley 2007)(Figure 12). When comparing Arctic grayling and prey fish, grayling appear to incorporate more terrestrial derived nutrients given their diet on average appears to be less enriched with $\delta^{13}C$ (Hoeinghaus and Zeug 2008). Our results align with previous studies that highlight

low level producers such as aquatic invertebrates as lowest in $\delta^{15}N$ while top predators such as bull trout exhibit the highest $\delta^{15}N$ levels (Alvarez and Ward 2019)(Figure 12).

It appears that competition for similar dietary resources is not the strongest driver of dietary interactions in the Parsnip watershed. Though most taxa overlap in terms of dietary breadth, core species diets appear significantly different. Differences in habitat use and stream temperature have been shown to influence bull trout spatial distributions and thus consequent interactions with prey species similar to Arctic grayling, this would likely affect the predator prey interactions between the species (Heinle et al. 2021).

*6.3.4 Limitations and Future Research*

Limitations of the study primarily resulted from lack of sampling reservoir dietary inputs, like kokanee (*Oncorhynchus nerka*). Additionally, more sampling of fish at similar trophic levels to Arctic grayling would allow us to better estimate the influence of predation on grayling in the watershed and potentially conducted mixed source models to specify percent contributions to bull trout diet. Future research and analyses will build on these existing results to strengthen inference in the results of analyses. Combining stable isotope analysis with telemetry data may also allow us to investigate dietary preferences by life history and movement rate. More metrics set out by Layman et al. (2007) could be applied to our isoplots in order to measure other aspects of trophic relations such as evenness of species breadth and average degree of trophic diversity within the food webs. These metrics would help identify outliers and can be used to determine where gaps lie in the data. Future research should also quantify the importance of different prey sources to bull trout and grayling. These future directions will continue to address knowledge gaps in order to further understand the trophic interactions driving population and community structure in the Parsnip watershed.

## 7. Recommendations

In the fourth and final year of the project (field season of 2021), we will:

- Deploy up to 10 acoustic receivers in key sites where they were lost in 2020. This will be done as soon as flow decrease to levels that allow for safe working conditions (<400 $m^3$/sec measured at the Water Survey of Canada hydrometric station in the lower Parsnip River).

- Deploy 33 acoustic transmitters left over from last year in Arctic grayling and as sentinel tags for detection efficiency monitoring.

- Download existing temperature data loggers and take down the temperature monitoring network.

- Download existing acoustic receivers and take down the acoustic monitoring network.

- Evaluate project progress with respect to the priority action # 9 (PEA.RLR.S03.RI.09) of the *Peace Region Rivers, Lakes, and Reservoirs Action Plan* (FWCP 2020), as well as make suggestions for follow-up monitoring, enhancement, and/or conservation actions.

## 8. Acknowledgements

A large number of people provided critical support to different phases of this project: Julian Napoleon, Daniel Scurfield, Rioghnach Steiner, Grayson Vanderbyl, Cale Babey, Daniel Larson, Luc Turcotte, Douglas Thompson, John Orlowsky, Kendra Robinson, Bruna Gonçalves, Daniel Erasmus, Brian Smith, Tom Wilms, Nikolaus Gantner, Ian Spendlow, Ray Pillipow, Zsolt Sary, John Hagen, Dawn Cowie, Michael Stamford, Duncan McColl, Jeff Strohm, Kari Van Ruskenveld, Ainsley Davison, and Hunter Gleason. The Ministry of Forests, Lands, Natural Resource Operations and Rural Development kindly provided us with helicopter access to remote sites of the study area. This project is funded by the Fish and Wildlife Compensation Program (FWCP). The FWCP is a partnership between BC Hydro, the Province of BC, Fisheries and Oceans Canada, First Nations and public stakeholders to conserve and enhance fish and wildlife in watersheds impacted by BC Hydro dams. This research took place in the traditional territory of Tse'khene First Nation.

## 9. References

Abrams, A. E. I., A. M. Rous, J. L. Brooks, M. J. Lawrence, J. D. Midwood, S. E. Doka, and S. J. Cooke. 2018. Comparing immobilization, recovery, and stress indicators associated with electric fish handling gloves and a portable electrosedation system. Transactions of the American Fisheries Society 147:390–399.

Alvarez, J.S., Ward, D.M. 2019. Predation on wild and hatchery salmon by non-native brown trout (*Salmo trutta*) in the Trinity River, California. Ecology of Freshwater Fish. DOI: 10.1111/eff.12476

Allen, A. M., and N. J. Singh. 2016. Linking movement ecology with wildlife management and conservation. Frontiers in Ecology and Evolution 3:1–13.

Ballard. S and J.M. Shrimpton. 2009. Summary Report of Arctic Grayling Management and Conservation 2009. A synopsis of the information available on Arctic grayling in

the Omineca region of northern British Columbia and identification of additional information needs. Peace/Williston Fish and Wildlife Compensation Program Report No. 337.

Bearhop, S., C. E. Adams, S. Waldron, R. A. Fuller, and H. Macleod. 2004. Determining trophic niche width: a novel approach using stable isotope analysis. Journal of Animal Ecology 73:1007–1012.

Beauchamp, D.A., Tassell, J.V. 2001. Modeling Seasonal Trophic Interactions of Adfluvial Bull Trout in Lake Billy Chinook, Oregon. Transactions of the American Fisheries Society. 130(2): 204-216.

Beaudry P. and Associates, EDI Environmental Dynamics Inc. 2000. Parsnip River Watershed Restoration Plan and Priority Assessment Project. Report prepared for: Canadian Forest Products Ltd., 5162 Northwood Pulp Mill Road, Prince George, BC.

Blackman, B. G. 2002a. The distribution and relative abundance of Arctic grayling (Thymallus arcticus) in the Parsnip, Anzac and Table rivers. Peace/Williston Fish and Wildlife Compensation Program, Report No. 254. 15pp.

Blackman, B. G. 2002b. Radio Telemetry Studies of Arctic Grayling Migrations to Overwinter, Spawning and Summer Feeding Areas in the Parsnip River Watershed 1996-1997. Peace/Williston Fish and Wildlife Compensation Program, Report No. 263.

Brownscombe, J., Griffin, L., Chapman, J., Morley, D., Acosta, A., Crossin, G., Iverson, S., Adams, A., Cooke, S., Danylchuk, A. (2019). A practical method to account for variation in detection range in acoustic telemetry arrays to accurately quantify the spatial ecology of aquatic animals Methods in Ecology and Evolution

Byorth, P., Kaya, C., and Dwyer, W. 1996. High-temperature tolerances of fluvial Arctic grayling and comparisons with summer river temperatures of the Big Hole River, Montana. Fisheries Society.

Clarke, A. D., K. H. Telmer, and M. Shrimpton. J. 2007. Elemental analysis of otoliths, fin rays and scales: A comparison of bony structures to provide population and life-history information for the Arctic grayling (Thymallus arcticus). Ecology of Freshwater Fish 16:354– 361.

Conrad, O., Bechtel, B., Bock, M., Dietrich, H., Fischer, E., Gerlitz, L., Wehberg, J., Wichmann, V., and Bohner, J. (2015): System for Automated Geoscientific Analyses (SAGA) v. 2.1.4, Geosci. Model Dev., 8, 1991-2007, doi:10.5194/gmd-8-1991-2015.

Cooke, S. J., E. G. Martins, D. P. Struthers, L. F. G. Gutowsky, M. Power, S. E. Doka, J. M. Dettmers, D. A. Crook, M. C. Lucas, C. M. Holbrook, and C. C. Krueger. 2016. A

moving target—incorporating knowledge of the spatial ecology of fish into the assessment and management of freshwater fish populations. Environmental Monitoring and Assessment 188:239.

Coutant, C. C. 1977. Compilation of temperature preference data. Journal of the Fisheries Research Board of Canada 34: 739-745.

Cressie, N., Frey, J., Harch, B., and Smith, M. 2006. Spatial prediction on a river network. J Agric Biological Environ Statistics 11(2): 127–150. doi:10.1198/108571106x110649.

Cutting, K.A., W.F. Cross, M.L. Anderson, and E.G. Reese. 2016. Seasonal Change in Trophic Niche of Adfluvial Arctic Grayling (Thymallus arcticus) and Coexisting Fishes in a High Elevation Lake System. PLoS ONE. 11(5):e0156187.

Dale, M. R. T. & Fortin, M-J. 2014. Spatial Analysis: A Guide for Ecologists. Cambridge University Press, Cambridge, UK.

Evangelista, C., Bioche, A., Lecerf, A., Cucherousset, J. 2014. Ecological opportunities and intraspecific competition alter trophic niche specialization in an opportunistic stream predator. Journal of Animal Ecology. 83(5): 1025-1034.

Flávio, H., and Baktoft, H. 2020. actel: Standardised analysis of acoustic telemetry data from animals moving through receiver arrays. Methods in Ecology and Evolution. doi:10.1111/2041-210x.13503.

France, R.L. 1995. Differentiation between littoral and pelagic food webs in lakes using table carbon isotopes. Limnology and Oceanography. 40(7): 1310-1313.

Fullerton, A.H., Torgersen, C.E., Lawler, J.J., Faux, R.N., Steel, E.A., Beechie, T.J., Ebersole, J.L., and Leibowitz, S.G. 2015. Rethinking the longitudinal stream temperature paradigm: region-wide comparison of thermal infrared imagery reveals unexpected complexity of river temperatures. Hydrological Processes. 29(22): 4719–4737. doi:10.1002/hyp.10506.

FWCP. 2014. Peace Basin: Streams Action Plan. Page 27.

Guy, C.S., McMahon, T.E., Fredenberg, W.A., Smith, C.J., Garfield, D.W., Cox, B.S. 2011. Diet Overlap of Top-Level Predators in Recent Sympatry: Bull Trout and Nonnative Lake Trout. Journal of Fish and Wildlife Management. 2(2): 183-189.

Hagen, J., and M. Stamford. 2017. FWCP Arctic Grayling Monitoring Framework for the Williston Reservoir Watershed. Fish and Wildlife Compensation Program - Peace Region, Prince George.

Hagen, J., and S. Webber. 2019. Limiting Factors, Enhancement Potential, Critical Habitats, and Conservation Status for Bull Trout of the Williston Reservoir

Watershed: Information Synthesis and Recommended Monitoring Framework. Fish and Wildlife Compensation Program - Peace Region, Prince George.

Hagen, J., S. Williamson, M. D. Stamford, and R. Pillipow. 2015. Critical Habitats for Bull Trout and Arctic Grayling within the Parsnip River and Pack River watersheds. Report prepared for: McLeod Lake Indian Band, Sekani Drive, McLeod Lake, BC.

Harrison, P.M., Gutowsky, L.F.G., Martins, E.G., Ward, T.D., Patterson, D.A., Cooke, S.J., M. Power. 2017. Individual isotopic specializations predict subsequent inter-individual variation in movement in a freshwater fish. Ecology. 98(3): 608-615.

Hastings, A., S. Petrovskii, and A. Morozov. 2011. Spatial ecology across scales. Biology Letters 7:163–165.

Hawkshaw, S. C. F., M. P. Gillingham, and J. M. Shrimpton. 2014. Habitat characteristics affecting occurrence of a fluvial species in a watershed altered by a large reservoir. Ecology of Freshwater Fish 23:383–394.

Heinle, K.B., Eby, L.A., Muhlfeld, C.C., Steed, A., Jones, L., D'Angelo, V., Whiteley, A.R., and Hebblewhite, M. 2021. Influence of water temperature and biotic interactions on the distribution of westslope cutthroat trout (Oncorhynchus clarkii lewisi) in a population stronghold under climate change. Canadian Journal of Fisheries and Aquatic Sciences 99(999): 1–13. doi:10.1139/cjfas-2020-0099.

Hoeinghaus, D.J., Zeug, S.C. 2008. Can stable isotope ratios provide for community-wide measures of trophic structure? Comment. Ecological Society of America. 89(8): 2353-2357.

Hughes, N.F. 1992. Ranking of Feeding Position by Drift-Feeding Arctic Grayling (*Thymallus arcticus*) in Dominance Hierarchies. Canadian Journal of Fisheries and Aquatic Sciences. 49: 1994-1998.

IPCC. 2014. Climate Change 2014: Synthesis Report. Contribution of Working Groups I, II and III to the Fifth Assessment Report of the Intergovernmental Panel on Climate Change. Edited by Core Writing Team, R.K. Pachauri, and L.A. Meyer. Intergovernmental Panel on Climate Change, Geneva, Switzerland.

Isaak, D. J., C. H. Luce, B. E. Rieman, D. E. Nagel, E. E. Peterson, D. L. Horan, S. Parkes, and G. L. Chandler. 2010. Effects of climate change and wildfire on stream temperatures and salmonid thermal habitat in a mountain river network. Ecological Applications 20:1350–1371.

Isaak, Daniel J., Horan, Dona L., and Wollrab, Sherry P. 2013. A simple protocol using underwater epoxy to install annual temperature monitoring sites in rivers and

streams. General Technical Report RMRS-GTR-314. U.S. Department of Agriculture, Forest Service, Rocky Mountain Research Station, Fort Collins, CO.

Isaak, D.J., Peterson, E.E., Hoef, J.M.V., Wenger, S.J., Falke, J.A., Torgersen, C.E., Sowder, C., Steel, E.A., Fortin, M., Jordan, C.E., Ruesch, A.S., Som, N., and Monestiez, P. 2014. Applications of spatial statistical network models to stream data. Wiley Interdisciplinary Reviews: Water 1(3): 277–294.

Isaak, D.J., Young, M.K., Nagel, D.E., Horan, D.L., and Groce, M.C. 2015. The cold-water climate shield: delineating refugia for preserving salmonid fishes through the 21st century. Global Change Biol 21(7): 2540–2553.

Isaak, D.J., Wenger, S.J., and Young, M.K. 2017. Big biology meets microclimatology: defining thermal niches of ectotherms at landscape scales for conservation planning. Ecological Applications 27(3): 977–990. doi:10.1002/eap.1501.

Isaak, D.J., Luce, C.H., Chandler, G.L., Horan, D.L., and Wollrab, S.P. 2018. Principal components of thermal regimes in mountain river networks. Hydrological and Earth System Sciences 22(12): 6225–6240. doi:10.5194/hess-22-6225-2018.

Jackson, A.L., R., Inger, Parnell, A.C., and S. Bearhop. 2011. Comparing isotopic niche widths among and within communities: SIBER - Stable Isotope Bayesian Ellipses in R. Journal of Animal Ecology. 80(1): 595-602.

Josse, J., and Husson, F. 2016. missMDA : A Package for Handling Missing Values in Multivariate Data Analysis. Journal of Statistical Software 70(1).

Kattwinkel M, Szöcs E. 2018 openSTARS: open source implementation of the STARS ArcGIS toolbox. See https://github.com/MiKatt/openSTARS.

Kéry, M., and Schaub, M. 2012. Bayesian Population Analysis using WinBUGS.

Kurylyk, B. L., K. T. B. MacQuarrie, T. Linnansaari, R. A. Cunjak, and R. A. Curry. 2015. Preserving, augmenting, and creating cold-water thermal refugia in rivers: concepts derived from research on the Miramichi River, New Brunswick (Canada). Ecohydrology 8:1095–1108.

Larkin, P.A. 1956. Interspecific Competition and Population Control in Freshwater Fish. Journal of the Fisheries Research Board of Canada. 13(3). 327-342.

Lashmar, M. and Ptolemy, J. 2002. Williston watershed Arctic grayling. Wildlife at Risk in Britich Columbia brochure. ISBN 0-7726-7705-0 B.C. Ministry of Water, Land, and Air Protection.

Layman, C.A., D.A. Arrington, C.G. Montaña, and D.M. Post. 2007. Can stable isotope ratios provide for community wide measures of trophic structure? The Ecological Society of America. 88(1):42-48.

Lucas, M. C., and E. Baras. 2001. Migration of Freshwater Fishes. Blackwell Science Ltd, Oxford.

Magnan, P., Fitzgerald, G.J. 1984. Mechanisms responsible for the niche shift of brook charr, *Salvelinus fontinalis* Mitchill , when living sympatrically with creek chub, *Semotilus atromaculatus* Mitchill. Canadian Journal of Zoology. 62(8): 1548-1555.

Marsha, A.L., Steel, E.A., and Fullerton, A.H. 2021. Modeling thermal metrics of importance for native vs non-native fish across stream networks to provide insight for watershed-scale fisheries management. Freshwater Science: 000–000. doi:10.1086/713038.

McPhail, J.D., Baxter, J.S. 1996. A review of bull trout (*Salvelinus confluentus*) life history and habitat use in relation to compensation and improvement opportunities. British Columbia Ministry of Environment, Lands and Parks, Fisheries Management Report No. 104: 40p.

Melnychuk, M. 2012. Detection efficiency in telemetry studies, Definitions and evaluation methods. Telemetry Techniques: A User Guide to Fisheries Research.

Milinsky, M. 1982. Optimal Foraging: The Influence of Intraspecific Competition on Diet Selection. Behavioral Ecology and Sociobiology. 11: 109-115.

Moore, J.W., Kenagy, G.J. 2004. Consumption of shrews *Sorex spp*. by Arctic Grayling, *Thymallus arcticus*. Canadian Field Naturalist. 118(1): 111-114.

Morash, A.J., Speers-Roesch, B., Andrew, S., and Currie, S. 2021. The physiological ups and downs of thermal variability in temperate freshwater ecosystems. Journal of Fish Biology. doi:10.1111/jfb.14655.

Neteler M, Bowman MH, Landa M, Metz M. 2012 GRASS GIS: a multi-purpose open source GIS. Environmental Modeling and Software. 31: 124 –130. doi:10.1016/j. envsoft.2011.11.014.

Niella, Y., Flavio, H., Smoothey A., Aarestrup, K., Taylor, M., Peddemors, V., and Harcourt, R. 2020. Refined Shortest Paths (RSP): Incorporation of topography in space use estimation from node-based telemetry data. Methods in Ecology and Ecolution. doi:10.1111/2041-210X.13484

Northcote, T.G. 1993. A review of management and enhancement options for Arctic grayling (Thymallus arcticus) with special reference to the Williston Reservoir in

British Columbia. British Columbia Ministry of Environment, Lands and Parks, Fisheries Management Branch. Report no. 101:69p.

Ogburn, M. B., A.-L. Harrison, F. G. Whoriskey, S. J. Cooke, J. E. Mills Flemming, and L. G. Torres. 2017. Addressing challenges in the application of animal movement ecology to aquatic conservation and management. Frontiers in Marine Science 4:70.

Peterson, E.E., and Hoef, J.M.V. 2010. A mixed-model moving-average approach to geostatistical modeling in stream networks. Ecology 91(3): 644–651. doi:10.1890/08-1668.1.

Post, D. M. 2002. Using stable isotopes to estimate trophic position: models, methods, and assumptions. Ecology 83:703–718.

R Development Core Team. 2020. R: A Language and Environment for Statistical Computing, R Foundation for Statistical Computing: Vienna, Austria. ISBN 3-900051-07-0.

Ridout, M., and Linkie, M. 2009. Estimating overlap of daily activity patterns from camera trap data. Journal of Agriculture, Biological, and Environmental Statistics 14(3), 322-337.

Royle, J. A., A. K. Fuller, and C. Sutherland. 2017. Unifying population and landscape ecology with spatial capture-recapture. Ecography 41:444–456.

Schmidt, D., O'Brien, J. 1982. Planktivorous Feeding Ecology of Arctic Grayling (*Thymallus arcticus*). Canadian Journal of Aquatic Sciences. 39(1): 475-482.

Semmens, B.X., Ward, E.J., Moore, J.W., Darimont, C.T. 2009. Quantifying Inter- and Intra-Population Niche Variability Using Hierarchical Bayesian Stable Isotope Mixing Models. PLoS ONE. 4(7): e6187

Som, N.A., Monestiez, P., Hoef, J.M.V., Zimmerman, D.L., and Peterson, E.E. 2014. Spatial sampling on streams: principles for inference on aquatic networks. Environmetrics 25(5): 306–323.

Sowder, C., and Steel, E.A. 2012. A Note on the Collection and Cleaning of Water Temperature Data. Water 4(3): 597–606.

Stamford, M., J. Hagen, and S. Williamson. 2017. Limiting Factors, Enhancement Potential, Conservation Status, and Critical Habitats for Arctic Grayling in the Williston Reservoir Watershed, and Information Gaps Limiting Potential Conservation and Enhancement Actions. Fish and Wildlife Compensation Program - Peace Region, Prince George.

Stamford, M. D., and E.B. Taylor. 2005. Population subdivision and genetic signatures of demographic changes in Arctic grayling (Thymallus arcticus) from an impounded watershed. Canadian Journal of Fisheries and Aquatic Sciences 62: 2548–2559.

Stewart, D. B., N. J. Mochnacz, C. D. Sawatzky, T. J. Carmichael, and J. D. Reist. 2007a. Fish diets and food webs in the Northwest Territories: bull trout (Salvelinus confluentus). Canadian Manuscript Report of Fisheries and Aquatic Sciences. Pages vi–18p.

Stewart, D. B., N. J. Mochnacz, J. D. Reist, T. J. Carmichael, and C. D. Sawatzky. 2007b. Fish diets and food webs in the Northwest Territories: Arctic grayling (Thymallus arcticus). Canadian Manuscript Report of Fisheries and Aquatic Sciences. Pages vi–21p.

Hoef, J.M.V., Peterson, E.E., Clifford, D., and Shah, R. 2014. SSN : An R Package for Spatial Statistical Modeling on Stream Networks. Journal of Statistical Software 56(3).

Tyers, M. 2017. riverdist: River Network Distance Computation and Applications. R package version 0.15.0.

Wagner, G. F., S. J. Cooke, R. S. Brown, and K. A. Deters. 2011. Surgical implantation techniques for electronic tags in fish. Reviews in Fish Biology and Fisheries 21:71–81.

Waldock, C., Dornelas, M., and Bates, A.E. 2018. Temperature-Driven Biodiversity Change: Disentangling Space and Time. Bioscience.

Ward, T. D., J. W. Brownscombe, L. F. G. Gutowsky, R. Ballagh, N. Sakich, D. McLean, G. Quesnel, S. Gambhir, C. M. O'Connor, and S. J. Cooke. 2017. Electric fish handling gloves provide effective immobilization and do not impede reflex recovery of adult largemouth bass. North American Journal of Fisheries Management 37:652–659.

Ward, A.J., Webster, M.M., Hart, P.J. 2006. Intraspecific food competition in fishes. Fish and Fisheries. 7(4): 231-261.

Whiteley, A.R. 2007. Trophic polymorphism in a riverine fish: morphological, dietary and genetic analysis of mountain whitefish. Biological Journal of the Linnean Society. 92(2): 253-267.

Wrona, F.J., Davies, R.W., Linton, L., Wilkialis, J. 1981. Competition and coexistence between *Glossiphonia complanata* and *Helobdella stagnis* (*Glossiphoniidae: Hirudinoidea*). Oecologia. 48: 133-137

Woods, H.A., Dillon, M.E., and Pincebourde, S. 2015. The roles of microclimatic diversity and of behavior in mediating the responses of ectotherms to climate change. Journal of Thermal Biology 54: 86 97. doi:10.1016/j.jtherbio.2014.10.002.

Zimmerman, D.L. 2006. Optimal network design for spatial prediction, covariance parameter estimation, and empirical prediction. Environmetrics 17(6): 635–652. doi:10.1002/env.769.

Zuev, I.V., Shulepina, S.P., Trofimova, E.A., Zotina, T.A. 2016. Seasonal Changes in Feeding and Relative Condition Factors of Arctic Grayling (Thymallus arcticus) in a Stretch of the Middle Reaches of the Yenisei River. Contemporary Problems of Ecology. 10(3): 250-258.

**Table 1.** Predictor covariates, variance components for the final spatial stream network models. Predictor covariates, variance components for the final spatial stream network models. Variance Components comprise the variogram models used for kriging in the SSNM predictions. awat: Average Weekly Average Temperature; awcoef: Average Weekly Coefficient of Variation; avTmpA: Average Air Temperature; H2OAreaA: Reach Contributing Area; and RMSPE: Root Mean Square Prediction Error.

| Final Model Specification | | | |
|---|---|---|---|
| Year | Formula | Variance Components | RMSPE |
| 2019 | awat ~ avTmpA + H2OAreaA | Spherical.tailup + Exponential.taildown + Gaussian.Euclid + Nugget | 0.467553150 |
| 2019 | awcoef ~ avTmpA + H2OAreaA | LinearSill.tailup + LinearSill.taildown + Nugget | 0.005138688 |
| 2020 | awat ~ avTmpA + H2OAreaA | Epanech.tailup + Spherical.taildown + Nugget | 1.172844456 |
| 2020 | awcoef ~ avTmpA + H2OAreaA | Spherical.tailup + LinearSill.taildown + Nugget | 0.007984360 |

**Table 2.** Number of samples collected throughout the study by watershed and sample type. Samples were collected from June to September 2018, 2019 and 2020.

| Sample/Stream | Anzac | Hominka | Missinka | Table | Other | Total |
|---|---|---|---|---|---|---|
| Muscle | 47 | 14 | 12 | 35 | 16 | 124 |
| Adipose | 30 | 34 | 15 | 35 | 5 | 118 |
| Invertebrates | 10 | 8 | 6 | 6 | 0 | 30 |
| Prey Fish | 15 | 9 | 4 | 11 | 2 | 41 |
| Terrestrial Veg. | 21 | 18 | 16 | 15 | 0 | 70 |
| Periphyton | 4 | 5 | 4 | 3 | 0 | 16 |
| Total | 127 | 88 | 57 | 105 | 23 | 401 |

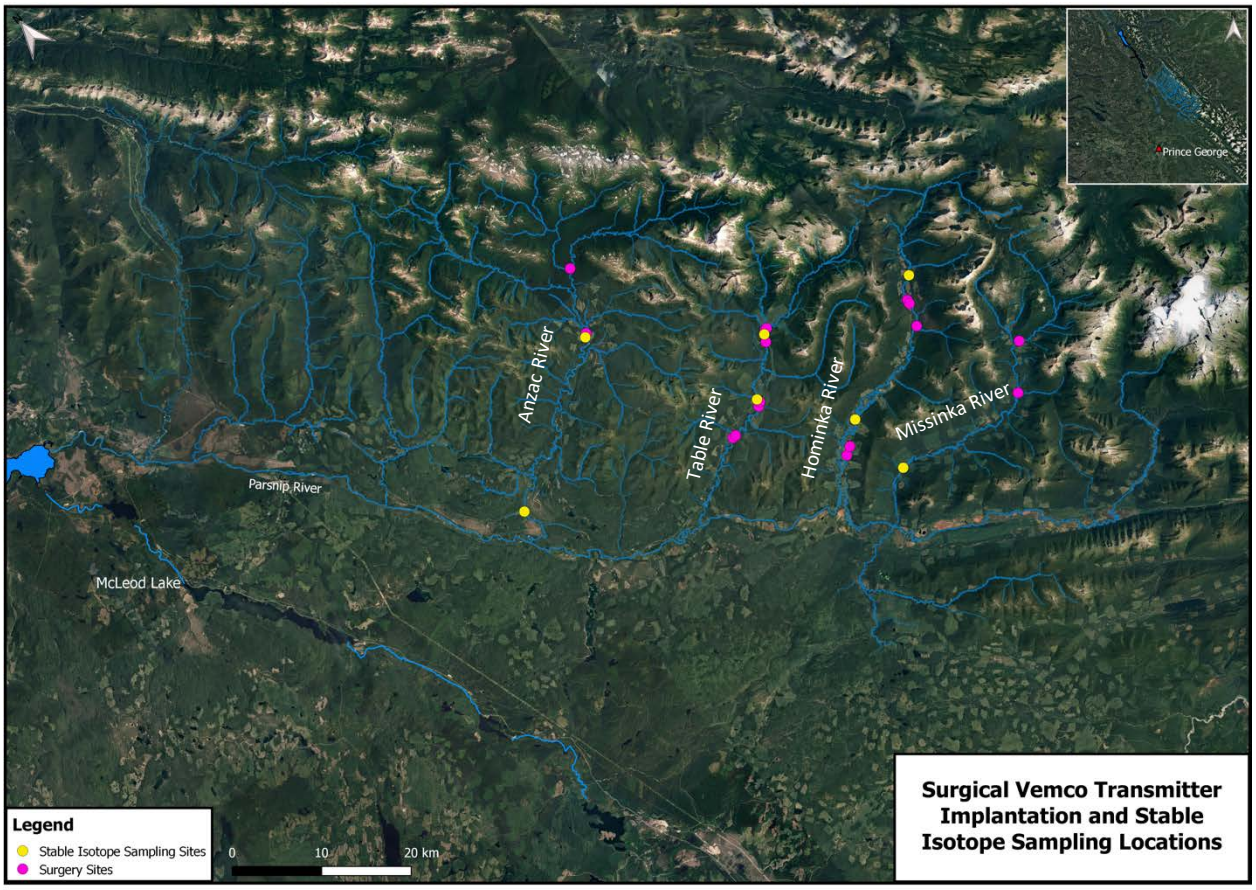


**Figure 1.** Locations of tag implantation surgery sites, and stable isotope sampling sites.

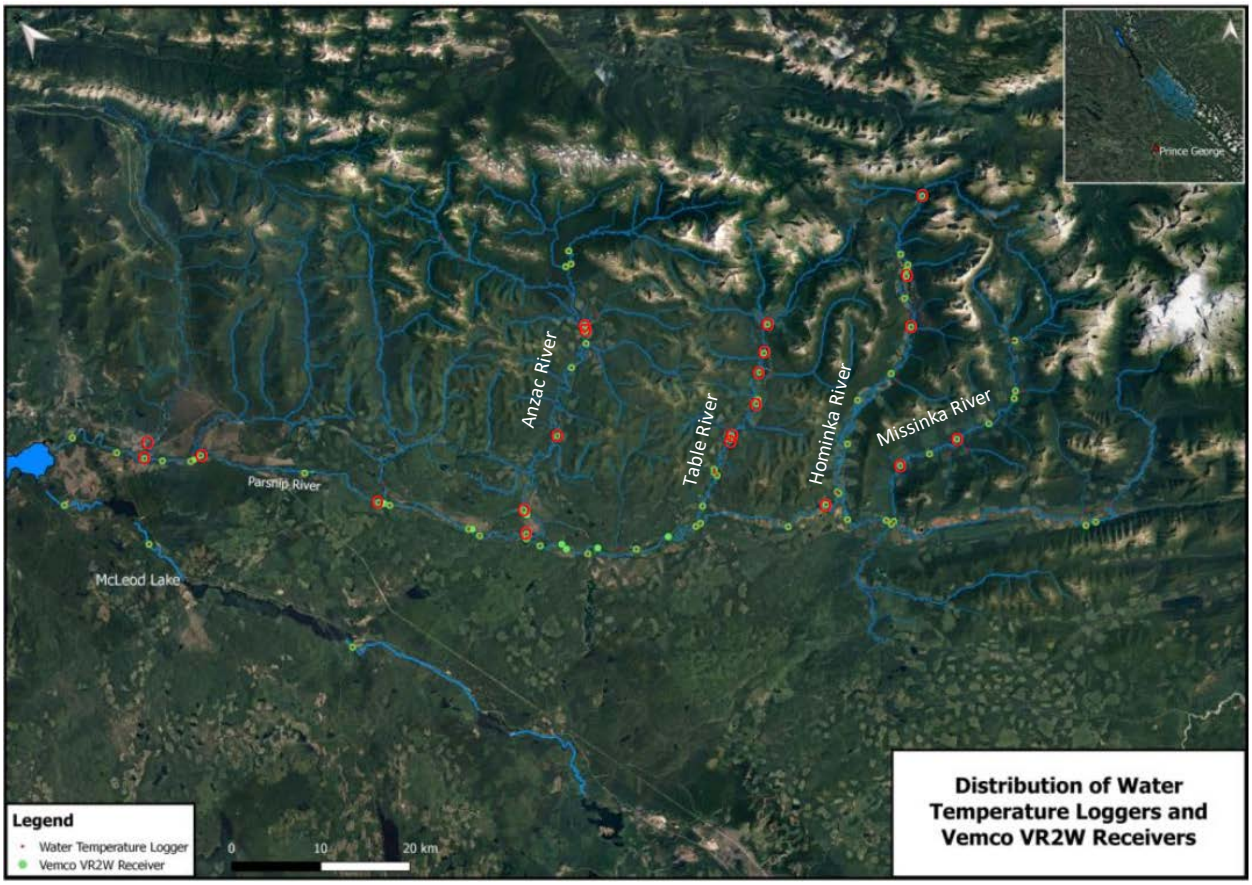


**Figure 2.** Location of all temperature loggers and Vemco VR2W acoustic receivers in the Parsnip River and Pack River Watersheds. Receivers lost in the 2020 spring freshet are circled in red.

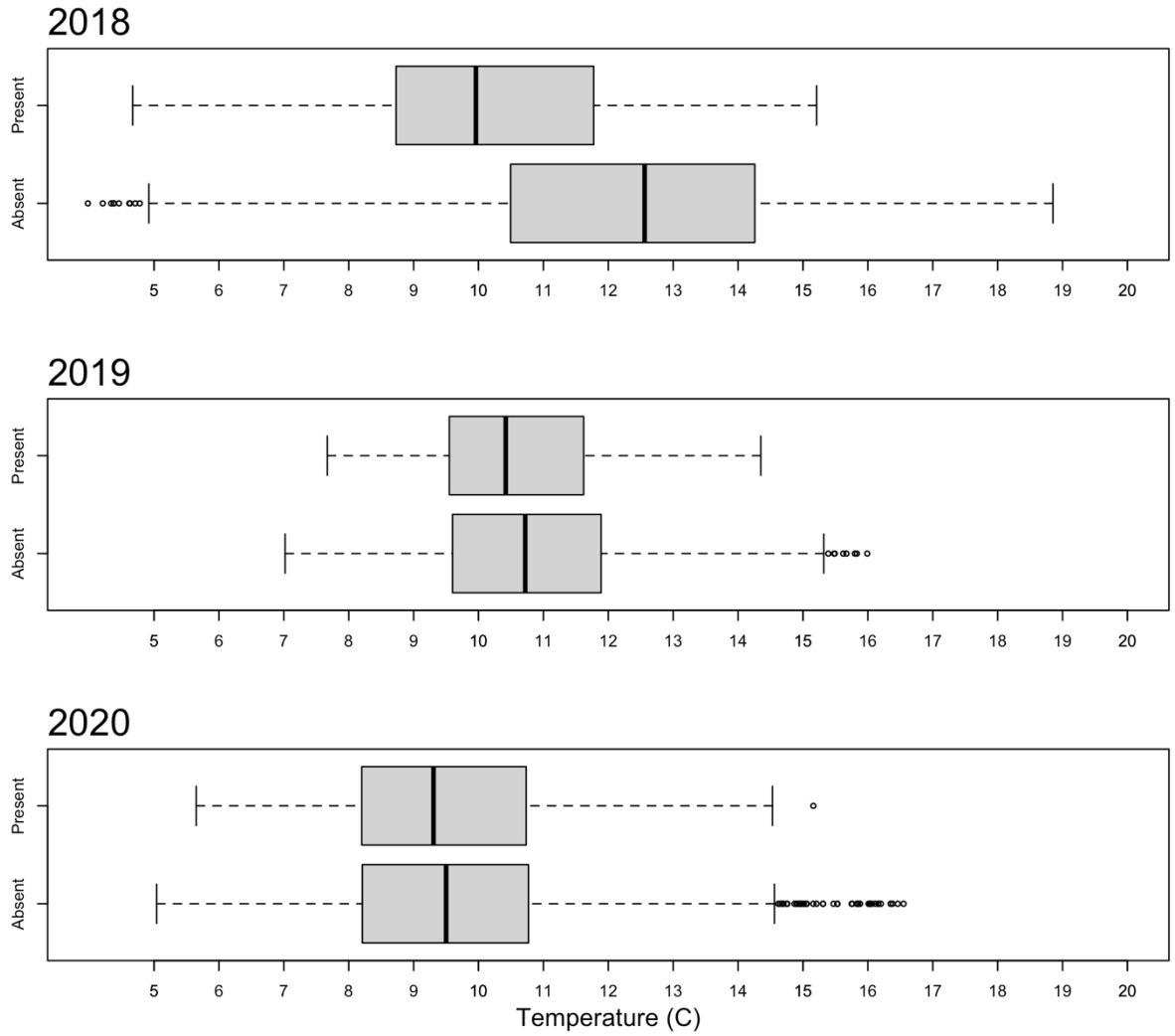


**Figure 3.** Box and whisker plots depicting Arctic grayling presence (detected at acoustic receiver on a day) or absence (not detected at acoustic receiver on a day) in relation to mean daily temperature recorded at a select number of acoustic receivers with attached temperature loggers (n=15 in 2018, n=40 in 2019, n=25 in 2020).

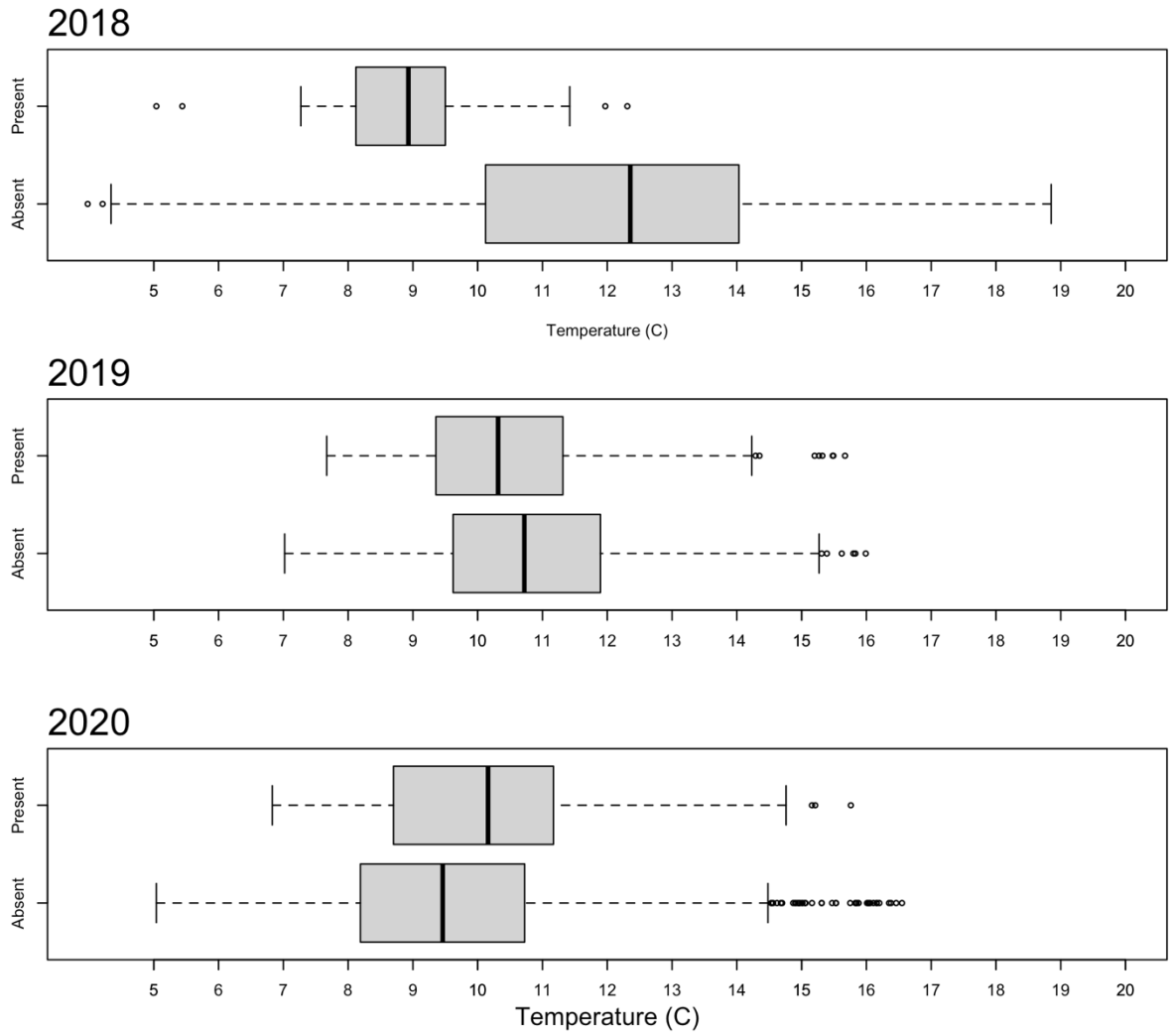


**Figure 4.** Box and whisker plots depicting bull trout detection temperature (mean daily temperature at acoustic detection) and water temperature for a select number of acoustic receivers with attached temperature loggers (n=40 in 2019, n=25 in 2020).

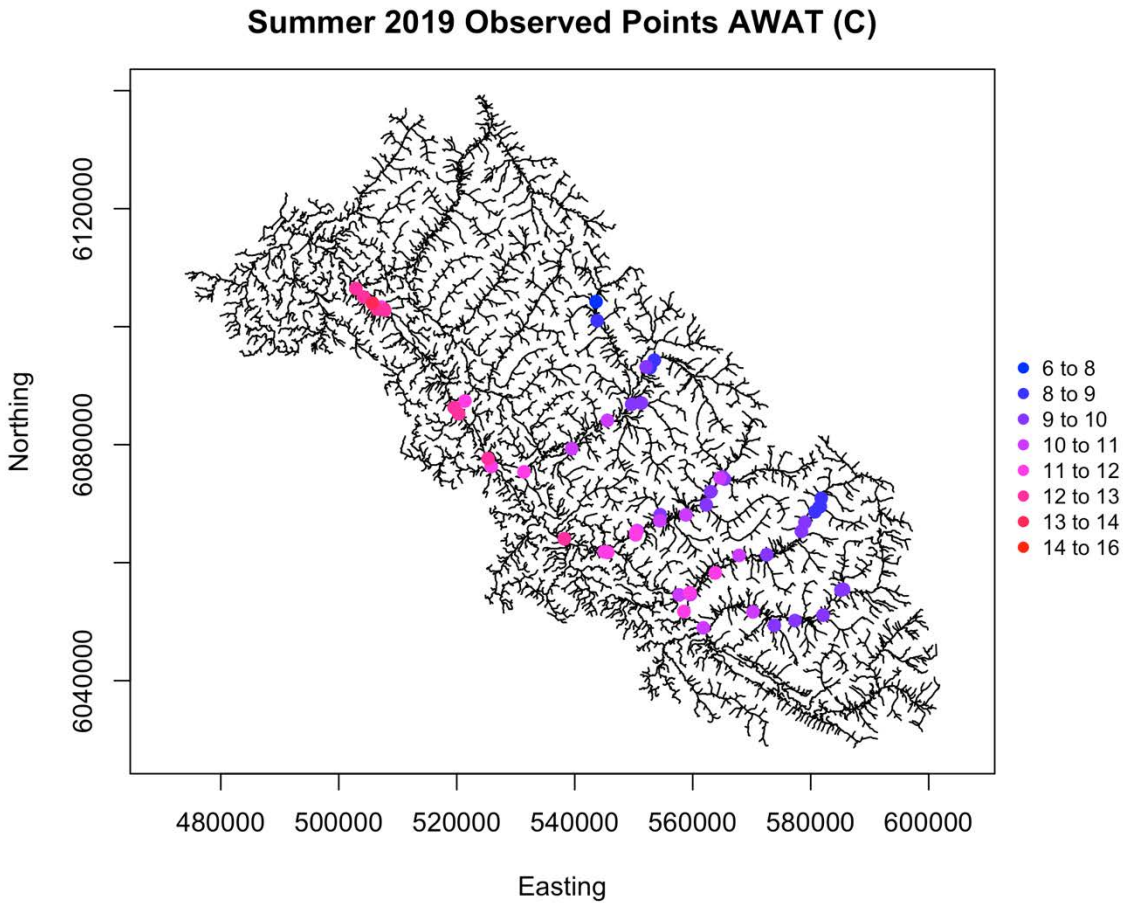


**Figure 5.** Observation points used in the 2019 Spatial Stream Network Models (n=57). The depicted temperature metric is average weekly average temperature (AWAT) during the trophic feeding window (July 1st - September 15th) for Arctic grayling.

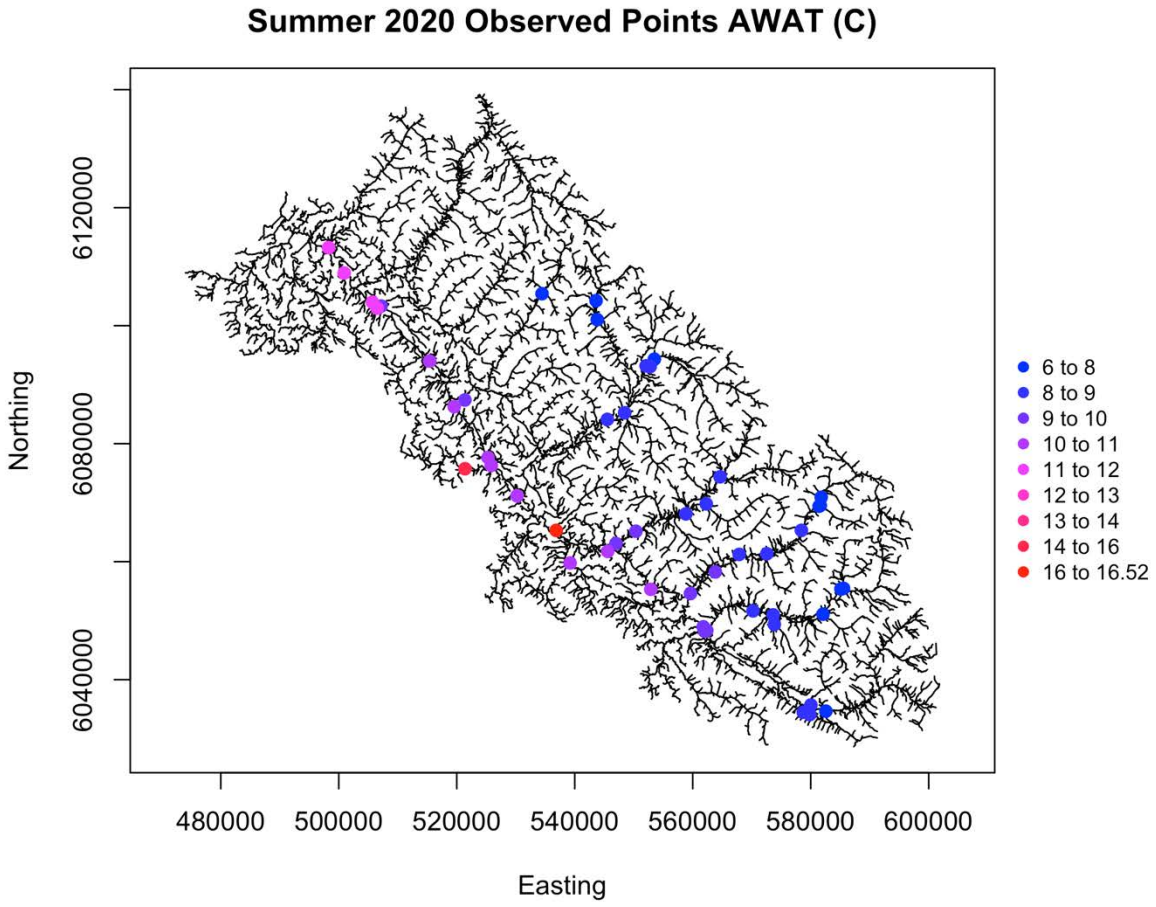


**Figure 6.** Observation points used in the 2020 Spatial Stream Network Models (n=51). The depicted temperature metric is average weekly average temperature (AWAT) during the trophic feeding window (July 1st - September 15th) for Arctic grayling.

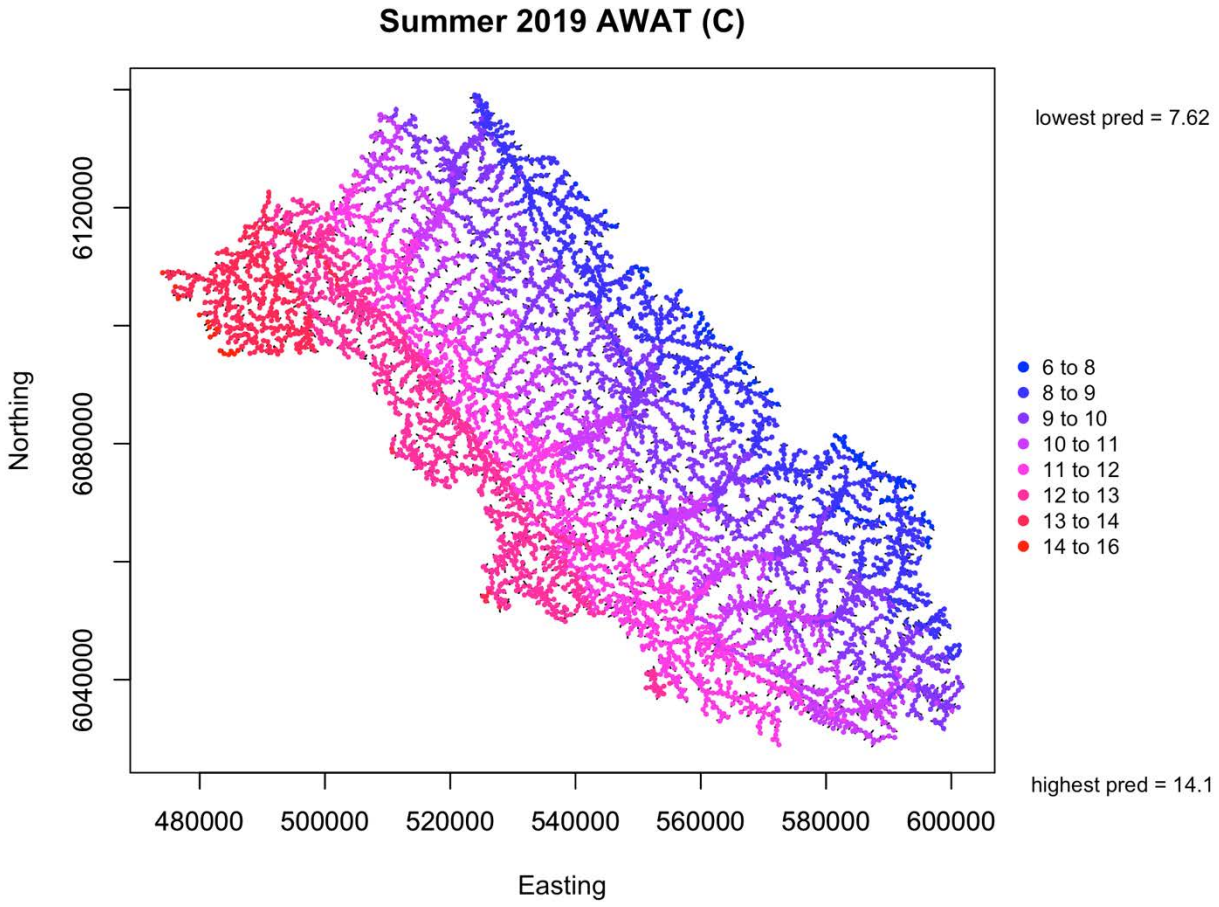


**Figure 7.** Spatial Stream Network Model predictions for the response metric average weekly average temperature (AWAT) in degrees Celsius for the trophic feeding window (July 1st - September 15th) for Arctic grayling in 2019. Predictions were created at 1km resolution.

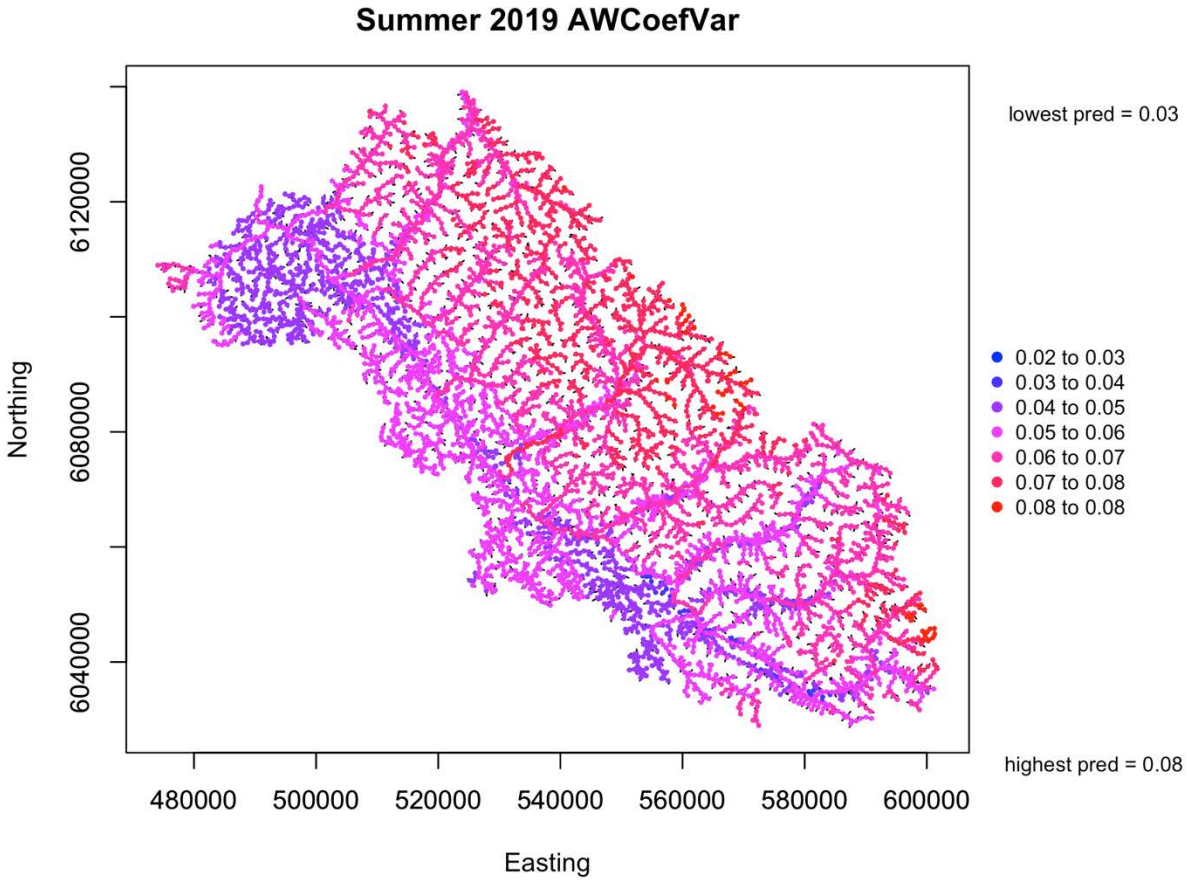


**Figure 8.** Spatial Stream Network Model predictions for the response metric average weekly coefficient of variation (AWCoefVar) in degrees Celsius for the trophic feeding window (July 1st - September 15th) for Arctic grayling in 2019. Predictions were created at 1km resolution.

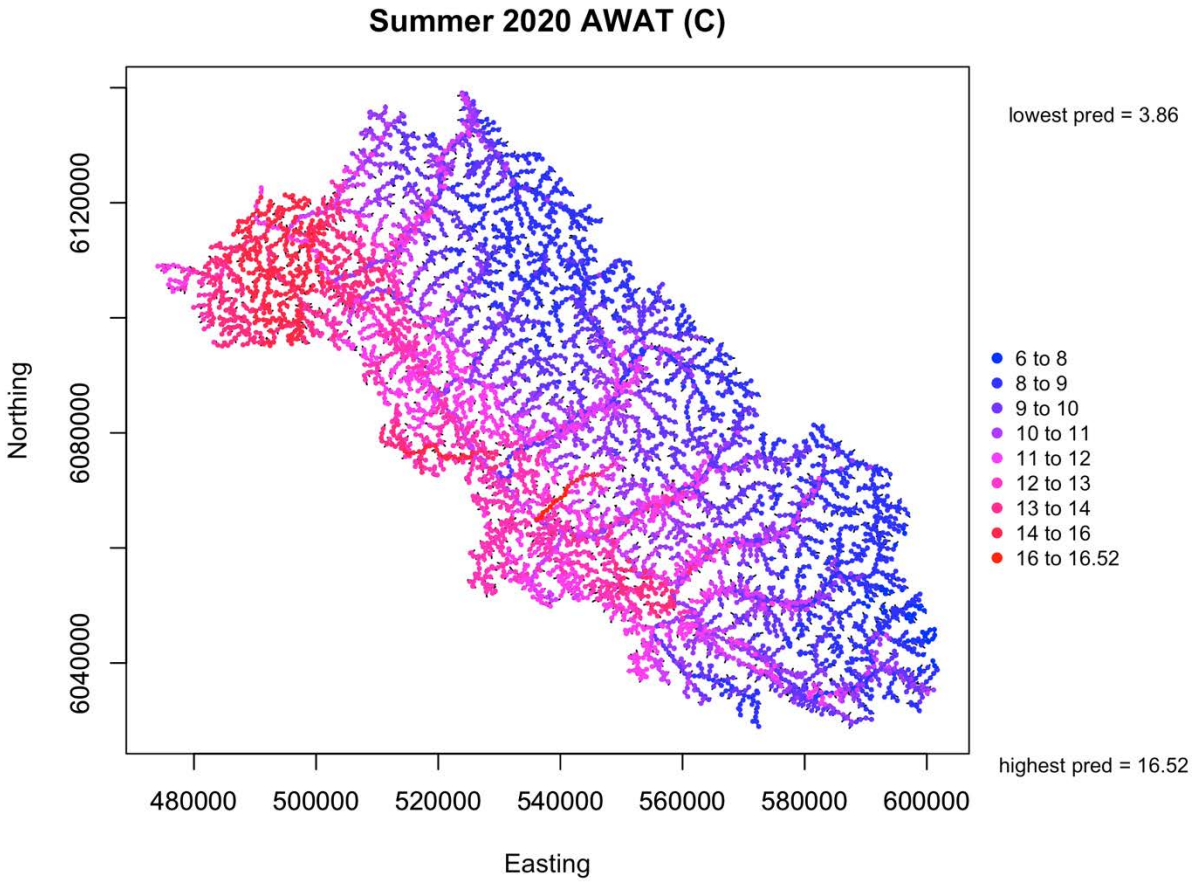


**Figure 9.** Spatial Stream Network Model predictions for the response metric average weekly average temperature (AWAT) in degrees Celsius for the trophic feeding window (July 1st - September 15th) for Arctic grayling in 2020. Predictions were created at 1km resolution.

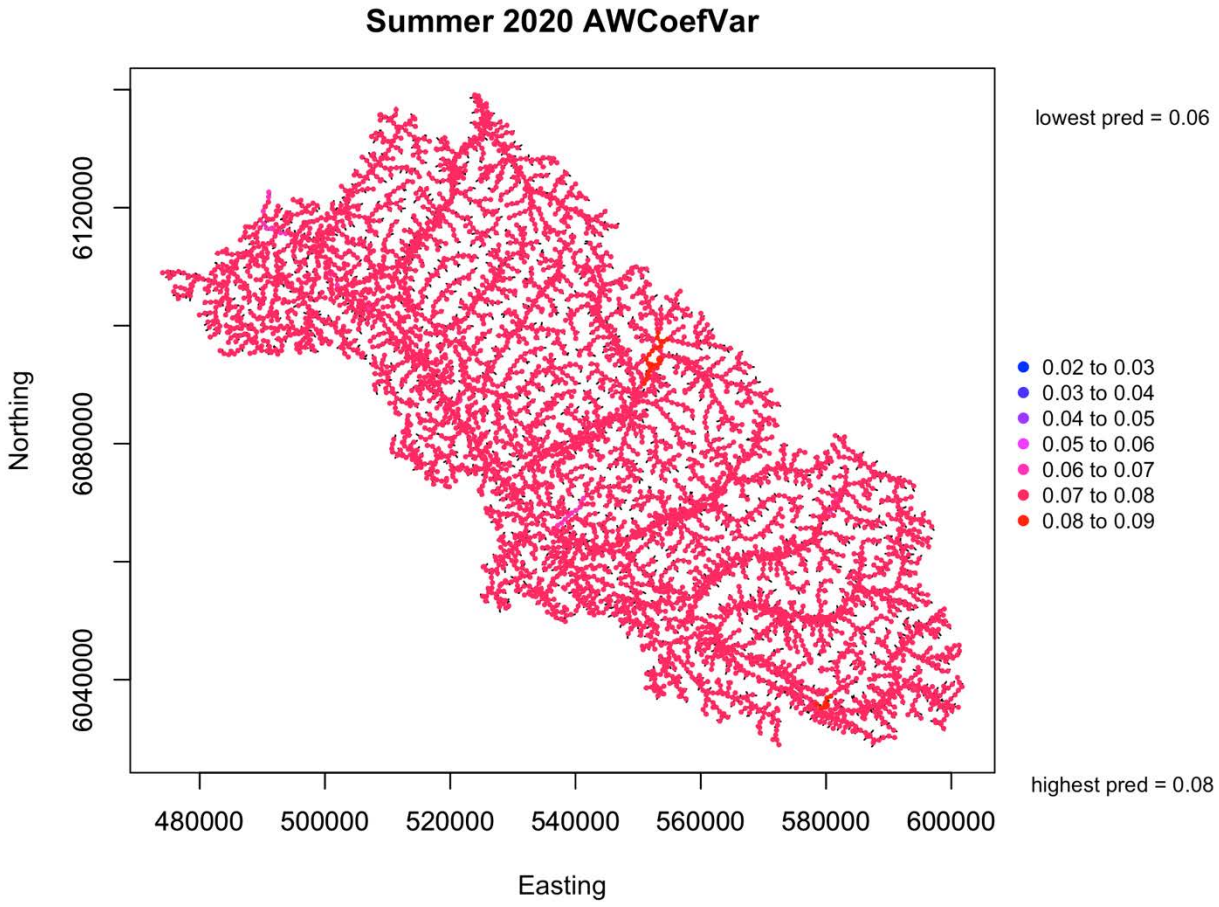


**Figure 10.** Spatial Stream Network Model predictions for the response metric average weekly coefficient of variation (AWCoefVar) in degrees Celsius for the trophic feeding window (July 1st - September 15th) for Arctic grayling in 2020. Predictions were created at 1km resolution.

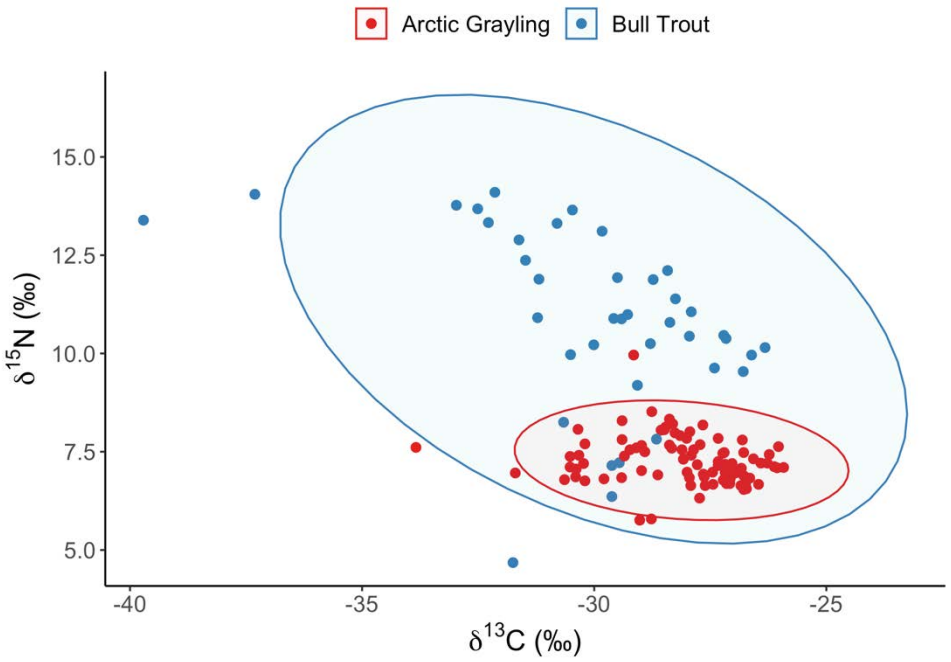


**Figure 11.** Isotope biplot fitted with 95% ellipses quantifying summer isotopic niche occupied by both Arctic grayling and bull trout within the Parsnip River watershed. Isotopic signatures were derived from muscle tissue collected over the 2018, 2019 and 2020 field seasons (bull trout n=41, Arctic grayling n= 85).

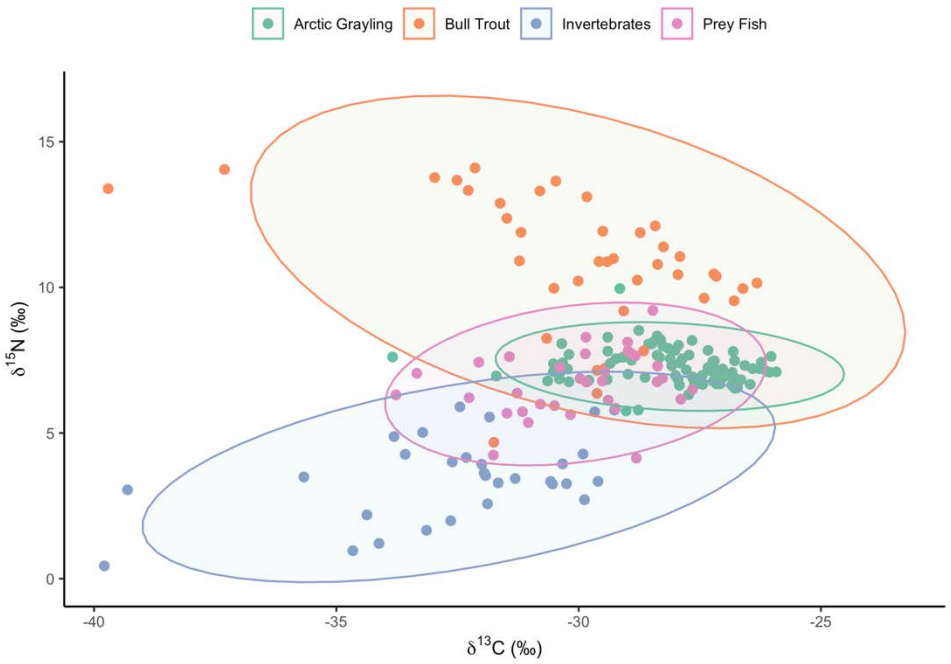


**Figure 12.** Isotope biplot fitted with 95% ellipses quantifying summer isotopic niche area occupied Arctic grayling, bull trout, prey fish and aquatic invertebrates within the Parsnip system. Isotopic signatures were derived from muscle samples or whole organism (prey fish, invertebrates) collected over the 2018, 2019, and 2020 field seasons (Arctic grayling n=86, bull trout n= 41, prey fish n=33, invertebrates n=29).

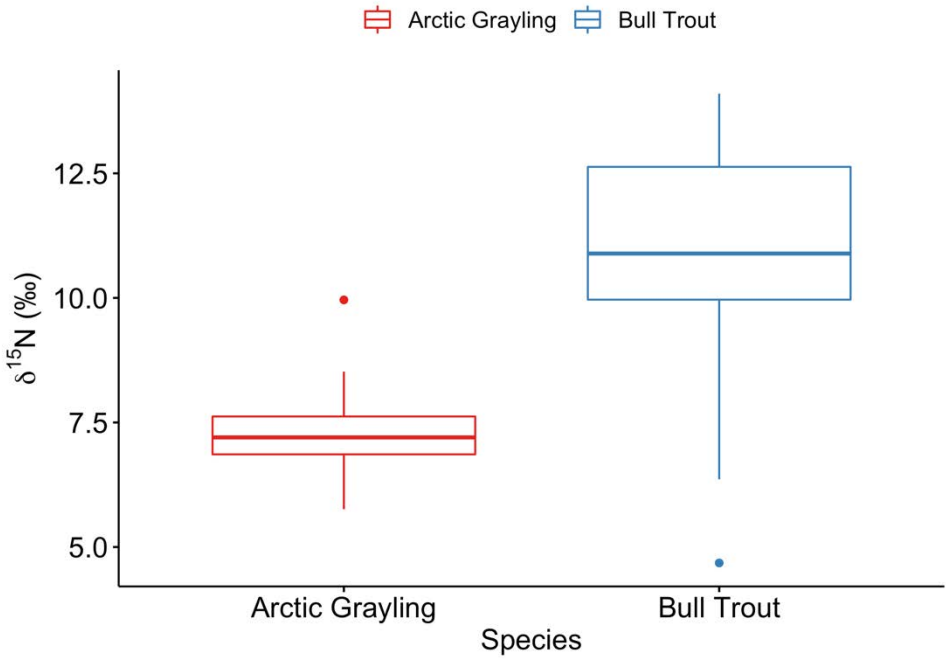


**Figure 13.** Box and whisker plot depicting the distribution of $\delta^{15}N$ values from sampled Arctic grayling and bull trout in the Parsnip watershed (bull trout n= 41; Arctic grayling n=86).

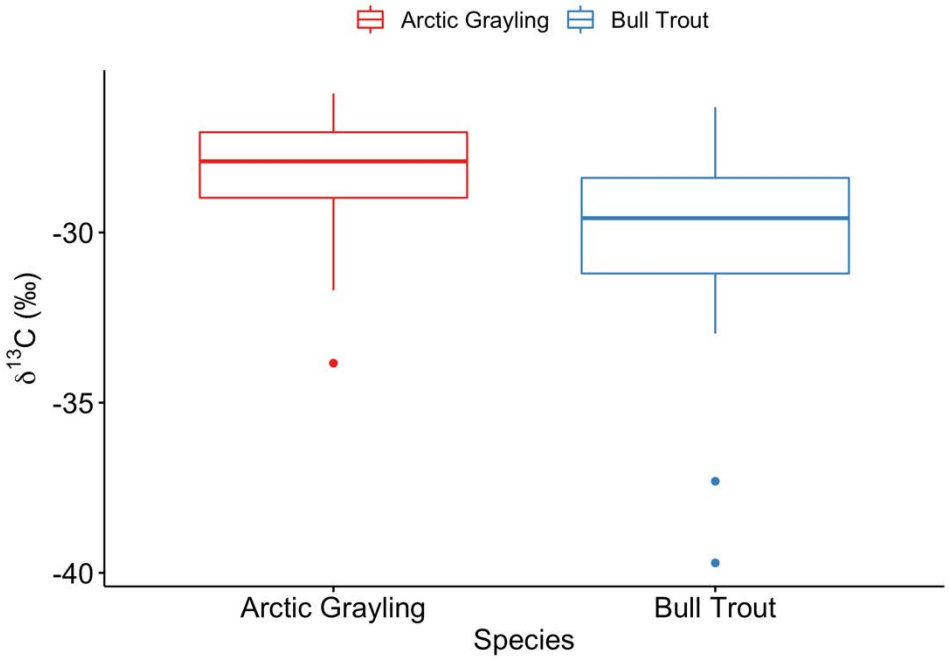


**Figure 14.** Box and whisker plot depicting the distribution of δ13C values from sampled Arctic grayling and bull trout in the Parsnip watershed (bull trout n= 41; Arctic grayling n=86).

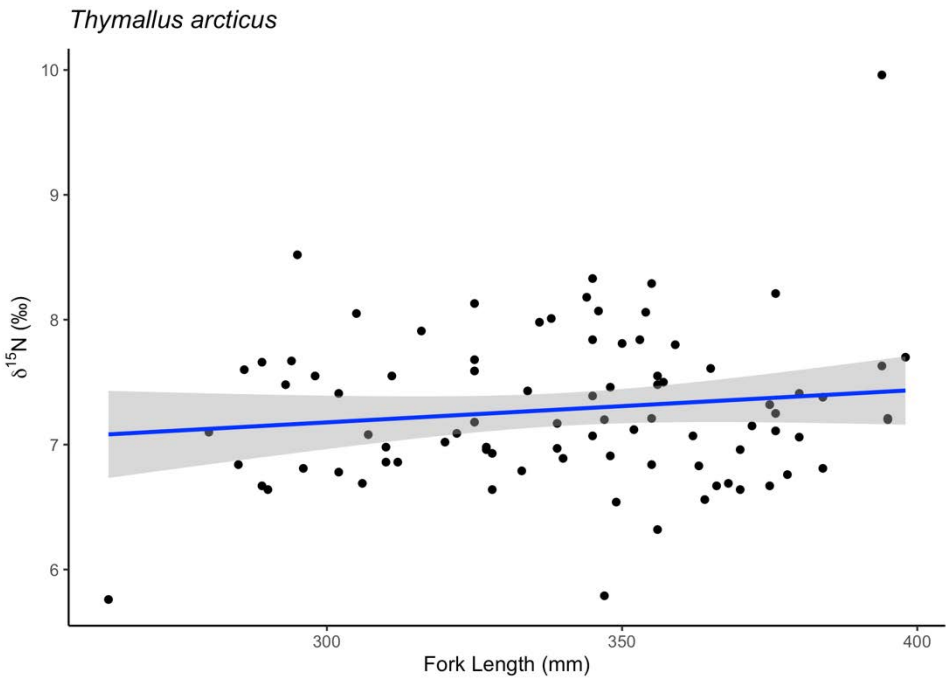


**Figure 15.** $\delta^{15}N$ in muscle tissue as a function of fork length in Arctic grayling. Muscle samples were collected in the Parsnip watershed during the summers of 2018, 2019 and 2020 (n= 86, y = 6.915x + 290, p=0.22, $R^2$ = 0.006).

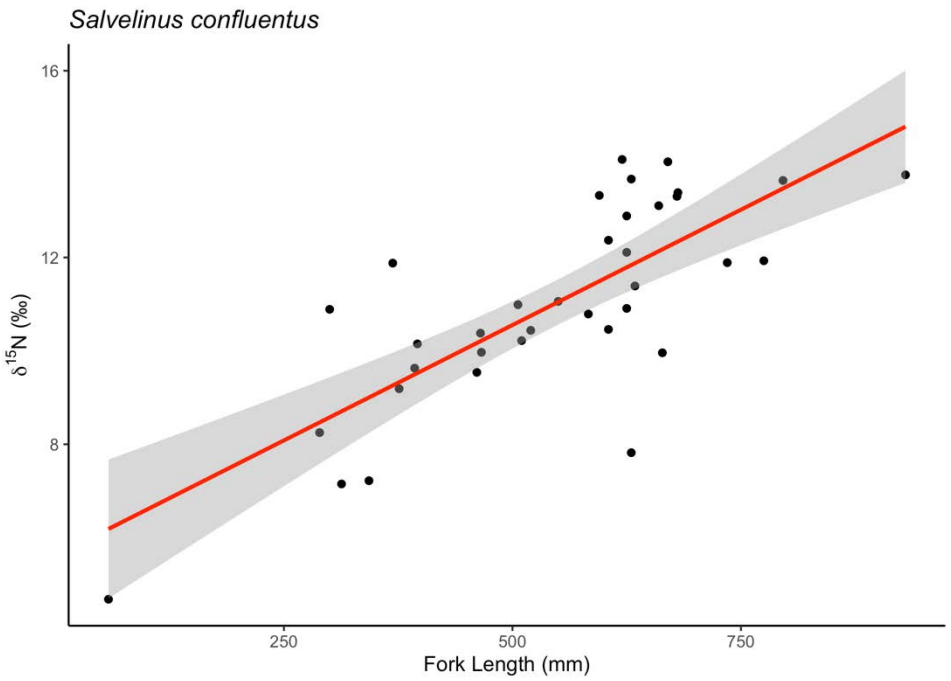


**Figure 16.** $\delta^{15}N$ in muscle tissue as a function of fork length in bull trout. Muscle samples were collected in the Parsnip watershed during the summers of 2018, 2019 and 2020 (n= 41, y= 0.0098x + 5.61, $p<0.001$, $R^2 = 0.58$).

**Appendix A. Telemetry Figures.**

This appendix accompanies the report Spatial Ecology of Arctic Grayling in the Parsnip Core Area (FWCP Peace Project No. PEA-F21-F-3178). This document contains the figures and tables referenced in *Section 5.2.1 – Telemetry Results*.

Each section is presented with a brief explanation of how to interpret the corresponding set of figures.

**Contents**

**Appendix A.1 – Individual detection history plots – Arctic grayling**

Figures in this section depict the spatial location of individual tags over the duration of that tag's active deployment. Tags with limited movement histories have been filtered out.

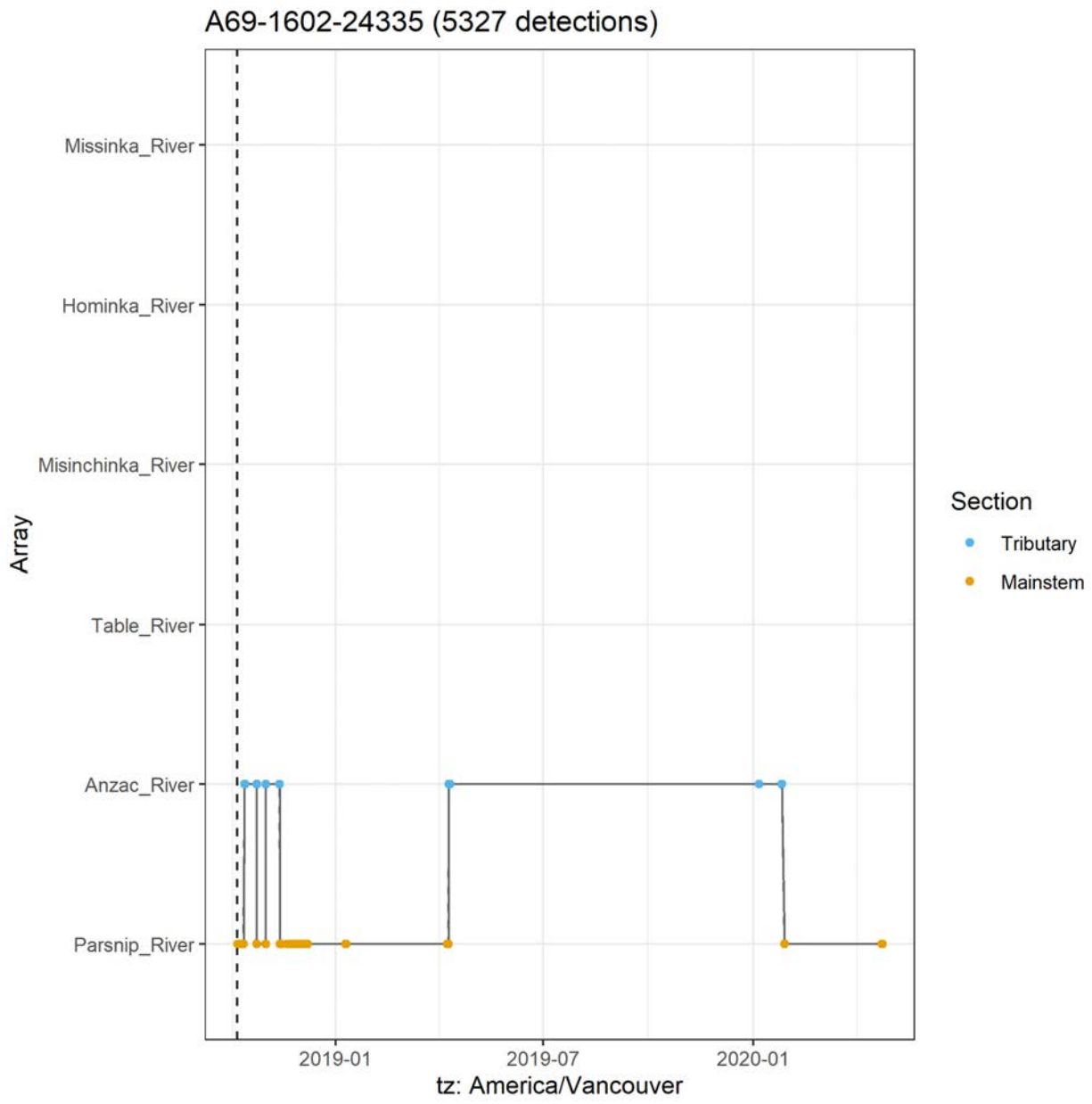
A69-1602-24335 (5327 detections)
Missinka_River
Hominka_River
Misinchinka_River
Table_River
Anzac_River
Parsnip_River
Array
2019-01
2019-07
2020-01
tz: America/Vancouver
Section
Tributary
Mainstem

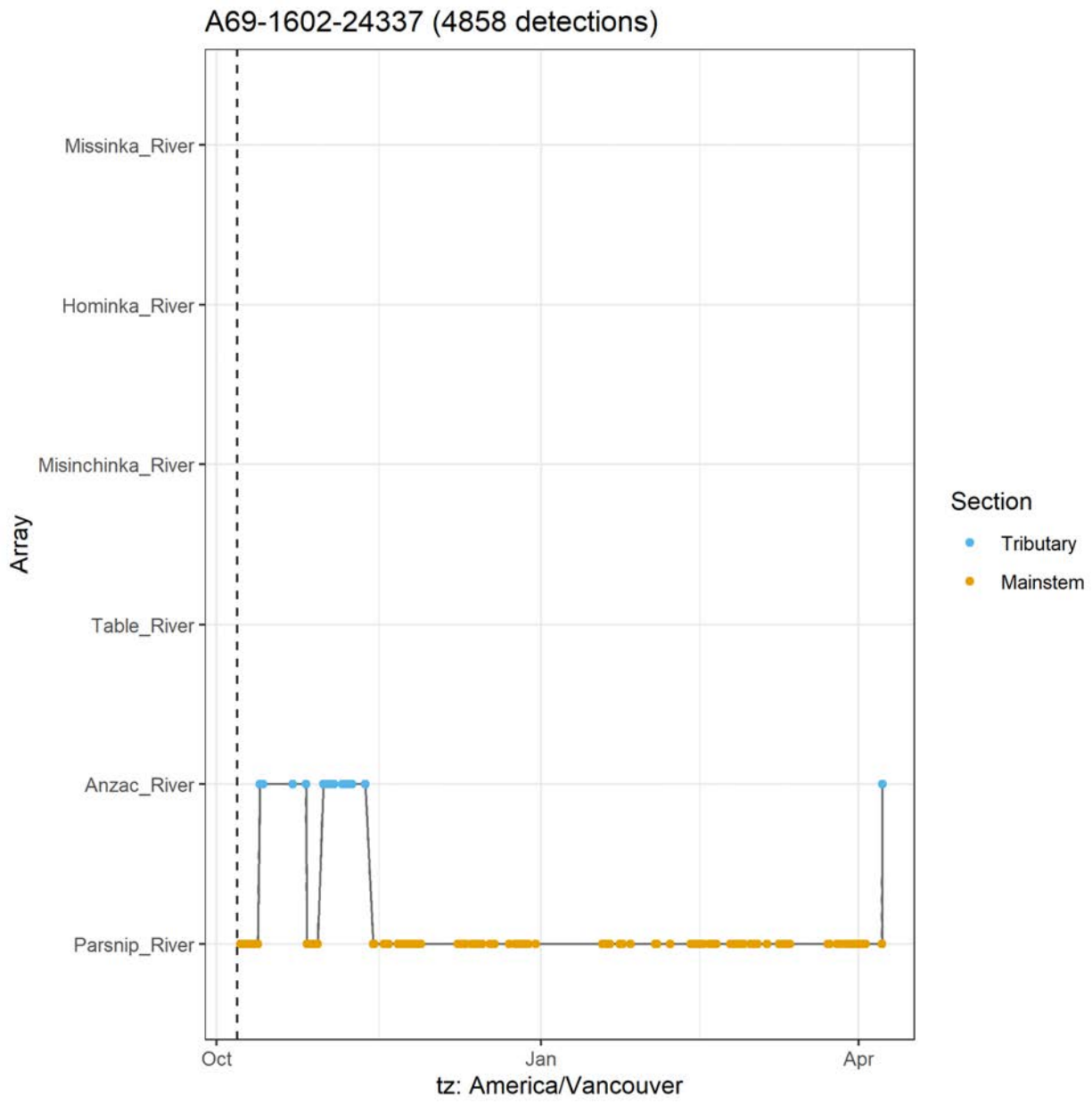
A69-1602-24337 (4858 detections)
Missinka_River
Hominka_River
Misinchinka_River
Table_River
Anzac_River
Parsnip_River
Array
Oct
Jan
Apr
tz: America/Vancouver
Section
Tributary
Mainstem

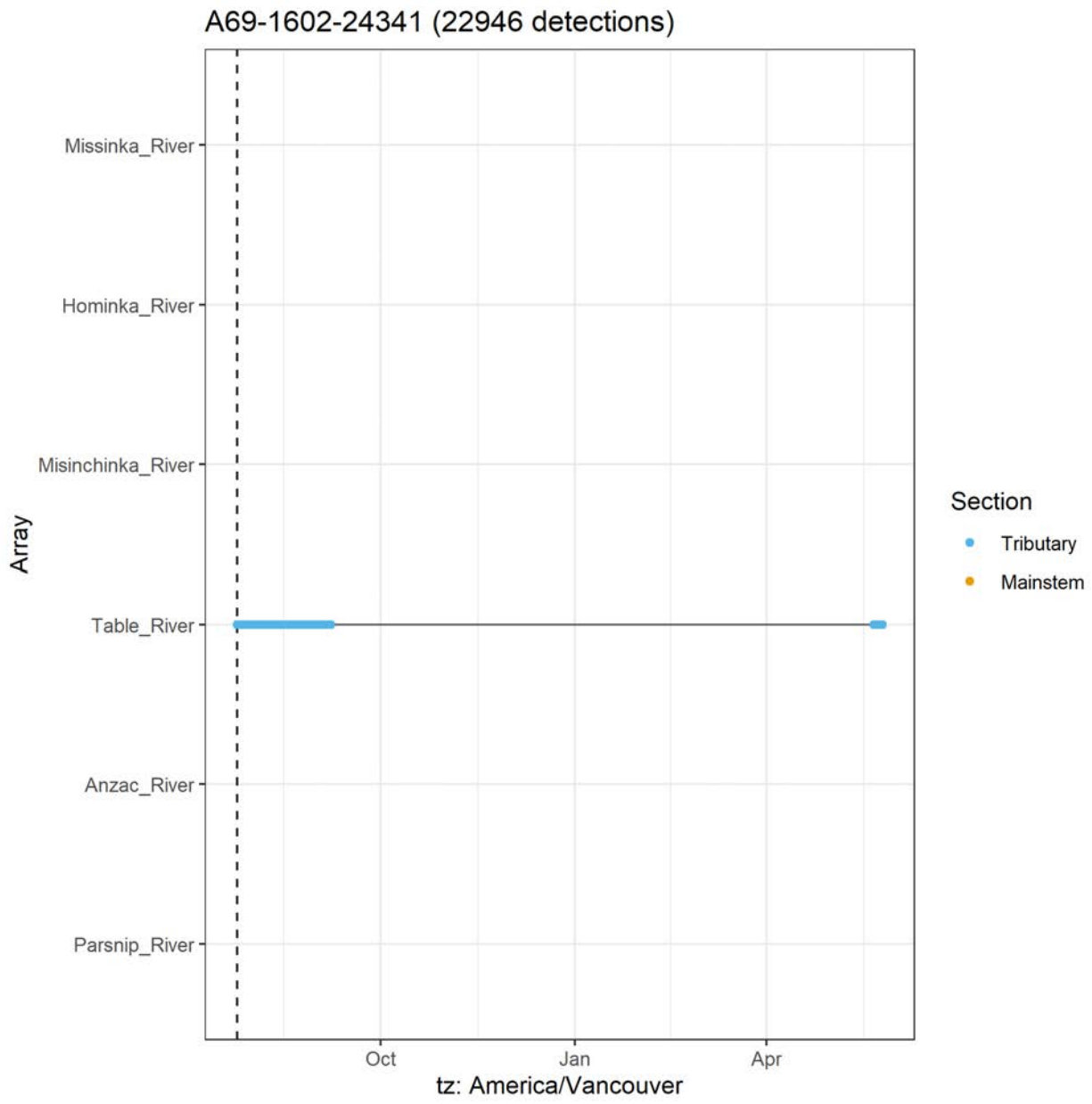
A69-1602-24341 (22946 detections)
Missinka_River
Hominka_River
Misinchinka_River
Table_River
Anzac_River
Parsnip_River
Array
Oct
Jan
Apr
tz: America/Vancouver
Section
Tributary
Mainstem

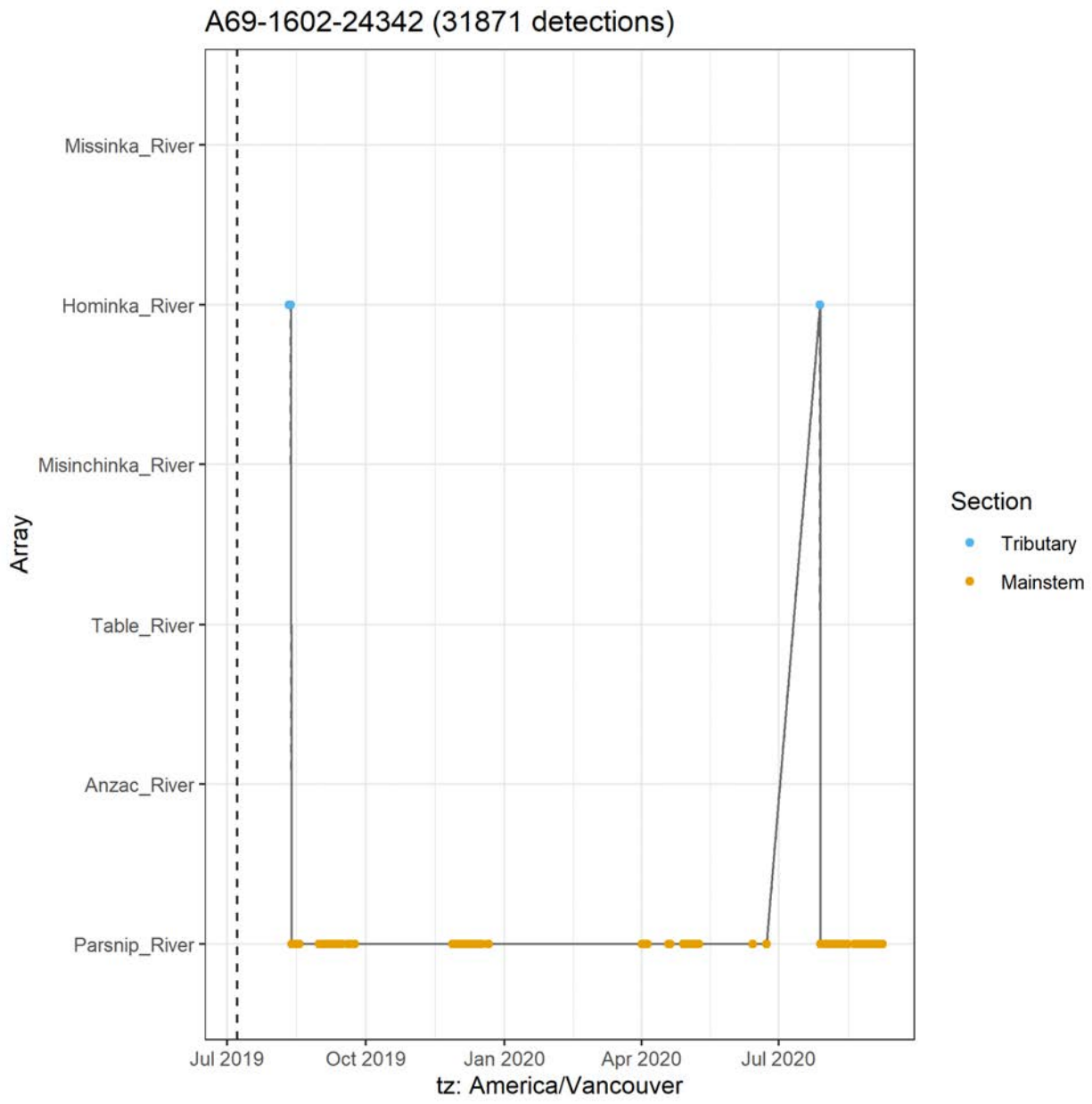
A69-1602-24342 (31871 detections)
Missinka_River
Hominka_River
Misinchinka_River
Table_River
Anzac_River
Parsnip_River
Array
Jul 2019
Oct 2019
Jan 2020
Apr 2020
Jul 2020
tz: America/Vancouver
Section
Tributary
Mainstem

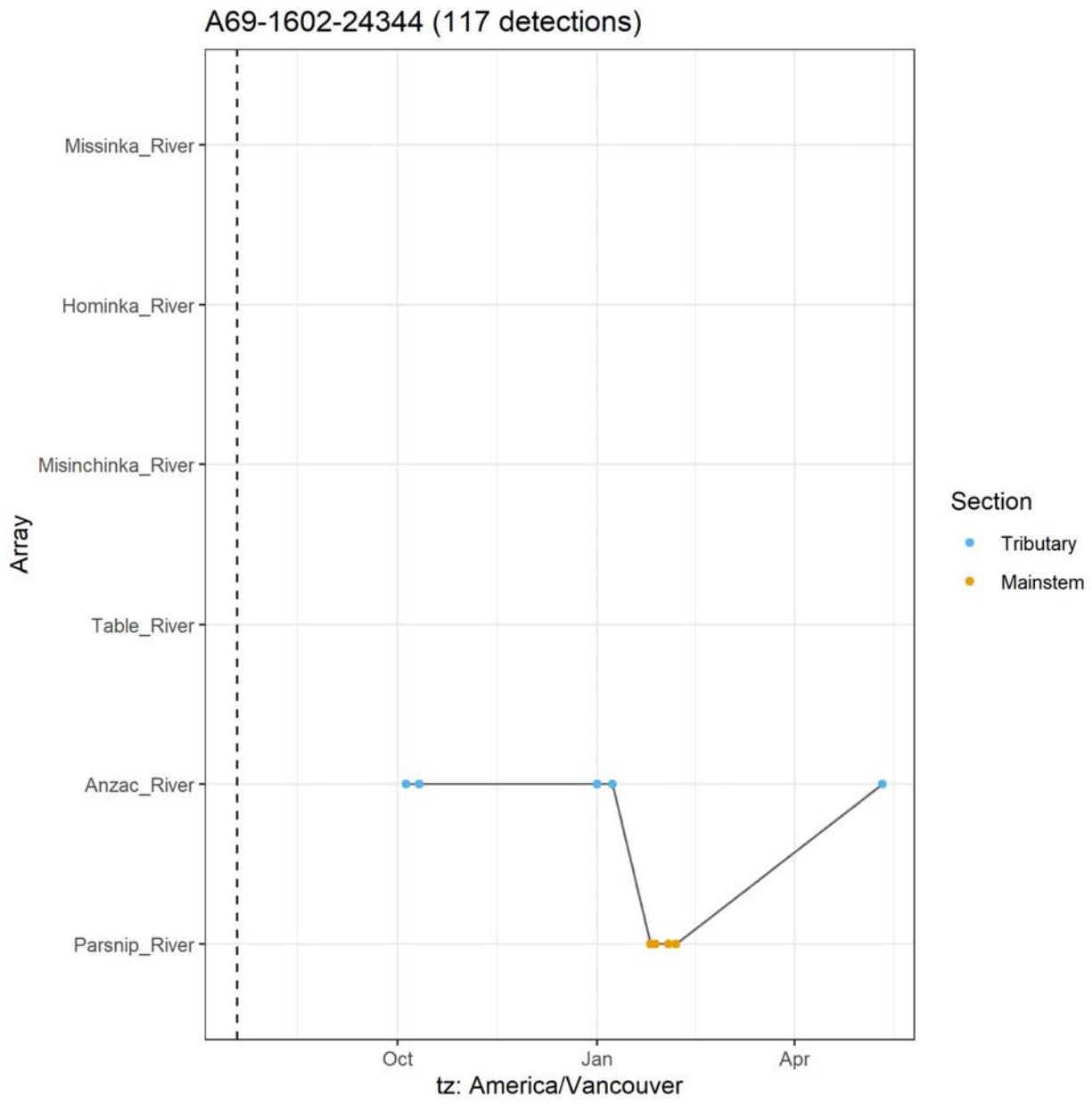
A69-1602-24344 (117 detections)
Missinka_River
Hominka_River
Misinchinka_River
Table_River
Anzac_River
Parsnip_River
Array
Oct
Jan
Apr
tz: America/Vancouver
Section
Tributary
Mainstem

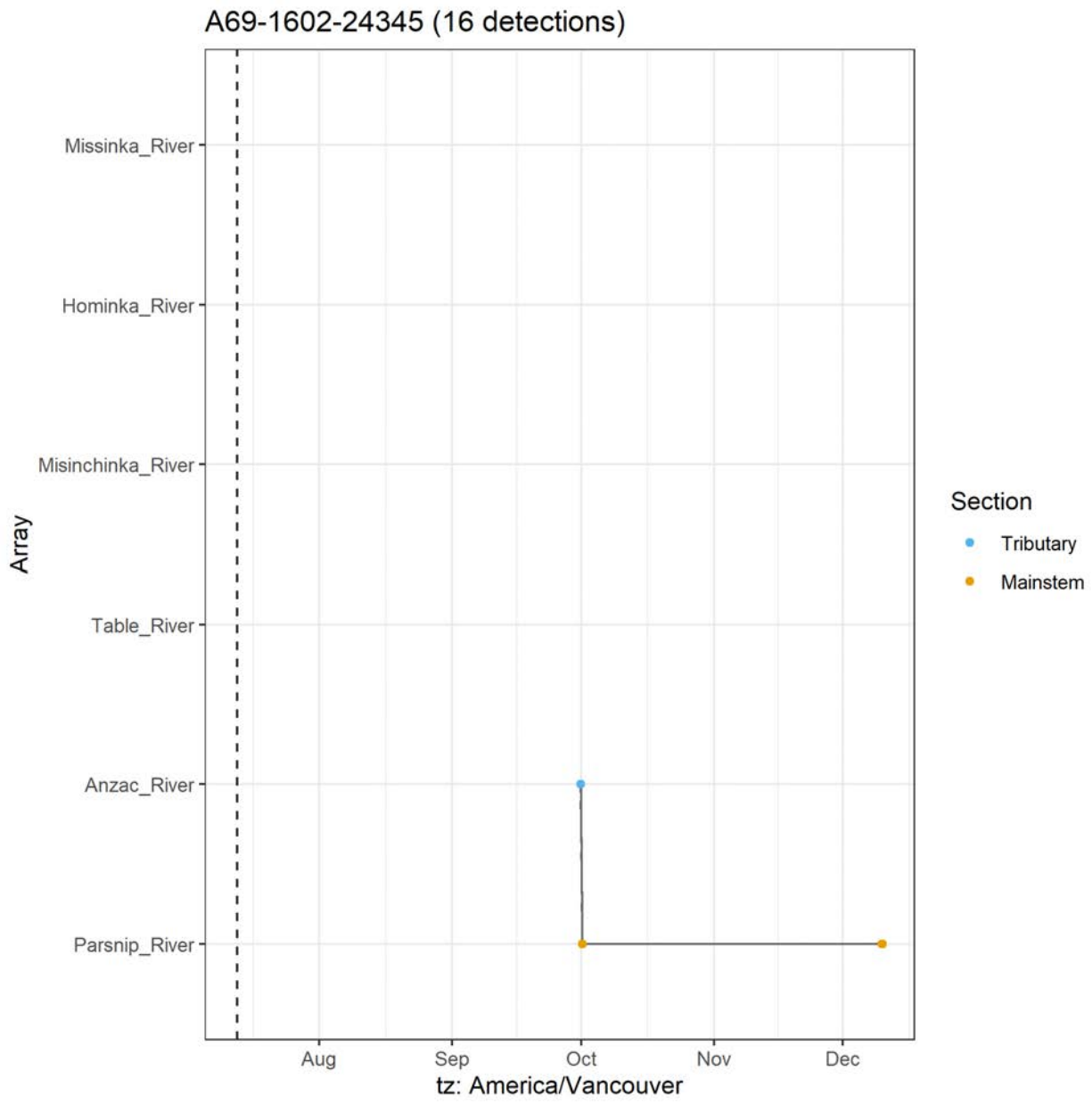
A69-1602-24345 (16 detections)
Missinka_River
Hominka_River
Misinchinka_River
Table_River
Anzac_River
Parsnip_River
Array
Aug
Sep
Oct
Nov
Dec
tz: America/Vancouver
Section
Tributary
Mainstem

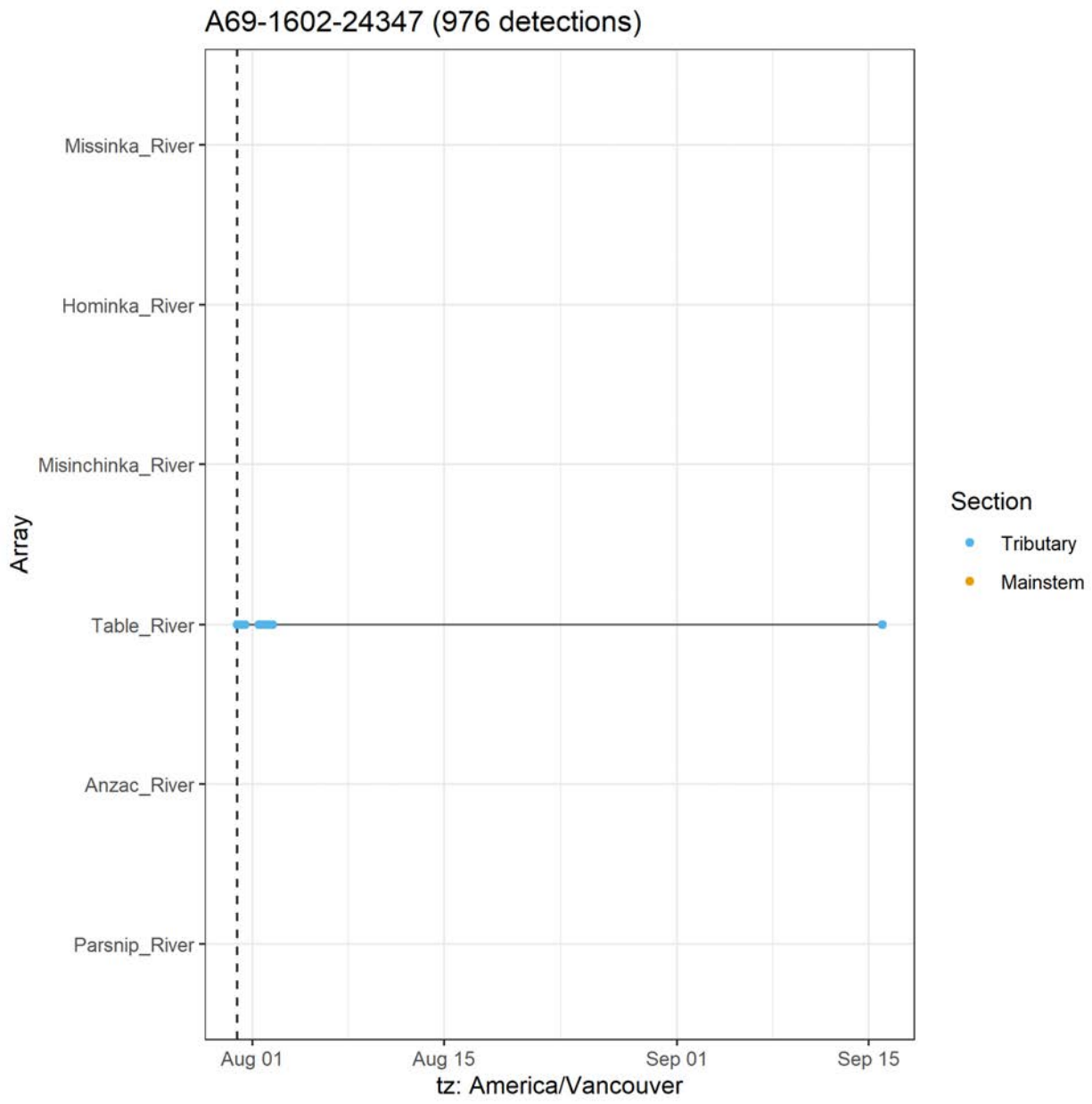
A69-1602-24347 (976 detections)
Missinka_River
Hominka_River
Misinchinka_River
Table_River
Anzac_River
Parsnip_River
Array
Aug 01
Aug 15
Sep 01
Sep 15
tz: America/Vancouver
Section
Tributary
Mainstem

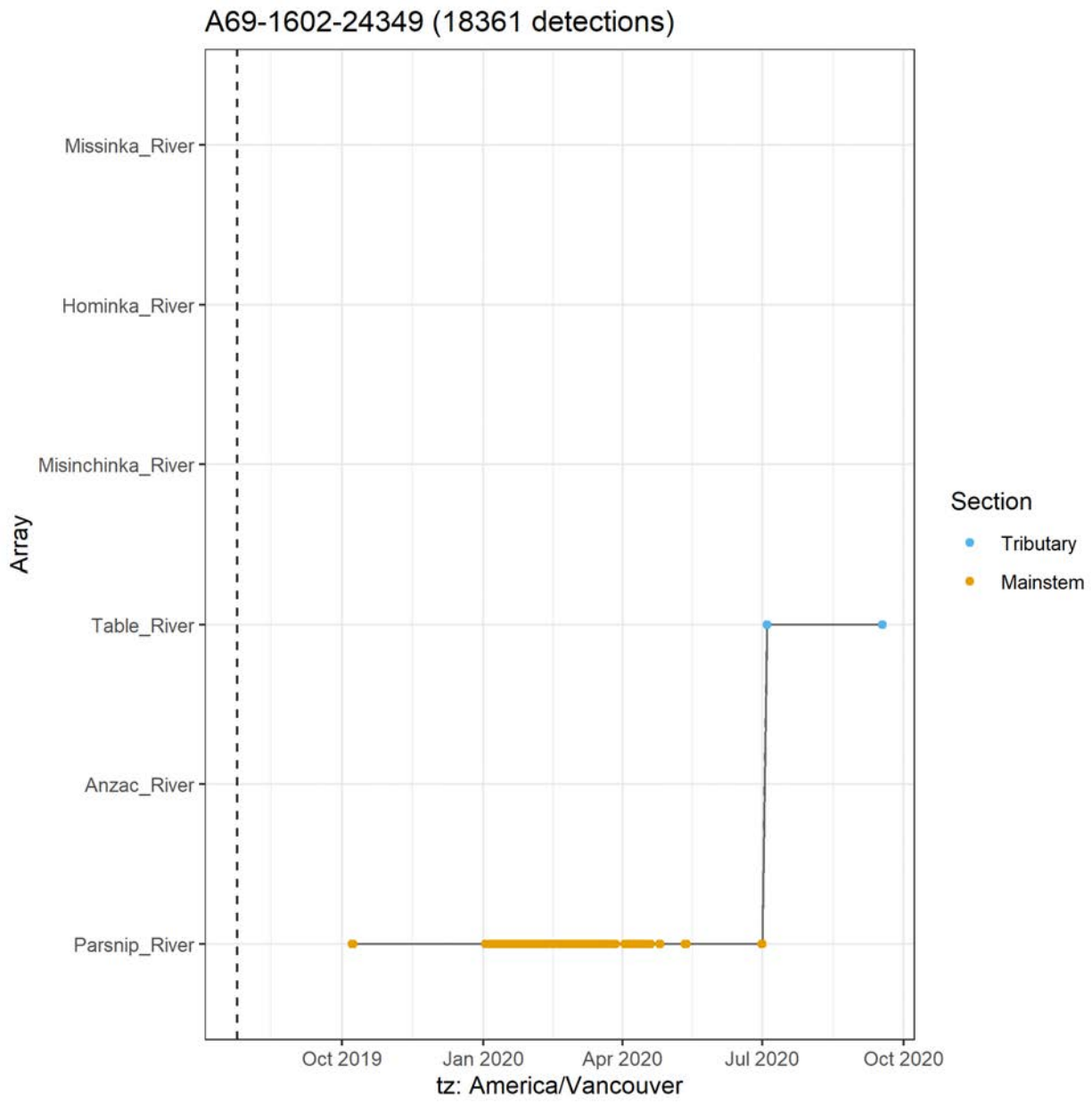
A69-1602-24349 (18361 detections)
Missinka_River
Hominka_River
Misinchinka_River
Table_River
Anzac_River
Parsnip_River
Array
Oct 2019
Jan 2020
Apr 2020
Jul 2020
Oct 2020
tz: America/Vancouver
Section
Tributary
Mainstem

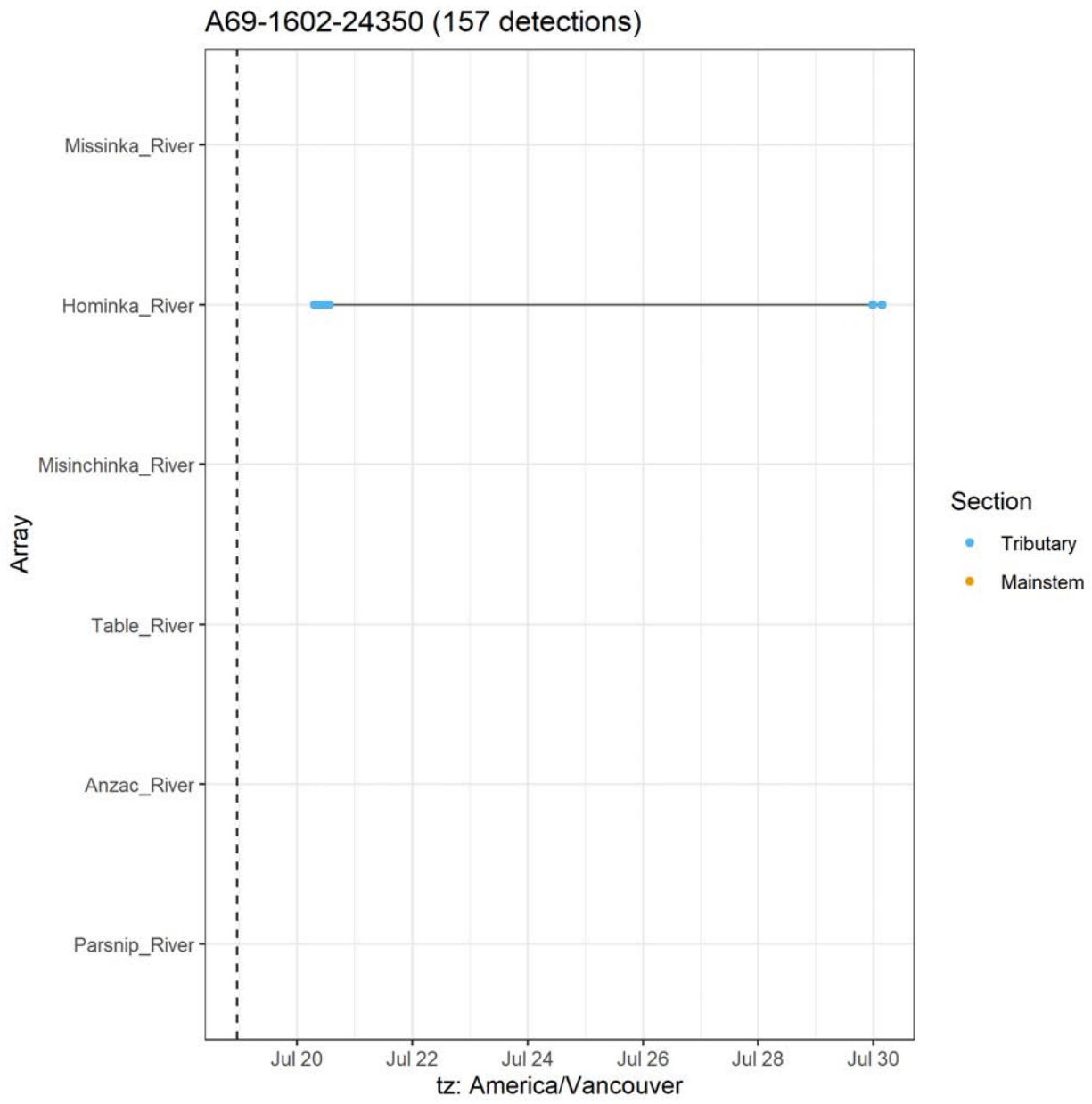
A69-1602-24350 (157 detections)
Missinka_River
Hominka_River
Misinchinka_River
Table_River
Anzac_River
Parsnip_River
Array
Jul 20
Jul 22
Jul 24
Jul 26
Jul 28
Jul 30
tz: America/Vancouver
Section
Tributary
Mainstem

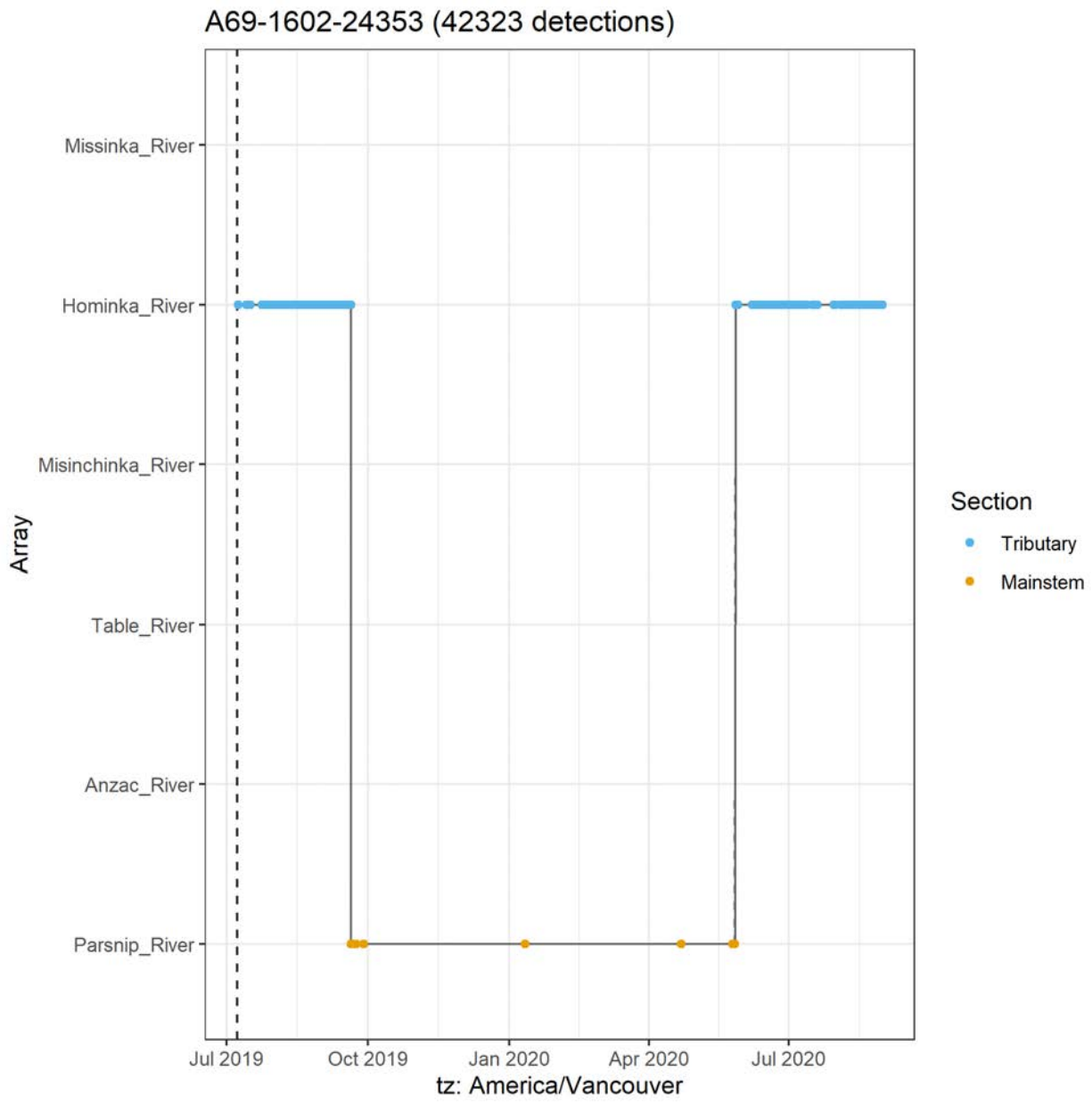
A69-1602-24353 (42323 detections)
Missinka_River
Hominka_River
Misinchinka_River
Table_River
Anzac_River
Parsnip_River
Array
Jul 2019
Oct 2019
Jan 2020
Apr 2020
Jul 2020
tz: America/Vancouver
Section
Tributary
Mainstem

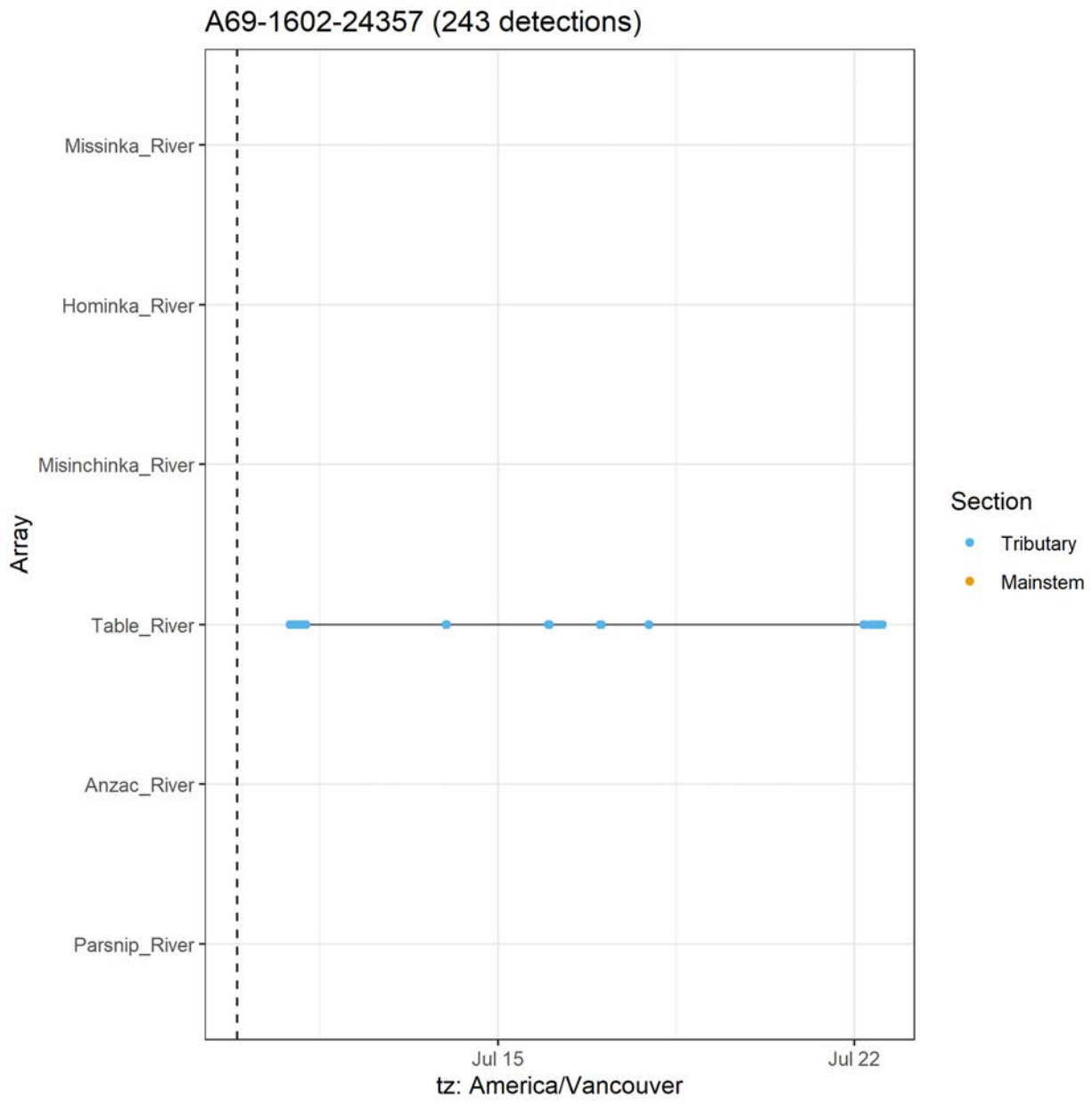
A69-1602-24357 (243 detections)
Missinka_River
Hominka_River
Misinchinka_River
Table_River
Anzac_River
Parsnip_River
Array
Jul 15
Jul 22
tz: America/Vancouver
Section
Tributary
Mainstem

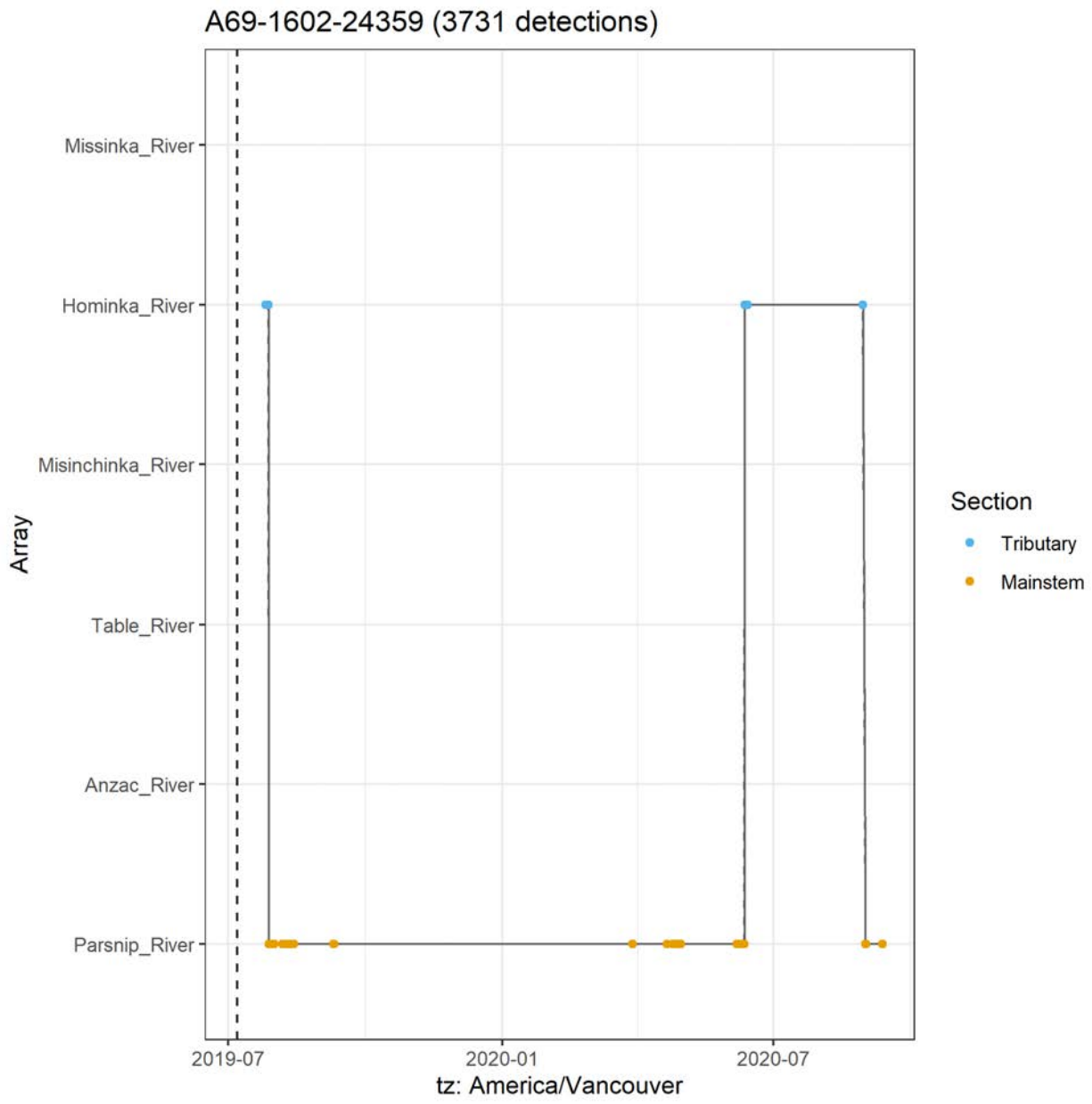
A69-1602-24359 (3731 detections)
Missinka_River
Hominka_River
Misinchinka_River
Table_River
Anzac_River
Parsnip_River
Array
2019-07
2020-01
2020-07
tz: America/Vancouver
Section
Tributary
Mainstem

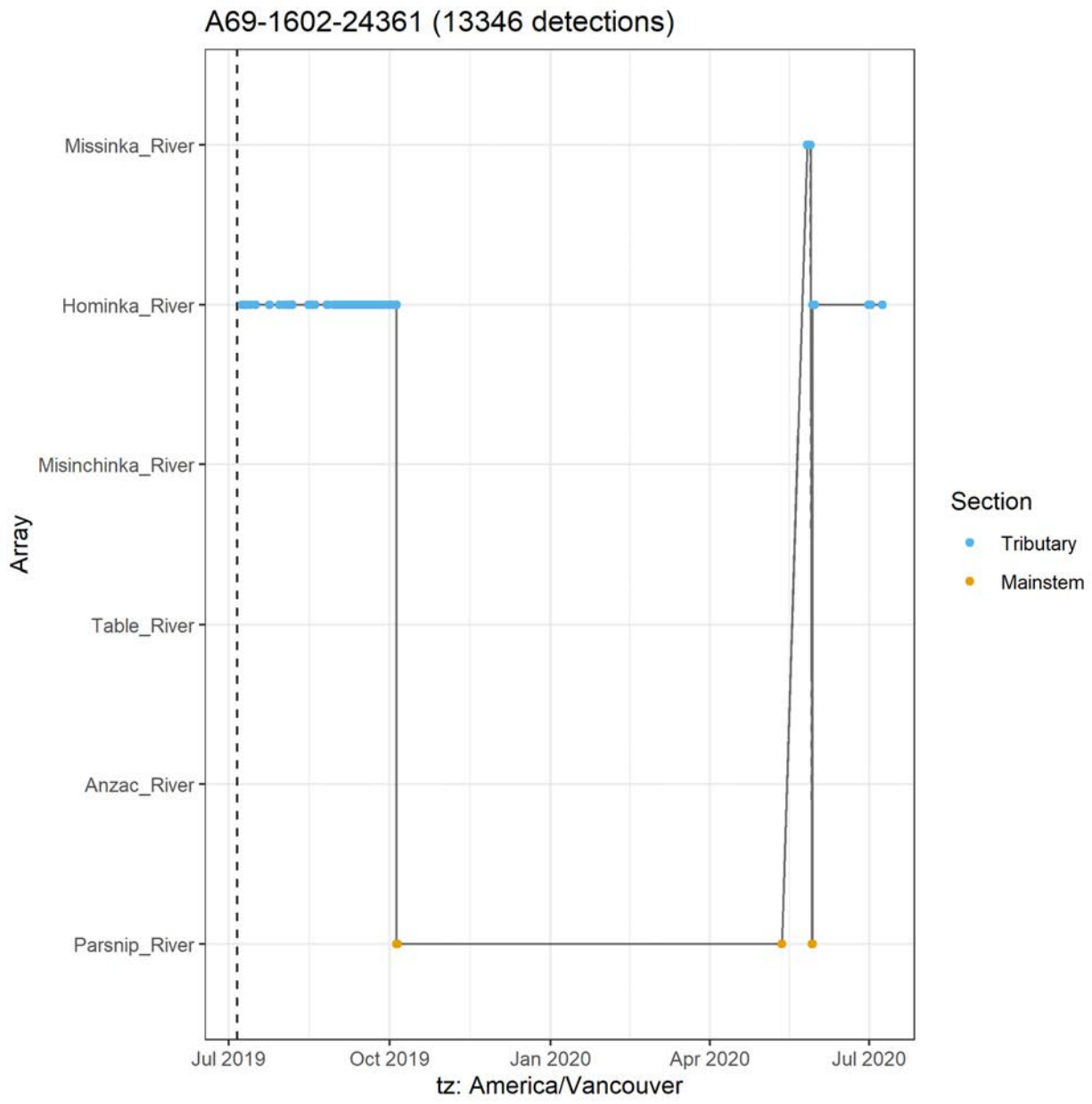
A69-1602-24361 (13346 detections)
Missinka_River
Hominka_River
Misinchinka_River
Table_River
Anzac_River
Parsnip_River
Array
Jul 2019
Oct 2019
Jan 2020
Apr 2020
Jul 2020
tz: America/Vancouver
Section
Tributary
Mainstem

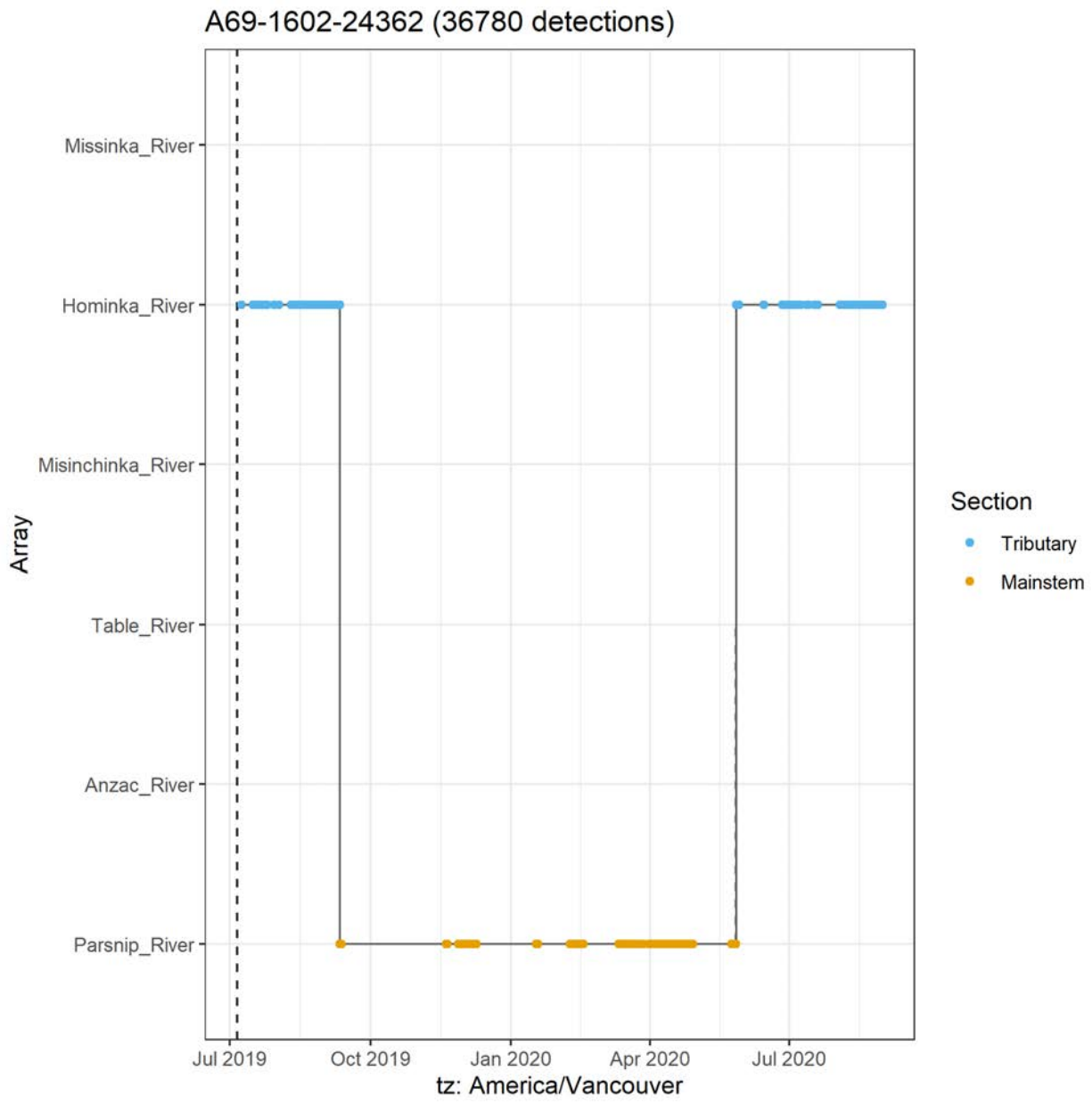
A69-1602-24362 (36780 detections)
Missinka_River
Hominka_River
Misinchinka_River
Table_River
Anzac_River
Parsnip_River
Array
Jul 2019
Oct 2019
Jan 2020
Apr 2020
Jul 2020
tz: America/Vancouver
Section
Tributary
Mainstem

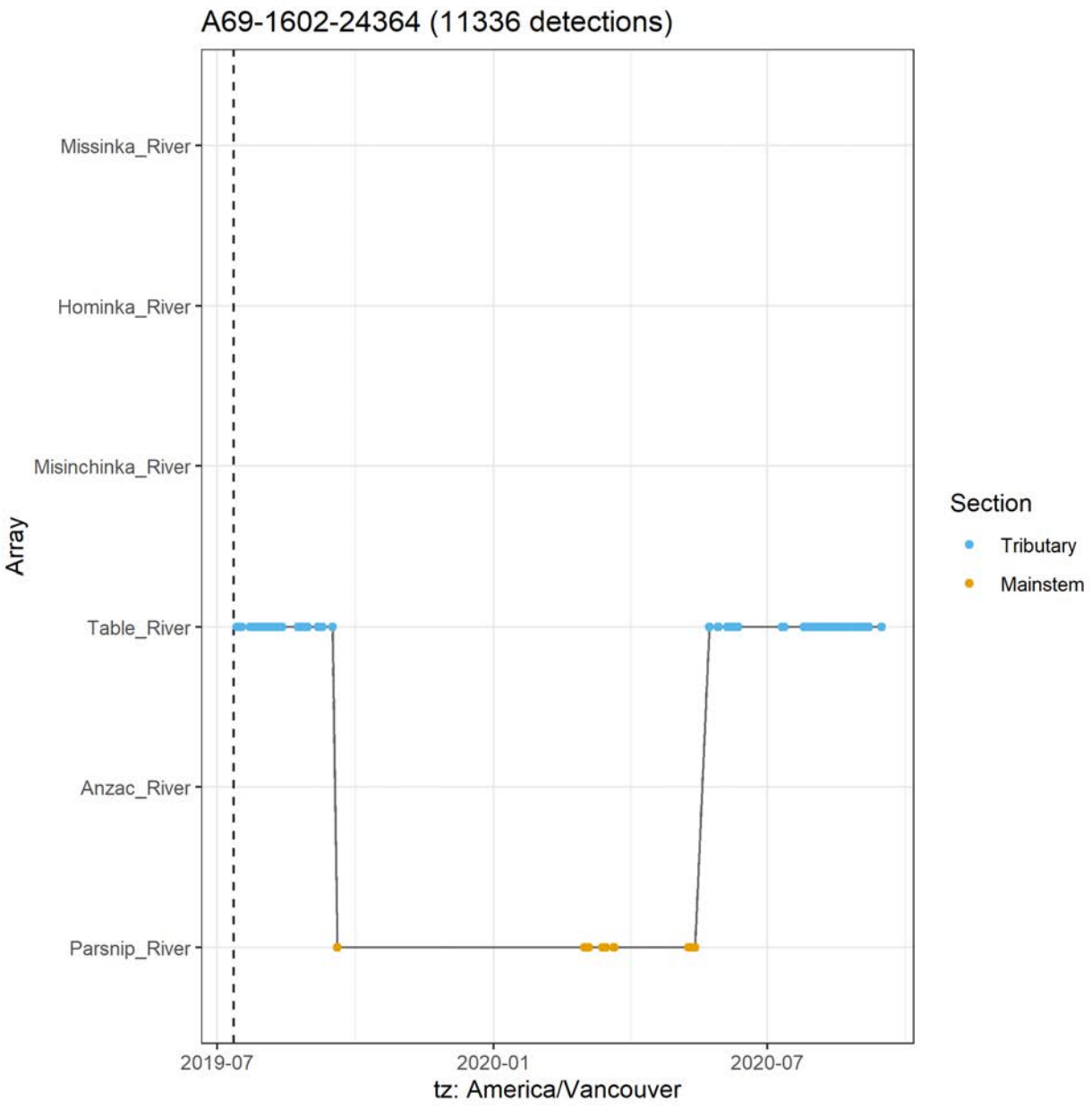
A69-1602-24364 (11336 detections)
Missinka_River
Hominka_River
Misinchinka_River
Table_River
Anzac_River
Parsnip_River
Array
2019-07
2020-01
2020-07
tz: America/Vancouver
Section
Tributary
Mainstem

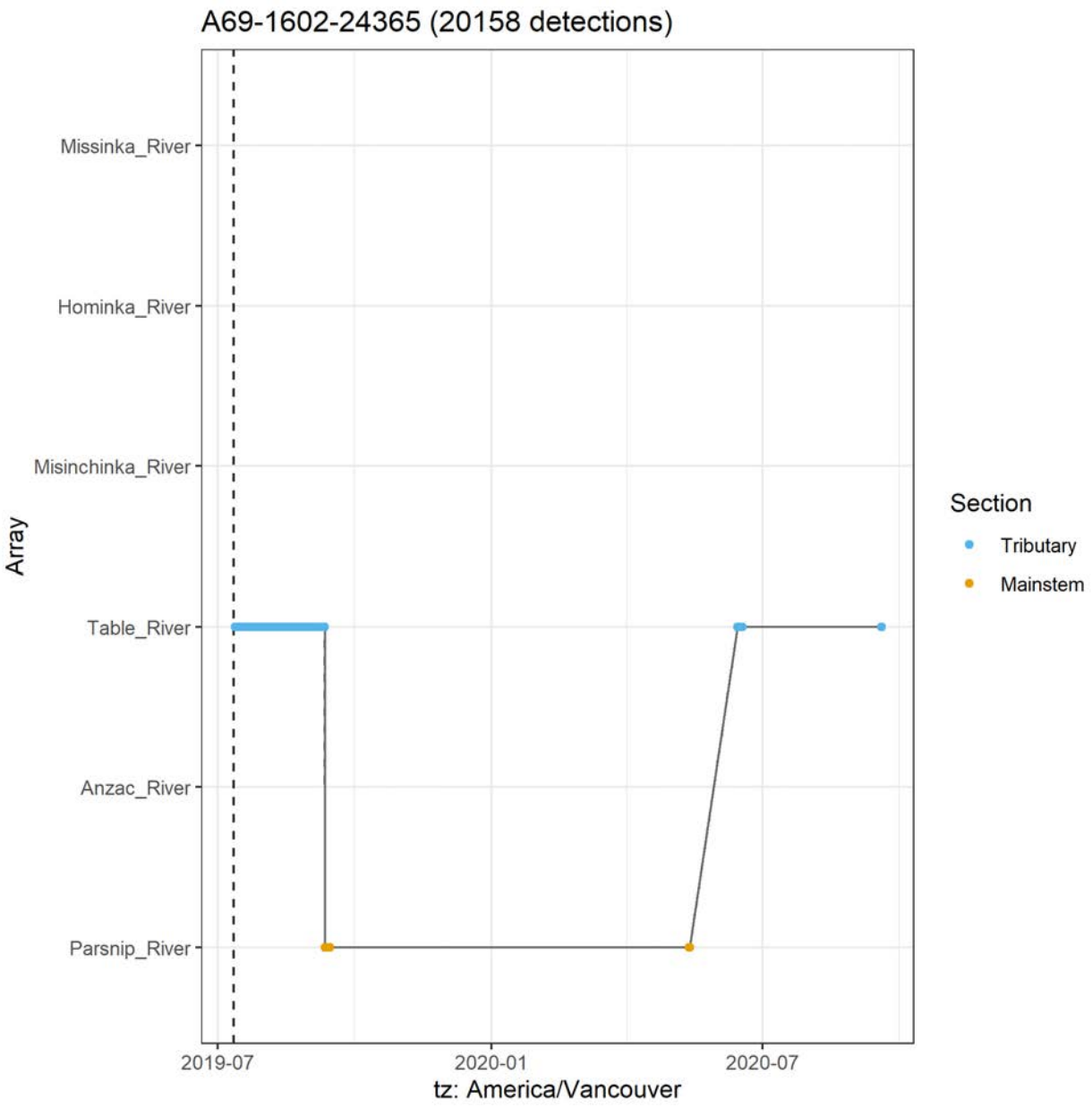
A69-1602-24365 (20158 detections)
Missinka_River
Hominka_River
Misinchinka_River
Table_River
Anzac_River
Parsnip_River
Array
2019-07
2020-01
2020-07
tz: America/Vancouver
Section
Tributary
Mainstem

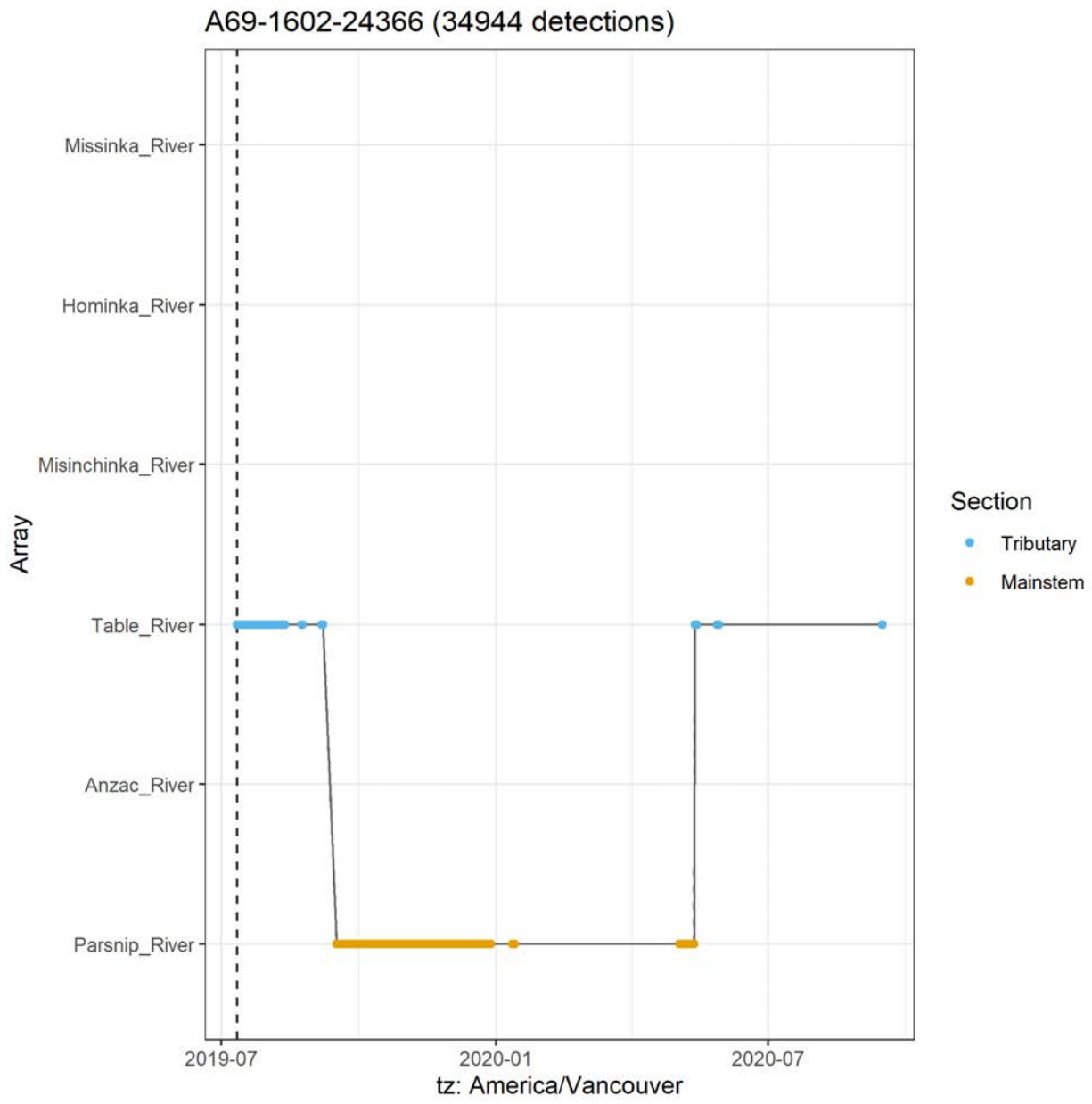
A69-1602-24366 (34944 detections)
Missinka_River
Hominka_River
Misinchinka_River
Table_River
Anzac_River
Parsnip_River
Array
2019-07
2020-01
2020-07
tz: America/Vancouver
Section
Tributary
Mainstem

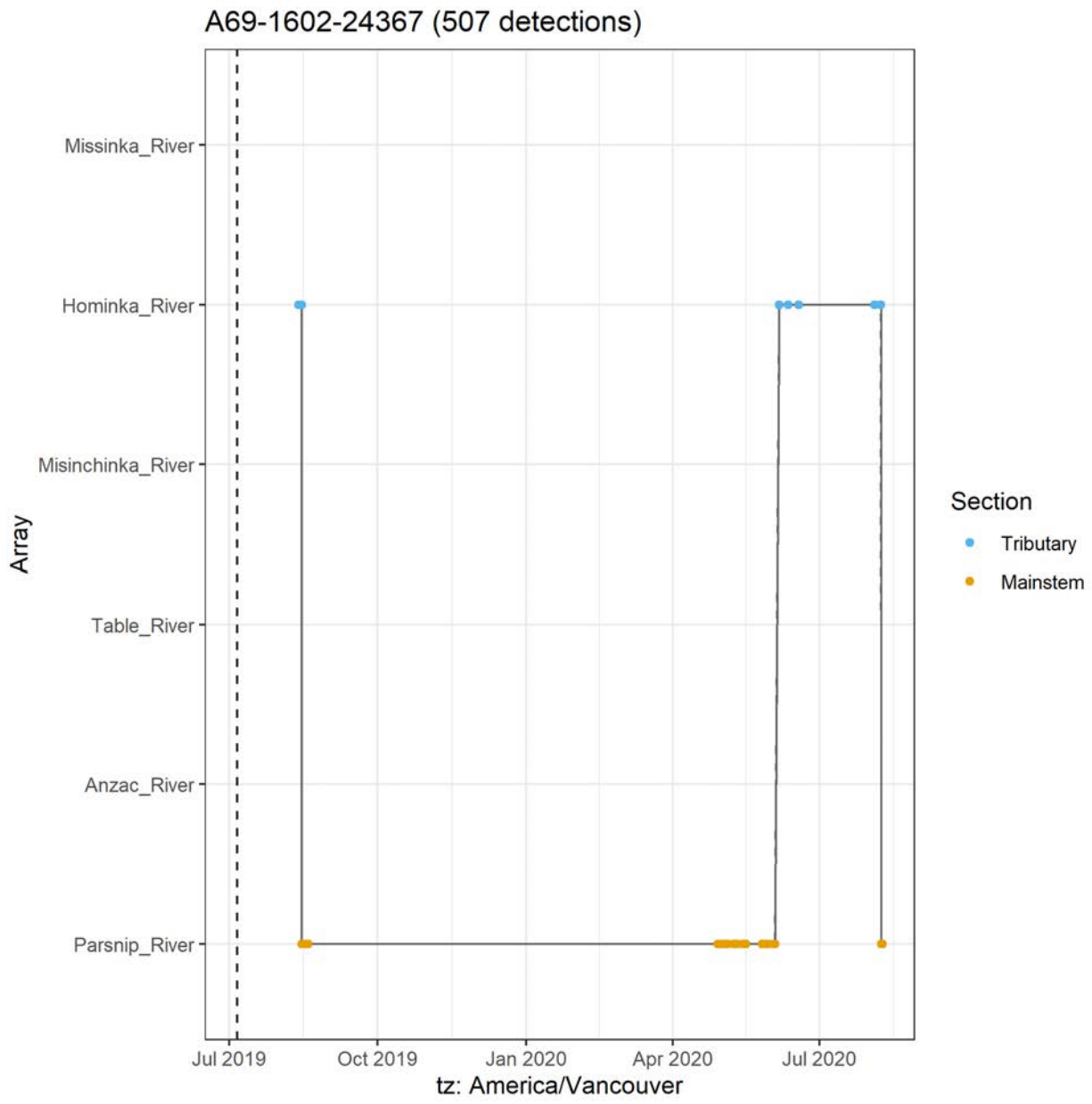
A69-1602-24367 (507 detections)
Missinka_River
Hominka_River
Misinchinka_River
Table_River
Anzac_River
Parsnip_River
Array
Jul 2019
Oct 2019
Jan 2020
Apr 2020
Jul 2020
tz: America/Vancouver
Section
Tributary
Mainstem

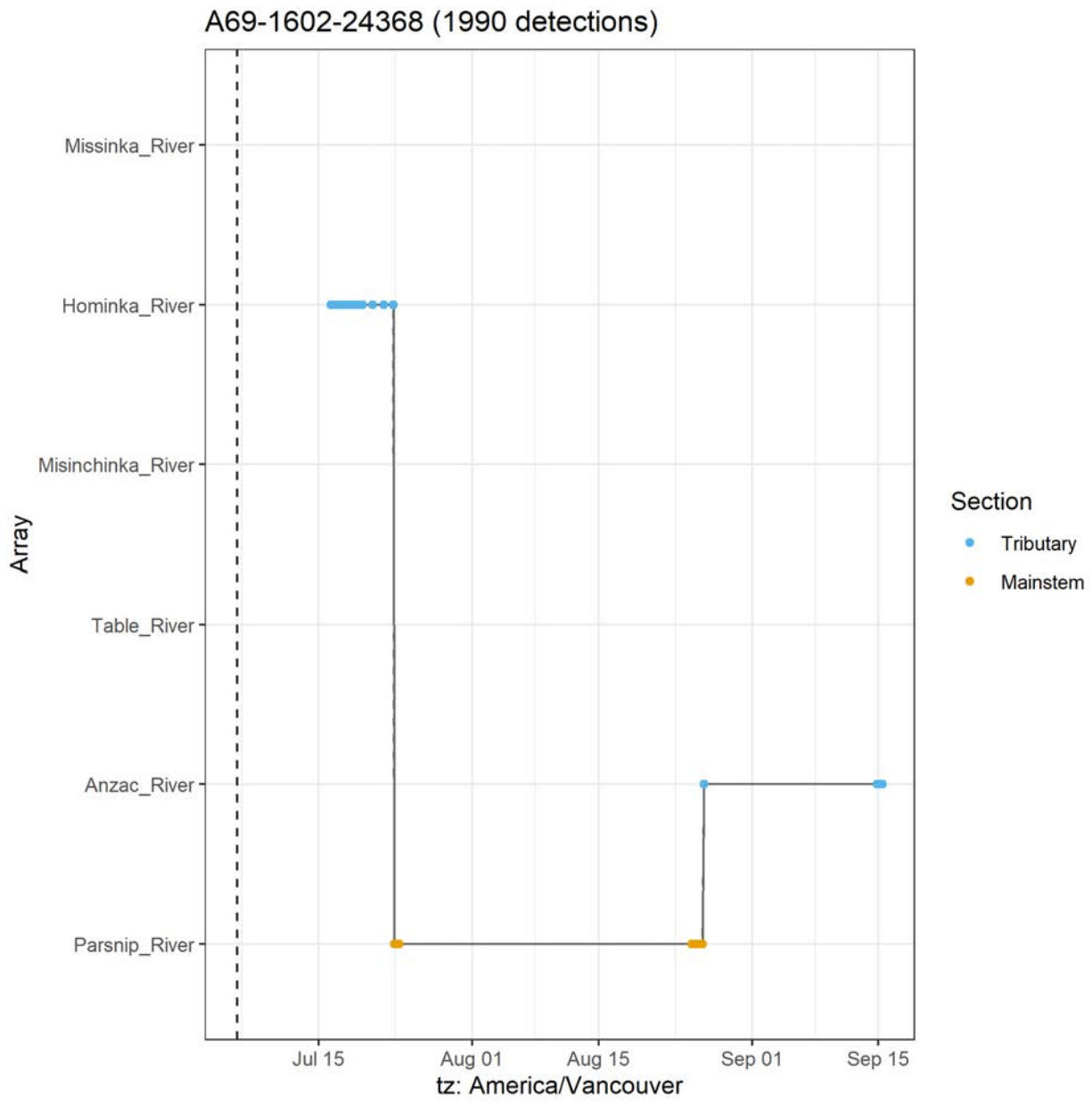
A69-1602-24368 (1990 detections)
Missinka_River
Hominka_River
Misinchinka_River
Table_River
Anzac_River
Parsnip_River
Array
Jul 15
Aug 01
Aug 15
Sep 01
Sep 15
tz: America/Vancouver
Section
Tributary
Mainstem

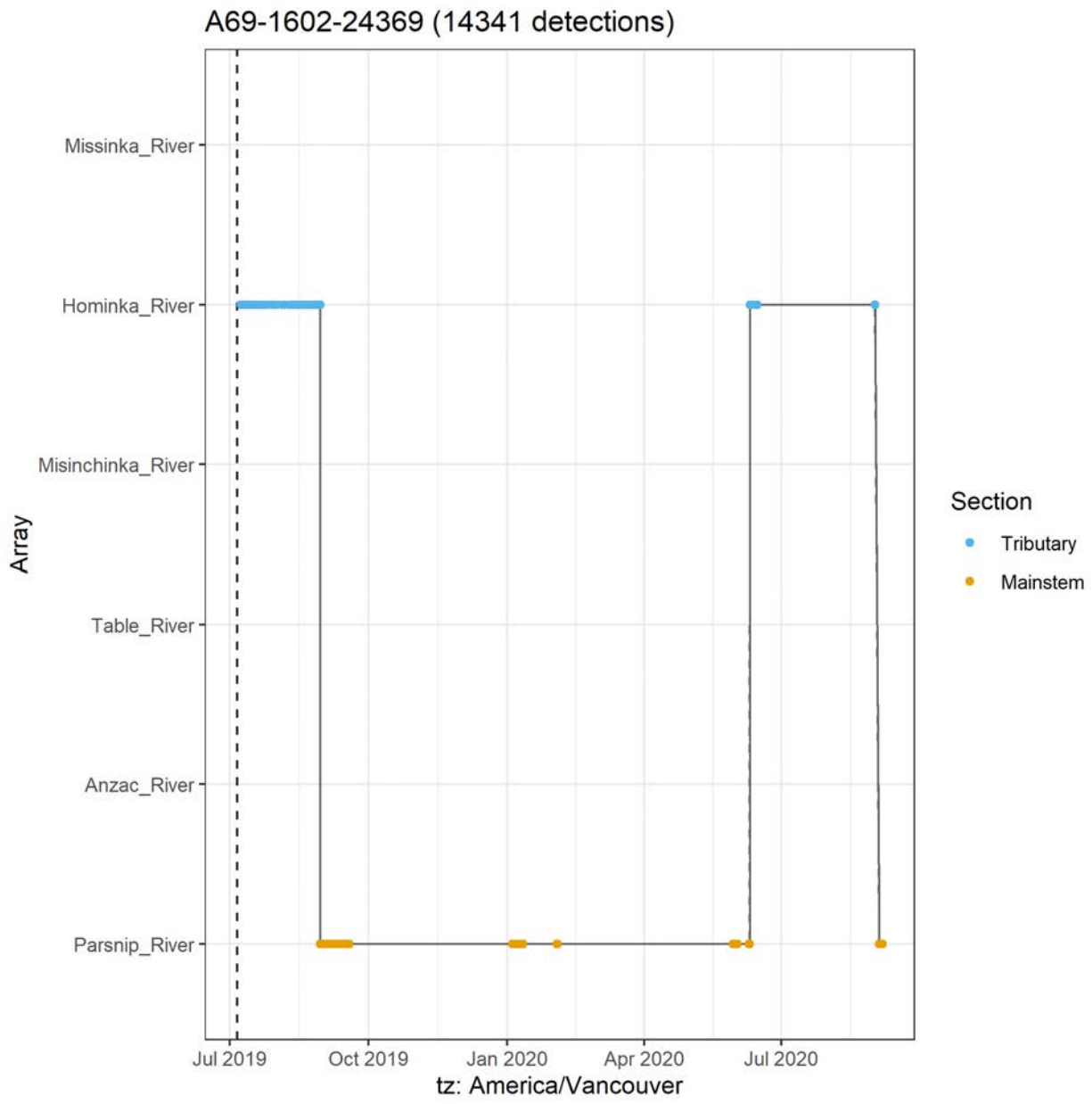
A69-1602-24369 (14341 detections)
Missinka_River
Hominka_River
Misinchinka_River
Table_River
Anzac_River
Parsnip_River
Array
Jul 2019
Oct 2019
Jan 2020
Apr 2020
Jul 2020
tz: America/Vancouver
Section
Tributary
Mainstem

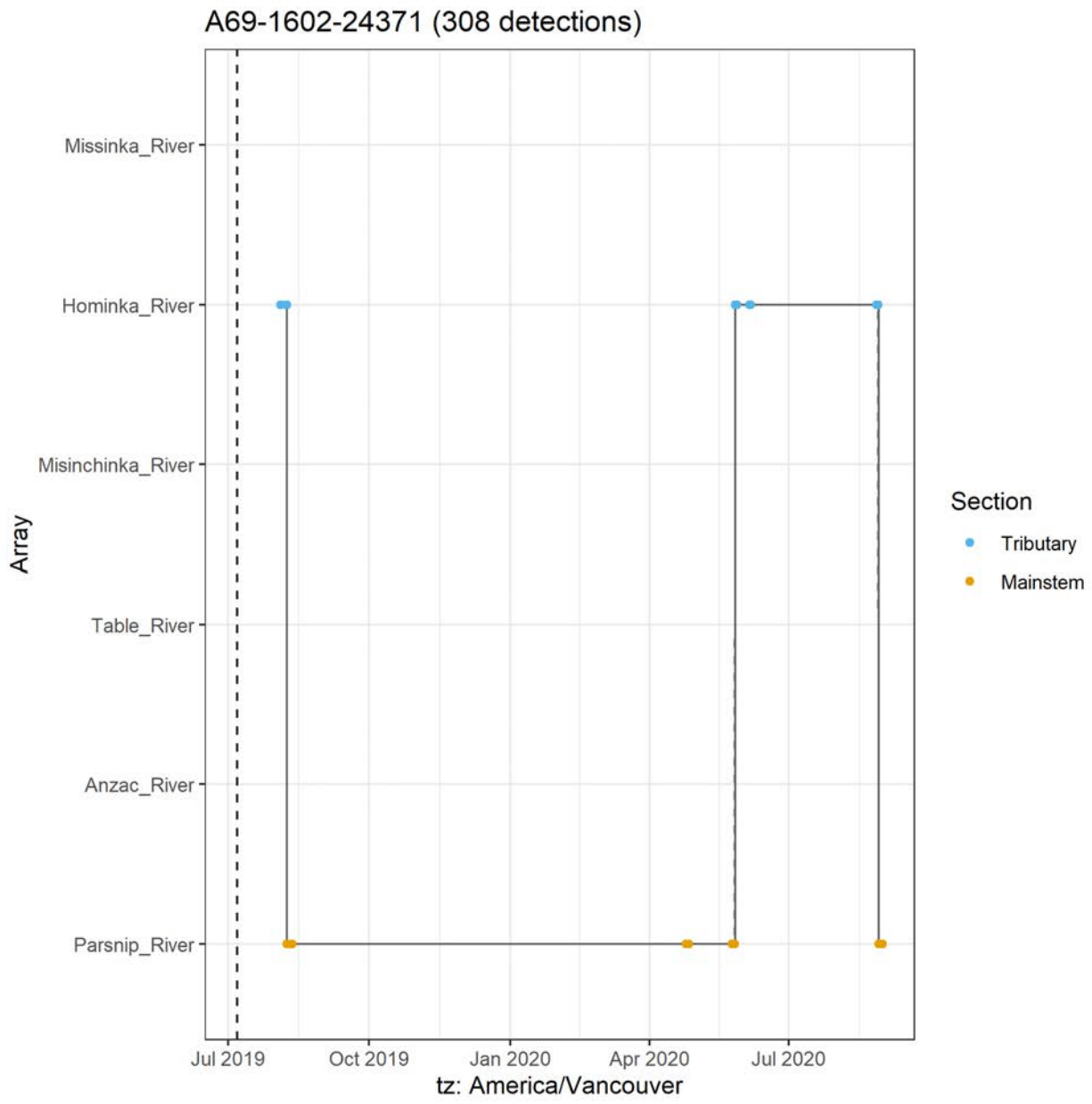
A69-1602-24371 (308 detections)
Missinka_River
Hominka_River
Misinchinka_River
Table_River
Anzac_River
Parsnip_River
Array
Jul 2019
Oct 2019
Jan 2020
Apr 2020
Jul 2020
tz: America/Vancouver
Section
Tributary
Mainstem

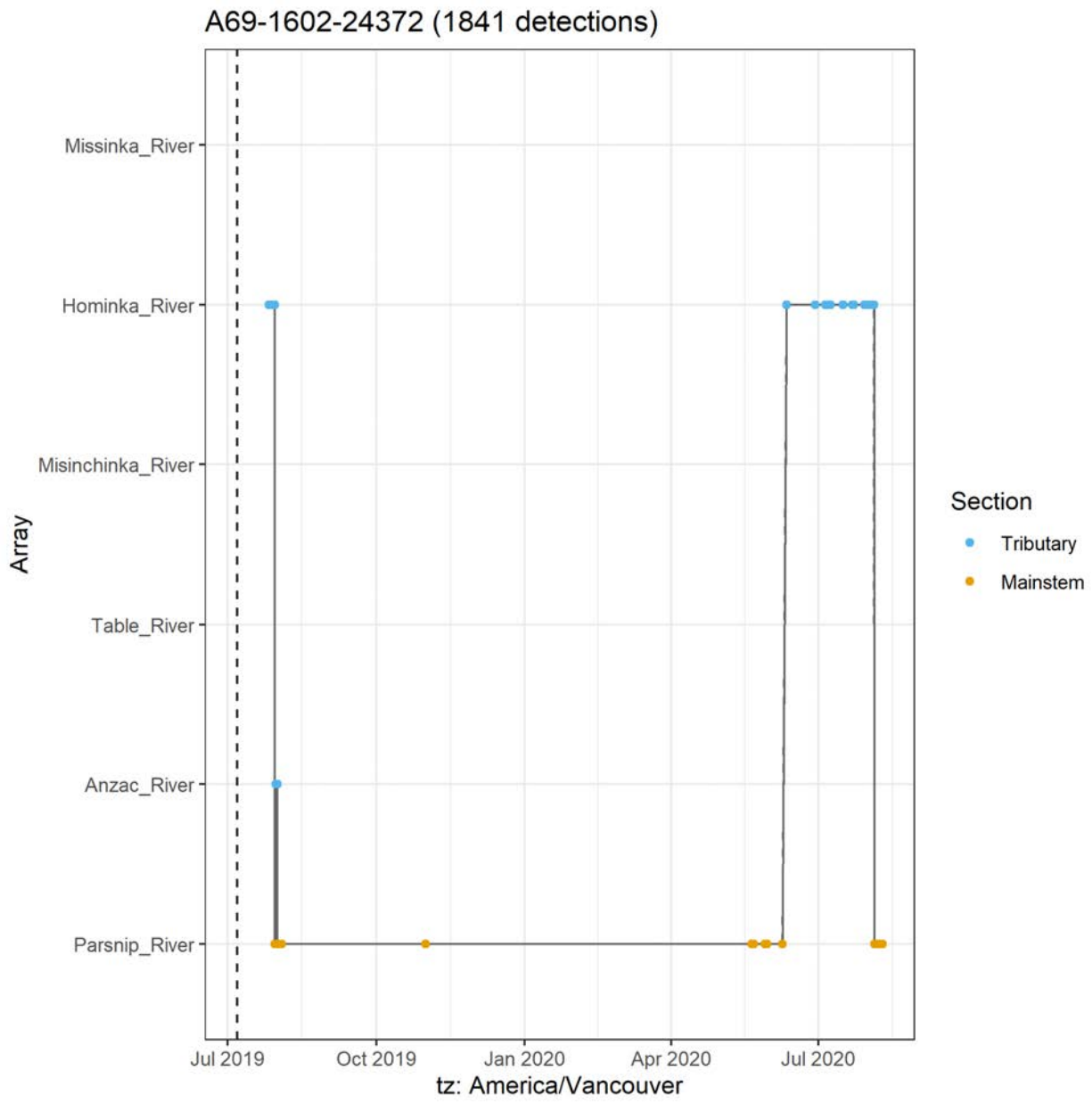
A69-1602-24372 (1841 detections)
Missinka_River
Hominka_River
Misinchinka_River
Table_River
Anzac_River
Parsnip_River
Array
Jul 2019
Oct 2019
Jan 2020
Apr 2020
Jul 2020
tz: America/Vancouver
Section
Tributary
Mainstem

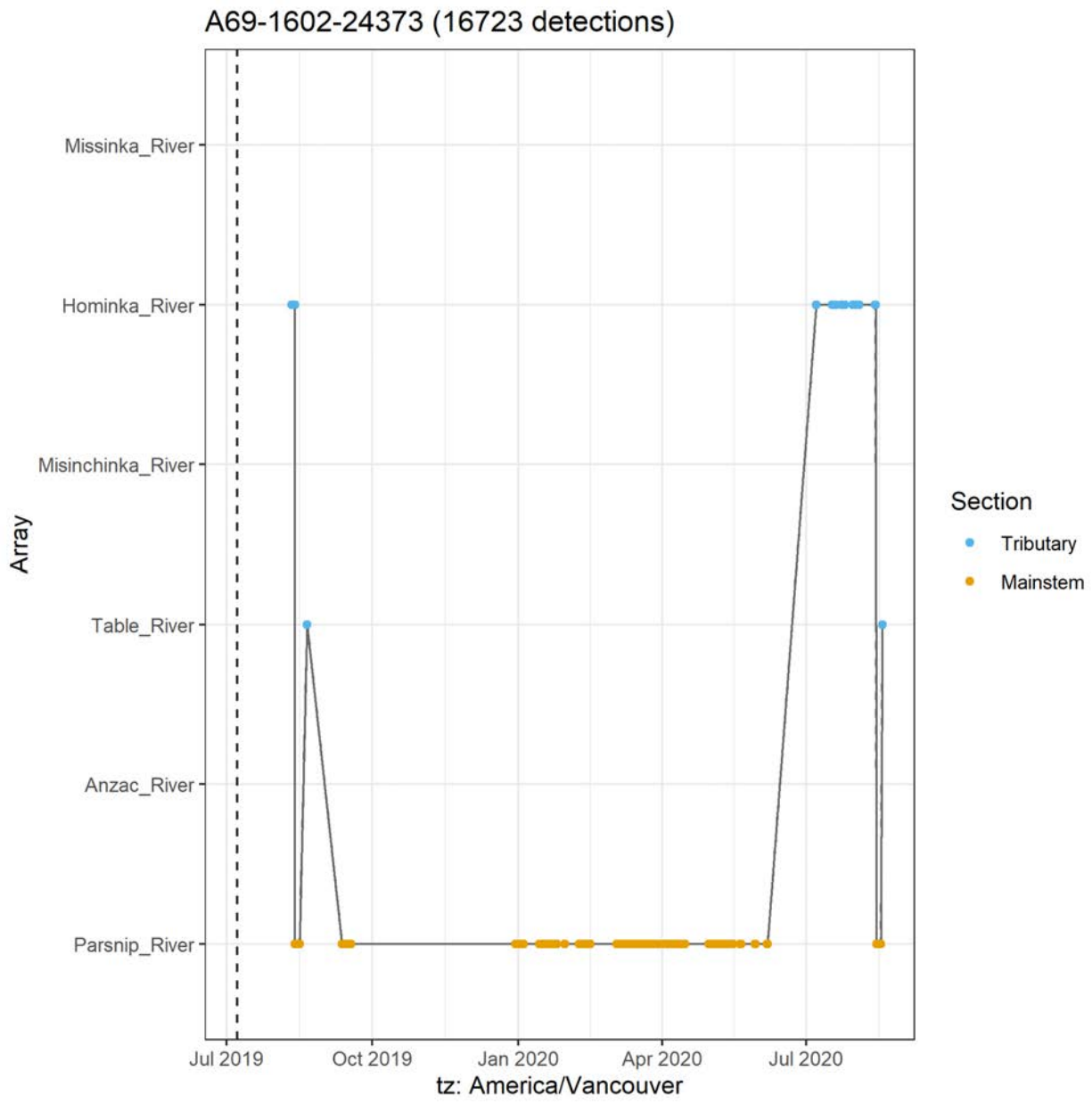
A69-1602-24373 (16723 detections)
Missinka_River
Hominka_River
Misinchinka_River
Table_River
Anzac_River
Parsnip_River
Array
Jul 2019
Oct 2019
Jan 2020
Apr 2020
Jul 2020
tz: America/Vancouver
Section
Tributary
Mainstem

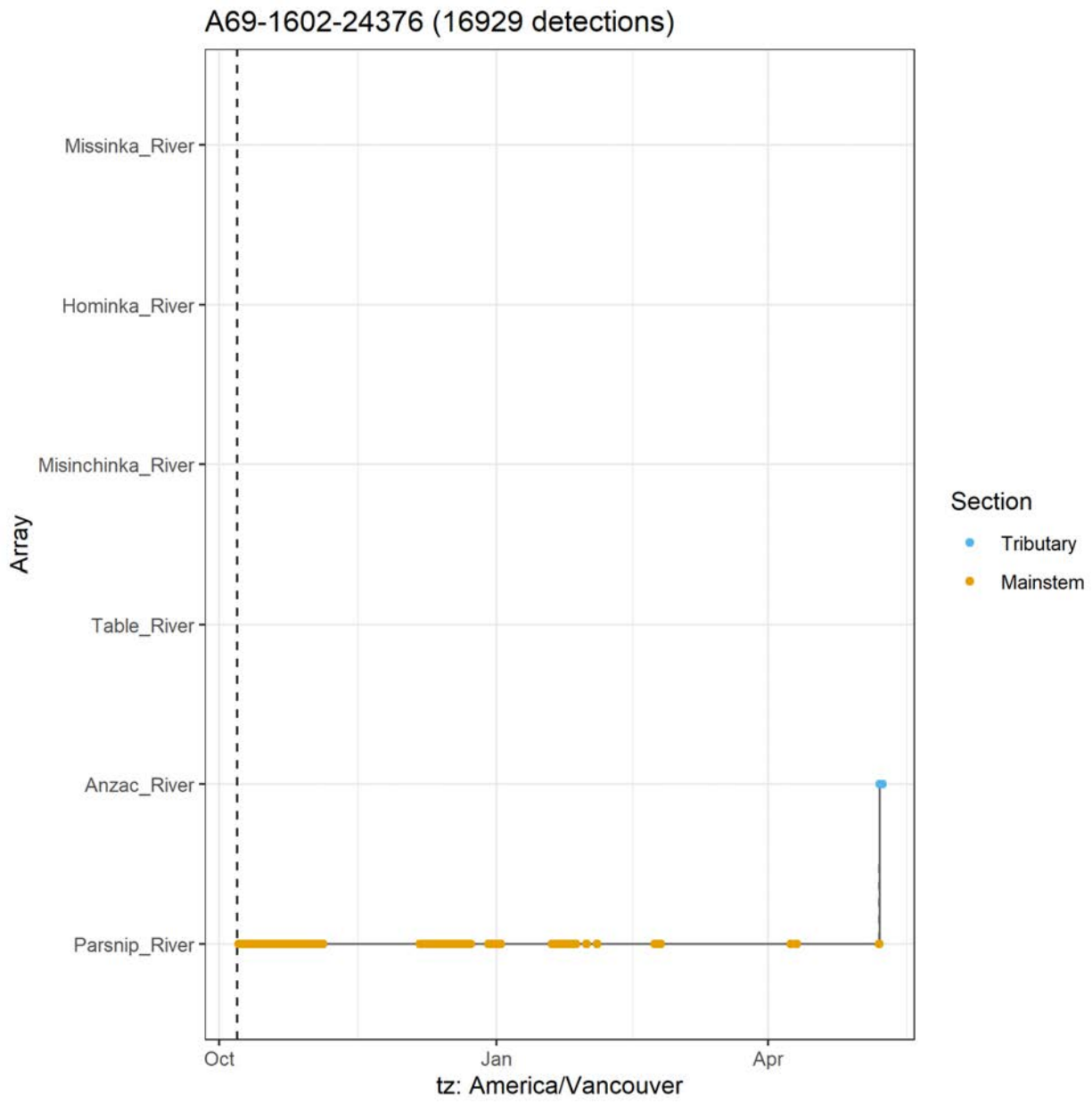
A69-1602-24376 (16929 detections)
Missinka_River
Hominka_River
Misinchinka_River
Table_River
Anzac_River
Parsnip_River
Array
Oct
Jan
Apr
tz: America/Vancouver
Section
Tributary
Mainstem

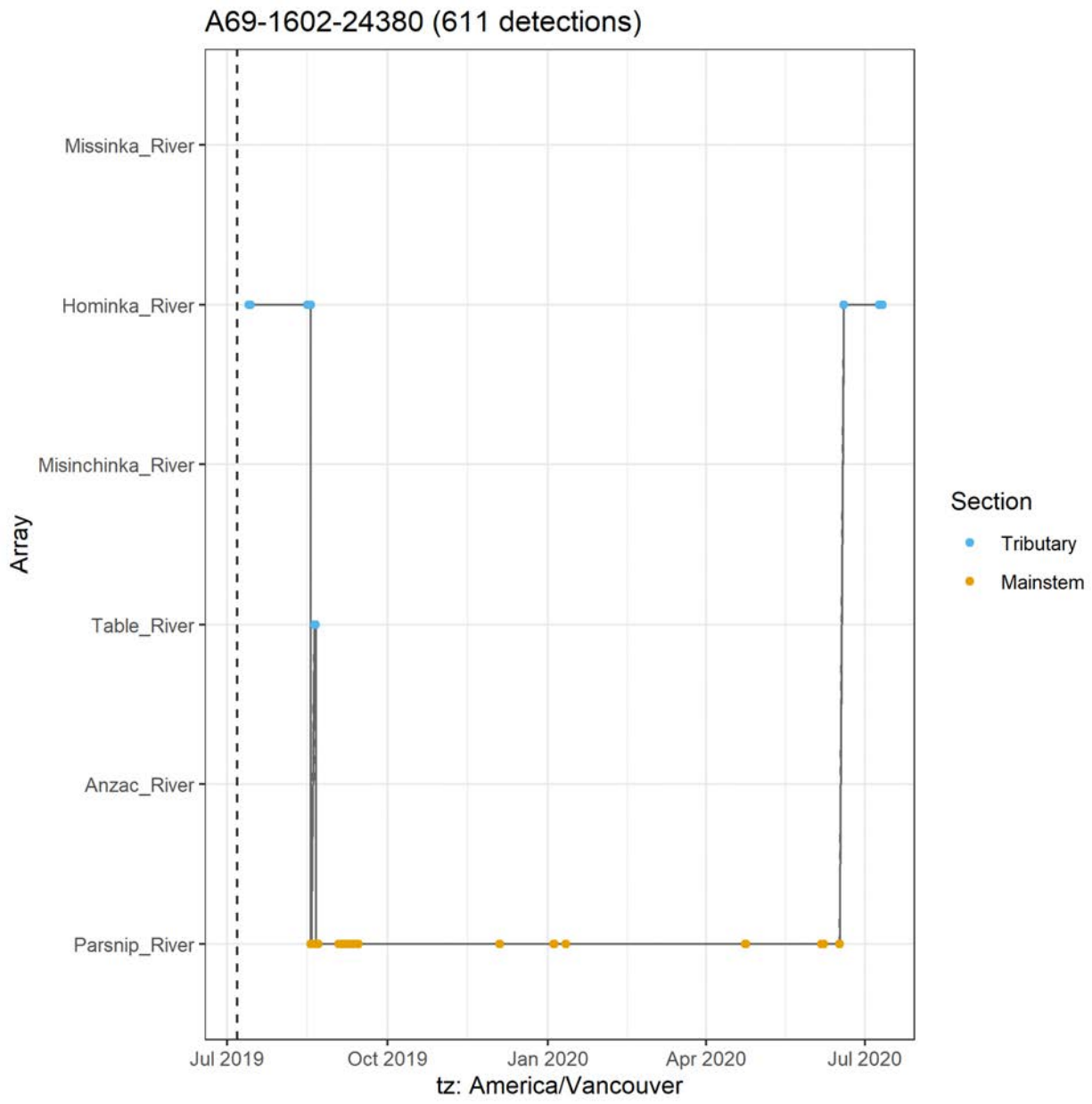
A69-1602-24380 (611 detections)
Missinka_River
Hominka_River
Misinchinka_River
Table_River
Anzac_River
Parsnip_River
Array
Jul 2019
Oct 2019
Jan 2020
Apr 2020
Jul 2020
tz: America/Vancouver
Section
Tributary
Mainstem

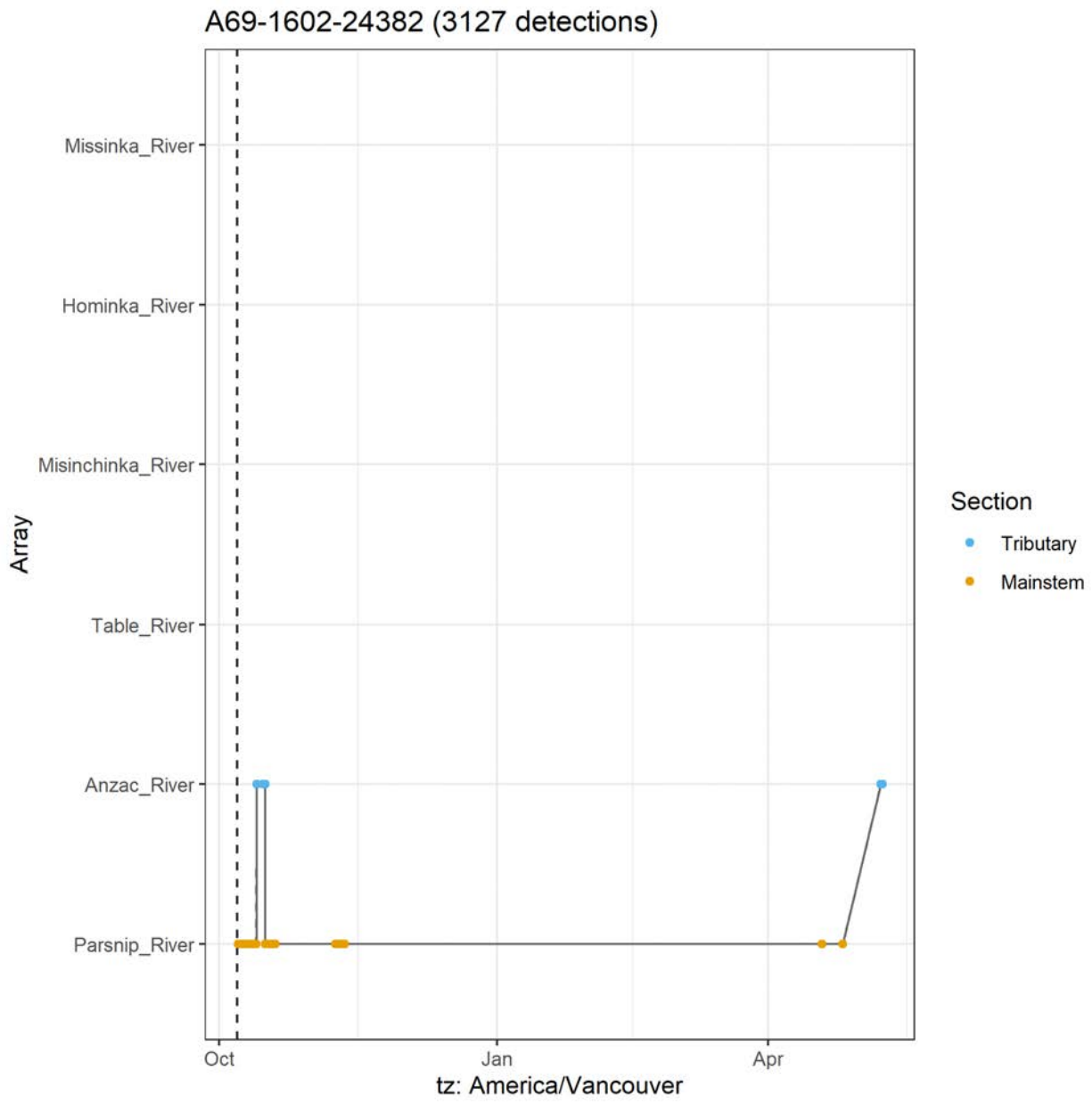
A69-1602-24382 (3127 detections)
Missinka_River
Hominka_River
Misinchinka_River
Table_River
Anzac_River
Parsnip_River
Array
Oct
Jan
Apr
tz: America/Vancouver
Section
Tributary
Mainstem

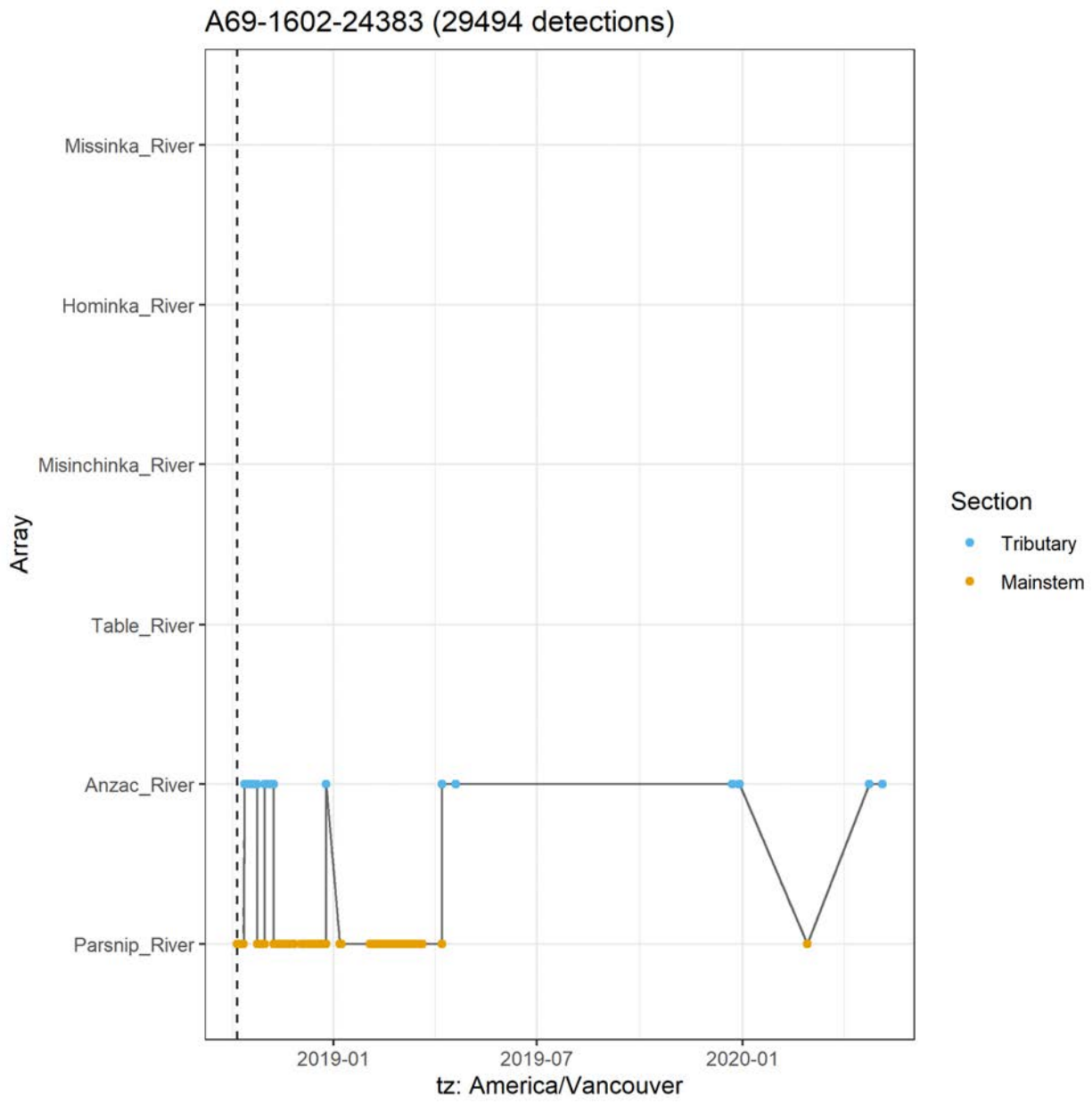
A69-1602-24383 (29494 detections)
Missinka_River
Hominka_River
Misinchinka_River
Table_River
Anzac_River
Parsnip_River
Array
2019-01
2019-07
2020-01
tz: America/Vancouver
Section
Tributary
Mainstem

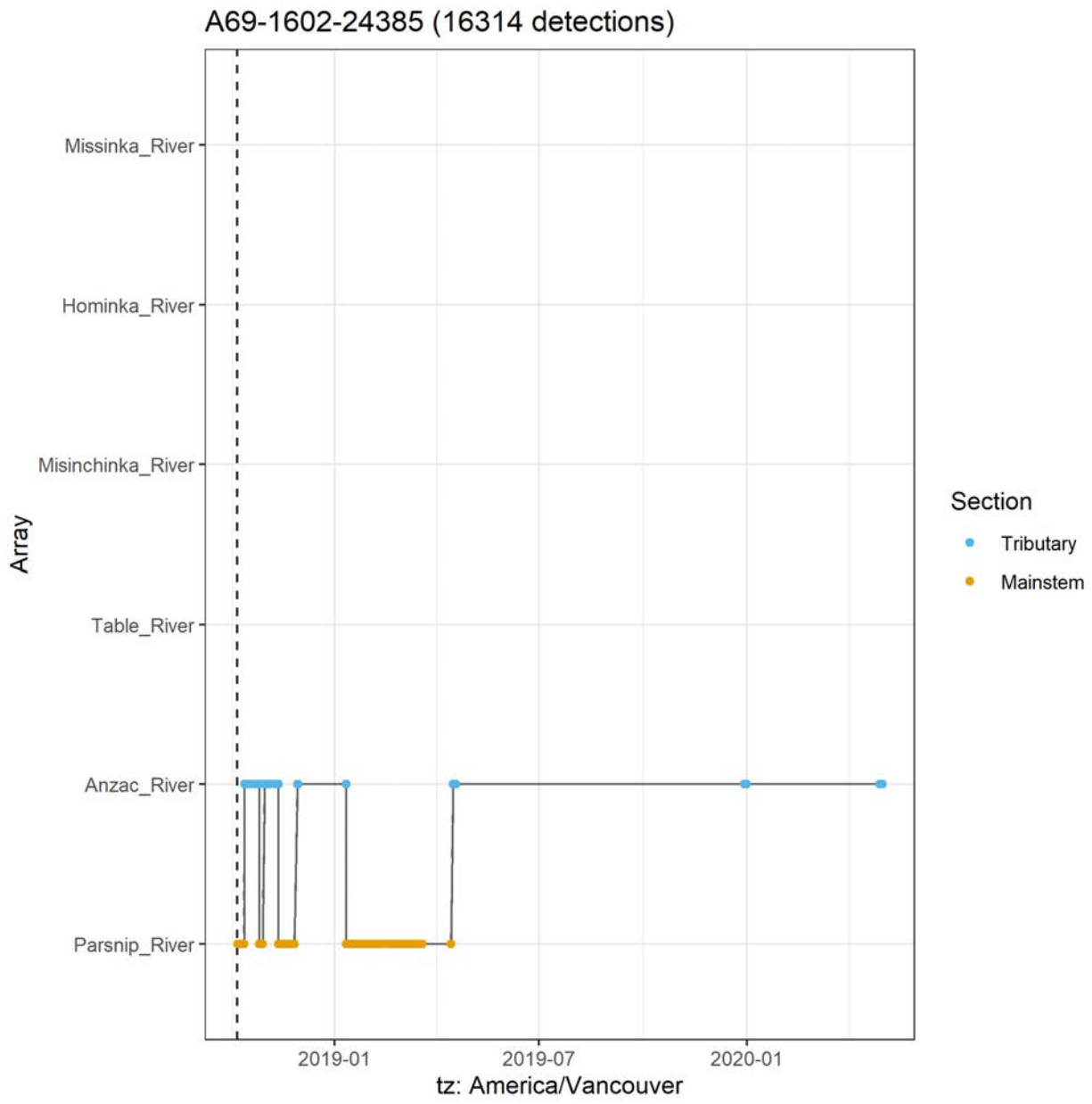
A69-1602-24385 (16314 detections)
Missinka_River
Hominka_River
Misinchinka_River
Table_River
Anzac_River
Parsnip_River
Array
2019-01
2019-07
2020-01
tz: America/Vancouver
Section
Tributary
Mainstem

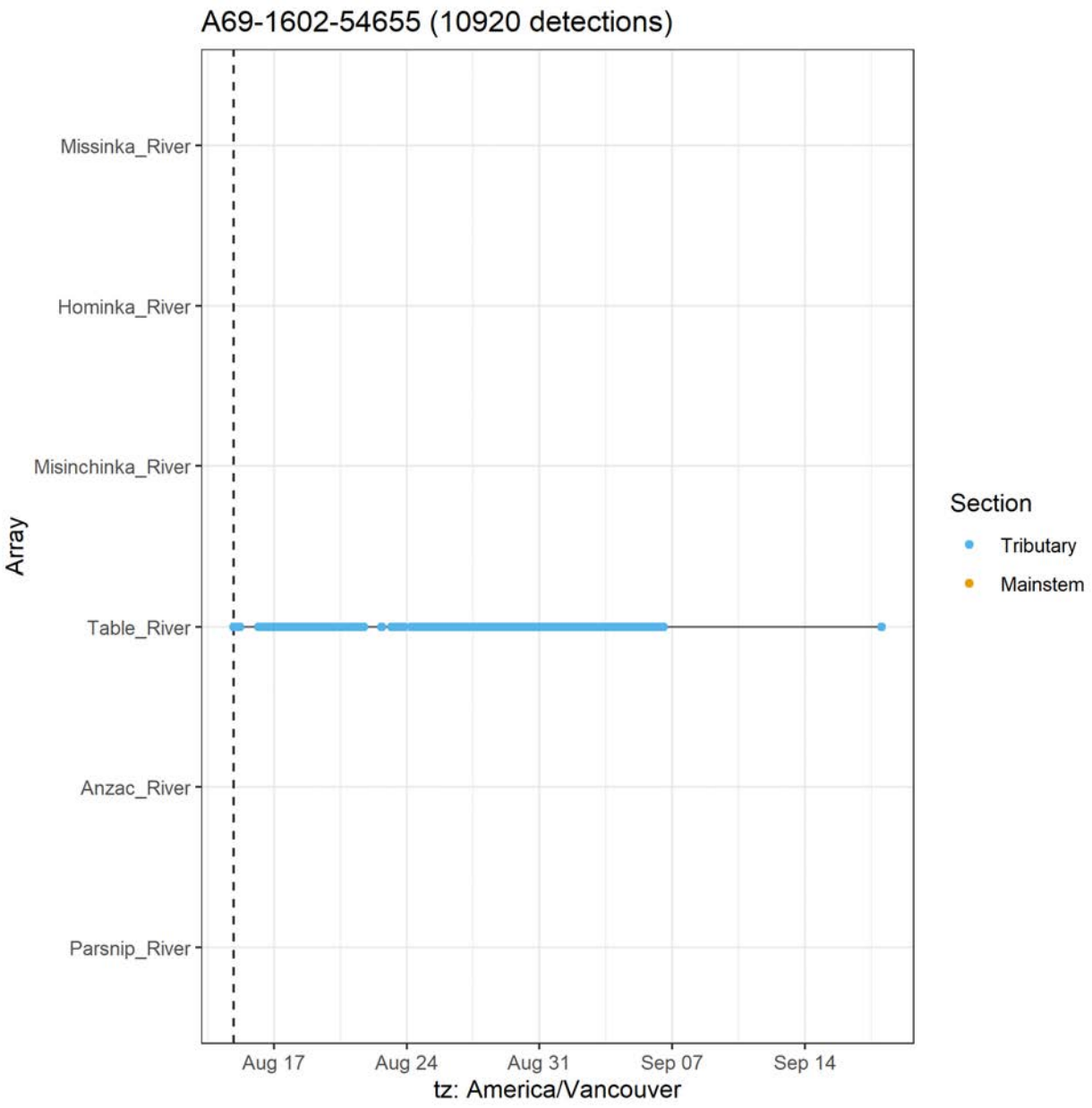
A69-1602-54655 (10920 detections)
Missinka_River
Hominka_River
Misinchinka_River
Table_River
Anzac_River
Parsnip_River
Array
Aug 17
Aug 24
Aug 31
Sep 07
Sep 14
tz: America/Vancouver
Section
Tributary
Mainstem

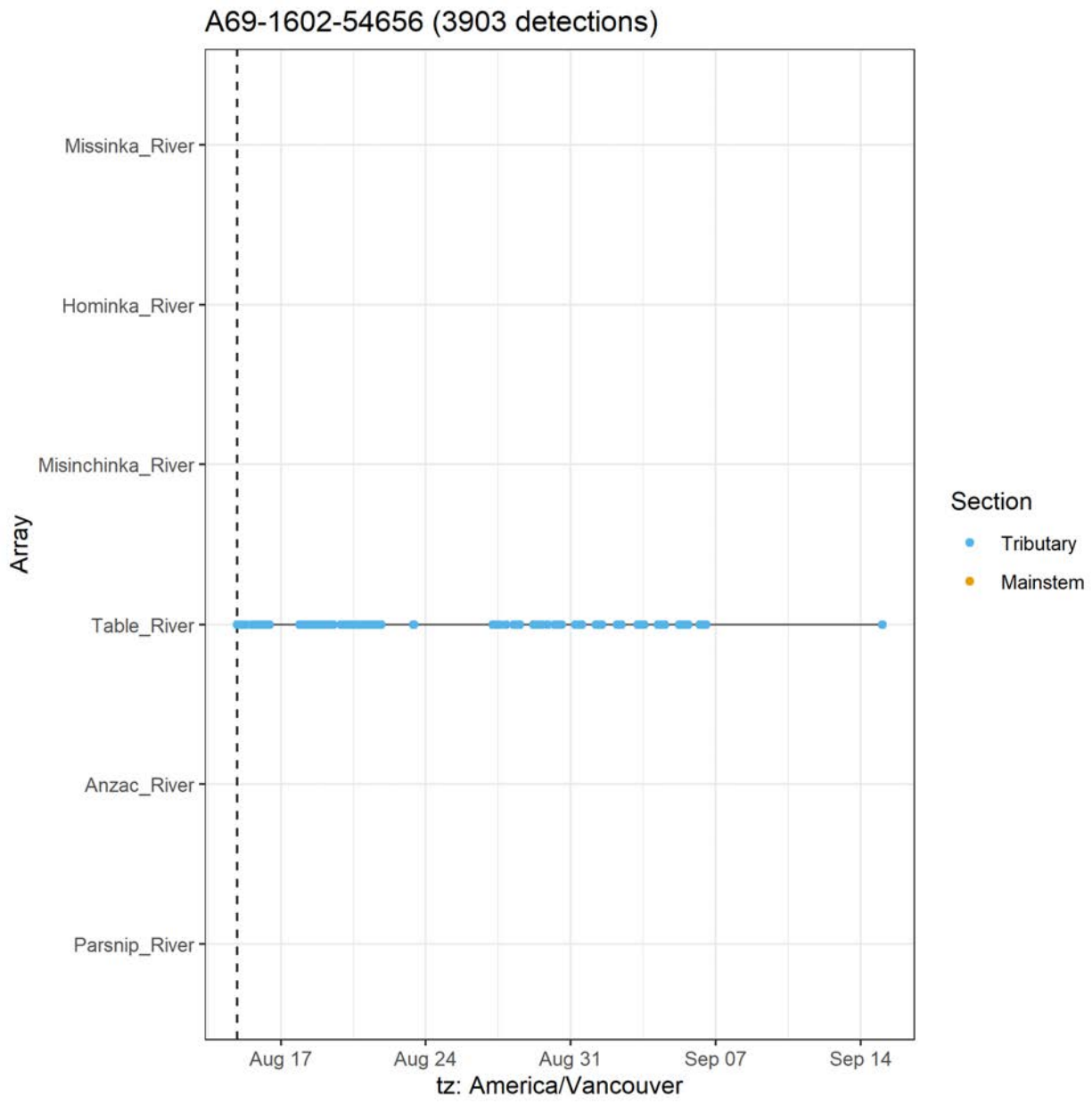
A69-1602-54656 (3903 detections)
Missinka_River
Hominka_River
Misinchinka_River
Table_River
Anzac_River
Parsnip_River
Array
Aug 17
Aug 24
Aug 31
Sep 07
Sep 14
tz: America/Vancouver
Section
Tributary
Mainstem

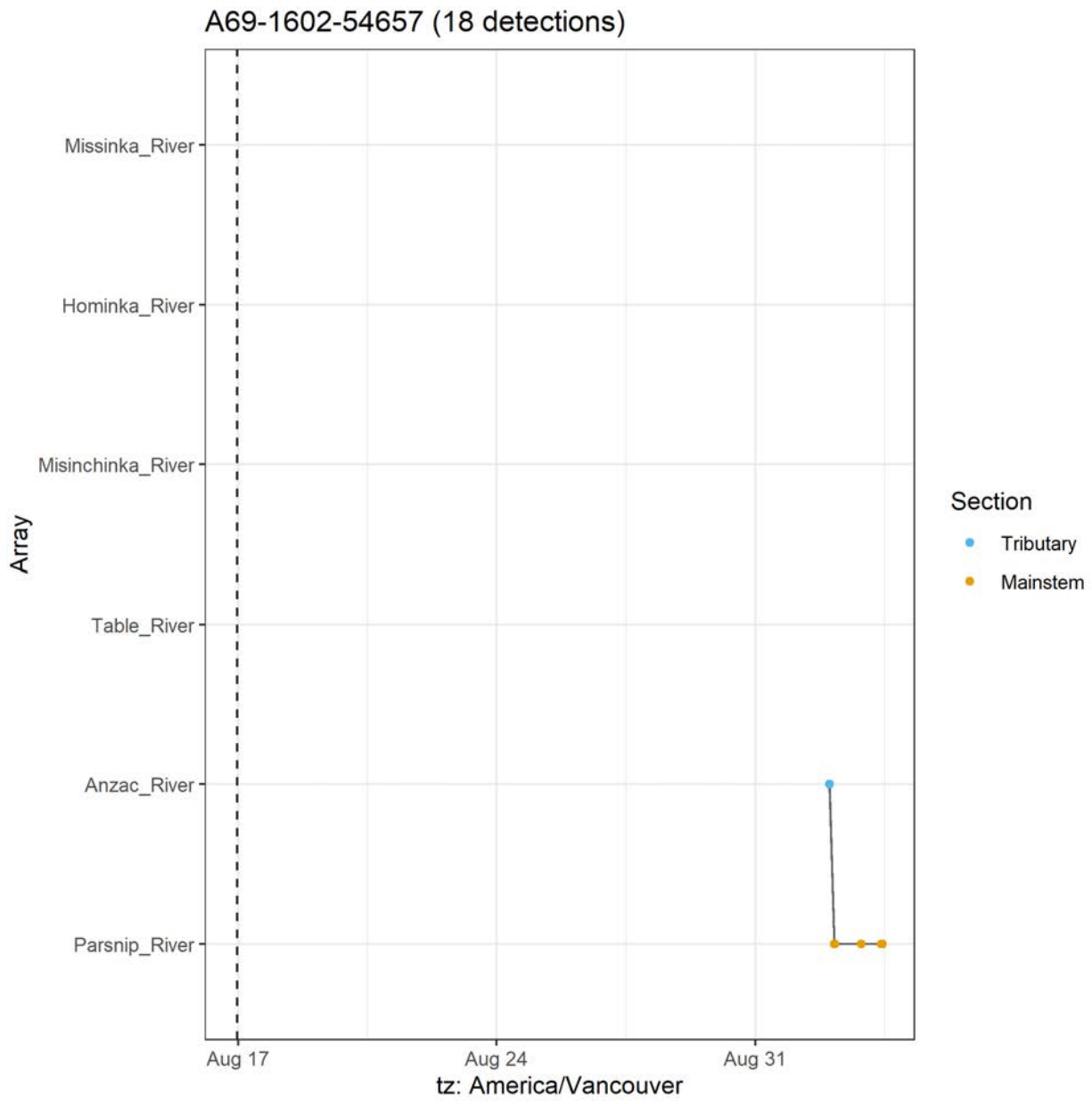
A69-1602-54657 (18 detections)
Missinka_River
Hominka_River
Misinchinka_River
Table_River
Anzac_River
Parsnip_River
Array
Aug 17
Aug 24
Aug 31
tz: America/Vancouver
Section
Tributary
Mainstem

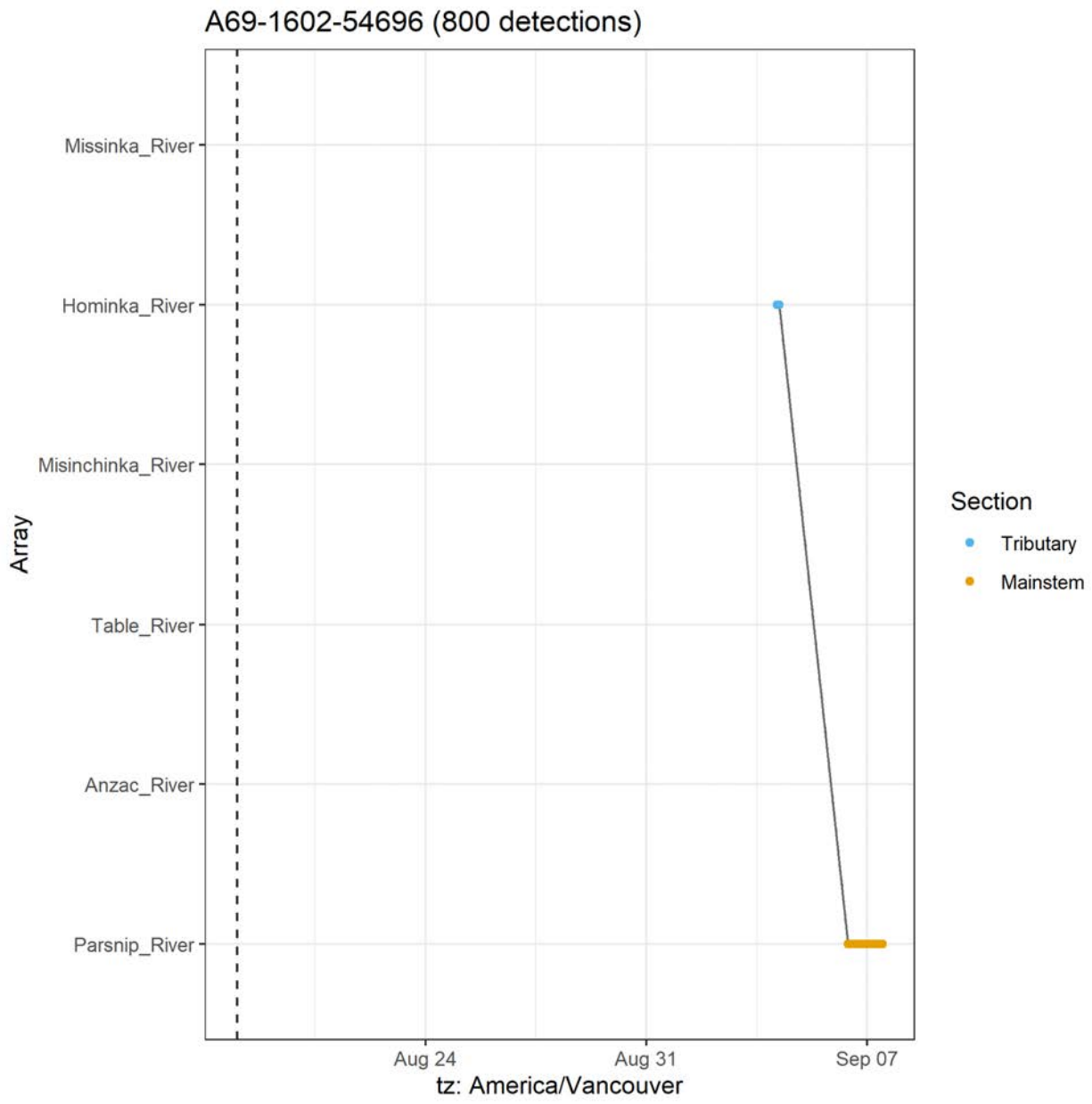
A69-1602-54696 (800 detections)
Missinka_River
Hominka_River
Misinchinka_River
Table_River
Anzac_River
Parsnip_River
Array
Aug 24
Aug 31
Sep 07
tz: America/Vancouver
Section
Tributary
Mainstem

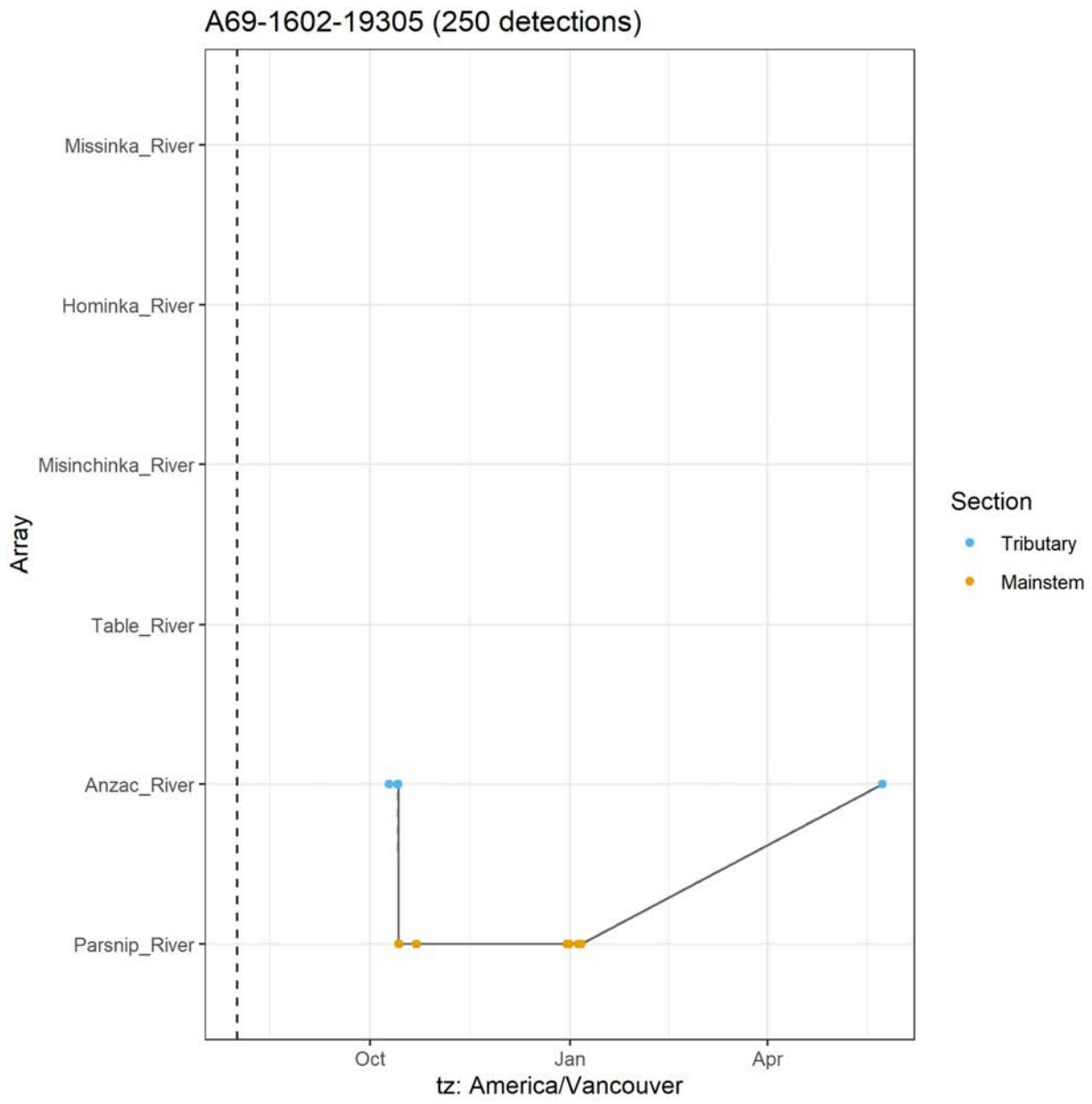
A69-1602-19305 (250 detections)
Missinka_River
Hominka_River
Misinchinka_River
Table_River
Anzac_River
Parsnip_River
Array
Oct
Jan
Apr
tz: America/Vancouver
Section
Tributary
Mainstem

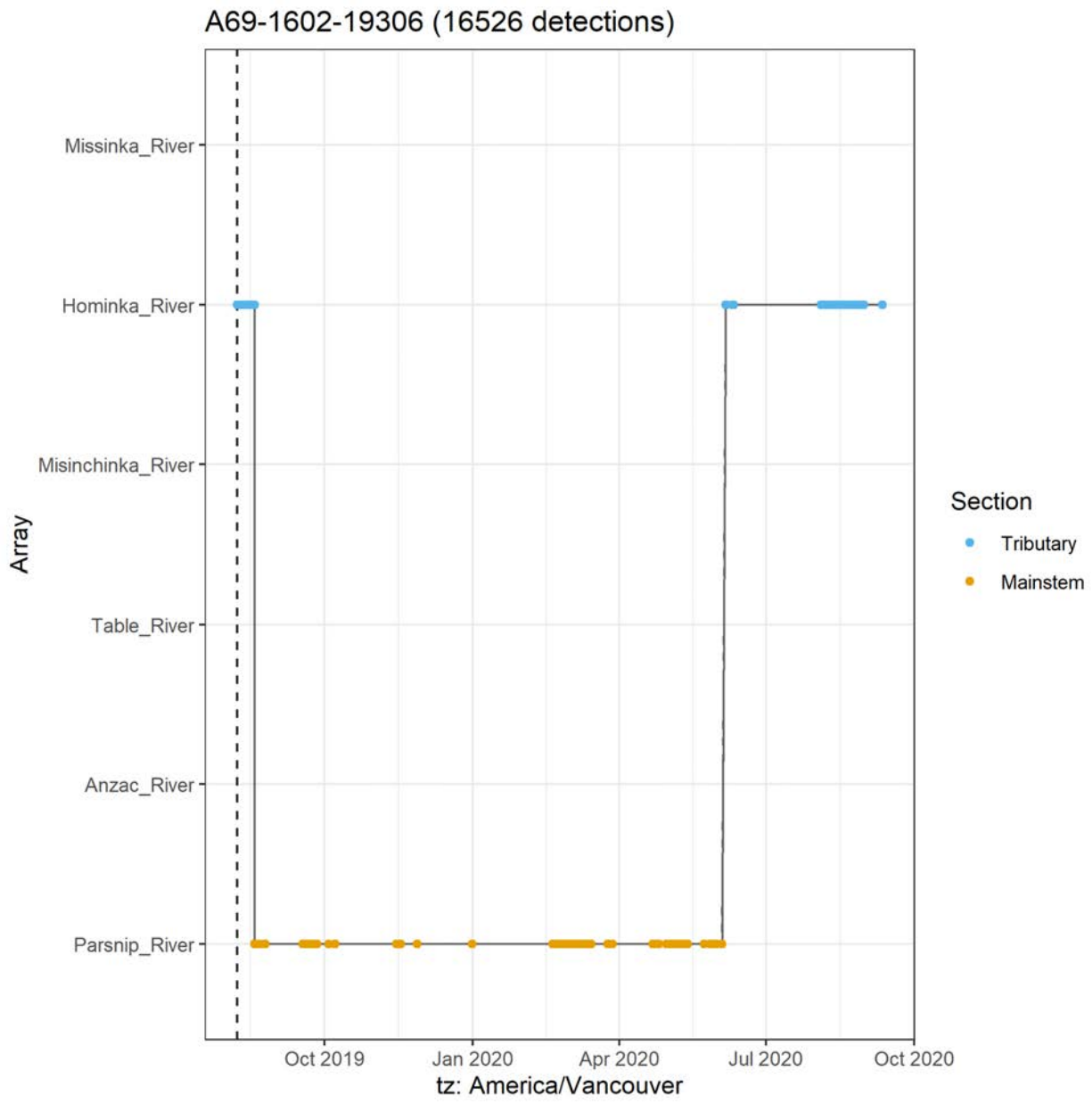
A69-1602-19306 (16526 detections)
Missinka_River
Hominka_River
Misinchinka_River
Table_River
Anzac_River
Parsnip_River
Array
Oct 2019
Jan 2020
Apr 2020
Jul 2020
Oct 2020
tz: America/Vancouver
Section
Tributary
Mainstem

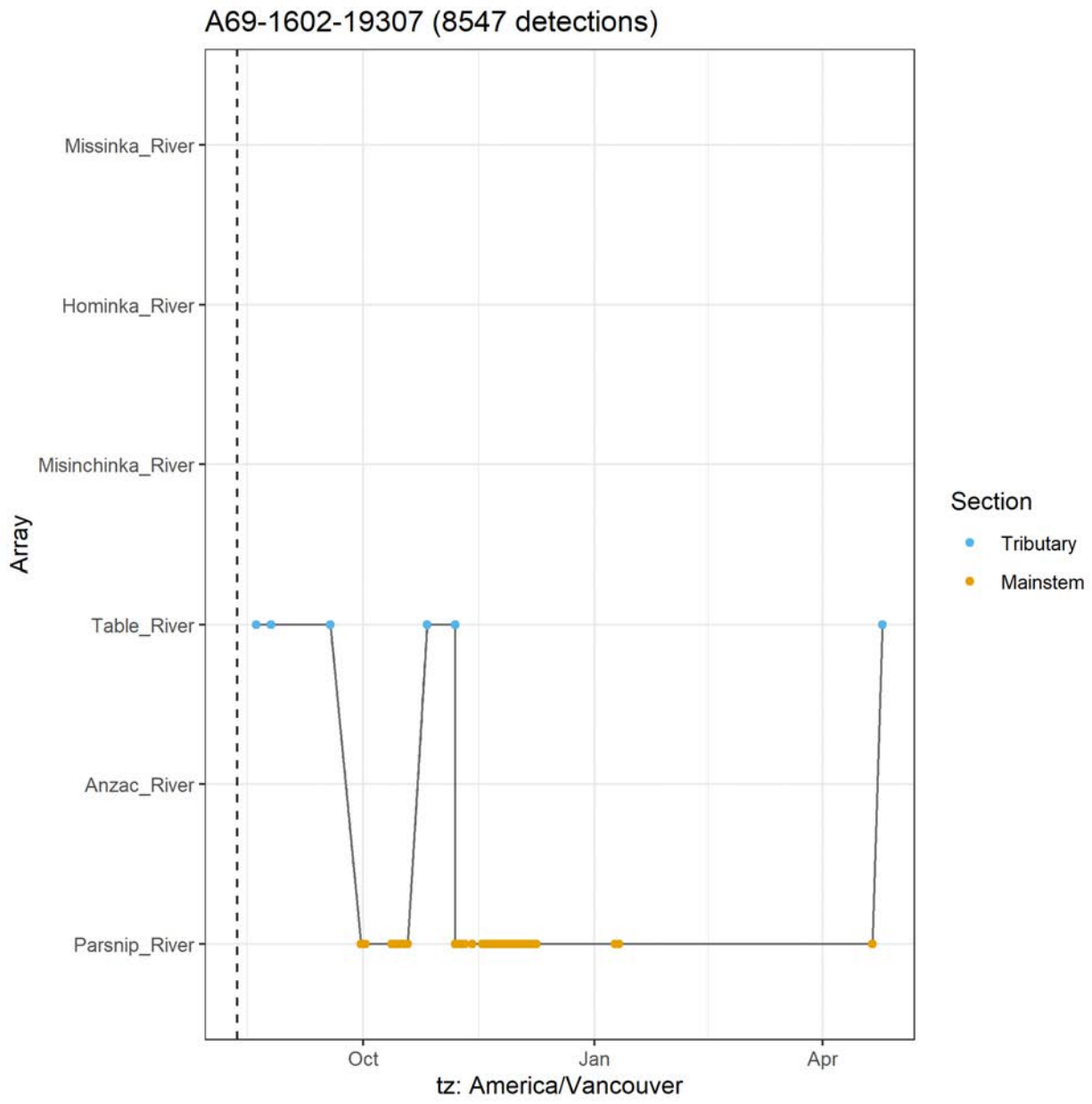
A69-1602-19307 (8547 detections)
Missinka_River
Hominka_River
Misinchinka_River
Table_River
Anzac_River
Parsnip_River
Array
Oct
Jan
Apr
tz: America/Vancouver
Section
Tributary
Mainstem

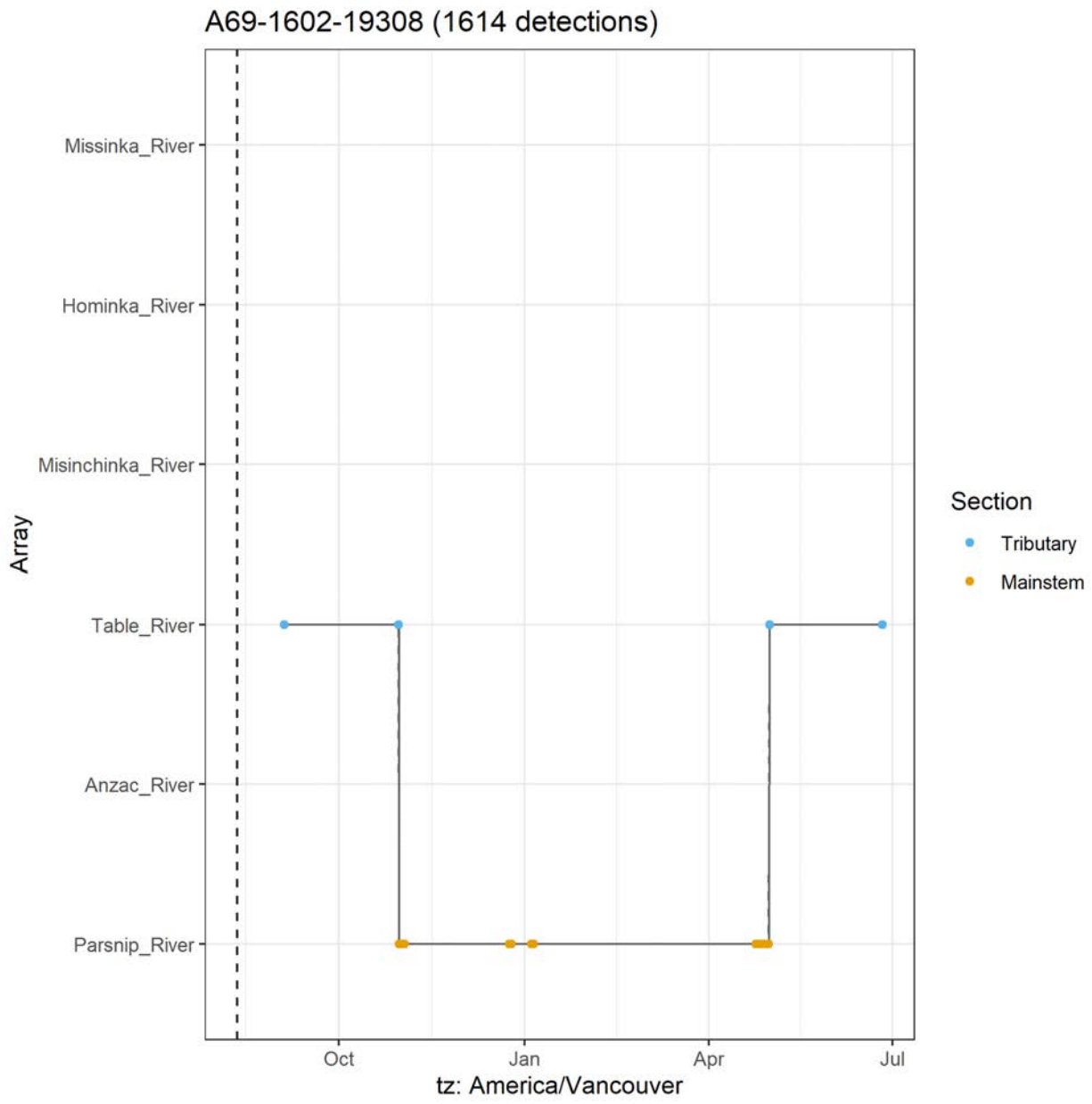
A69-1602-19308 (1614 detections)
Missinka_River
Hominka_River
Misinchinka_River
Table_River
Anzac_River
Parsnip_River
Array
Oct
Jan
Apr
Jul
tz: America/Vancouver
Section
Tributary
Mainstem

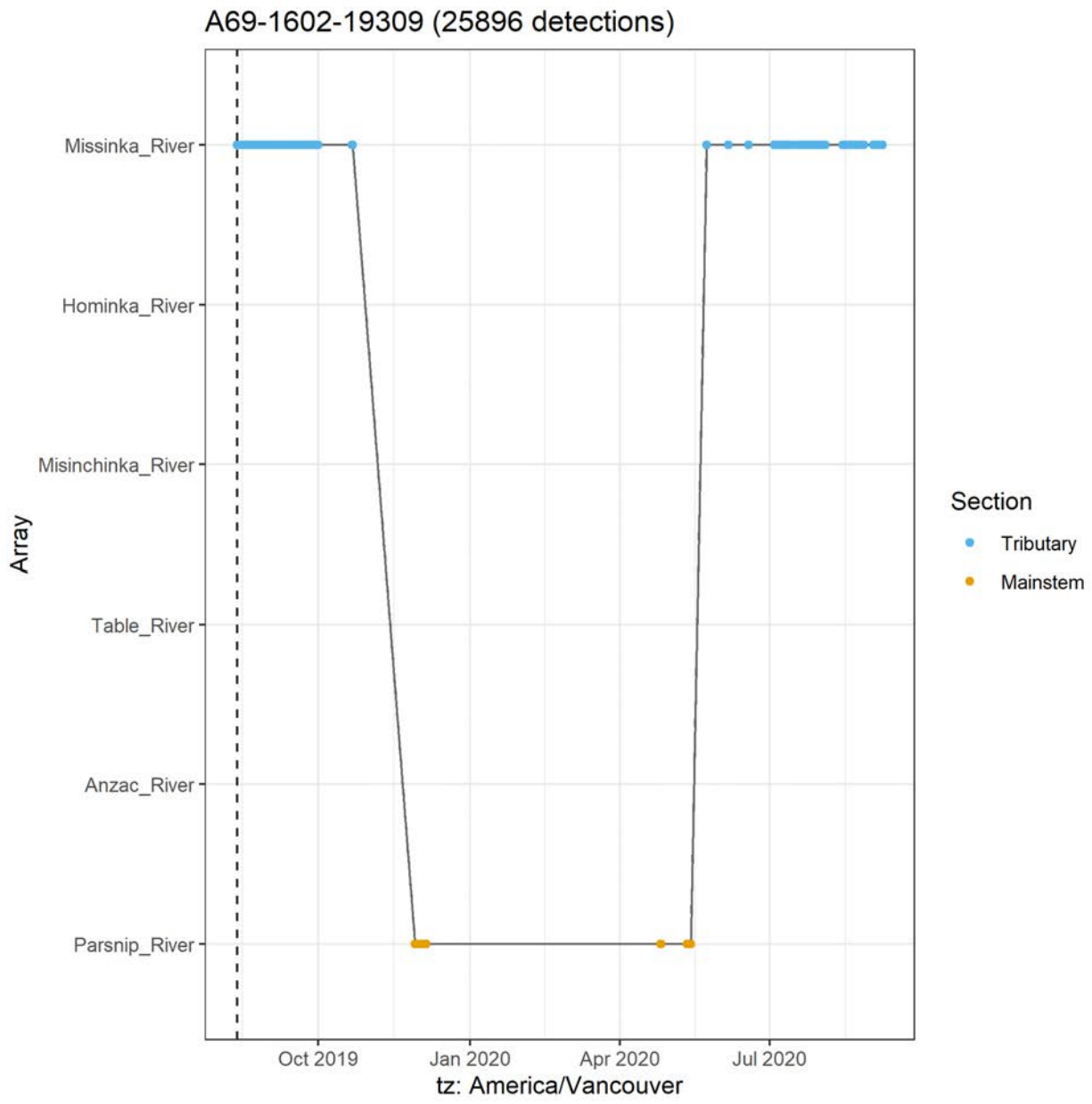
A69-1602-19309 (25896 detections)
Missinka_River
Hominka_River
Misinchinka_River
Table_River
Anzac_River
Parsnip_River
Array
Oct 2019
Jan 2020
Apr 2020
Jul 2020
tz: America/Vancouver
Section
Tributary
Mainstem

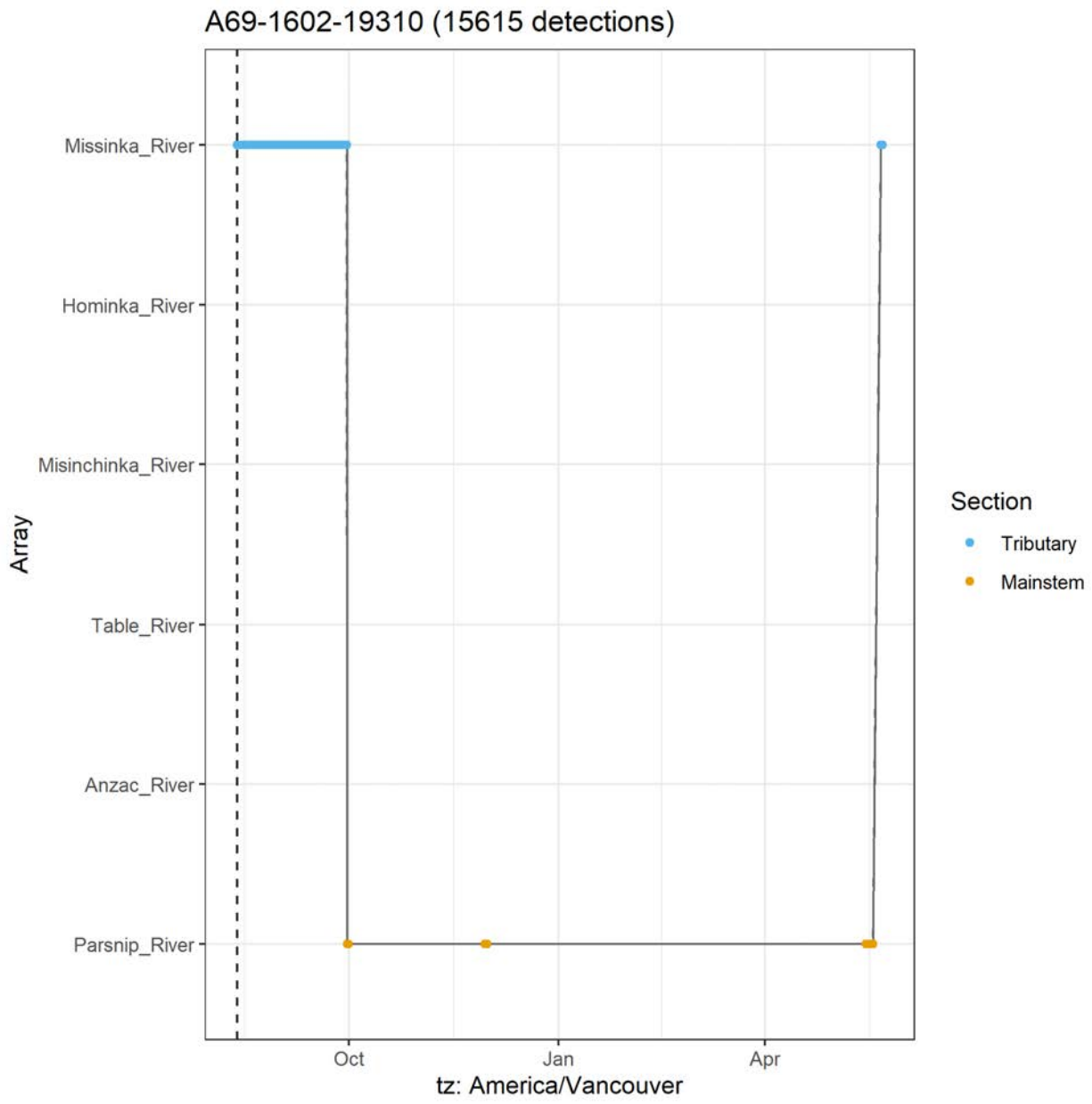
A69-1602-19310 (15615 detections)
Missinka_River
Hominka_River
Misinchinka_River
Table_River
Anzac_River
Parsnip_River
Array
Oct
Jan
Apr
tz: America/Vancouver
Section
Tributary
Mainstem

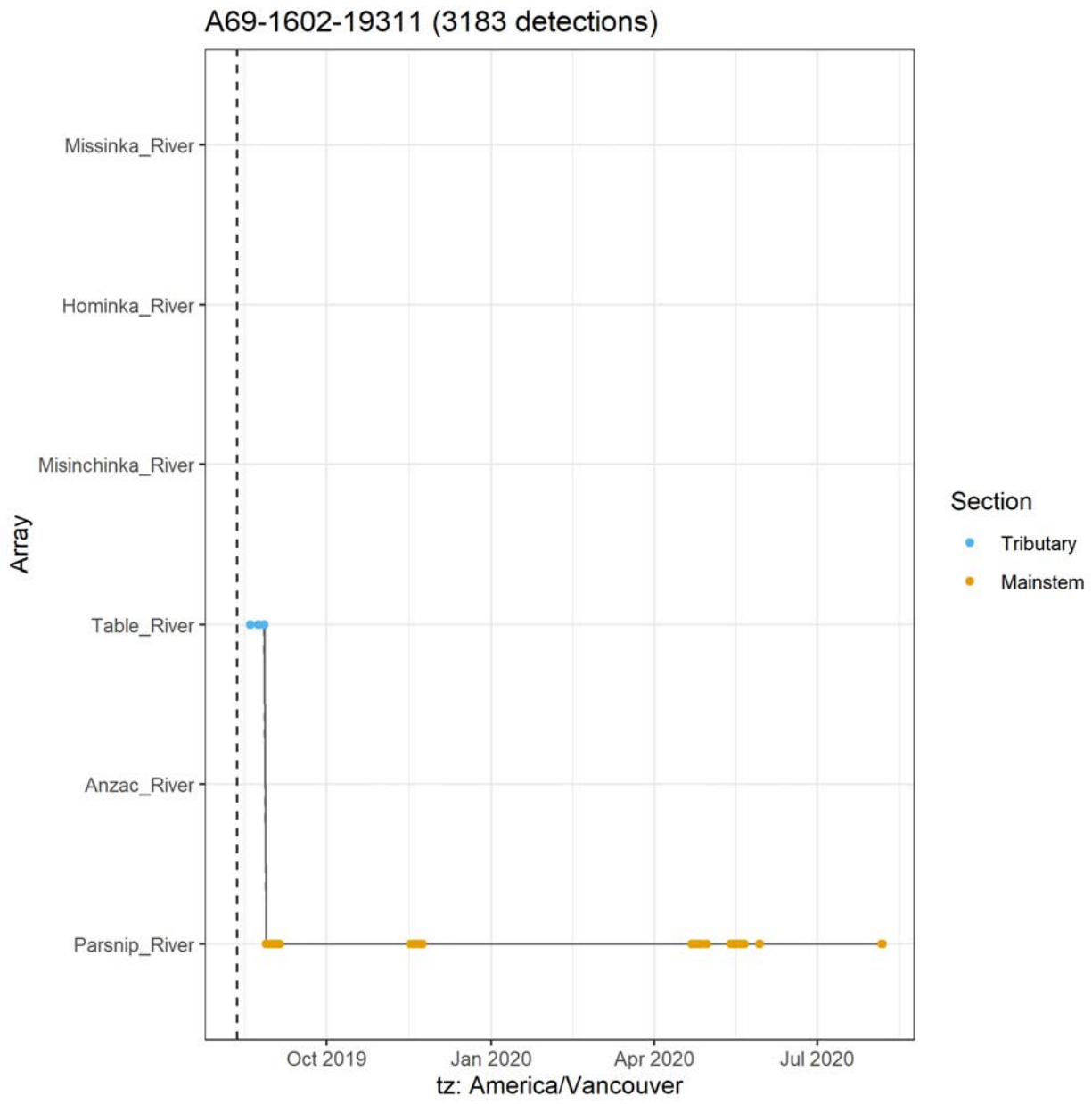
A69-1602-19311 (3183 detections)
Missinka_River
Hominka_River
Misinchinka_River
Table_River
Anzac_River
Parsnip_River
Array
Oct 2019
Jan 2020
Apr 2020
Jul 2020
tz: America/Vancouver
Section
Tributary
Mainstem

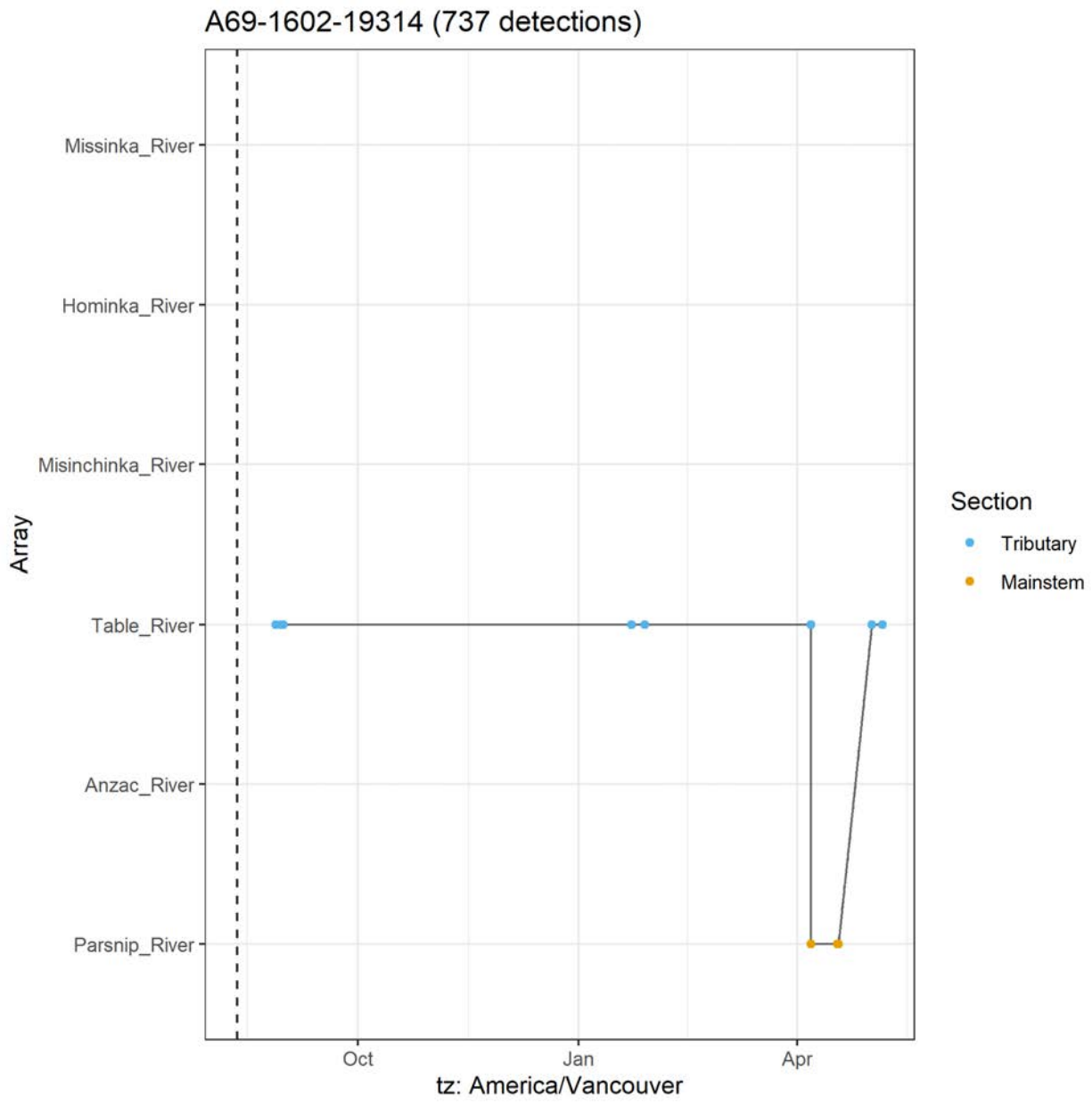
A69-1602-19314 (737 detections)
Missinka_River
Hominka_River
Misinchinka_River
Table_River
Anzac_River
Parsnip_River
Array
Oct
Jan
Apr
tz: America/Vancouver
Section
Tributary
Mainstem

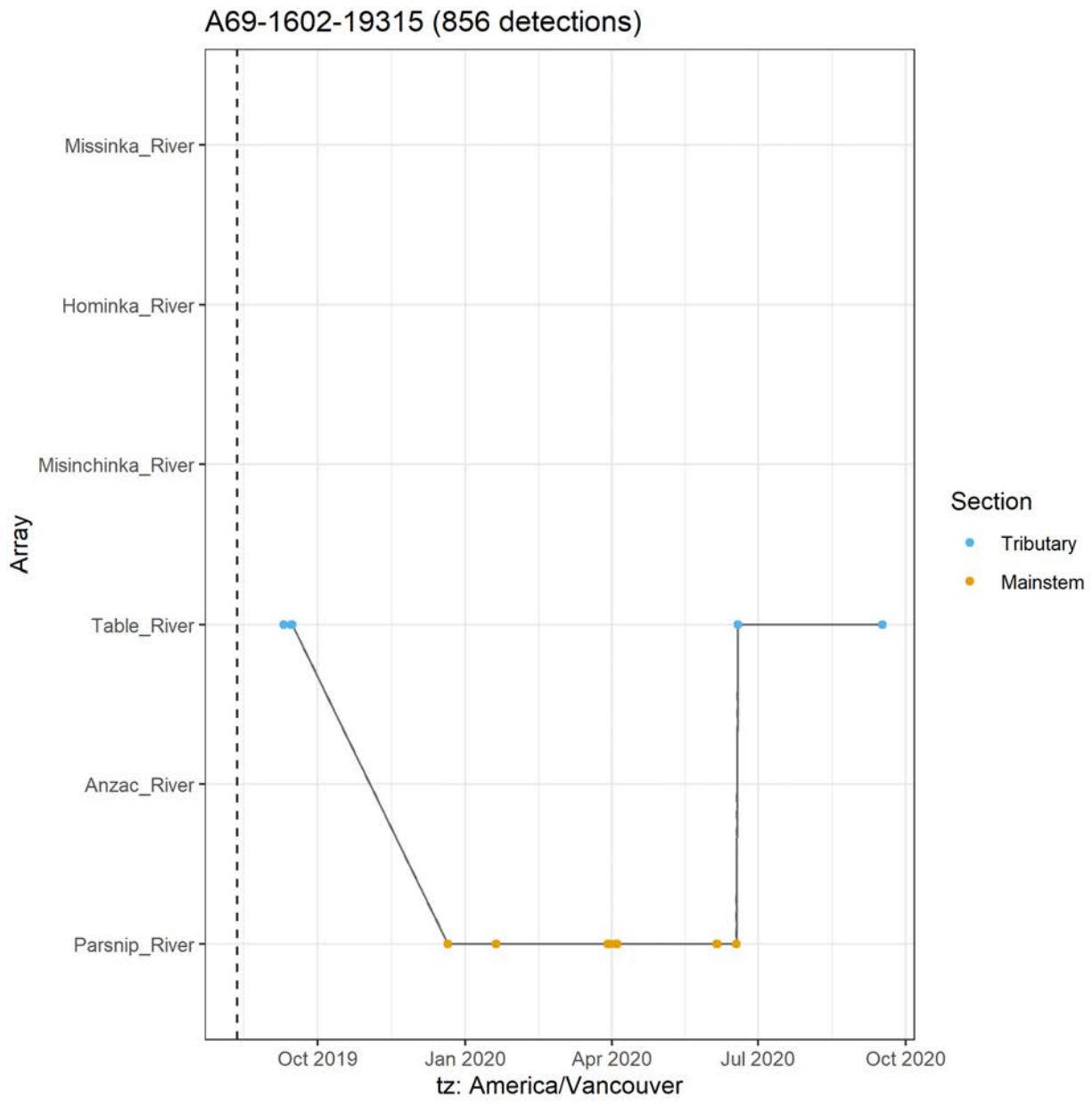
A69-1602-19315 (856 detections)
Missinka_River
Hominka_River
Misinchinka_River
Table_River
Anzac_River
Parsnip_River
Array
Oct 2019
Jan 2020
Apr 2020
Jul 2020
Oct 2020
tz: America/Vancouver
Section
Tributary
Mainstem

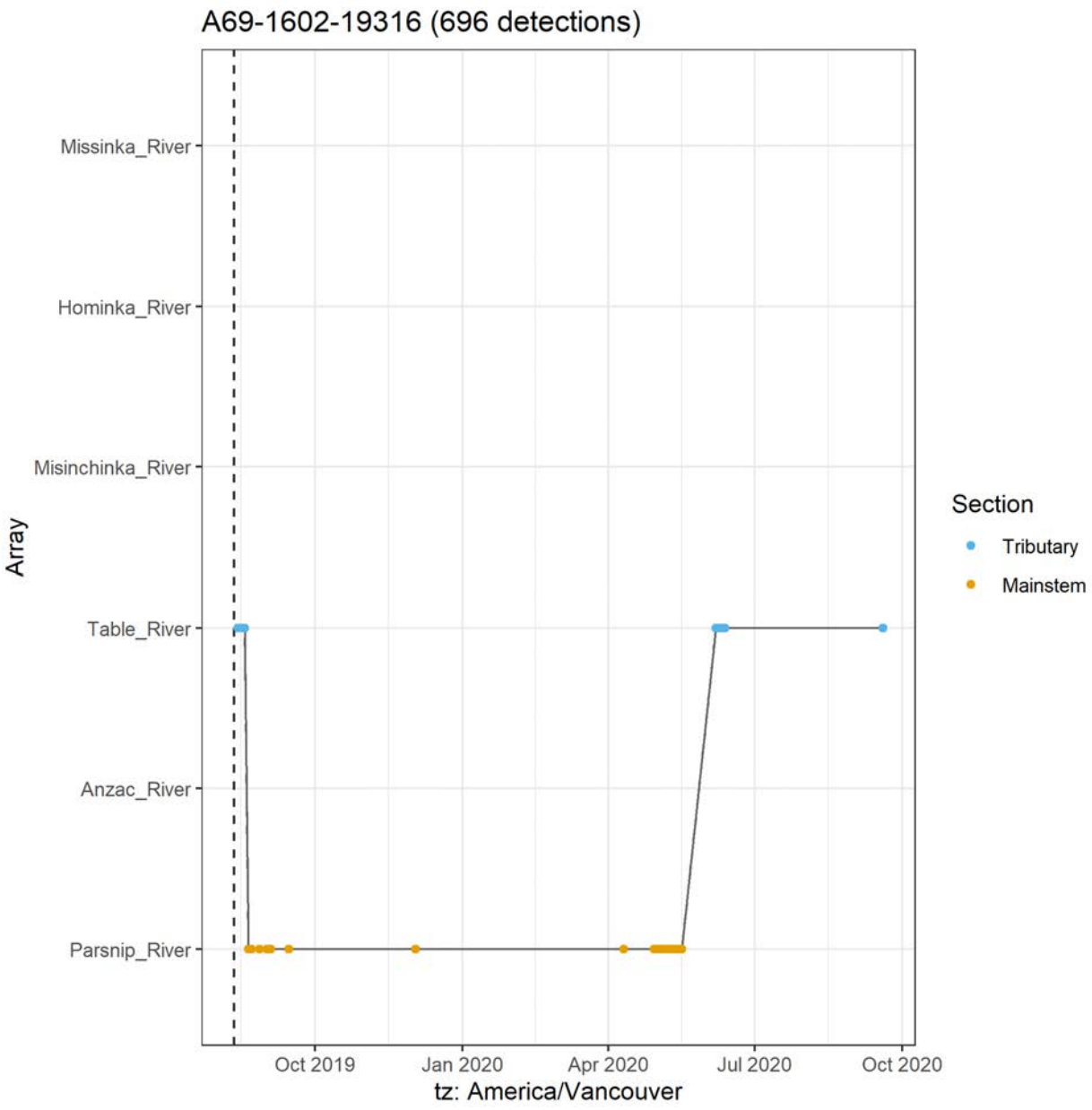
A69-1602-19316 (696 detections)
Missinka_River
Hominka_River
Misinchinka_River
Table_River
Anzac_River
Parsnip_River
Array
Oct 2019
Jan 2020
Apr 2020
Jul 2020
Oct 2020
tz: America/Vancouver
Section
Tributary
Mainstem

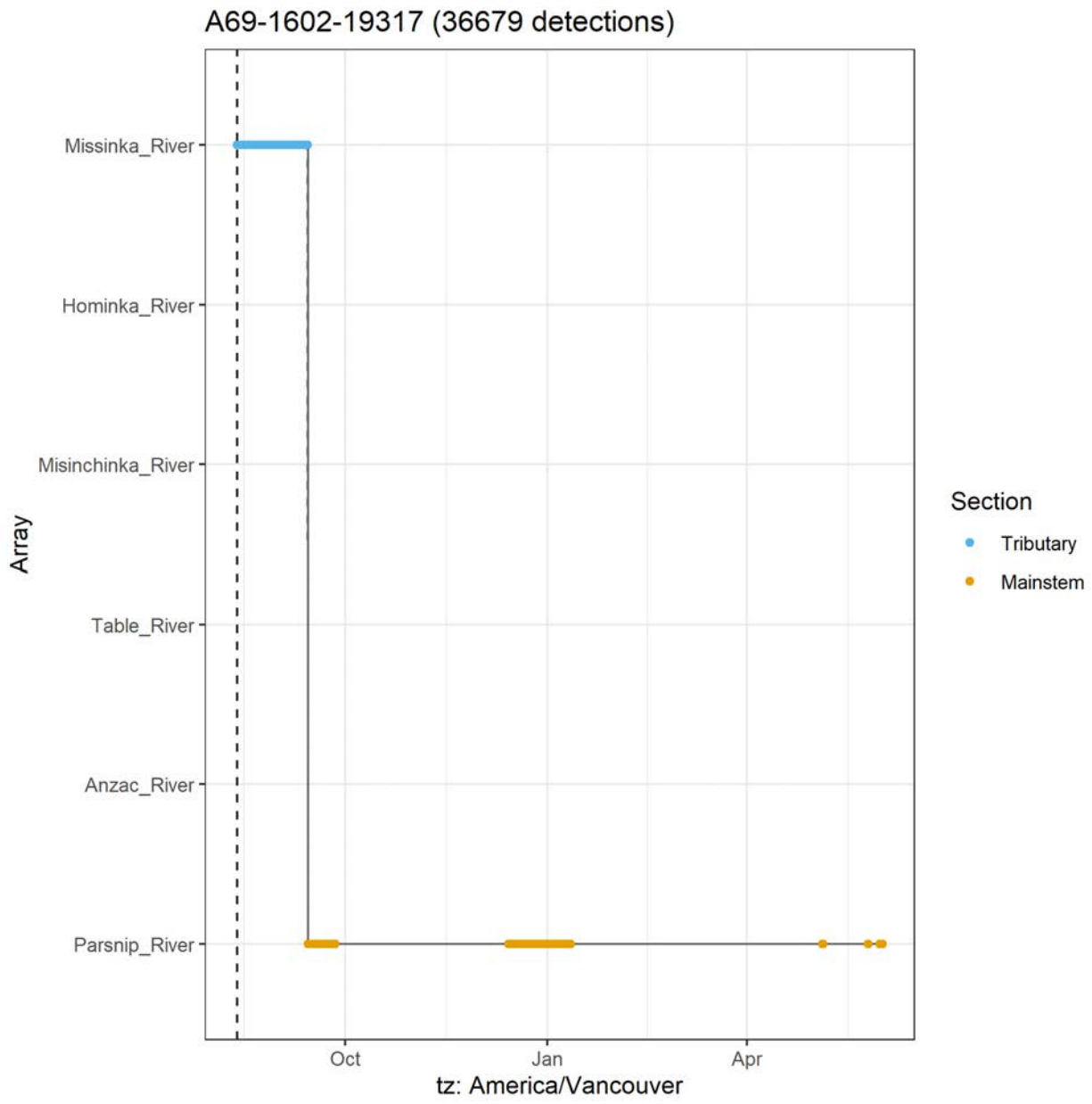
A69-1602-19317 (36679 detections)
Missinka_River
Hominka_River
Misinchinka_River
Table_River
Anzac_River
Parsnip_River
Array
Oct
Jan
Apr
tz: America/Vancouver
Section
Tributary
Mainstem

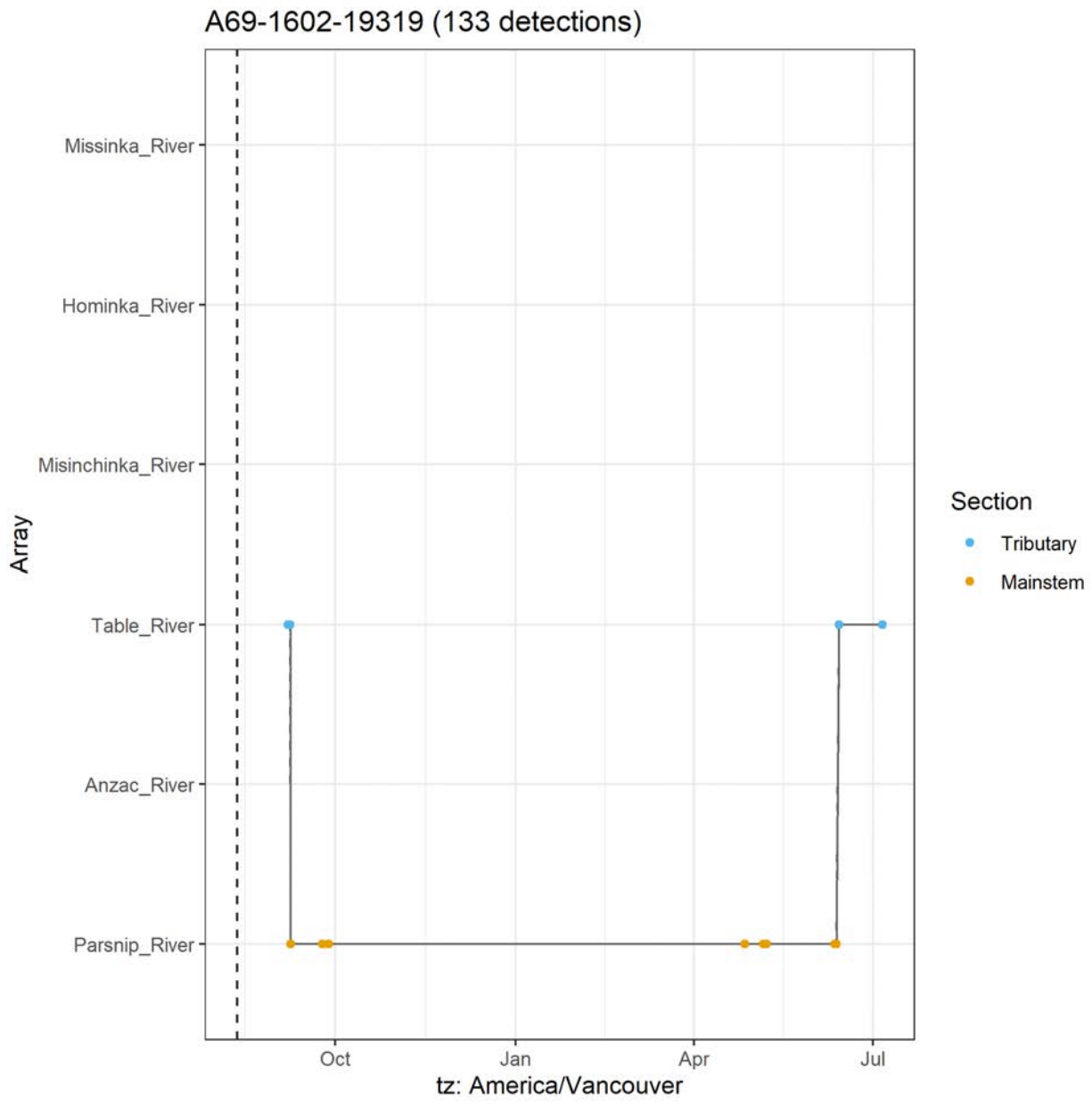
A69-1602-19319 (133 detections)
Missinka_River
Hominka_River
Misinchinka_River
Table_River
Anzac_River
Parsnip_River
Array
Oct
Jan
Apr
Jul
tz: America/Vancouver
Section
Tributary
Mainstem

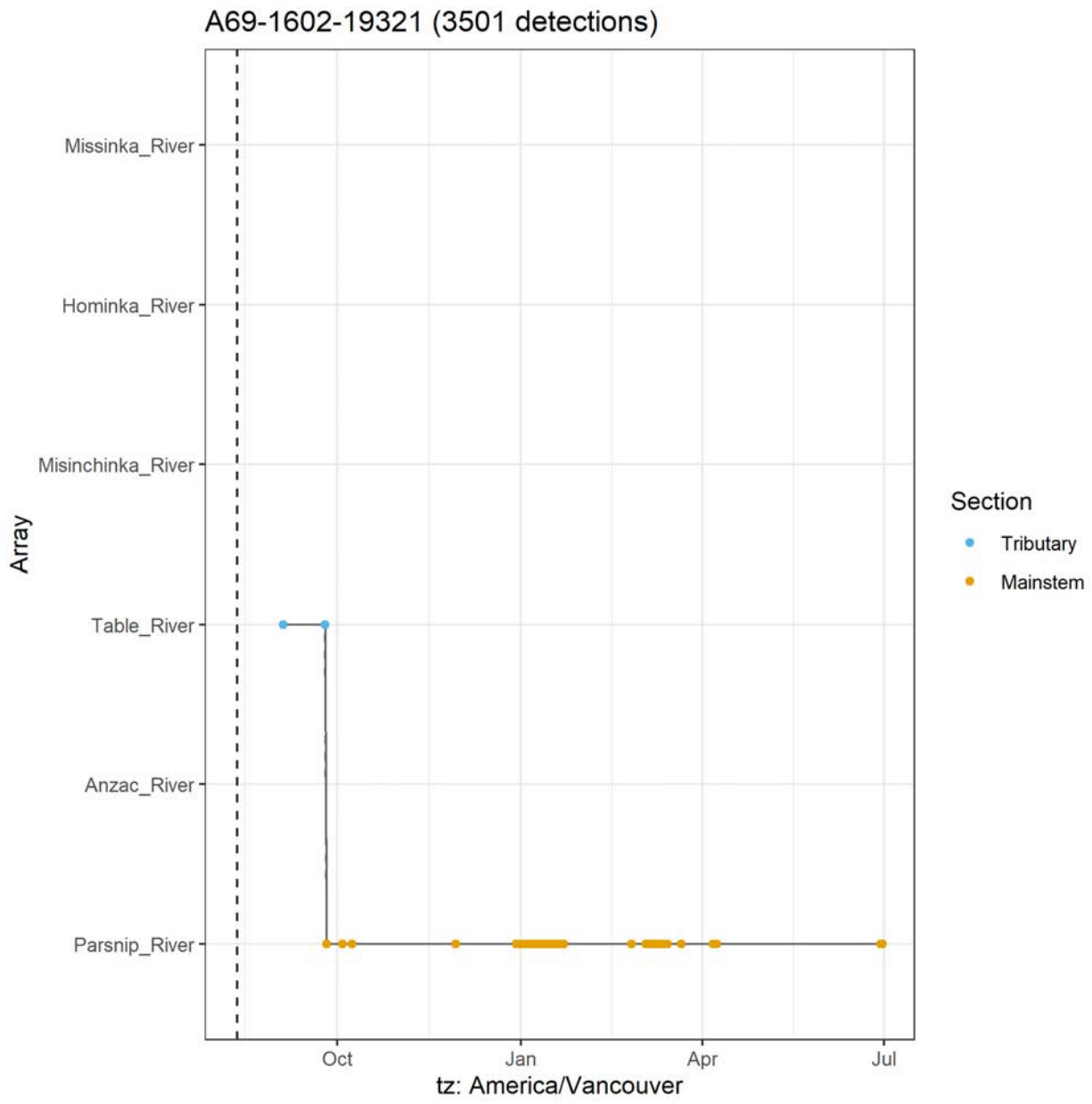
A69-1602-19321 (3501 detections)
Missinka_River
Hominka_River
Misinchinka_River
Table_River
Anzac_River
Parsnip_River
Array
Oct
Jan
Apr
Jul
tz: America/Vancouver
Section
Tributary
Mainstem

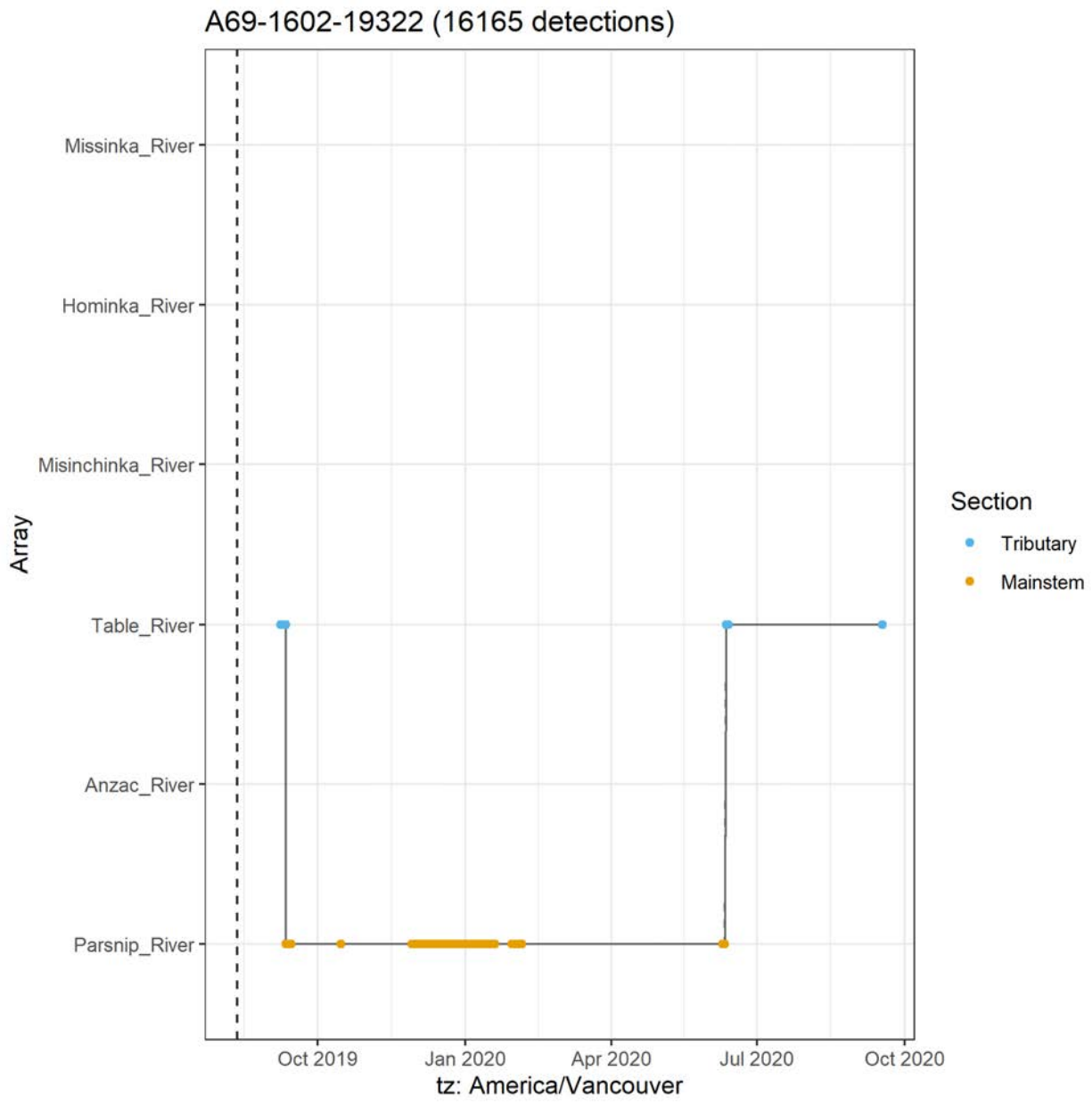
A69-1602-19322 (16165 detections)
Missinka_River
Hominka_River
Misinchinka_River
Table_River
Anzac_River
Parsnip_River
Array
Oct 2019
Jan 2020
Apr 2020
Jul 2020
Oct 2020
tz: America/Vancouver
Section
Tributary
Mainstem

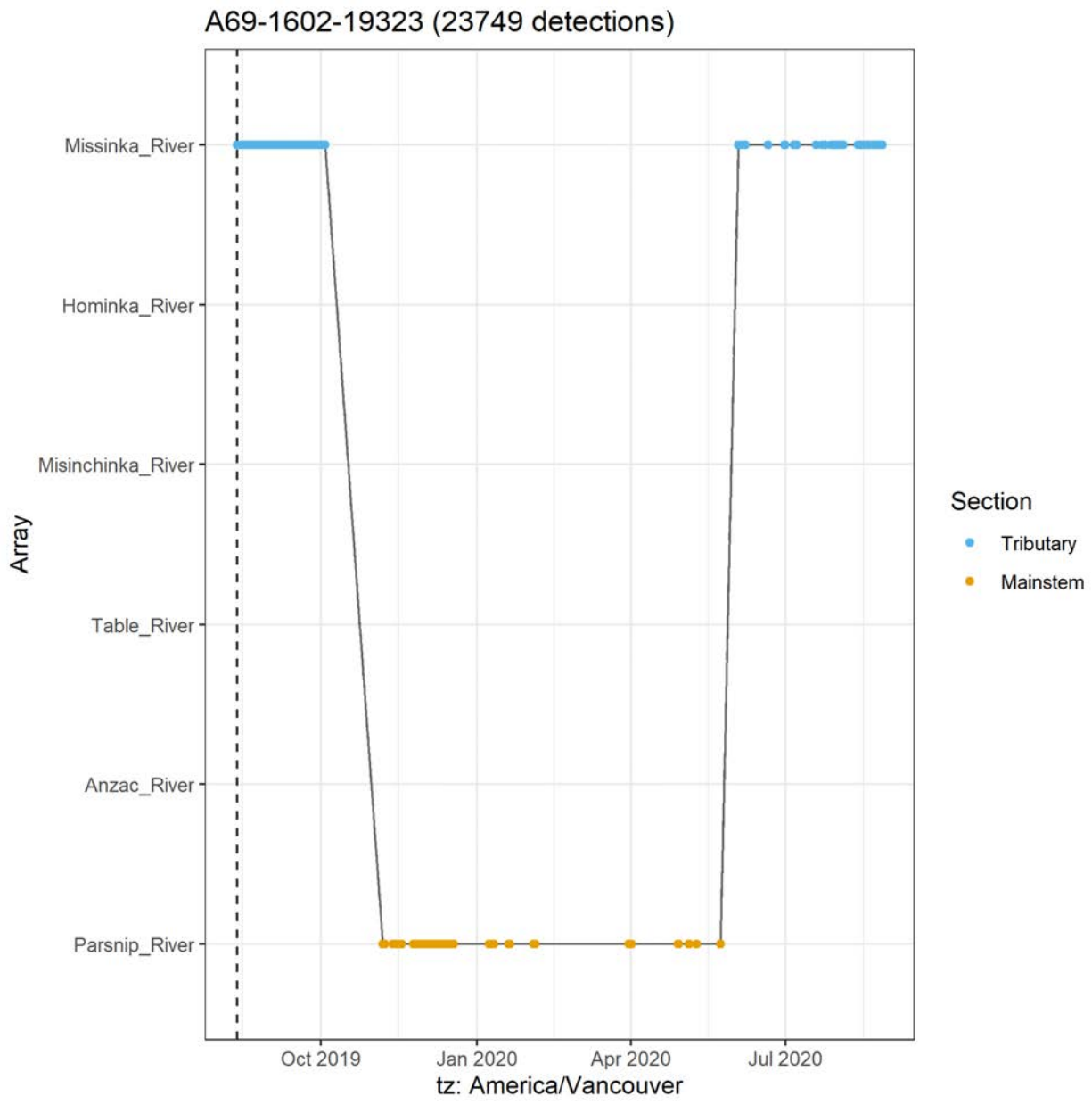
A69-1602-19323 (23749 detections)
Missinka_River
Hominka_River
Misinchinka_River
Table_River
Anzac_River
Parsnip_River
Array
Oct 2019
Jan 2020
Apr 2020
Jul 2020
tz: America/Vancouver
Section
Tributary
Mainstem

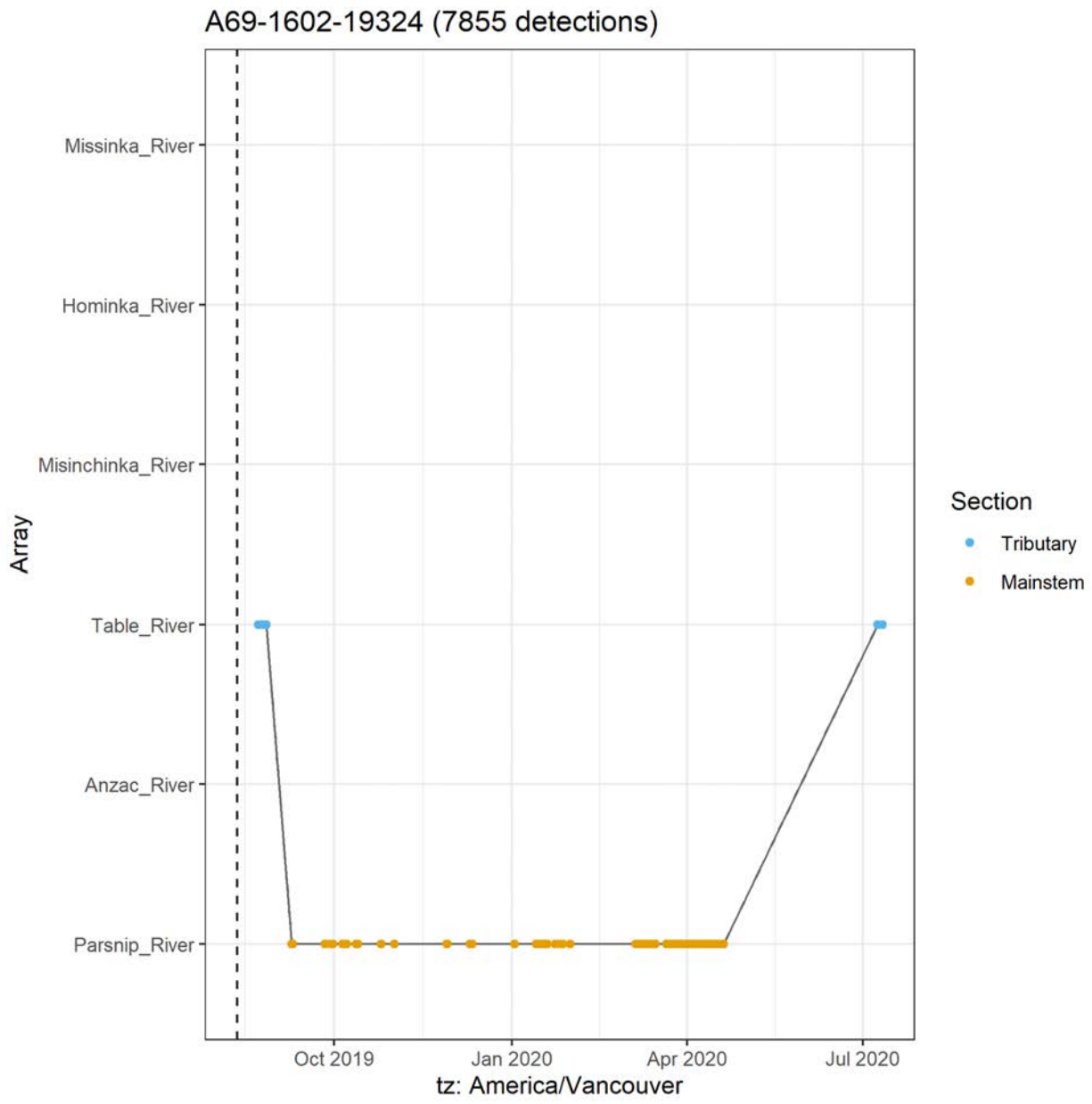
A69-1602-19324 (7855 detections)
Missinka_River
Hominka_River
Misinchinka_River
Table_River
Anzac_River
Parsnip_River
Array
Oct 2019
Jan 2020
Apr 2020
Jul 2020
tz: America/Vancouver
Section
Tributary
Mainstem

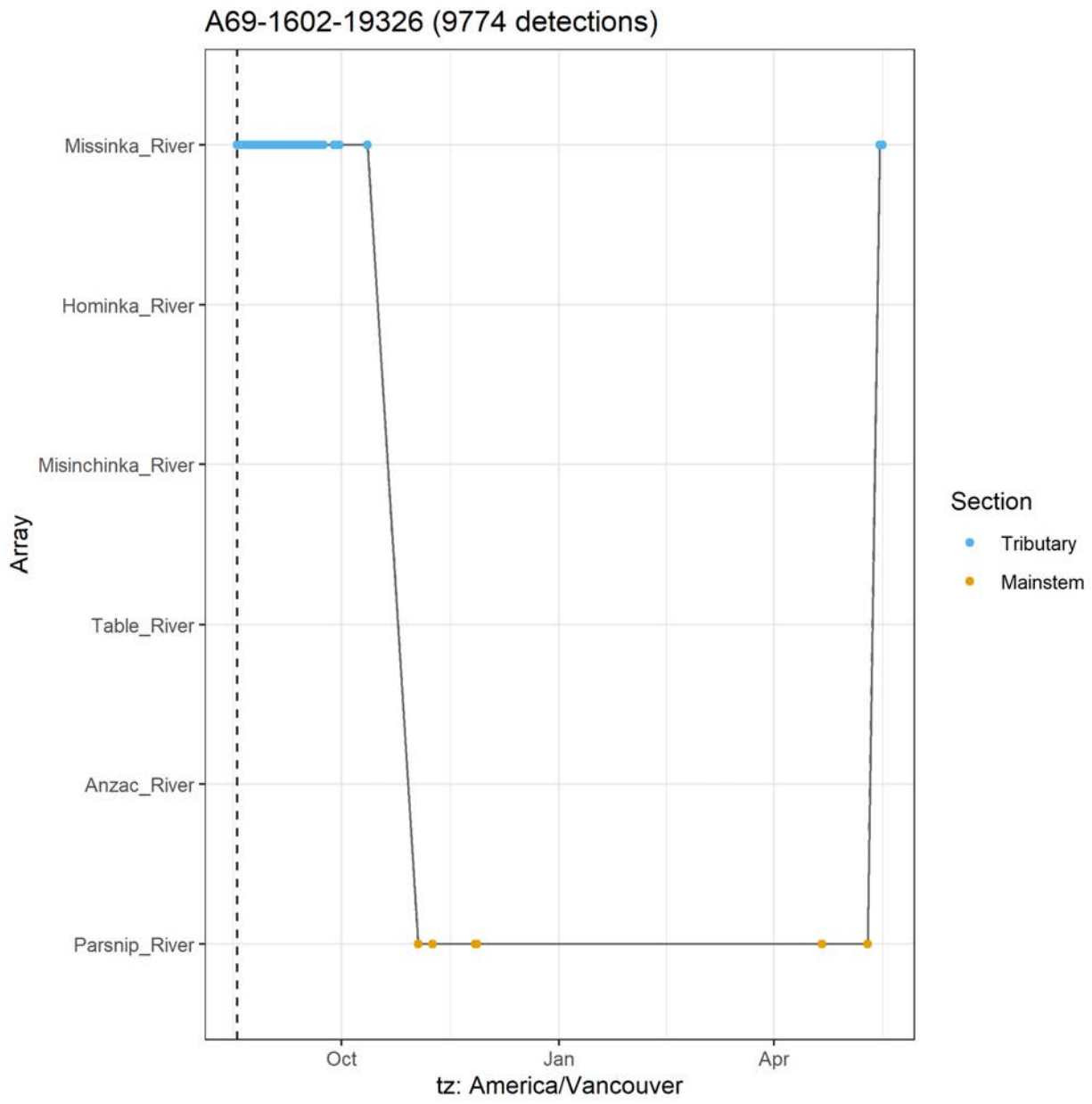
A69-1602-19326 (9774 detections)
Missinka_River
Hominka_River
Misinchinka_River
Table_River
Anzac_River
Parsnip_River
Array
Oct
Jan
Apr
tz: America/Vancouver
Section
Tributary
Mainstem

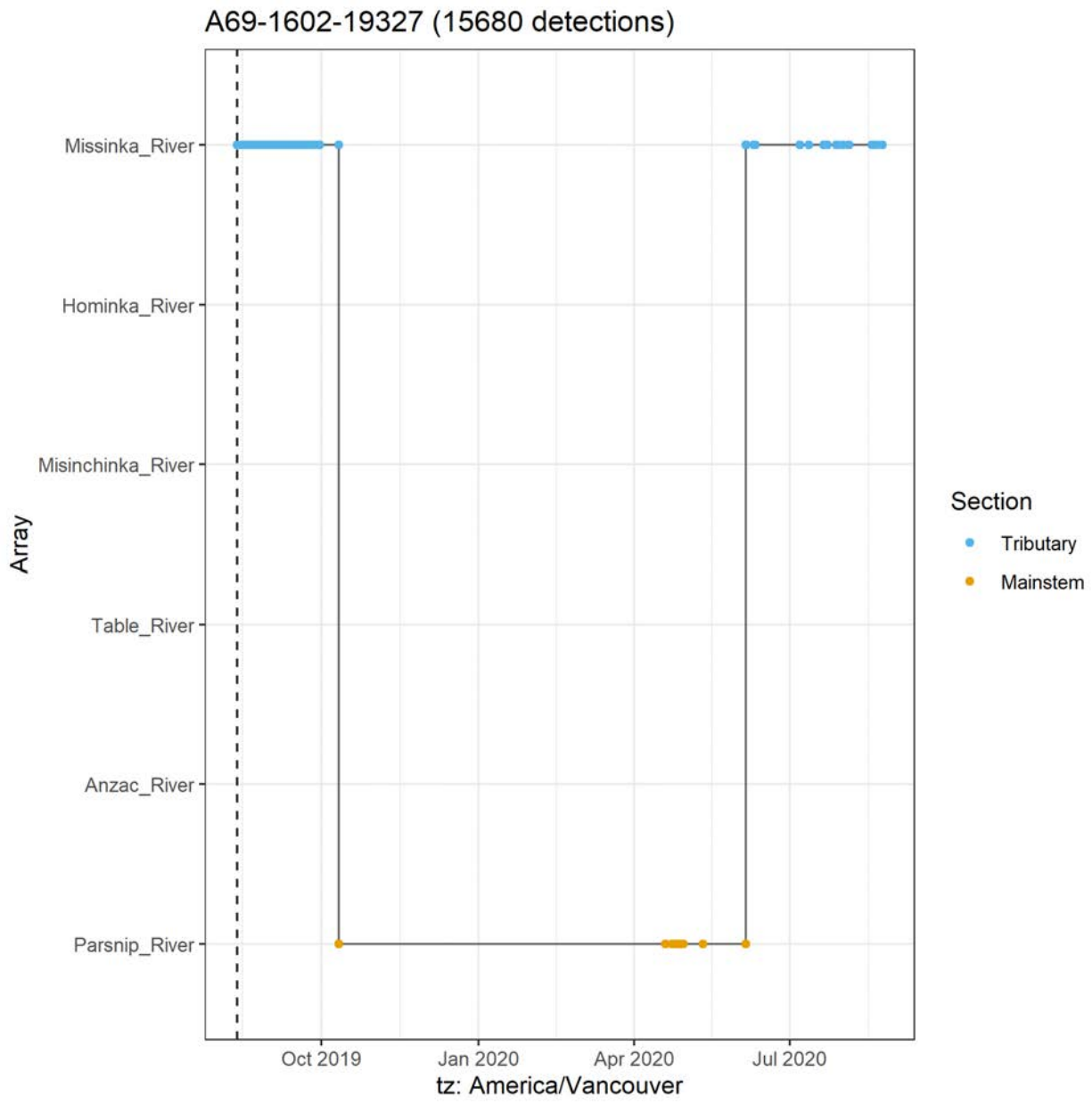
A69-1602-19327 (15680 detections)
Missinka_River
Hominka_River
Misinchinka_River
Table_River
Anzac_River
Parsnip_River
Array
Oct 2019
Jan 2020
Apr 2020
Jul 2020
tz: America/Vancouver
Section
Tributary
Mainstem

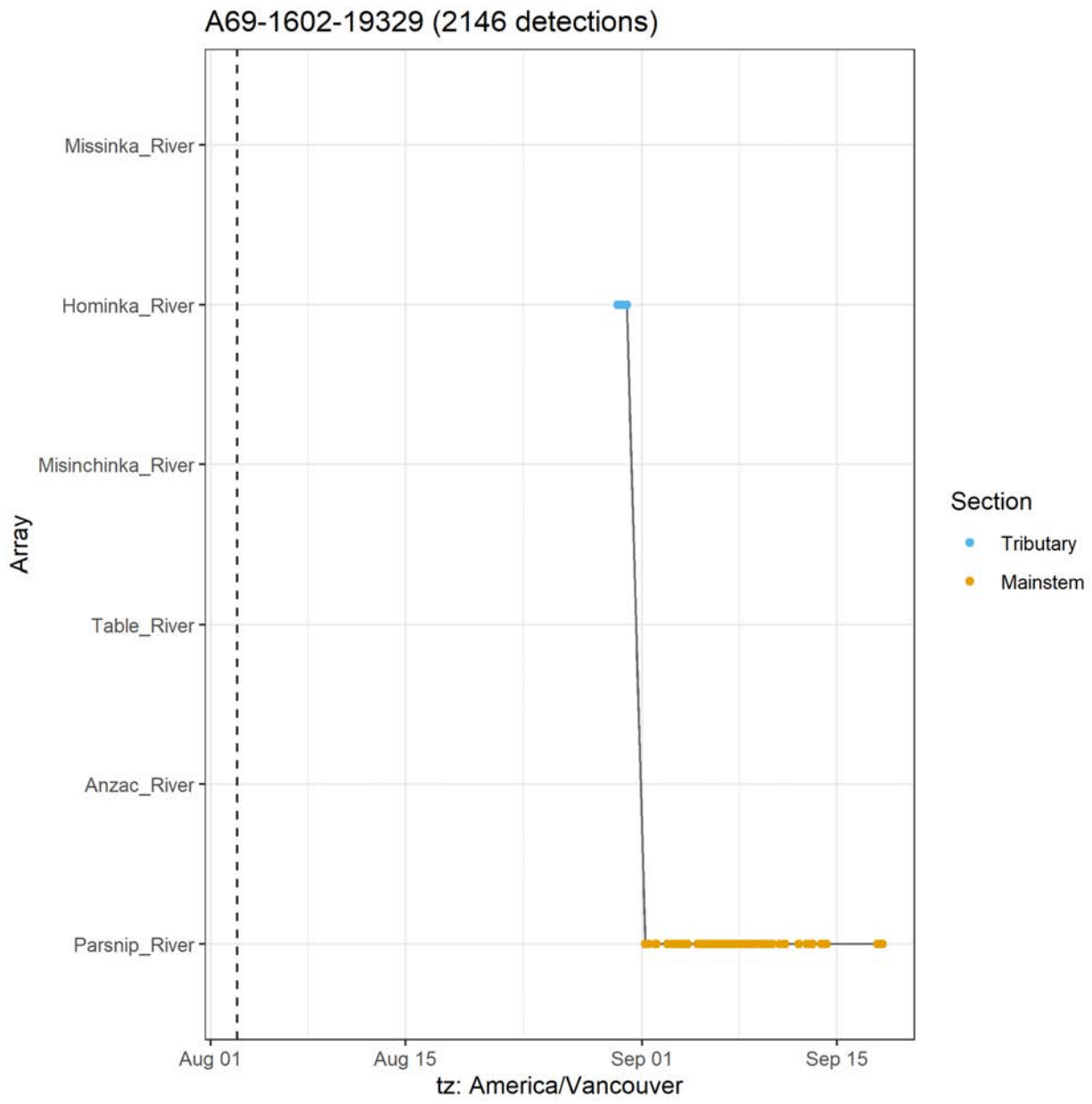
A69-1602-19329 (2146 detections)
Missinka_River
Hominka_River
Misinchinka_River
Table_River
Anzac_River
Parsnip_River
Array
Aug 01
Aug 15
Sep 01
Sep 15
tz: America/Vancouver
Section
Tributary
Mainstem

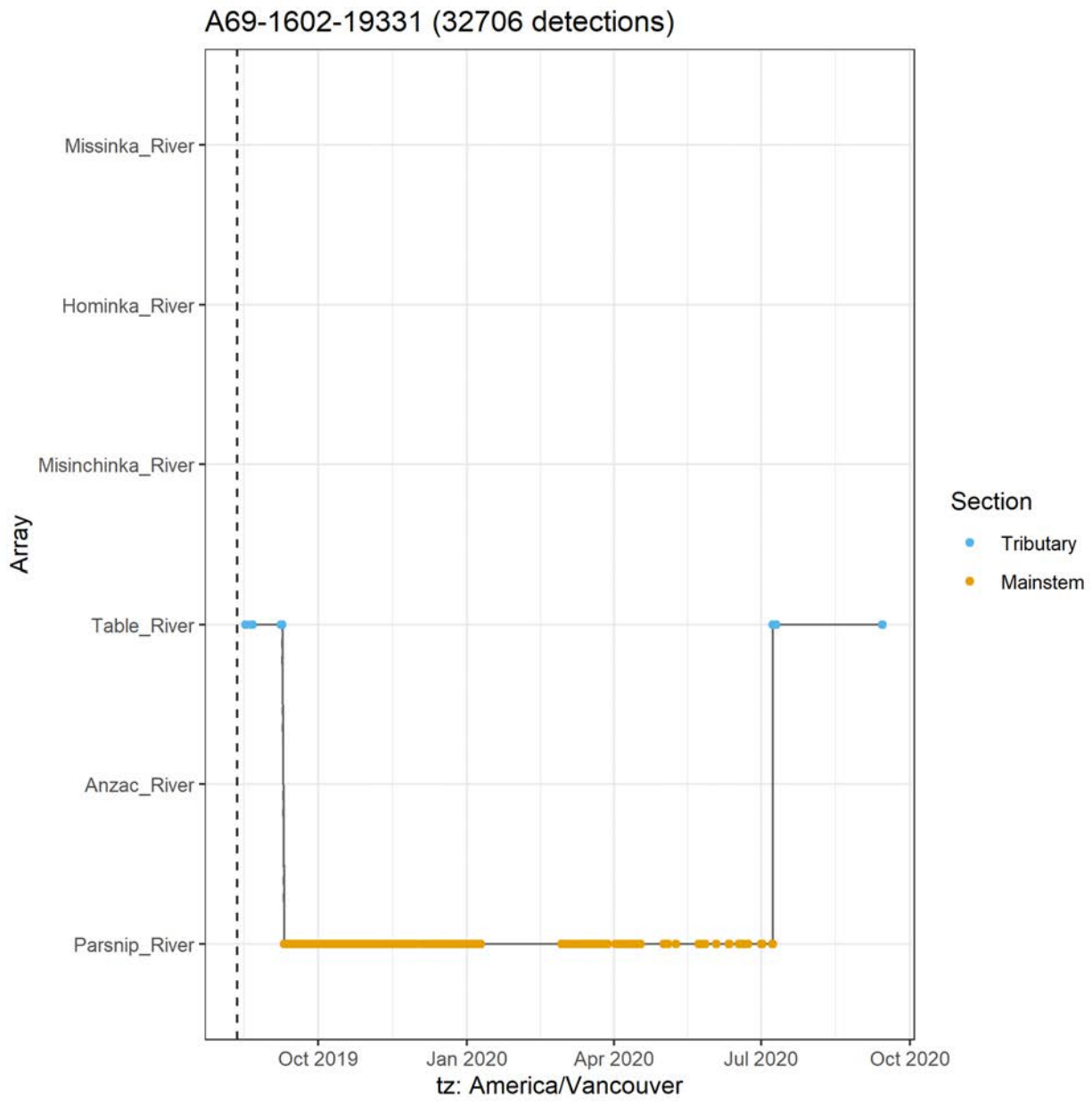
A69-1602-19331 (32706 detections)
Missinka_River
Hominka_River
Misinchinka_River
Table_River
Anzac_River
Parsnip_River
Array
Oct 2019
Jan 2020
Apr 2020
Jul 2020
Oct 2020
tz: America/Vancouver
Section
Tributary
Mainstem

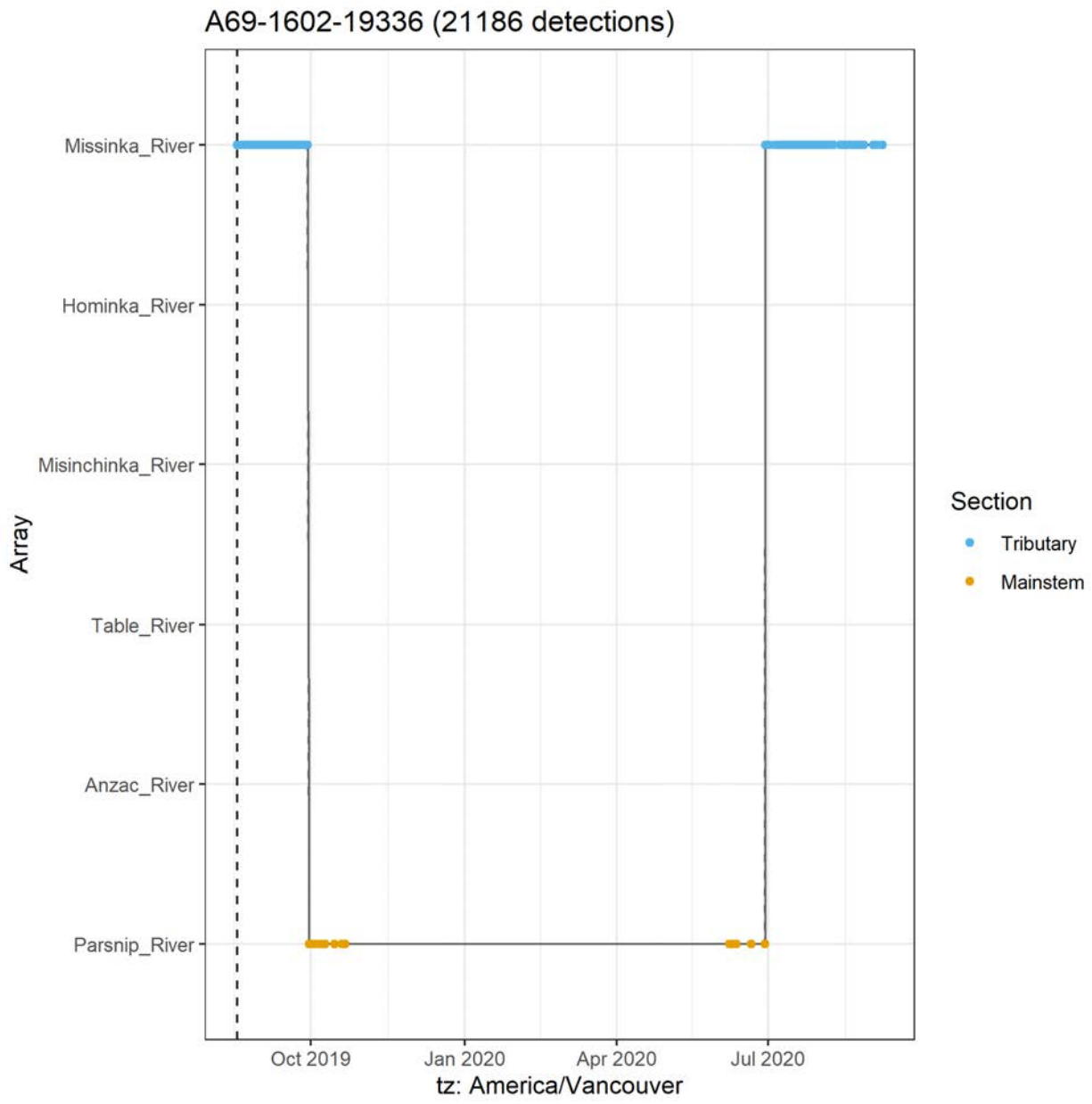
A69-1602-19336 (21186 detections)
Missinka_River
Hominka_River
Misinchinka_River
Table_River
Anzac_River
Parsnip_River
Array
Oct 2019
Jan 2020
Apr 2020
Jul 2020
tz: America/Vancouver
Section
Tributary
Mainstem

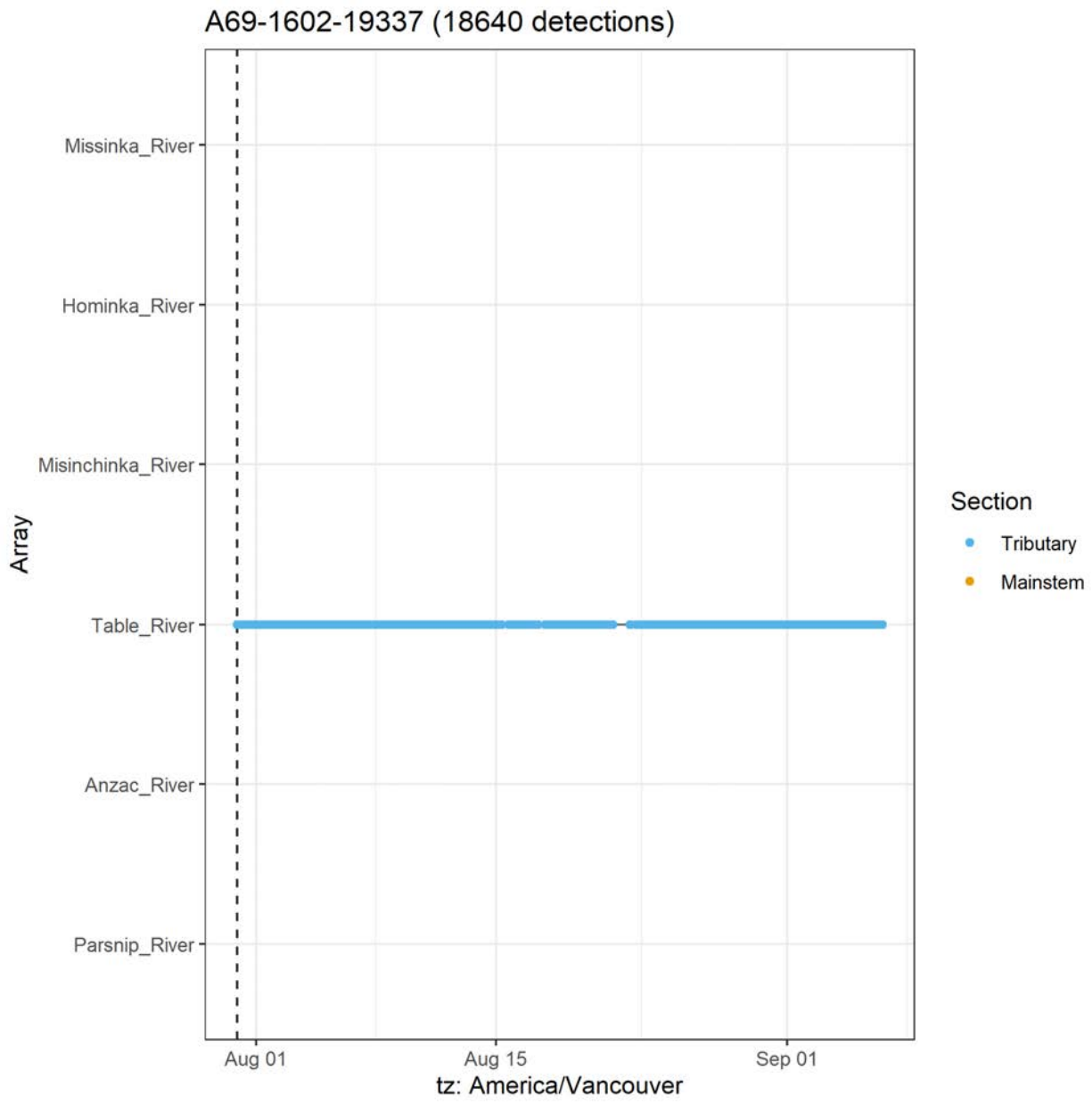
A69-1602-19337 (18640 detections)
Missinka_River
Hominka_River
Misinchinka_River
Table_River
Anzac_River
Parsnip_River
Array
Aug 01
Aug 15
Sep 01
tz: America/Vancouver
Section
Tributary
Mainstem

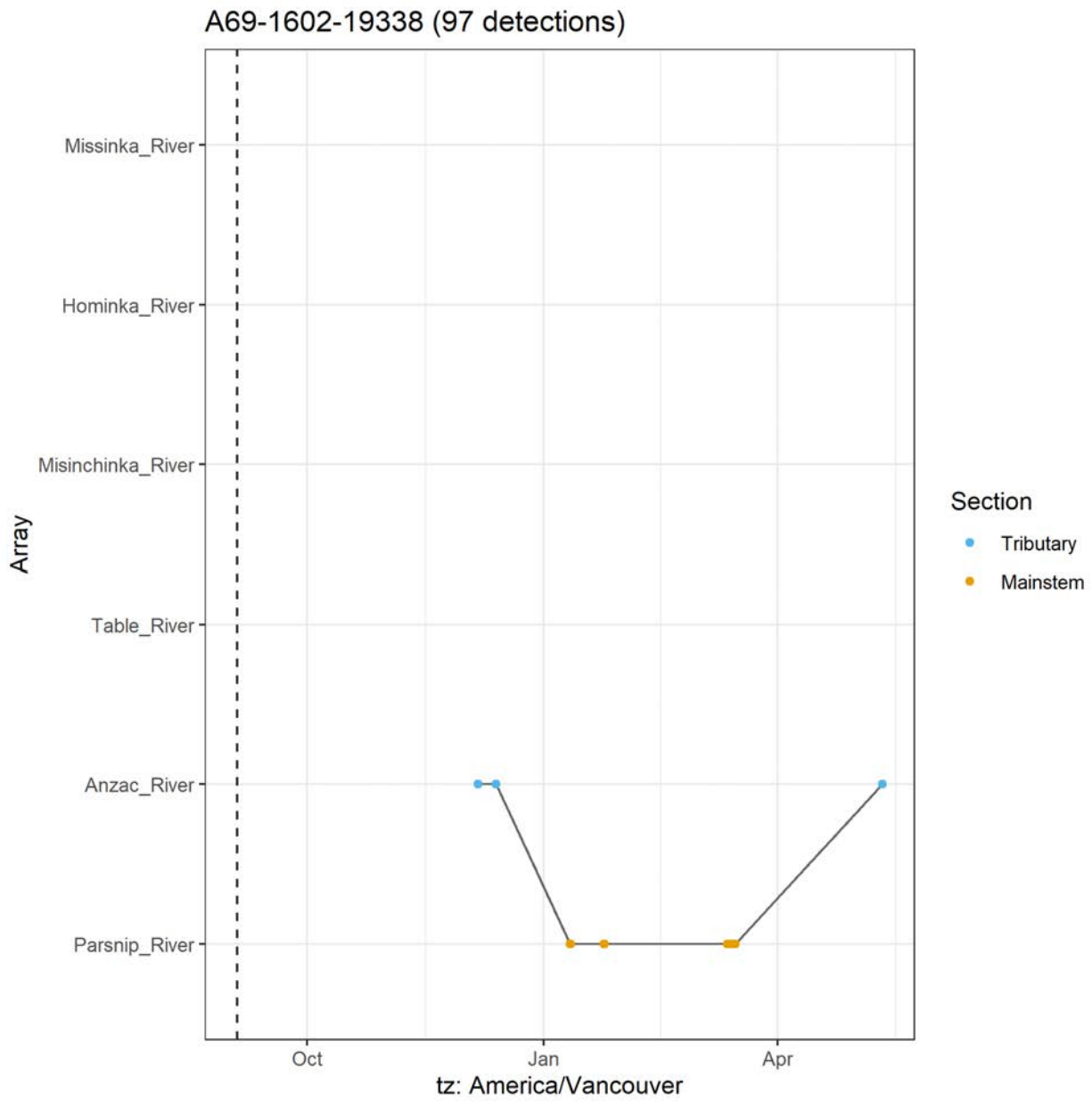
A69-1602-19338 (97 detections)
Missinka_River
Hominka_River
Misinchinka_River
Table_River
Anzac_River
Parsnip_River
Array
Oct
Jan
Apr
tz: America/Vancouver
Section
Tributary
Mainstem

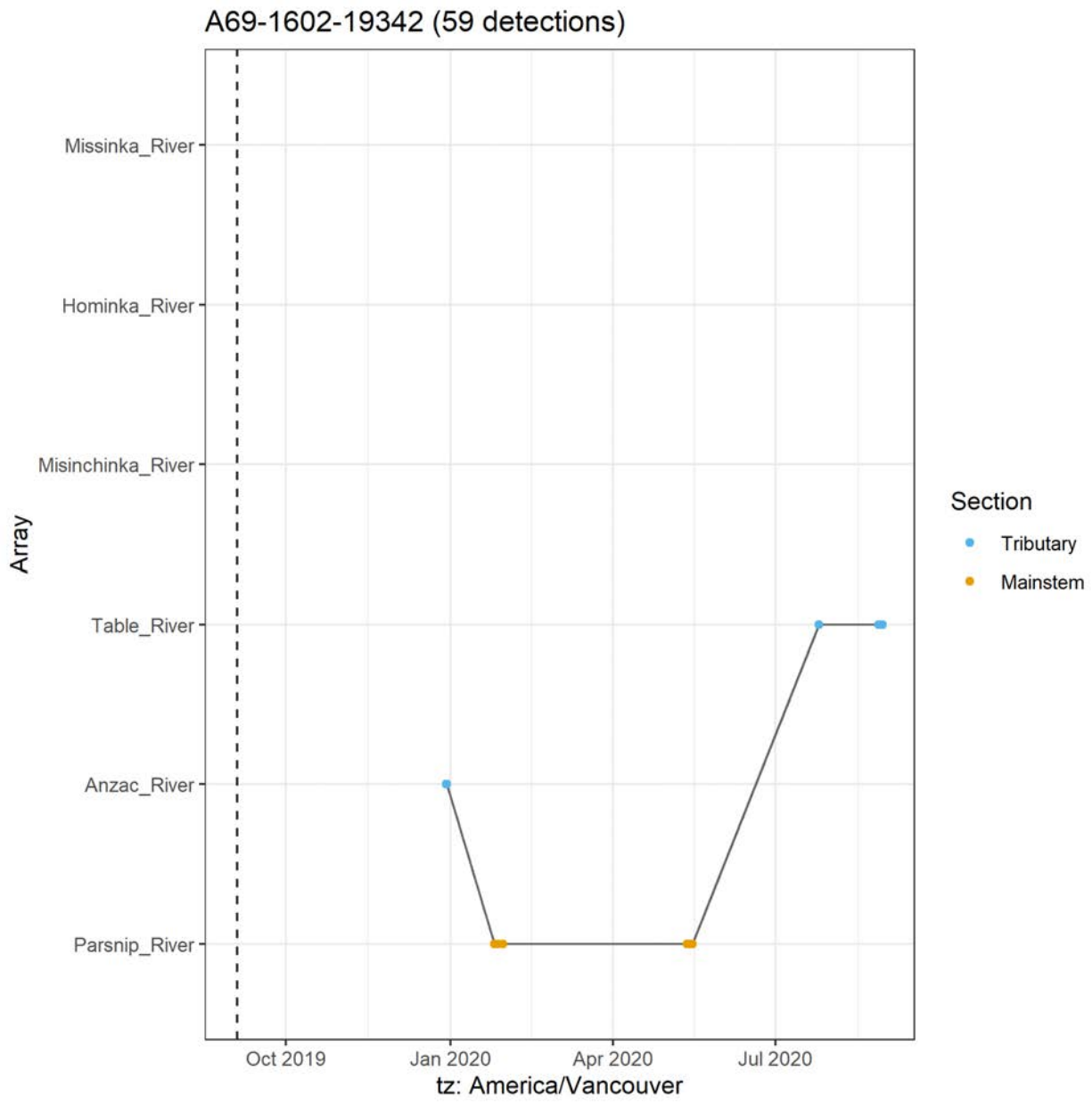
A69-1602-19342 (59 detections)
Missinka_River
Hominka_River
Misinchinka_River
Table_River
Anzac_River
Parsnip_River
Array
Oct 2019
Jan 2020
Apr 2020
Jul 2020
tz: America/Vancouver
Section
Tributary
Mainstem

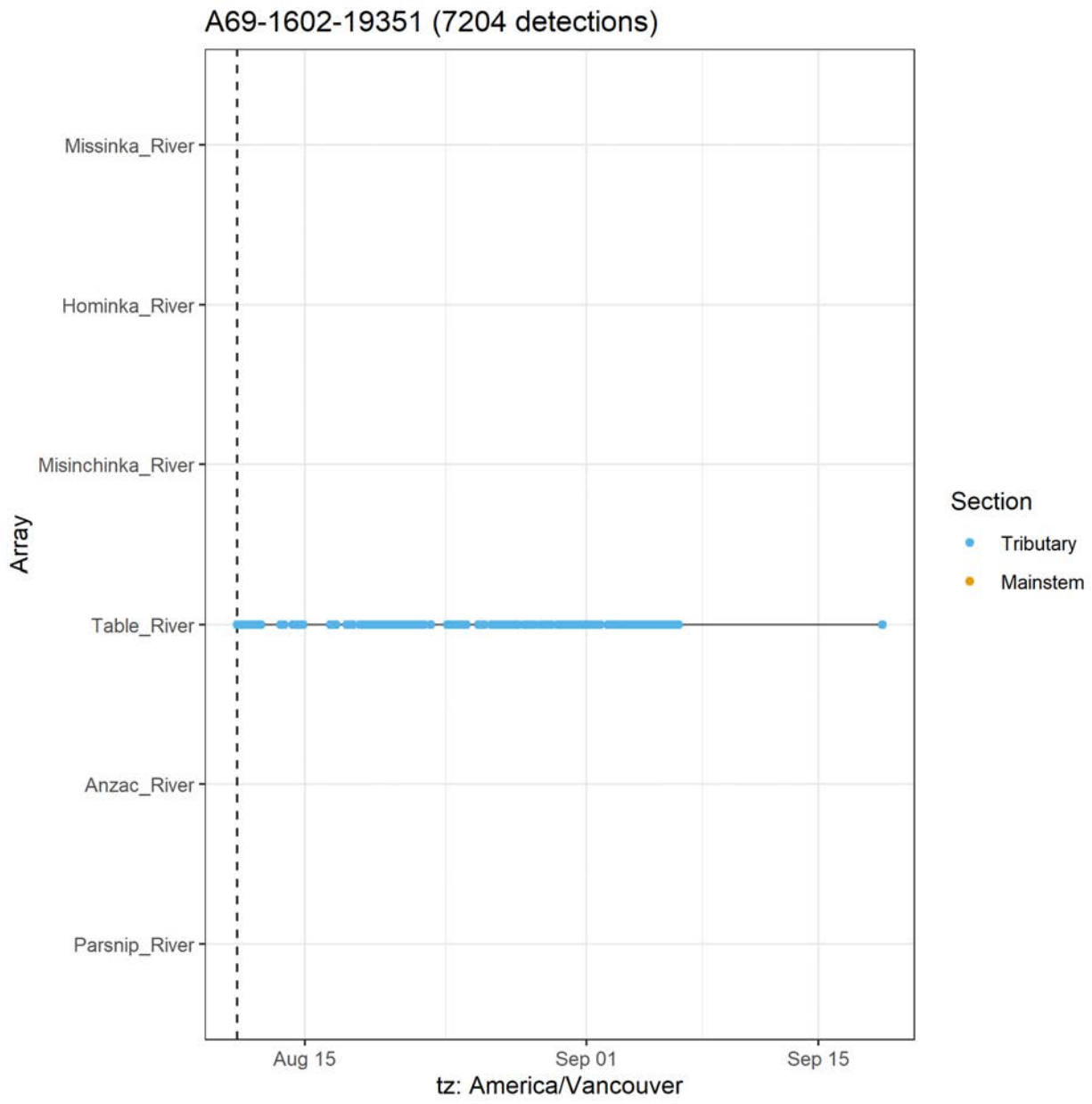
A69-1602-19351 (7204 detections)
Missinka_River
Hominka_River
Misinchinka_River
Table_River
Anzac_River
Parsnip_River
Array
Aug 15
Sep 01
Sep 15
tz: America/Vancouver
Section
Tributary
Mainstem

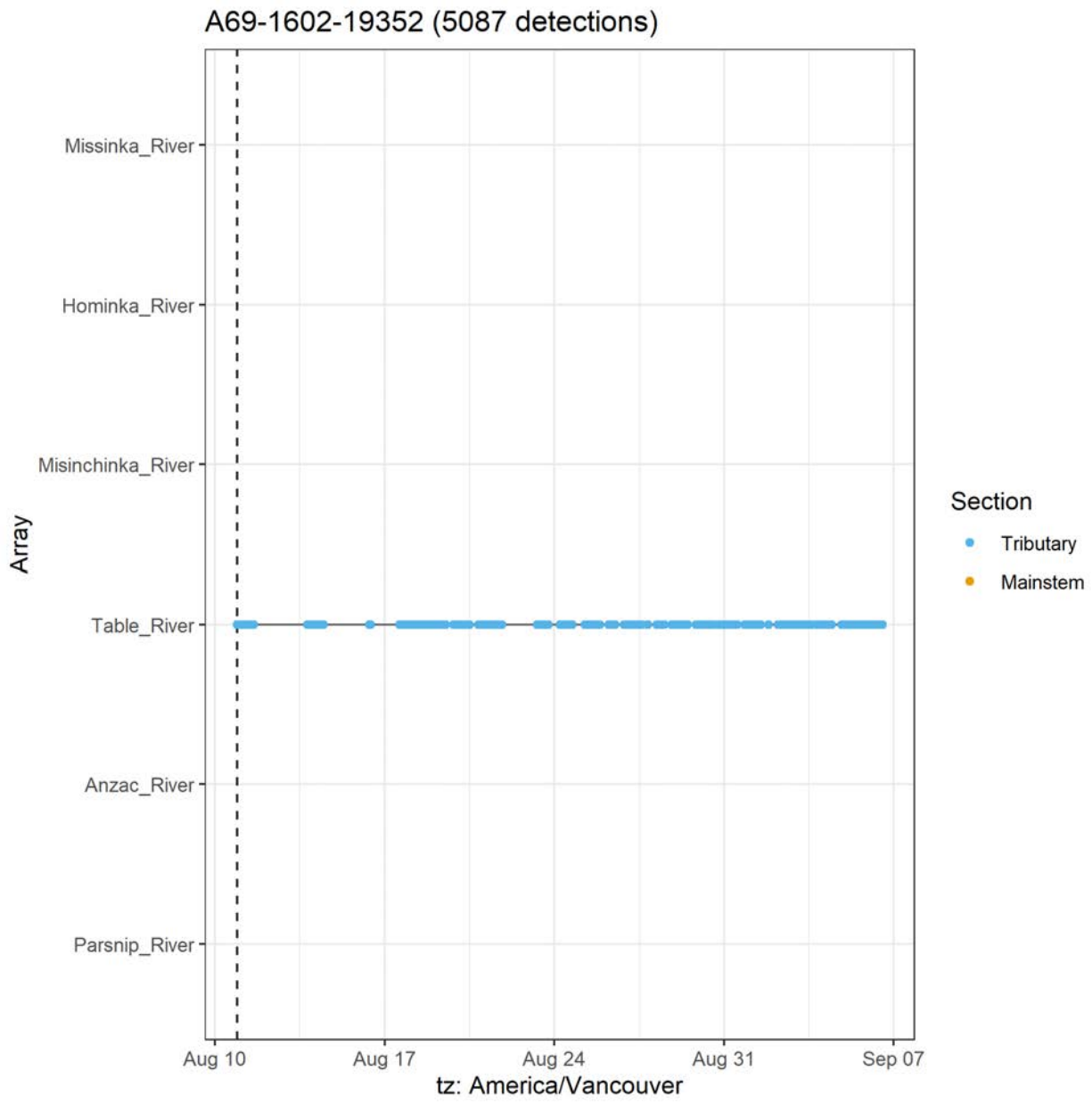
A69-1602-19352 (5087 detections)
Missinka_River
Hominka_River
Misinchinka_River
Table_River
Anzac_River
Parsnip_River
Array
Aug 10
Aug 17
Aug 24
Aug 31
Sep 07
tz: America/Vancouver
Section
Tributary
Mainstem

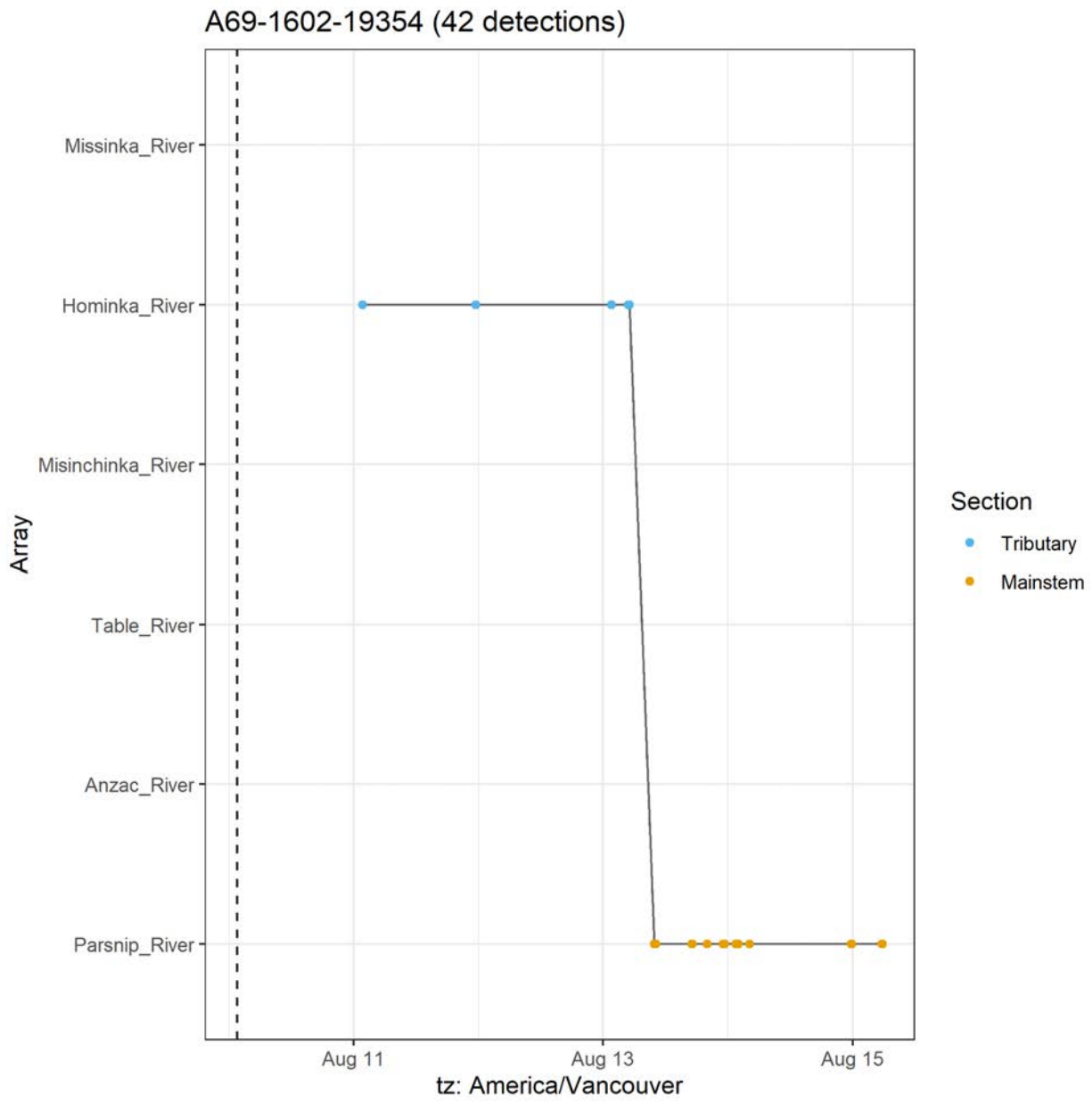
A69-1602-19354 (42 detections)
Missinka_River
Hominka_River
Misinchinka_River
Table_River
Anzac_River
Parsnip_River
Array
Aug 11
Aug 13
Aug 15
tz: America/Vancouver
Section
Tributary
Mainstem

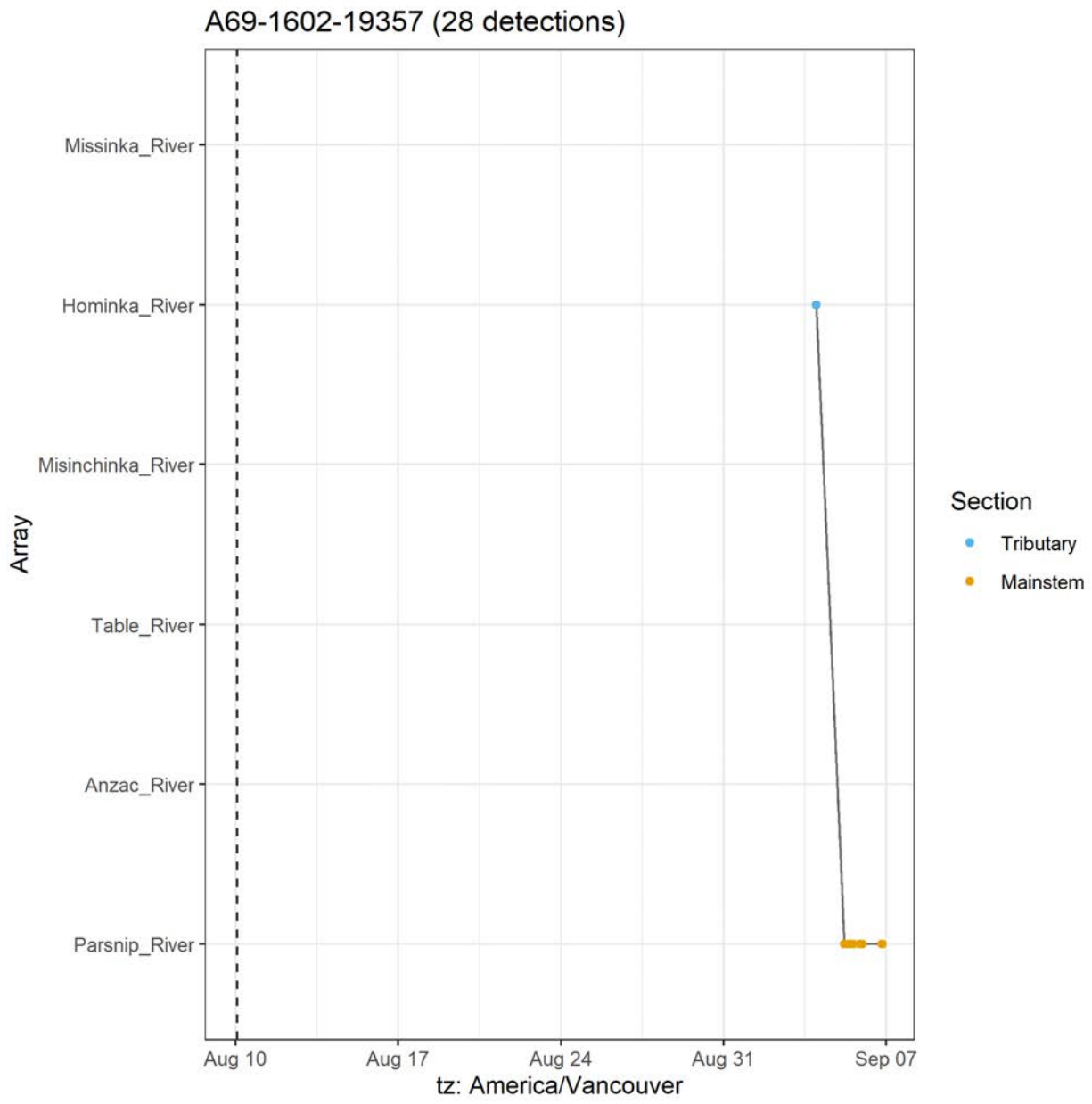
A69-1602-19357 (28 detections)
Missinka_River
Hominka_River
Misinchinka_River
Table_River
Anzac_River
Parsnip_River
Array
Aug 10
Aug 17
Aug 24
Aug 31
Sep 07
tz: America/Vancouver
Section
Tributary
Mainstem

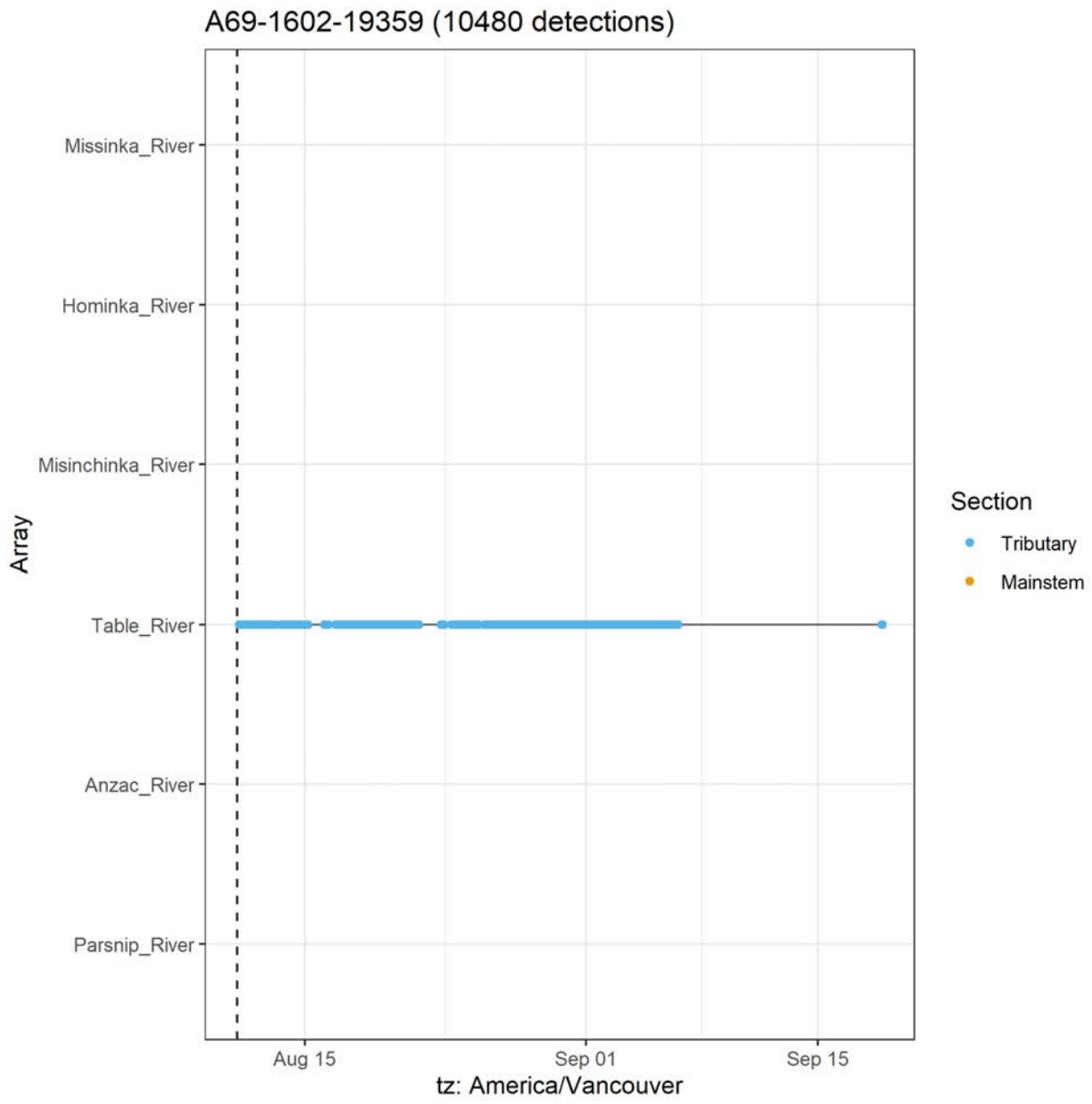
A69-1602-19359 (10480 detections)
Missinka_River
Hominka_River
Misinchinka_River
Table_River
Anzac_River
Parsnip_River
Array
Aug 15
Sep 01
Sep 15
tz: America/Vancouver
Section
Tributary
Mainstem

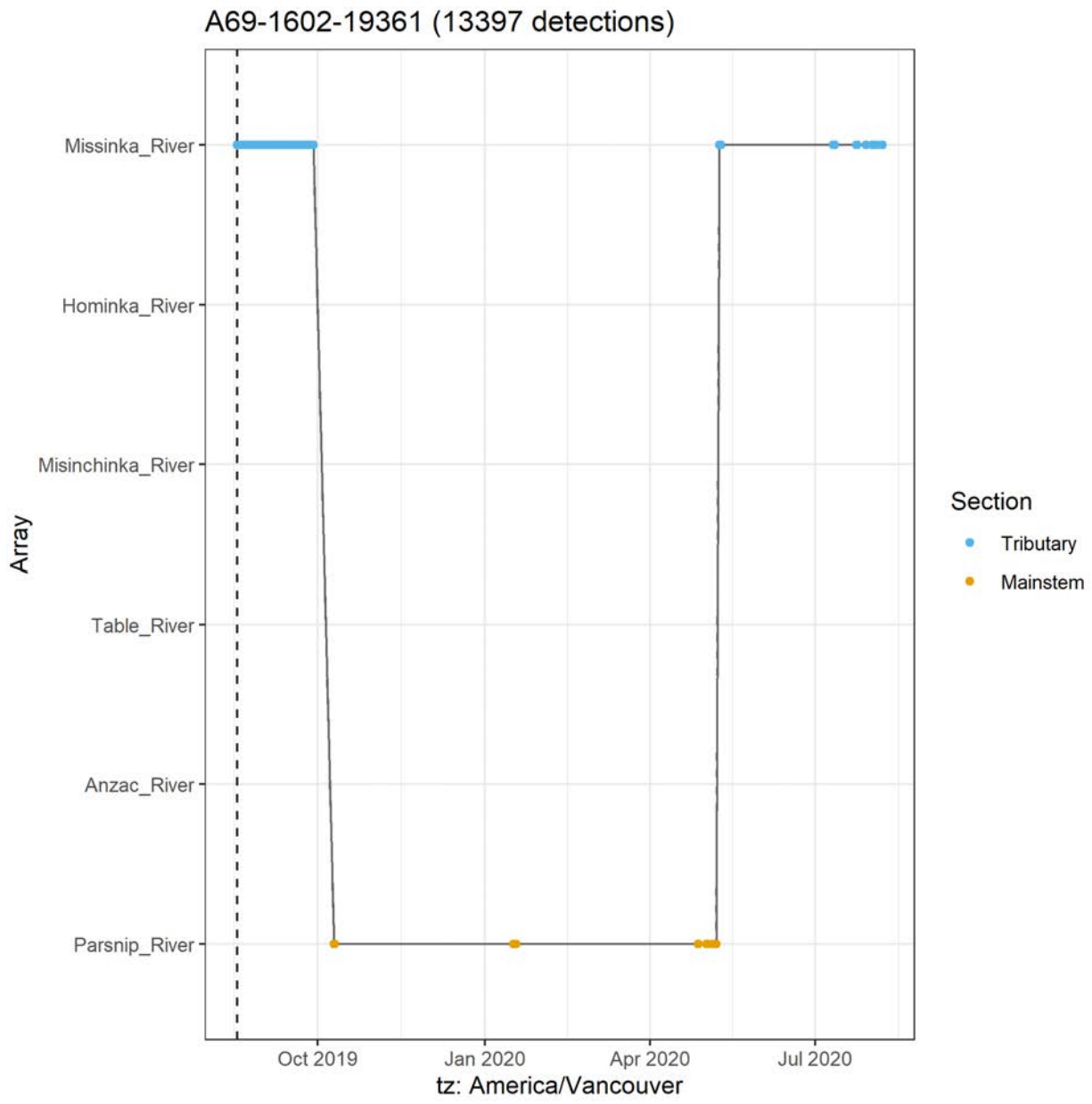
A69-1602-19361 (13397 detections)
Missinka_River
Hominka_River
Misinchinka_River
Table_River
Anzac_River
Parsnip_River
Array
Oct 2019
Jan 2020
Apr 2020
Jul 2020
tz: America/Vancouver
Section
Tributary
Mainstem

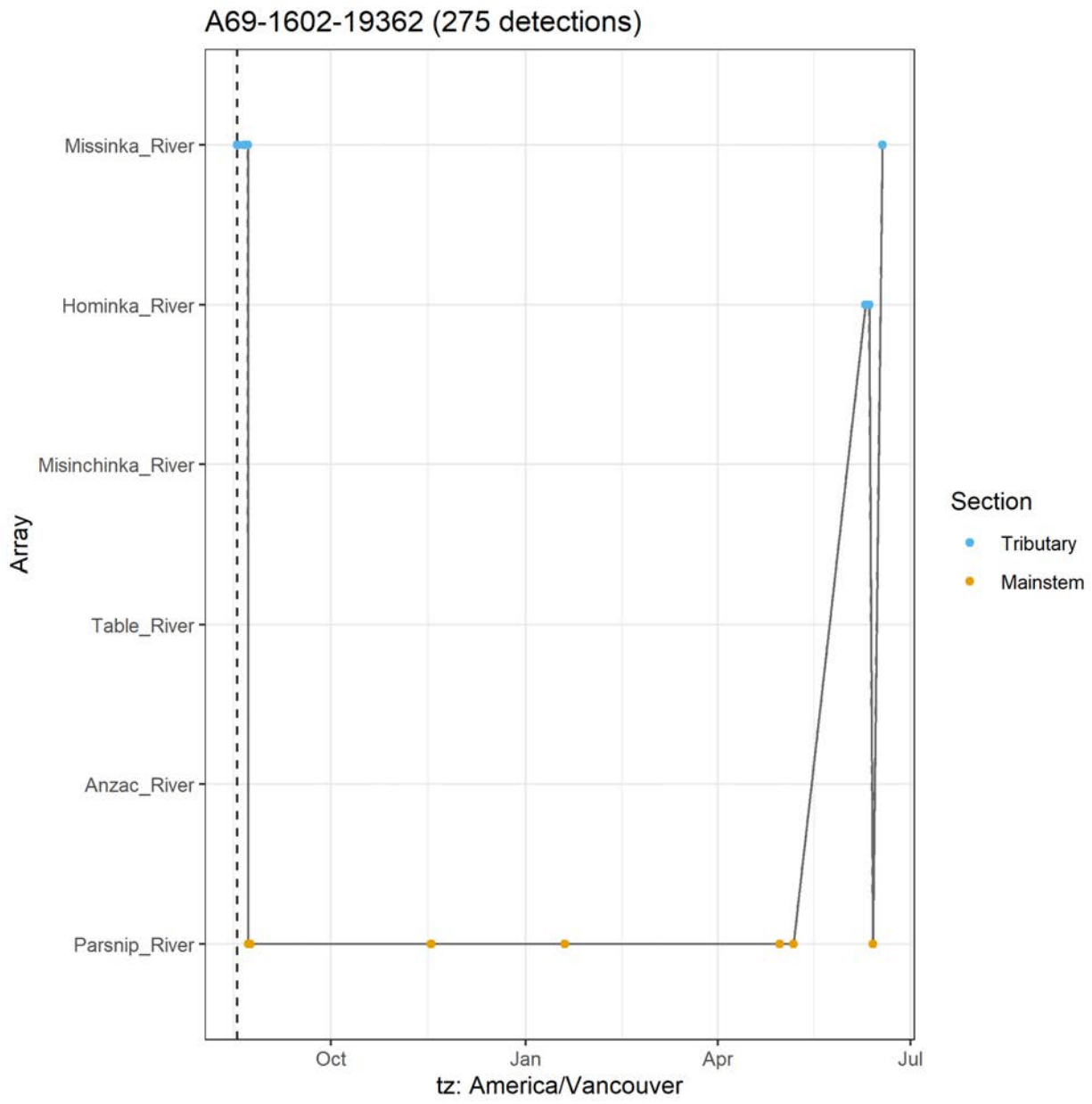
A69-1602-19362 (275 detections)
Missinka_River
Hominka_River
Misinchinka_River
Table_River
Anzac_River
Parsnip_River
Array
Oct
Jan
Apr
Jul
tz: America/Vancouver
Section
Tributary
Mainstem

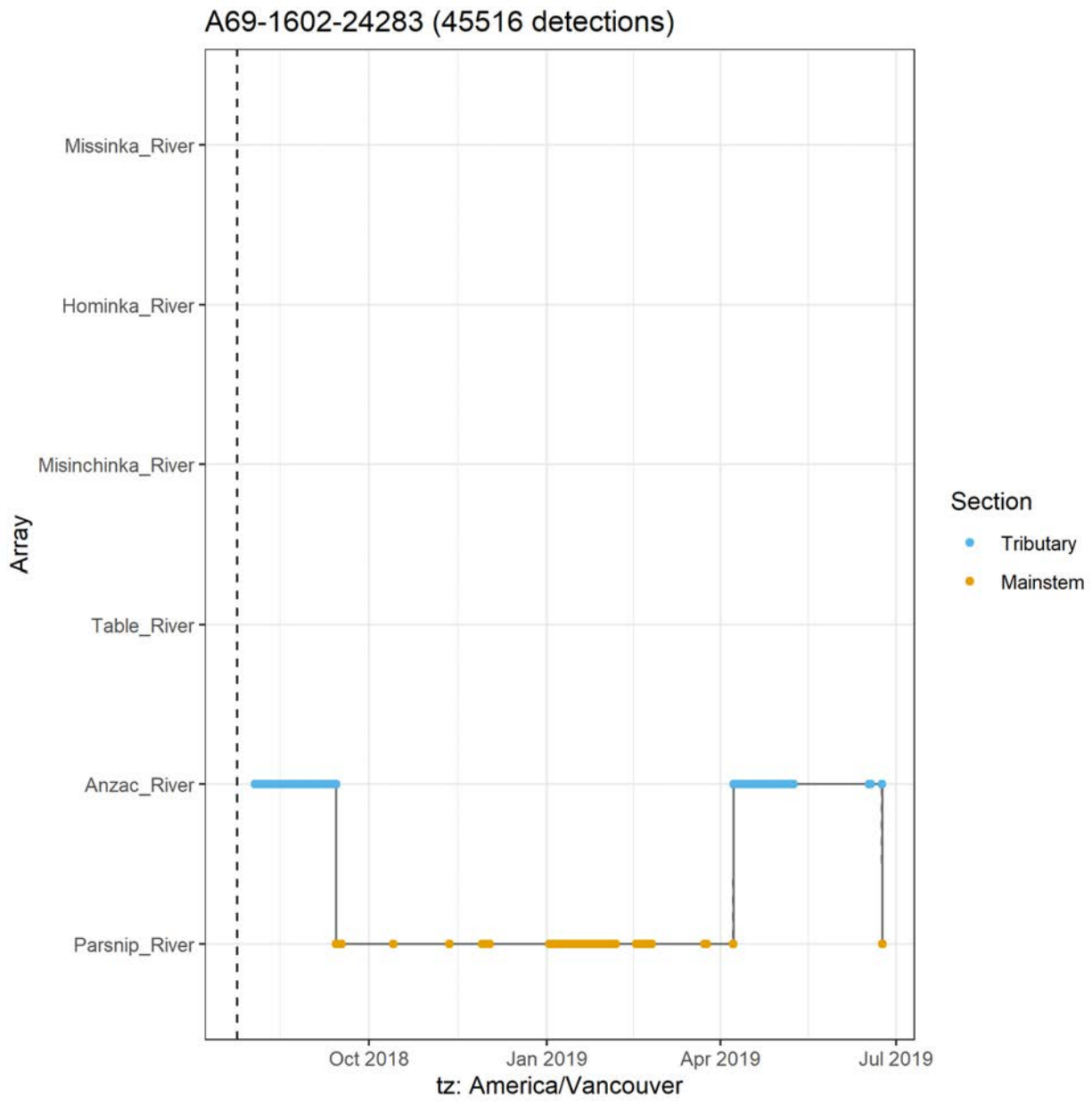
A69-1602-24283 (45516 detections)
Missinka_River
Hominka_River
Misinchinka_River
Table_River
Anzac_River
Parsnip_River
Array
Oct 2018
Jan 2019
Apr 2019
Jul 2019
tz: America/Vancouver
Section
Tributary
Mainstem

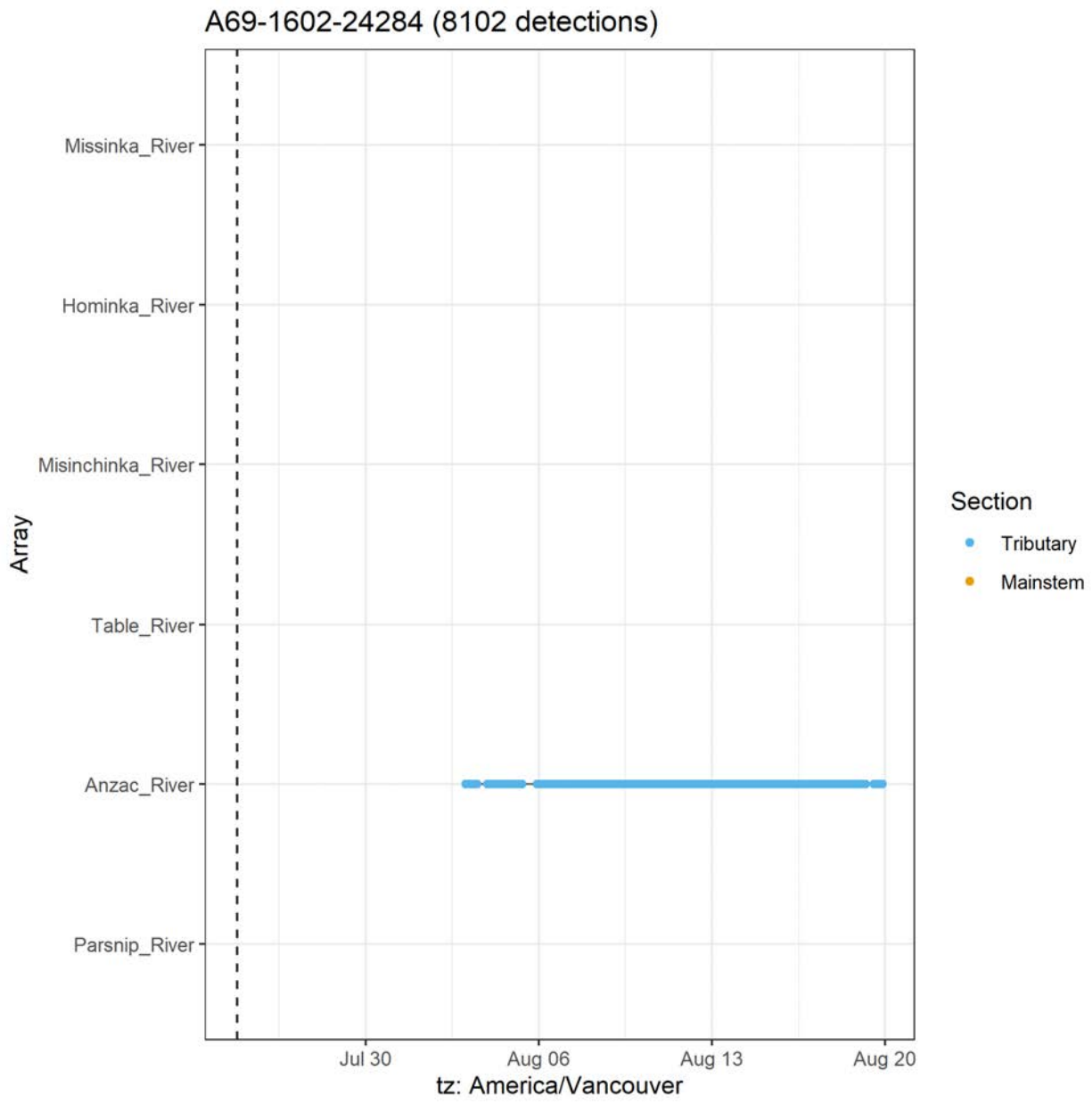
A69-1602-24284 (8102 detections)
Missinka_River
Hominka_River
Misinchinka_River
Table_River
Anzac_River
Parsnip_River
Array
Jul 30
Aug 06
Aug 13
Aug 20
tz: America/Vancouver
Section
Tributary
Mainstem

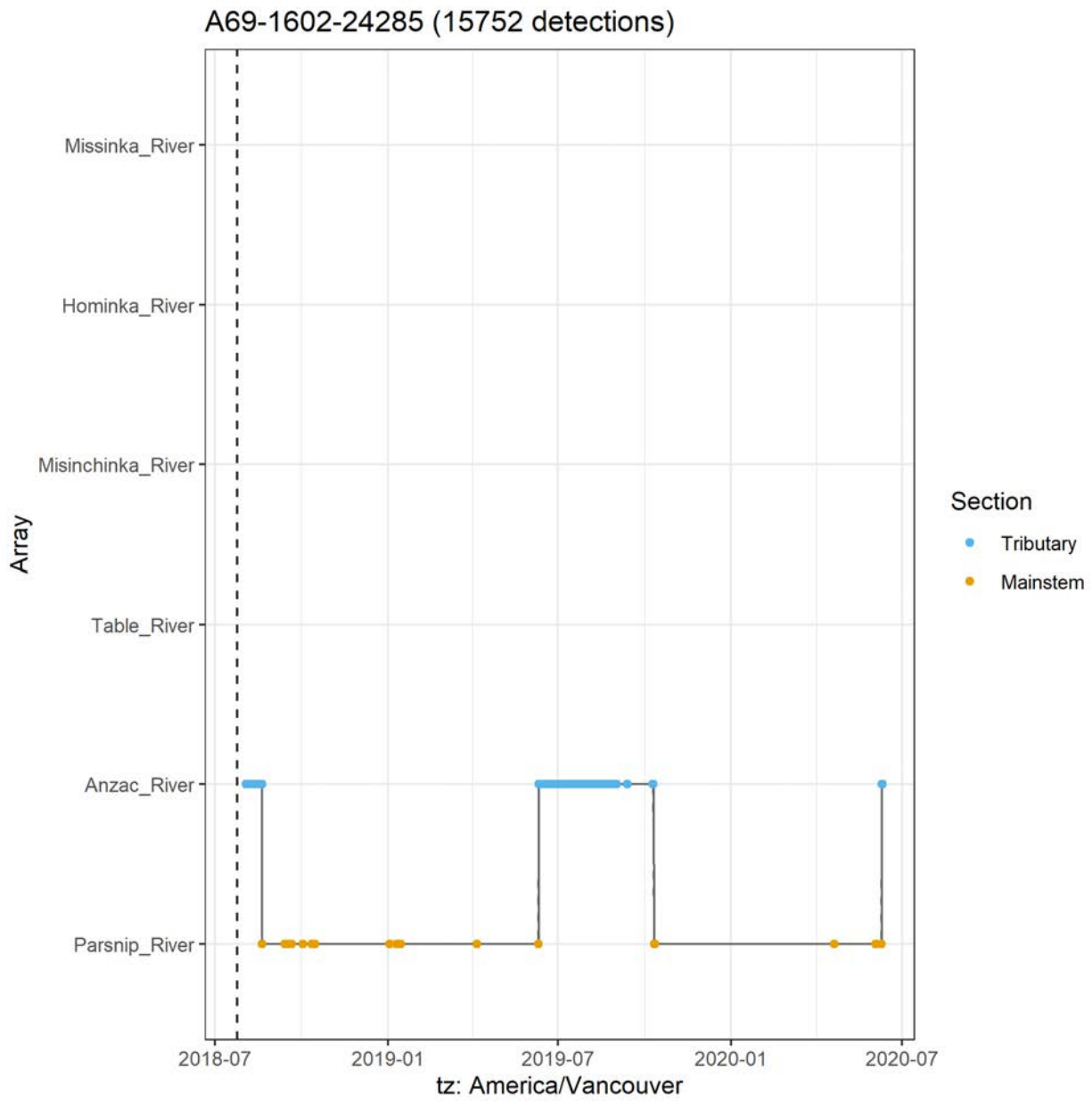
A69-1602-24285 (15752 detections)
Missinka_River
Hominka_River
Misinchinka_River
Table_River
Anzac_River
Parsnip_River
Array
2018-07
2019-01
2019-07
2020-01
2020-07
tz: America/Vancouver
Section
Tributary
Mainstem

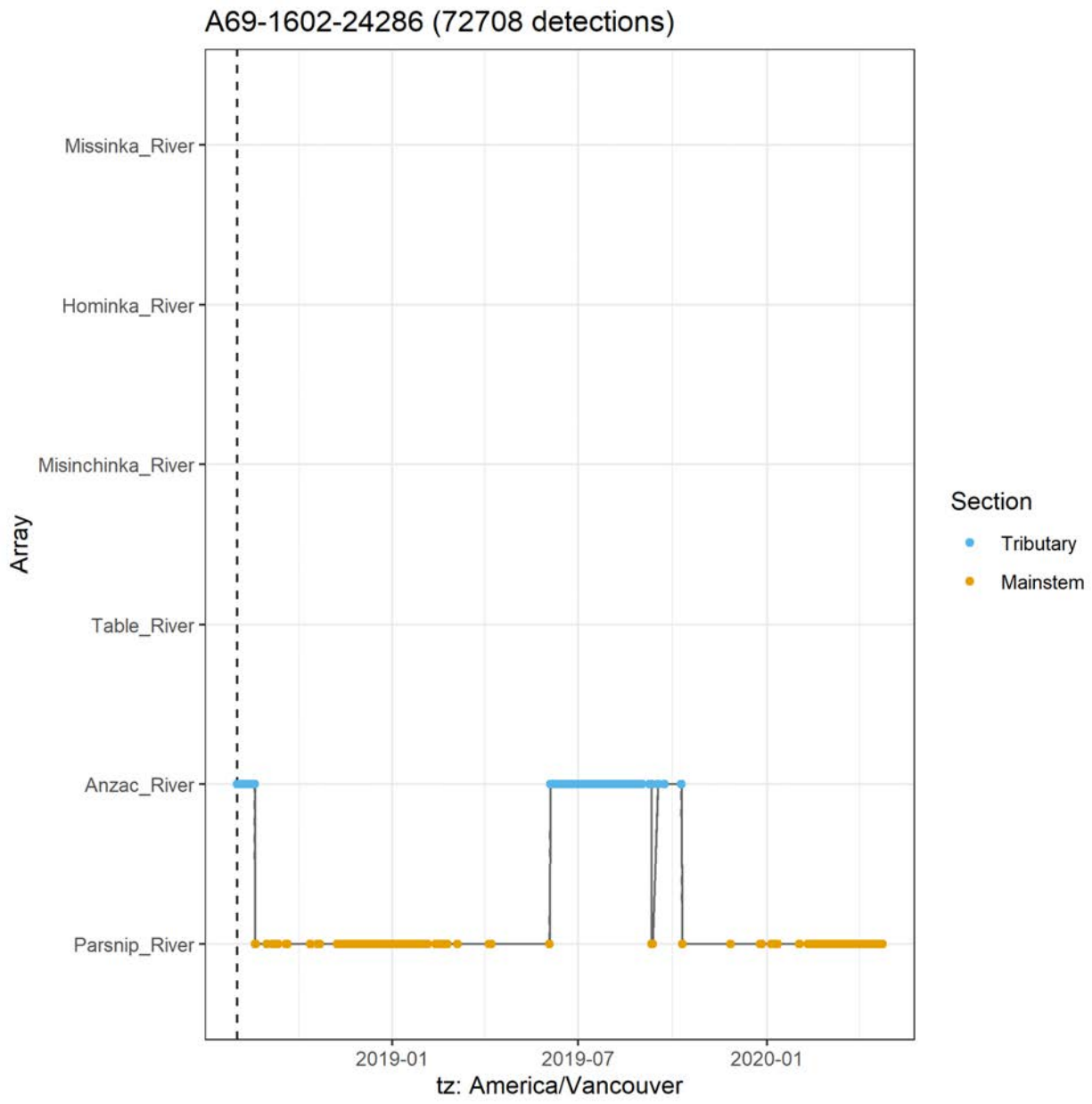
A69-1602-24286 (72708 detections)
Missinka_River
Hominka_River
Misinchinka_River
Table_River
Anzac_River
Parsnip_River
Array
2019-01
2019-07
2020-01
tz: America/Vancouver
Section
Tributary
Mainstem

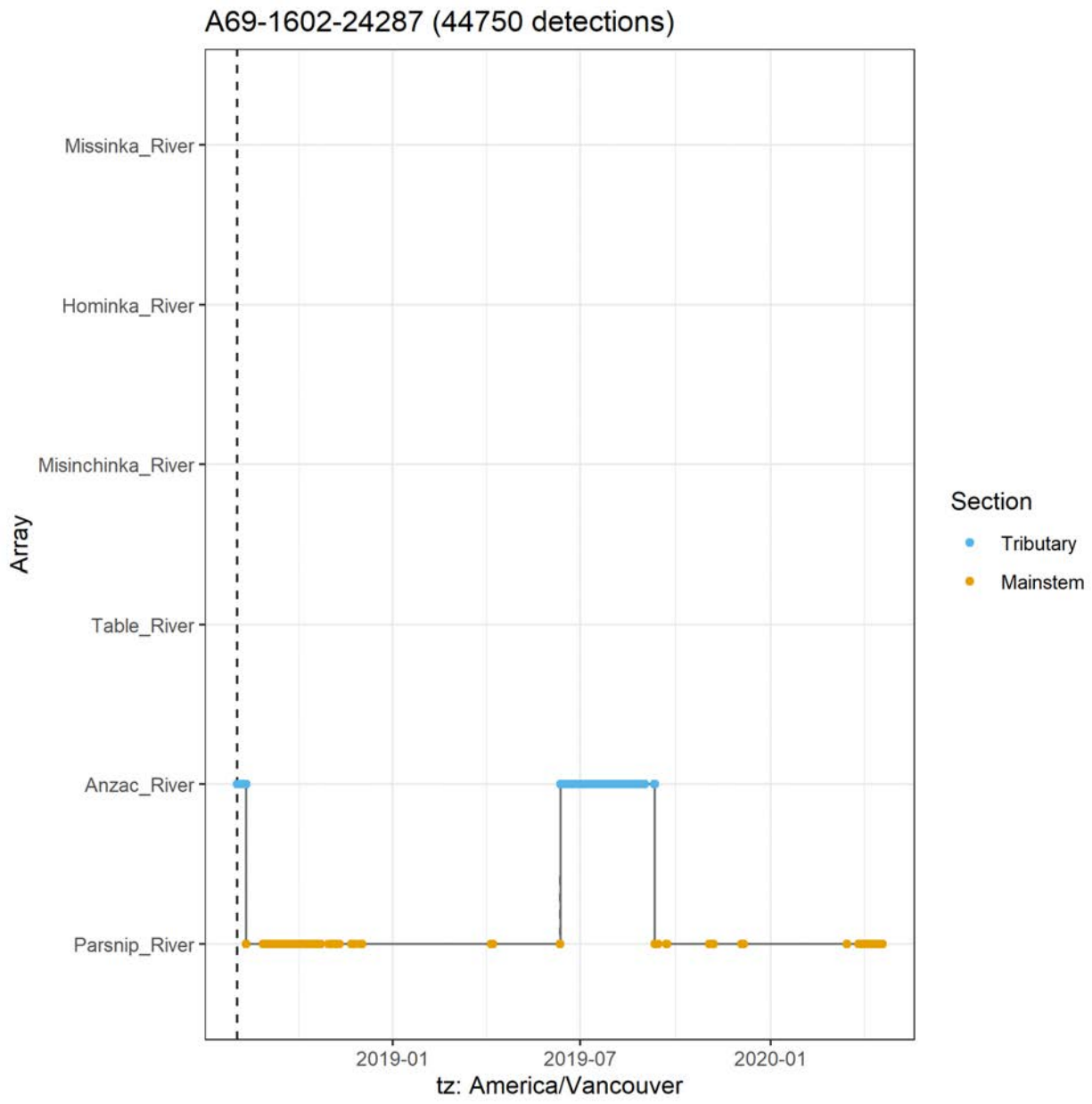
A69-1602-24287 (44750 detections)
Missinka_River
Hominka_River
Misinchinka_River
Table_River
Anzac_River
Parsnip_River
Array
2019-01
2019-07
2020-01
tz: America/Vancouver
Section
Tributary
Mainstem

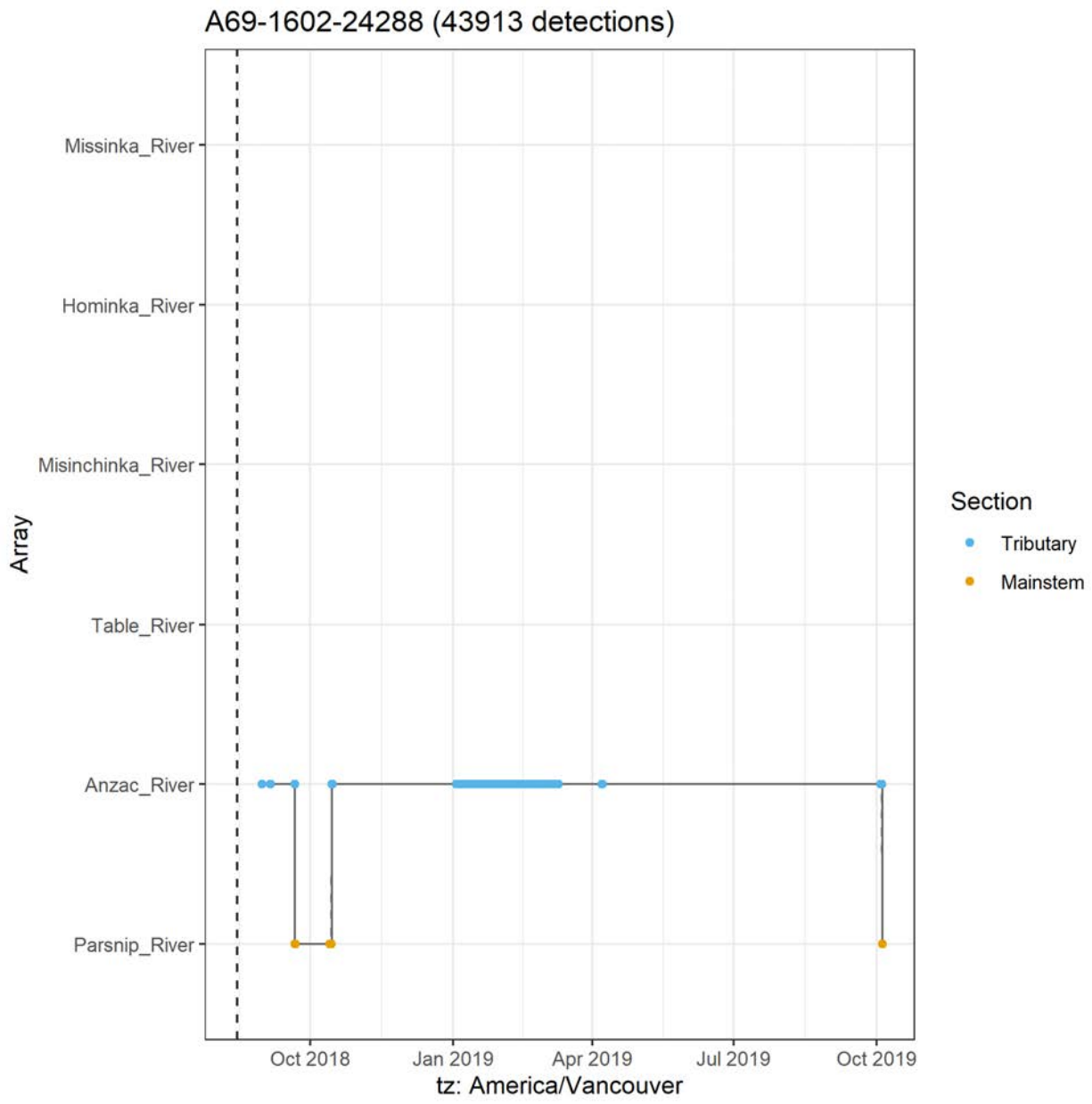
A69-1602-24288 (43913 detections)
Missinka_River
Hominka_River
Misinchinka_River
Table_River
Anzac_River
Parsnip_River
Array
Oct 2018
Jan 2019
Apr 2019
Jul 2019
Oct 2019
tz: America/Vancouver
Section
Tributary
Mainstem

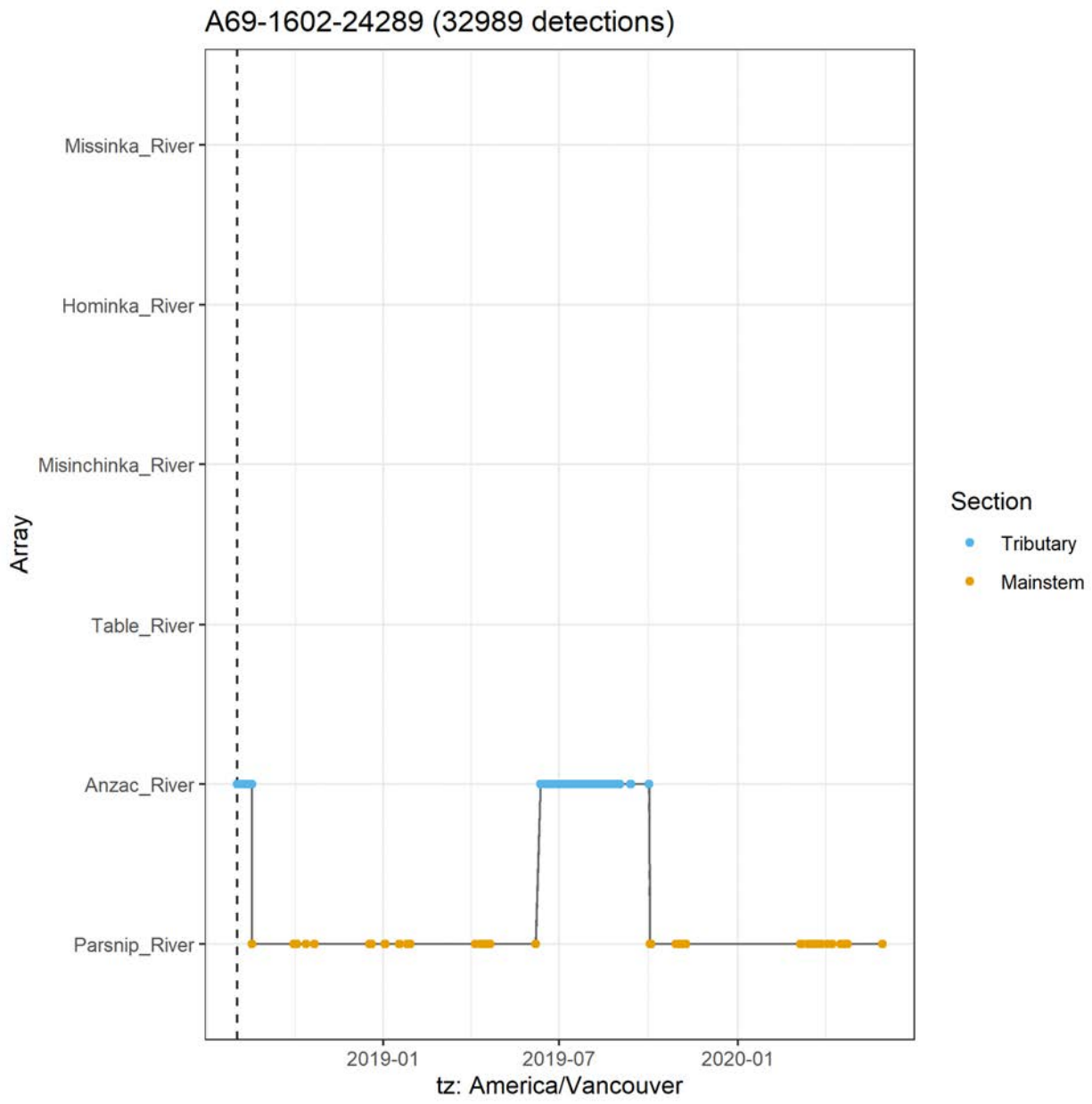
A69-1602-24289 (32989 detections)
Missinka_River
Hominka_River
Misinchinka_River
Table_River
Anzac_River
Parsnip_River
Array
2019-01
2019-07
2020-01
tz: America/Vancouver
Section
Tributary
Mainstem

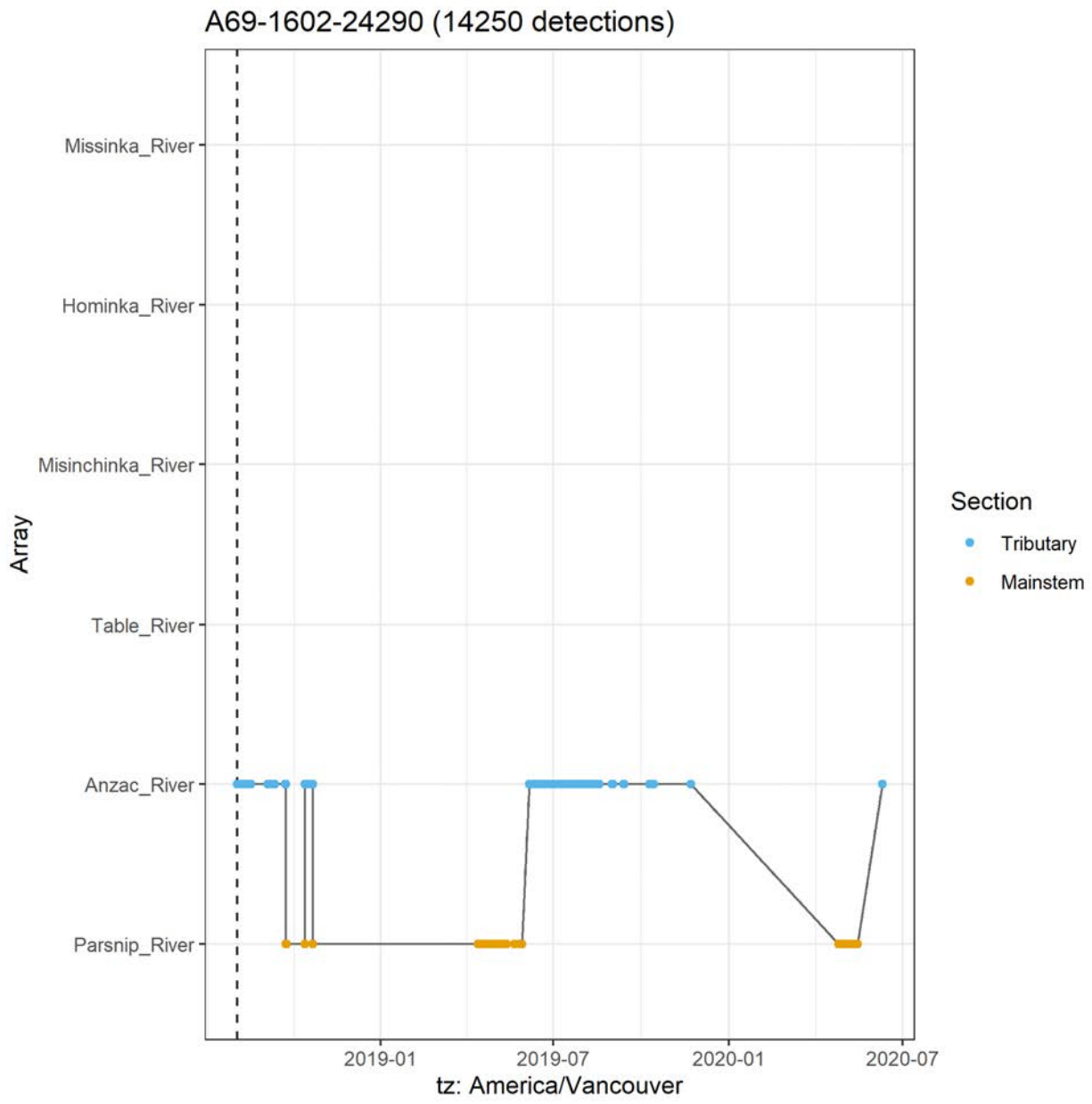
A69-1602-24290 (14250 detections)
Missinka_River
Hominka_River
Misinchinka_River
Table_River
Anzac_River
Parsnip_River
Array
2019-01
2019-07
2020-01
2020-07
tz: America/Vancouver
Section
Tributary
Mainstem

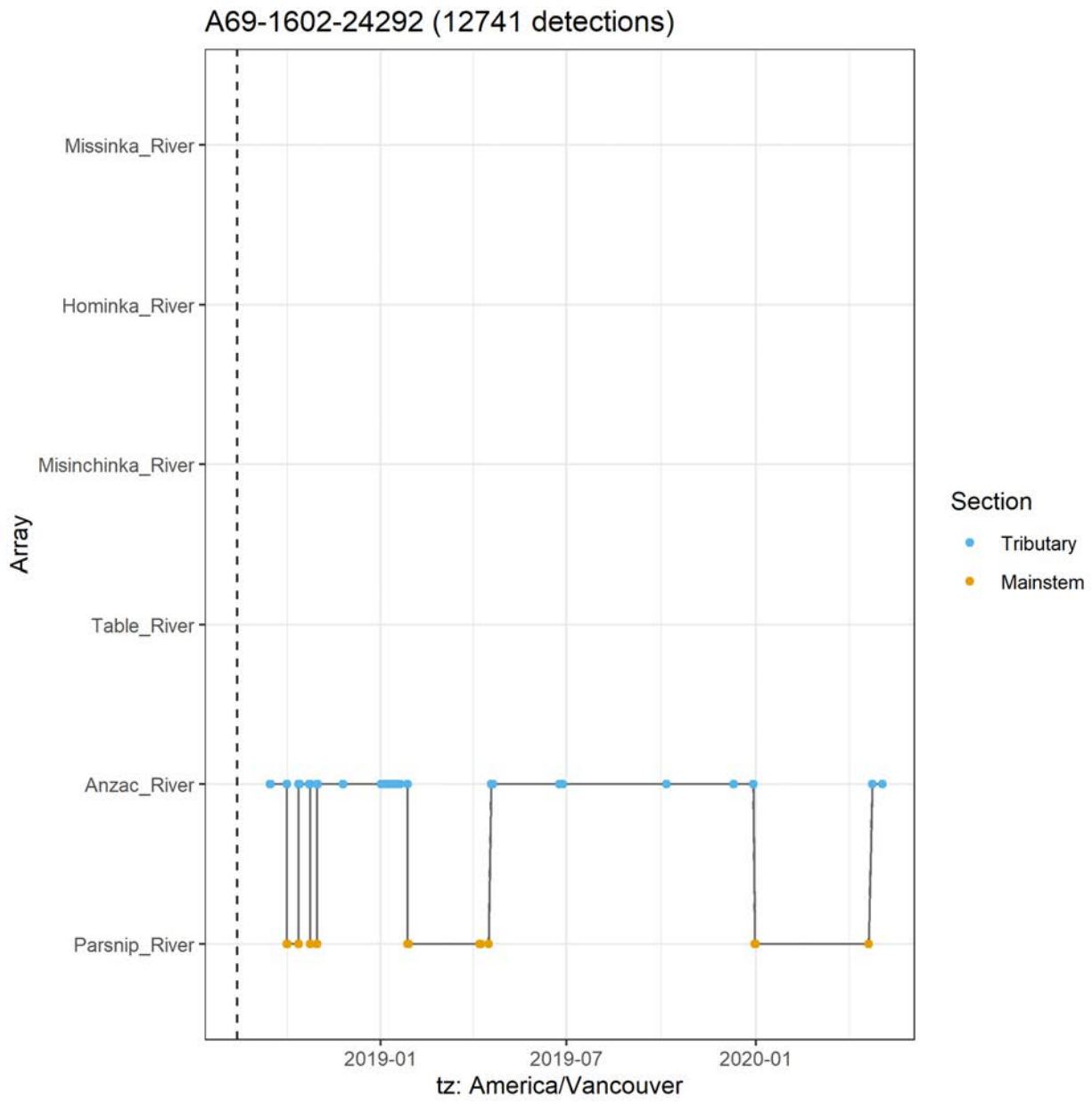
A69-1602-24292 (12741 detections)
Missinka_River
Hominka_River
Misinchinka_River
Table_River
Anzac_River
Parsnip_River
Array
2019-01
2019-07
2020-01
tz: America/Vancouver
Section
Tributary
Mainstem

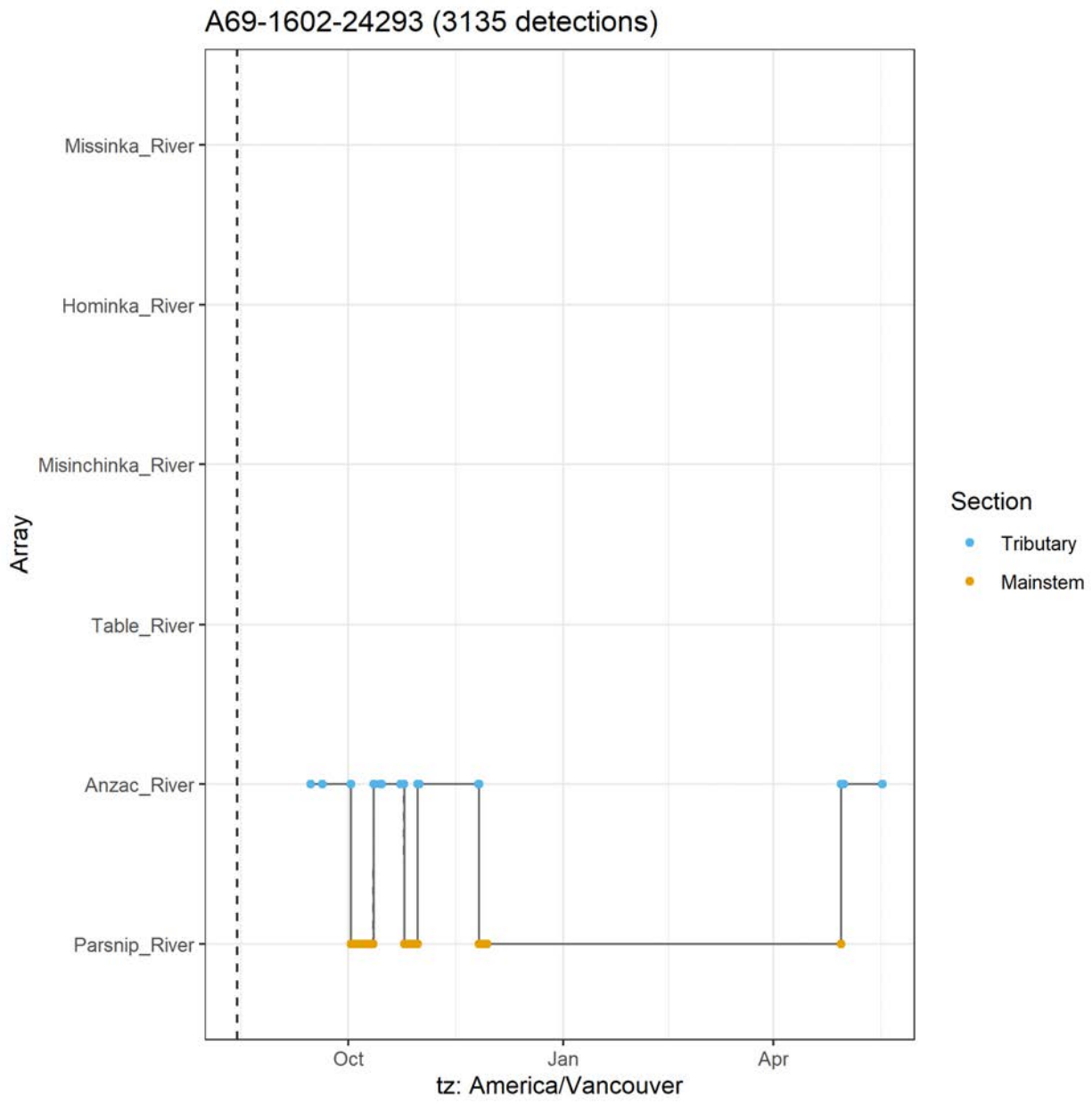
A69-1602-24293 (3135 detections)
Missinka_River
Hominka_River
Misinchinka_River
Table_River
Anzac_River
Parsnip_River
Array
Oct
Jan
Apr
tz: America/Vancouver
Section
Tributary
Mainstem

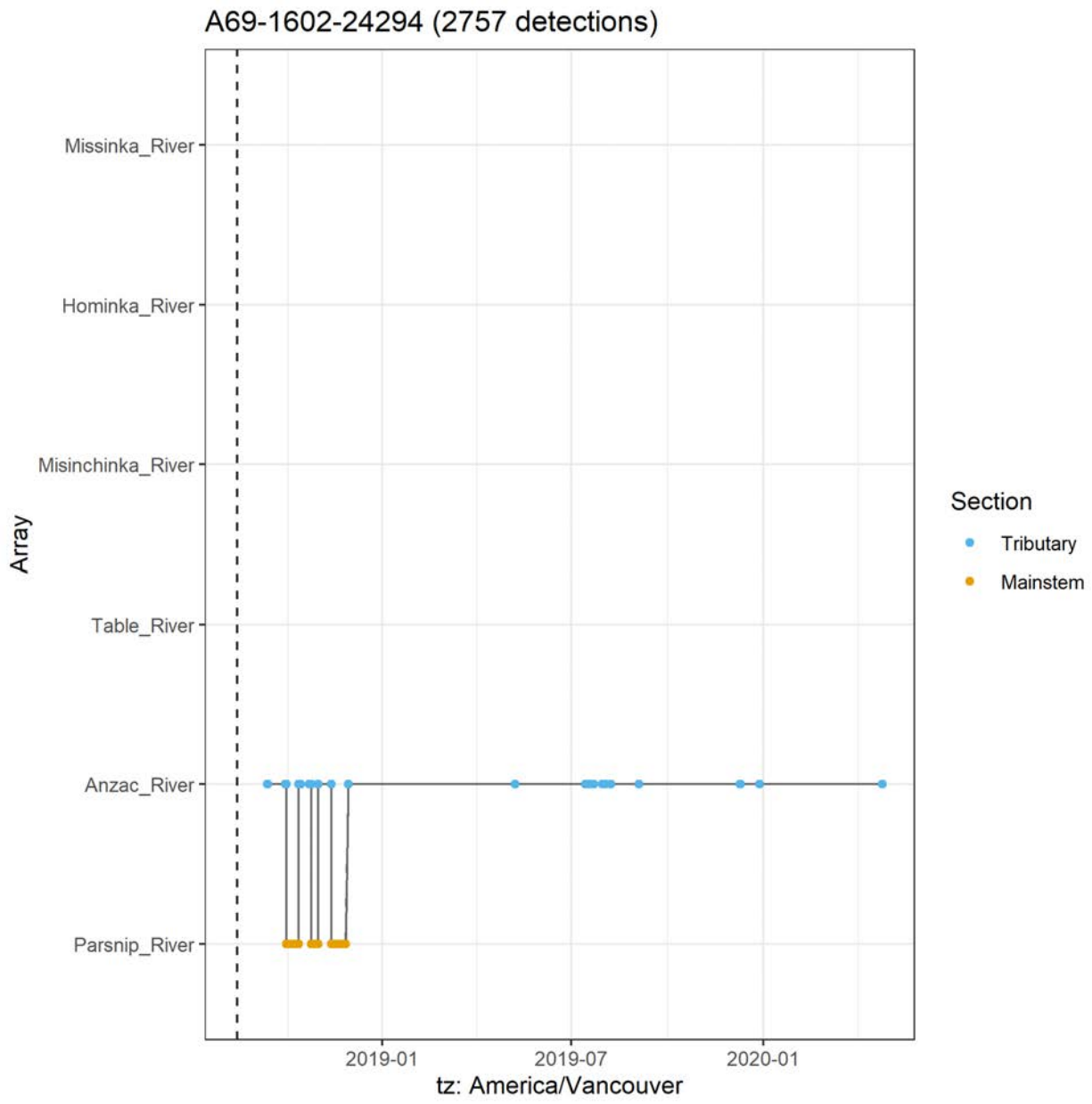
A69-1602-24294 (2757 detections)
Missinka_River
Hominka_River
Misinchinka_River
Table_River
Anzac_River
Parsnip_River
Array
2019-01
2019-07
2020-01
tz: America/Vancouver
Section
Tributary
Mainstem

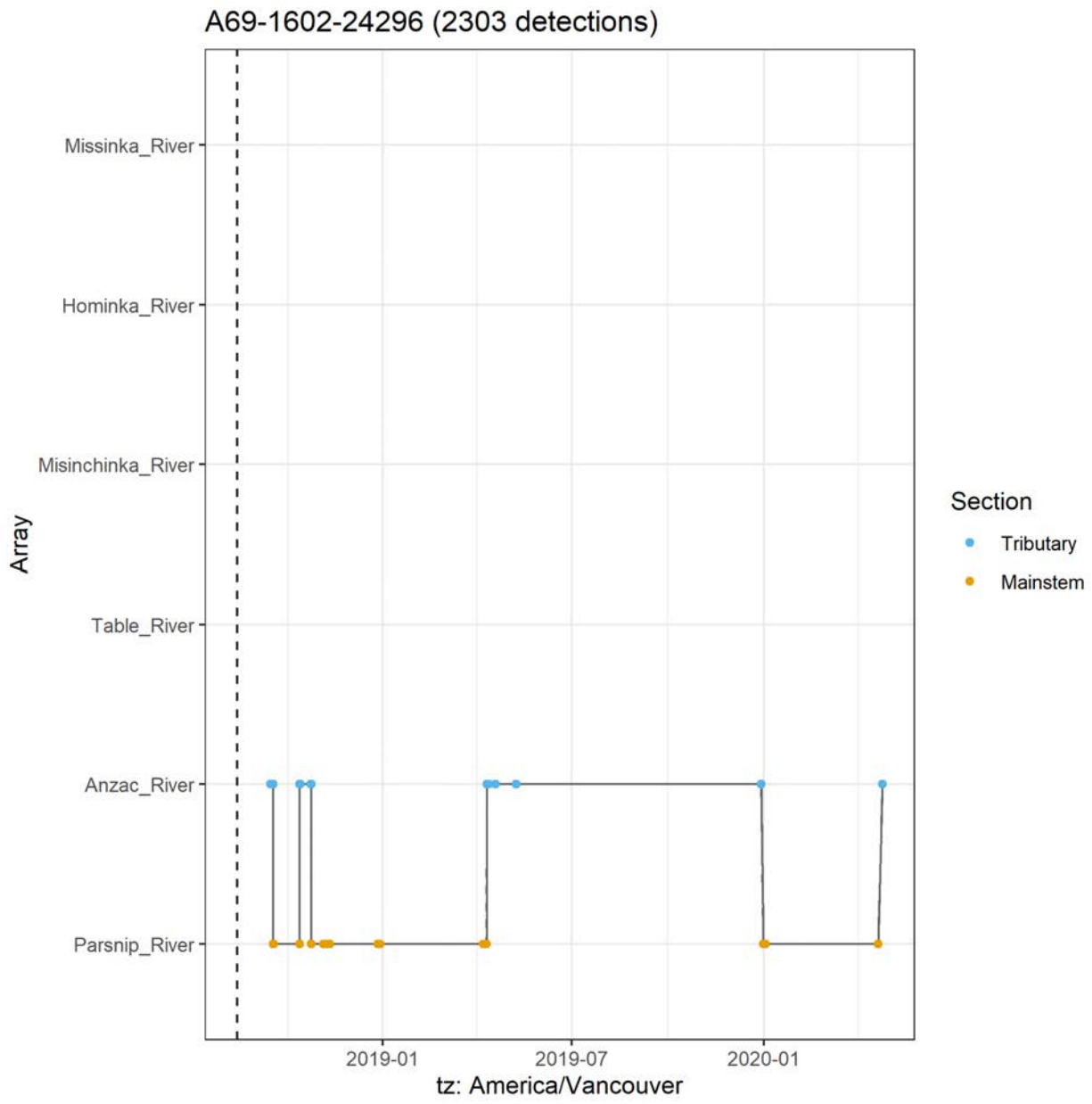
A69-1602-24296 (2303 detections)
Missinka_River
Hominka_River
Misinchinka_River
Table_River
Anzac_River
Parsnip_River
Array
2019-01
2019-07
2020-01
tz: America/Vancouver
Section
Tributary
Mainstem

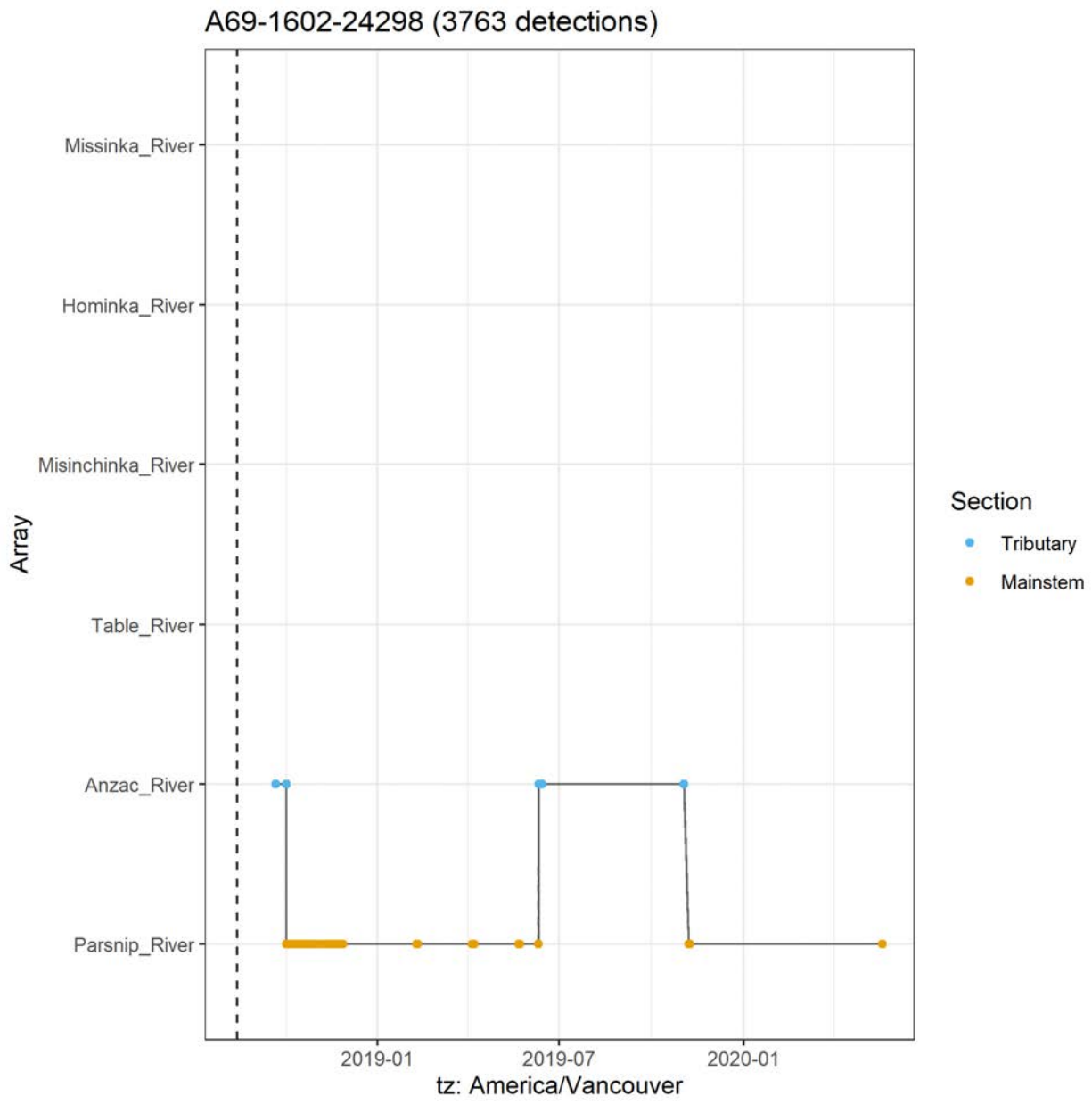
A69-1602-24298 (3763 detections)
Missinka_River
Hominka_River
Misinchinka_River
Table_River
Anzac_River
Parsnip_River
Array
2019-01
2019-07
2020-01
tz: America/Vancouver
Section
Tributary
Mainstem

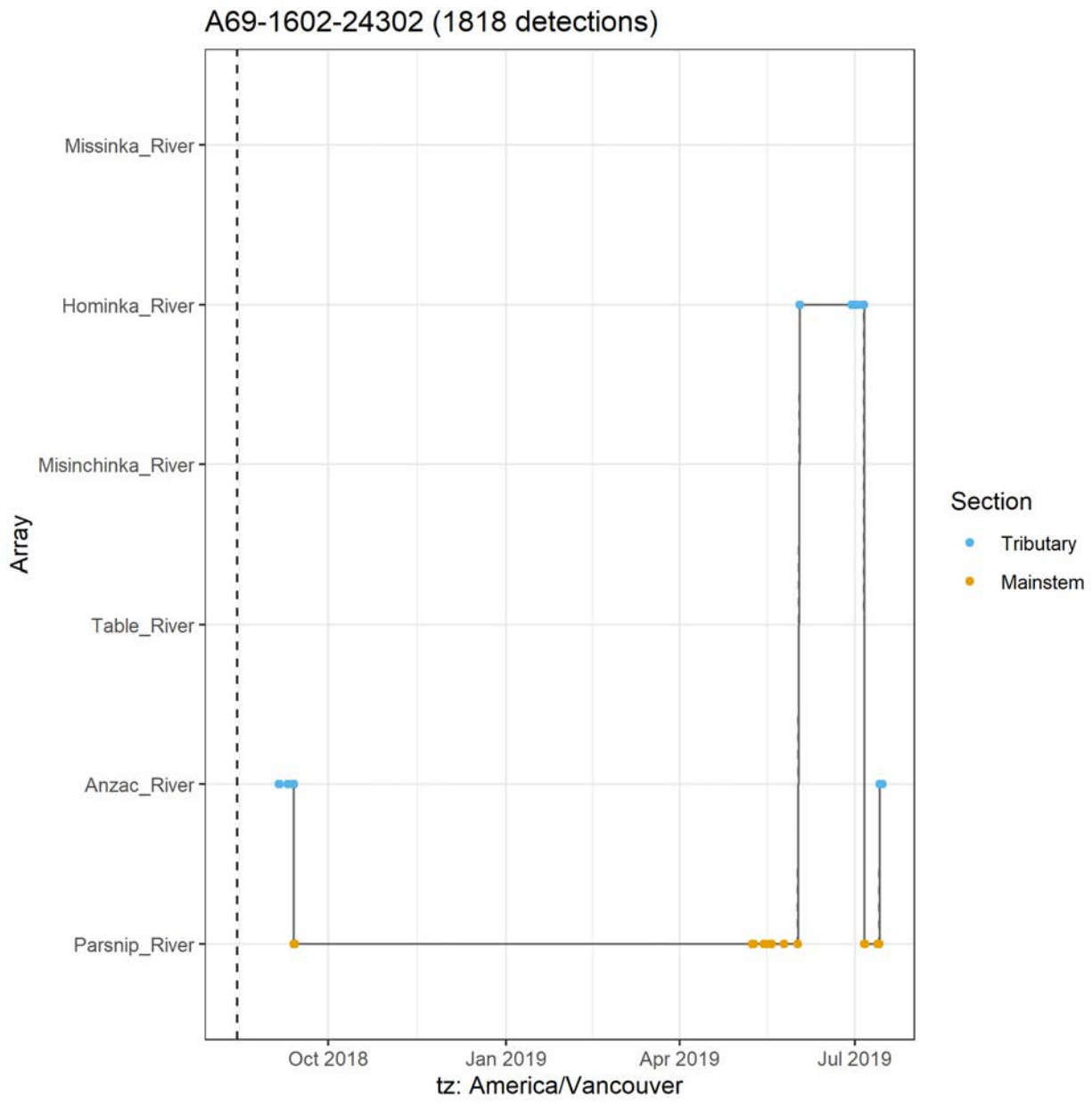
A69-1602-24302 (1818 detections)
Missinka_River
Hominka_River
Misinchinka_River
Table_River
Anzac_River
Parsnip_River
Array
Oct 2018
Jan 2019
Apr 2019
Jul 2019
tz: America/Vancouver
Section
Tributary
Mainstem

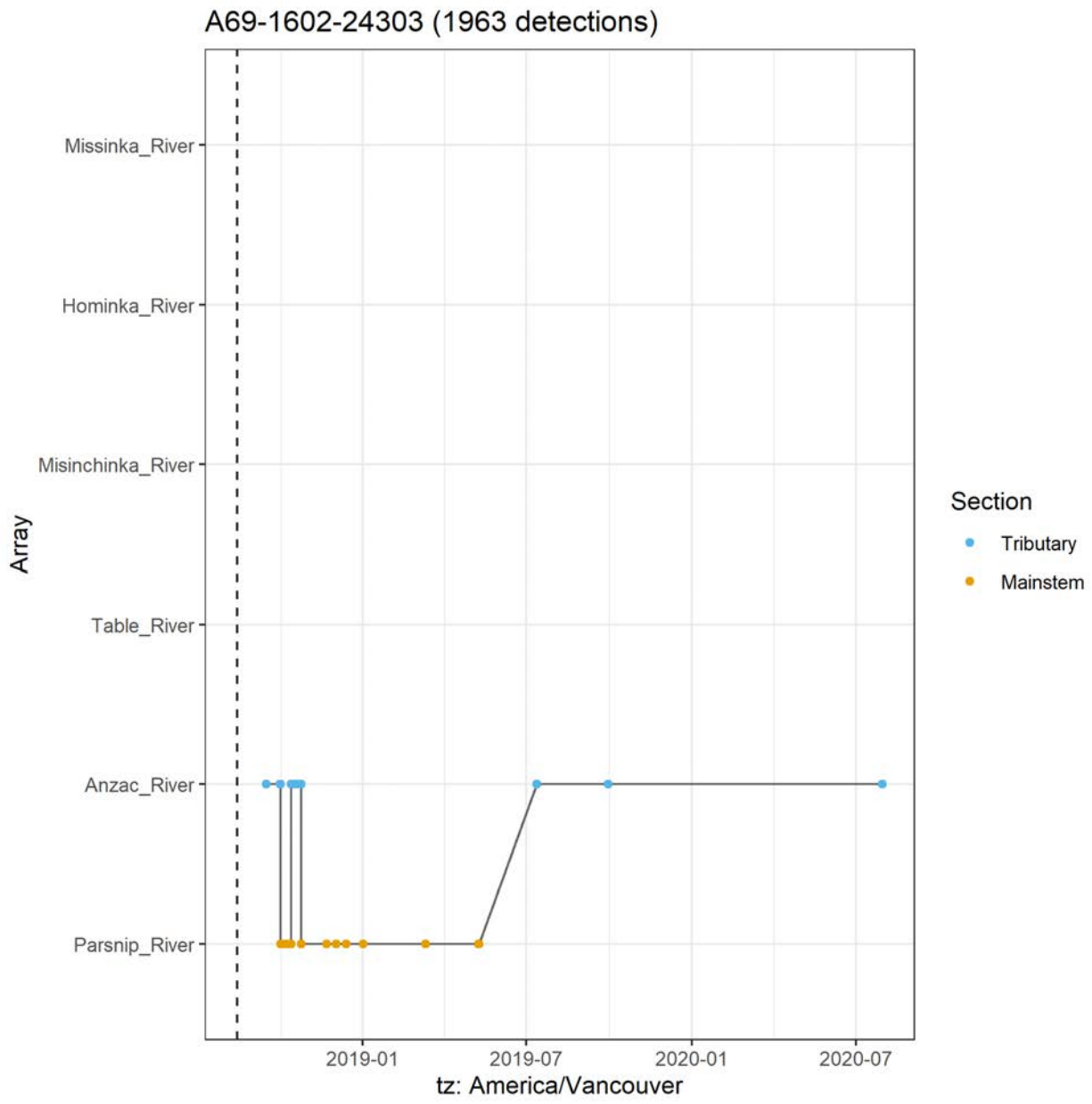
A69-1602-24303 (1963 detections)
Missinka_River
Hominka_River
Misinchinka_River
Table_River
Anzac_River
Parsnip_River
Array
2019-01
2019-07
2020-01
2020-07
tz: America/Vancouver
Section
Tributary
Mainstem

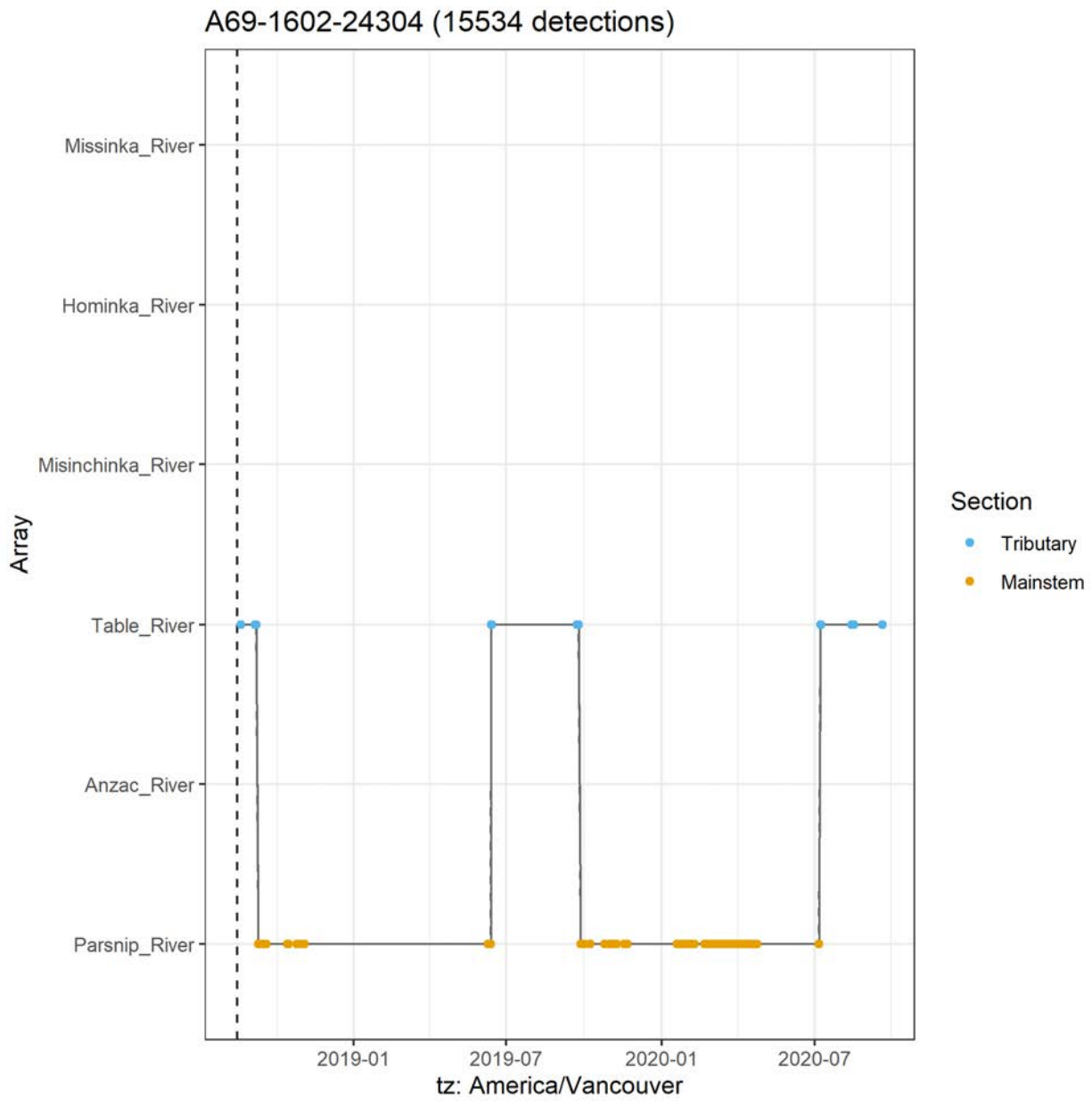
A69-1602-24304 (15534 detections)
Missinka_River
Hominka_River
Misinchinka_River
Table_River
Anzac_River
Parsnip_River
Array
2019-01
2019-07
2020-01
2020-07
tz: America/Vancouver
Section
Tributary
Mainstem

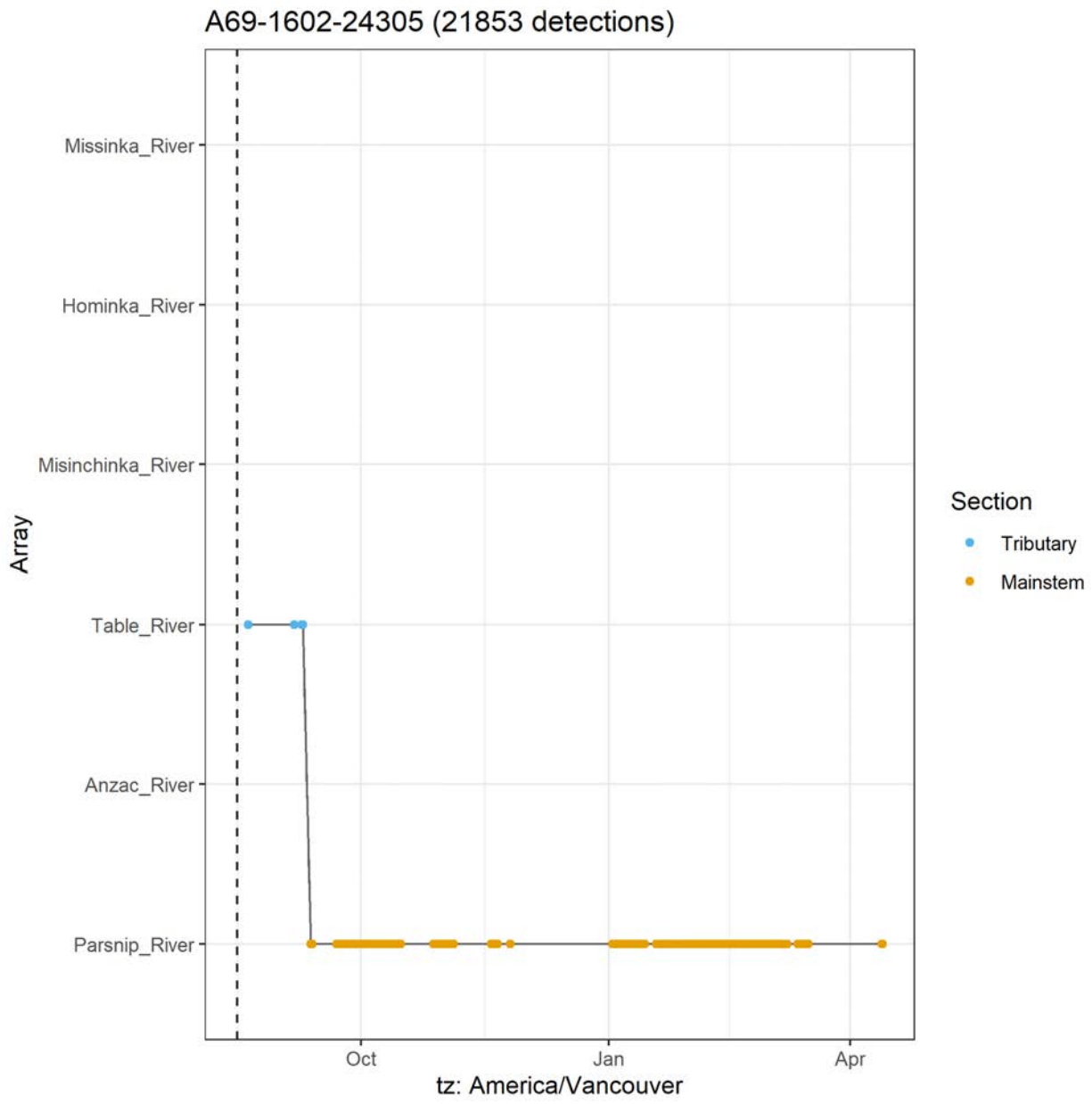
A69-1602-24305 (21853 detections)
Missinka_River
Hominka_River
Misinchinka_River
Table_River
Anzac_River
Parsnip_River
Array
Oct
Jan
Apr
tz: America/Vancouver
Section
Tributary
Mainstem

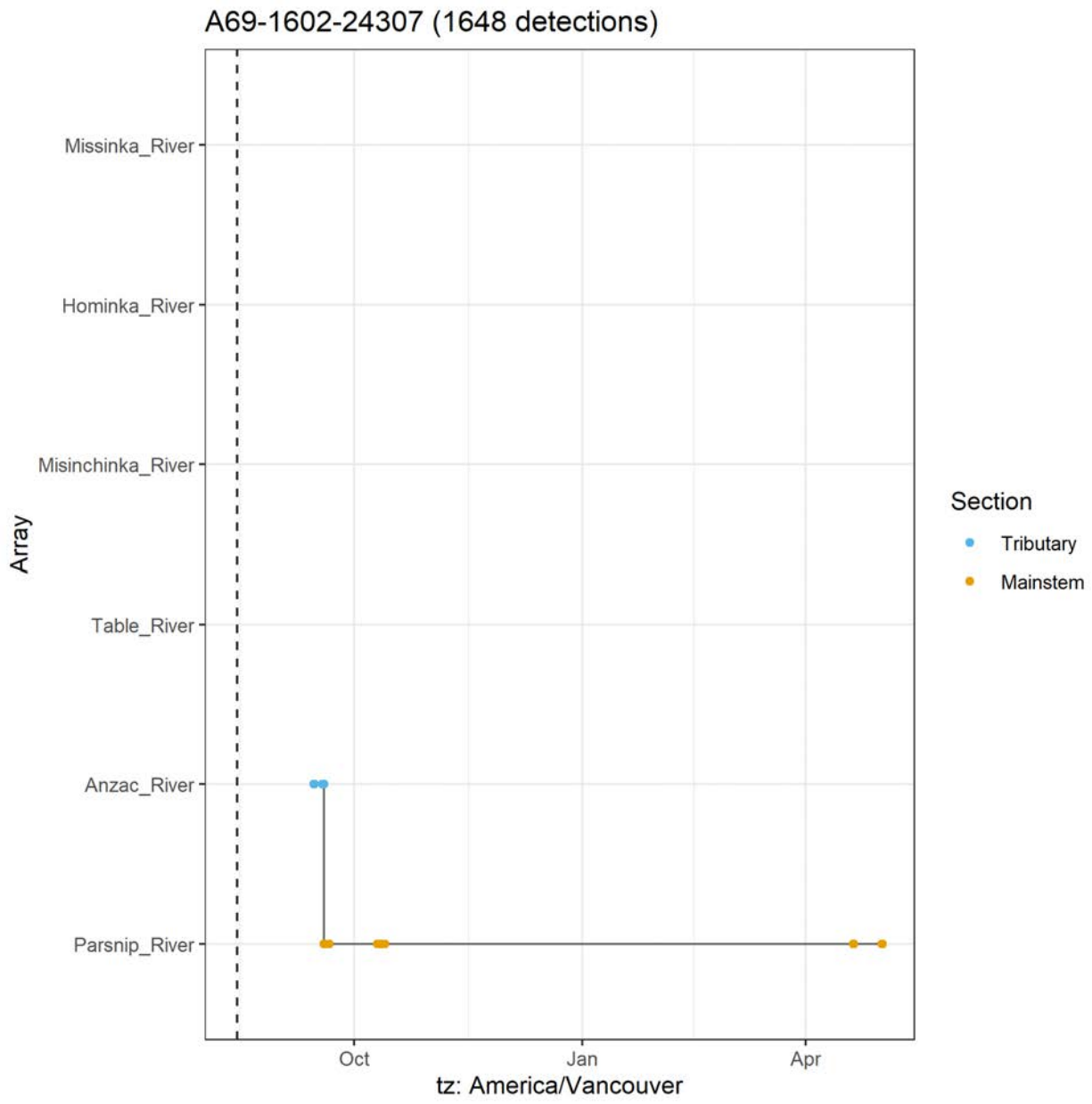
A69-1602-24307 (1648 detections)
Missinka_River
Hominka_River
Misinchinka_River
Table_River
Anzac_River
Parsnip_River
Array
Oct
Jan
Apr
tz: America/Vancouver
Section
Tributary
Mainstem

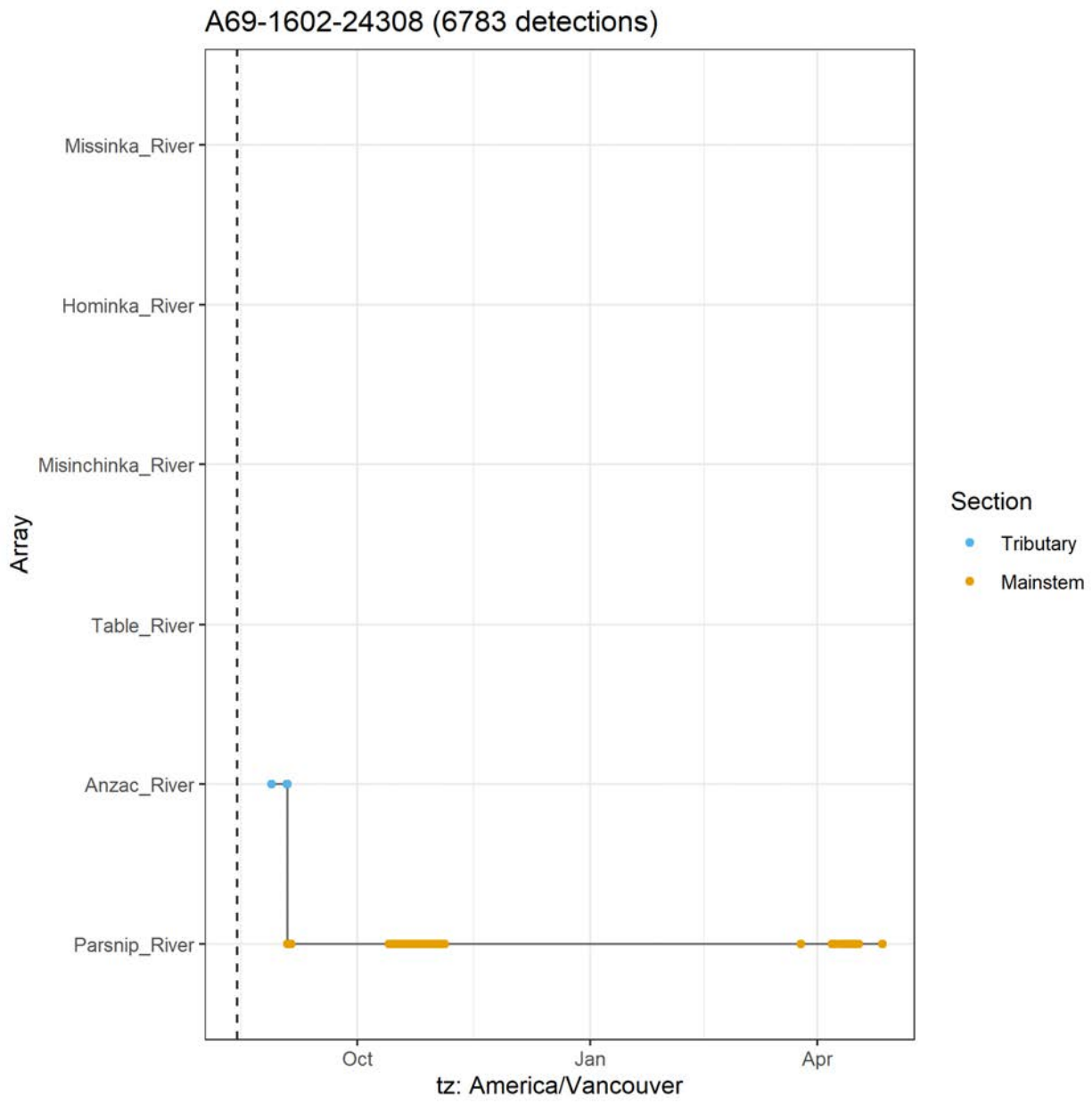
A69-1602-24308 (6783 detections)
Missinka_River
Hominka_River
Misinchinka_River
Table_River
Anzac_River
Parsnip_River
Array
Oct
Jan
Apr
tz: America/Vancouver
Section
Tributary
Mainstem

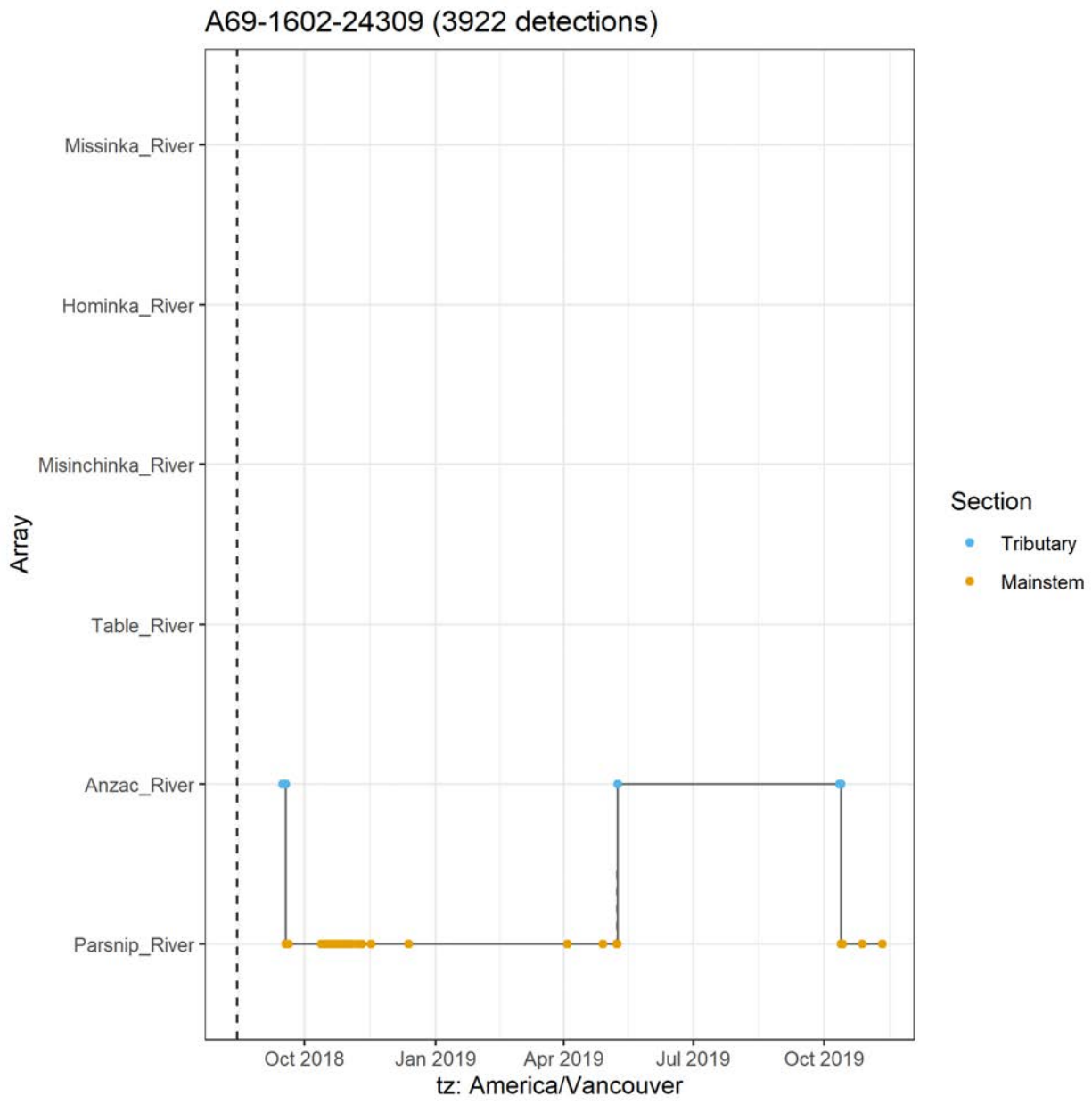
A69-1602-24309 (3922 detections)
Missinka_River
Hominka_River
Misinchinka_River
Table_River
Anzac_River
Parsnip_River
Array
Oct 2018
Jan 2019
Apr 2019
Jul 2019
Oct 2019
tz: America/Vancouver
Section
Tributary
Mainstem

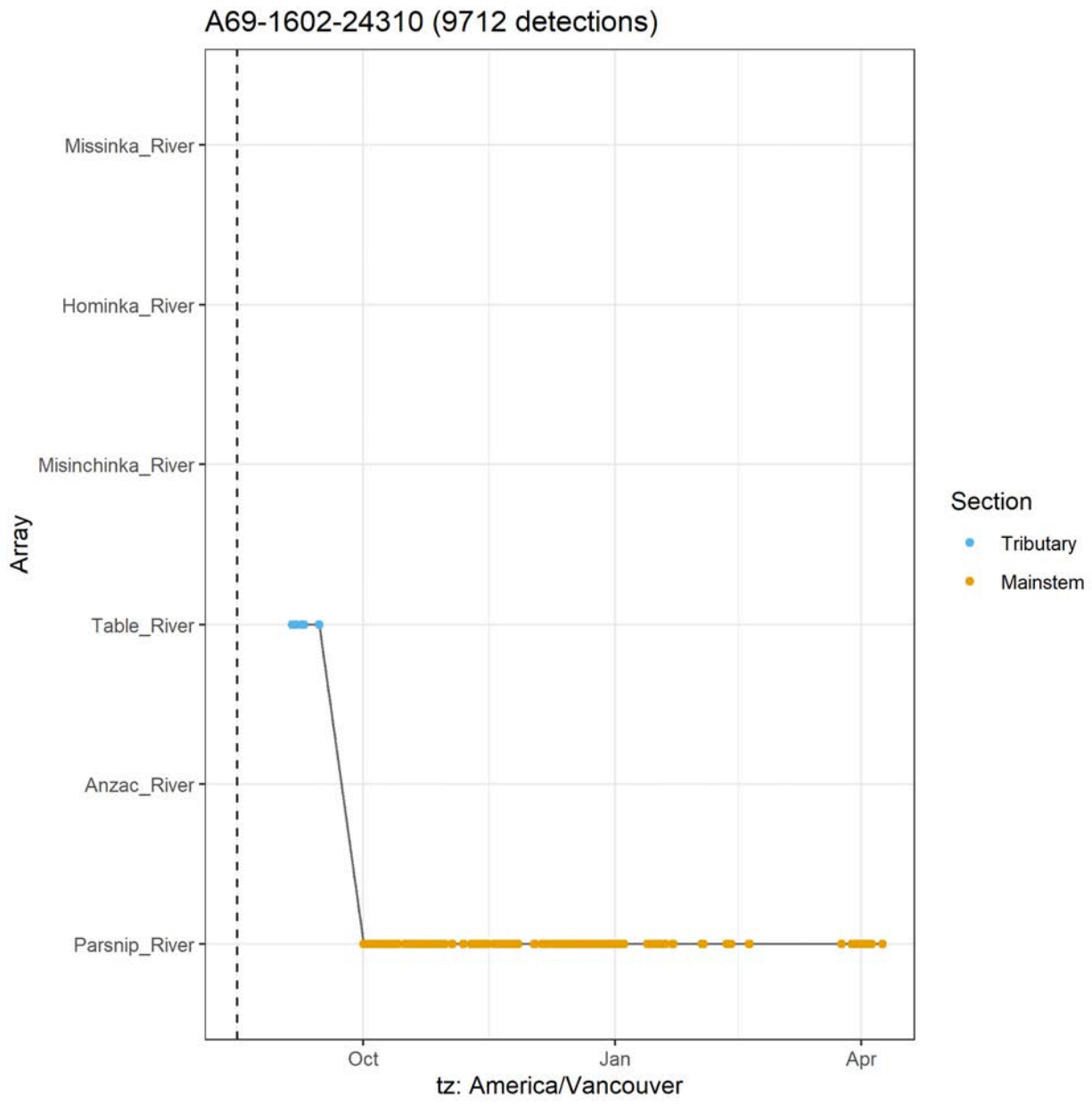
A69-1602-24310 (9712 detections)
Missinka_River
Hominka_River
Misinchinka_River
Table_River
Anzac_River
Parsnip_River
Array
Oct
Jan
Apr
tz: America/Vancouver
Section
Tributary
Mainstem

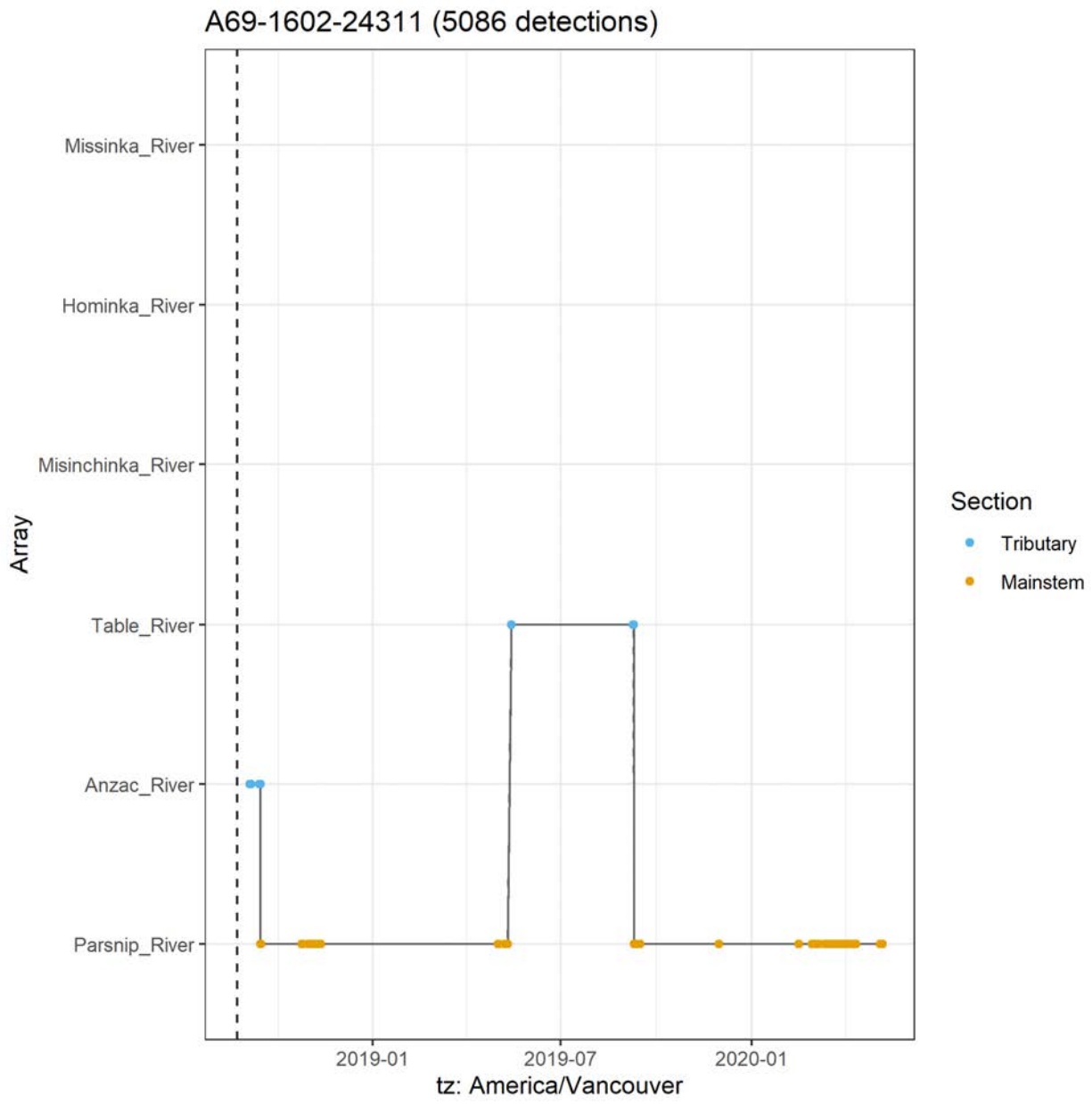
A69-1602-24311 (5086 detections)
Missinka_River
Hominka_River
Misinchinka_River
Table_River
Anzac_River
Parsnip_River
Array
2019-01
2019-07
2020-01
tz: America/Vancouver
Section
Tributary
Mainstem

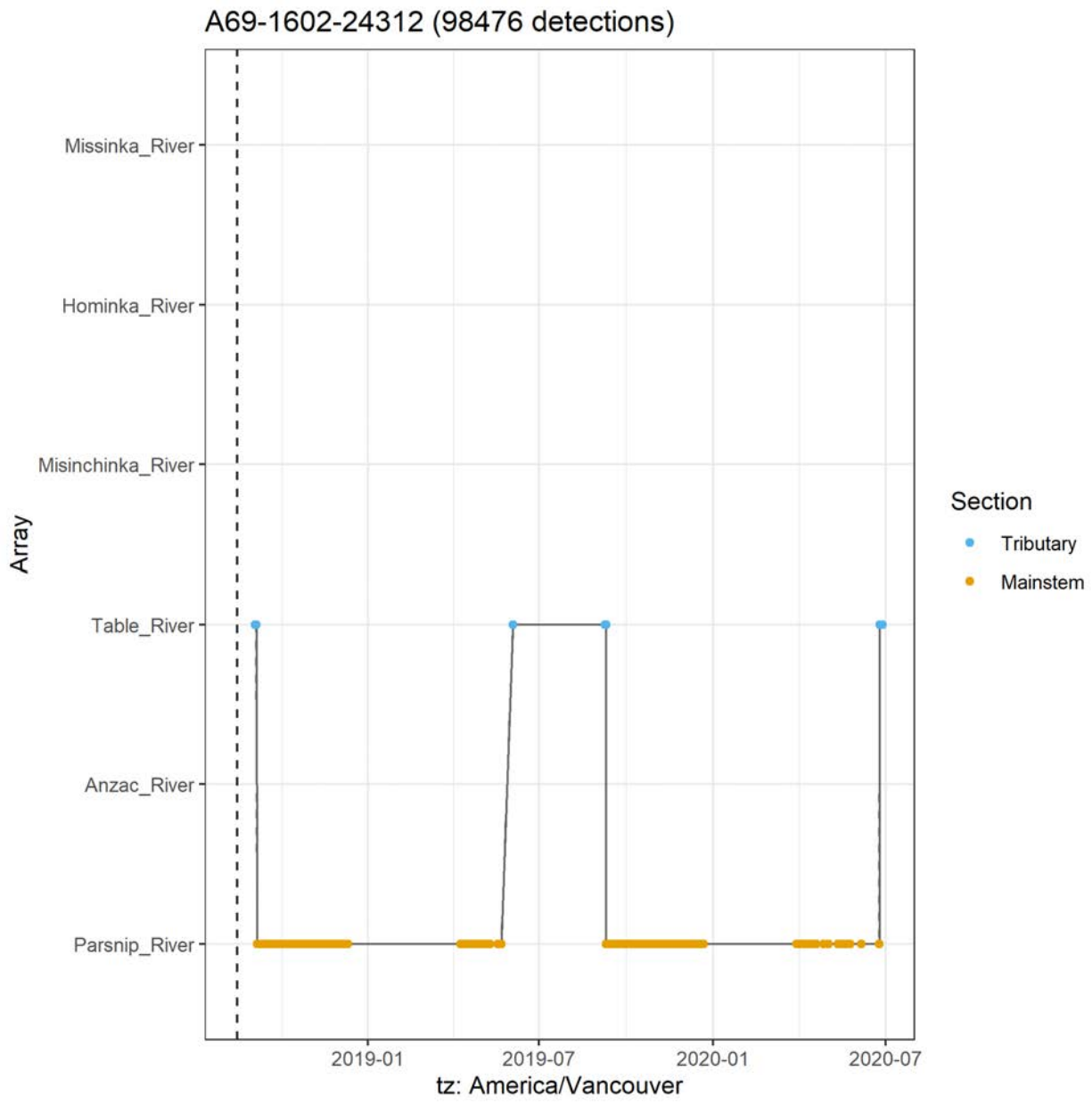
A69-1602-24312 (98476 detections)
Missinka_River
Hominka_River
Misinchinka_River
Table_River
Anzac_River
Parsnip_River
Array
2019-01
2019-07
2020-01
2020-07
tz: America/Vancouver
Section
Tributary
Mainstem

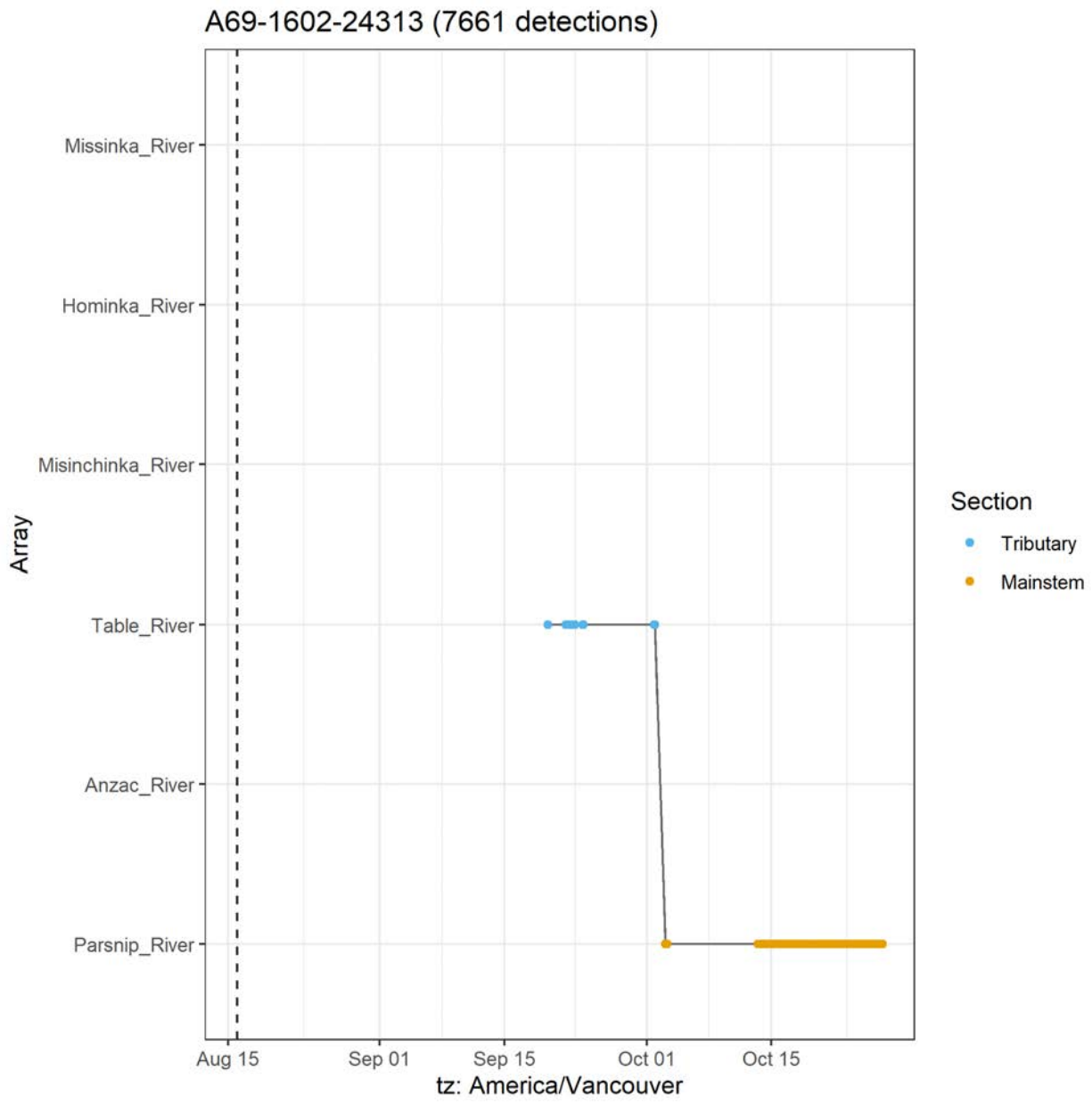
A69-1602-24313 (7661 detections)
Missinka_River
Hominka_River
Misinchinka_River
Table_River
Anzac_River
Parsnip_River
Array
Aug 15
Sep 01
Sep 15
Oct 01
Oct 15
tz: America/Vancouver
Section
Tributary
Mainstem

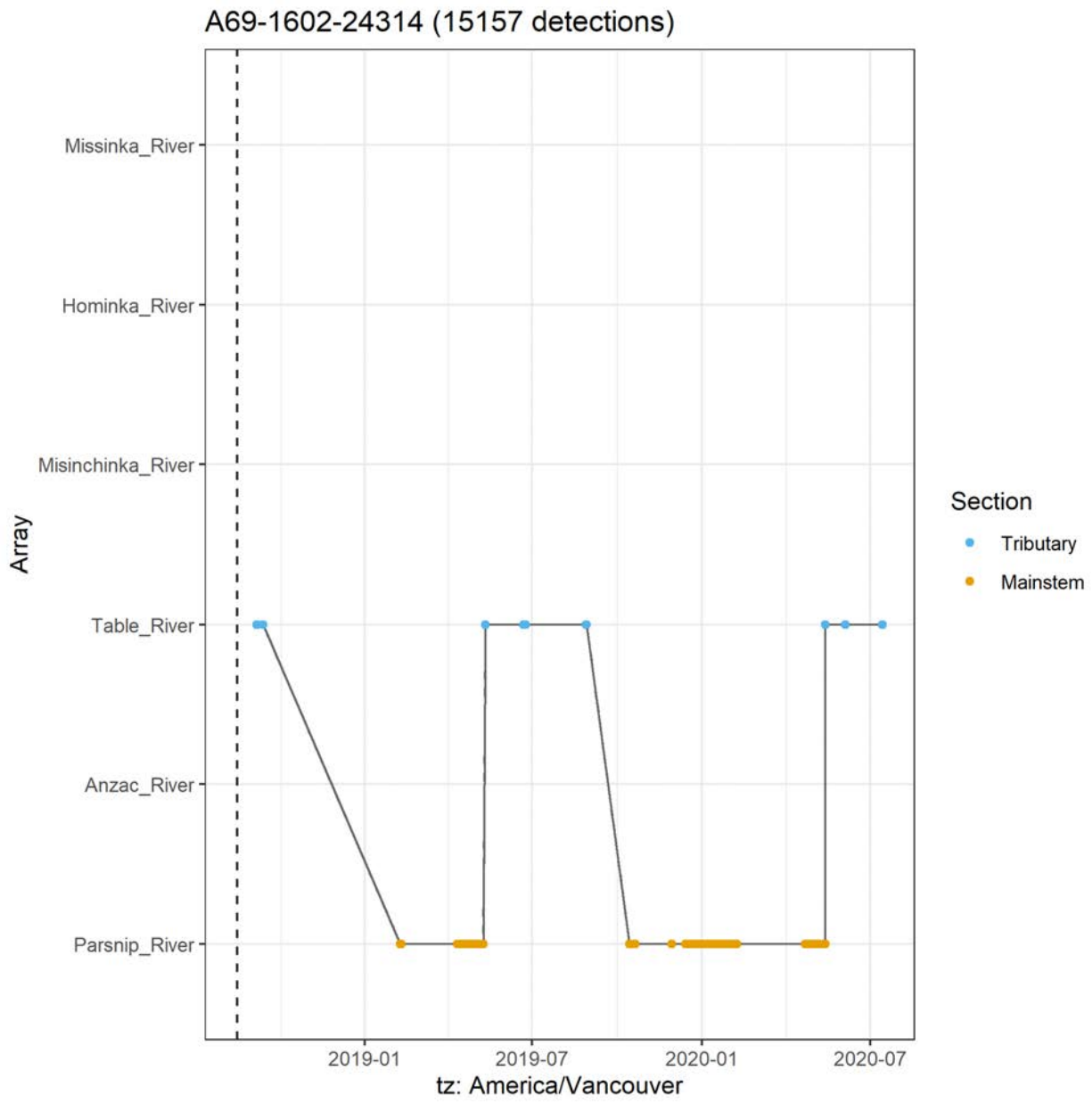
A69-1602-24314 (15157 detections)
Missinka_River
Hominka_River
Misinchinka_River
Table_River
Anzac_River
Parsnip_River
Array
2019-01
2019-07
2020-01
2020-07
tz: America/Vancouver
Section
Tributary
Mainstem

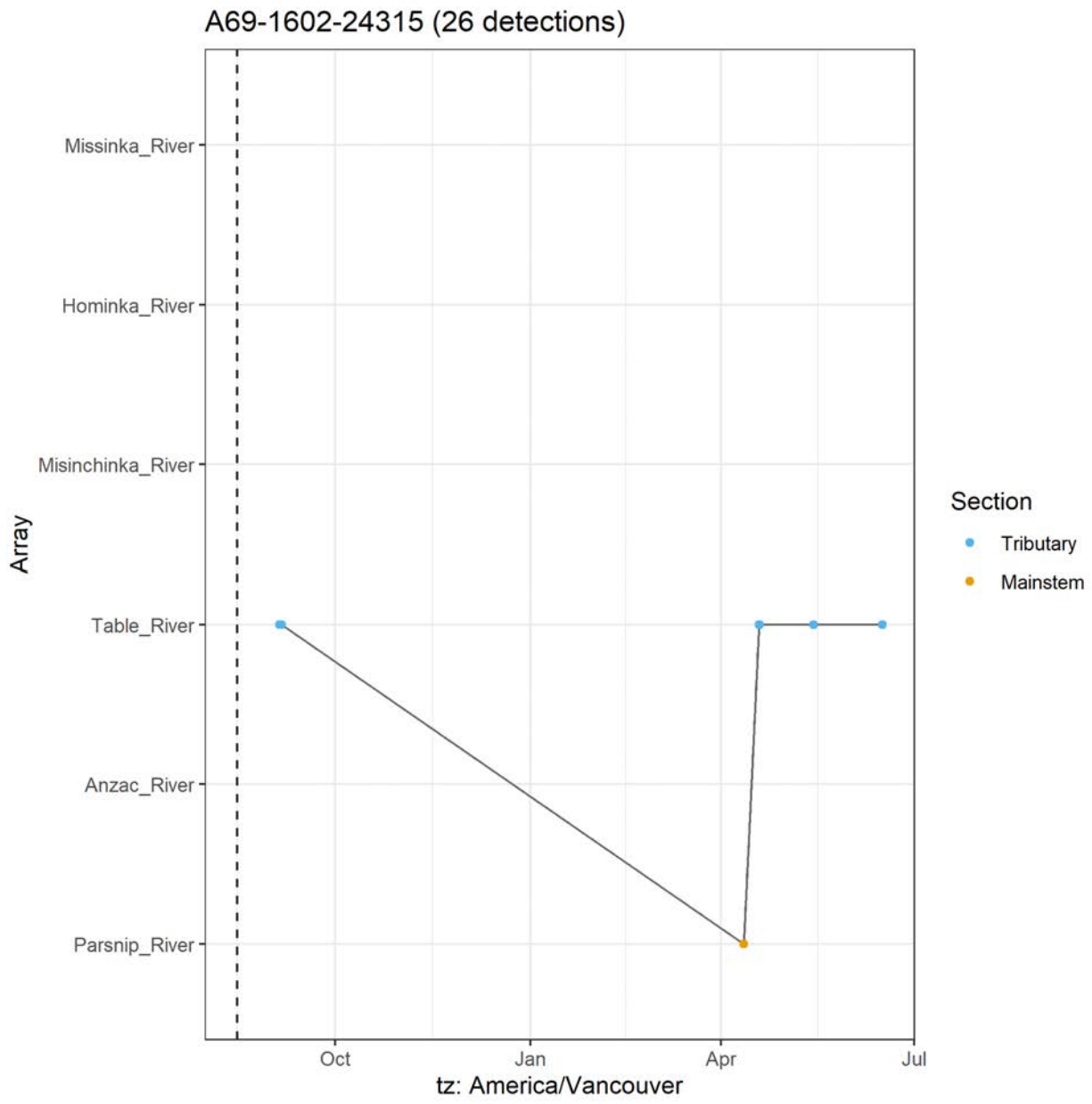
A69-1602-24315 (26 detections)
Missinka_River
Hominka_River
Misinchinka_River
Table_River
Anzac_River
Parsnip_River
Array
Oct
Jan
Apr
Jul
tz: America/Vancouver
Section
Tributary
Mainstem

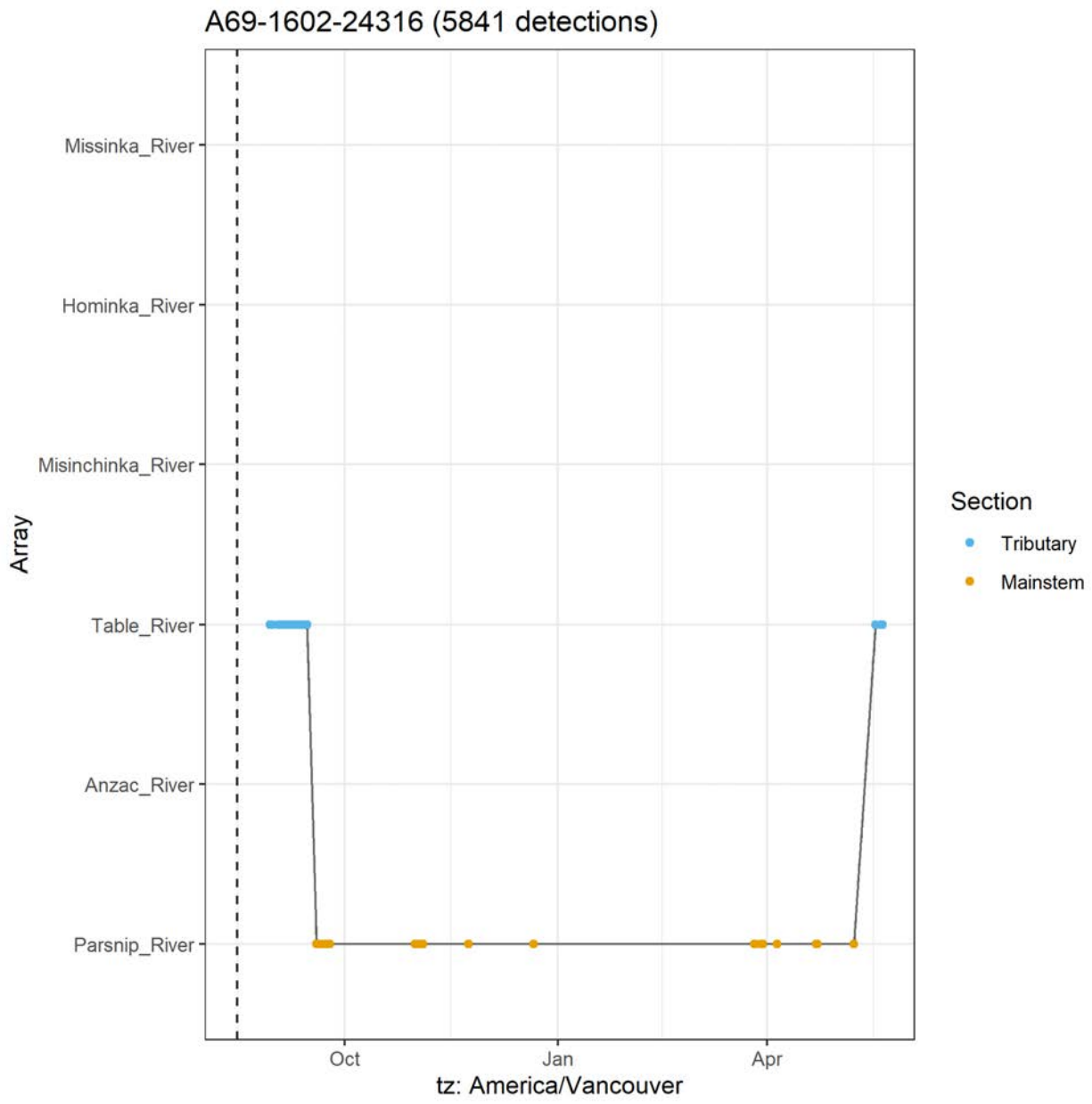
A69-1602-24316 (5841 detections)
Missinka_River
Hominka_River
Misinchinka_River
Table_River
Anzac_River
Parsnip_River
Array
Oct
Jan
Apr
tz: America/Vancouver
Section
Tributary
Mainstem

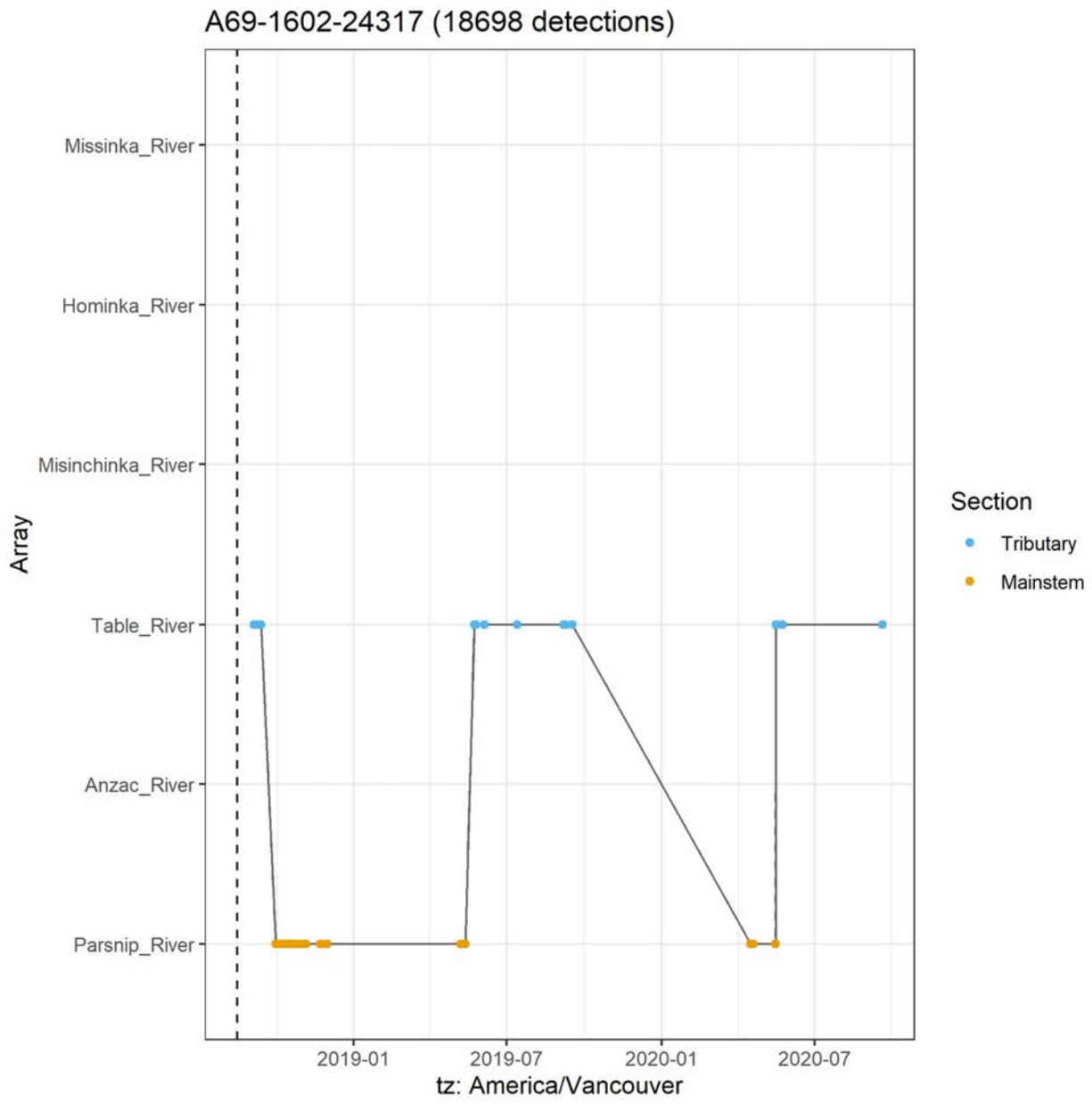
A69-1602-24317 (18698 detections)
Missinka_River
Hominka_River
Misinchinka_River
Table_River
Anzac_River
Parsnip_River
Array
2019-01
2019-07
2020-01
2020-07
tz: America/Vancouver
Section
Tributary
Mainstem

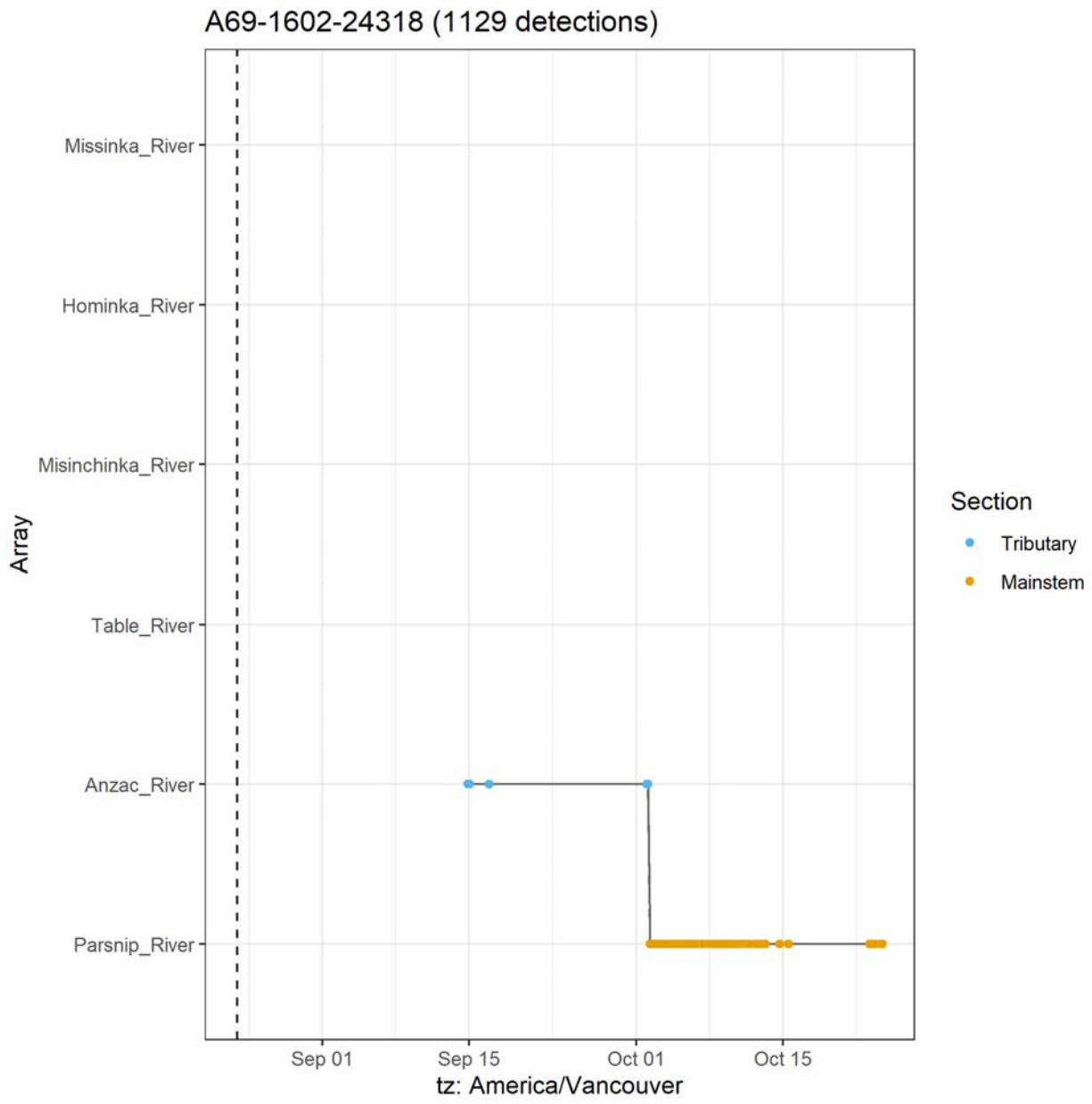
A69-1602-24318 (1129 detections)
Missinka_River
Hominka_River
Misinchinka_River
Table_River
Anzac_River
Parsnip_River
Array
Sep 01
Sep 15
Oct 01
Oct 15
tz: America/Vancouver
Section
Tributary
Mainstem

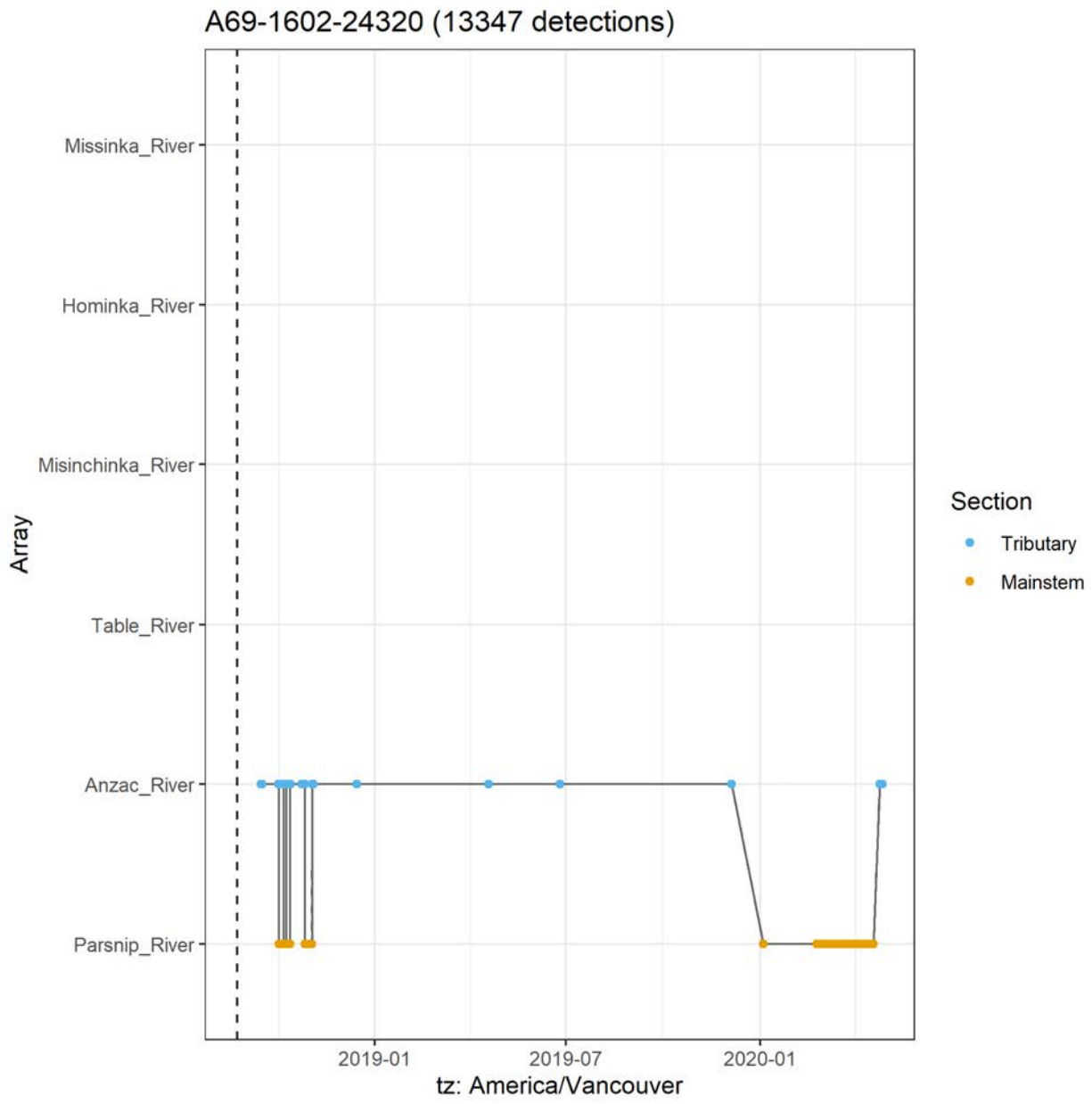
A69-1602-24320 (13347 detections)
Missinka_River
Hominka_River
Misinchinka_River
Table_River
Anzac_River
Parsnip_River
Array
2019-01
2019-07
2020-01
tz: America/Vancouver
Section
Tributary
Mainstem

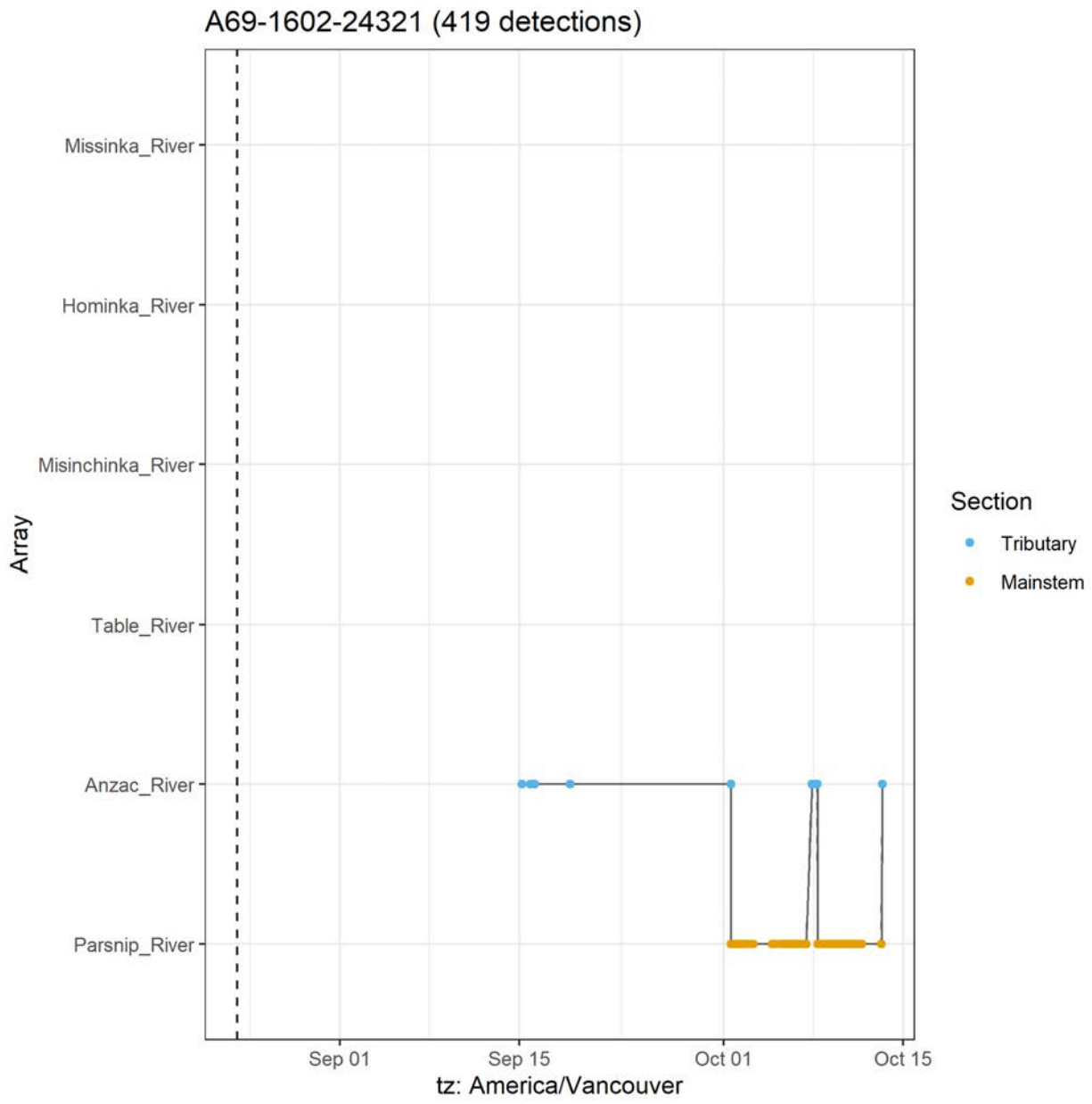
A69-1602-24321 (419 detections)
Missinka_River
Hominka_River
Misinchinka_River
Table_River
Anzac_River
Parsnip_River
Array
Sep 01
Sep 15
Oct 01
Oct 15
tz: America/Vancouver
Section
Tributary
Mainstem

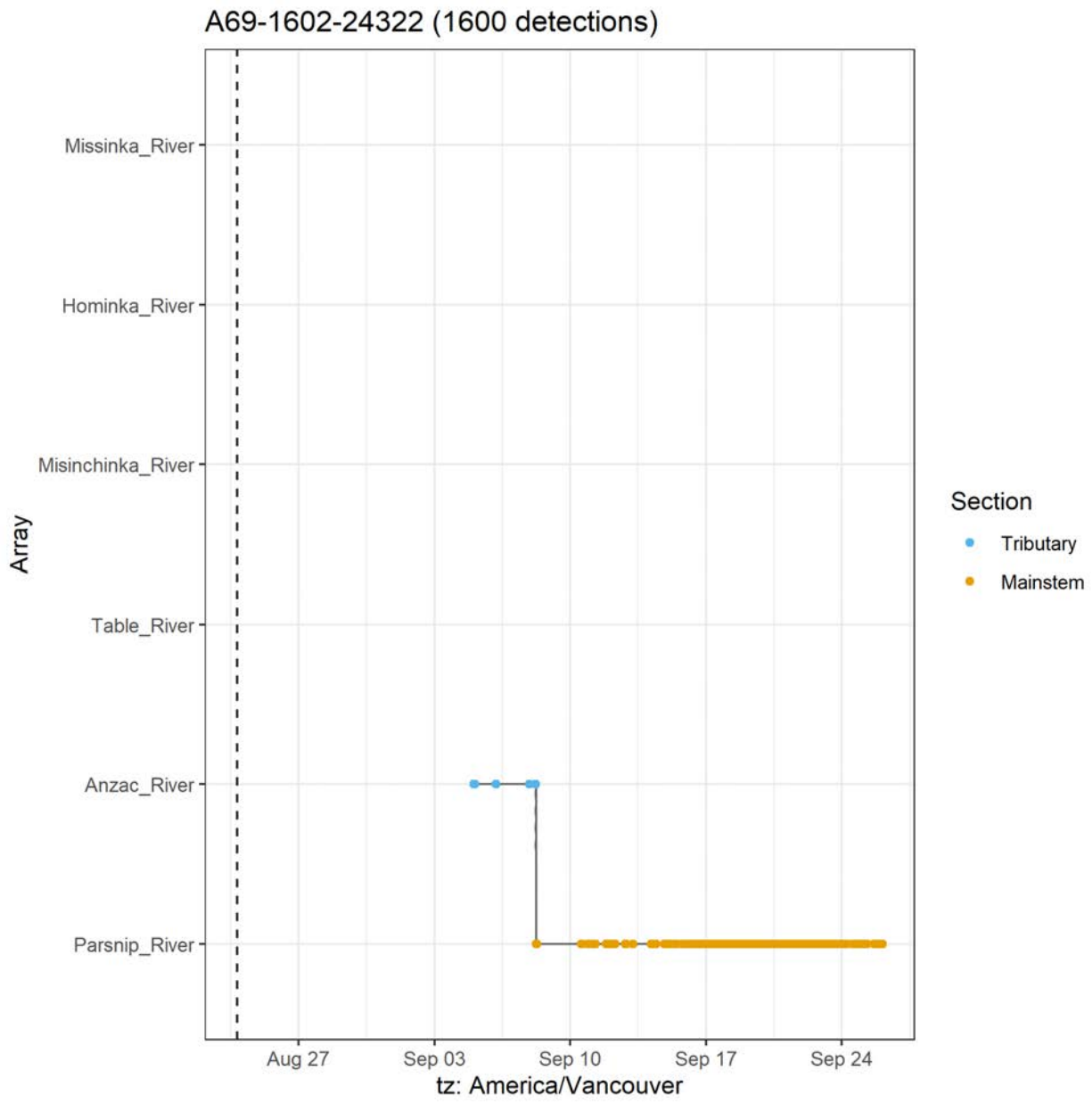
A69-1602-24322 (1600 detections)
Missinka_River
Hominka_River
Misinchinka_River
Table_River
Anzac_River
Parsnip_River
Array
Aug 27
Sep 03
Sep 10
Sep 17
Sep 24
tz: America/Vancouver
Section
Tributary
Mainstem

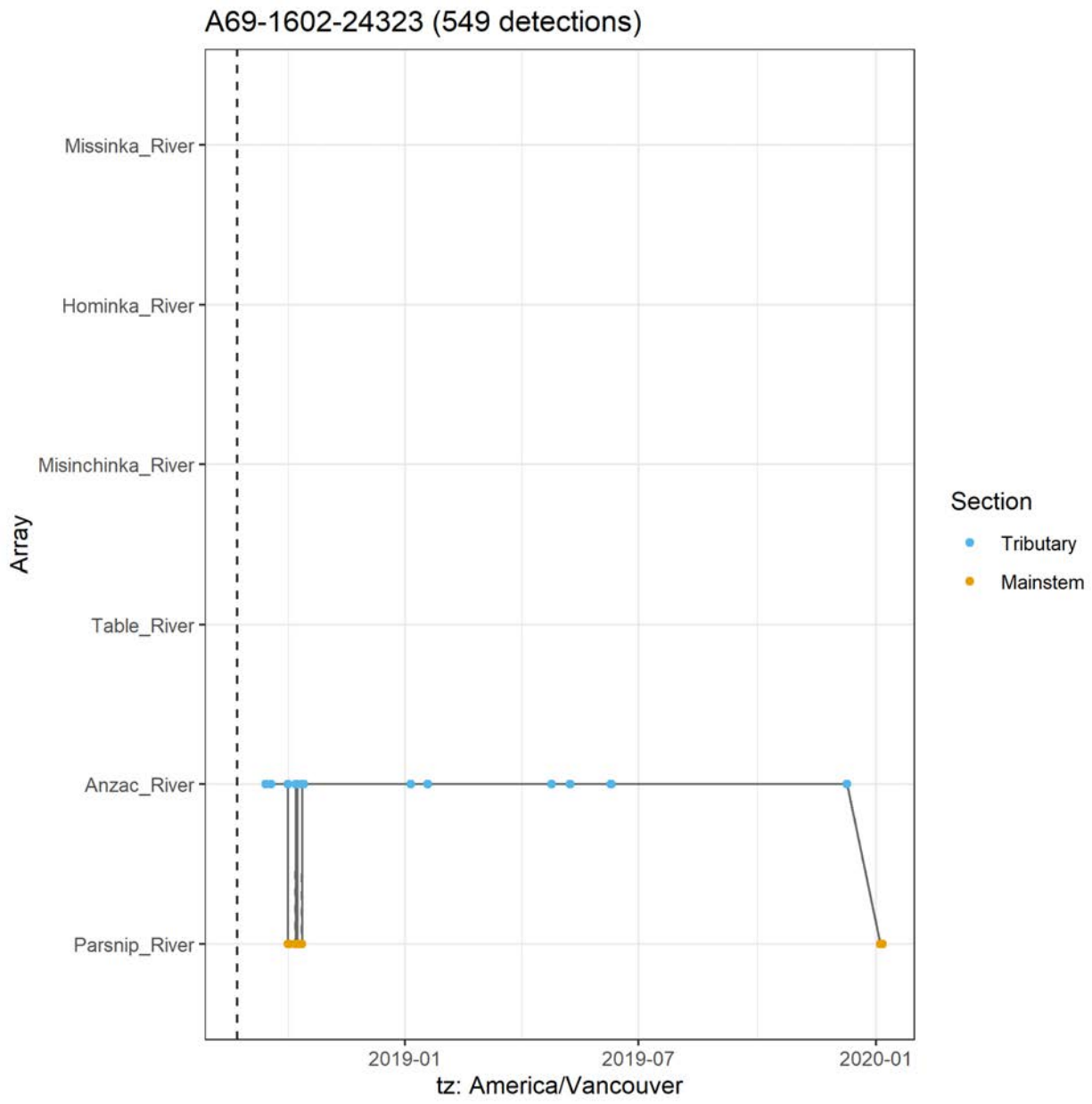
A69-1602-24323 (549 detections)
Missinka_River
Hominka_River
Misinchinka_River
Table_River
Anzac_River
Parsnip_River
Array
2019-01
2019-07
2020-01
tz: America/Vancouver
Section
Tributary
Mainstem

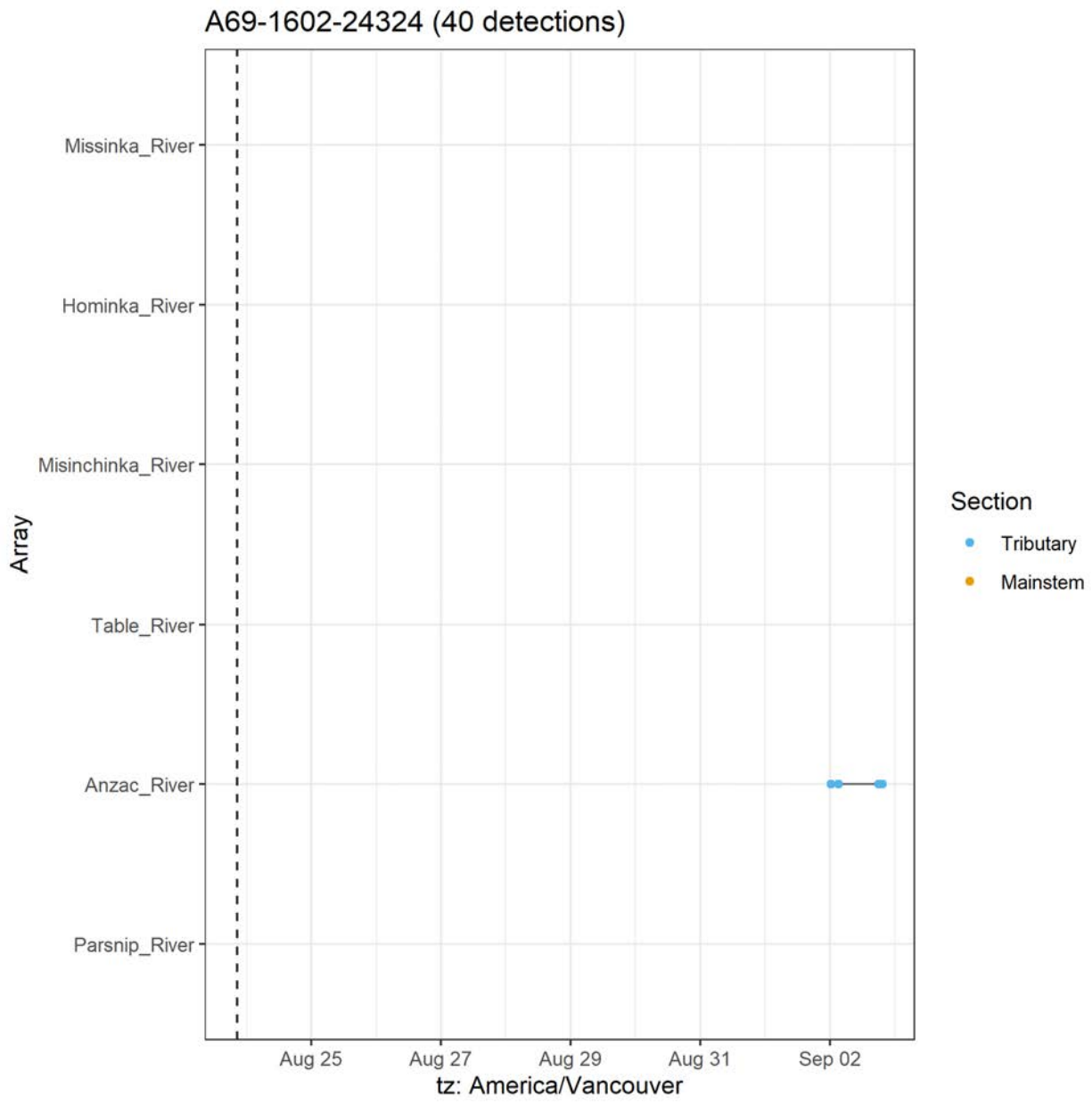
A69-1602-24324 (40 detections)
Missinka_River
Hominka_River
Misinchinka_River
Table_River
Anzac_River
Parsnip_River
Array
Aug 25
Aug 27
Aug 29
Aug 31
Sep 02
tz: America/Vancouver
Section
Tributary
Mainstem

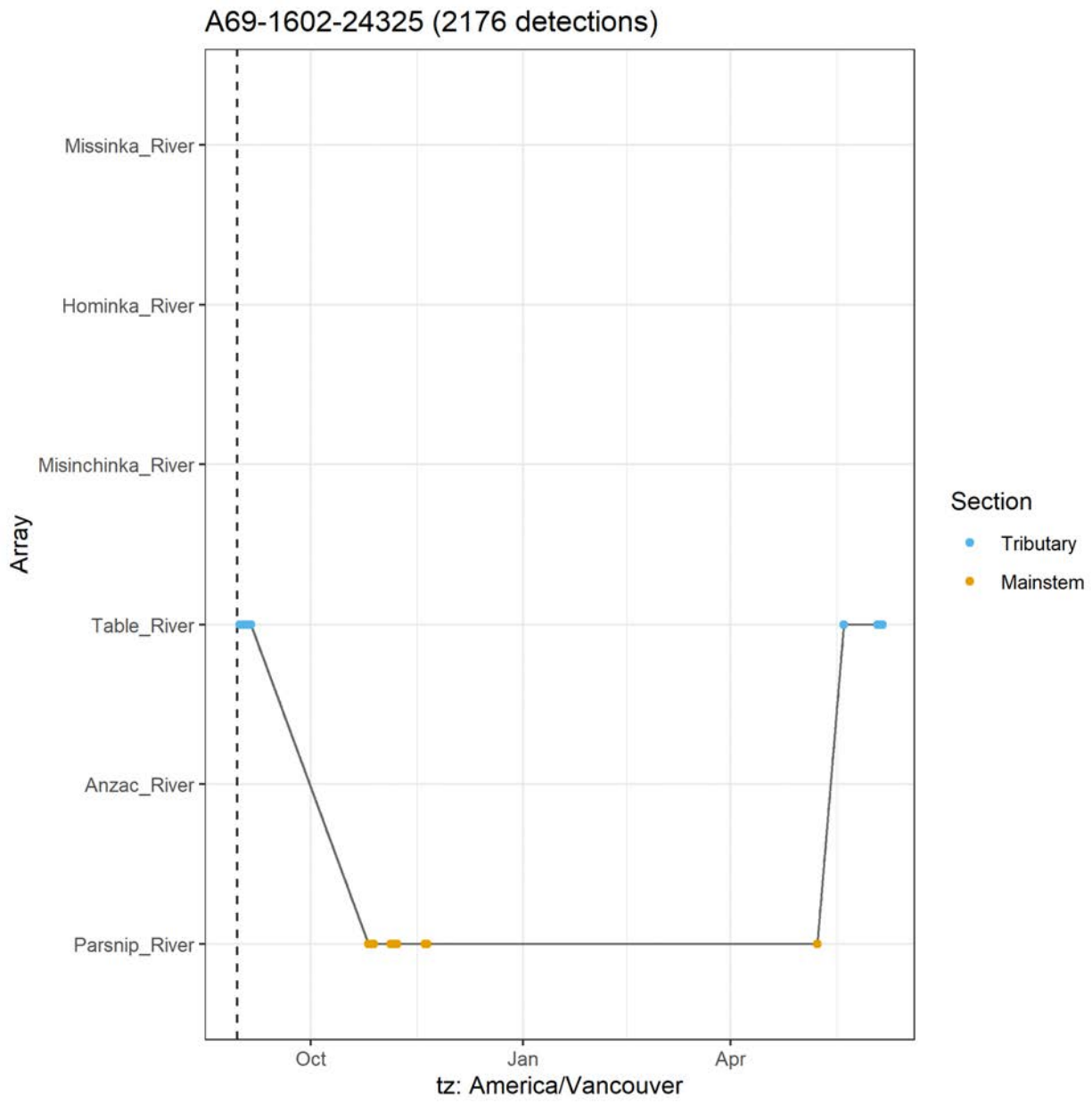
A69-1602-24325 (2176 detections)
Missinka_River
Hominka_River
Misinchinka_River
Table_River
Anzac_River
Parsnip_River
Array
Oct
Jan
Apr
tz: America/Vancouver
Section
Tributary
Mainstem

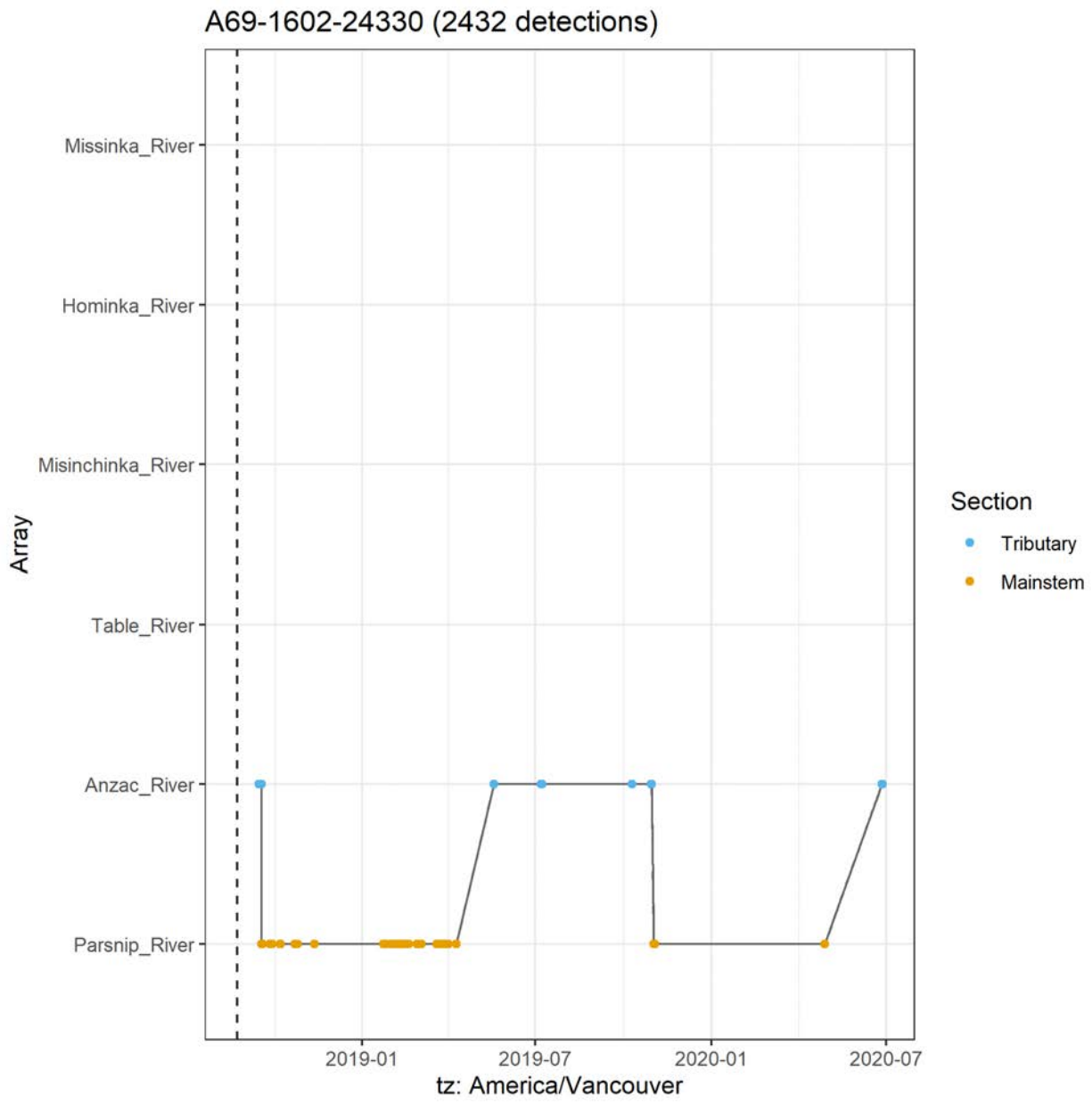
A69-1602-24330 (2432 detections)
Missinka_River
Hominka_River
Misinchinka_River
Table_River
Anzac_River
Parsnip_River
Array
2019-01
2019-07
2020-01
2020-07
tz: America/Vancouver
Section
Tributary
Mainstem

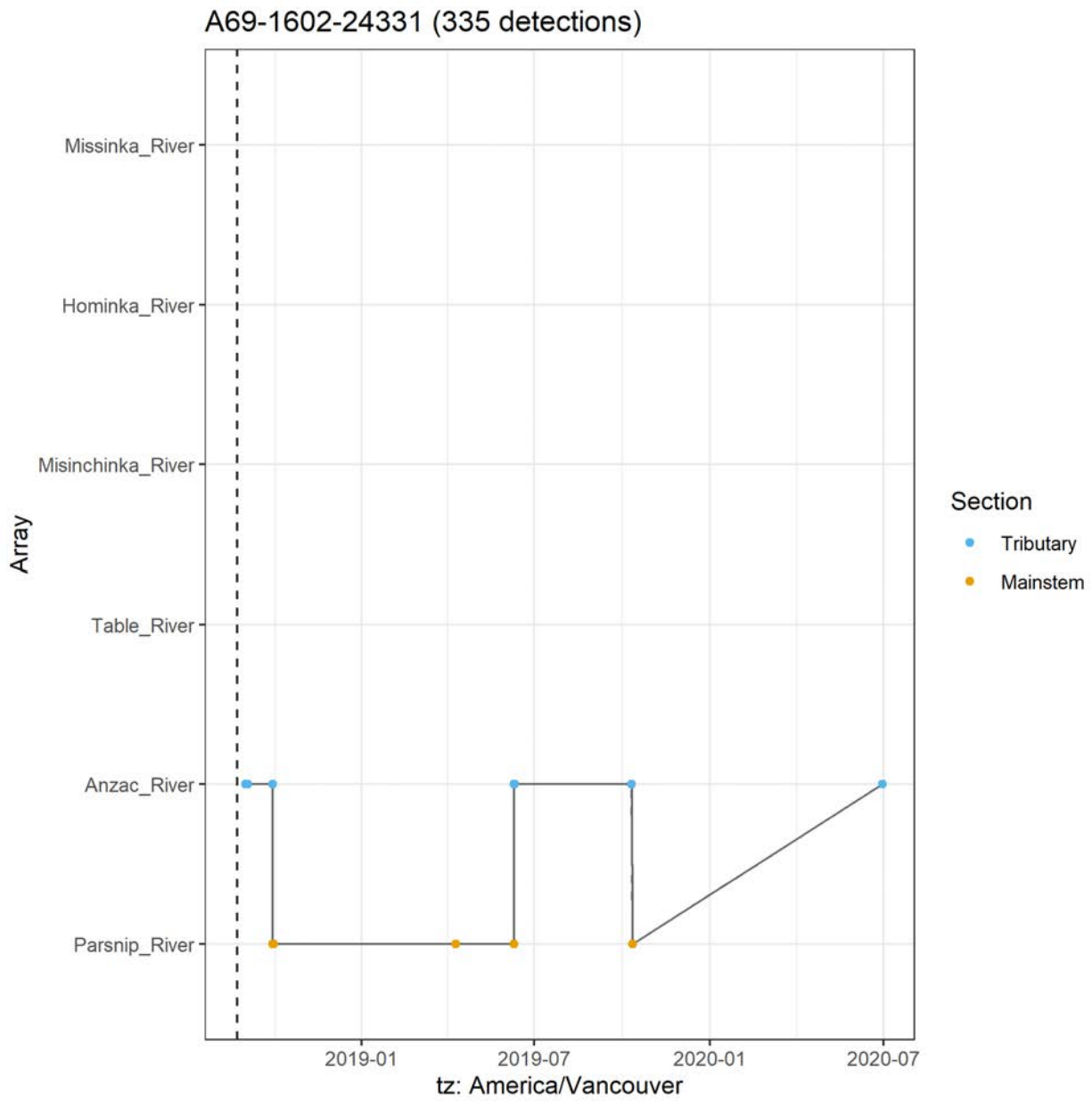
A69-1602-24331 (335 detections)
Missinka_River
Hominka_River
Misinchinka_River
Table_River
Anzac_River
Parsnip_River
Array
2019-01
2019-07
2020-01
2020-07
tz: America/Vancouver
Section
Tributary
Mainstem

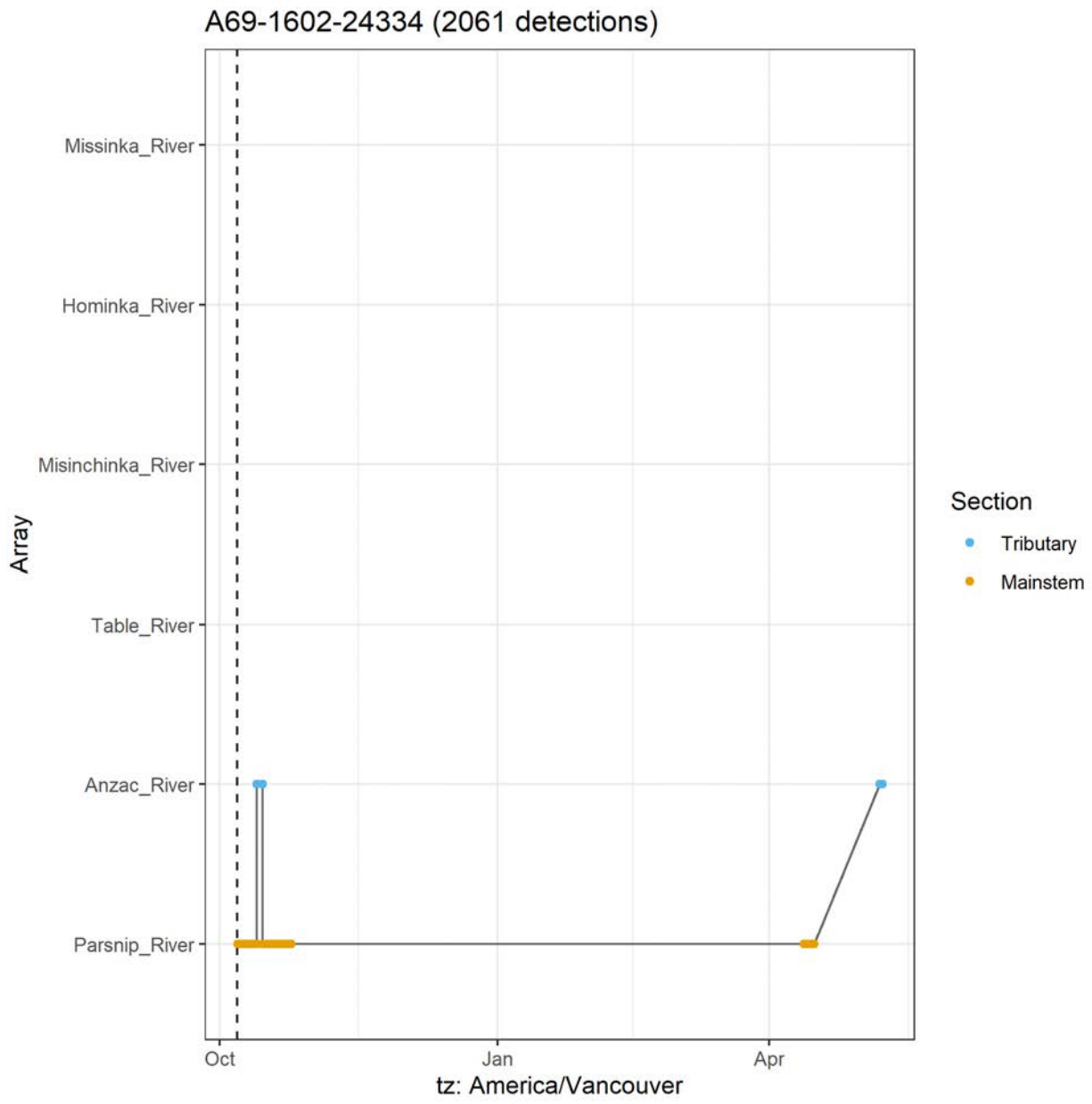
A69-1602-24334 (2061 detections)
Missinka_River
Hominka_River
Misinchinka_River
Table_River
Anzac_River
Parsnip_River
Array
Oct
Jan
Apr
tz: America/Vancouver
Section
Tributary
Mainstem

.

**Appendix A.1 – Individual detection history plots – Bull trout**

Figures in this section depict the spatial location of individual tags over the duration of that tag's active deployment. Tags with limited movement histories have been filtered out.

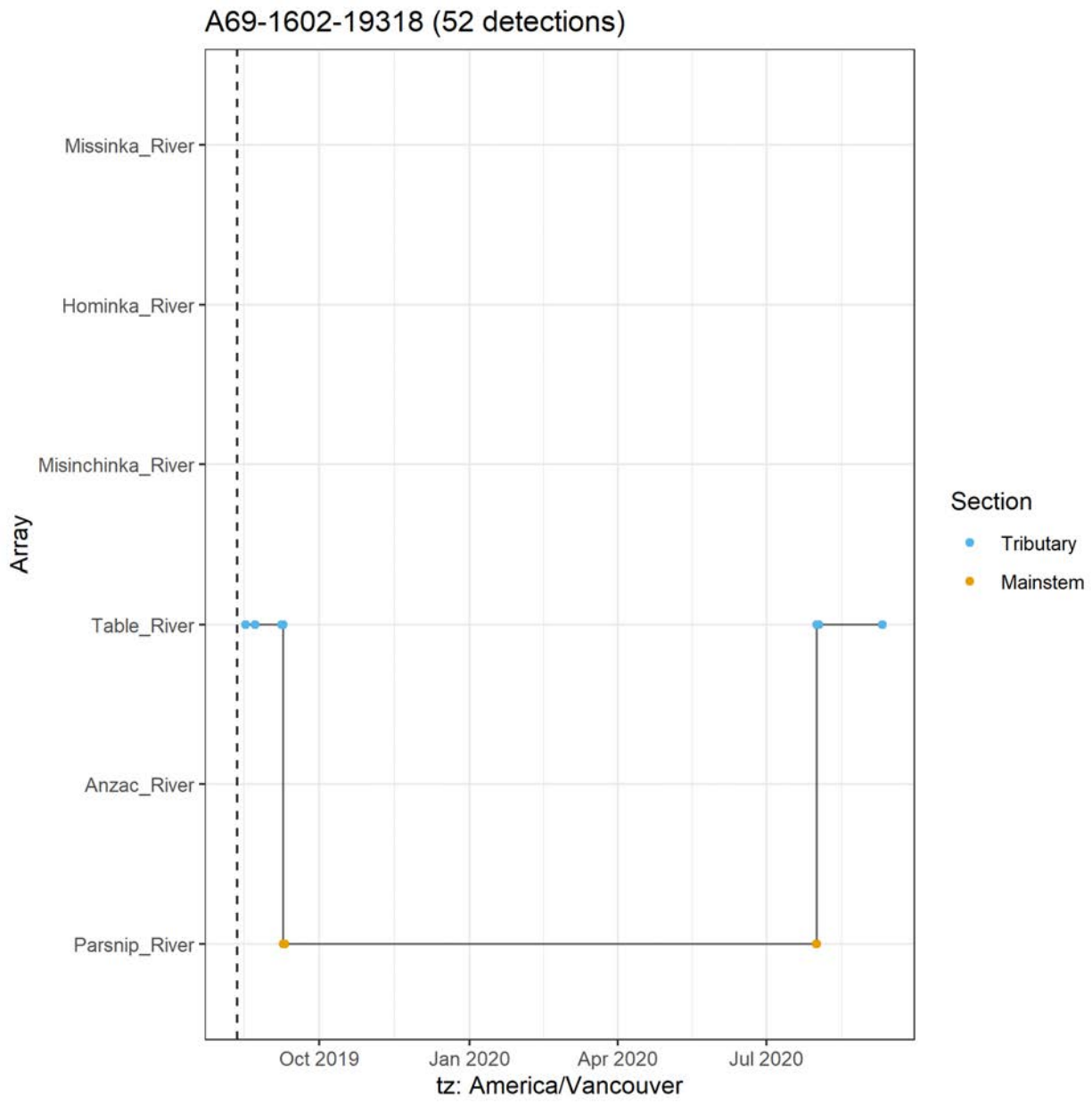
A69-1602-19318 (52 detections)
Missinka_River
Hominka_River
Misinchinka_River
Table_River
Anzac_River
Parsnip_River
Array
Oct 2019
Jan 2020
Apr 2020
Jul 2020
tz: America/Vancouver
Section
Tributary
Mainstem

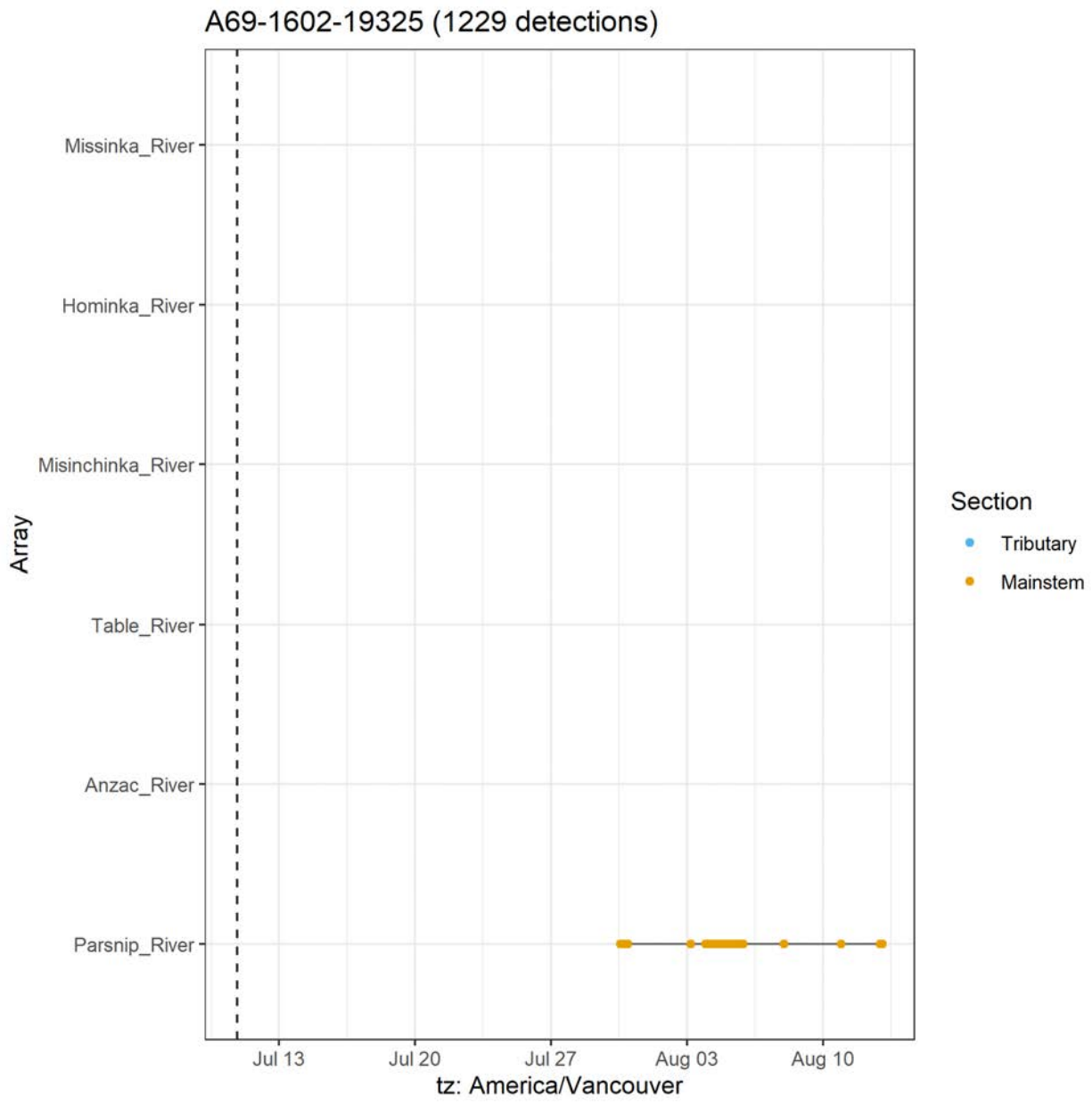
A69-1602-19325 (1229 detections)
Missinka_River
Hominka_River
Misinchinka_River
Table_River
Anzac_River
Parsnip_River
Array
Jul 13
Jul 20
Jul 27
Aug 03
Aug 10
tz: America/Vancouver
Section
Tributary
Mainstem

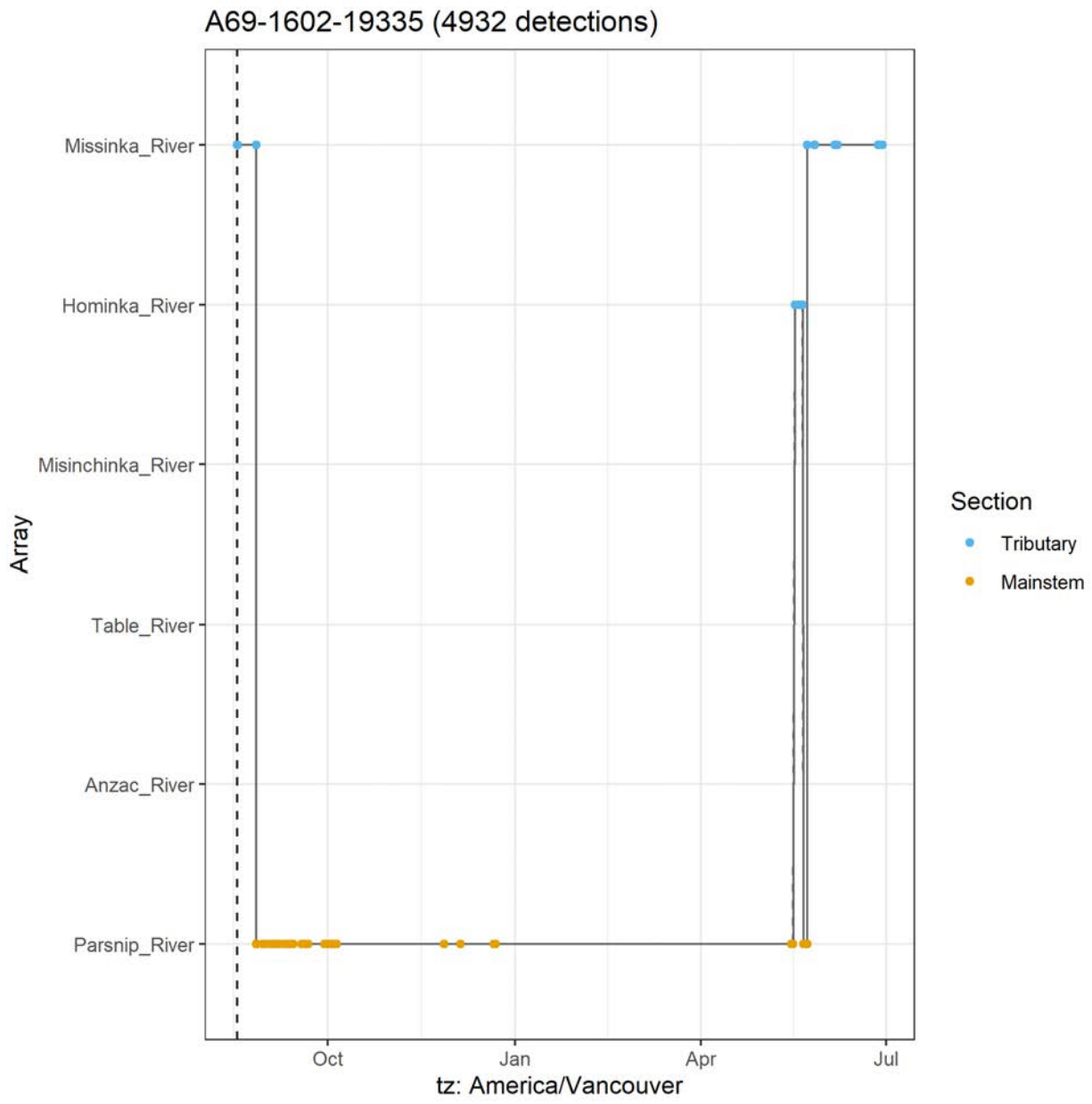
A69-1602-19335 (4932 detections)
Missinka_River
Hominka_River
Misinchinka_River
Table_River
Anzac_River
Parsnip_River
Array
Oct
Jan
Apr
Jul
tz: America/Vancouver
Section
Tributary
Mainstem

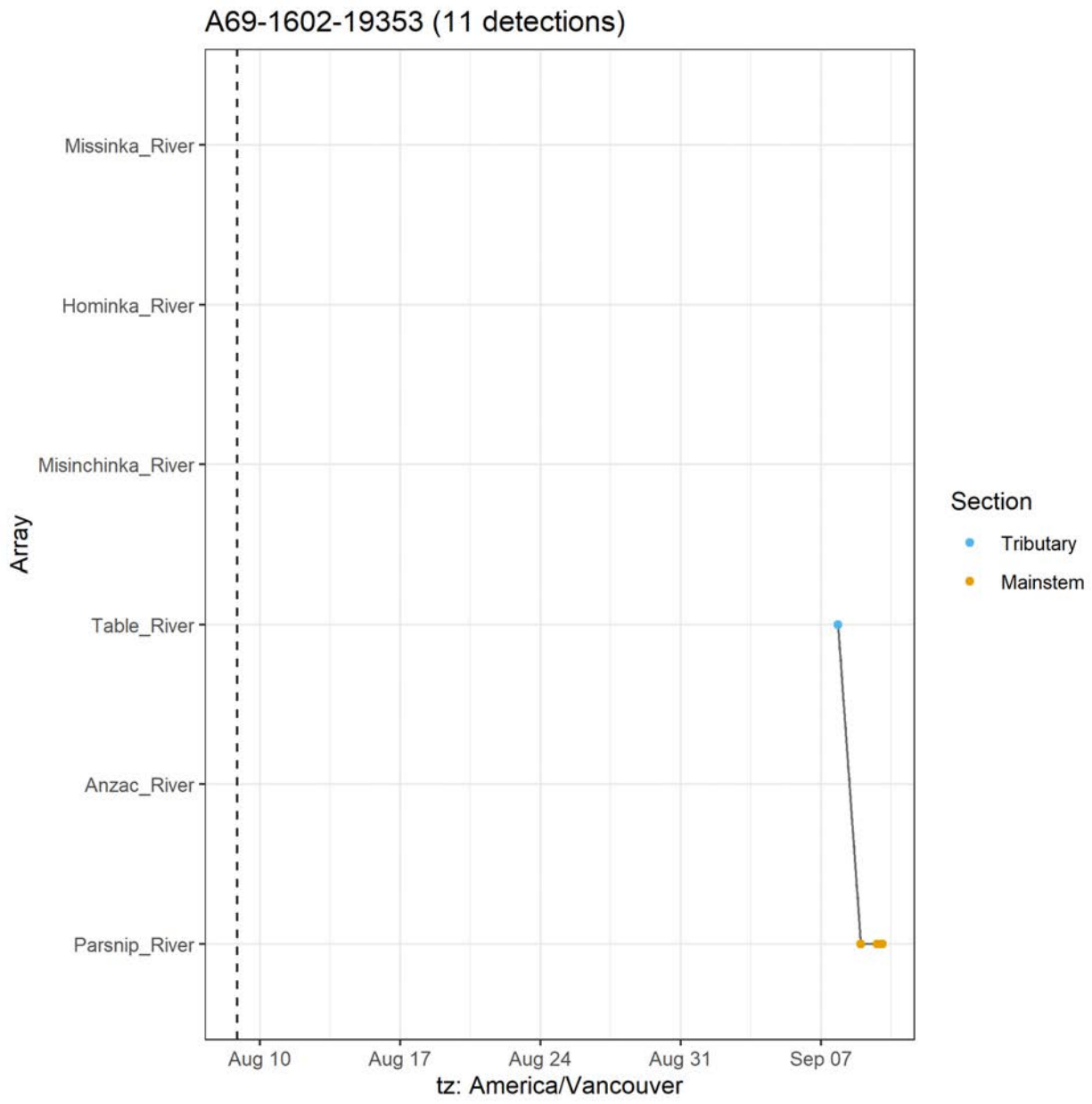
A69-1602-19353 (11 detections)
Missinka_River
Hominka_River
Misinchinka_River
Table_River
Anzac_River
Parsnip_River
Array
Aug 10
Aug 17
Aug 24
Aug 31
Sep 07
tz: America/Vancouver
Section
Tributary
Mainstem

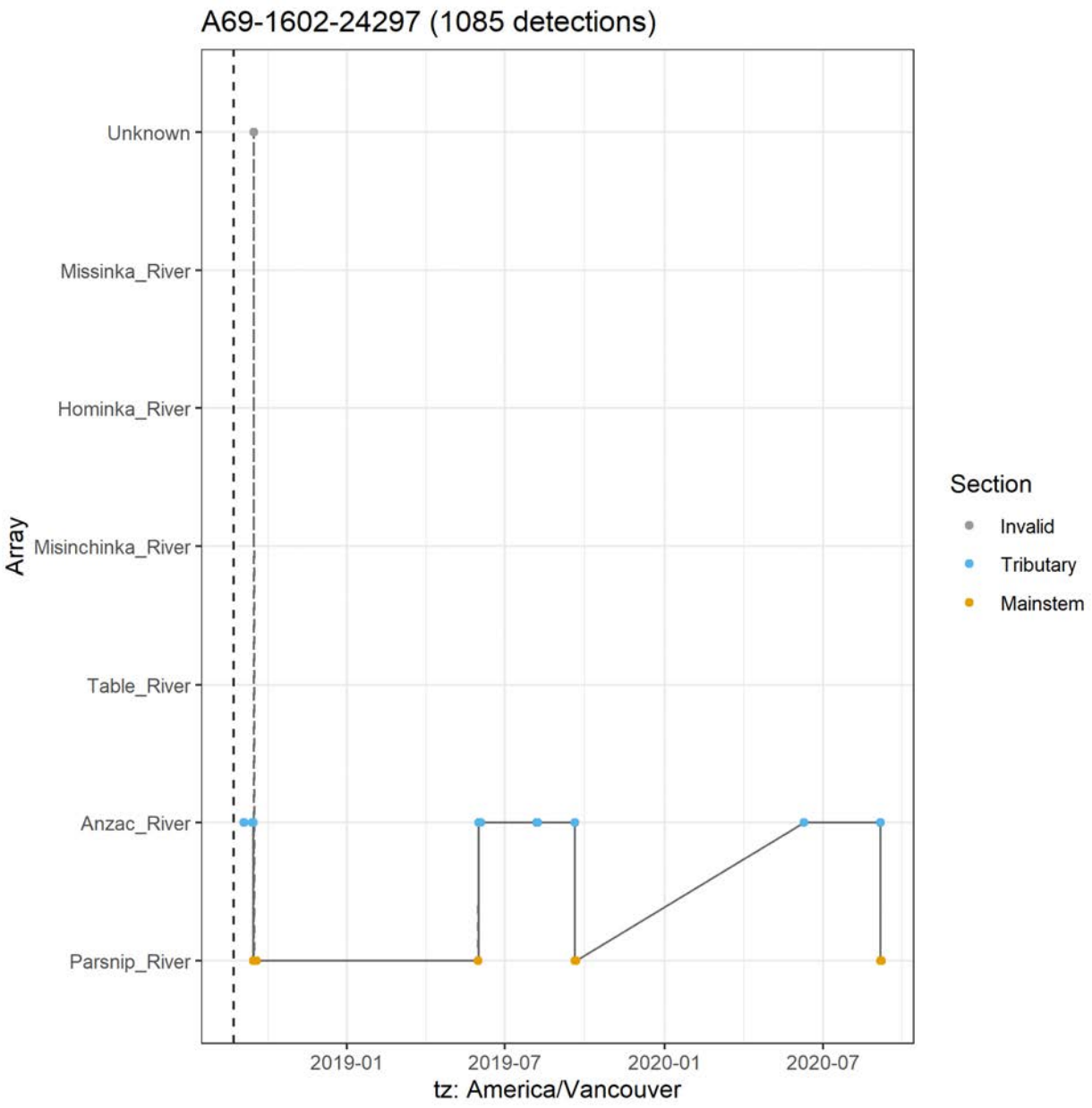
A69-1602-24297 (1085 detections)
Unknown
Missinka_River
Hominka_River
Misinchinka_River
Table_River
Anzac_River
Parsnip_River
Array
2019-01
2019-07
2020-01
2020-07
tz: America/Vancouver
Section
Invalid
Tributary
Mainstem

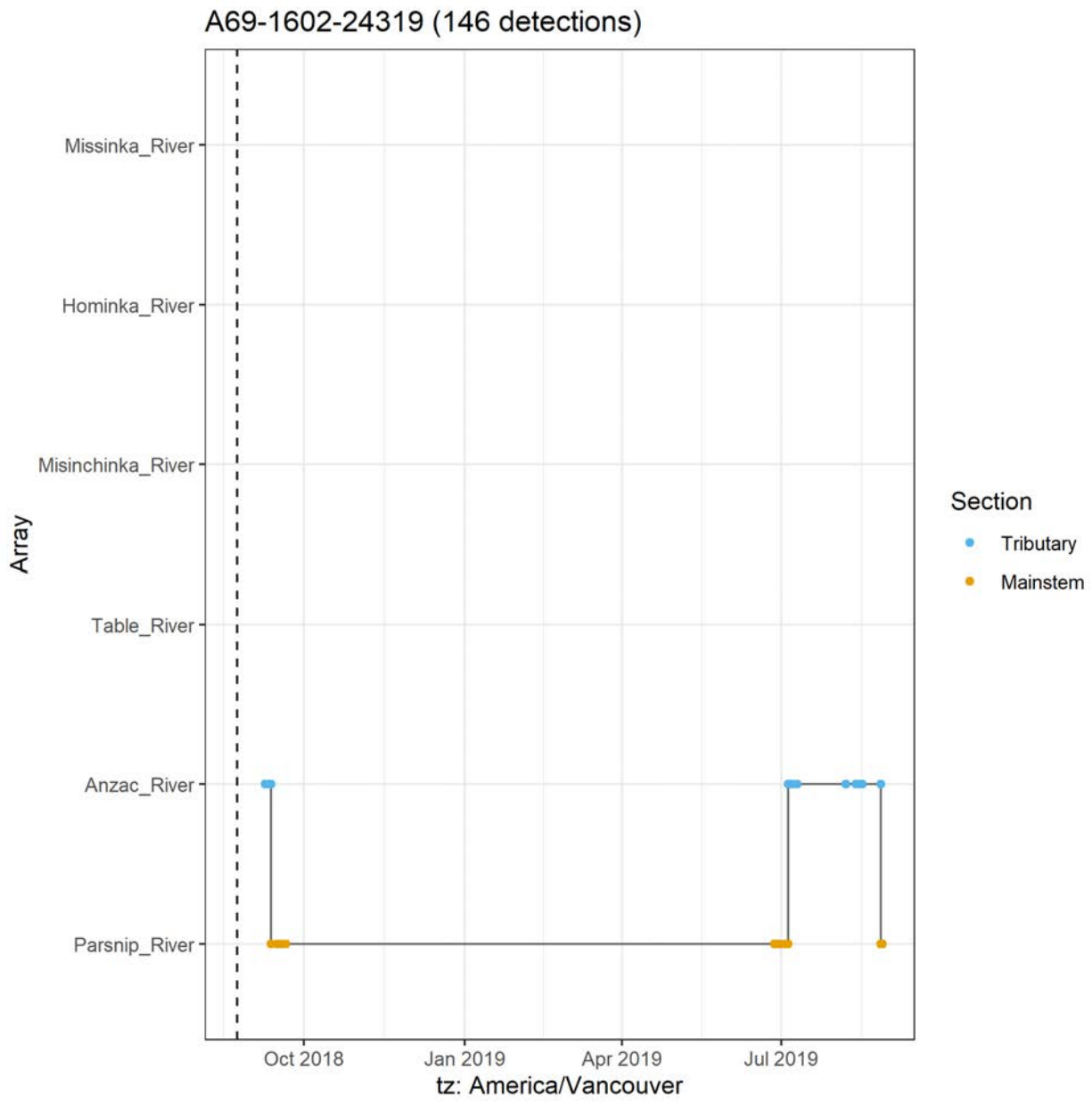
A69-1602-24319 (146 detections)
Missinka_River
Hominka_River
Misinchinka_River
Table_River
Anzac_River
Parsnip_River
Array
Oct 2018
Jan 2019
Apr 2019
Jul 2019
tz: America/Vancouver
Section
Tributary
Mainstem

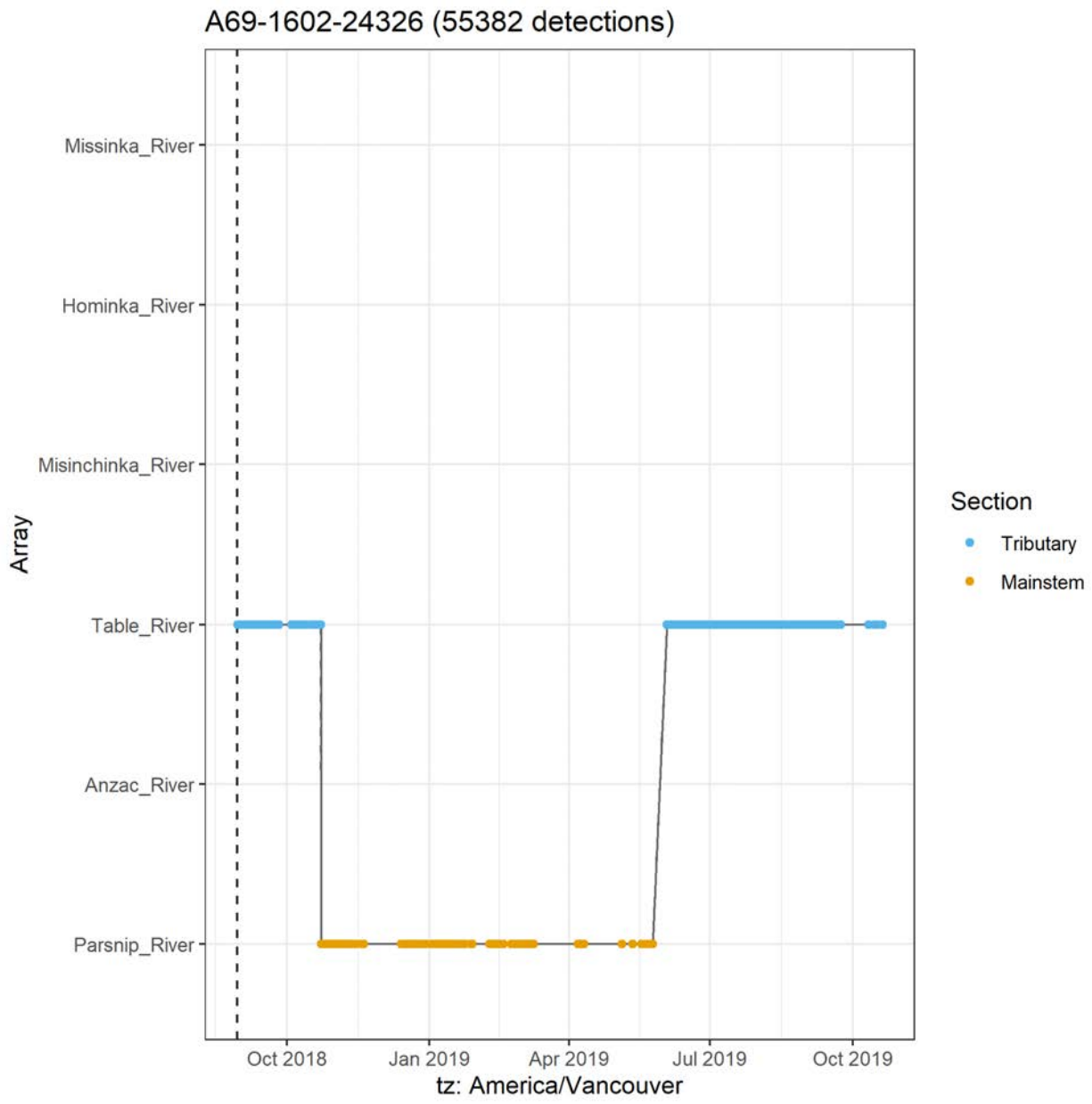
A69-1602-24326 (55382 detections)
Missinka_River
Hominka_River
Misinchinka_River
Table_River
Anzac_River
Parsnip_River
Array
Oct 2018
Jan 2019
Apr 2019
Jul 2019
Oct 2019
tz: America/Vancouver
Section
Tributary
Mainstem

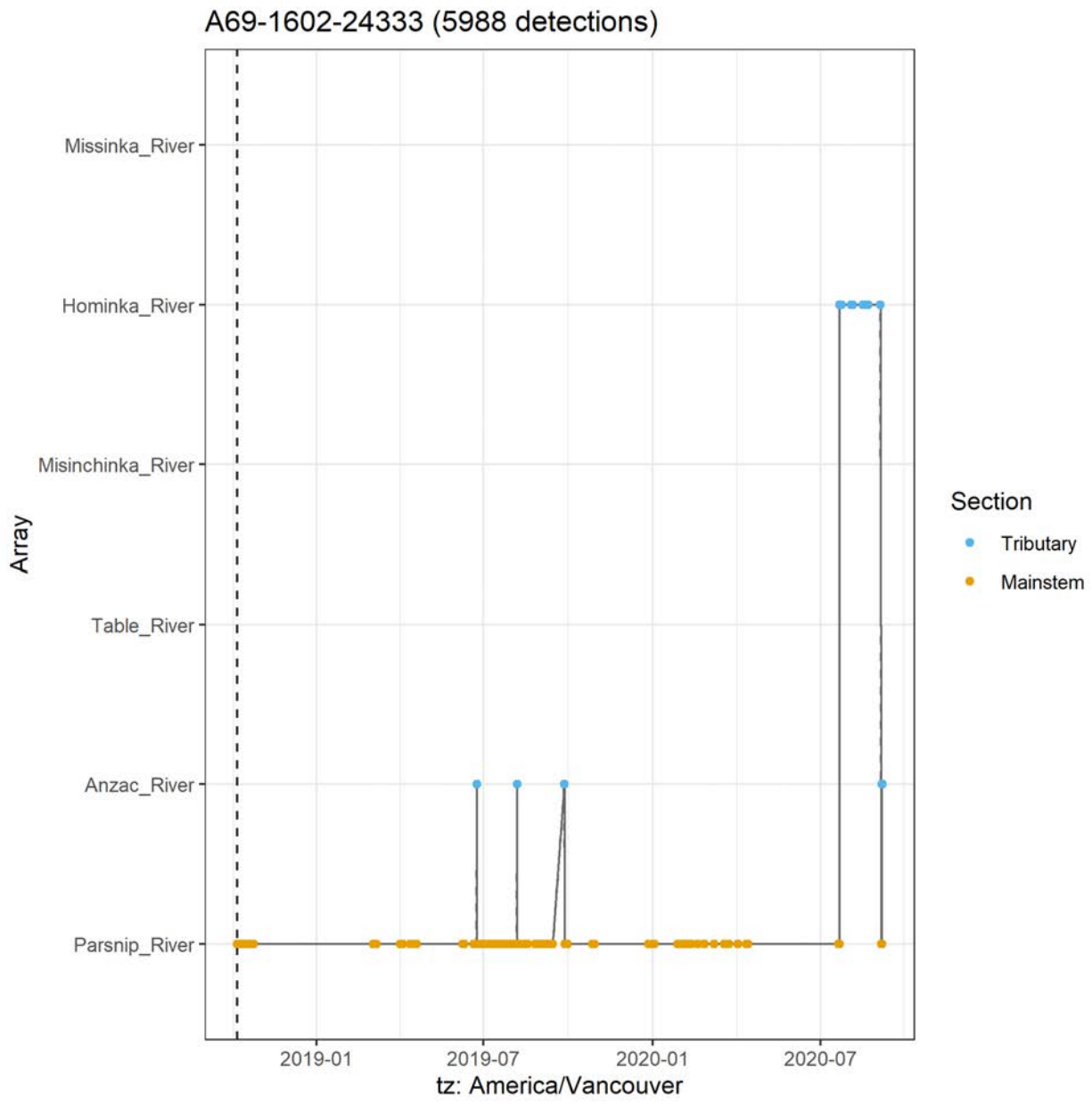
A69-1602-24333 (5988 detections)
Missinka_River
Hominka_River
Misinchinka_River
Table_River
Anzac_River
Parsnip_River
Array
2019-01
2019-07
2020-01
2020-07
tz: America/Vancouver
Section
Tributary
Mainstem

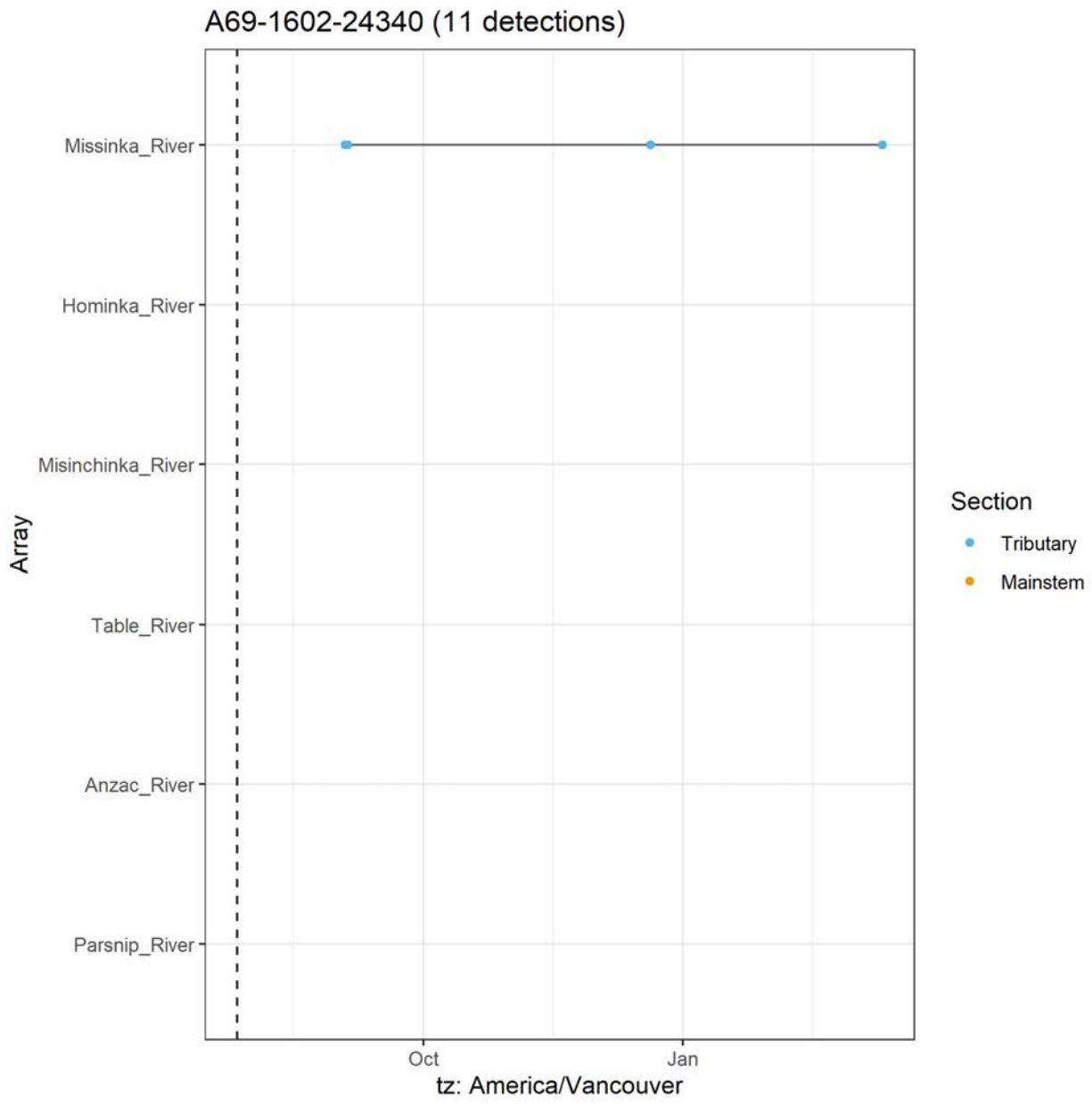
A69-1602-24340 (11 detections)
Missinka_River
Hominka_River
Misinchinka_River
Table_River
Anzac_River
Parsnip_River
Array
Oct
Jan
tz: America/Vancouver
Section
Tributary
Mainstem

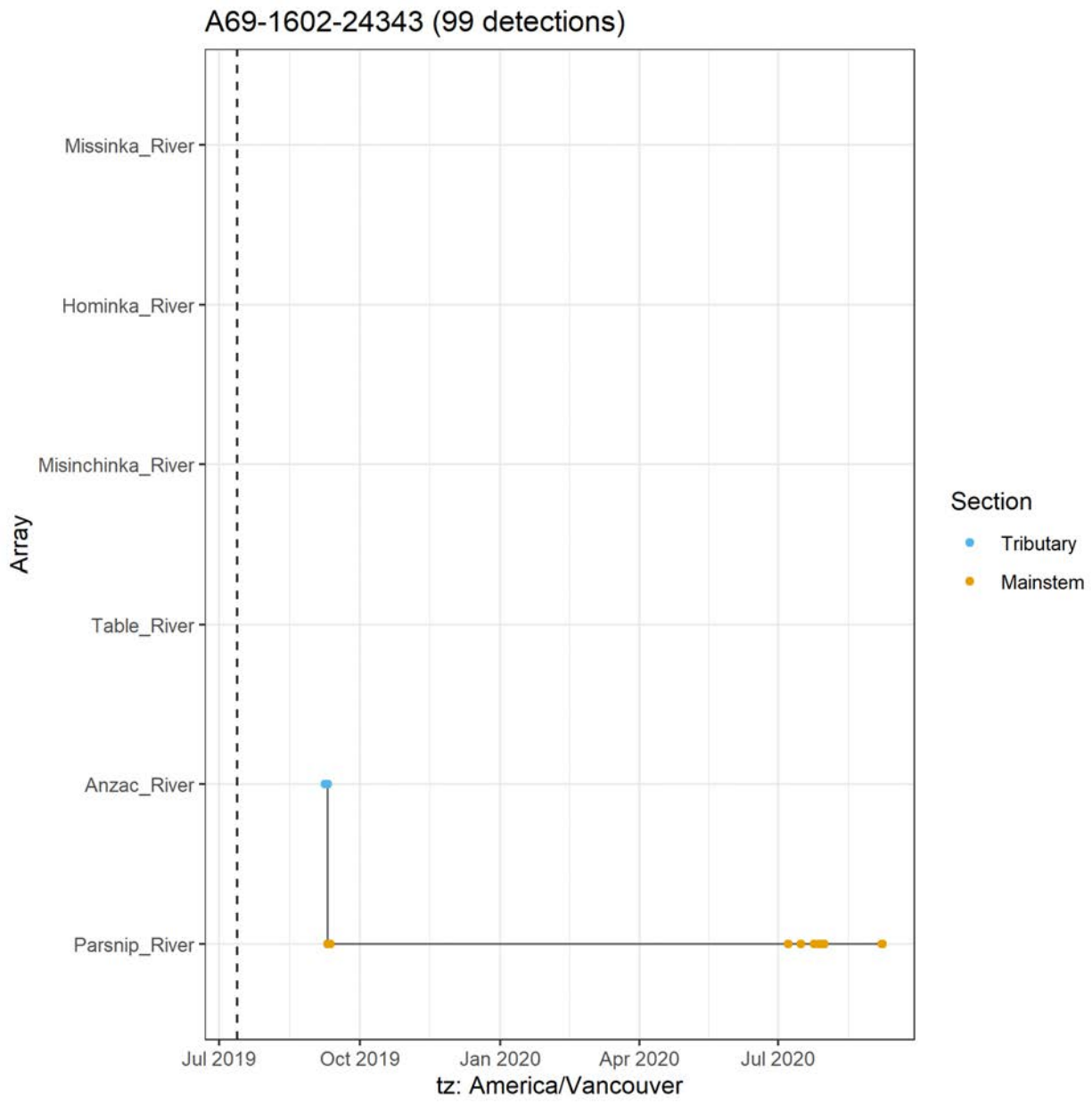
A69-1602-24343 (99 detections)
Missinka_River
Hominka_River
Misinchinka_River
Table_River
Anzac_River
Parsnip_River
Array
Jul 2019
Oct 2019
Jan 2020
Apr 2020
Jul 2020
tz: America/Vancouver
Section
Tributary
Mainstem

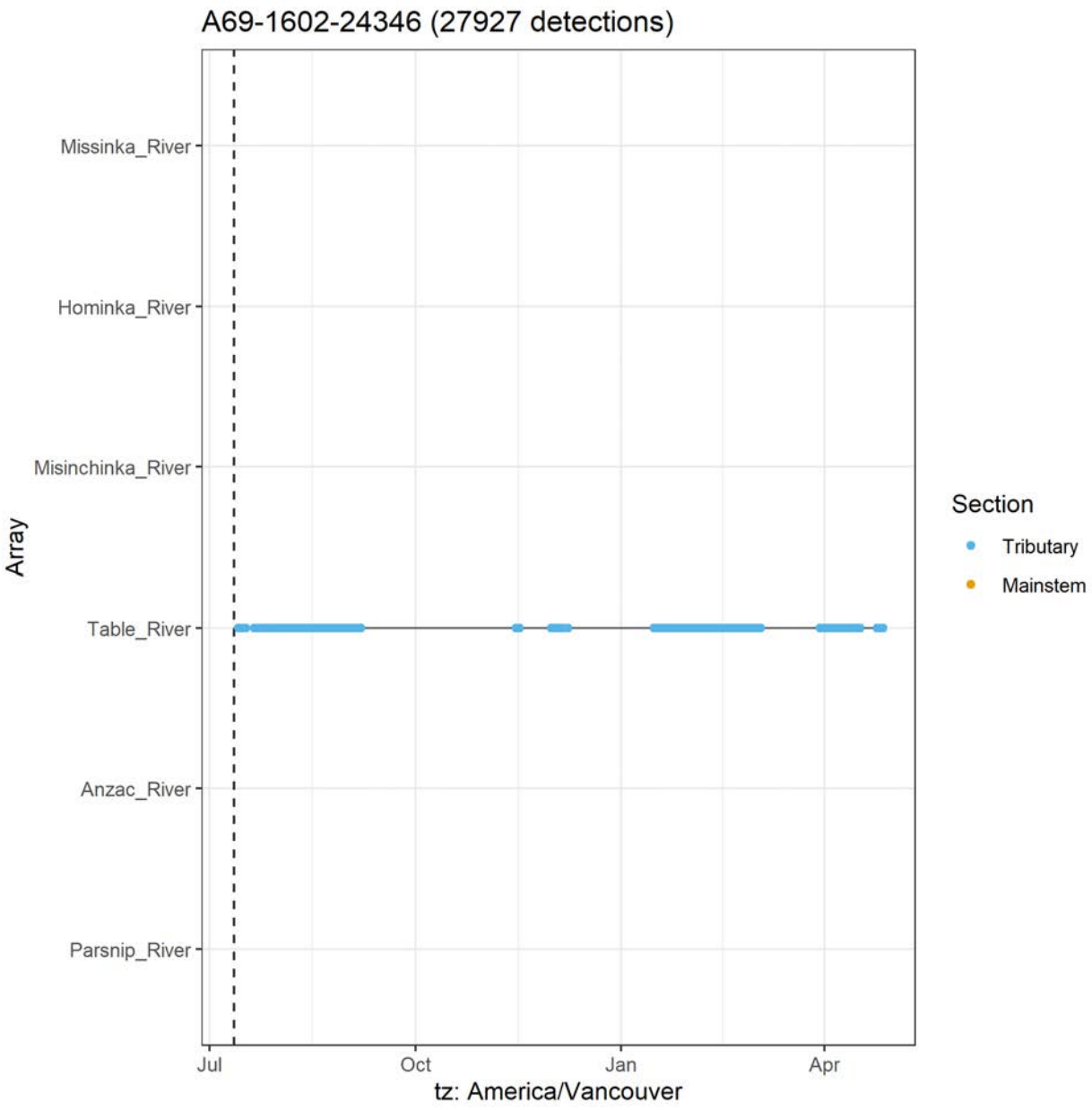
A69-1602-24346 (27927 detections)
Missinka_River
Hominka_River
Misinchinka_River
Table_River
Anzac_River
Parsnip_River
Array
Jul
Oct
Jan
Apr
tz: America/Vancouver
Section
Tributary
Mainstem

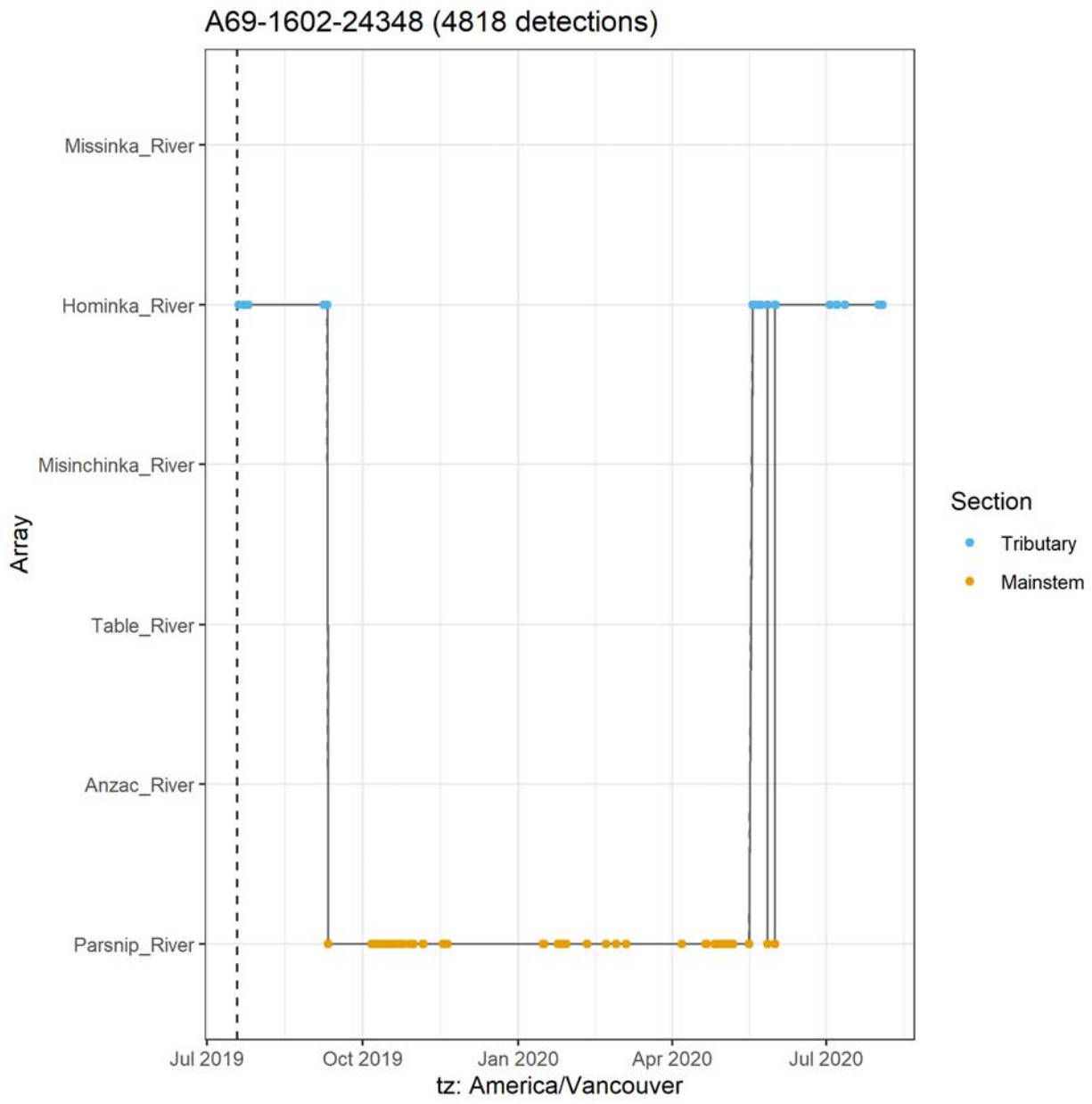
A69-1602-24348 (4818 detections)
Missinka_River
Hominka_River
Misinchinka_River
Table_River
Anzac_River
Parsnip_River
Array
Jul 2019
Oct 2019
Jan 2020
Apr 2020
Jul 2020
tz: America/Vancouver
Section
Tributary
Mainstem

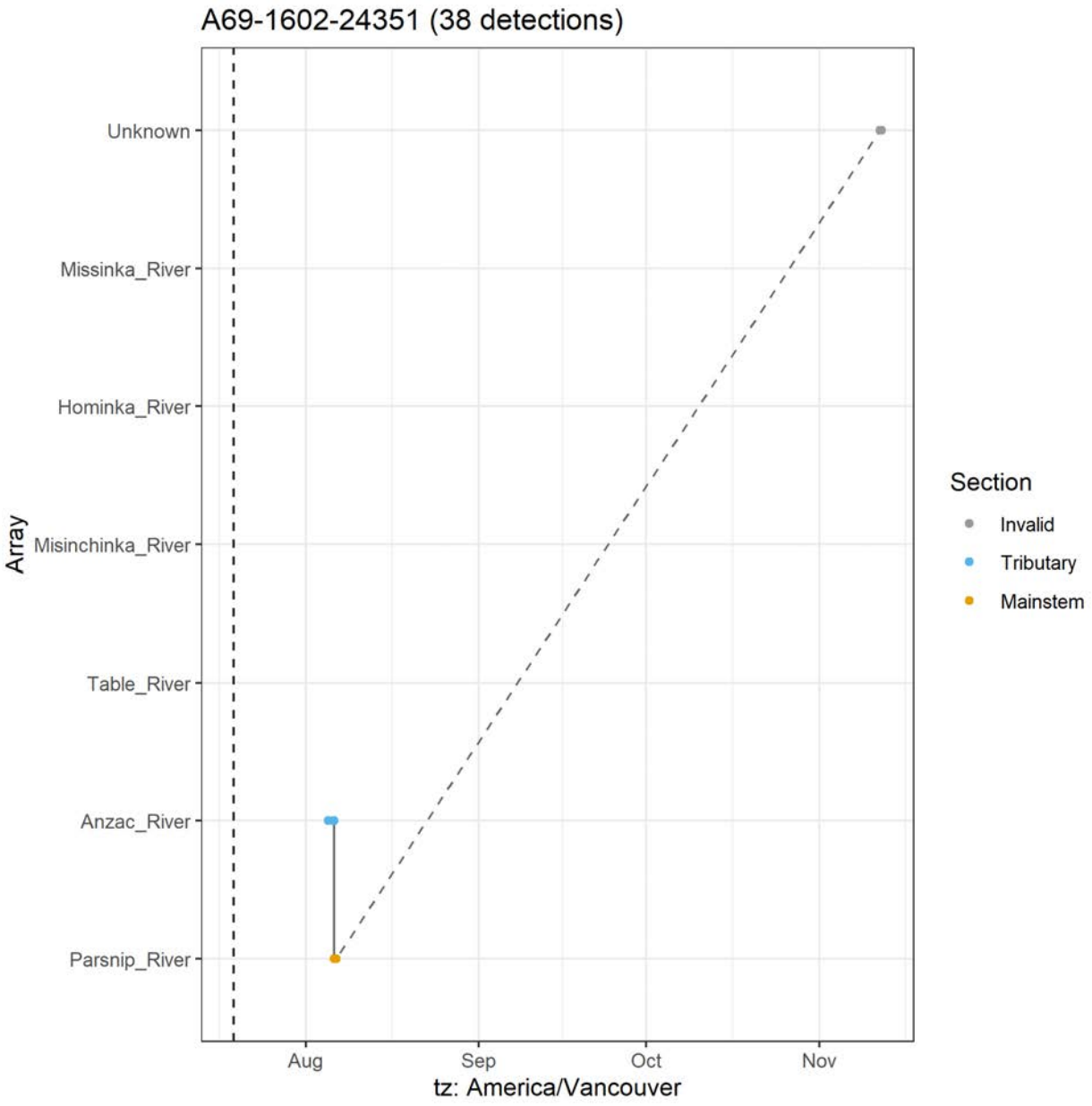
A69-1602-24351 (38 detections)
Unknown
Missinka_River
Hominka_River
Misinchinka_River
Table_River
Anzac_River
Parsnip_River
Array
Aug
Sep
Oct
Nov
tz: America/Vancouver
Section
Invalid
Tributary
Mainstem

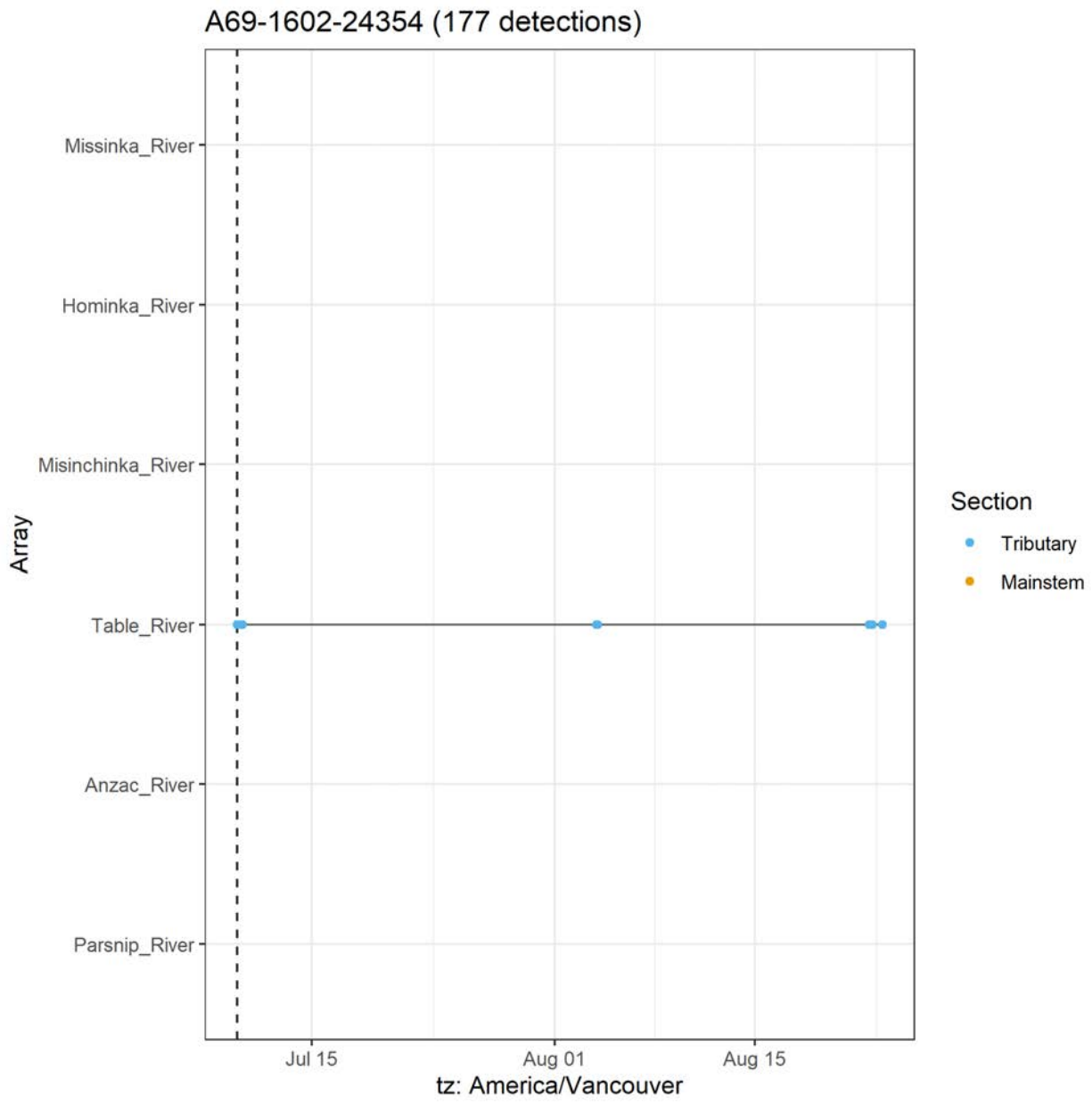
A69-1602-24354 (177 detections)
Missinka_River
Hominka_River
Misinchinka_River
Table_River
Anzac_River
Parsnip_River
Array
Jul 15
Aug 01
Aug 15
tz: America/Vancouver
Section
Tributary
Mainstem

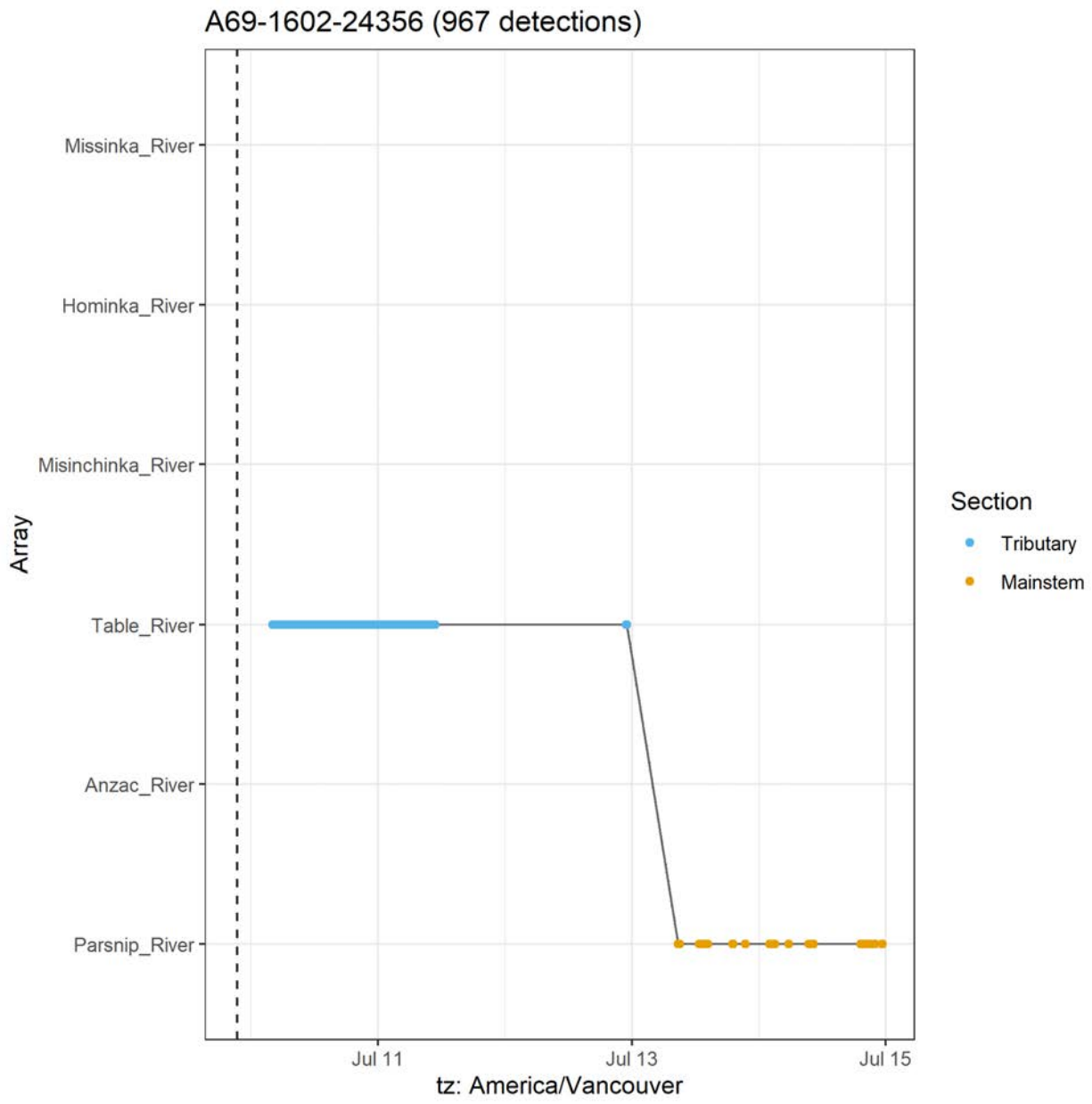
A69-1602-24356 (967 detections)
Missinka_River
Hominka_River
Misinchinka_River
Table_River
Anzac_River
Parsnip_River
Array
Jul 11
Jul 13
Jul 15
tz: America/Vancouver
Section
Tributary
Mainstem

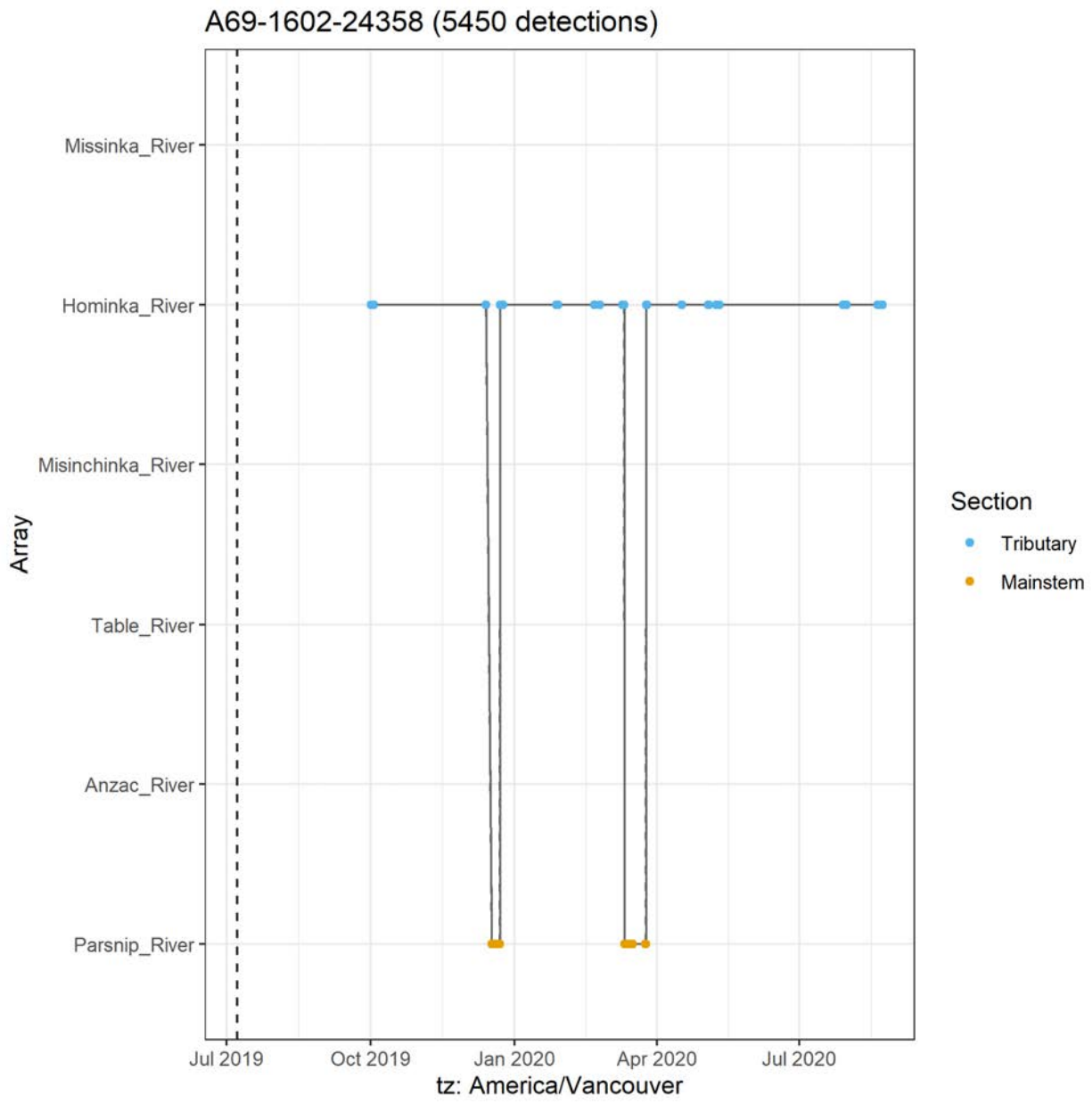
A69-1602-24358 (5450 detections)
Missinka_River
Hominka_River
Misinchinka_River
Table_River
Anzac_River
Parsnip_River
Array
Jul 2019
Oct 2019
Jan 2020
Apr 2020
Jul 2020
tz: America/Vancouver
Section
Tributary
Mainstem

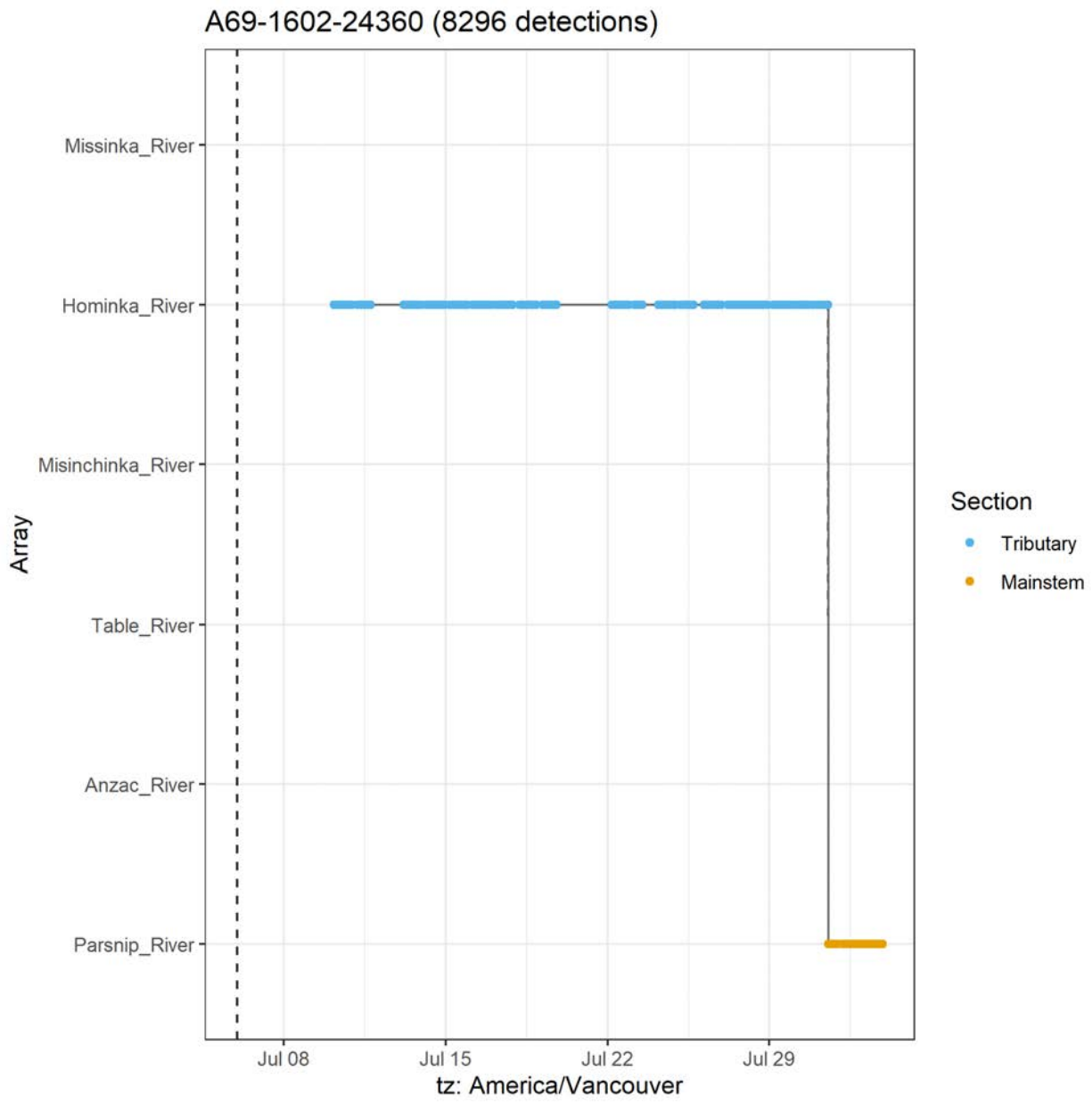
A69-1602-24360 (8296 detections)
Missinka_River
Hominka_River
Misinchinka_River
Table_River
Anzac_River
Parsnip_River
Array
Jul 08
Jul 15
Jul 22
Jul 29
tz: America/Vancouver
Section
Tributary
Mainstem

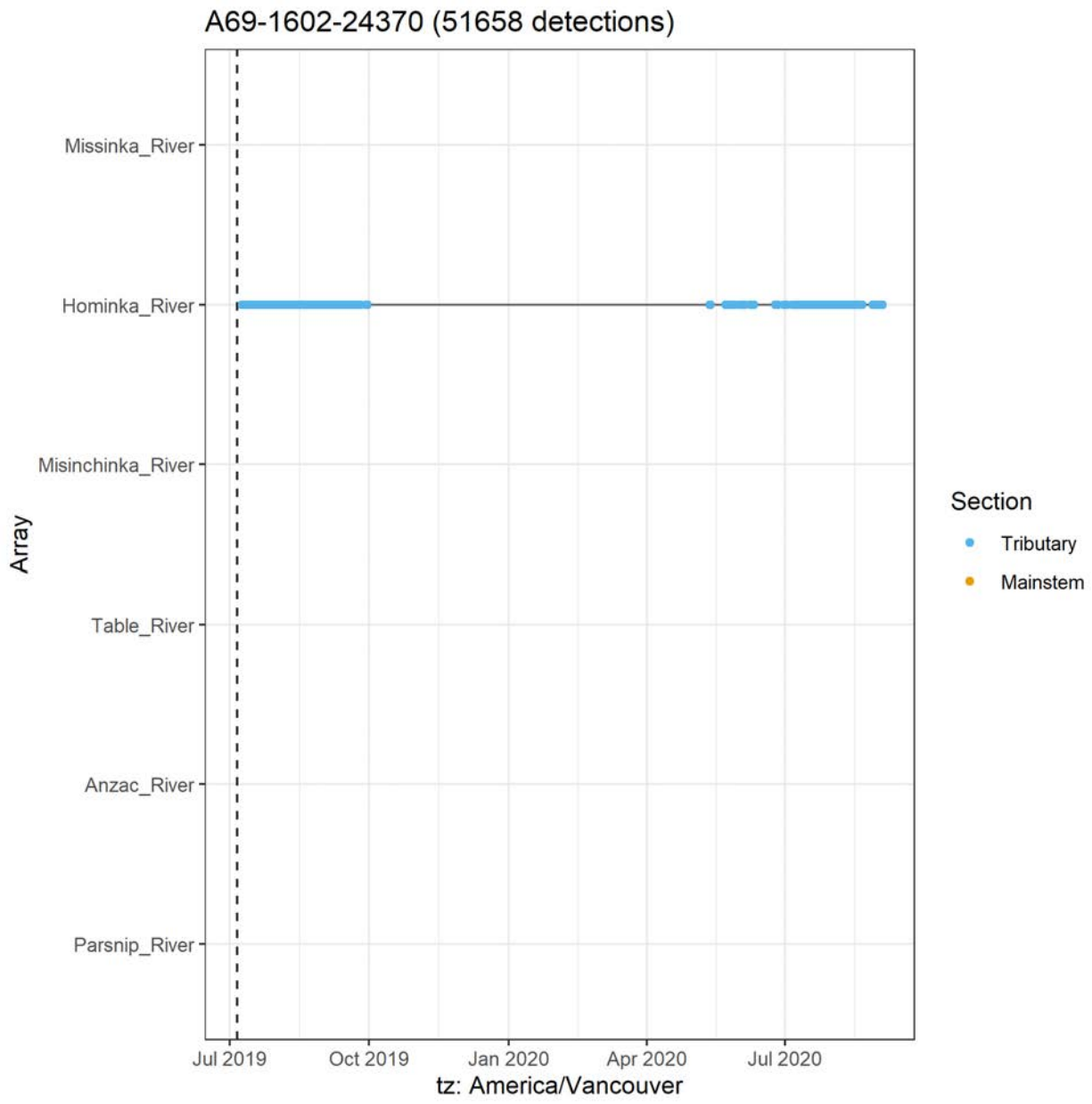
A69-1602-24370 (51658 detections)
Missinka_River
Hominka_River
Misinchinka_River
Table_River
Anzac_River
Parsnip_River
Array
Jul 2019
Oct 2019
Jan 2020
Apr 2020
Jul 2020
tz: America/Vancouver
Section
Tributary
Mainstem

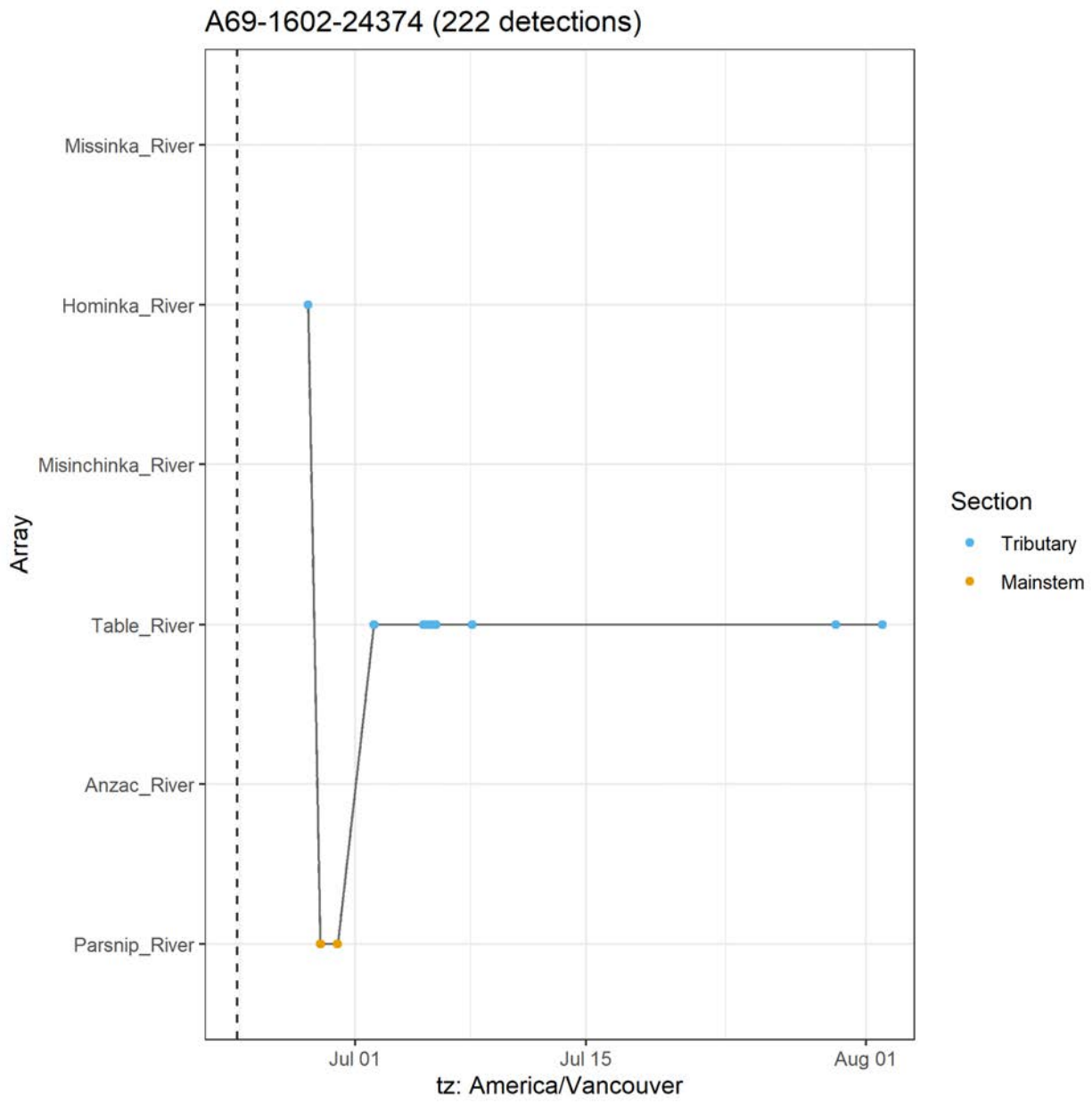
A69-1602-24374 (222 detections)
Missinka_River
Hominka_River
Misinchinka_River
Table_River
Anzac_River
Parsnip_River
Array
Jul 01
Jul 15
Aug 01
tz: America/Vancouver
Section
Tributary
Mainstem

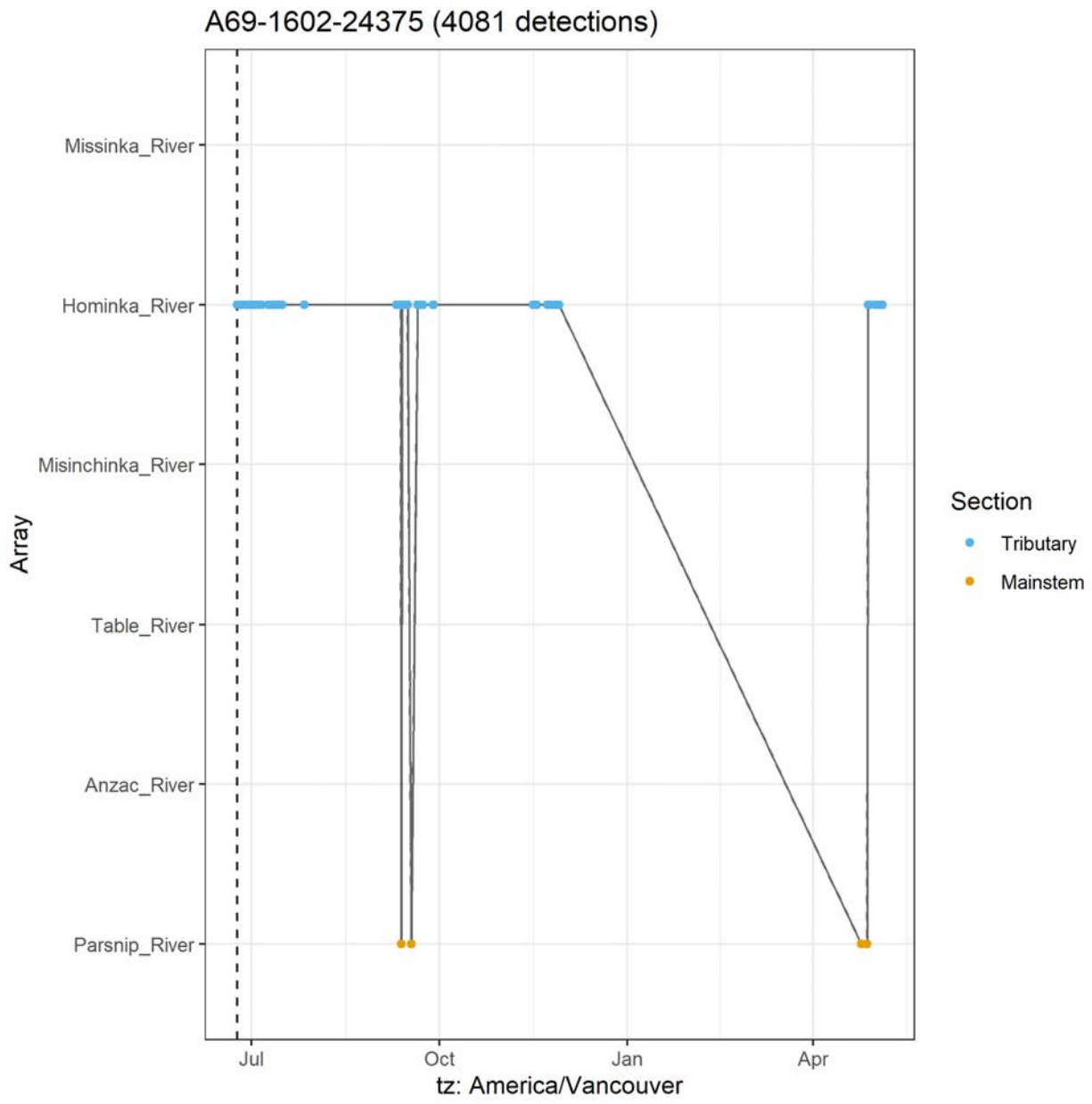
A69-1602-24375 (4081 detections)
Missinka_River
Hominka_River
Misinchinka_River
Table_River
Anzac_River
Parsnip_River
Array
Jul
Oct
Jan
Apr
tz: America/Vancouver
Section
Tributary
Mainstem

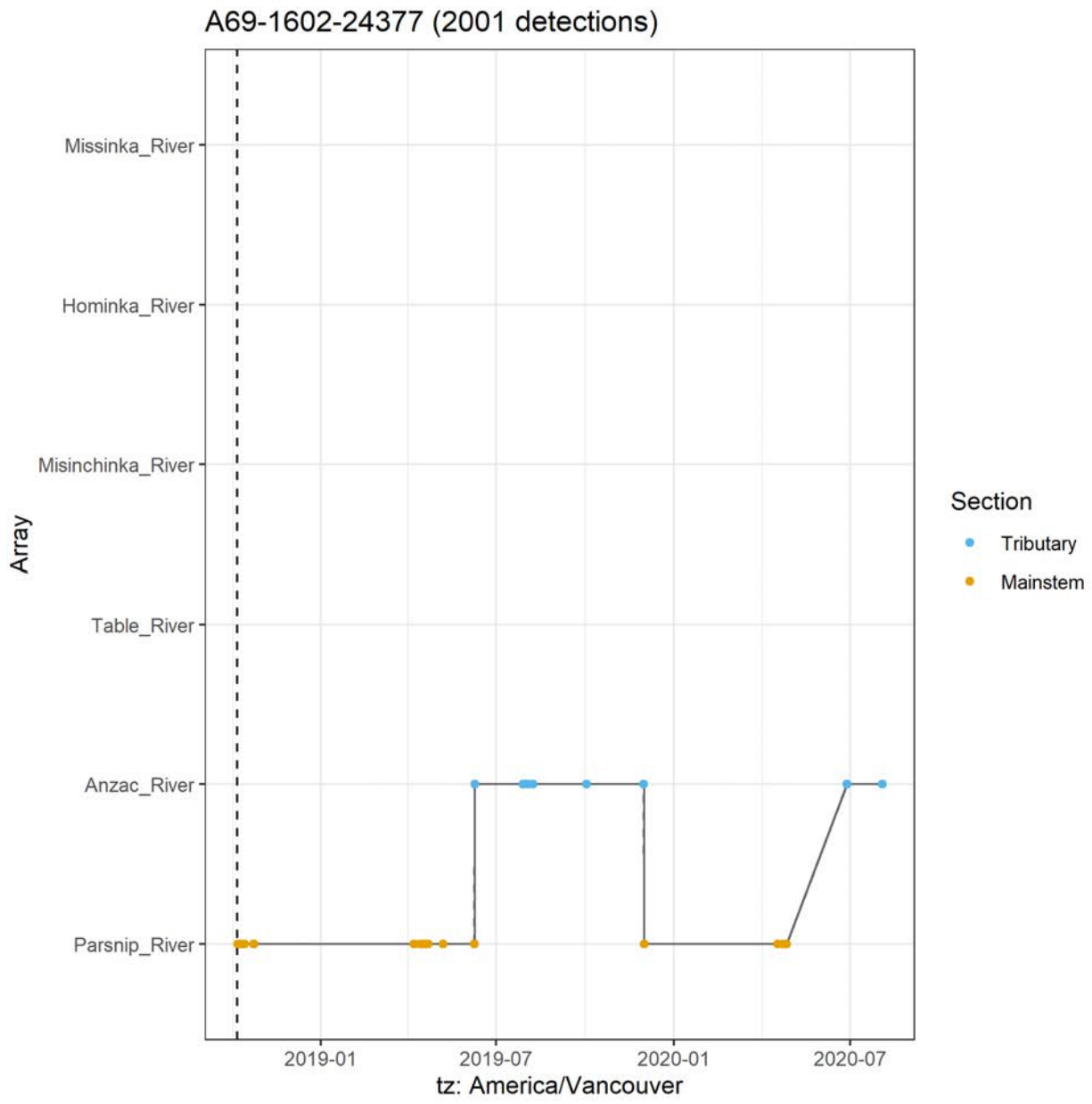
A69-1602-24377 (2001 detections)
Missinka_River
Hominka_River
Misinchinka_River
Table_River
Anzac_River
Parsnip_River
Array
2019-01
2019-07
2020-01
2020-07
tz: America/Vancouver
Section
Tributary
Mainstem

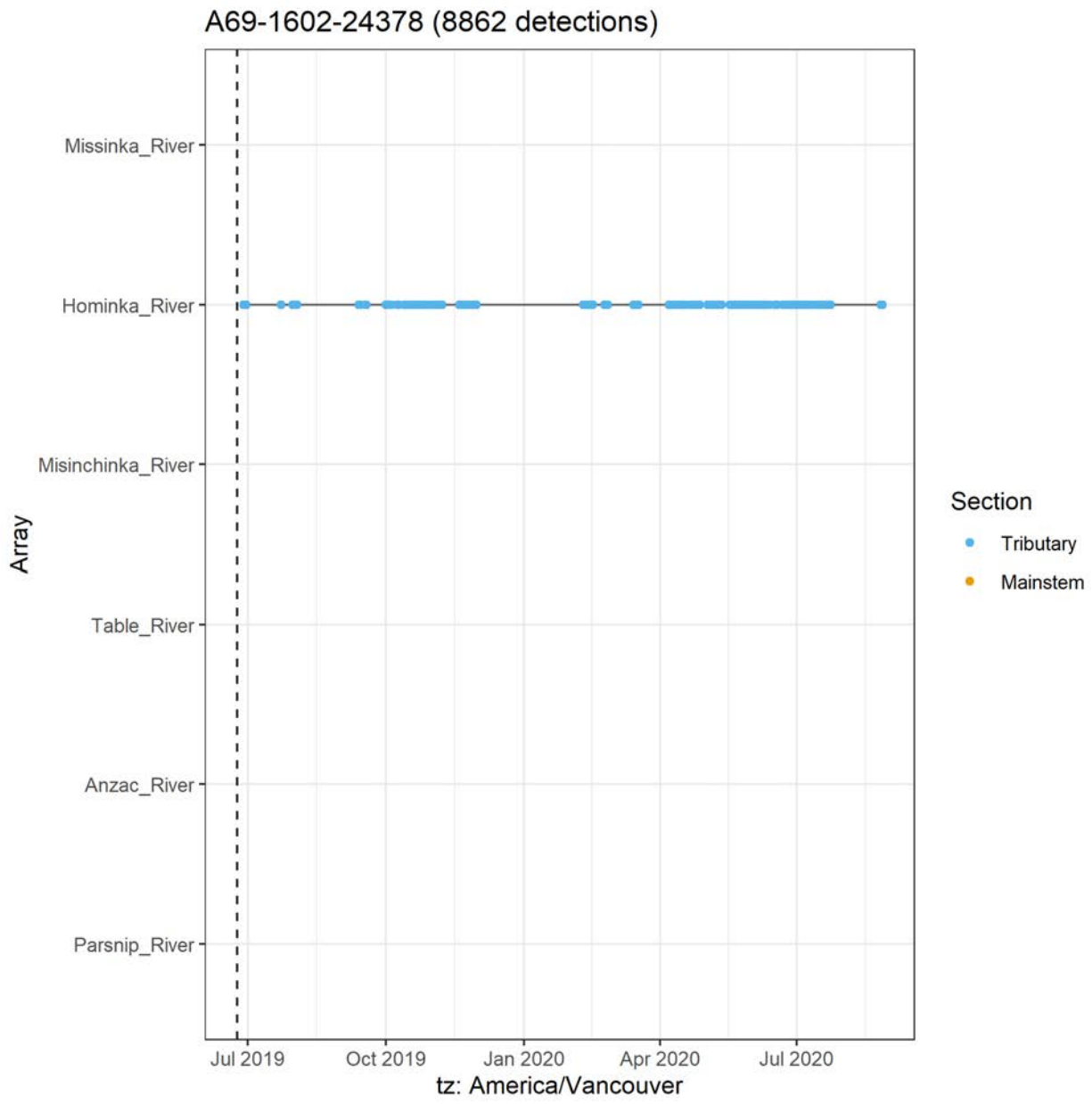
A69-1602-24378 (8862 detections)
Missinka_River
Hominka_River
Misinchinka_River
Table_River
Anzac_River
Parsnip_River
Array
Jul 2019
Oct 2019
Jan 2020
Apr 2020
Jul 2020
tz: America/Vancouver
Section
Tributary
Mainstem

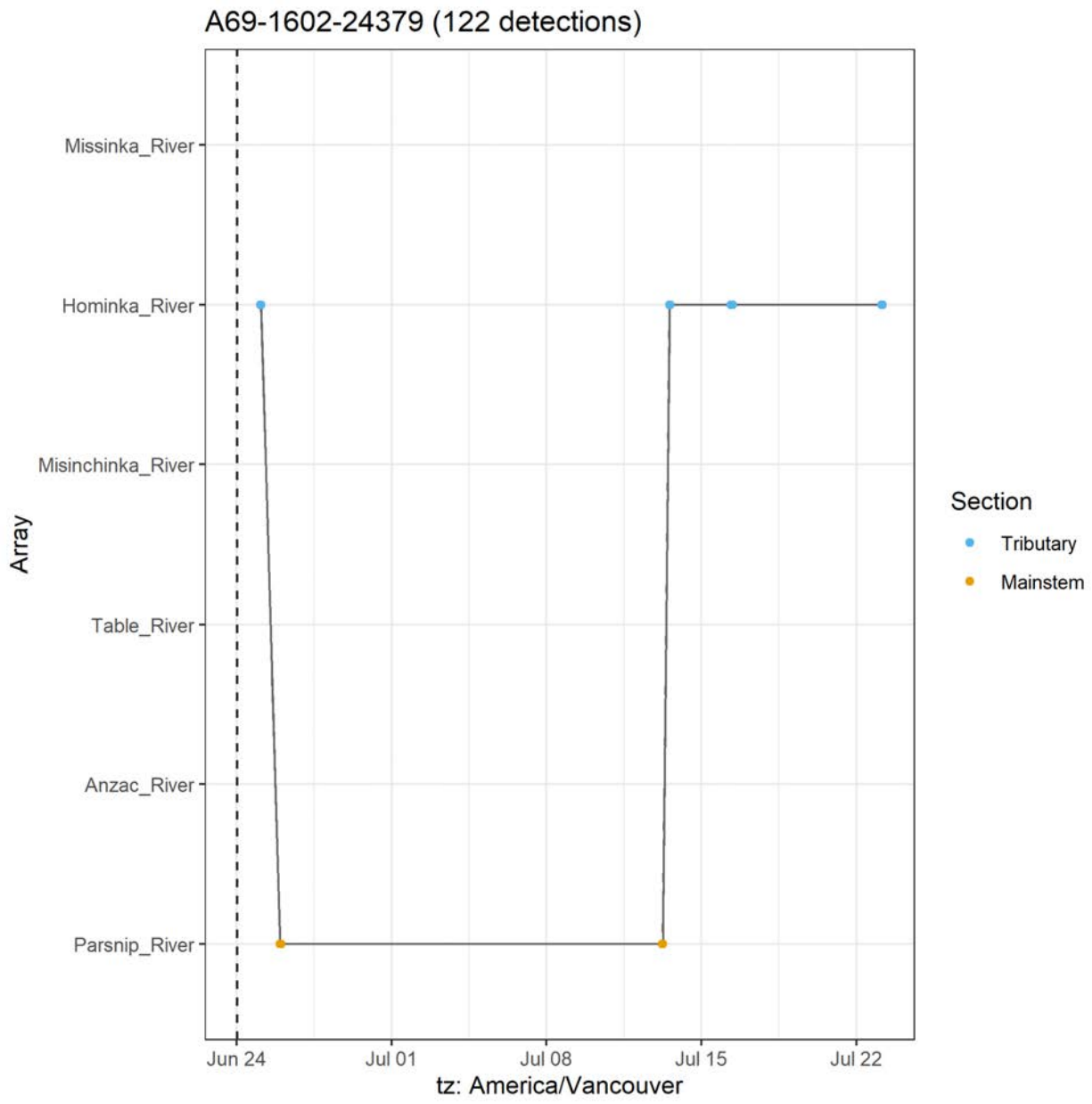
A69-1602-24379 (122 detections)
Missinka_River
Hominka_River
Misinchinka_River
Table_River
Anzac_River
Parsnip_River
Array
Jun 24
Jul 01
Jul 08
Jul 15
Jul 22
tz: America/Vancouver
Section
Tributary
Mainstem

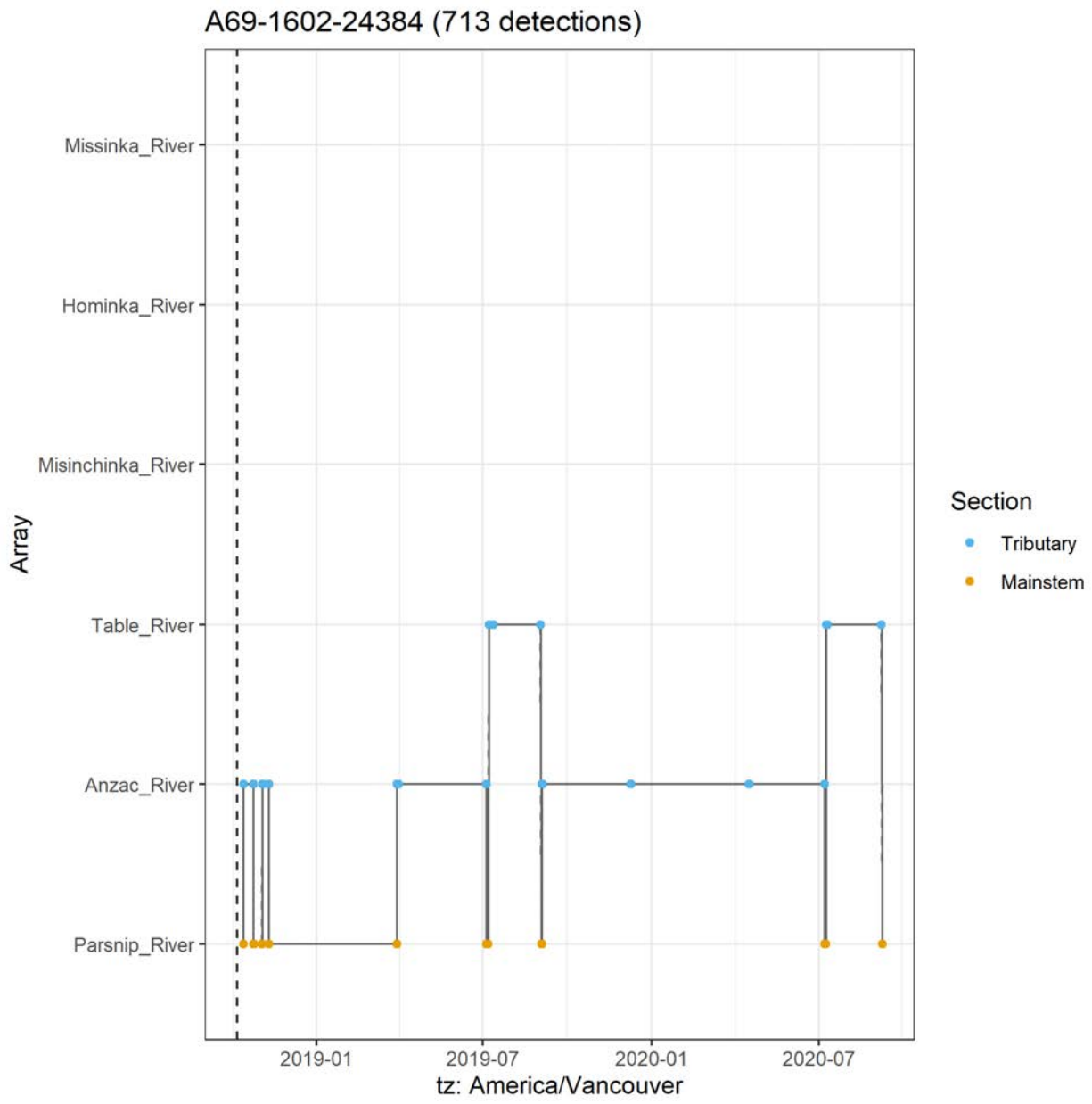
A69-1602-24384 (713 detections)
Missinka_River
Hominka_River
Misinchinka_River
Table_River
Anzac_River
Parsnip_River
Array
2019-01
2019-07
2020-01
2020-07
tz: America/Vancouver
Section
Tributary
Mainstem

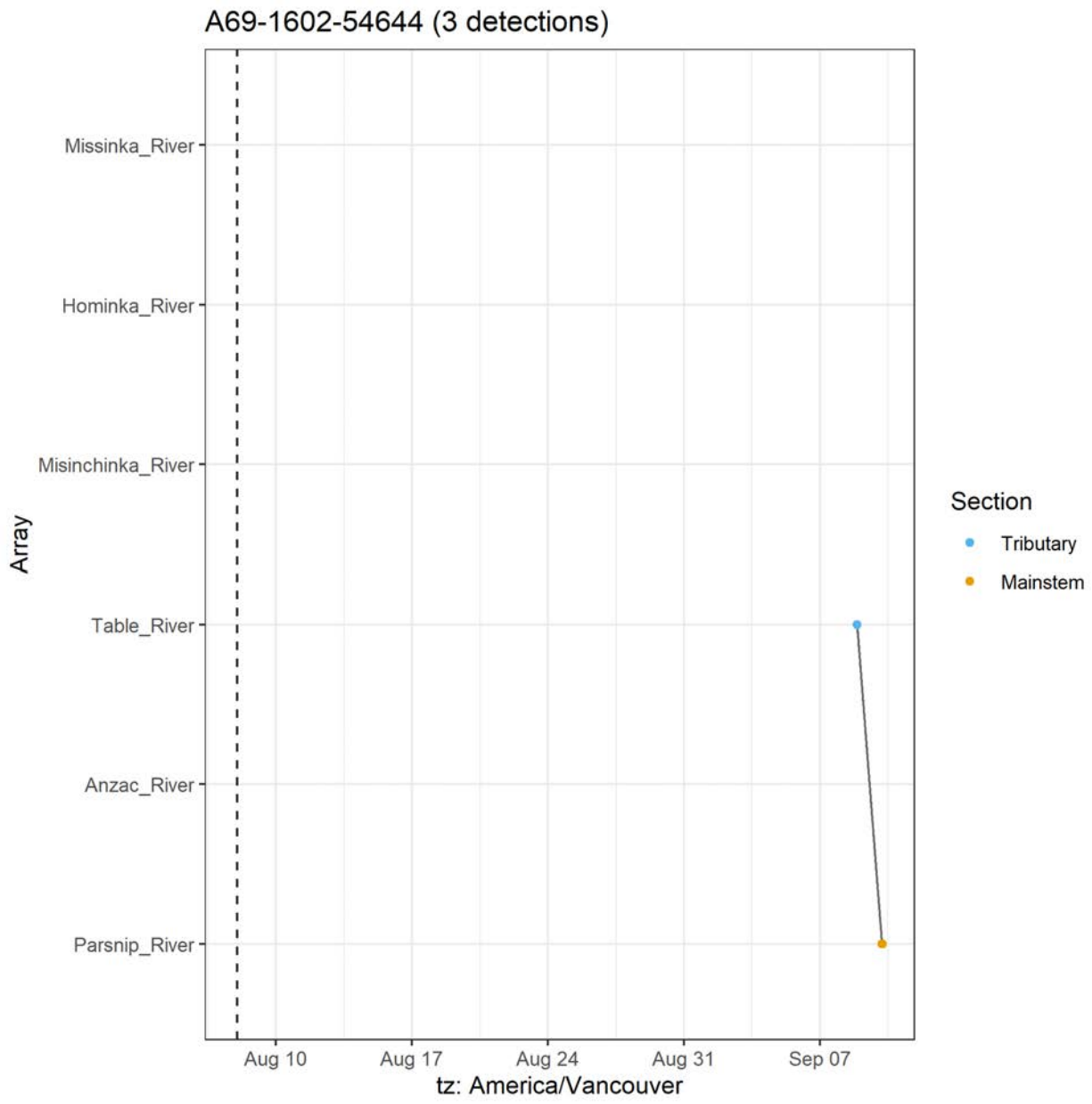
A69-1602-54644 (3 detections)
Missinka_River
Hominka_River
Misinchinka_River
Table_River
Anzac_River
Parsnip_River
Array
Aug 10
Aug 17
Aug 24
Aug 31
Sep 07
tz: America/Vancouver
Section
Tributary
Mainstem

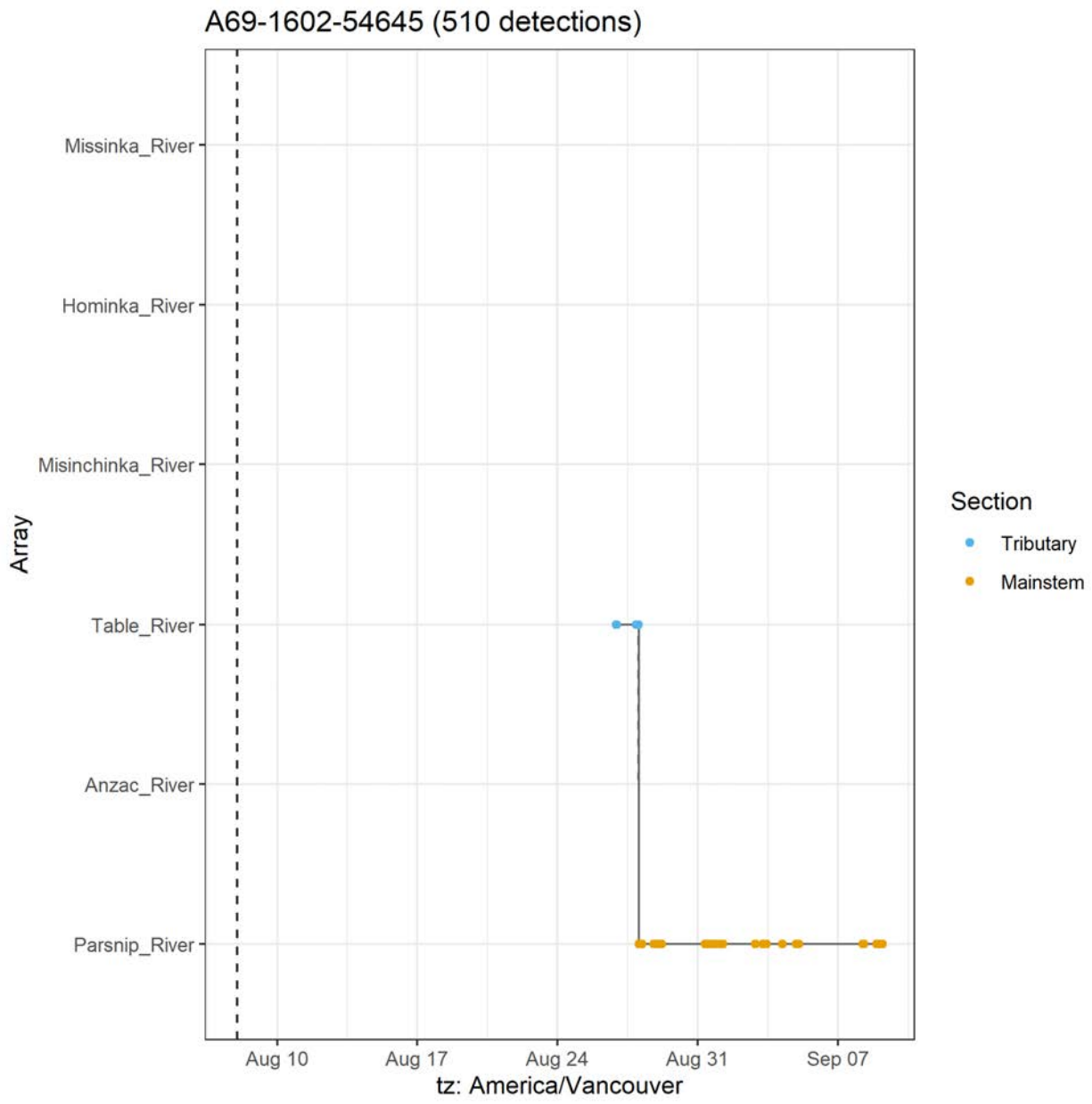
A69-1602-54645 (510 detections)
Missinka_River
Hominka_River
Misinchinka_River
Table_River
Anzac_River
Parsnip_River
Array
Aug 10
Aug 17
Aug 24
Aug 31
Sep 07
tz: America/Vancouver
Section
Tributary
Mainstem

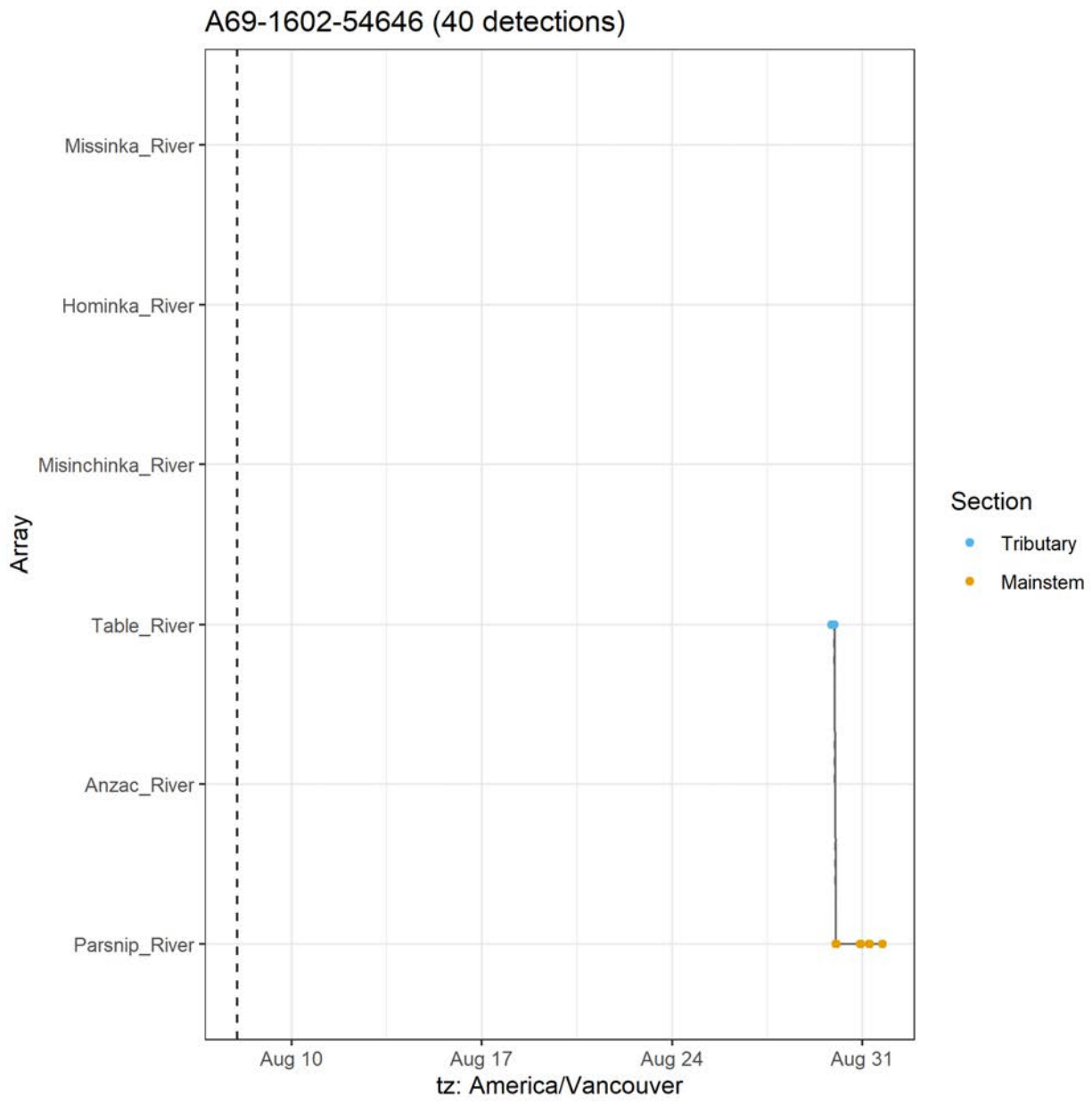
A69-1602-54646 (40 detections)
Missinka_River
Hominka_River
Misinchinka_River
Table_River
Anzac_River
Parsnip_River
Array
Aug 10
Aug 17
Aug 24
Aug 31
tz: America/Vancouver
Section
Tributary
Mainstem

.

**Appendix A.2 – Table of distances moved by individual - Arctic grayling**

These tables represent the results of the function getDistances() called in the package *RSP* (Niella et al. 2020). Each individual is represented by tag ID. Columns 'total distance moved' and 'average distance per event' represent the sum of all movements by an individual since being tagged with an acoustic transmitter and the average distance covered in each event, respectively. Each event, referred to in the analysis as a 'track', represents movements of fish lasting more than ten minutes but is capped at 24 hours. By default, this package assumes a 500 m detection range for acoustic receivers, which is preliminary and will be refined in future analyses. Tags with limited movement histories have been filtered out.

| Arctic grayling tag ID | Total distance moved (m) | Average distance per event (m) | Number of events in history ('tracks') |
|---|---|---|---|
| A69-1602-24283 | 20,090 | 1,339 | 15 |
| A69-1602-24284 | 1,306 | 1,306 | 1 |
| A69-1602-24285 | 19,405 | 693 | 28 |
| A69-1602-24286 | 51,604 | 1,779 | 29 |
| A69-1602-24287 | 51,808 | 2,878 | 18 |
| A69-1602-24289 | 32,676 | 1,167 | 28 |
| A69-1602-24290 | 24,126 | 536 | 45 |
| A69-1602-24288 | 45,244 | 6,463 | 7 |
| A69-1602-24292 | 51,841 | 3,240 | 16 |
| A69-1602-24293 | 35,536 | 3,948 | 9 |
| A69-1602-24294 | 23,093 | 1,215 | 19 |
| A69-1602-24295 | 3,739 | 1,870 | 2 |
| A69-1602-24296 | 42,758 | 2,851 | 15 |
| A69-1602-24298 | 225,395 | 10,733 | 21 |
| A69-1602-24302 | 67,179 | 6,107 | 11 |
| A69-1602-24303 | 29,276 | 2,252 | 13 |
| A69-1602-24307 | 26,649 | 4,441 | 6 |
| A69-1602-24308 | 35,827 | 4,478 | 8 |
| A69-1602-24309 | 73,853 | 8,206 | 9 |
| A69-1602-24304 | 37,603 | 1,213 | 31 |
| A69-1602-24305 | 9,559 | 683 | 14 |
| A69-1602-24310 | 1,238 | 54 | 23 |
| A69-1602-24312 | 81,300 | 3,387 | 24 |
| A69-1602-24313 | 6,983 | 1,746 | 4 |
| A69-1602-24314 | 66,883 | 4,180 | 16 |
| A69-1602-24315 | 11,159 | 2,790 | 4 |
| A69-1602-24316 | 11,339 | 810 | 14 |
| A69-1602-24317 | 22,741 | 1,516 | 15 |
| A69-1602-24311 | 66,263 | 2,651 | 25 |
| A69-1602-24318 | 11,970 | 2,394 | 5 |

| Arctic grayling tag ID | Total distance moved (m) | Average distance per event (m) | Number of events in history ('tracks') |
|---|---|---|---|
| A69-1602-24320 | 34,570 | 2,034 | 17 |
| A69-1602-24321 | 15,694 | 3,139 | 5 |
| A69-1602-24322 | 54,045 | 13,511 | 4 |
| A69-1602-24323 | 17,067 | 1,707 | 10 |
| A69-1602-24324 | 5,876 | 5,876 | 1 |
| A69-1602-24330 | 88,551 | 4,025 | 22 |
| A69-1602-24331 | 30,890 | 3,861 | 8 |
| A69-1602-24325 | 13,617 | 1,702 | 8 |
| A69-1602-24334 | 6,039 | 1,208 | 5 |
| A69-1602-24335 | 27,457 | 1,830 | 15 |
| A69-1602-24337 | 14,131 | 404 | 35 |
| A69-1602-24376 | 7,154 | 795 | 9 |
| A69-1602-24382 | 7,768 | 1,110 | 7 |
| A69-1602-24383 | 10,128 | 460 | 22 |
| A69-1602-24385 | 10,366 | 384 | 27 |
| A69-1602-24361 | 34,669 | 1,825 | 19 |
| A69-1602-24362 | 76,038 | 2,236 | 34 |
| A69-1602-24367 | 100,465 | 6,279 | 16 |
| A69-1602-24368 | 42,749 | 7,125 | 6 |
| A69-1602-24369 | 107,314 | 5,110 | 21 |
| A69-1602-24359 | 94,065 | 5,879 | 16 |
| A69-1602-24371 | 190,466 | 23,808 | 8 |
| A69-1602-24372 | 195,823 | 13,055 | 15 |
| A69-1602-24380 | 88,031 | 5,869 | 15 |
| A69-1602-24342 | 60,907 | 3,206 | 19 |
| A69-1602-24353 | 116,161 | 6,833 | 17 |
| A69-1602-24373 | 69,460 | 2,043 | 34 |
| A69-1602-24357 | 11,723 | 2,931 | 4 |
| A69-1602-24364 | 21,729 | 869 | 25 |
| A69-1602-24365 | 42,654 | 6,093 | 7 |

| Arctic grayling tag ID | Total distance moved (m) | Average distance per event (m) | Number of events in history ('tracks') |
|---|---|---|---|
| A69-1602-24366 | 7,738 | 430 | 18 |
| A69-1602-24344 | 511 | 102 | 5 |
| A69-1602-24350 | 5,176 | 2,588 | 2 |
| A69-1602-24349 | 13,700 | 979 | 14 |
| A69-1602-19304 | 653 | 653 | 1 |
| A69-1602-19305 | 25,658 | 3,665 | 7 |
| A69-1602-19306 | 69,022 | 2,157 | 32 |
| A69-1602-19307 | 2,179 | 198 | 11 |
| A69-1602-19308 | 36,186 | 6,031 | 6 |
| A69-1602-19311 | 7,184 | 718 | 10 |
| A69-1602-19314 | 2,694 | 449 | 6 |
| A69-1602-19315 | 33,346 | 3,705 | 9 |
| A69-1602-19316 | 23,165 | 1,930 | 12 |
| A69-1602-19319 | 28,627 | 3,578 | 8 |
| A69-1602-19321 | 20,279 | 1,560 | 13 |
| A69-1602-19322 | 56,057 | 7,007 | 8 |
| A69-1602-19324 | 20,547 | 893 | 23 |
| A69-1602-19331 | 38,293 | 1,160 | 33 |
| A69-1602-19309 | 1,369 | 62 | 22 |
| A69-1602-19310 | 29,888 | 5,978 | 5 |
| A69-1602-19317 | 17,070 | 2,439 | 7 |
| A69-1602-19323 | 27,066 | 873 | 31 |
| A69-1602-19327 | 15,377 | 961 | 16 |
| A69-1602-19326 | 5,994 | 545 | 11 |
| A69-1602-19336 | 84,088 | 4,004 | 21 |
| A69-1602-19345 | 24,137 | 24,137 | 1 |
| A69-1602-19361 | 33,089 | 2,206 | 15 |
| A69-1602-19362 | 47,281 | 5,253 | 9 |
| A69-1602-19338 | 511 | 102 | 5 |
| A69-1602-19342 | 20,276 | 2,897 | 7 |
| A69-1602-24345 | 6,912 | 3,456 | 2 |
| A69-1602-19347 | 11,154 | 5,577 | 2 |
| A69-1602-19329 | 24,583 | 8,194 | 3 |
| A69-1602-19354 | 81,992 | 40,996 | 2 |
| A69-1602-19357 | 39,685 | 19,842 | 2 |
| A69-1602-54657 | 28,764 | 28,764 | 1 |

**Appendix A.2 – Table of distances moved by individual - Bull trout**

These tables represent the results of the function getDistances() called in the package *RSP* (Niella et al. 2020). Each individual is represented by tag ID. Columns 'total distance moved' and 'average distance per event' represent the sum of all movements by an individual since being tagged with an acoustic transmitter and the average distance covered in each event, respectively. Each event, referred to in the analysis as a 'track', represents movements of fish lasting more than ten minutes but is capped at 24 hours. By default, this package assumes a 500 m detection range for acoustic receivers, which is being considered preliminary and will be refined in future analyses. Tags with limited movement histories have been filtered out.

| Bull trout tag ID | Total distance moved (m) | Average distance per event (m) | Number of events in history |
|---|---|---|---|
| A69-1602-24300 | 5,508 | 5,508 | 1 |
| A69-1602-24297 | 159,573 | 17,730 | 9 |
| A69-1602-24319 | 109,388 | 9,116 | 12 |
| A69-1602-24326 | 33,850 | 677 | 50 |
| A69-1602-24333 | 132,193 | 2,644 | 50 |
| A69-1602-24377 | 8,191 | 455 | 18 |
| A69-1602-24384 | 148,806 | 9,920 | 15 |
| A69-1602-24374 | 20,650 | 4,130 | 5 |
| A69-1602-24375 | 24,623 | 1,368 | 18 |
| A69-1602-24378 | 33,864 | 691 | 49 |
| A69-1602-24379 | 6,371 | 1,593 | 4 |
| A69-1602-24360 | 36,053 | 12,018 | 3 |
| A69-1602-24370 | 12,186 | 677 | 18 |
| A69-1602-24358 | 22,992 | 1,437 | 16 |
| A69-1602-24354 | 671 | 224 | 3 |
| A69-1602-24356 | 80,559 | 40,279 | 2 |
| A69-1602-24343 | 73,287 | 12,215 | 6 |
| A69-1602-24348 | 49,432 | 1,545 | 32 |
| A69-1602-24351 | 83,229 | 83,229 | 1 |
| A69-1602-19318 | 86,634 | 28,878 | 3 |
| A69-1602-19335 | 20,899 | 1,100 | 19 |
| A69-1602-54646 | 29,469 | 29,469 | 1 |
| A69-1602-54645 | 62,699 | 12,540 | 5 |
| A69-1602-54644 | 1,504 | 1,504 | 1 |
| A69-1602-19325 | 20,847 | 4,169 | 5 |
| A69-1602-19353 | 36,578 | 36,578 | 1 |

**Appendix A.3 – Individual track histories – Arctic grayling**

These plots represent a visualization of the 'tracks' calculated in package *RSP* (Niella et al 2020). Each plot represents the track history of one individual since being tagged with an acoustic transmitter. Tracks represent movement events that last longer than 10 minutes but are capped at 24 hours. Plots with a large number of tracks but a small spatial extent indicate frequently overlapping of tracks. By default, this package assumes a 500 m detection range for acoustic receivers, which is being considered preliminary and will be refined in future analyses. Tags with limited movement histories have been filtered out.

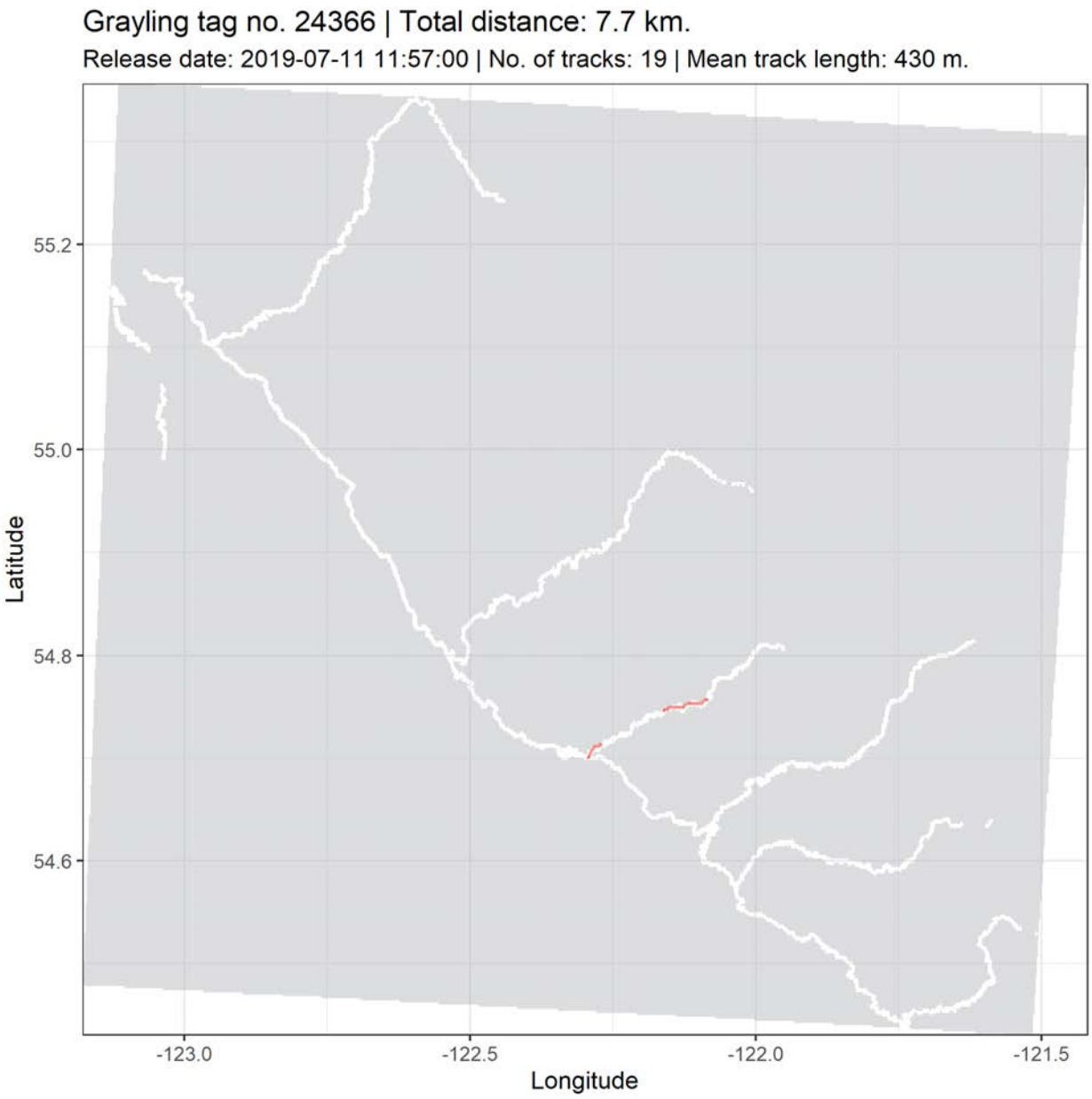
Grayling tag no. 24366 | Total distance: 7.7 km.
Release date: 2019-07-11 11:57:00 | No. of tracks: 19 | Mean track length: 430 m.
55.2
55.0
54.8
54.6
Latitude
-123.0
-122.5
-122.0
-121.5
Longitude

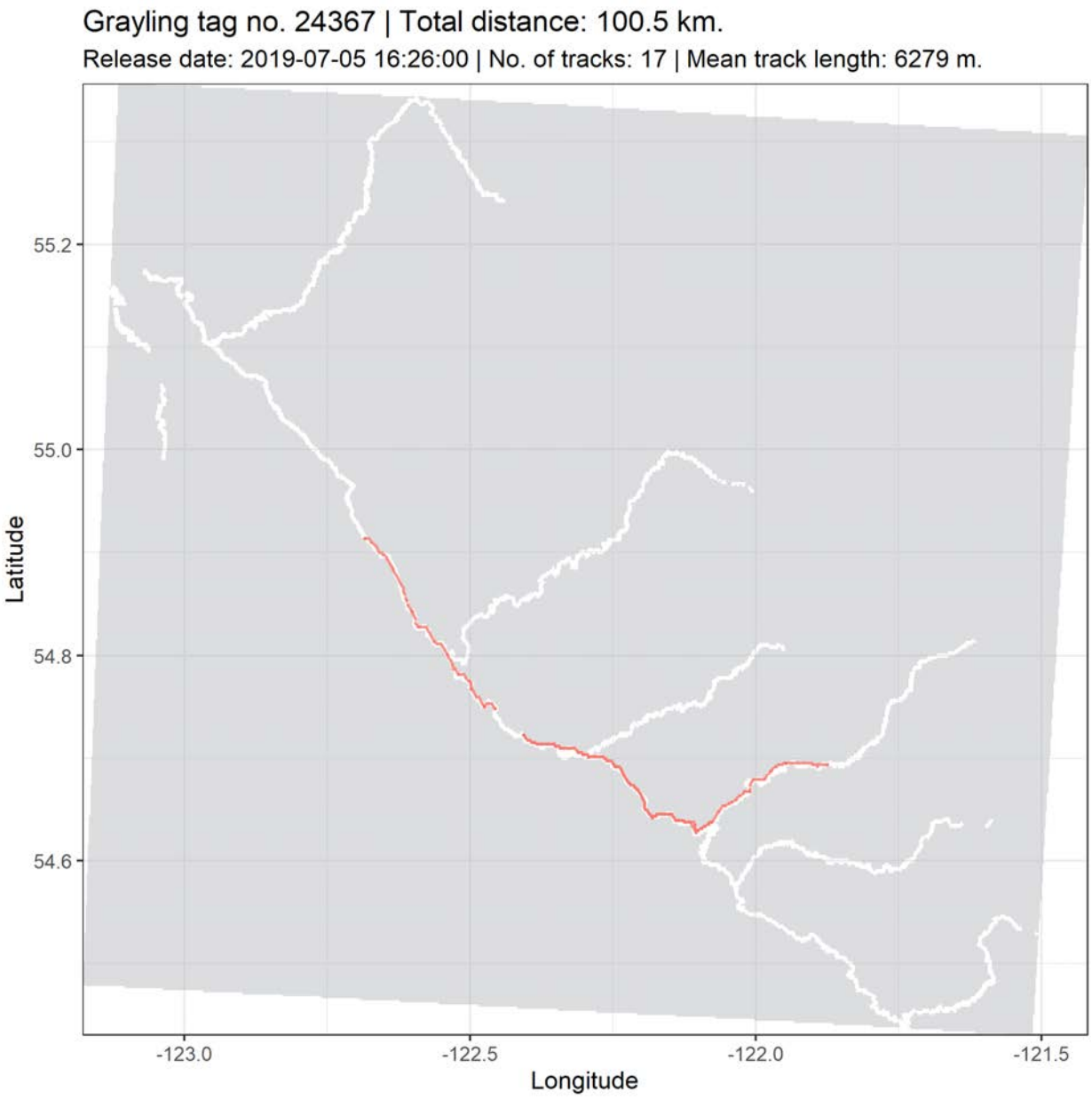
Grayling tag no. 24367 | Total distance: 100.5 km.
Release date: 2019-07-05 16:26:00 | No. of tracks: 17 | Mean track length: 6279 m.
55.2
55.0
54.8
54.6
Latitude
-123.0
-122.5
-122.0
-121.5
Longitude

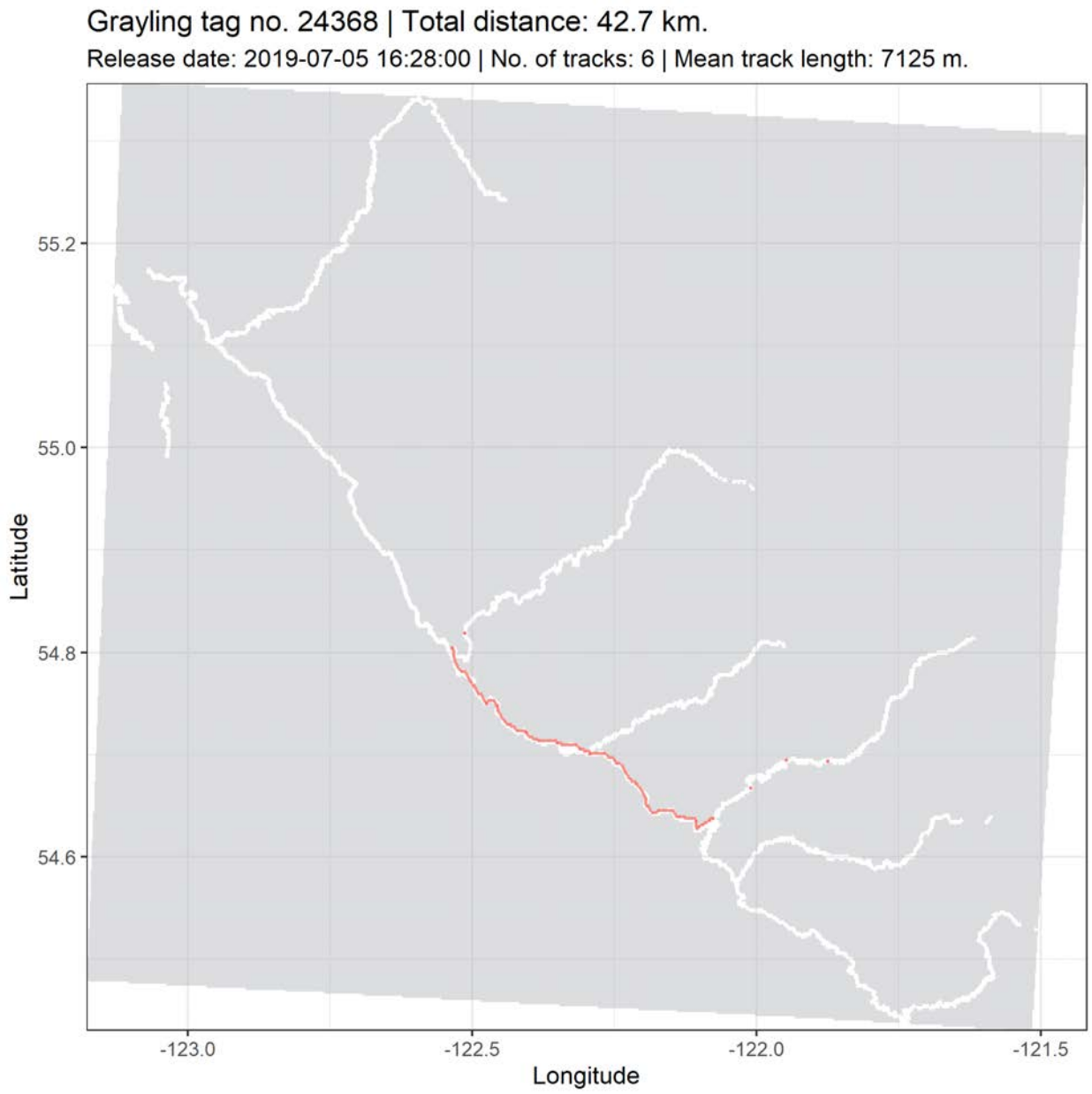
Grayling tag no. 24368 | Total distance: 42.7 km.
Release date: 2019-07-05 16:28:00 | No. of tracks: 6 | Mean track length: 7125 m.
55.2
55.0
54.8
54.6
Latitude
-123.0
-122.5
-122.0
-121.5
Longitude

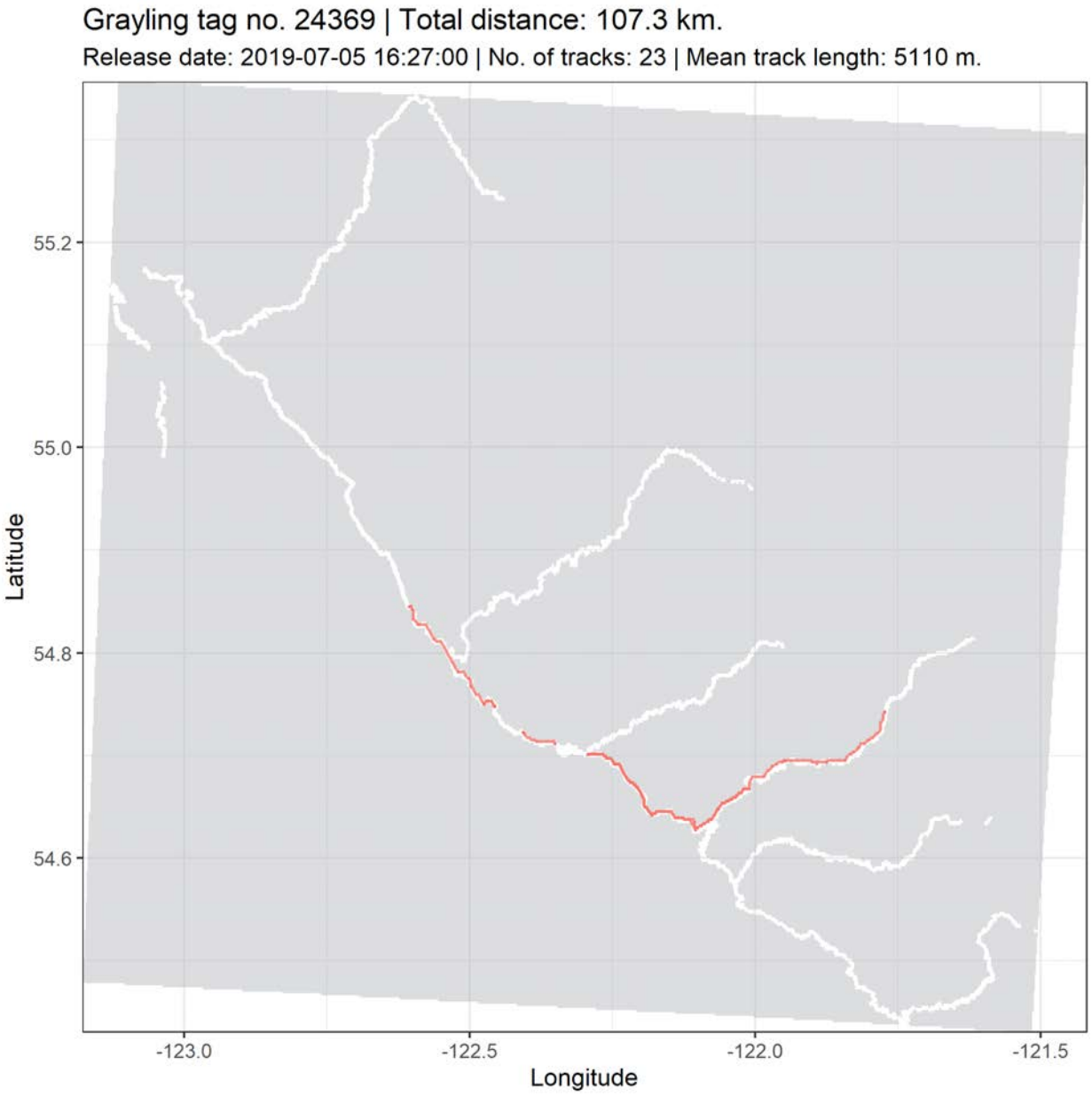
Grayling tag no. 24369 | Total distance: 107.3 km.
Release date: 2019-07-05 16:27:00 | No. of tracks: 23 | Mean track length: 5110 m.
55.2
55.0
54.8
54.6
Latitude
-123.0
-122.5
-122.0
-121.5
Longitude

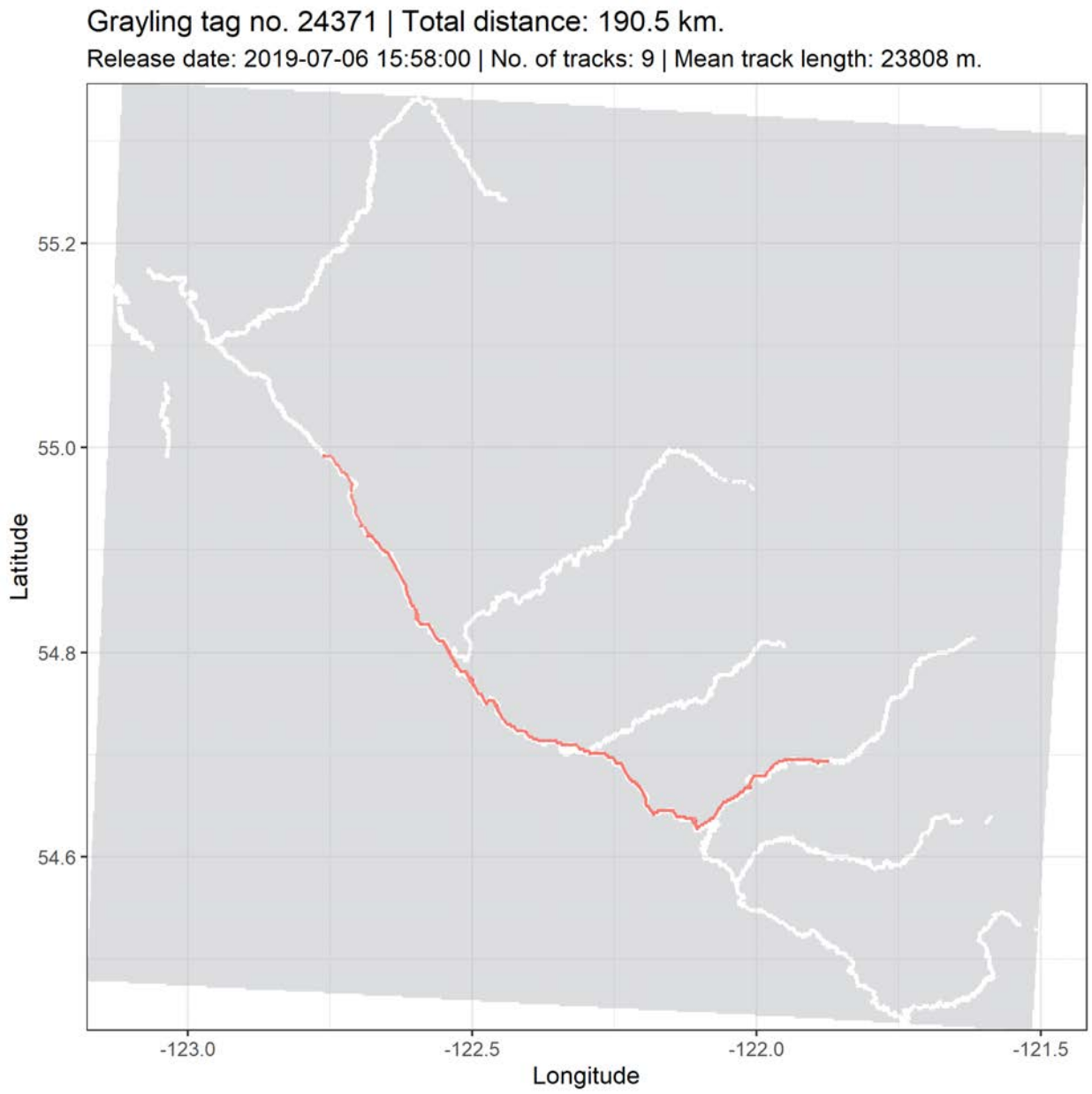
Grayling tag no. 24371 | Total distance: 190.5 km.
Release date: 2019-07-06 15:58:00 | No. of tracks: 9 | Mean track length: 23808 m.
55.2
55.0
54.8
54.6
Latitude
-123.0
-122.5
-122.0
-121.5
Longitude

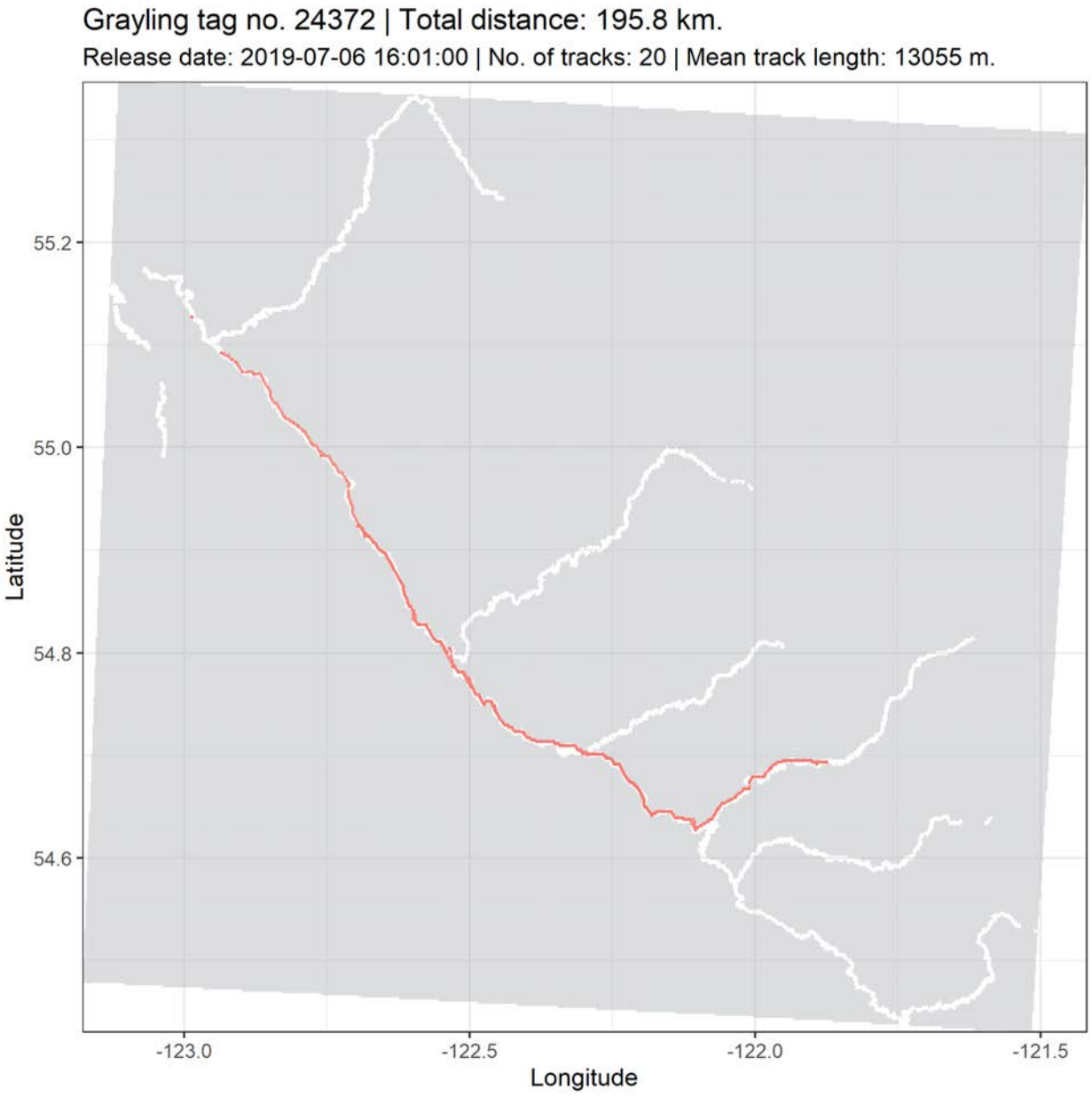
Grayling tag no. 24372 | Total distance: 195.8 km.
Release date: 2019-07-06 16:01:00 | No. of tracks: 20 | Mean track length: 13055 m.
55.2
55.0
54.8
54.6
Latitude
-123.0
-122.5
-122.0
-121.5
Longitude

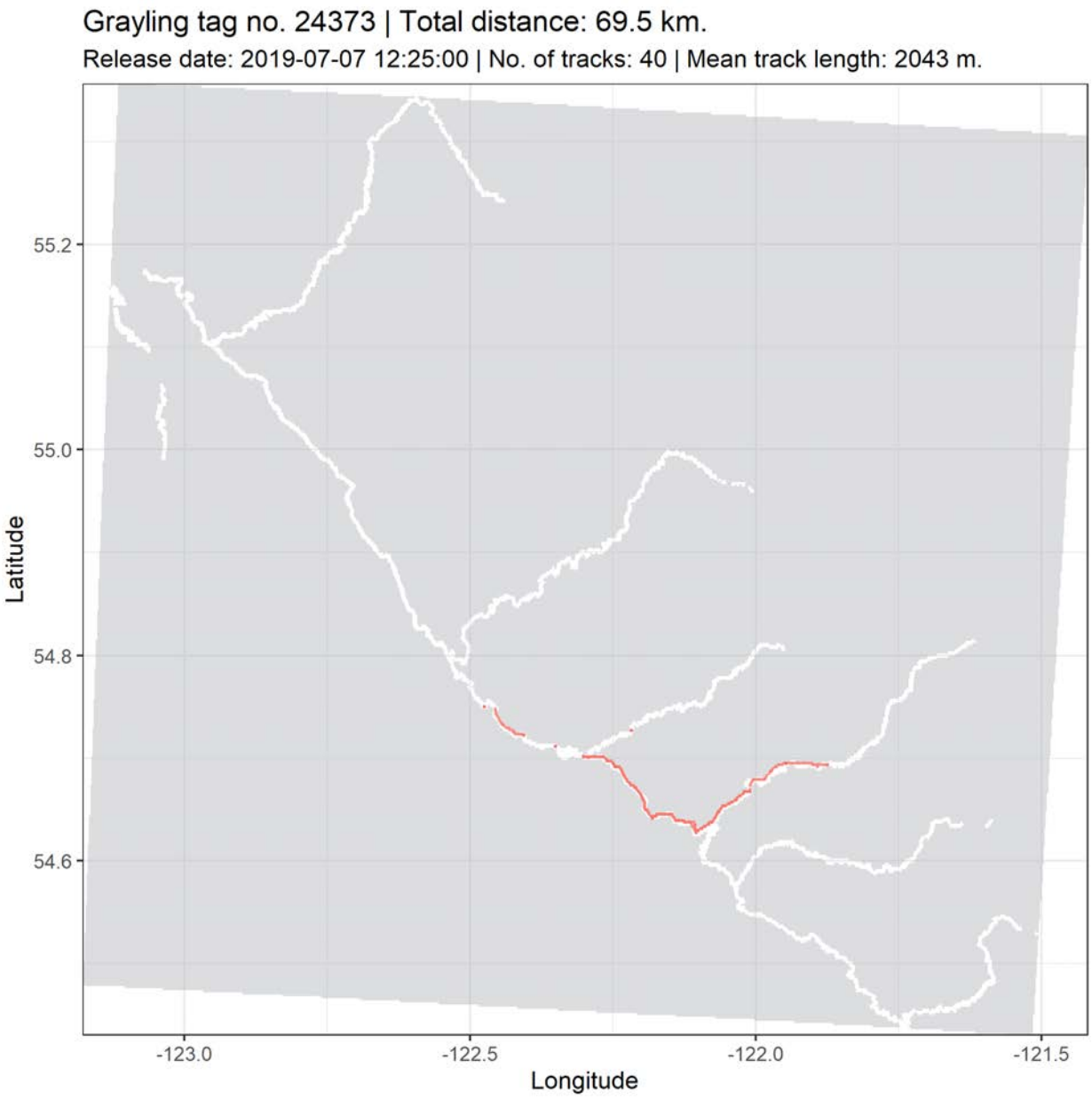
Grayling tag no. 24373 | Total distance: 69.5 km.
Release date: 2019-07-07 12:25:00 | No. of tracks: 40 | Mean track length: 2043 m.
55.2
55.0
54.8
54.6
Latitude
-123.0
-122.5
-122.0
-121.5
Longitude

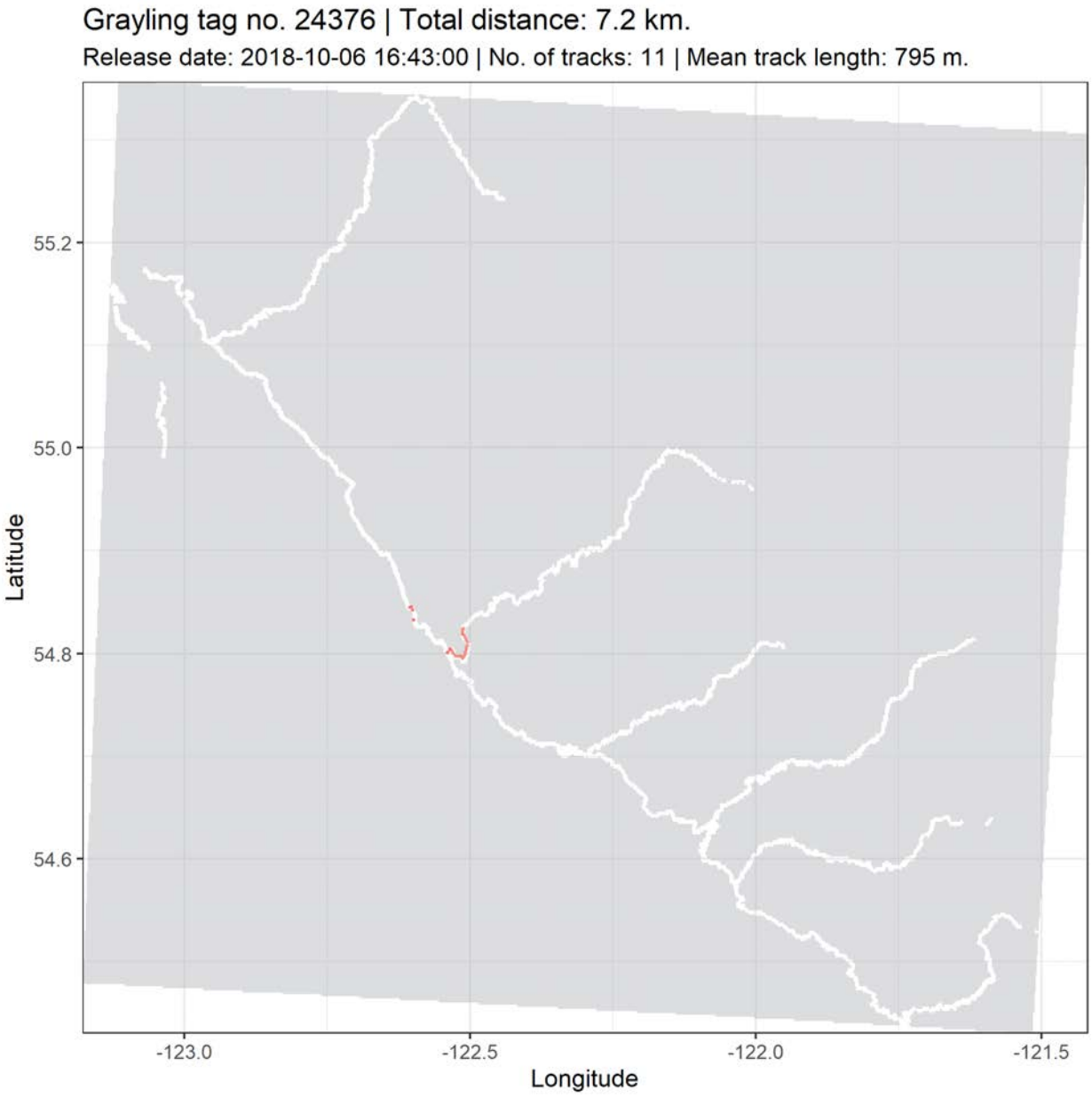
Grayling tag no. 24376 | Total distance: 7.2 km.
Release date: 2018-10-06 16:43:00 | No. of tracks: 11 | Mean track length: 795 m.
55.2
55.0
54.8
54.6
Latitude
-123.0
-122.5
-122.0
-121.5
Longitude

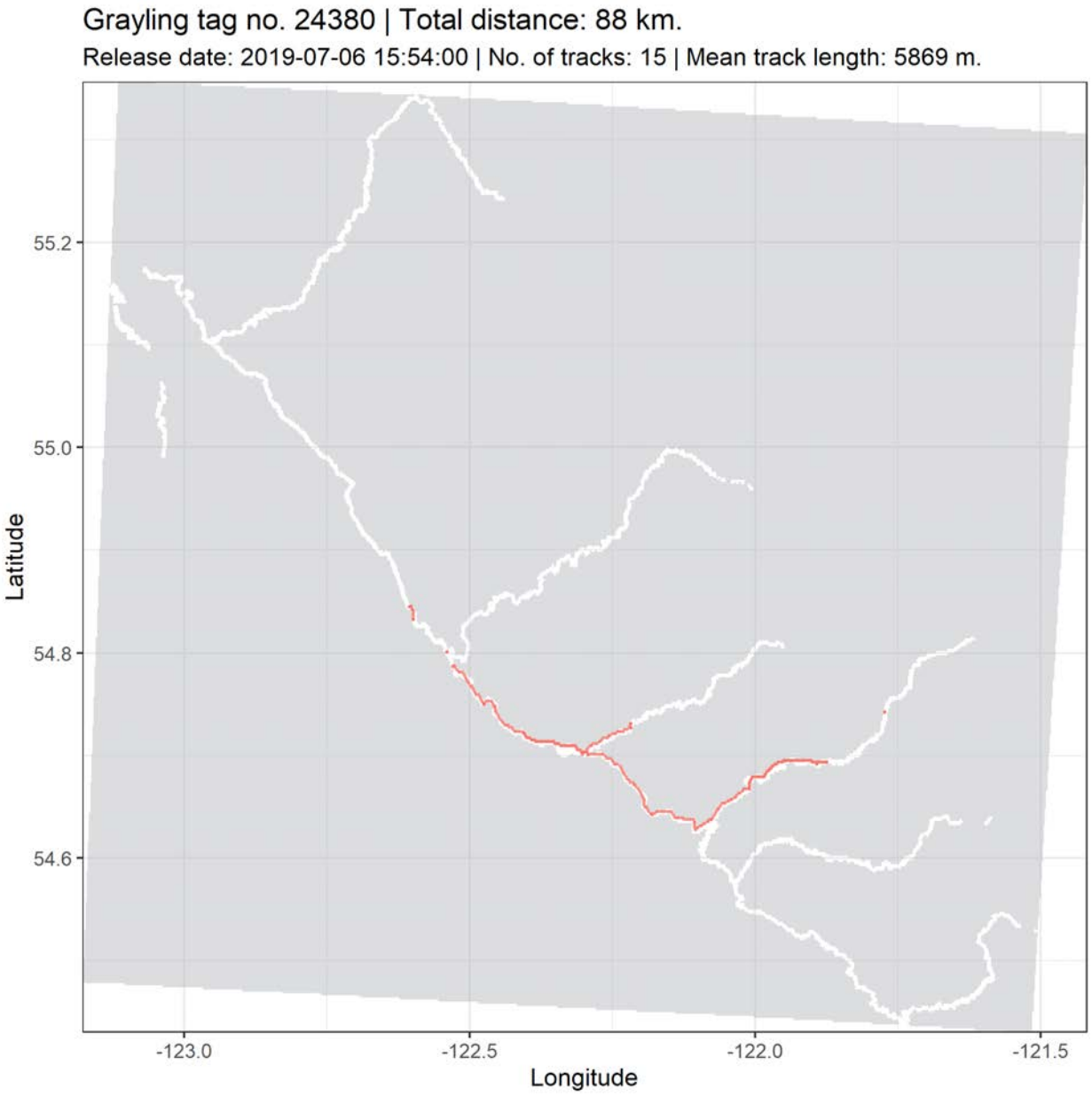
Grayling tag no. 24380 | Total distance: 88 km.
Release date: 2019-07-06 15:54:00 | No. of tracks: 15 | Mean track length: 5869 m.
55.2
55.0
54.8
54.6
Latitude
-123.0
-122.5
-122.0
-121.5
Longitude

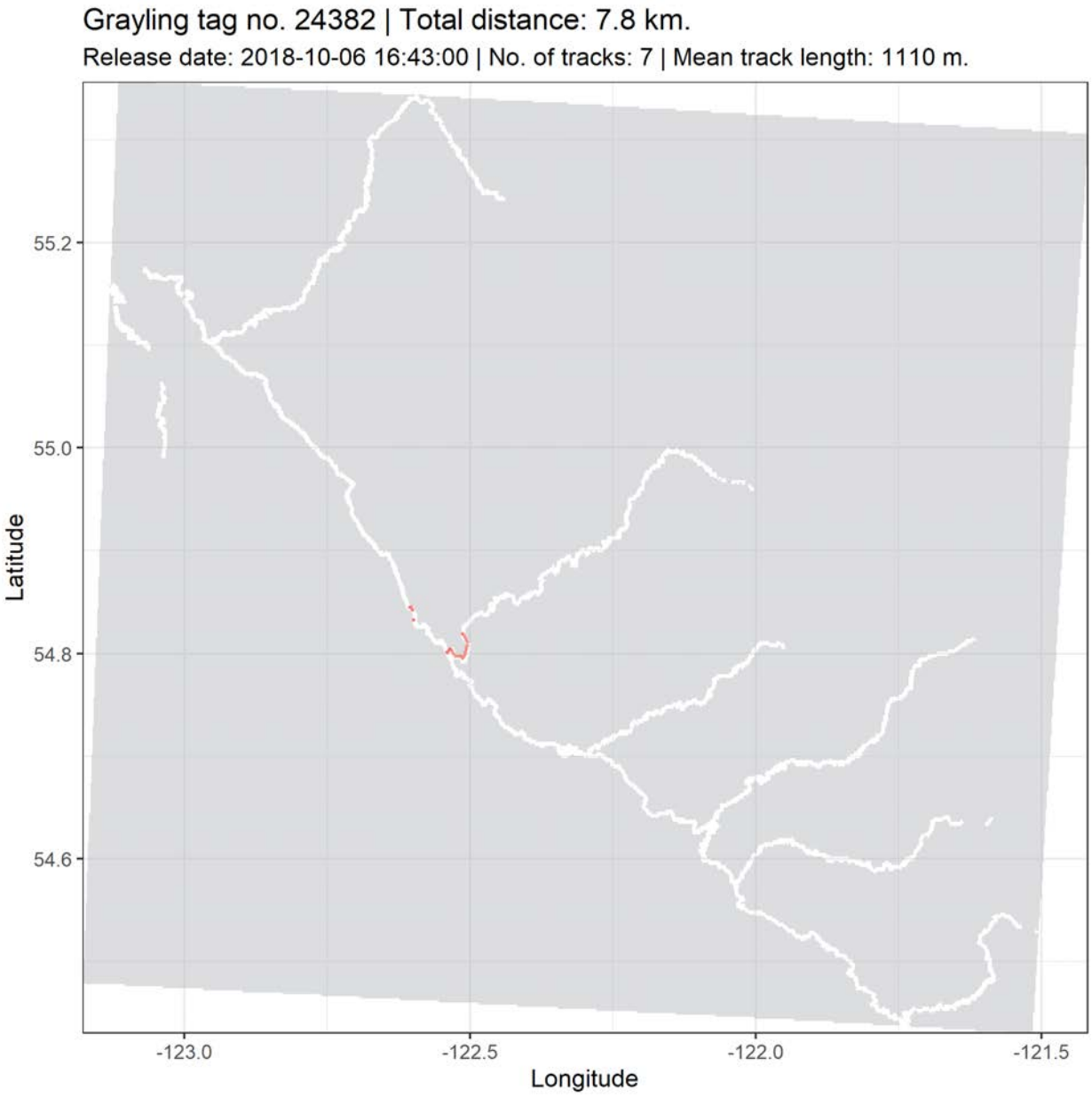
Grayling tag no. 24382 | Total distance: 7.8 km.
Release date: 2018-10-06 16:43:00 | No. of tracks: 7 | Mean track length: 1110 m.
55.2
55.0
54.8
54.6
Latitude
-123.0
-122.5
-122.0
-121.5
Longitude

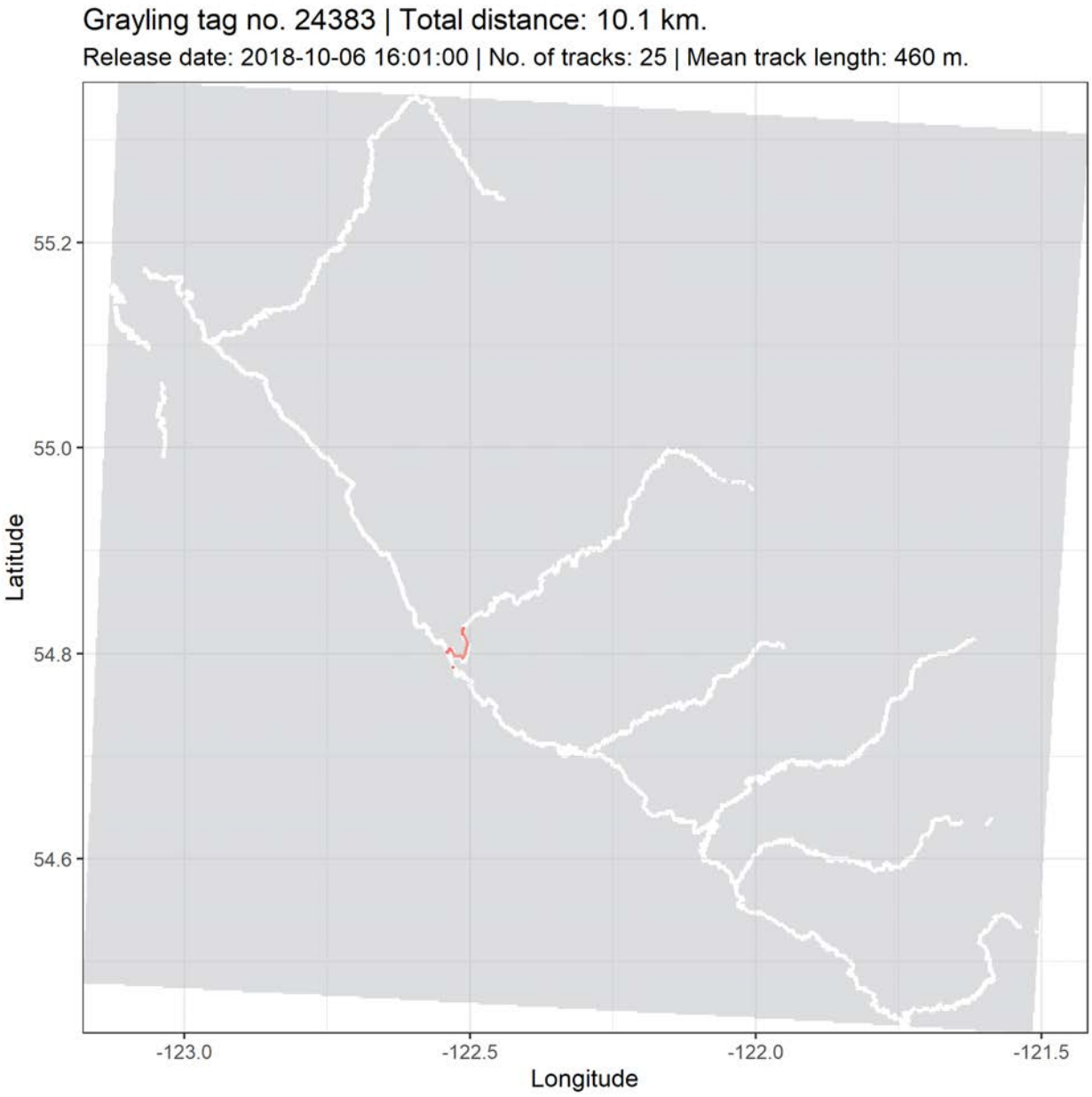
Grayling tag no. 24383 | Total distance: 10.1 km.
Release date: 2018-10-06 16:01:00 | No. of tracks: 25 | Mean track length: 460 m.
55.2
55.0
54.8
54.6
Latitude
-123.0
-122.5
-122.0
-121.5
Longitude

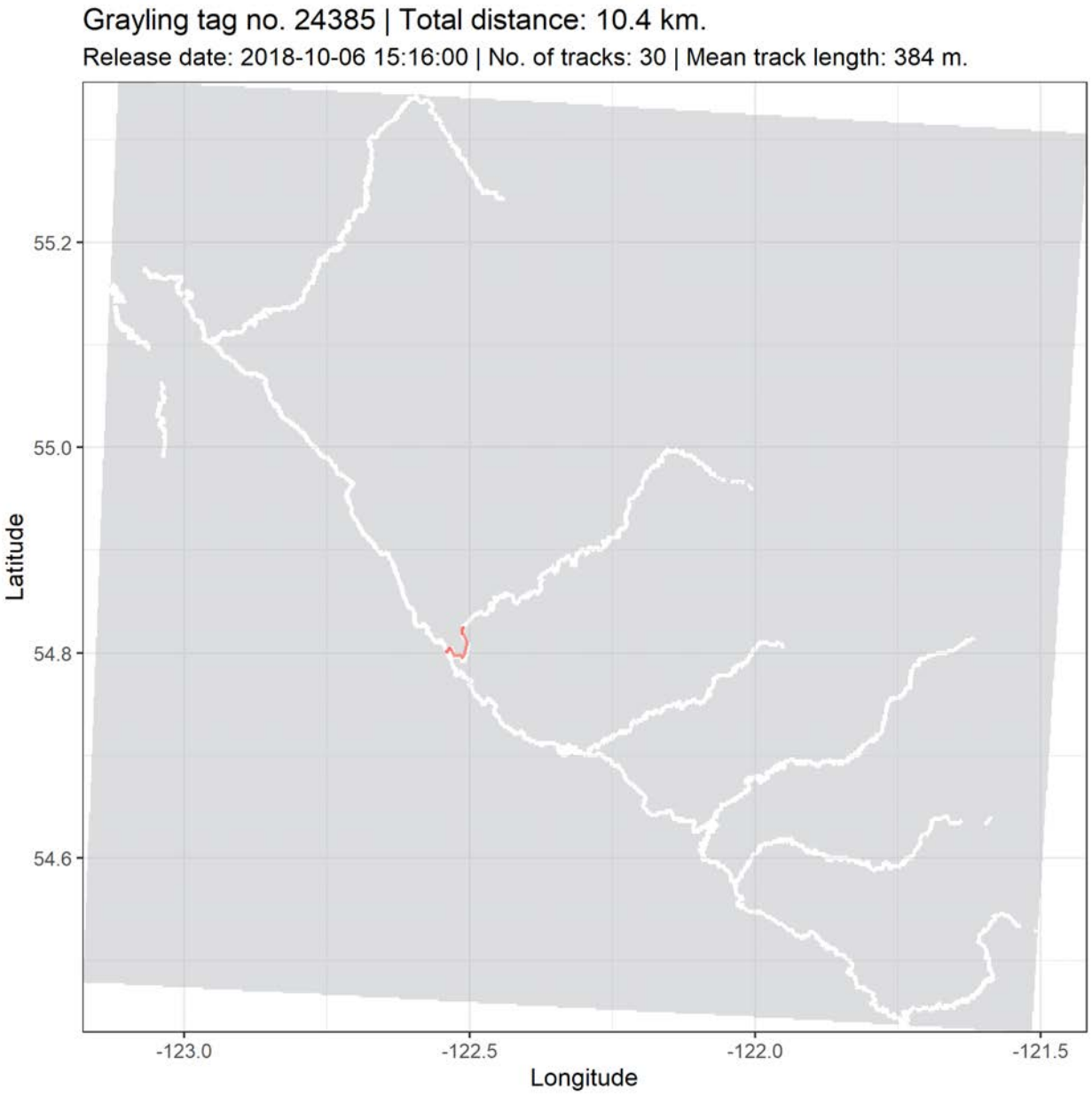
Grayling tag no. 24385 | Total distance: 10.4 km.
Release date: 2018-10-06 15:16:00 | No. of tracks: 30 | Mean track length: 384 m.
55.2
55.0
54.8
54.6
Latitude
-123.0
-122.5
-122.0
-121.5
Longitude

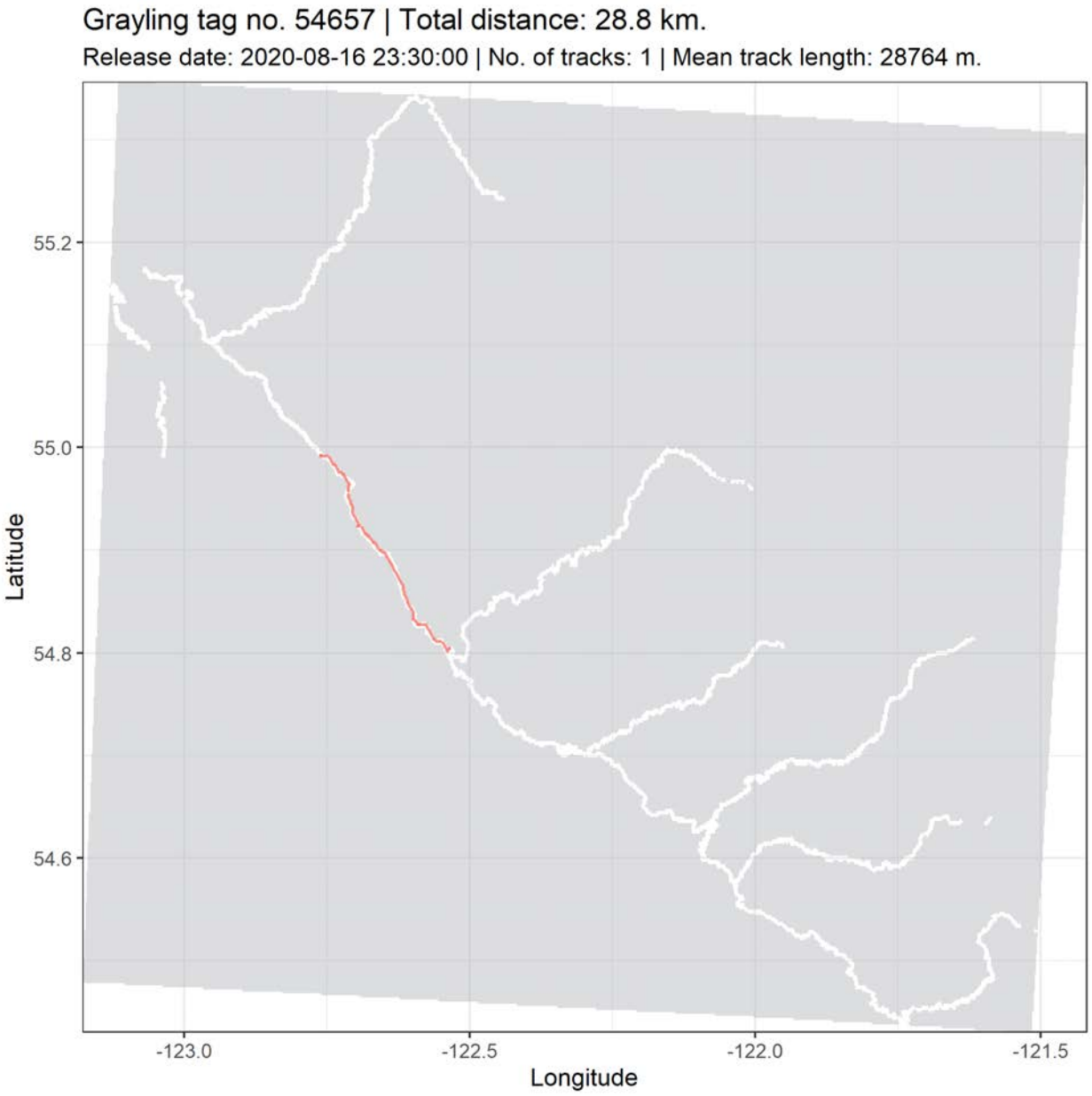
Grayling tag no. 54657 | Total distance: 28.8 km.
Release date: 2020-08-16 23:30:00 | No. of tracks: 1 | Mean track length: 28764 m.
55.2
55.0
54.8
54.6
Latitude
-123.0
-122.5
-122.0
-121.5
Longitude

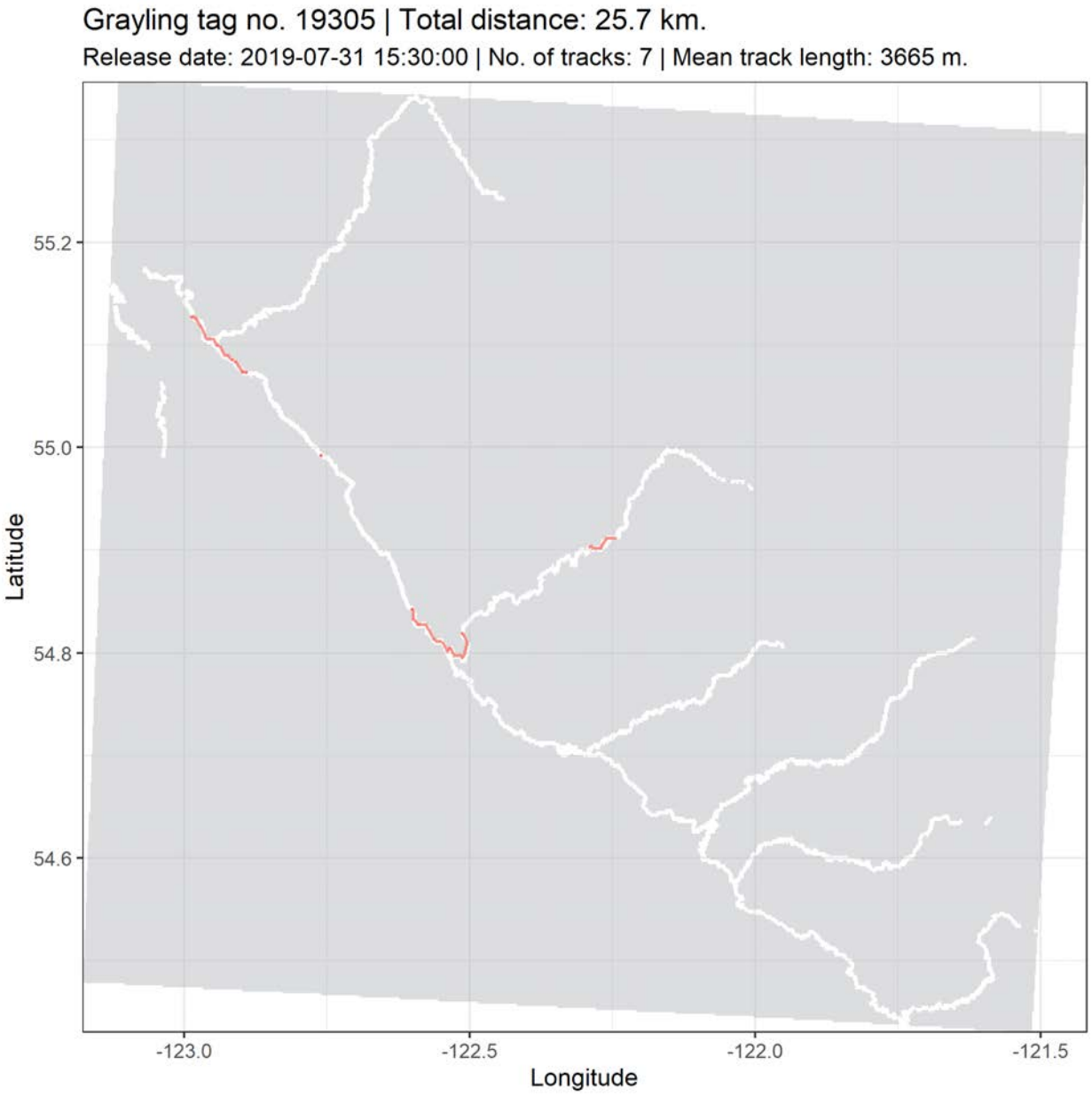
Grayling tag no. 19305 | Total distance: 25.7 km.
Release date: 2019-07-31 15:30:00 | No. of tracks: 7 | Mean track length: 3665 m.
55.2
55.0
54.8
54.6
Latitude
-123.0
-122.5
-122.0
-121.5
Longitude

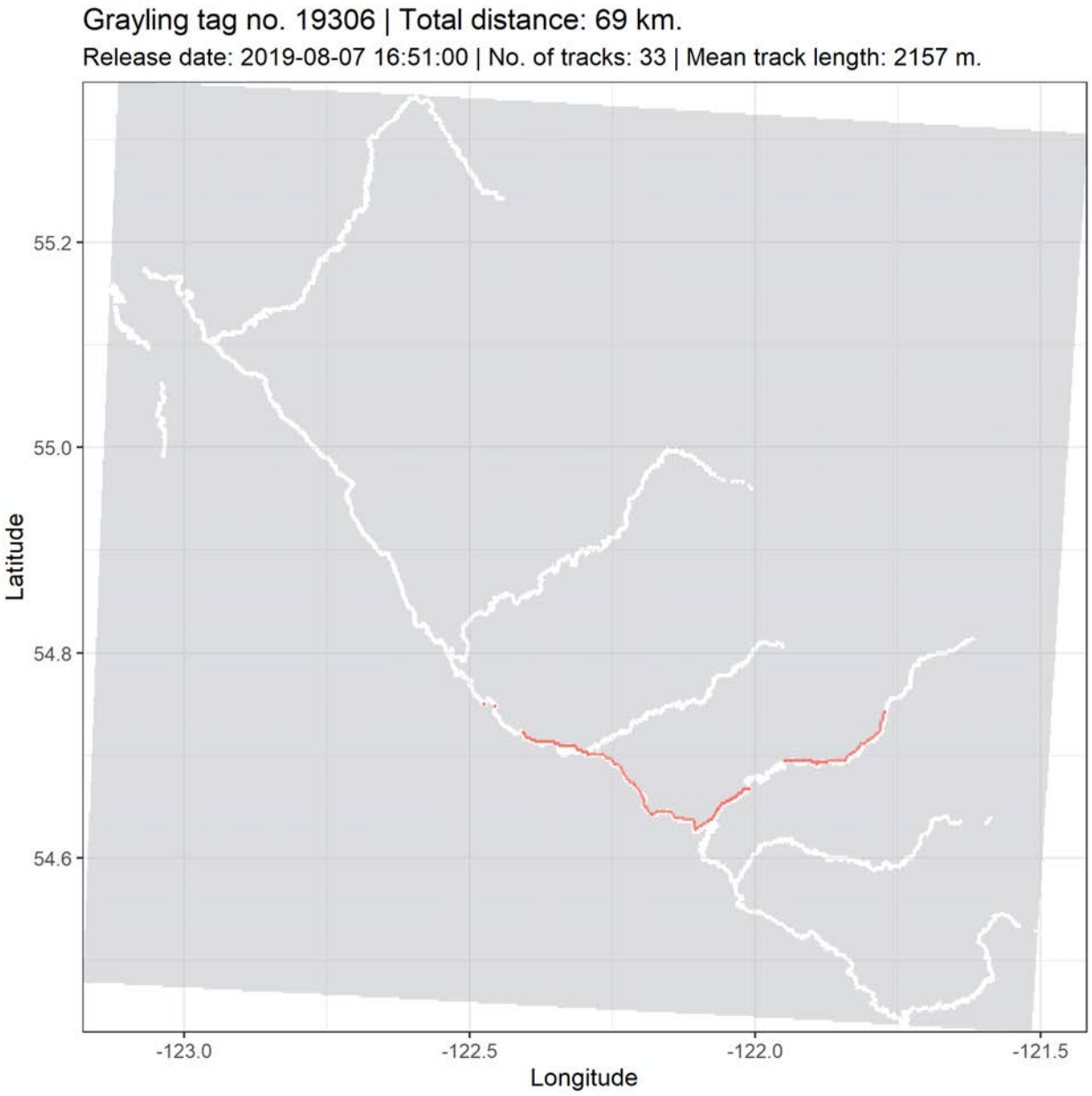
Grayling tag no. 19306 | Total distance: 69 km.
Release date: 2019-08-07 16:51:00 | No. of tracks: 33 | Mean track length: 2157 m.
55.2
55.0
54.8
54.6
Latitude
-123.0
-122.5
-122.0
-121.5
Longitude

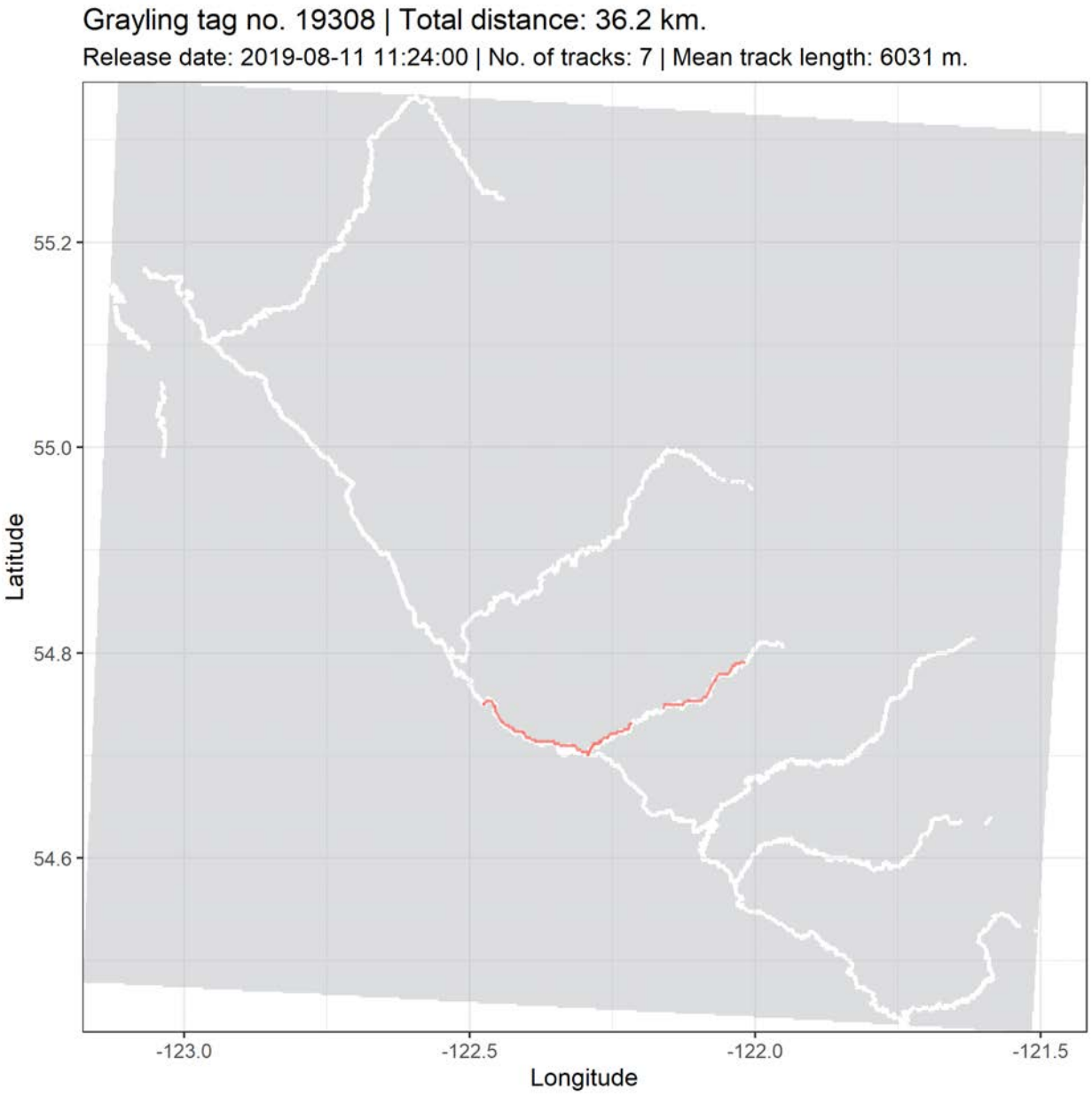
Grayling tag no. 19308 | Total distance: 36.2 km.
Release date: 2019-08-11 11:24:00 | No. of tracks: 7 | Mean track length: 6031 m.
55.2
55.0
54.8
54.6
Latitude
-123.0
-122.5
-122.0
-121.5
Longitude

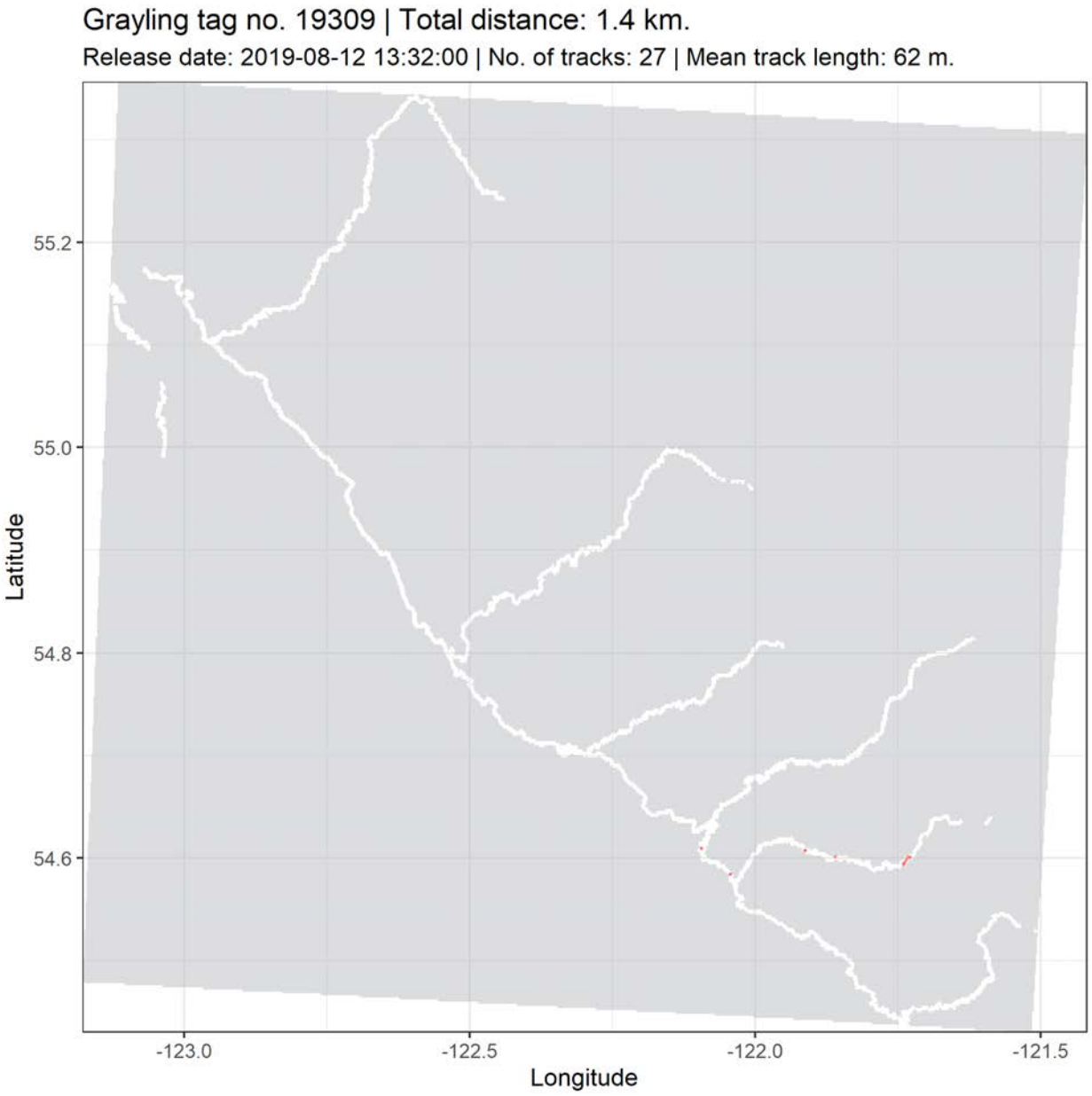
Grayling tag no. 19309 | Total distance: 1.4 km.
Release date: 2019-08-12 13:32:00 | No. of tracks: 27 | Mean track length: 62 m.
55.2
55.0
54.8
54.6
Latitude
-123.0
-122.5
-122.0
-121.5
Longitude

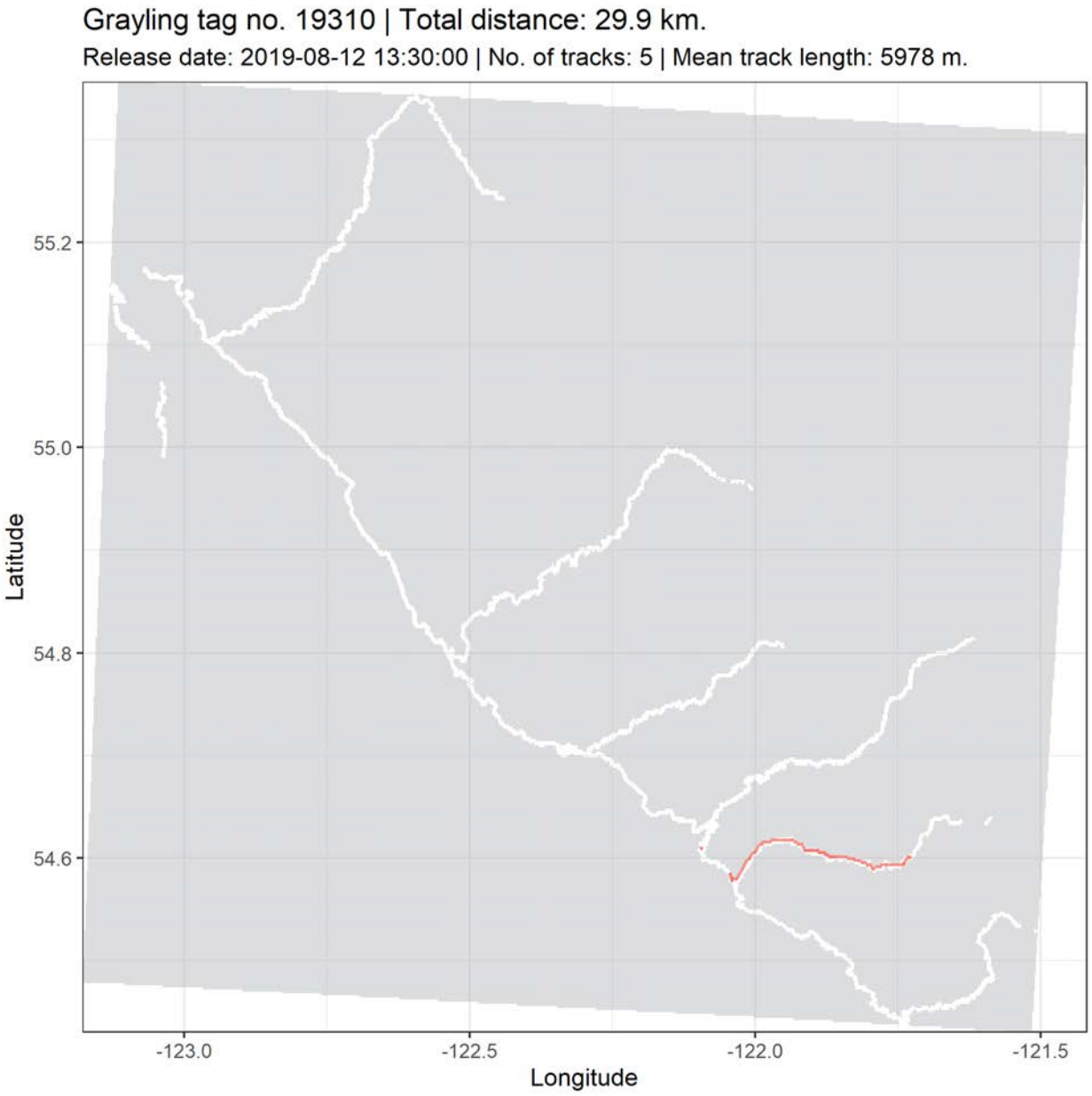
Grayling tag no. 19310 | Total distance: 29.9 km.
Release date: 2019-08-12 13:30:00 | No. of tracks: 5 | Mean track length: 5978 m.
55.2
55.0
54.8
54.6
Latitude
-123.0
-122.5
-122.0
-121.5
Longitude

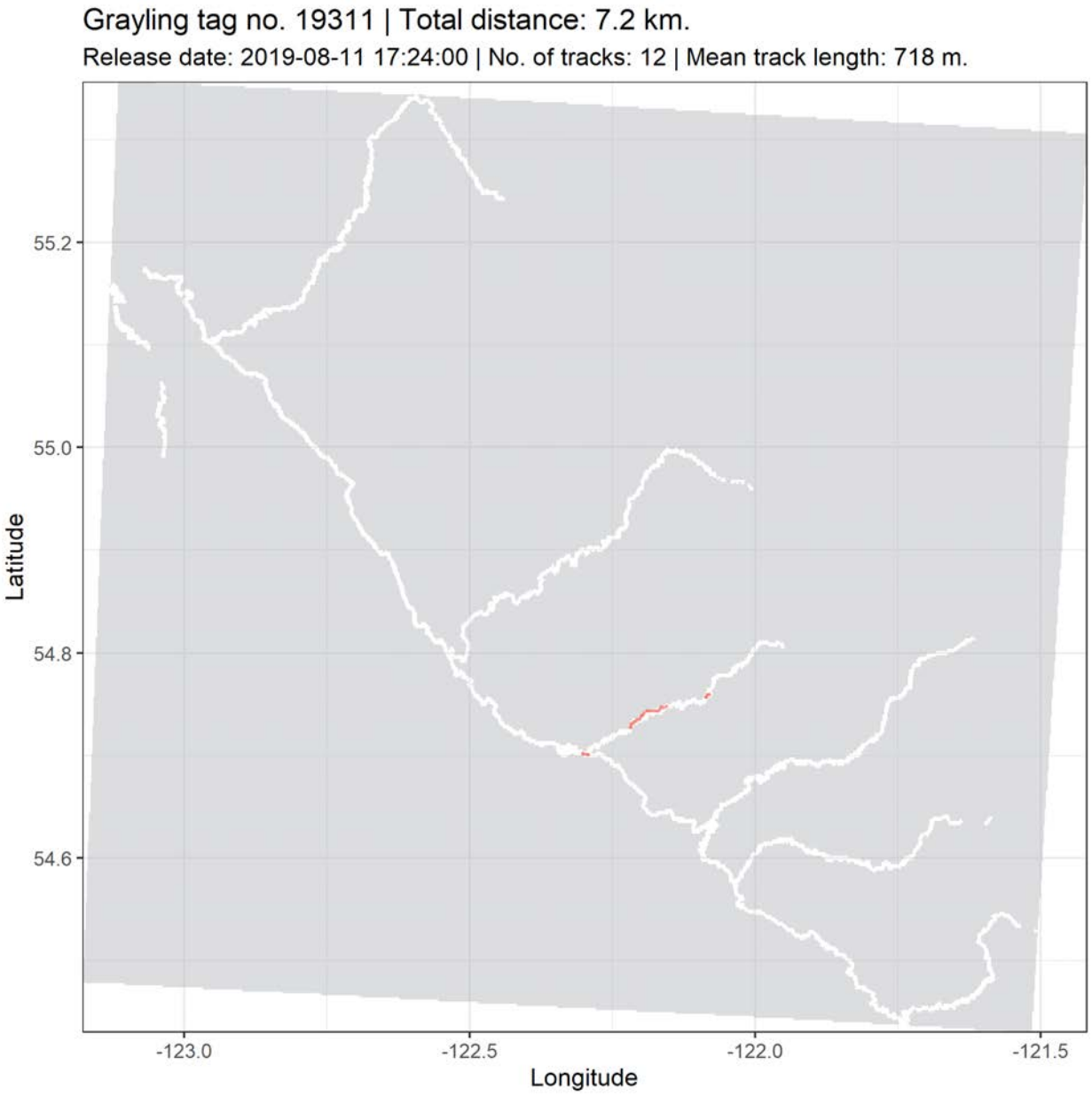
Grayling tag no. 19311 | Total distance: 7.2 km.
Release date: 2019-08-11 17:24:00 | No. of tracks: 12 | Mean track length: 718 m.
55.2
55.0
54.8
54.6
Latitude
-123.0
-122.5
-122.0
-121.5
Longitude

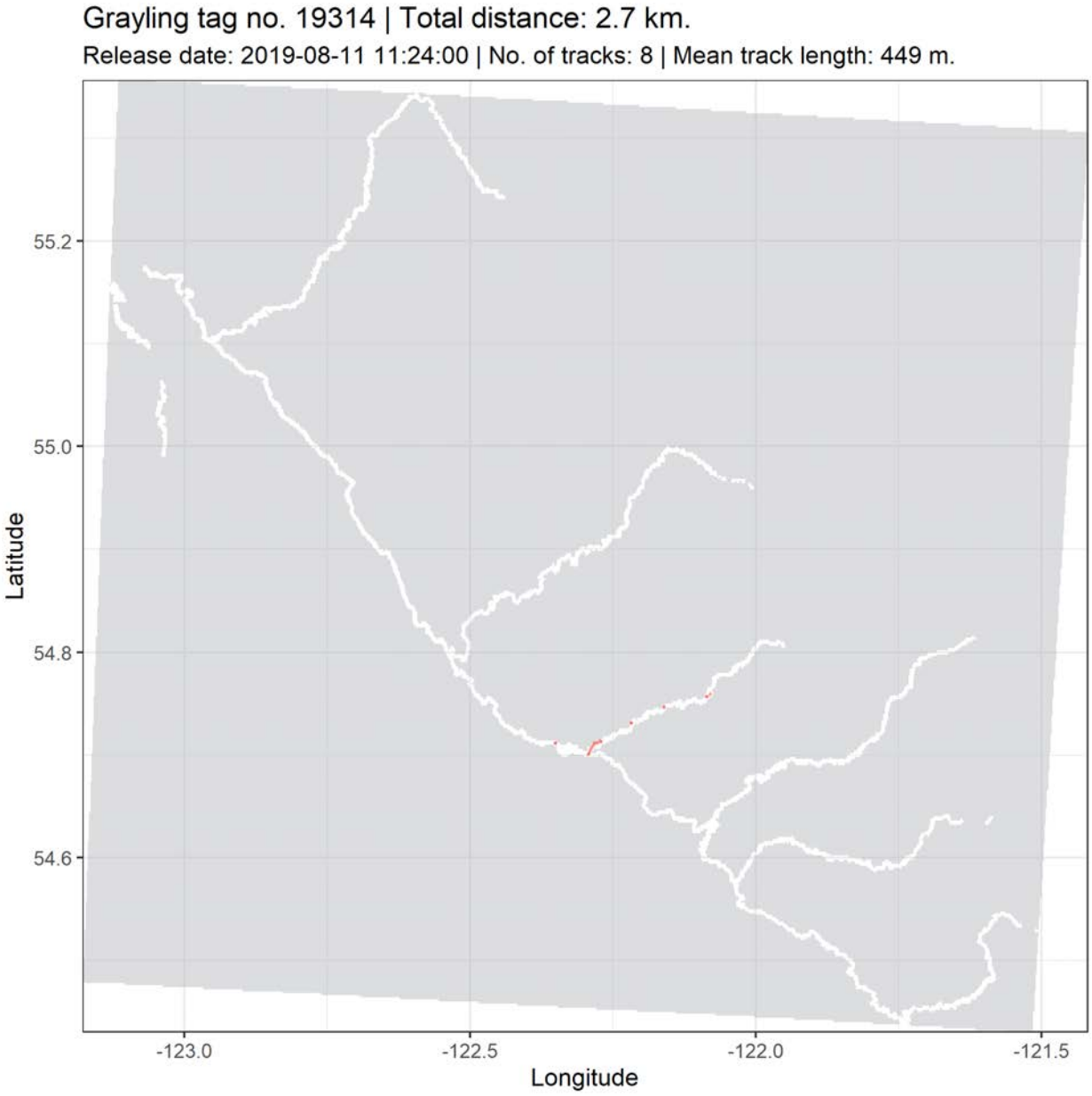
Grayling tag no. 19314 | Total distance: 2.7 km.
Release date: 2019-08-11 11:24:00 | No. of tracks: 8 | Mean track length: 449 m.
55.2
55.0
54.8
54.6
Latitude
-123.0
-122.5
-122.0
-121.5
Longitude

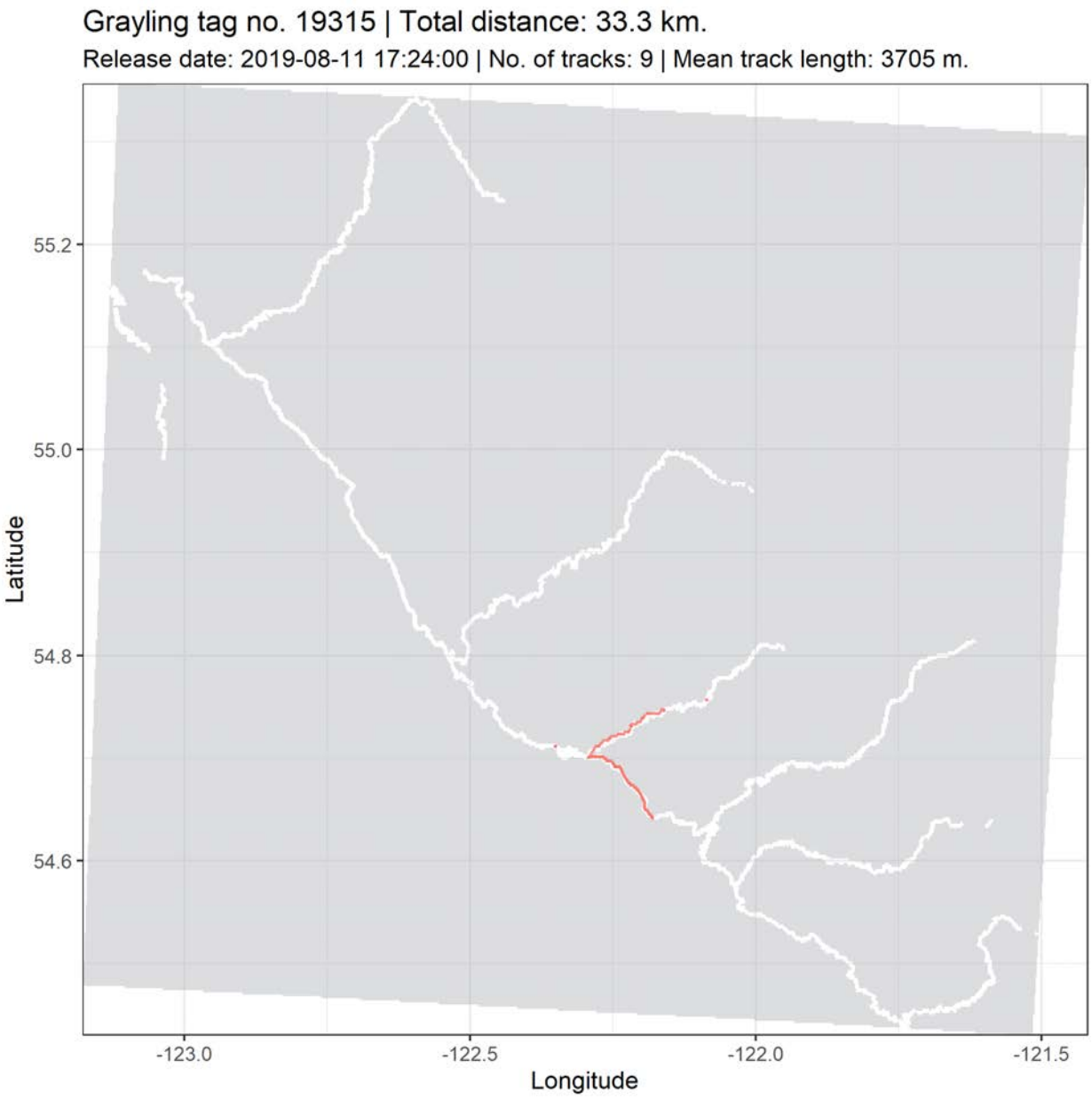
Grayling tag no. 19315 | Total distance: 33.3 km.
Release date: 2019-08-11 17:24:00 | No. of tracks: 9 | Mean track length: 3705 m.
55.2
55.0
54.8
54.6
Latitude
-123.0
-122.5
-122.0
-121.5
Longitude

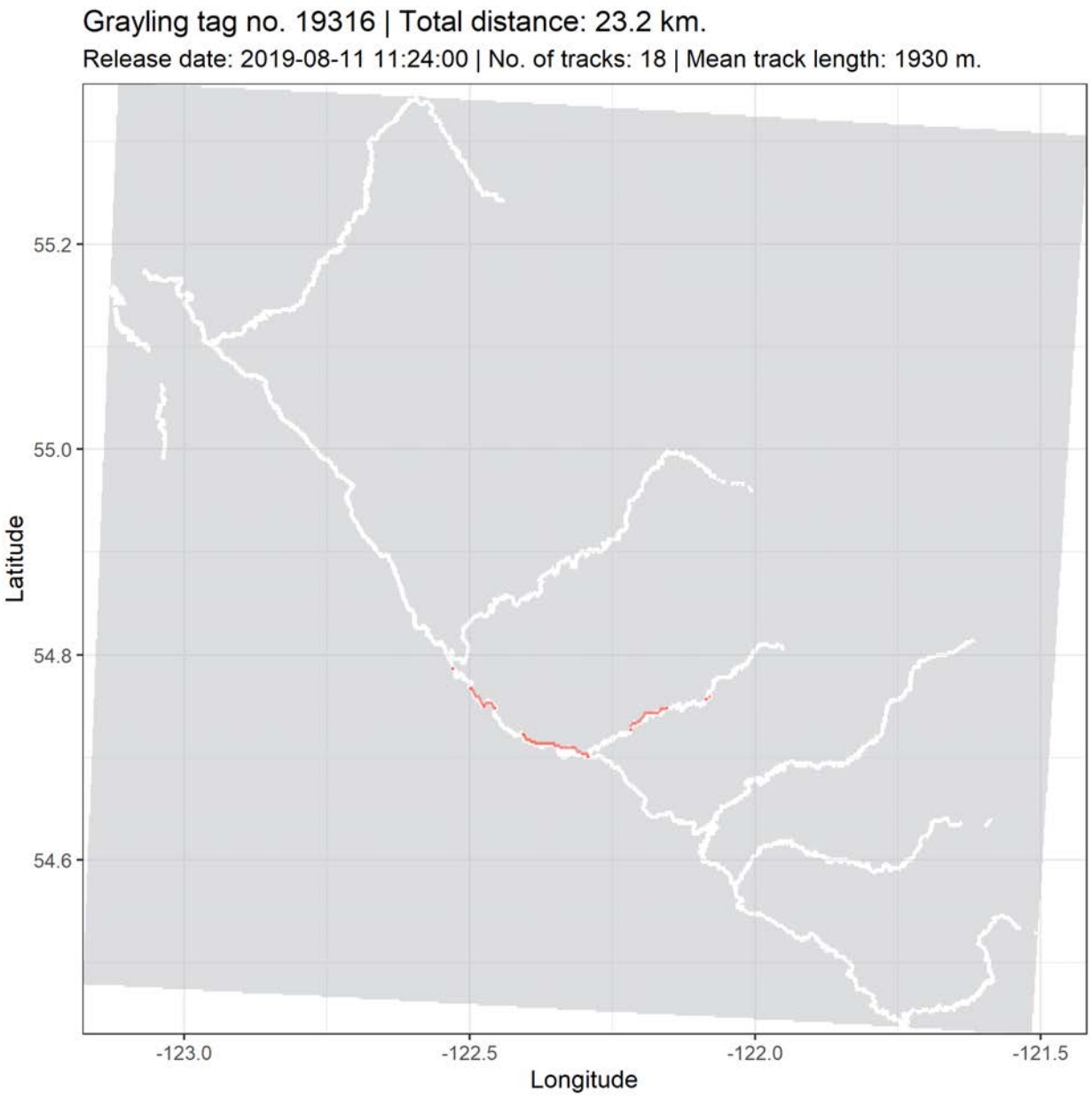
Grayling tag no. 19316 | Total distance: 23.2 km.
Release date: 2019-08-11 11:24:00 | No. of tracks: 18 | Mean track length: 1930 m.
55.2
55.0
54.8
54.6
Latitude
-123.0
-122.5
-122.0
-121.5
Longitude

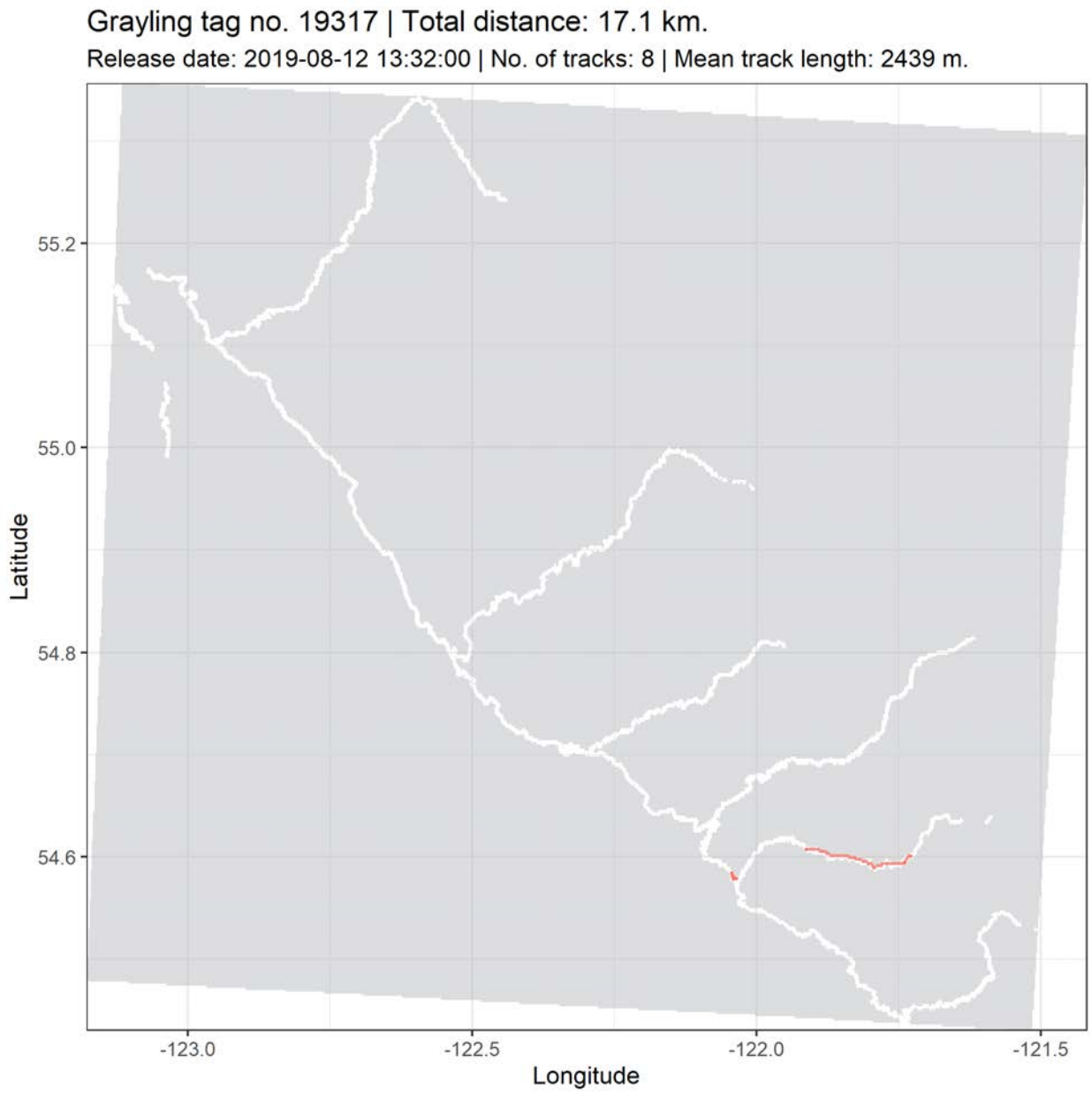
Grayling tag no. 19317 | Total distance: 17.1 km.
Release date: 2019-08-12 13:32:00 | No. of tracks: 8 | Mean track length: 2439 m.
55.2
55.0
54.8
54.6
Latitude
-123.0
-122.5
-122.0
-121.5
Longitude

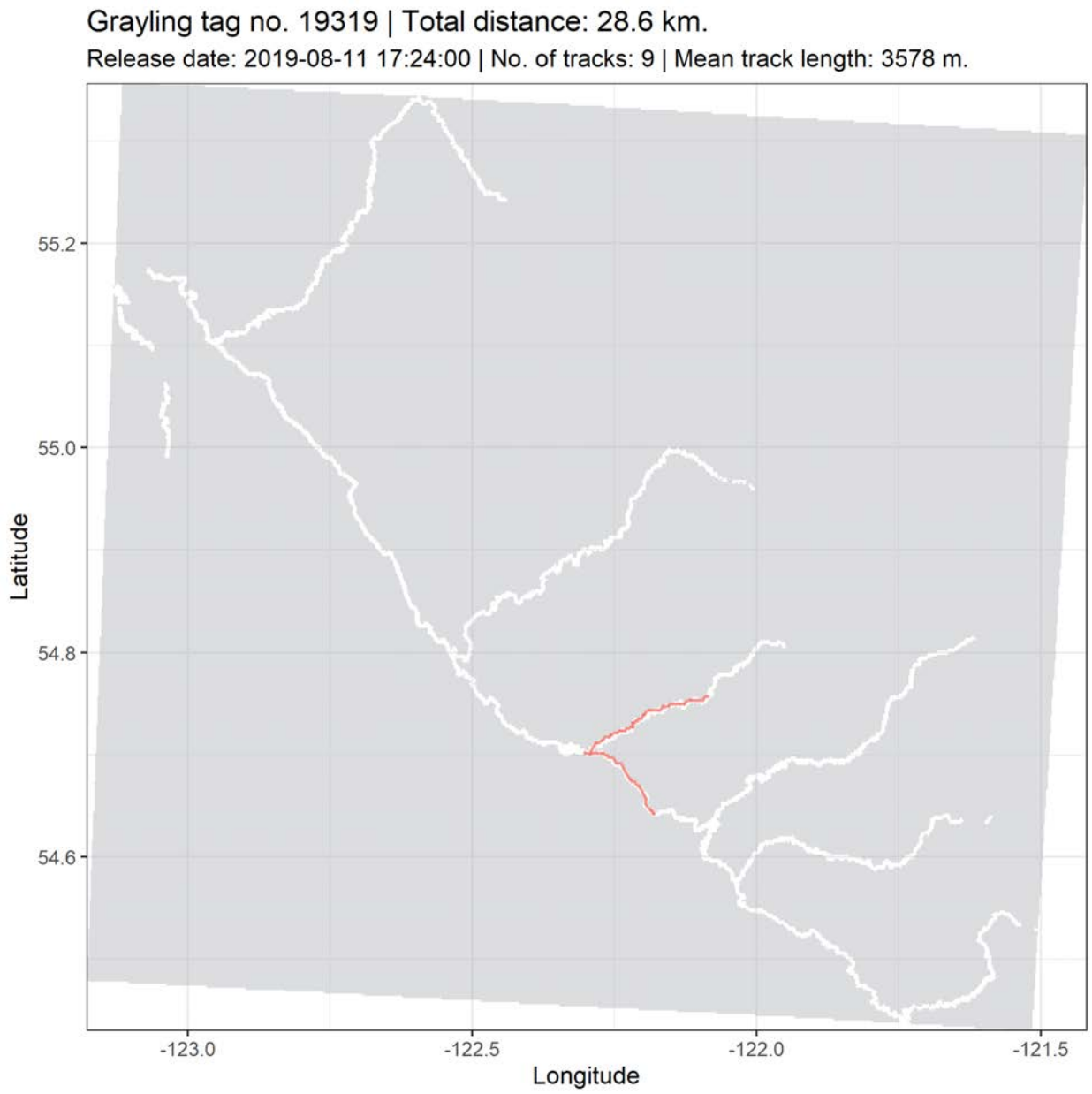
Grayling tag no. 19319 | Total distance: 28.6 km.
Release date: 2019-08-11 17:24:00 | No. of tracks: 9 | Mean track length: 3578 m.
55.2
55.0
54.8
54.6
Latitude
-123.0
-122.5
-122.0
-121.5
Longitude

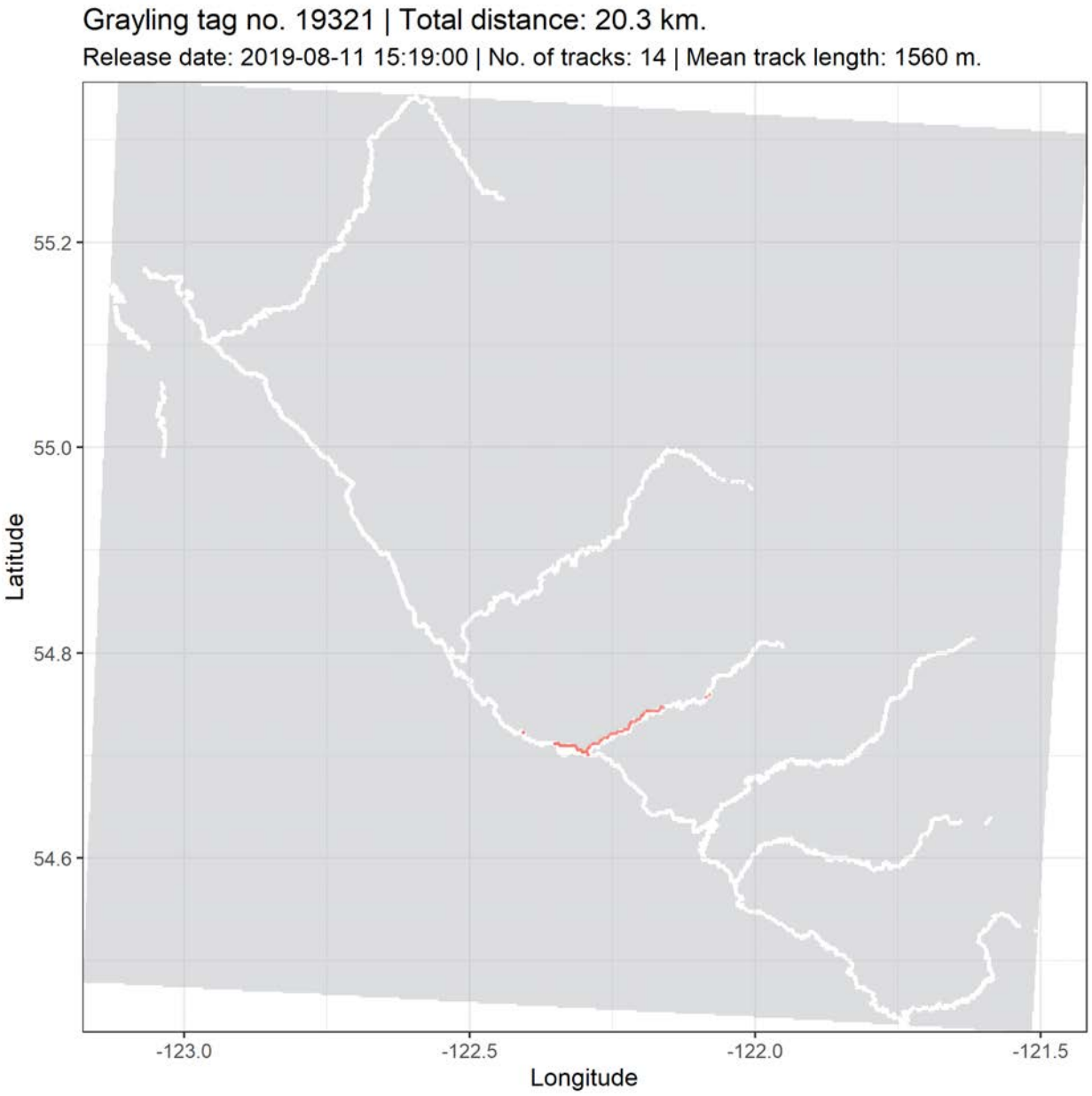
Grayling tag no. 19321 | Total distance: 20.3 km.
Release date: 2019-08-11 15:19:00 | No. of tracks: 14 | Mean track length: 1560 m.
55.2
55.0
54.8
54.6
Latitude
-123.0
-122.5
-122.0
-121.5
Longitude

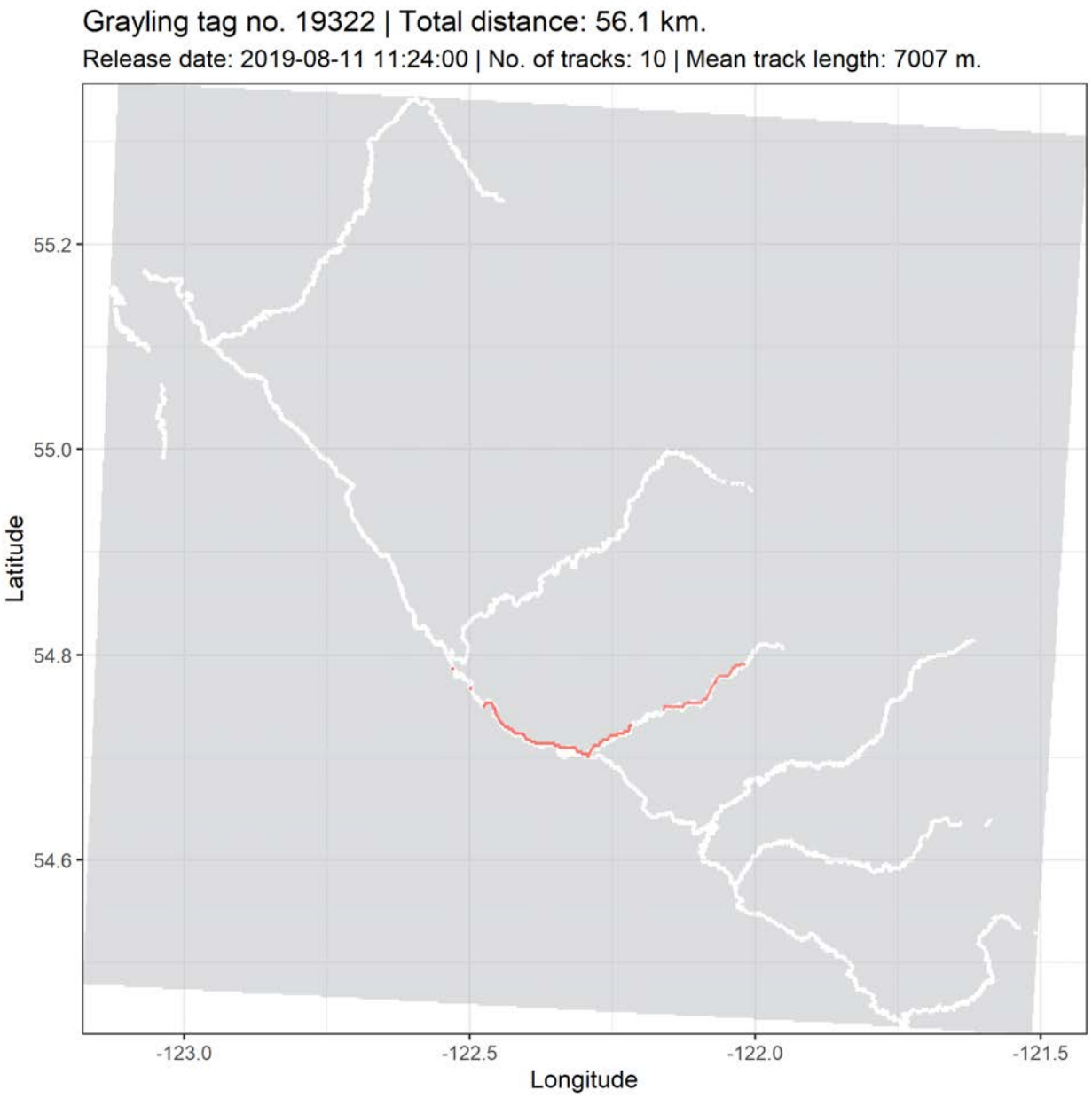
Grayling tag no. 19322 | Total distance: 56.1 km.
Release date: 2019-08-11 11:24:00 | No. of tracks: 10 | Mean track length: 7007 m.
55.2
55.0
54.8
54.6
Latitude
-123.0
-122.5
-122.0
-121.5
Longitude

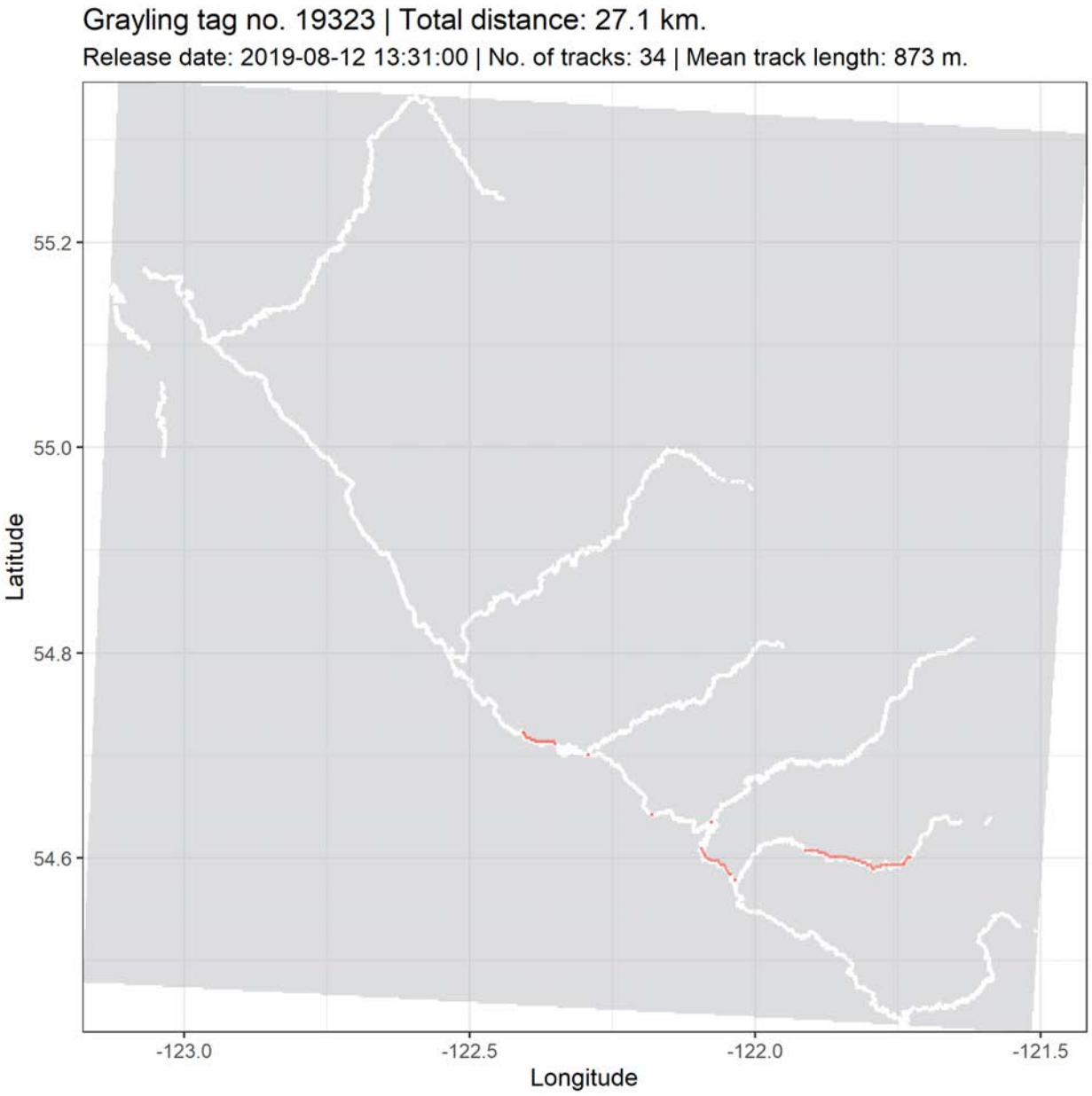
Grayling tag no. 19323 | Total distance: 27.1 km.
Release date: 2019-08-12 13:31:00 | No. of tracks: 34 | Mean track length: 873 m.
55.2
55.0
54.8
54.6
Latitude
-123.0
-122.5
-122.0
-121.5
Longitude

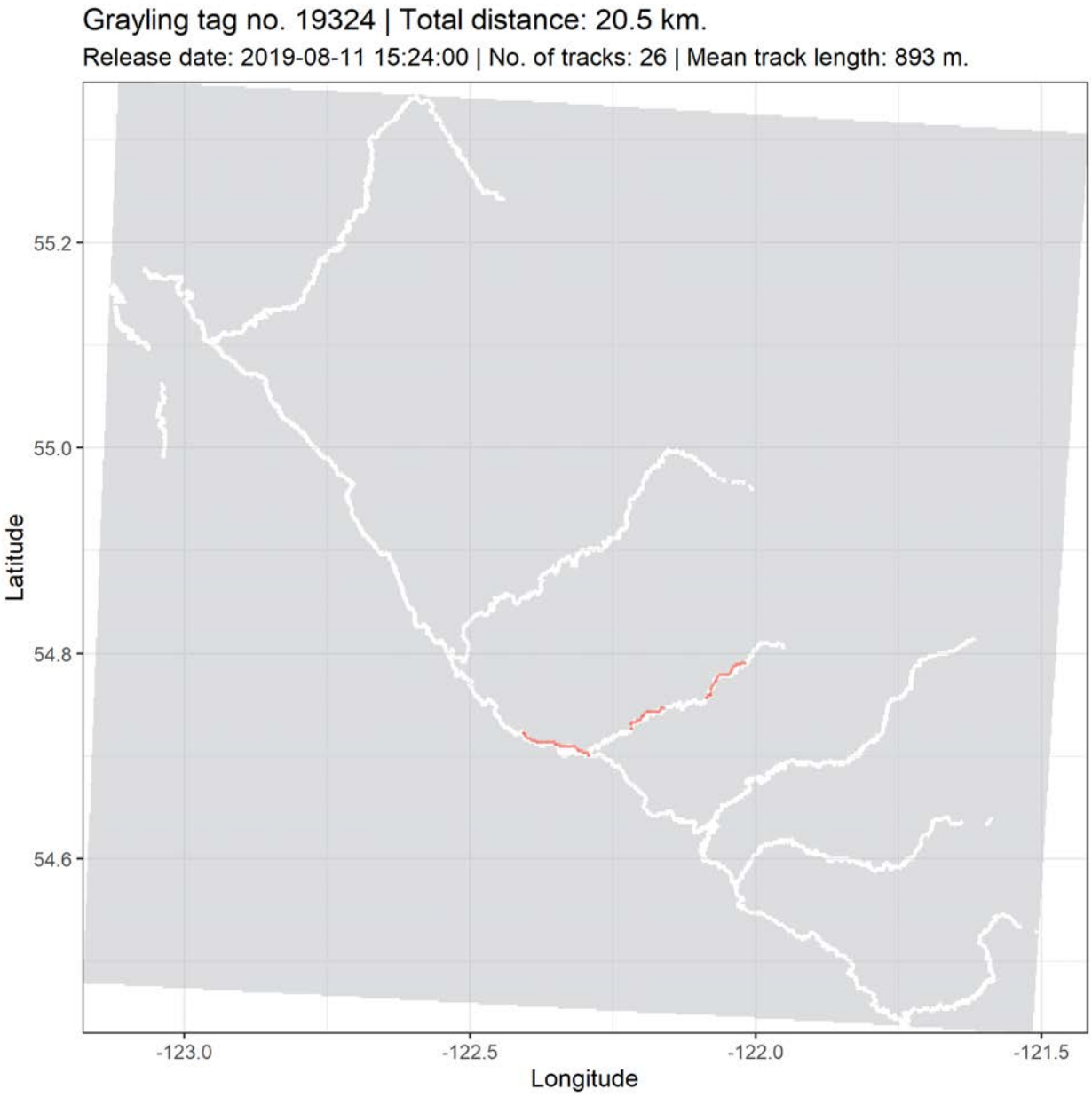
Grayling tag no. 19324 | Total distance: 20.5 km.
Release date: 2019-08-11 15:24:00 | No. of tracks: 26 | Mean track length: 893 m.
55.2
55.0
54.8
54.6
Latitude
-123.0
-122.5
-122.0
-121.5
Longitude

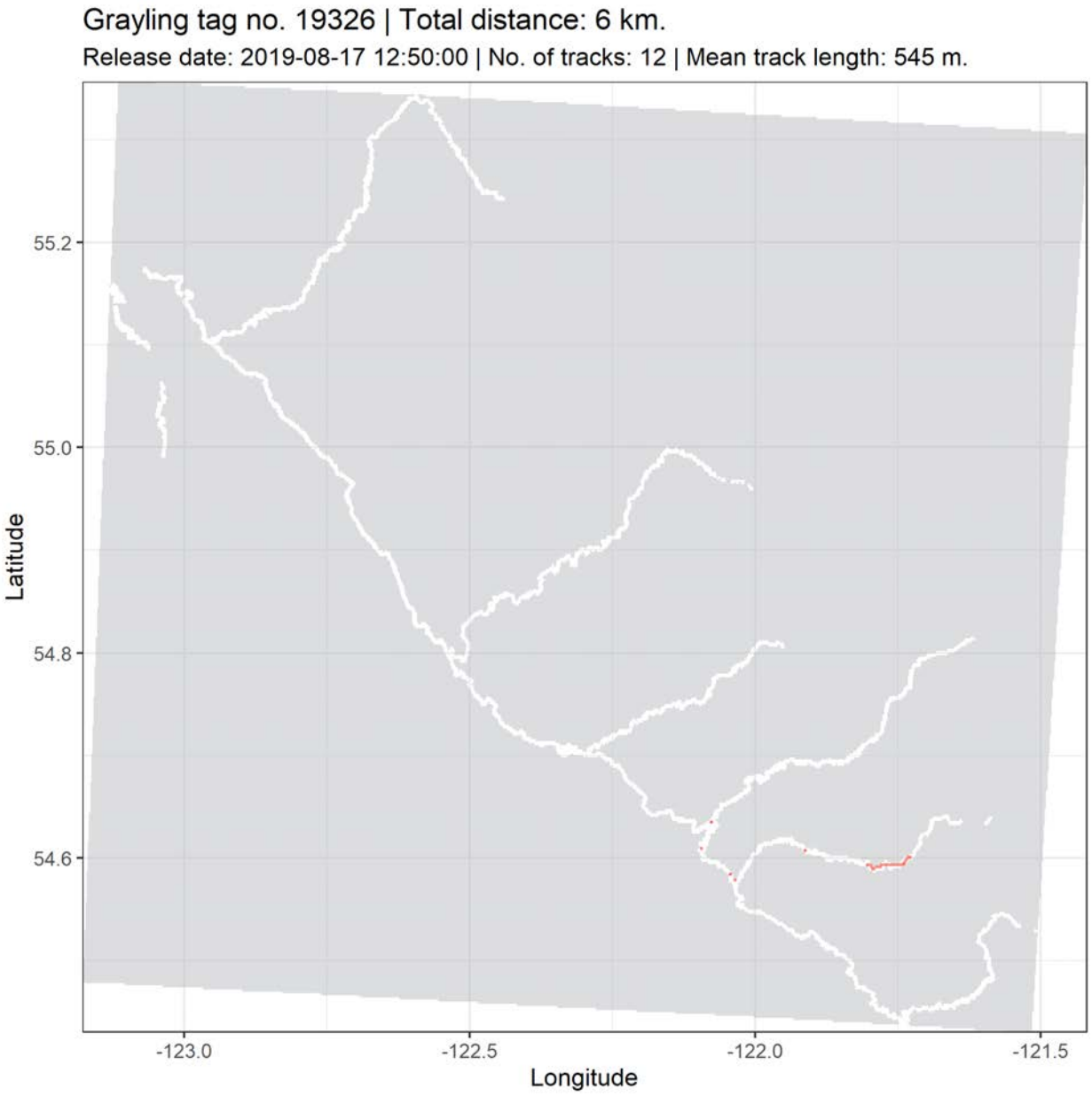
Grayling tag no. 19326 | Total distance: 6 km.
Release date: 2019-08-17 12:50:00 | No. of tracks: 12 | Mean track length: 545 m.
55.2
55.0
54.8
54.6
Latitude
-123.0
-122.5
-122.0
-121.5
Longitude

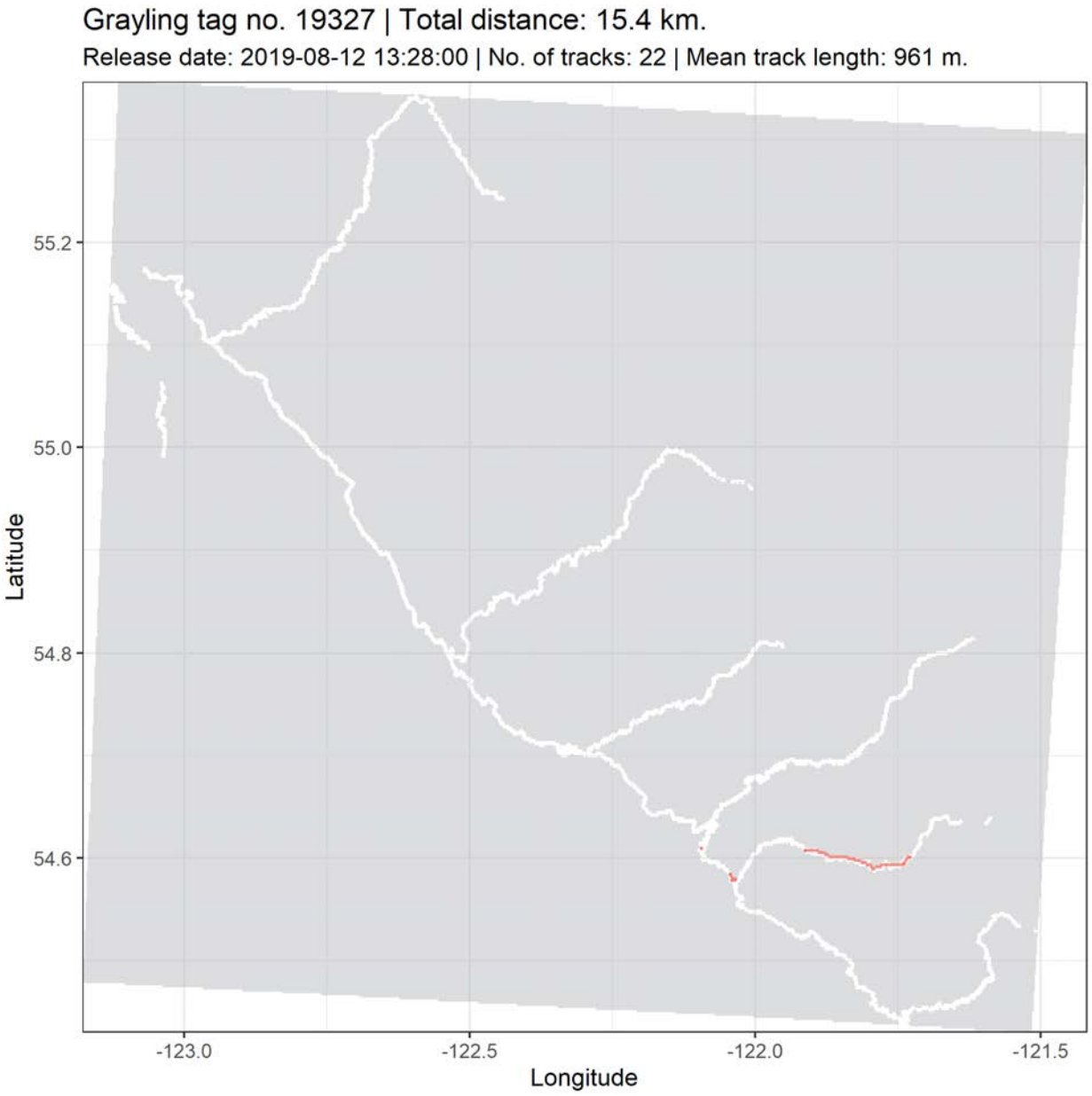
Grayling tag no. 19327 | Total distance: 15.4 km.
Release date: 2019-08-12 13:28:00 | No. of tracks: 22 | Mean track length: 961 m.
55.2
55.0
54.8
54.6
Latitude
-123.0
-122.5
-122.0
-121.5
Longitude

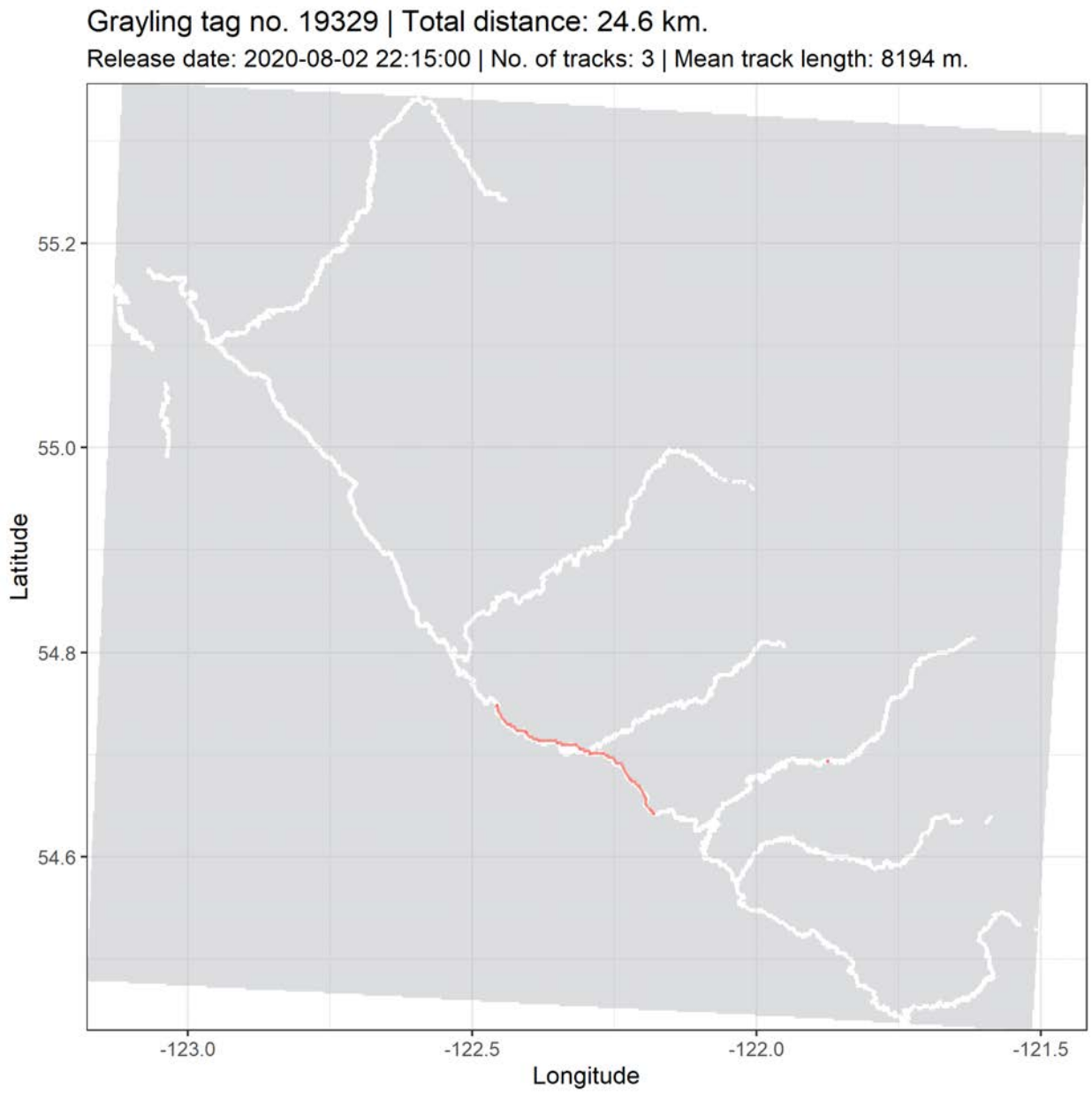
Grayling tag no. 19329 | Total distance: 24.6 km.
Release date: 2020-08-02 22:15:00 | No. of tracks: 3 | Mean track length: 8194 m.
55.2
55.0
54.8
54.6
Latitude
-123.0
-122.5
-122.0
-121.5
Longitude

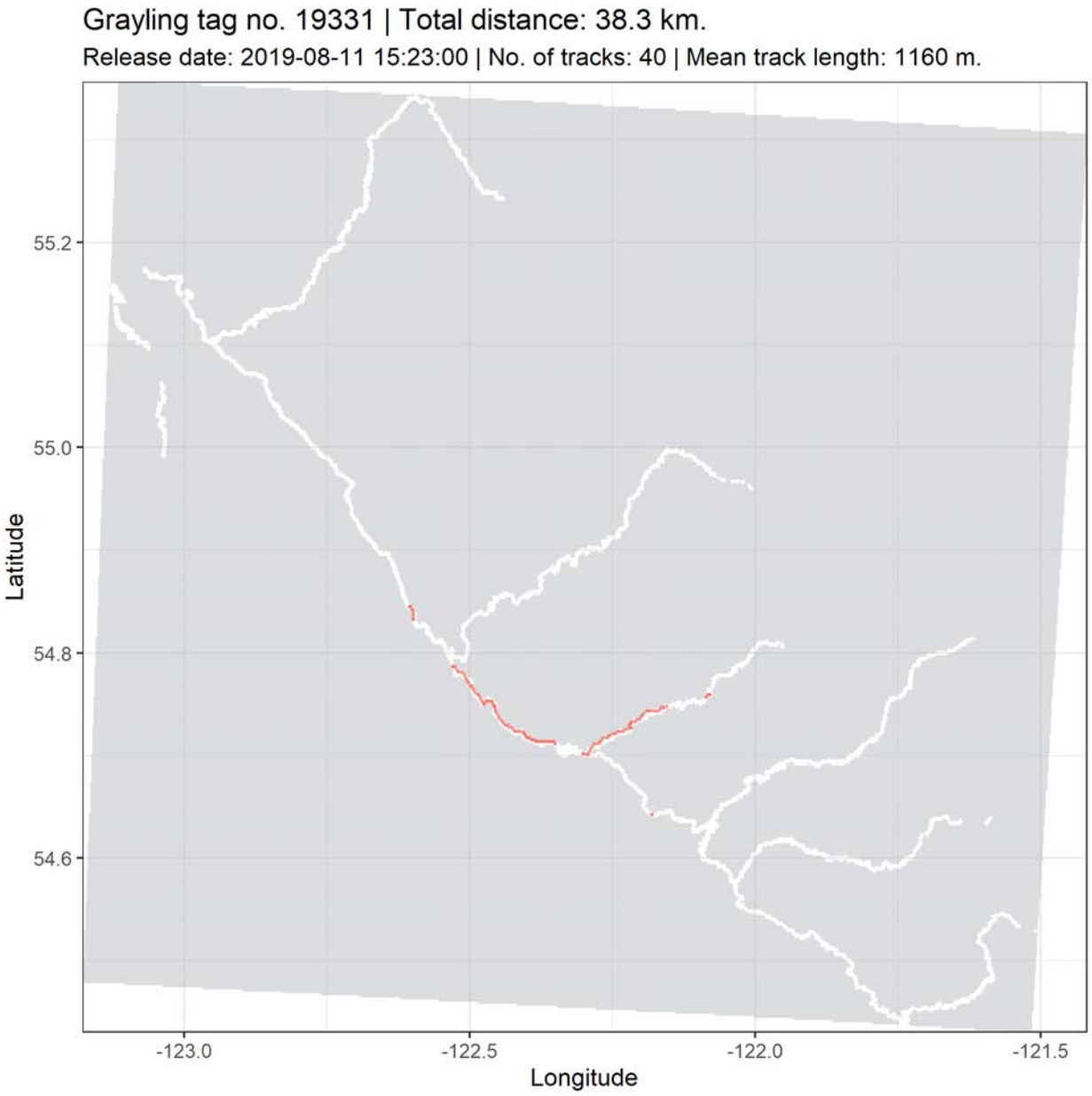
Grayling tag no. 19331 | Total distance: 38.3 km.
Release date: 2019-08-11 15:23:00 | No. of tracks: 40 | Mean track length: 1160 m.
55.2
55.0
54.8
54.6
Latitude
-123.0
-122.5
-122.0
-121.5
Longitude

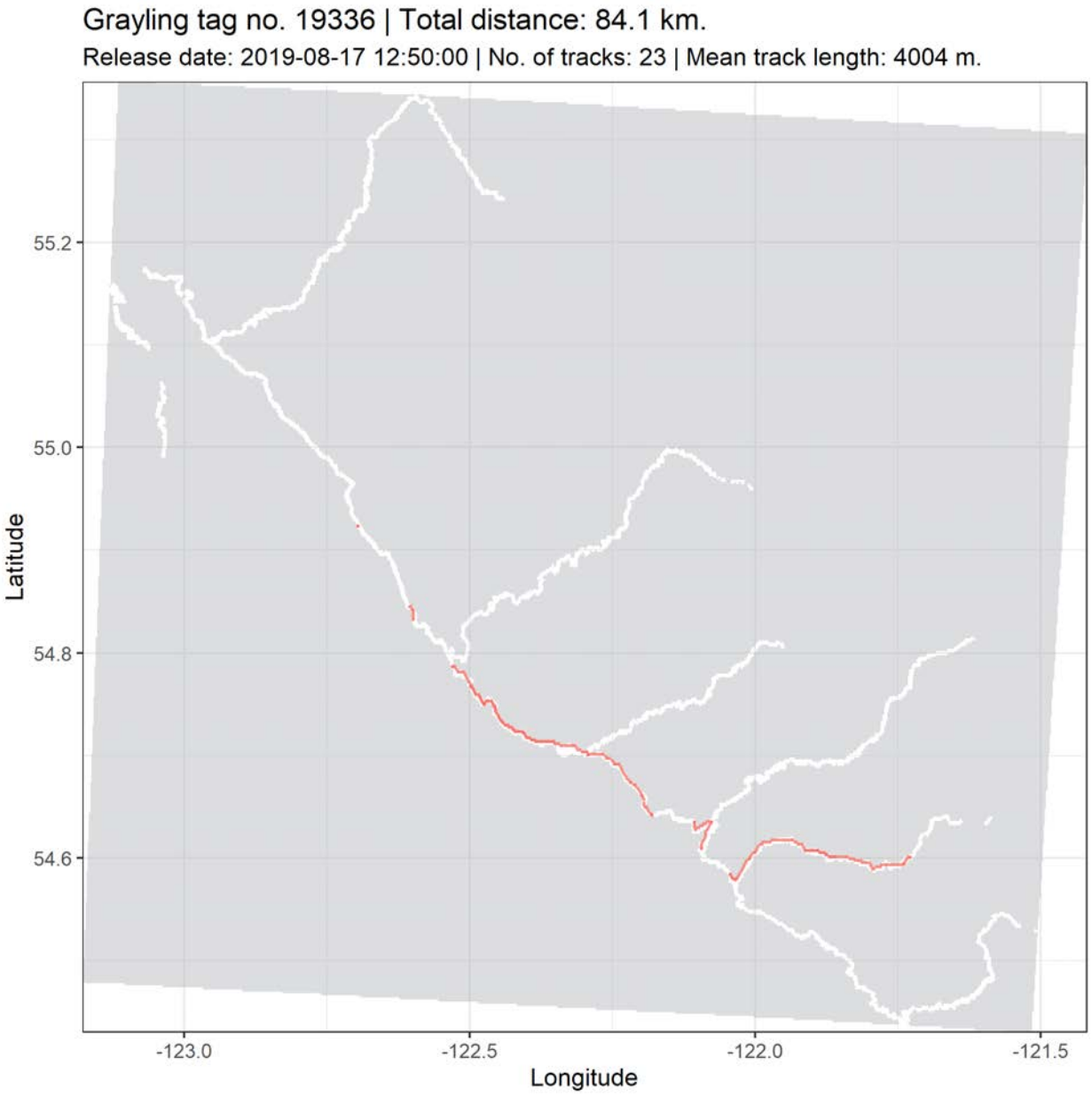
Grayling tag no. 19336 | Total distance: 84.1 km.
Release date: 2019-08-17 12:50:00 | No. of tracks: 23 | Mean track length: 4004 m.
55.2
55.0
54.8
54.6
Latitude
-123.0
-122.5
-122.0
-121.5
Longitude

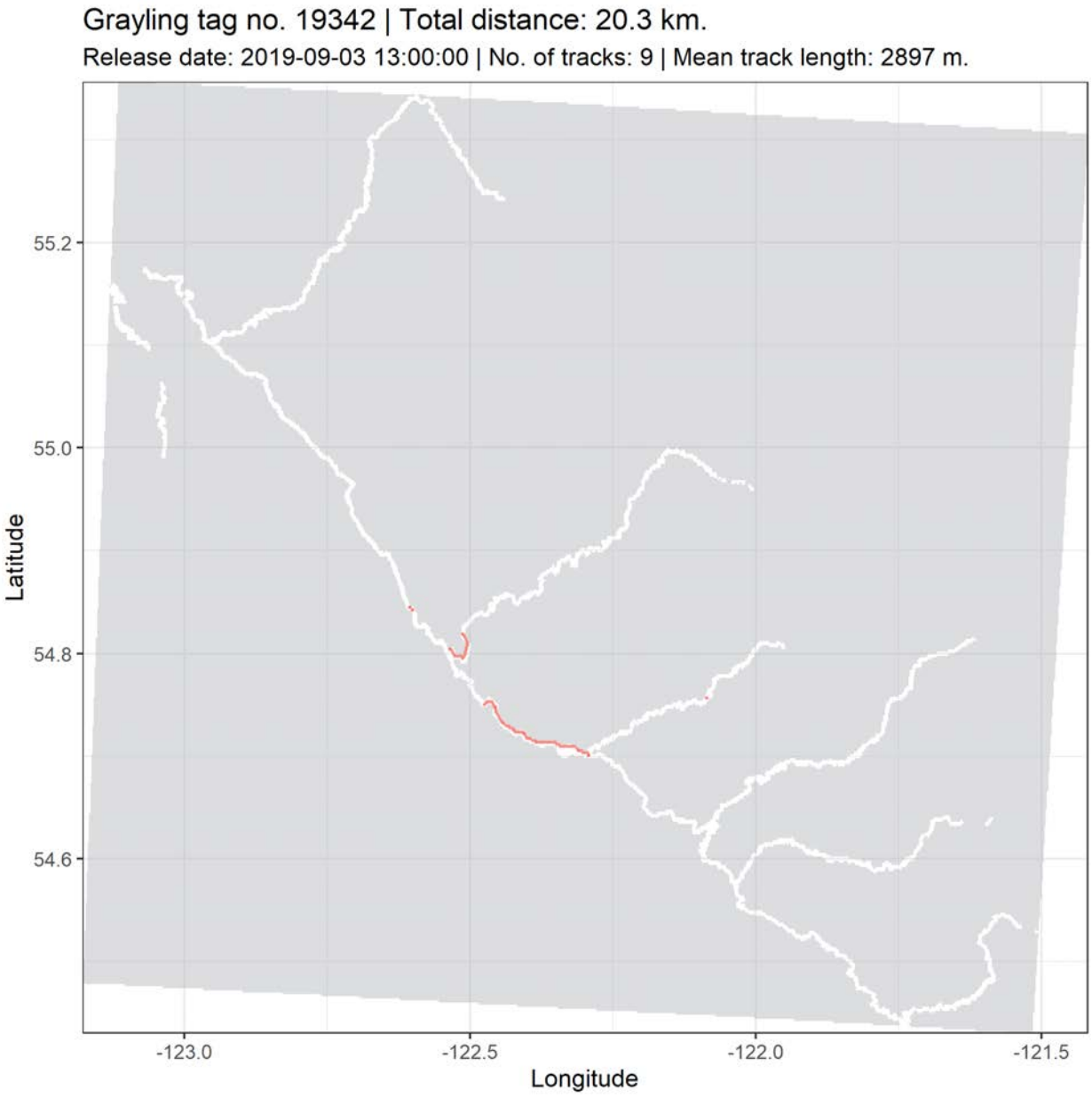
Grayling tag no. 19342 | Total distance: 20.3 km.
Release date: 2019-09-03 13:00:00 | No. of tracks: 9 | Mean track length: 2897 m.
55.2
55.0
54.8
54.6
Latitude
-123.0
-122.5
-122.0
-121.5
Longitude

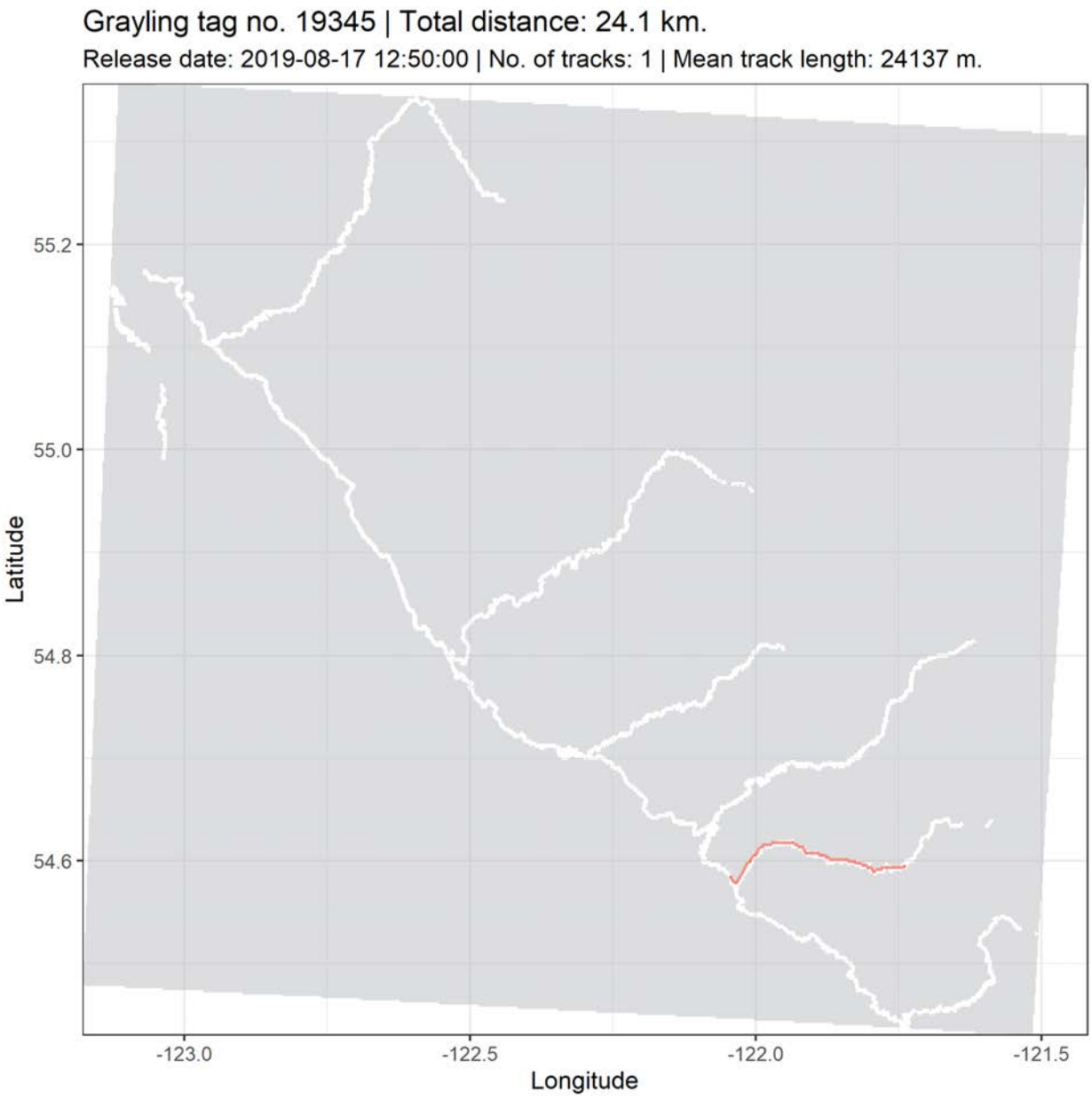
Grayling tag no. 19345 | Total distance: 24.1 km.
Release date: 2019-08-17 12:50:00 | No. of tracks: 1 | Mean track length: 24137 m.
55.2
55.0
54.8
54.6
Latitude
-123.0
-122.5
-122.0
-121.5
Longitude

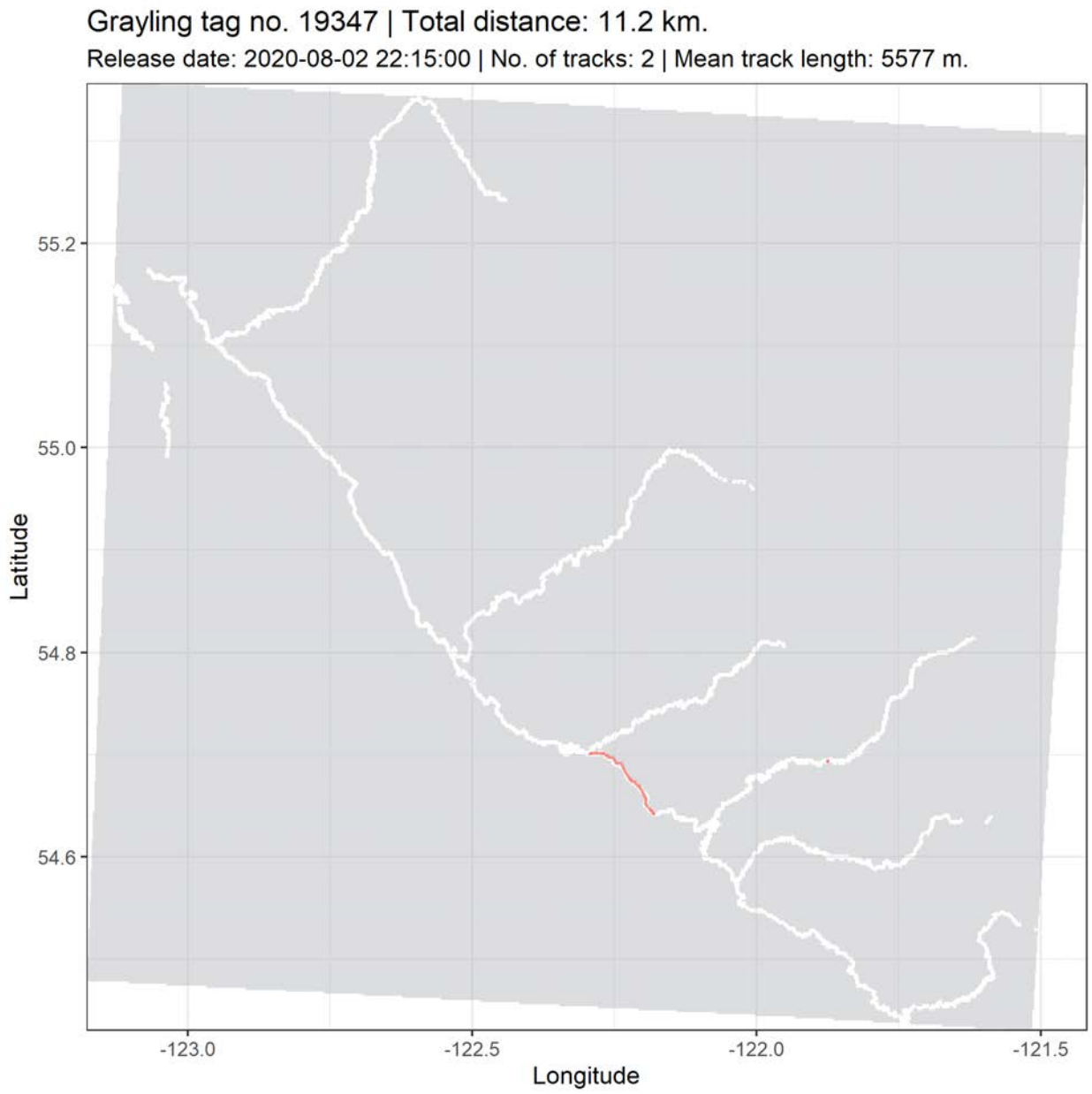
Grayling tag no. 19347 | Total distance: 11.2 km.
Release date: 2020-08-02 22:15:00 | No. of tracks: 2 | Mean track length: 5577 m.
55.2
55.0
54.8
54.6
Latitude
-123.0
-122.5
-122.0
-121.5
Longitude

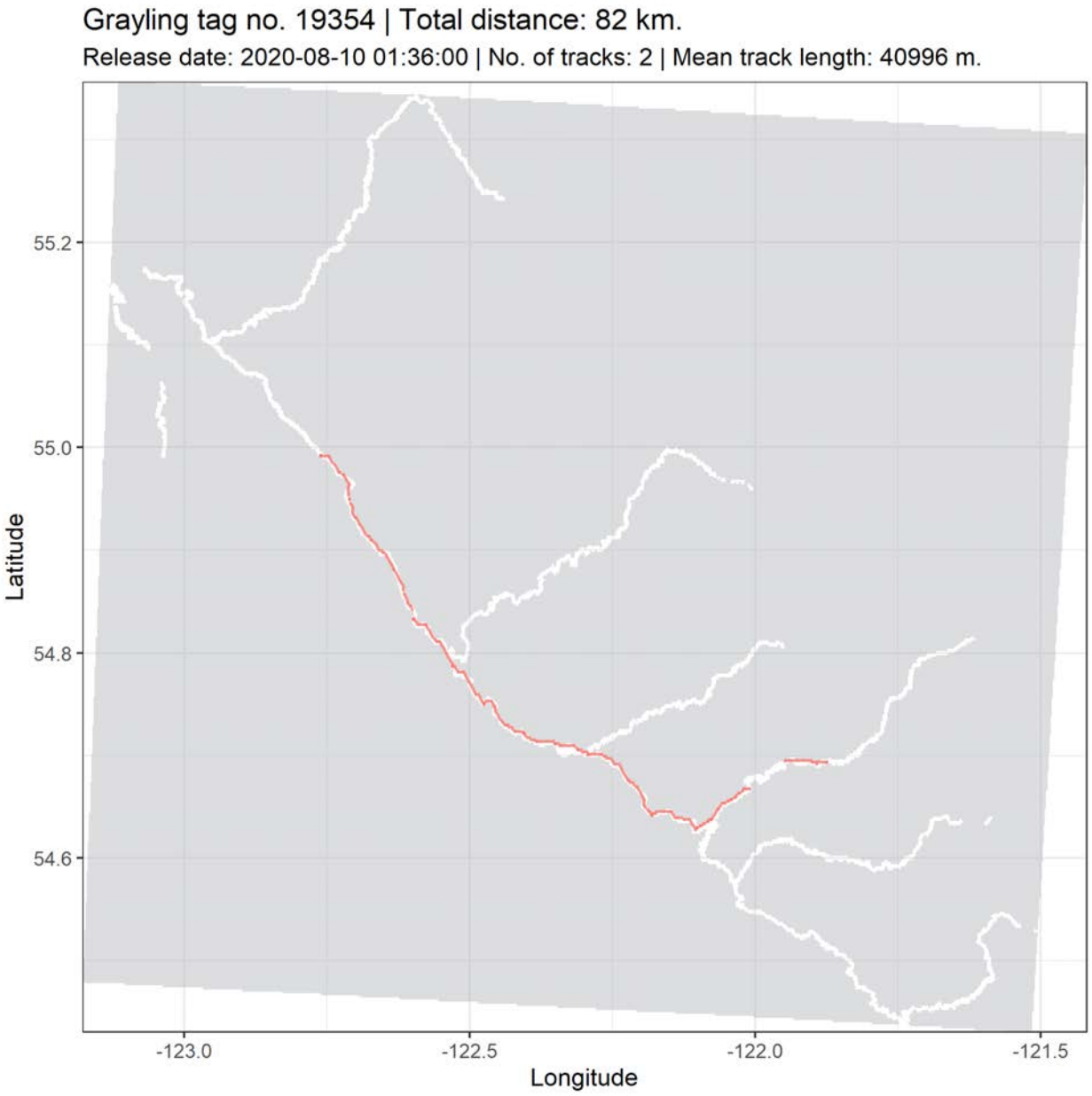
Grayling tag no. 19354 | Total distance: 82 km.
Release date: 2020-08-10 01:36:00 | No. of tracks: 2 | Mean track length: 40996 m.
55.2
55.0
54.8
54.6
Latitude
-123.0
-122.5
-122.0
-121.5
Longitude

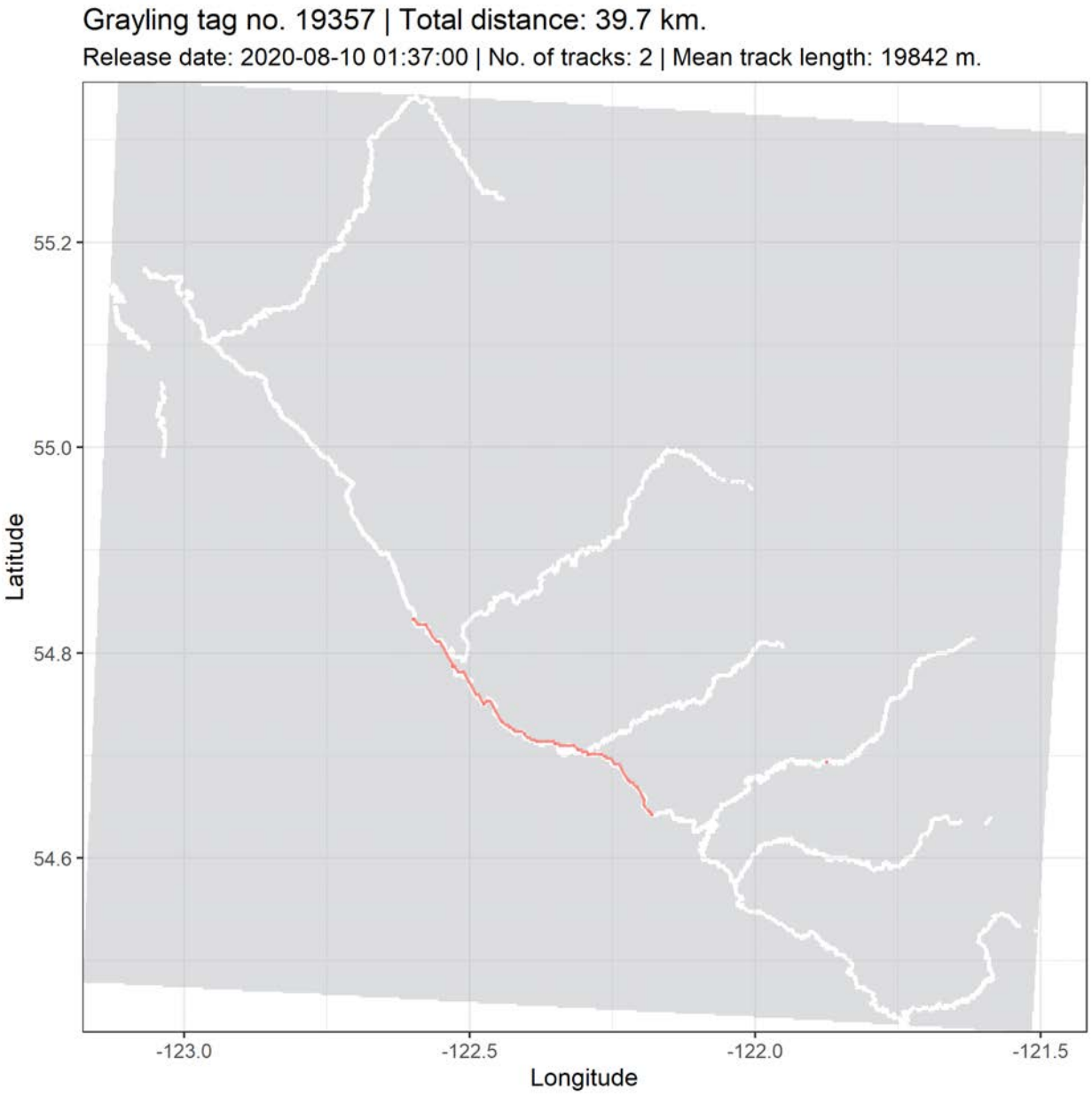
Grayling tag no. 19357 | Total distance: 39.7 km.
Release date: 2020-08-10 01:37:00 | No. of tracks: 2 | Mean track length: 19842 m.
55.2
55.0
54.8
54.6
Latitude
-123.0
-122.5
-122.0
-121.5
Longitude

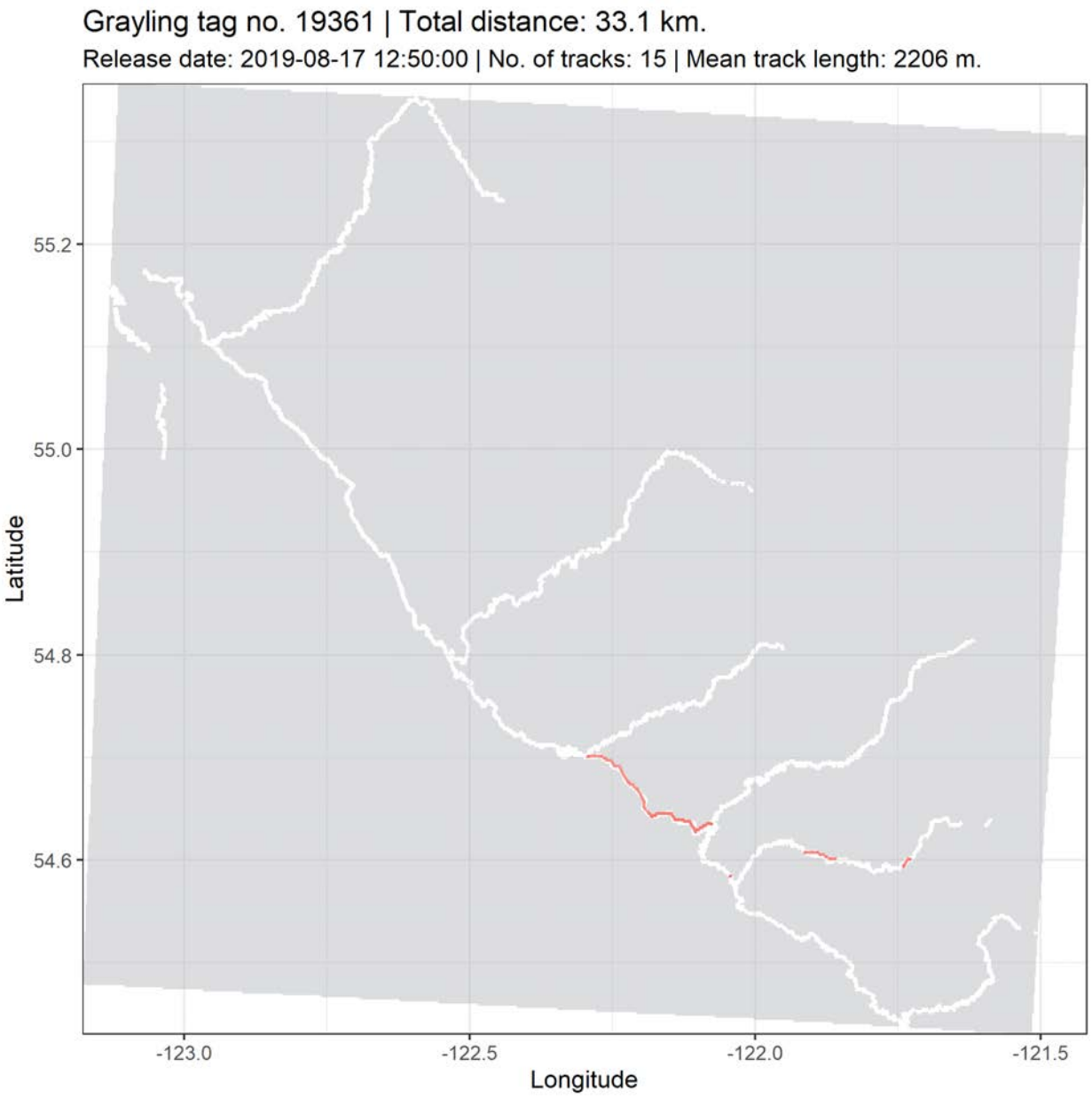
Grayling tag no. 19361 | Total distance: 33.1 km.
Release date: 2019-08-17 12:50:00 | No. of tracks: 15 | Mean track length: 2206 m.
55.2
55.0
54.8
54.6
Latitude
-123.0
-122.5
-122.0
-121.5
Longitude

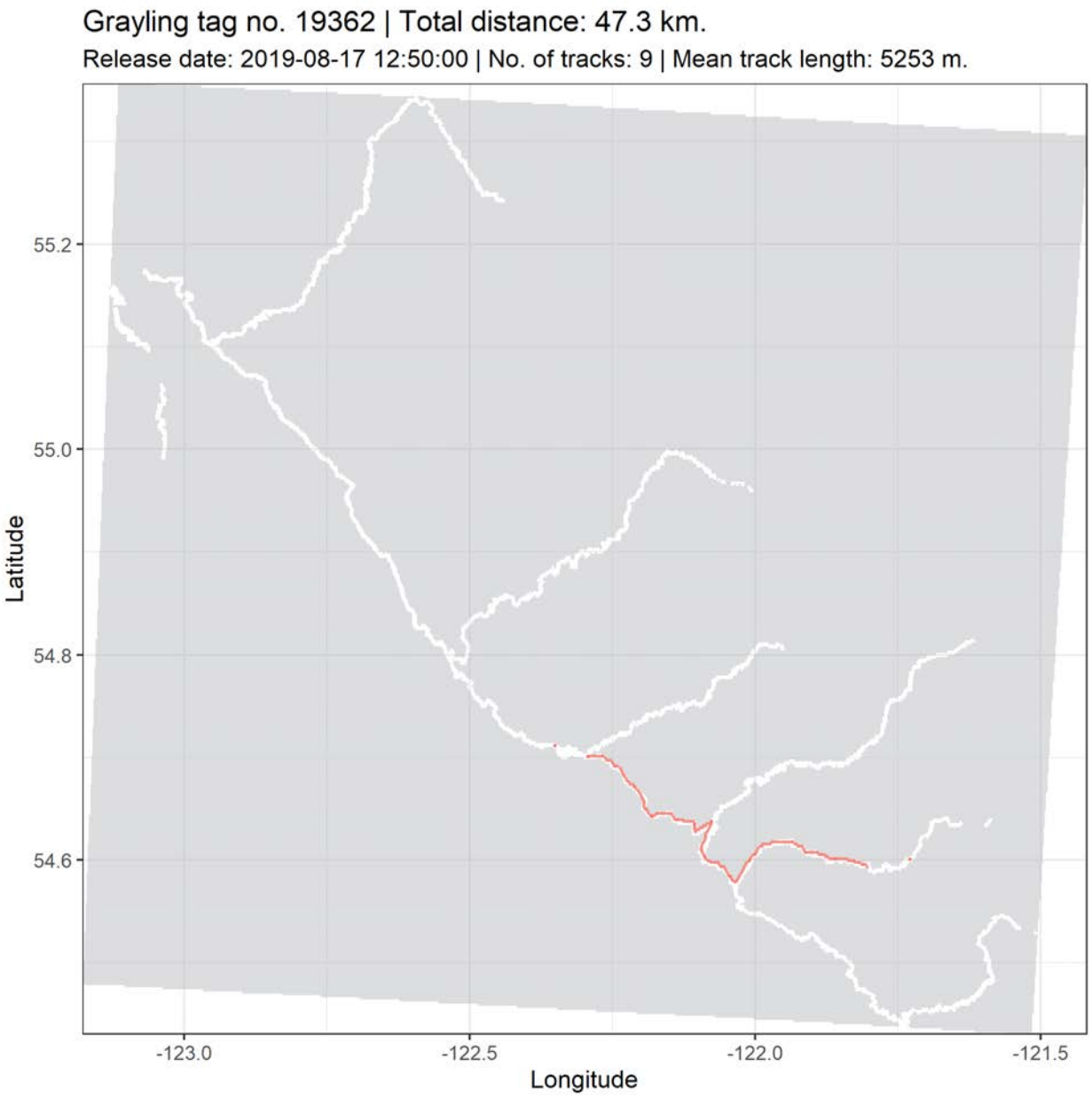
Grayling tag no. 19362 | Total distance: 47.3 km.
Release date: 2019-08-17 12:50:00 | No. of tracks: 9 | Mean track length: 5253 m.
55.2
55.0
54.8
54.6
Latitude
-123.0
-122.5
-122.0
-121.5
Longitude

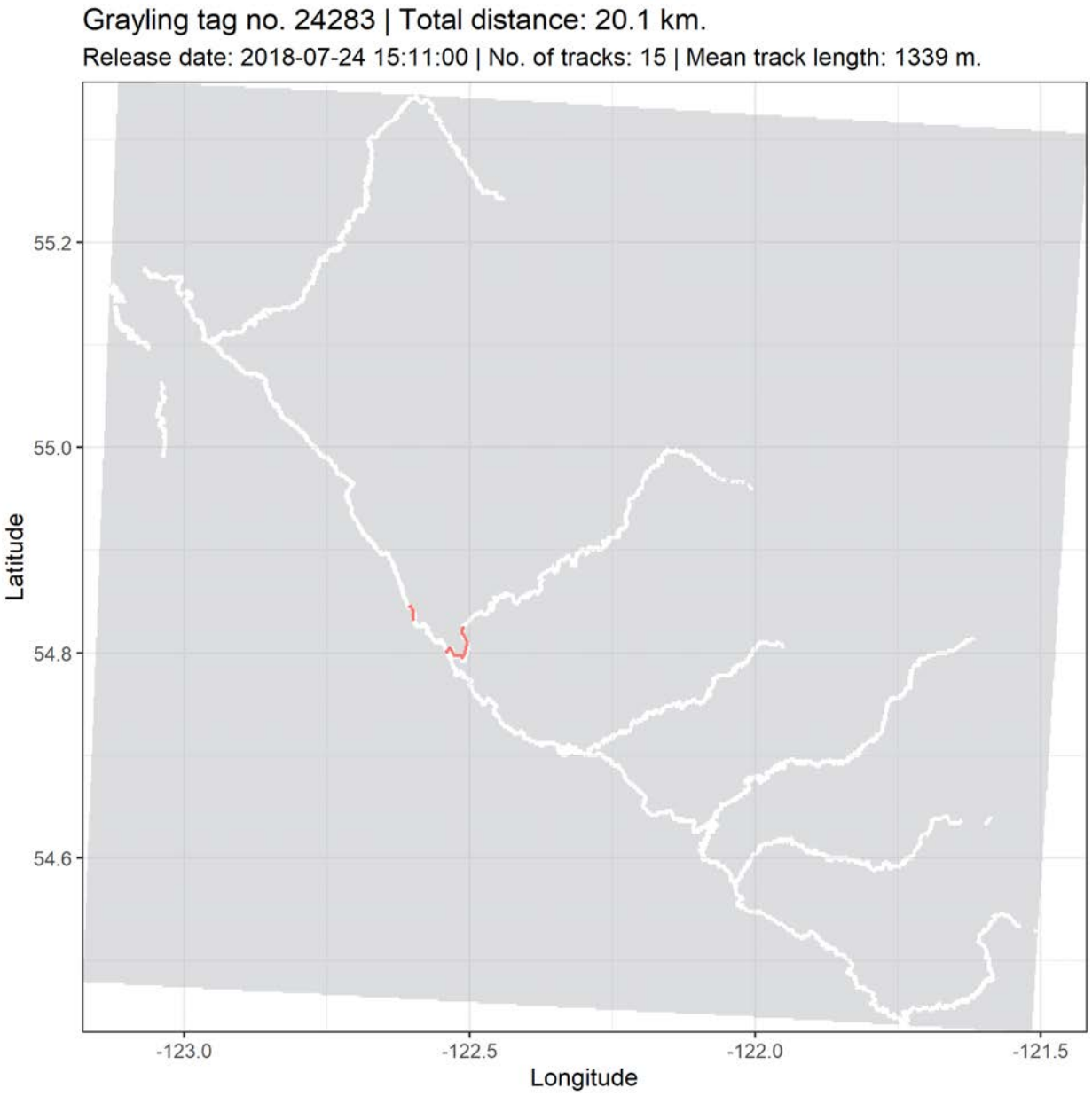
Grayling tag no. 24283 | Total distance: 20.1 km.
Release date: 2018-07-24 15:11:00 | No. of tracks: 15 | Mean track length: 1339 m.
55.2
55.0
54.8
54.6
Latitude
-123.0
-122.5
-122.0
-121.5
Longitude

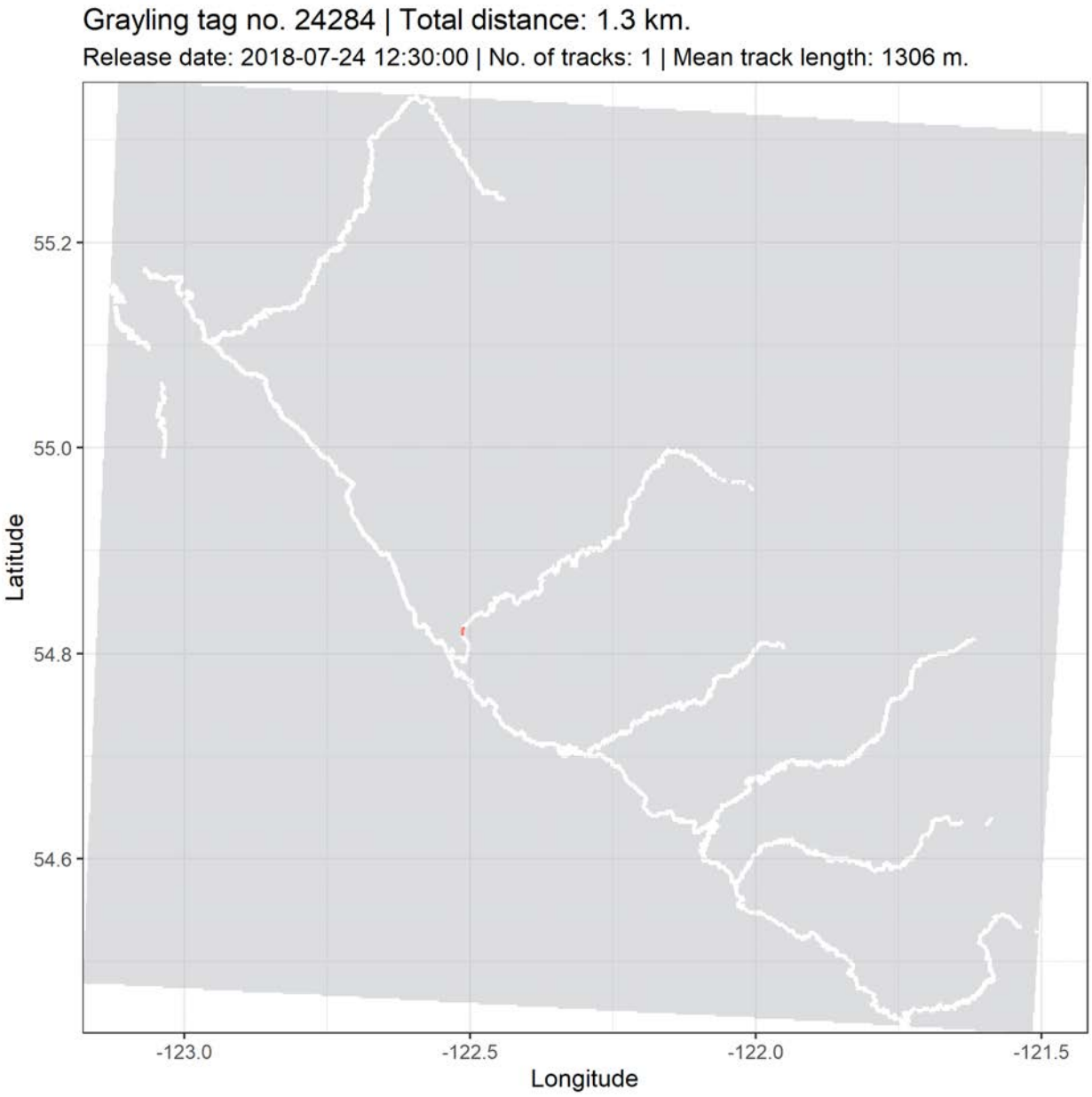
Grayling tag no. 24284 | Total distance: 1.3 km.
Release date: 2018-07-24 12:30:00 | No. of tracks: 1 | Mean track length: 1306 m.
55.2
55.0
54.8
54.6
Latitude
-123.0
-122.5
-122.0
-121.5
Longitude

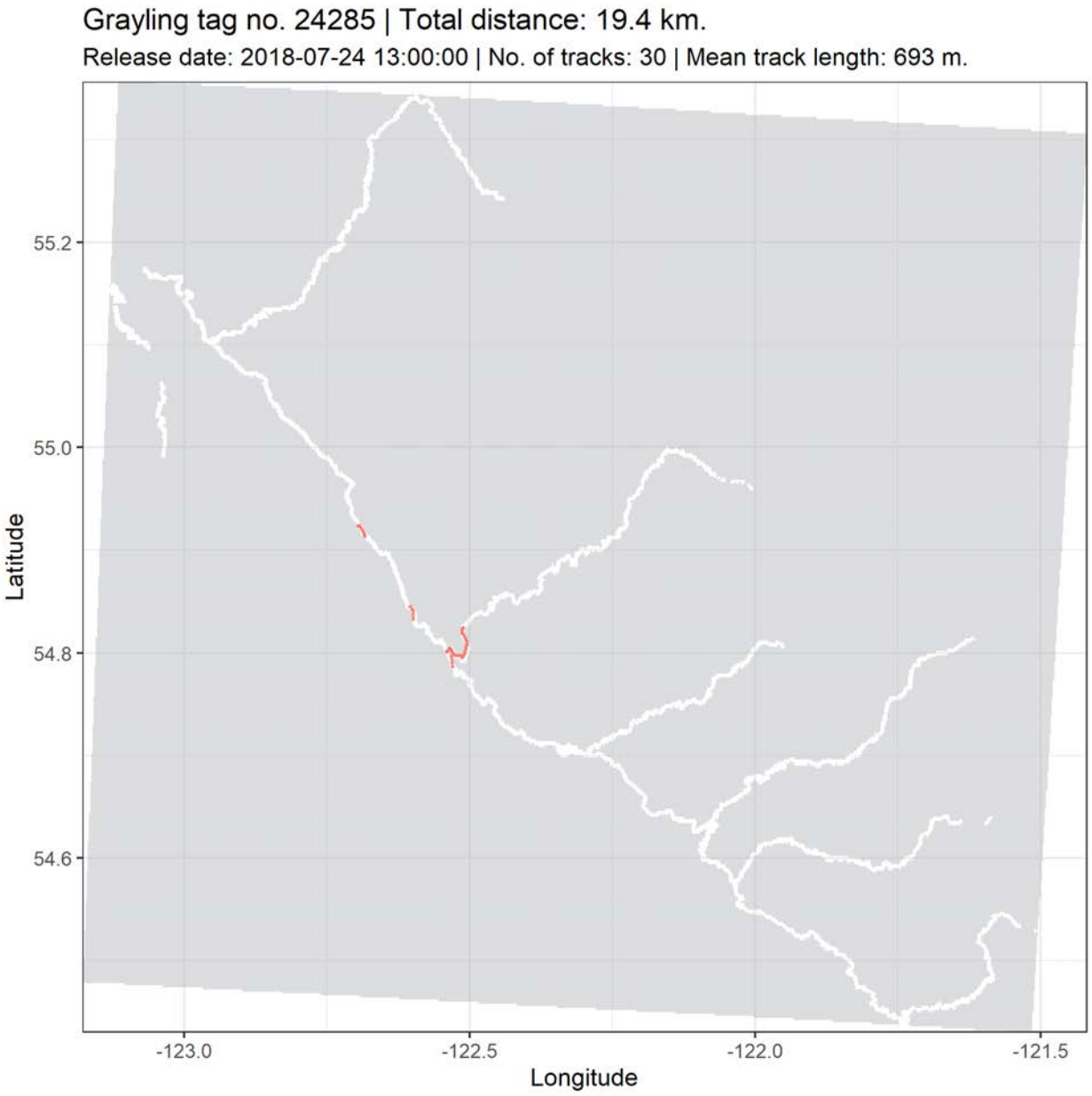
Grayling tag no. 24285 | Total distance: 19.4 km.
Release date: 2018-07-24 13:00:00 | No. of tracks: 30 | Mean track length: 693 m.
55.2
55.0
54.8
54.6
Latitude
-123.0
-122.5
-122.0
-121.5
Longitude

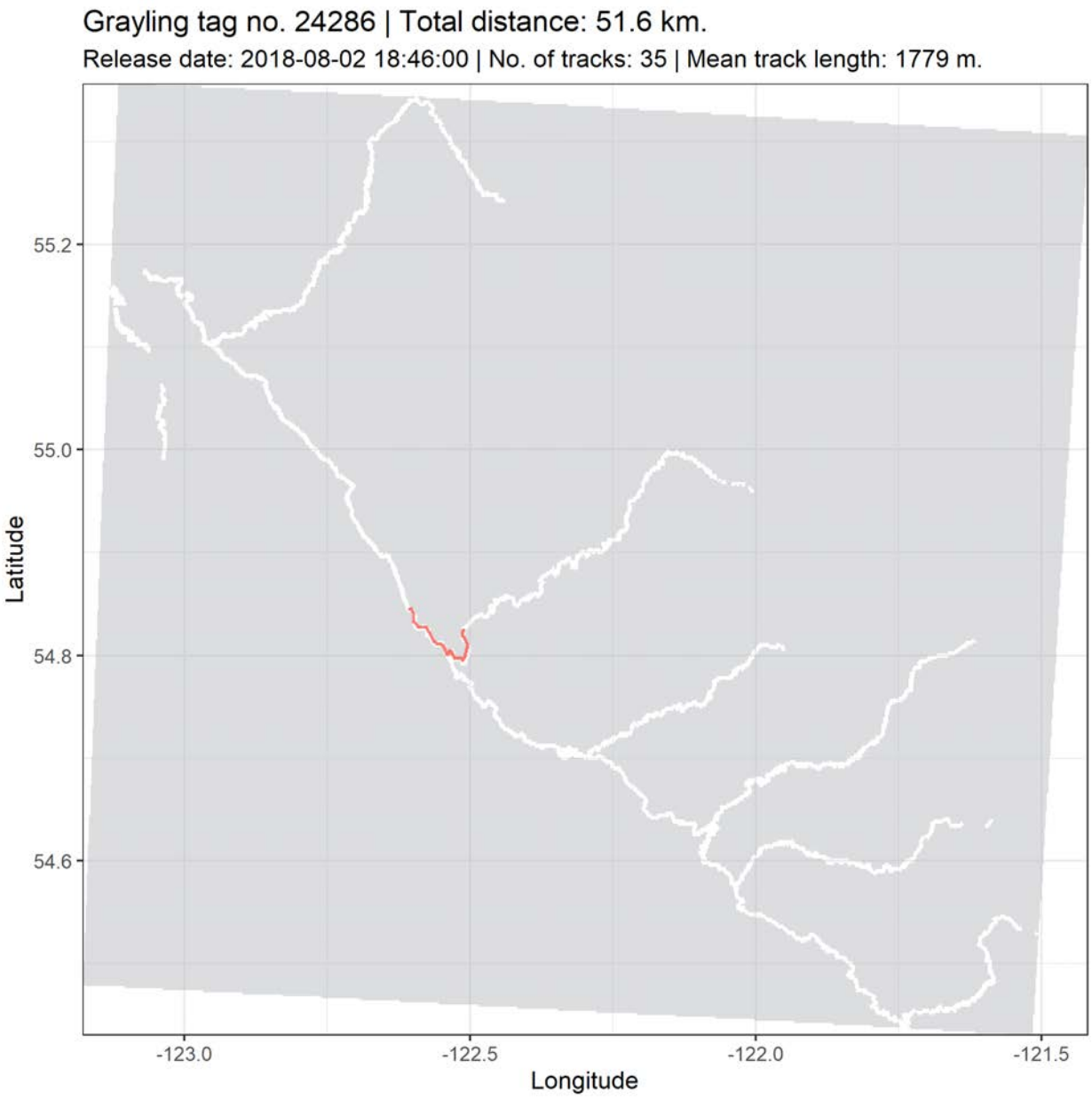
Grayling tag no. 24286 | Total distance: 51.6 km.
Release date: 2018-08-02 18:46:00 | No. of tracks: 35 | Mean track length: 1779 m.
55.2
55.0
54.8
54.6
Latitude
-123.0
-122.5
-122.0
-121.5
Longitude

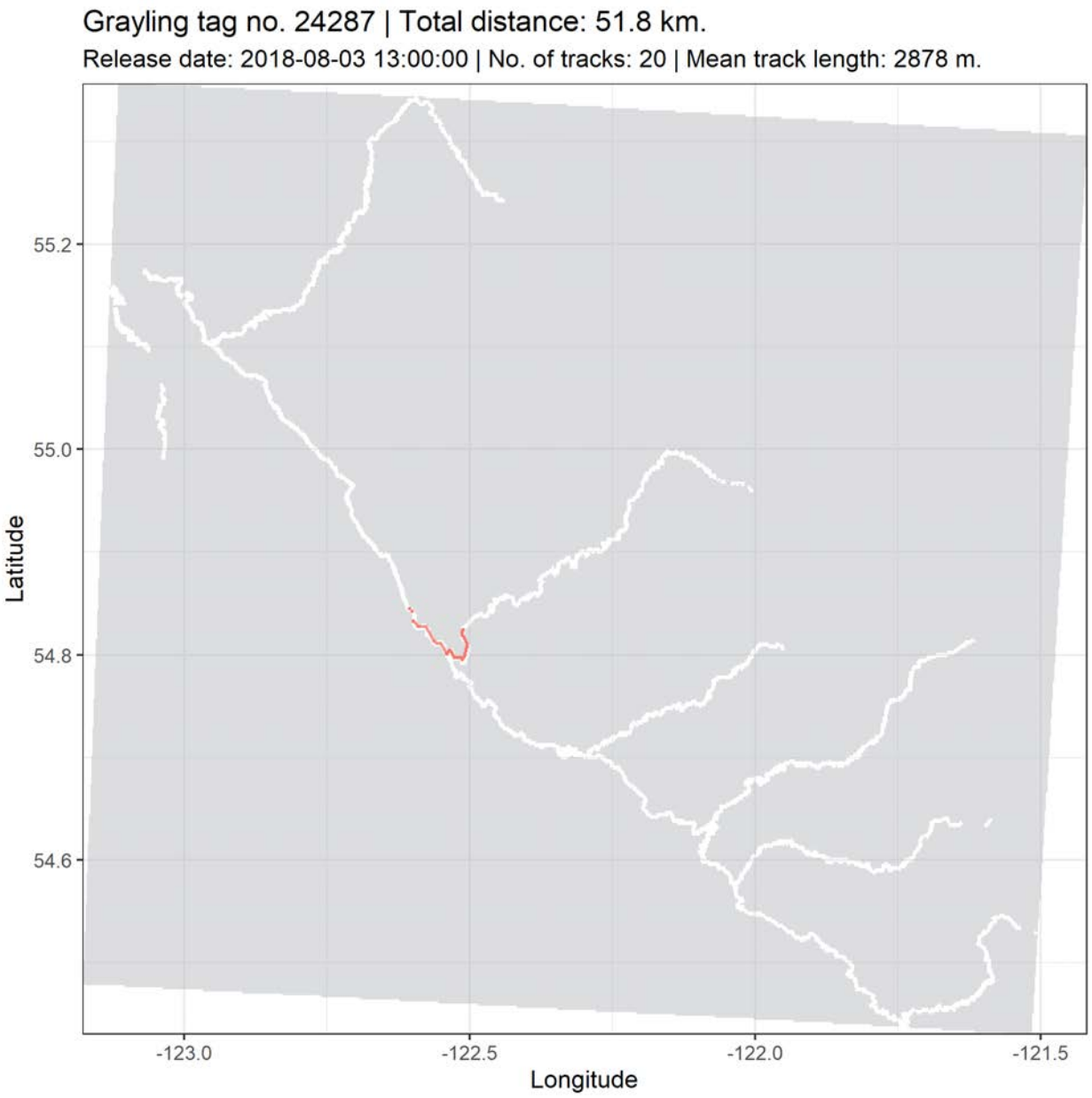
Grayling tag no. 24287 | Total distance: 51.8 km.
Release date: 2018-08-03 13:00:00 | No. of tracks: 20 | Mean track length: 2878 m.
55.2
55.0
54.8
54.6
Latitude
-123.0
-122.5
-122.0
-121.5
Longitude

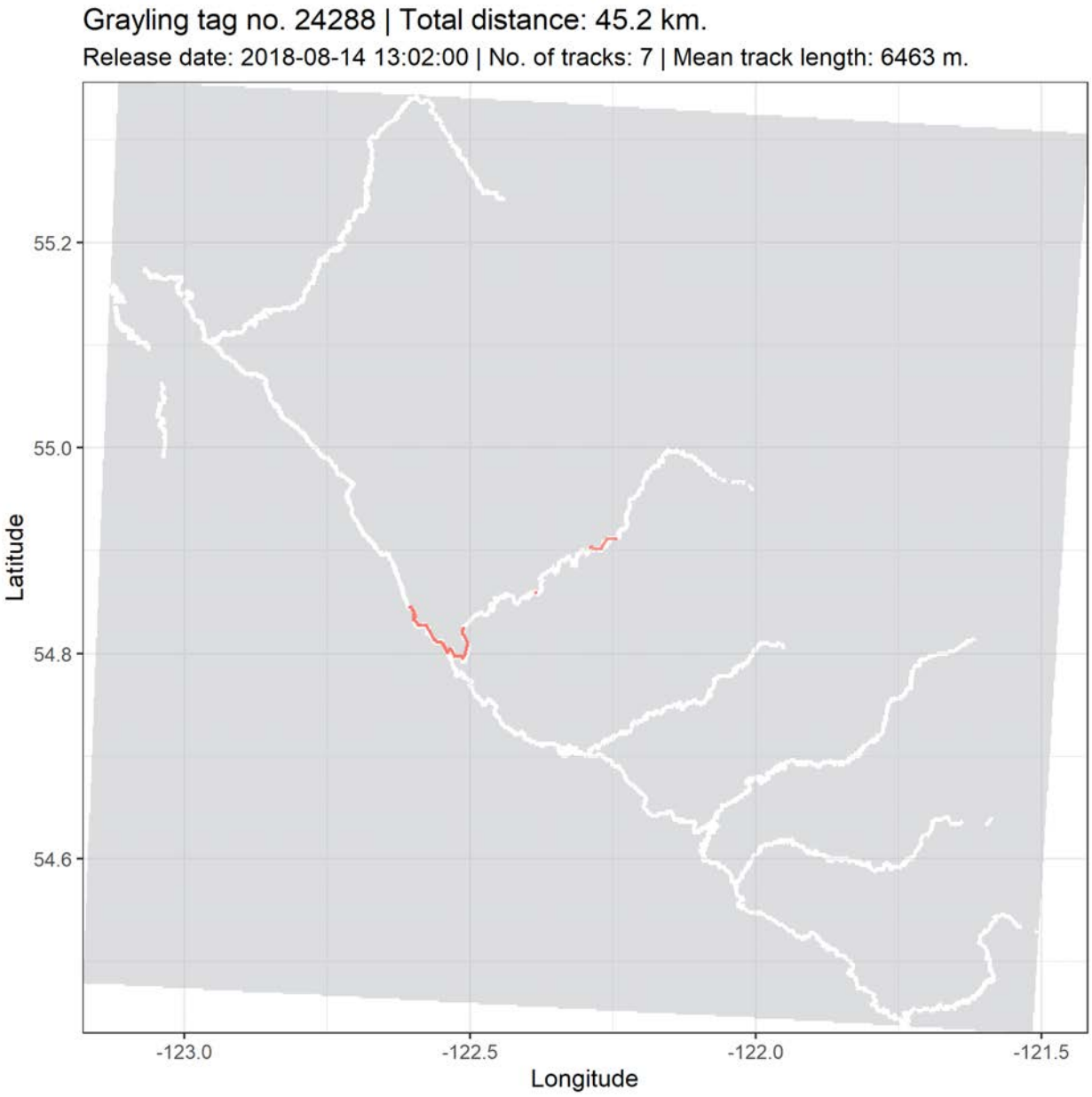
Grayling tag no. 24288 | Total distance: 45.2 km.
Release date: 2018-08-14 13:02:00 | No. of tracks: 7 | Mean track length: 6463 m.
55.2
55.0
54.8
54.6
Latitude
-123.0
-122.5
-122.0
-121.5
Longitude

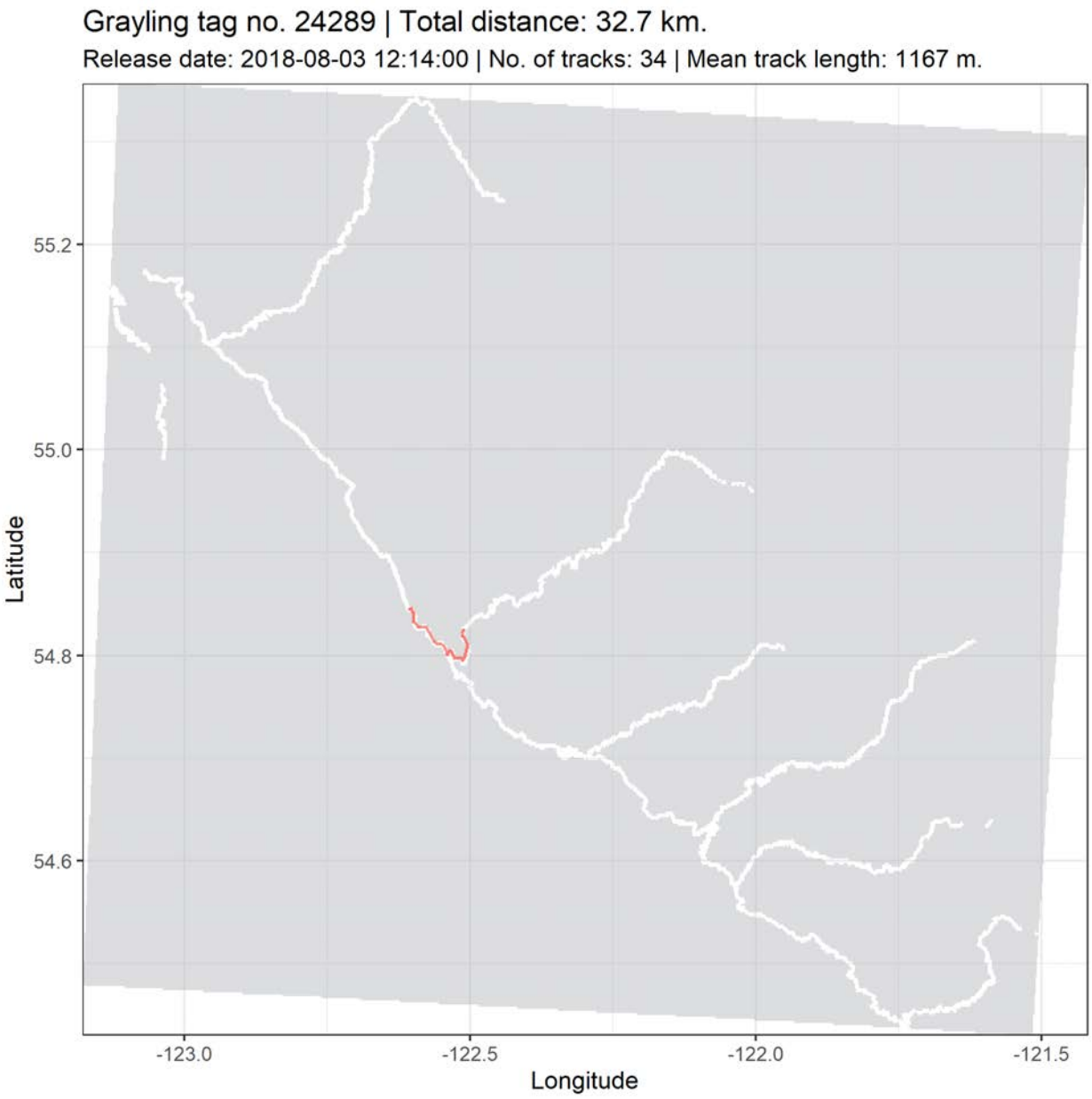
Grayling tag no. 24289 | Total distance: 32.7 km.
Release date: 2018-08-03 12:14:00 | No. of tracks: 34 | Mean track length: 1167 m.
55.2
55.0
54.8
54.6
Latitude
-123.0
-122.5
-122.0
-121.5
Longitude

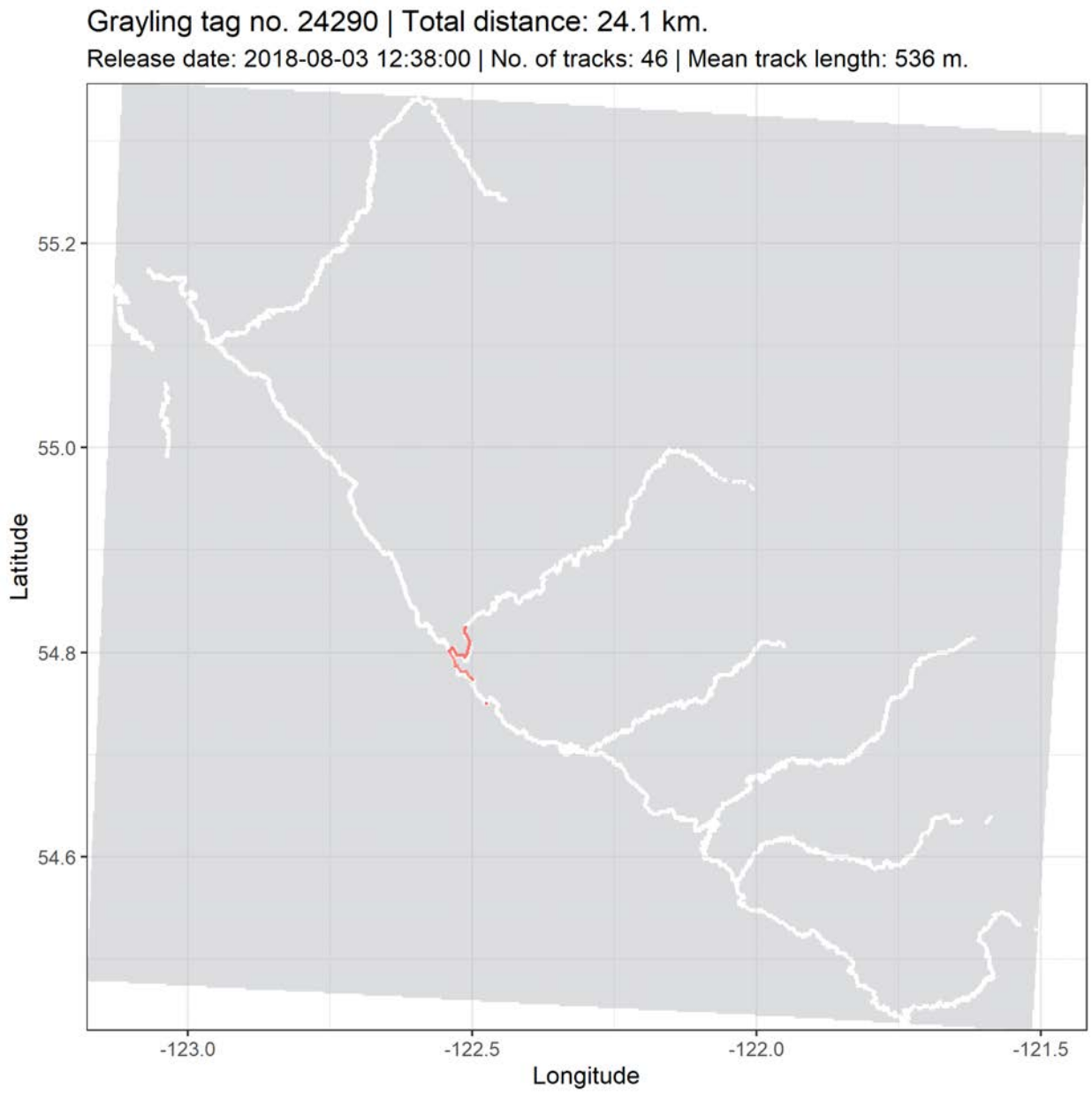
Grayling tag no. 24290 | Total distance: 24.1 km.
Release date: 2018-08-03 12:38:00 | No. of tracks: 46 | Mean track length: 536 m.
55.2
55.0
54.8
54.6
Latitude
-123.0
-122.5
-122.0
-121.5
Longitude

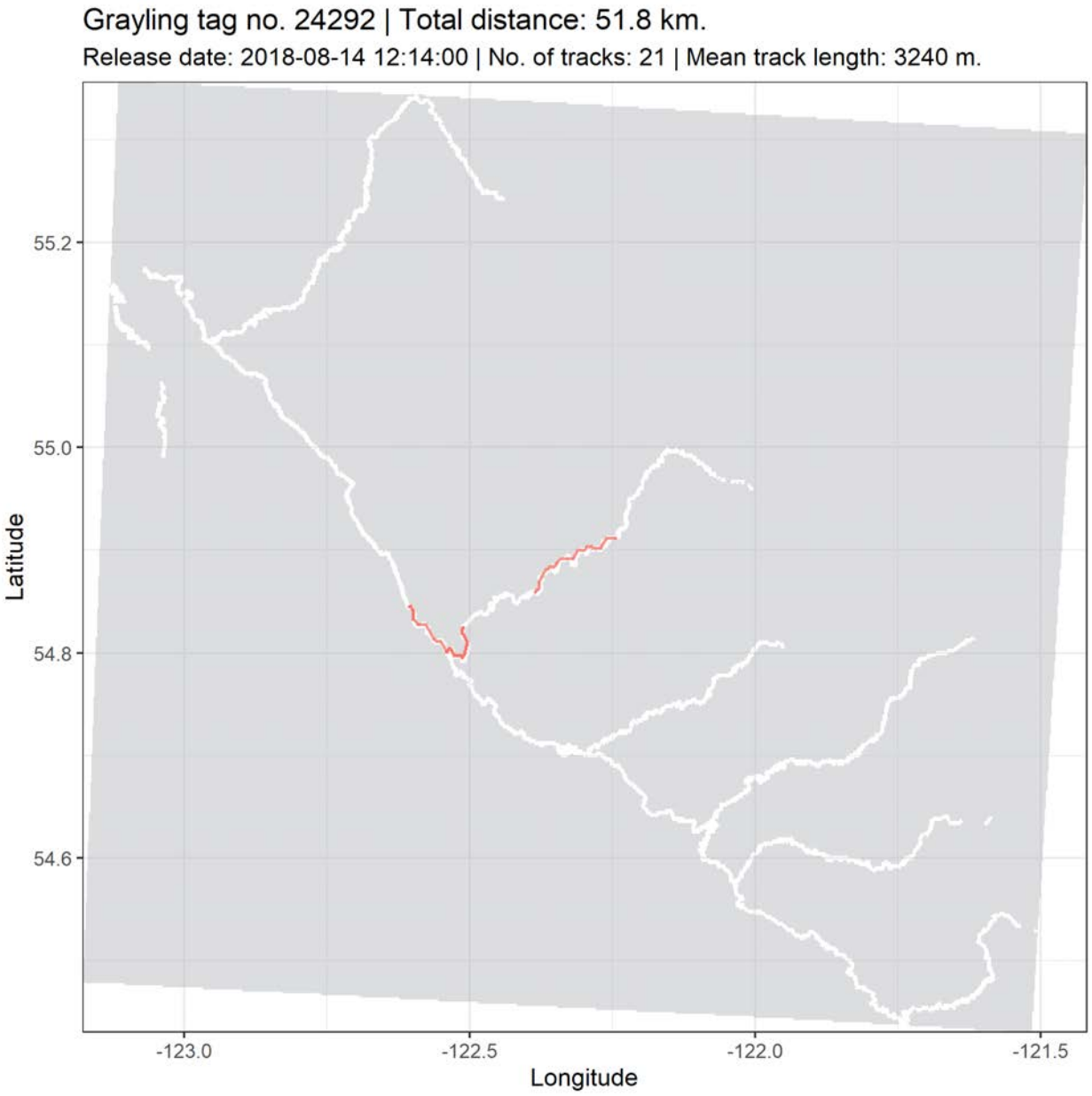
Grayling tag no. 24292 | Total distance: 51.8 km.
Release date: 2018-08-14 12:14:00 | No. of tracks: 21 | Mean track length: 3240 m.
55.2
55.0
54.8
54.6
Latitude
-123.0
-122.5
-122.0
-121.5
Longitude

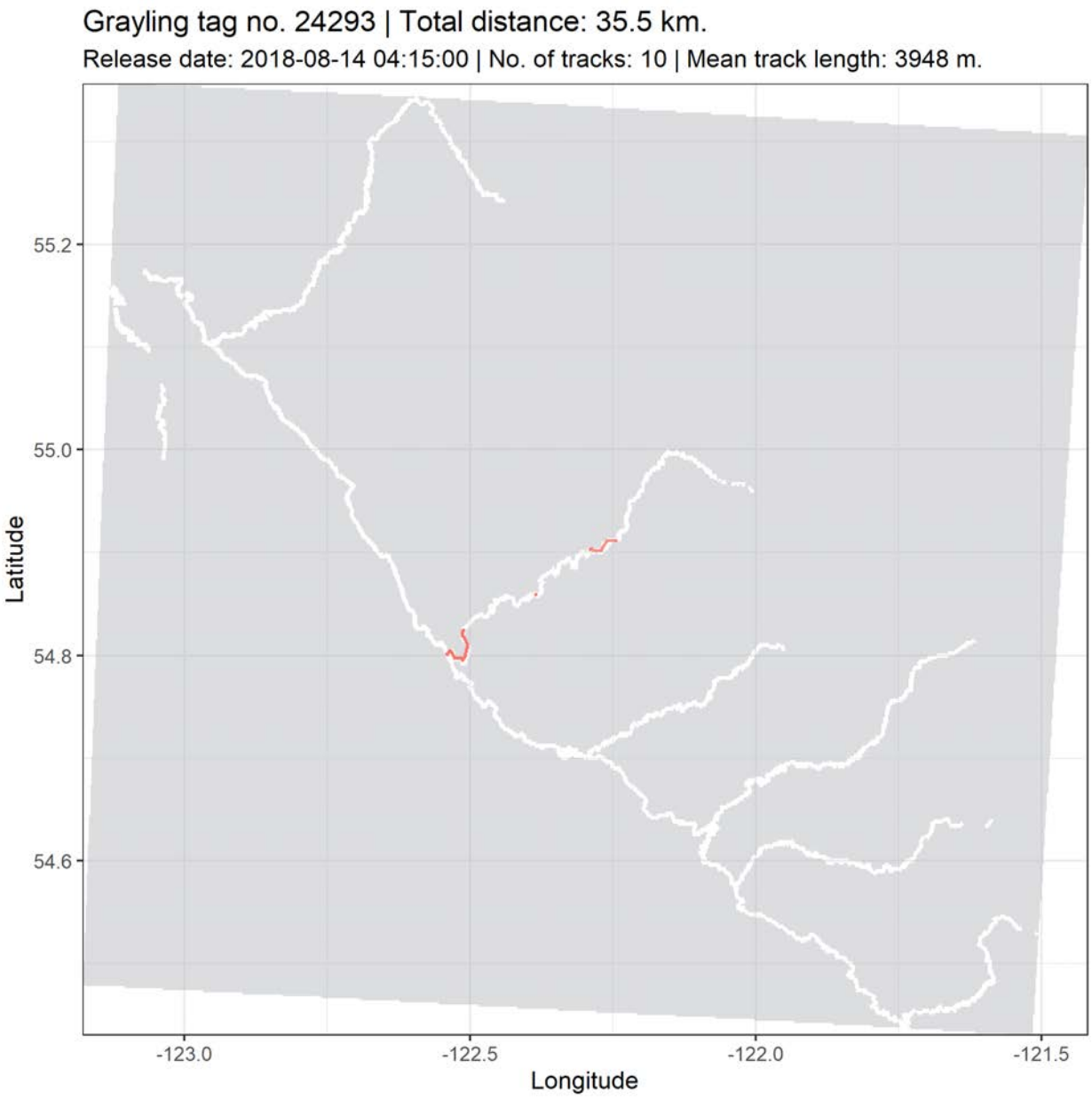
Grayling tag no. 24293 | Total distance: 35.5 km.
Release date: 2018-08-14 04:15:00 | No. of tracks: 10 | Mean track length: 3948 m.
55.2
55.0
54.8
54.6
Latitude
-123.0
-122.5
-122.0
-121.5
Longitude

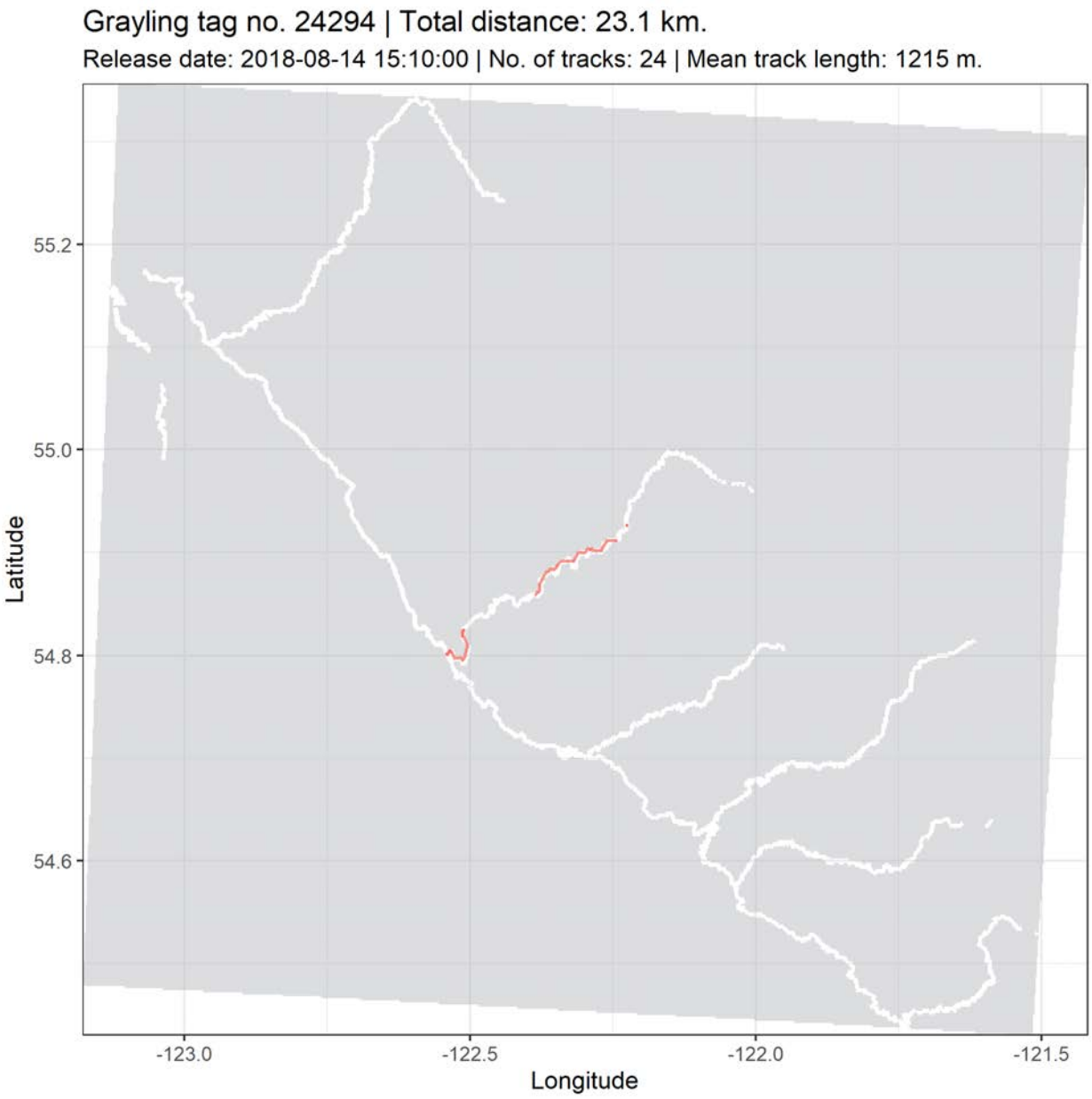
Grayling tag no. 24294 | Total distance: 23.1 km.
Release date: 2018-08-14 15:10:00 | No. of tracks: 24 | Mean track length: 1215 m.
55.2
55.0
54.8
54.6
Latitude
-123.0
-122.5
-122.0
-121.5
Longitude

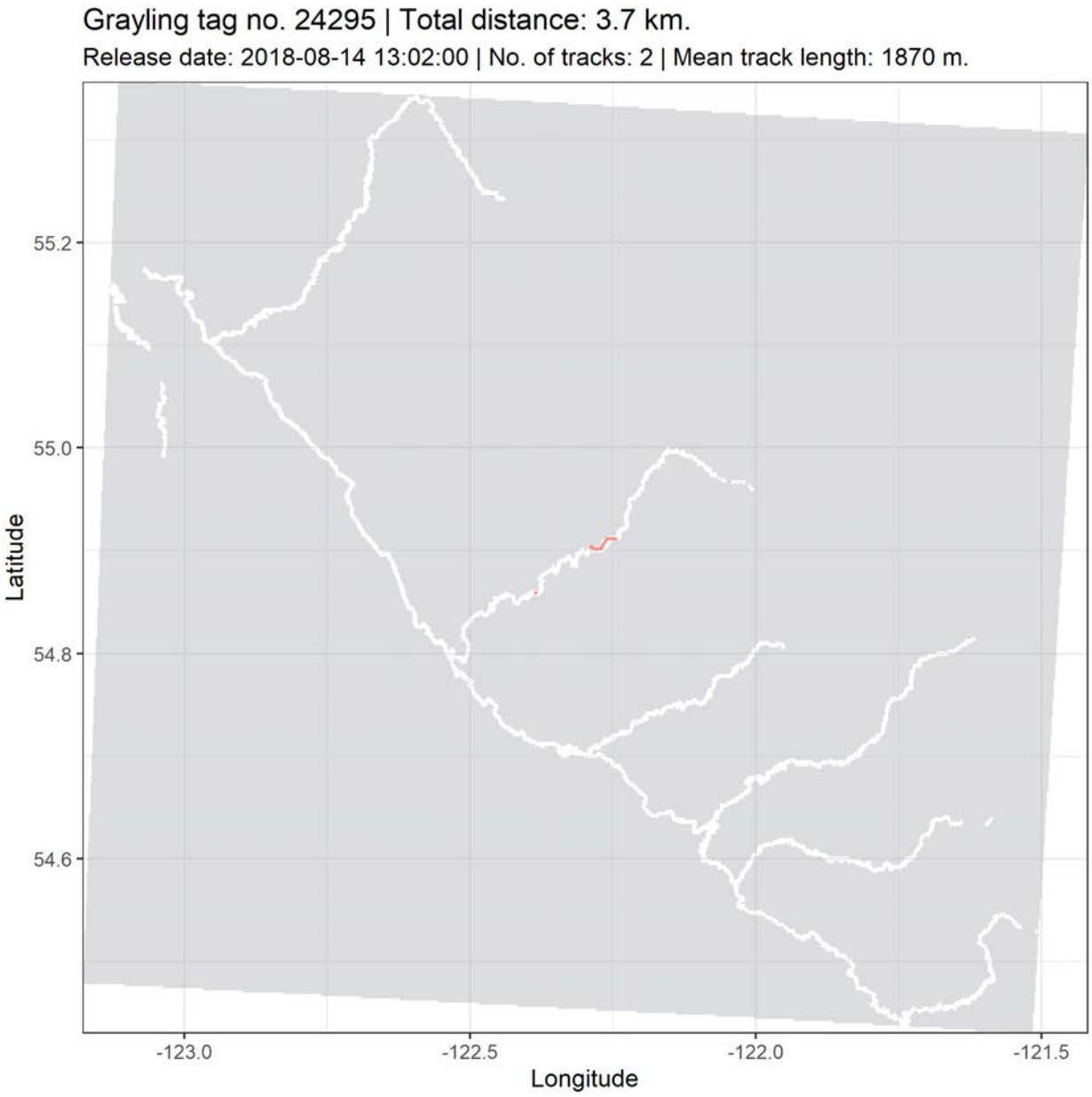
Grayling tag no. 24295 | Total distance: 3.7 km.
Release date: 2018-08-14 13:02:00 | No. of tracks: 2 | Mean track length: 1870 m.
55.2
55.0
54.8
54.6
Latitude
-123.0
-122.5
-122.0
-121.5
Longitude

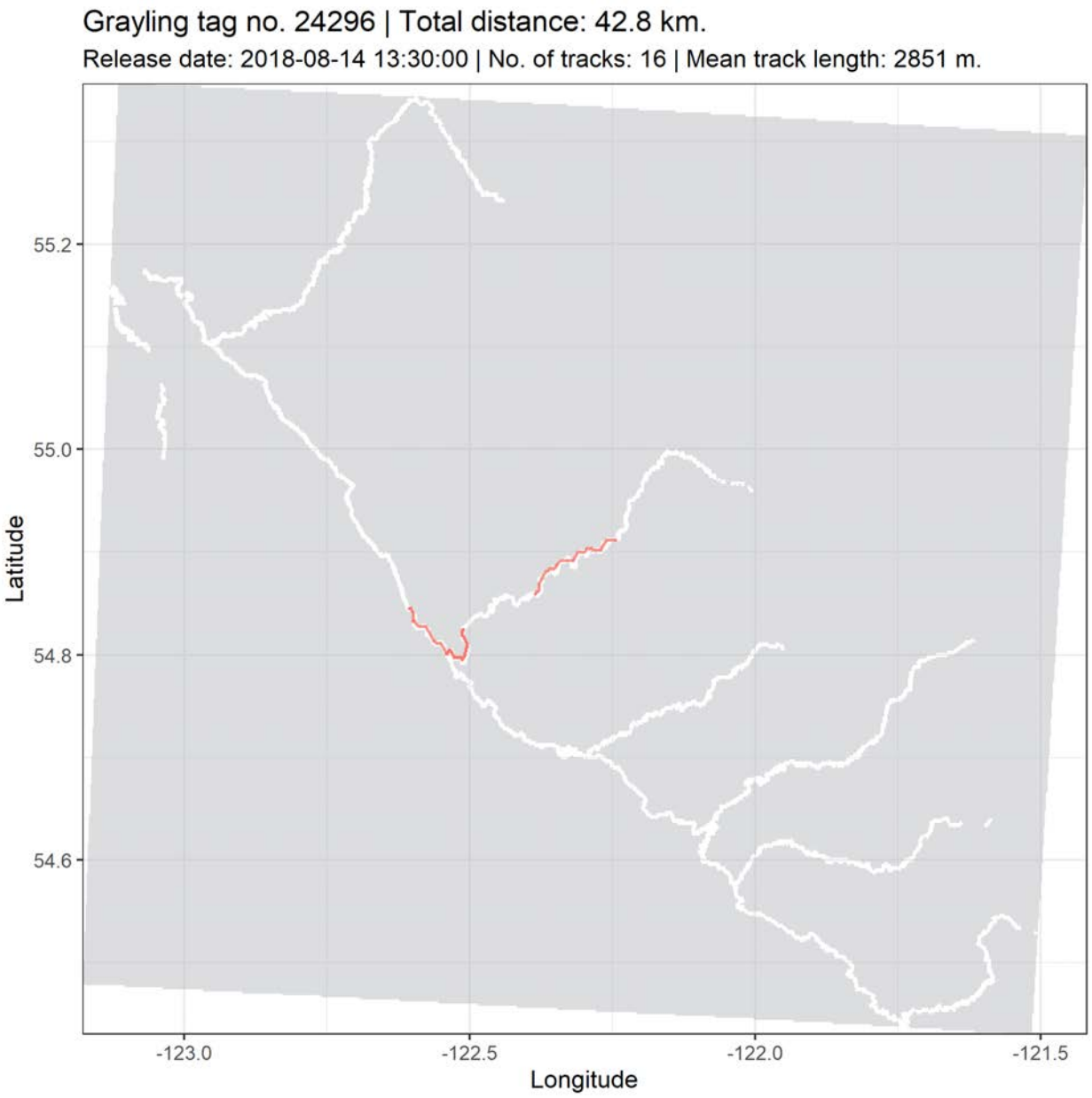
Grayling tag no. 24296 | Total distance: 42.8 km.
Release date: 2018-08-14 13:30:00 | No. of tracks: 16 | Mean track length: 2851 m.
55.2
55.0
54.8
54.6
Latitude
-123.0
-122.5
-122.0
-121.5
Longitude

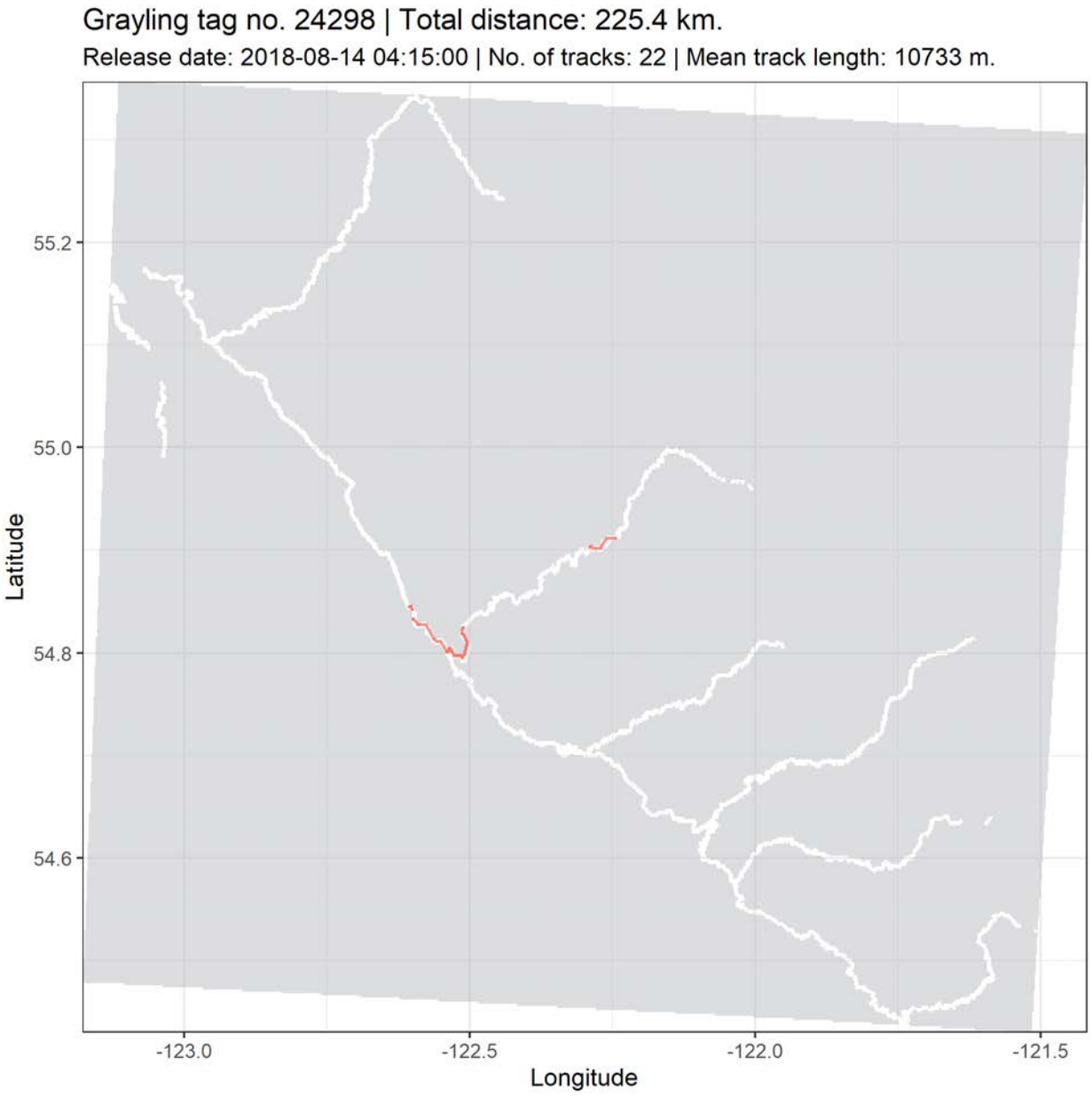
Grayling tag no. 24298 | Total distance: 225.4 km.
Release date: 2018-08-14 04:15:00 | No. of tracks: 22 | Mean track length: 10733 m.
55.2
55.0
54.8
54.6
Latitude
-123.0
-122.5
-122.0
-121.5
Longitude

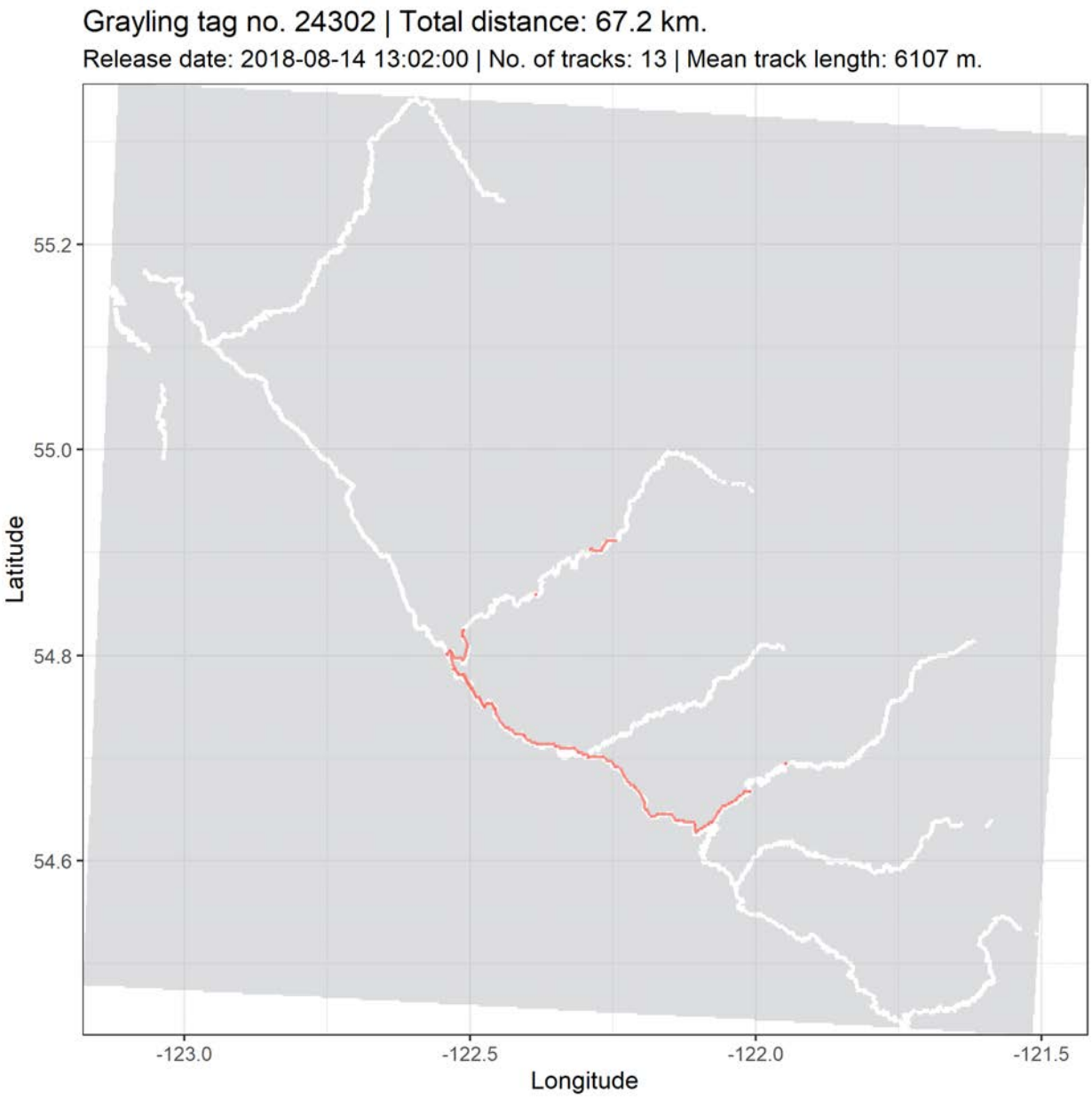
Grayling tag no. 24302 | Total distance: 67.2 km.
Release date: 2018-08-14 13:02:00 | No. of tracks: 13 | Mean track length: 6107 m.
55.2
55.0
54.8
54.6
Latitude
-123.0
-122.5
-122.0
-121.5
Longitude

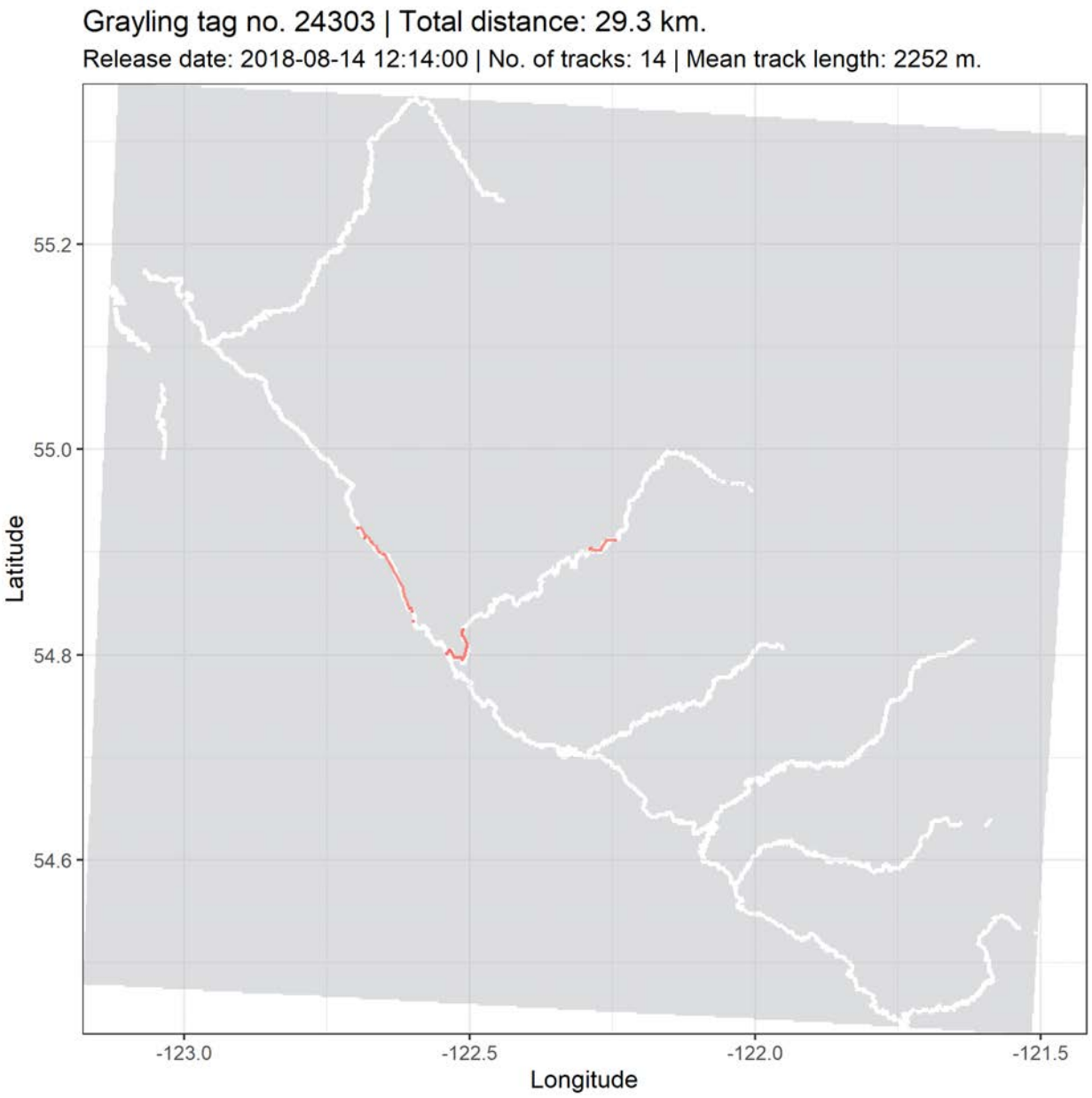
Grayling tag no. 24303 | Total distance: 29.3 km.
Release date: 2018-08-14 12:14:00 | No. of tracks: 14 | Mean track length: 2252 m.
55.2
55.0
54.8
54.6
Latitude
-123.0
-122.5
-122.0
-121.5
Longitude

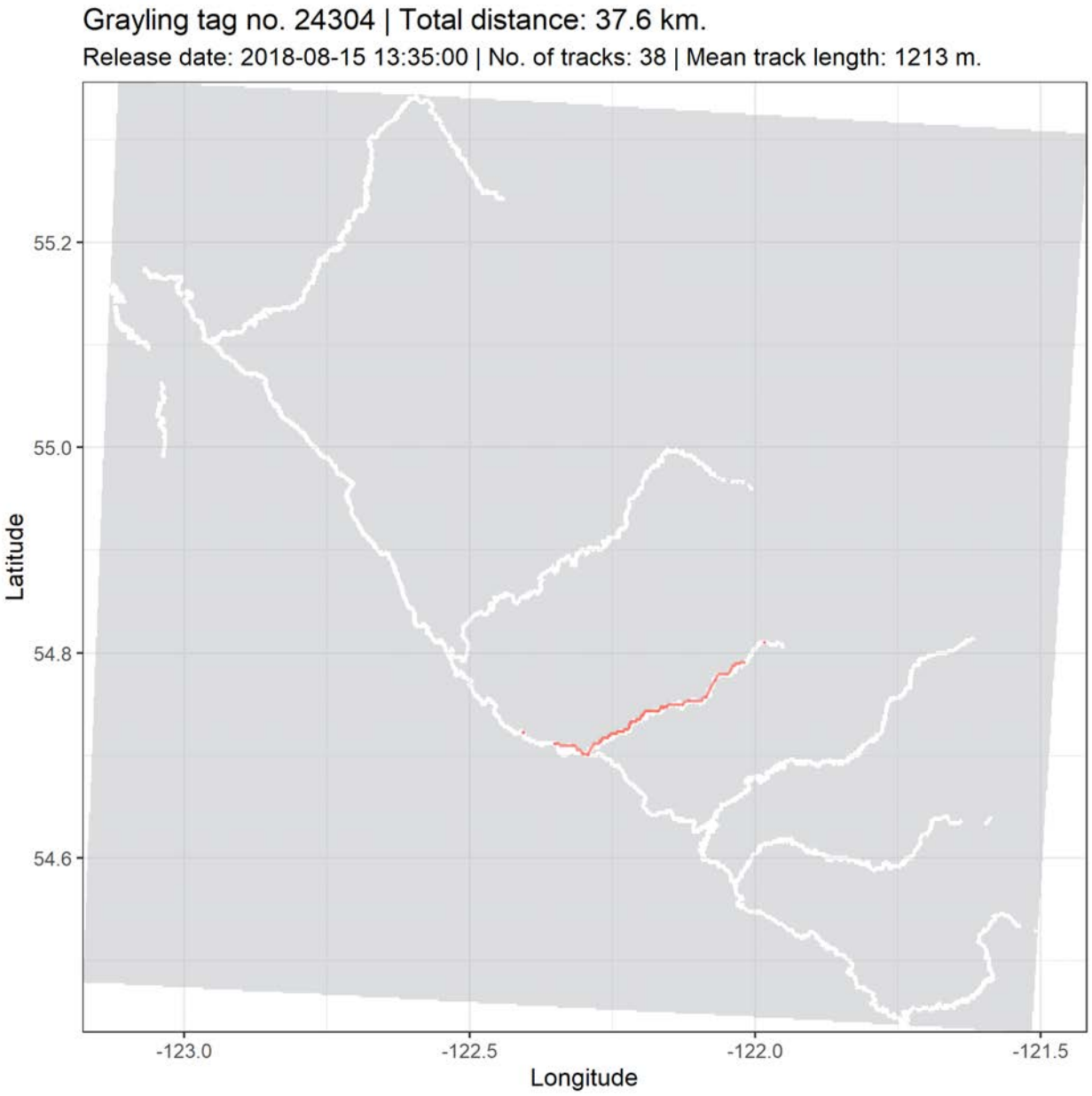
Grayling tag no. 24304 | Total distance: 37.6 km.
Release date: 2018-08-15 13:35:00 | No. of tracks: 38 | Mean track length: 1213 m.
55.2
55.0
54.8
54.6
Latitude
-123.0
-122.5
-122.0
-121.5
Longitude

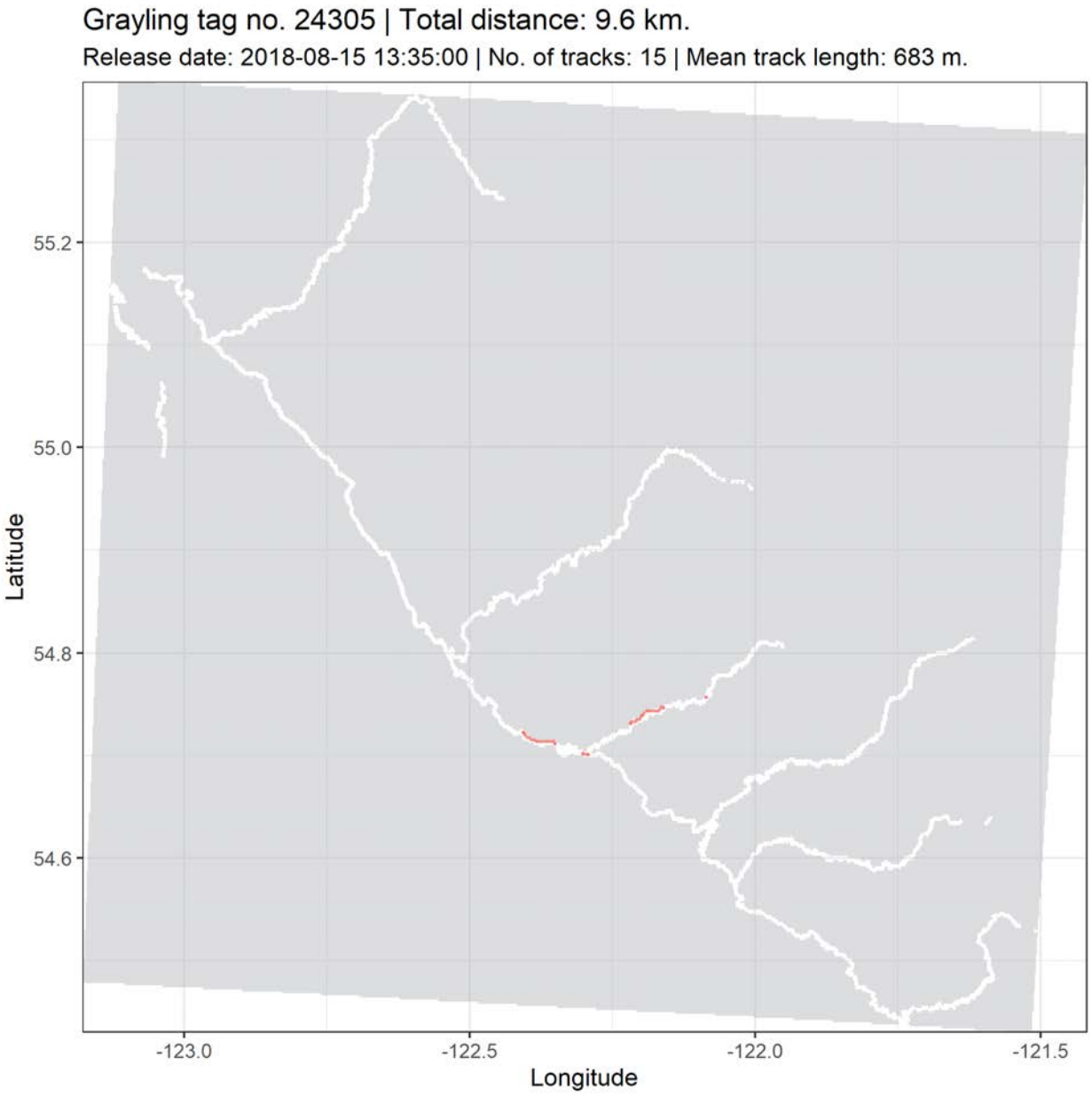
Grayling tag no. 24305 | Total distance: 9.6 km.
Release date: 2018-08-15 13:35:00 | No. of tracks: 15 | Mean track length: 683 m.
55.2
55.0
54.8
54.6
Latitude
-123.0
-122.5
-122.0
-121.5
Longitude

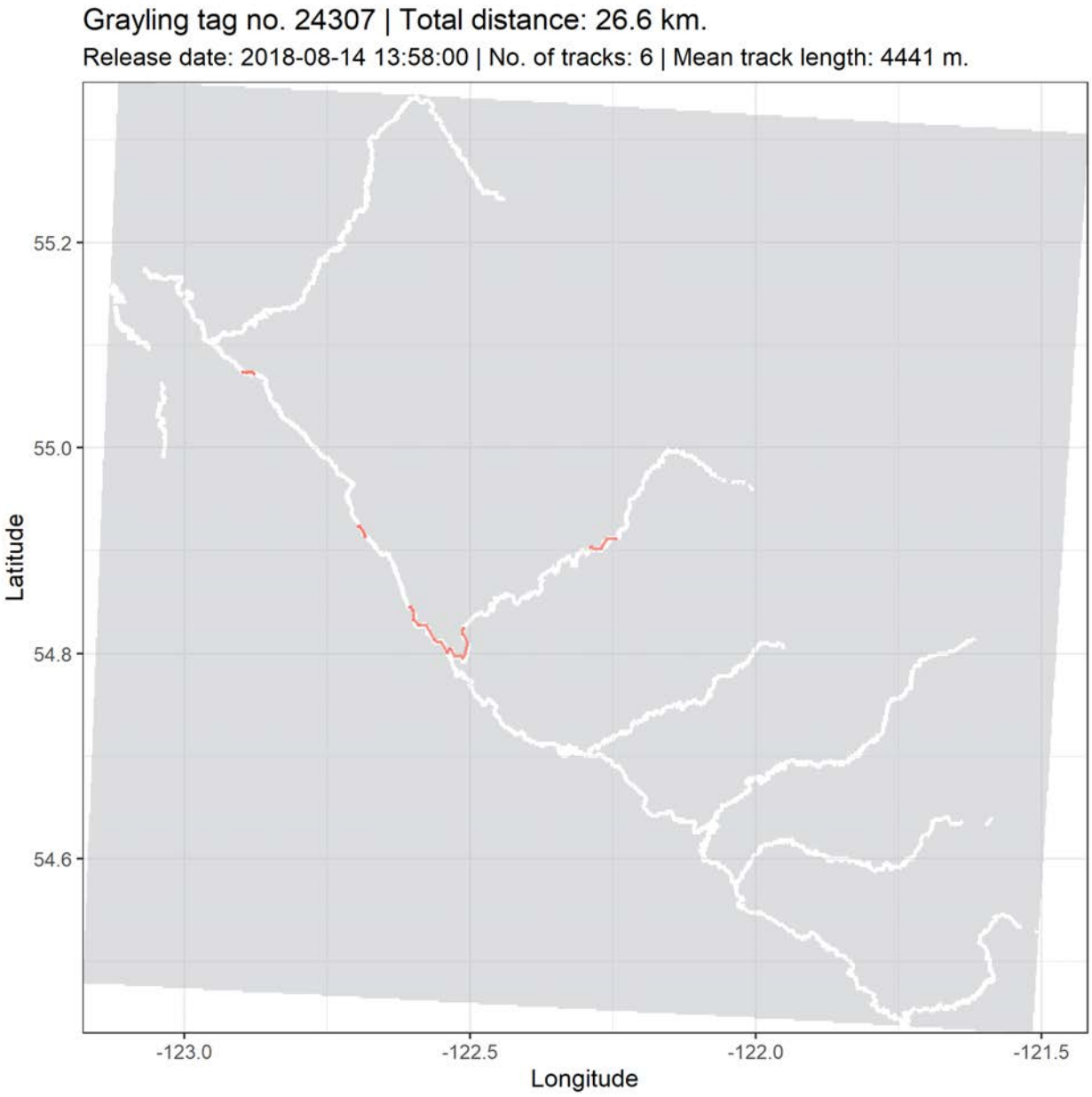
Grayling tag no. 24307 | Total distance: 26.6 km.
Release date: 2018-08-14 13:58:00 | No. of tracks: 6 | Mean track length: 4441 m.
55.2
55.0
54.8
54.6
Latitude
-123.0
-122.5
-122.0
-121.5
Longitude

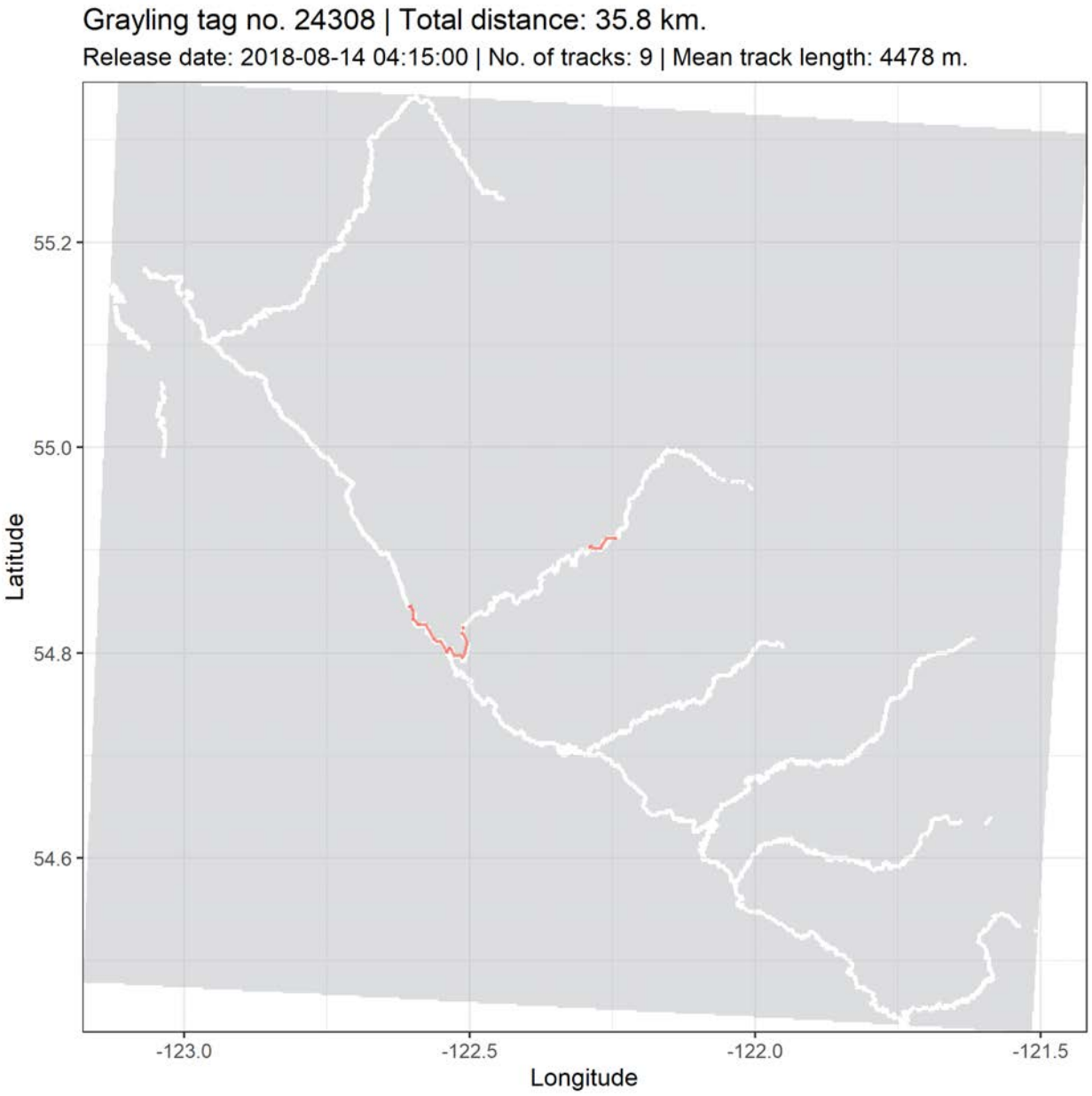
Grayling tag no. 24308 | Total distance: 35.8 km.
Release date: 2018-08-14 04:15:00 | No. of tracks: 9 | Mean track length: 4478 m.
55.2
55.0
54.8
54.6
Latitude
-123.0
-122.5
-122.0
-121.5
Longitude

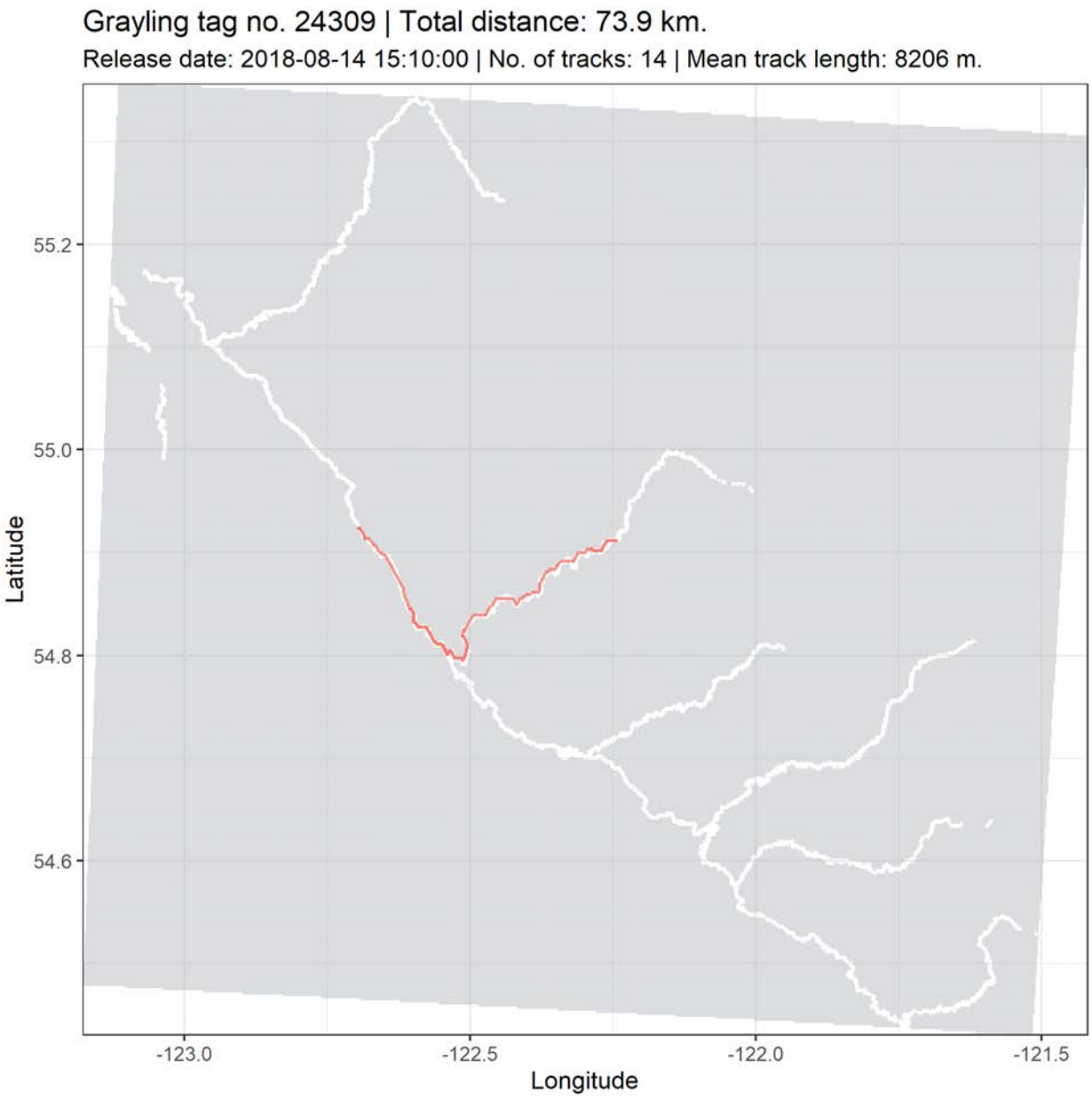
Grayling tag no. 24309 | Total distance: 73.9 km.
Release date: 2018-08-14 15:10:00 | No. of tracks: 14 | Mean track length: 8206 m.
55.2
55.0
54.8
54.6
Latitude
-123.0
-122.5
-122.0
-121.5
Longitude

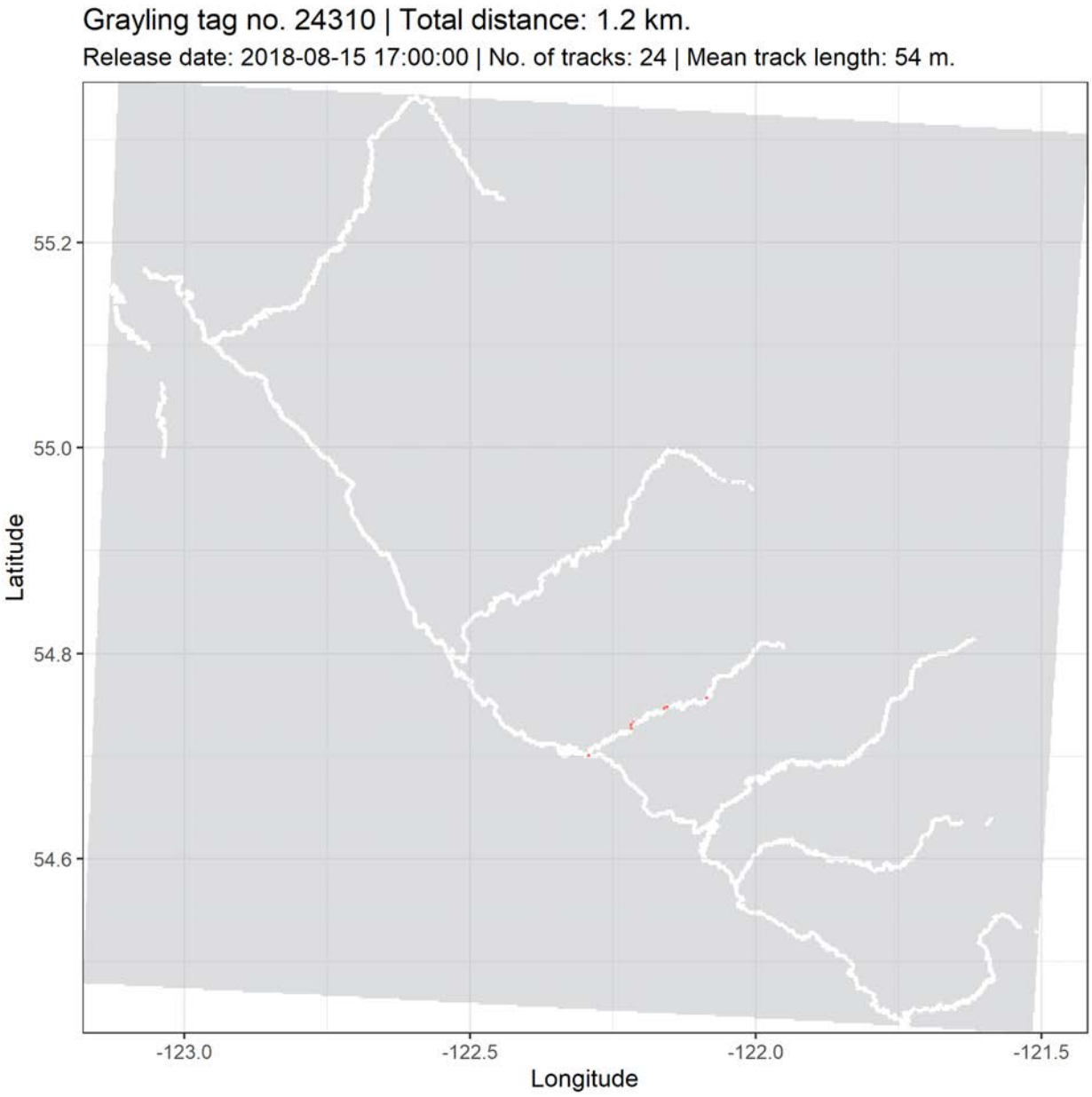
Grayling tag no. 24310 | Total distance: 1.2 km.
Release date: 2018-08-15 17:00:00 | No. of tracks: 24 | Mean track length: 54 m.
55.2
55.0
54.8
54.6
Latitude
-123.0
-122.5
-122.0
-121.5
Longitude

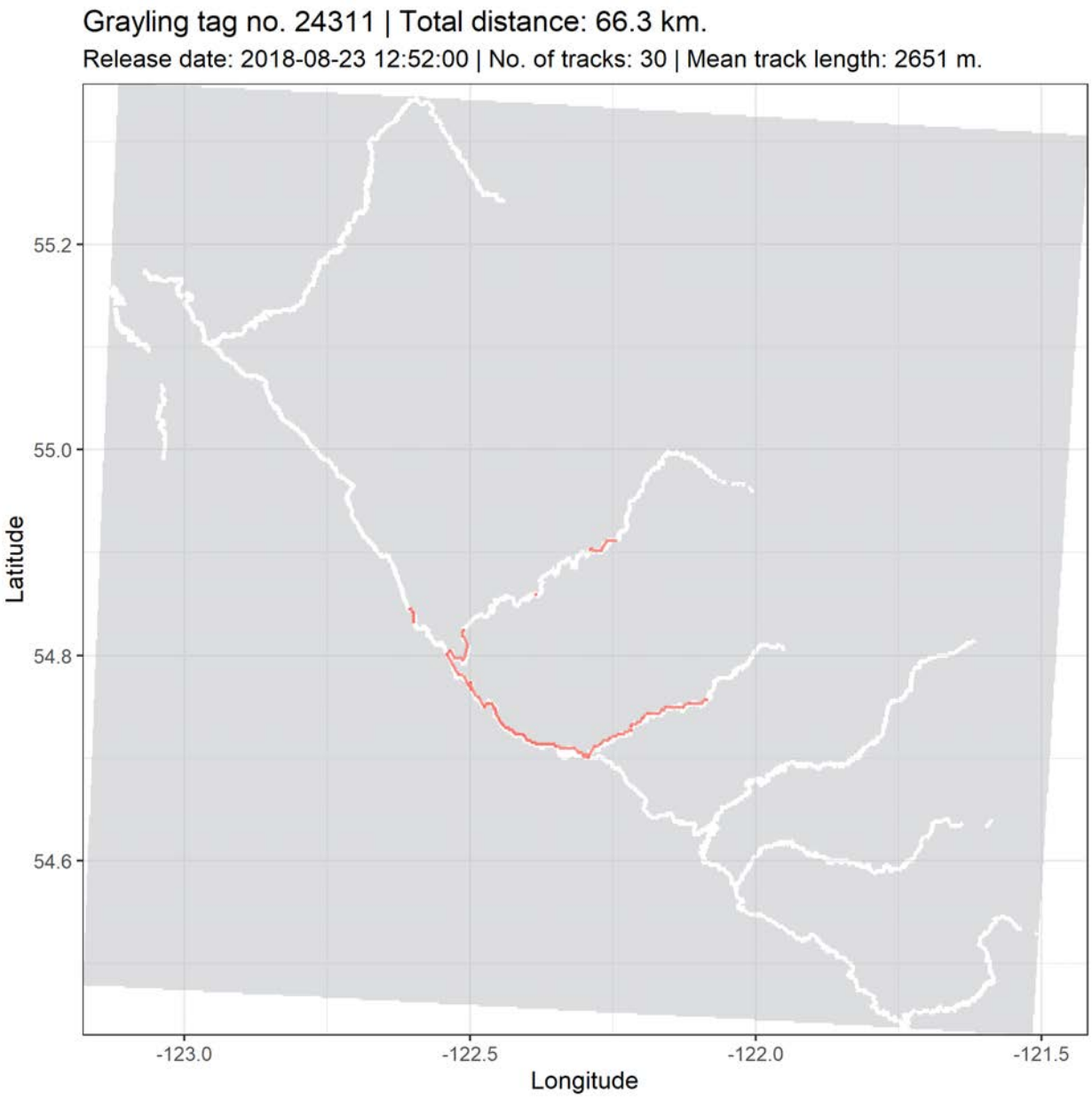
Grayling tag no. 24311 | Total distance: 66.3 km.
Release date: 2018-08-23 12:52:00 | No. of tracks: 30 | Mean track length: 2651 m.
55.2
55.0
54.8
54.6
Latitude
-123.0
-122.5
-122.0
-121.5
Longitude

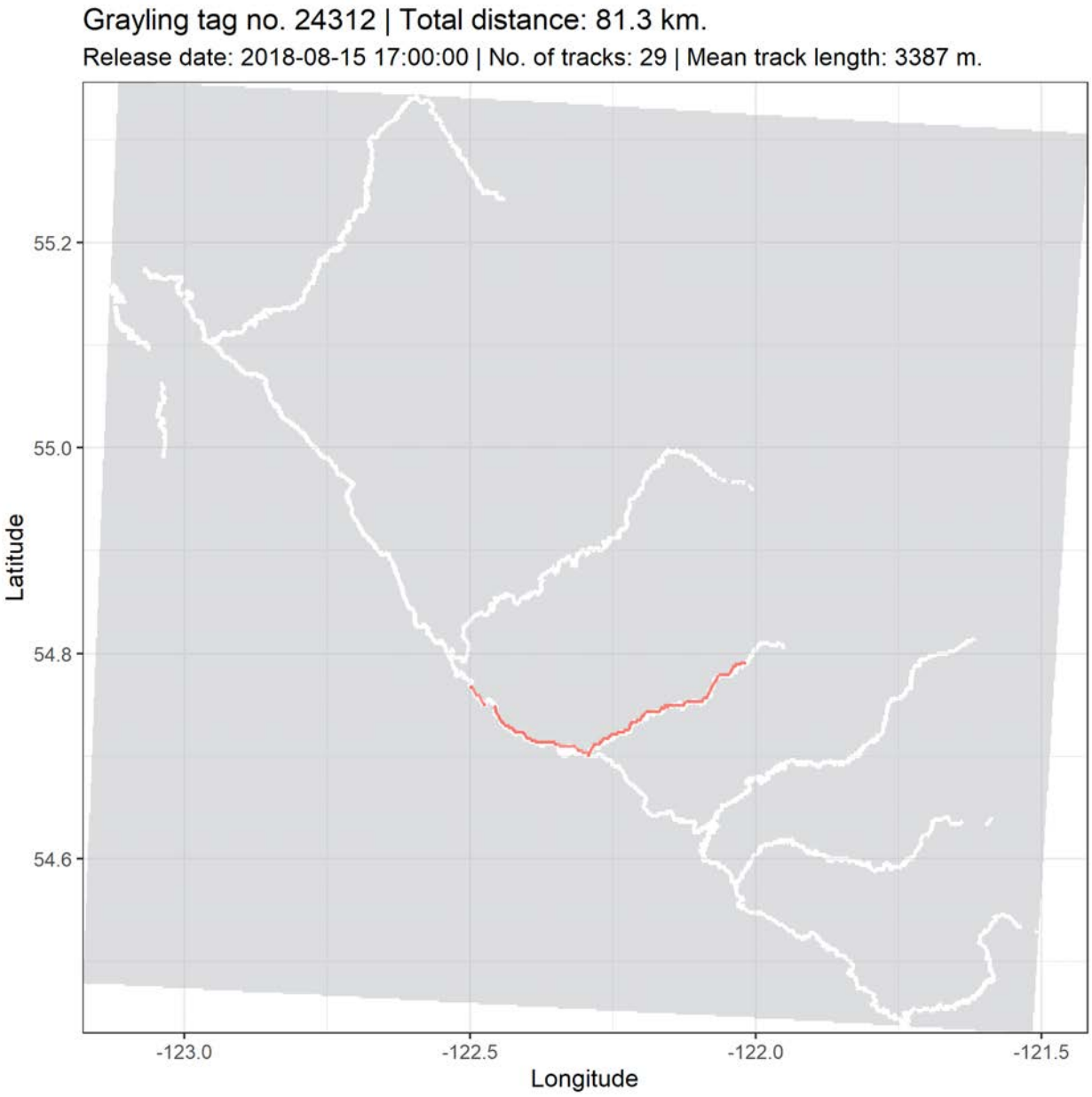
Grayling tag no. 24312 | Total distance: 81.3 km.
Release date: 2018-08-15 17:00:00 | No. of tracks: 29 | Mean track length: 3387 m.
55.2
55.0
54.8
54.6
Latitude
-123.0
-122.5
-122.0
-121.5
Longitude

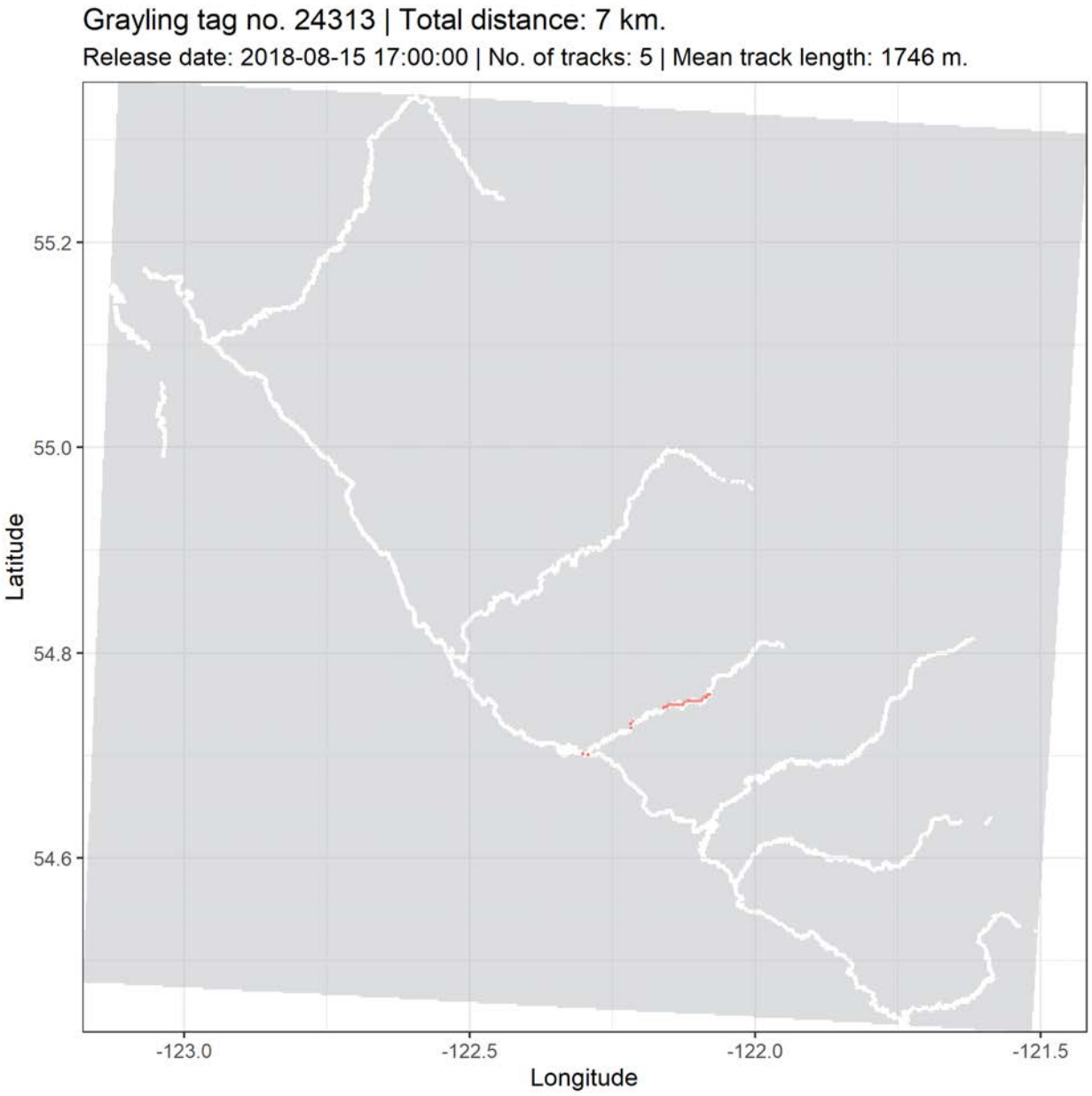
Grayling tag no. 24313 | Total distance: 7 km.
Release date: 2018-08-15 17:00:00 | No. of tracks: 5 | Mean track length: 1746 m.
55.2
55.0
54.8
54.6
Latitude
-123.0
-122.5
-122.0
-121.5
Longitude

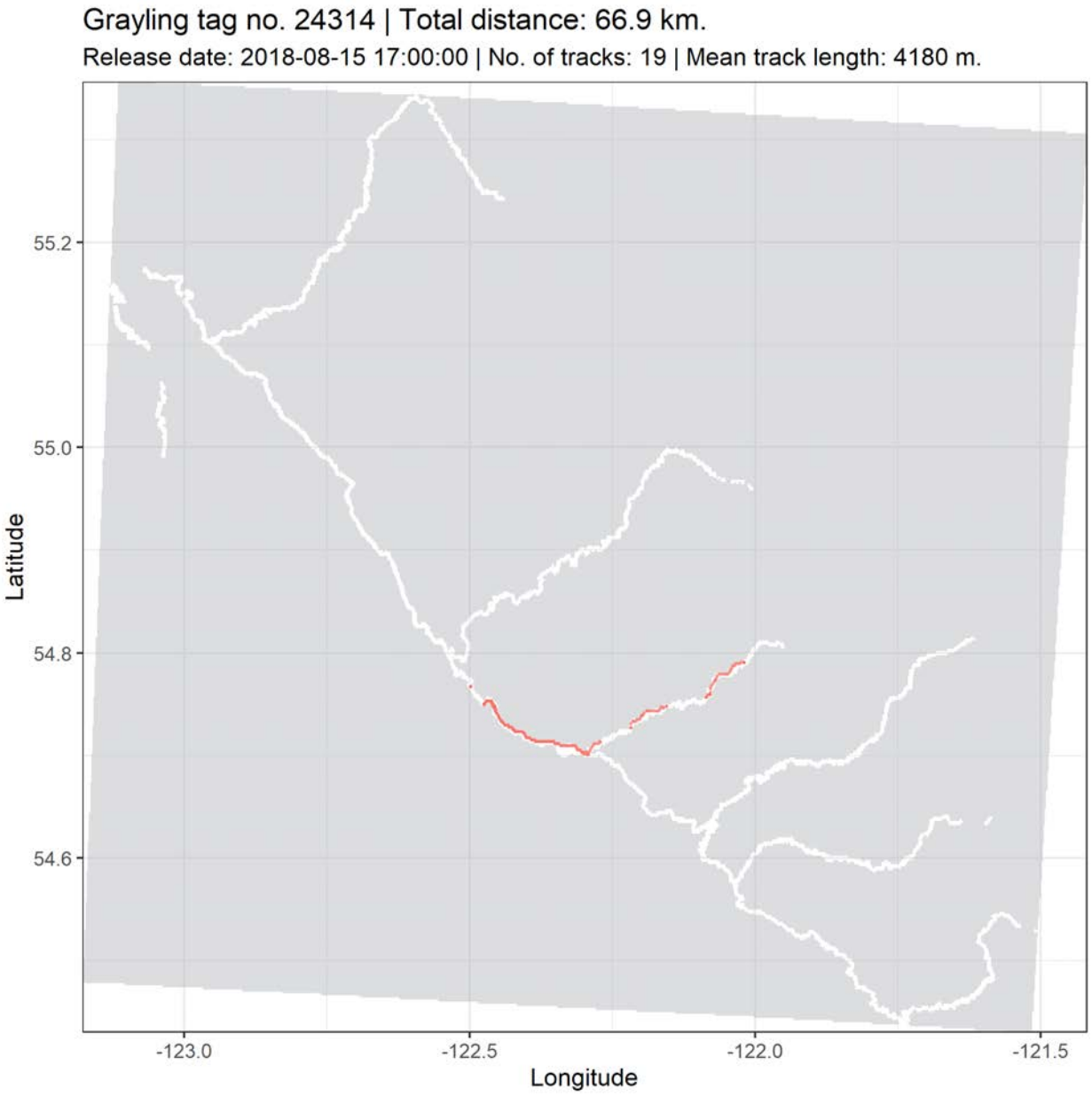
Grayling tag no. 24314 | Total distance: 66.9 km.
Release date: 2018-08-15 17:00:00 | No. of tracks: 19 | Mean track length: 4180 m.
55.2
55.0
54.8
54.6
Latitude
-123.0
-122.5
-122.0
-121.5
Longitude

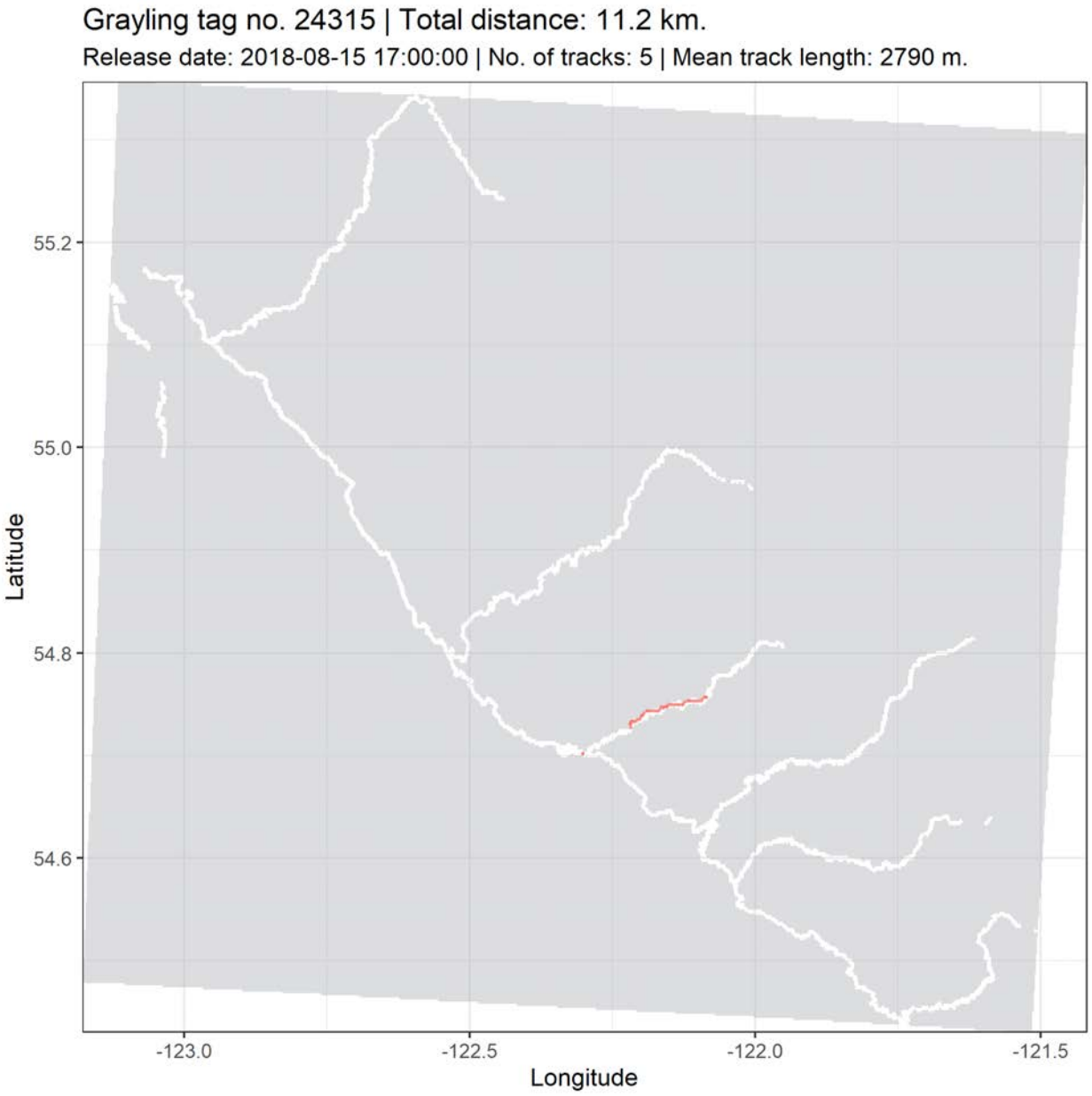
Grayling tag no. 24315 | Total distance: 11.2 km.
Release date: 2018-08-15 17:00:00 | No. of tracks: 5 | Mean track length: 2790 m.
55.2
55.0
54.8
54.6
Latitude
-123.0
-122.5
-122.0
-121.5
Longitude

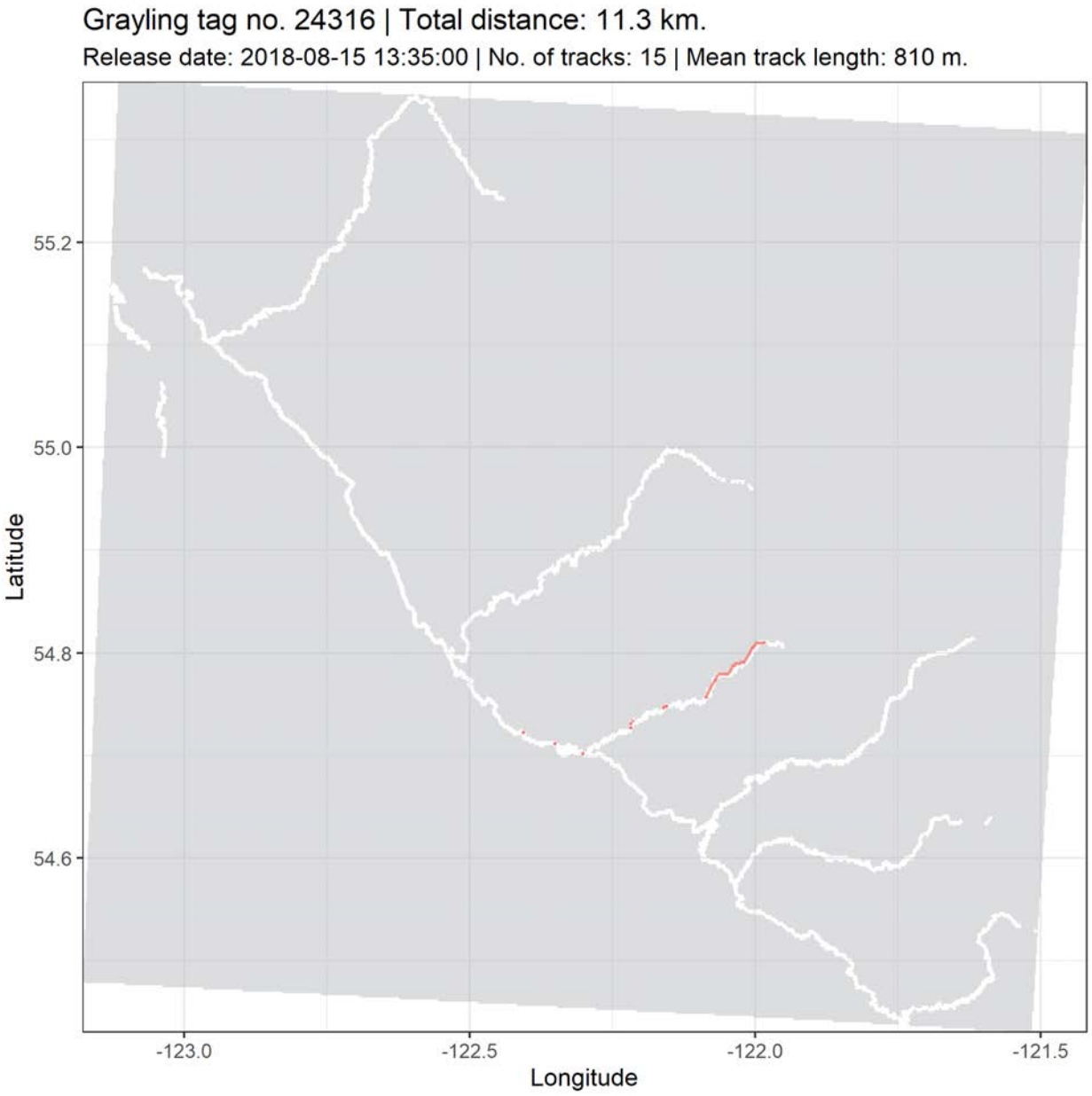
Grayling tag no. 24316 | Total distance: 11.3 km.
Release date: 2018-08-15 13:35:00 | No. of tracks: 15 | Mean track length: 810 m.
55.2
55.0
54.8
54.6
Latitude
-123.0
-122.5
-122.0
-121.5
Longitude

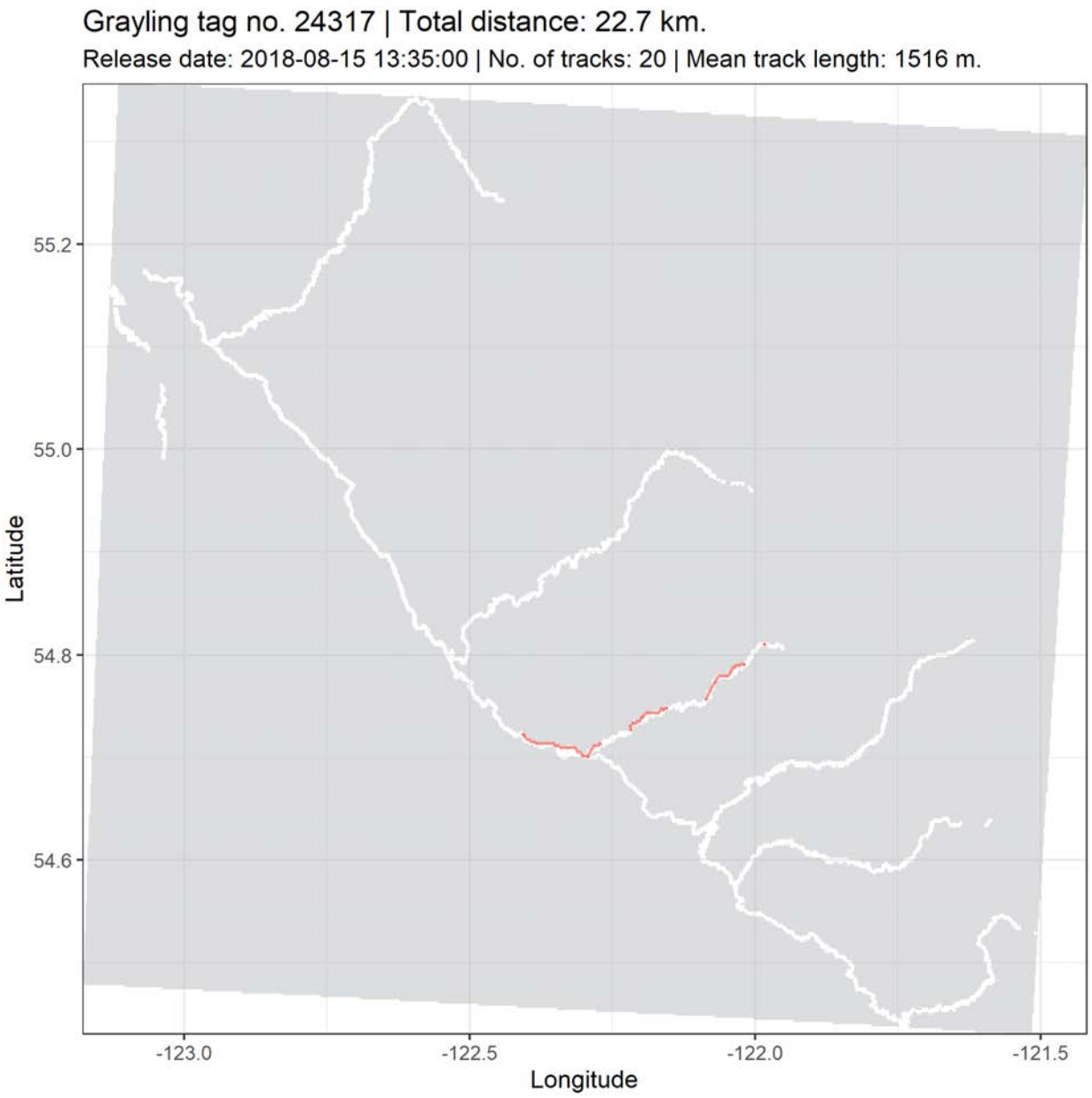
Grayling tag no. 24317 | Total distance: 22.7 km.
Release date: 2018-08-15 13:35:00 | No. of tracks: 20 | Mean track length: 1516 m.
55.2
55.0
54.8
54.6
Latitude
-123.0
-122.5
-122.0
-121.5
Longitude

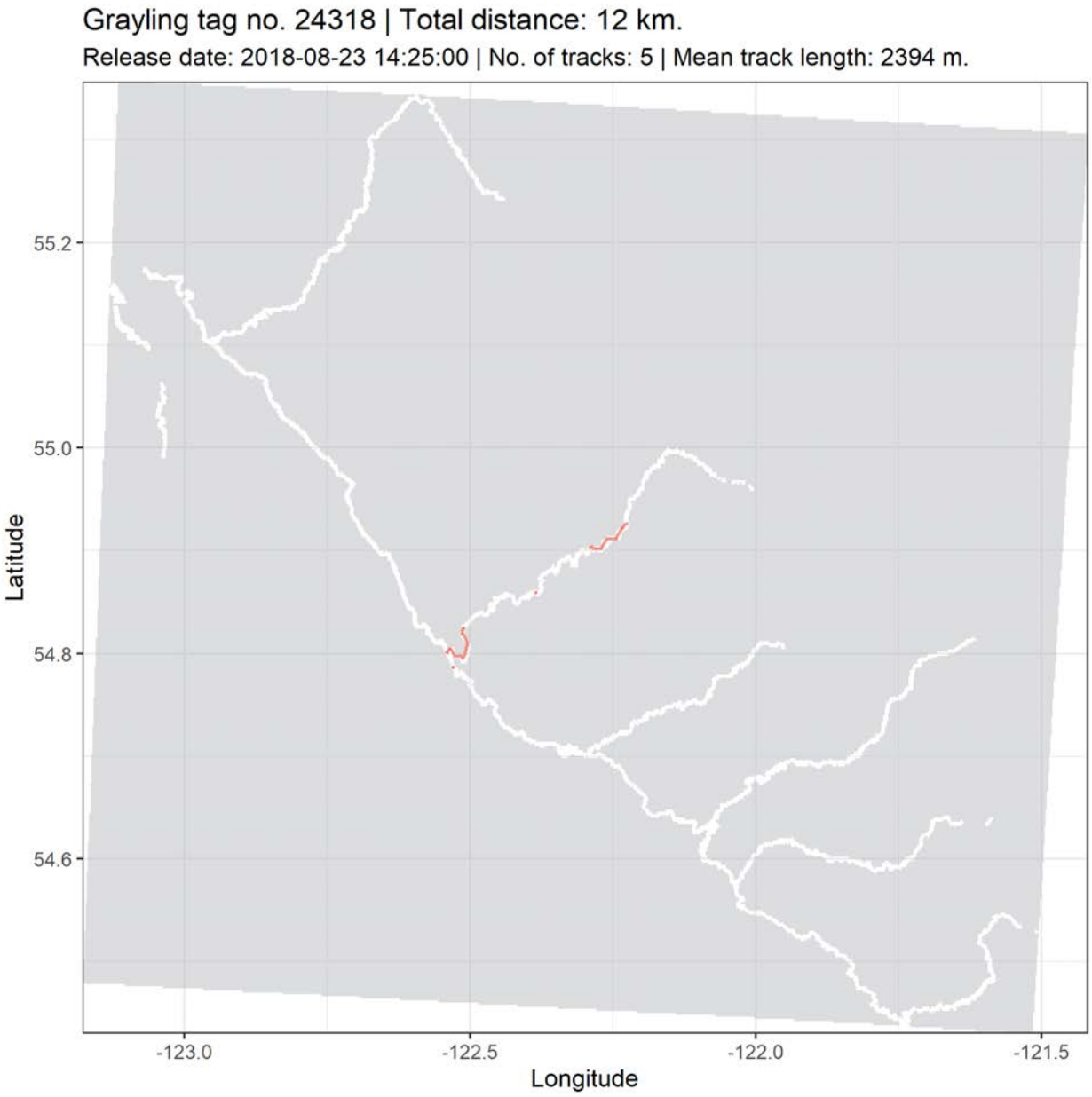
Grayling tag no. 24318 | Total distance: 12 km.
Release date: 2018-08-23 14:25:00 | No. of tracks: 5 | Mean track length: 2394 m.
55.2
55.0
54.8
54.6
Latitude
-123.0
-122.5
-122.0
-121.5
Longitude

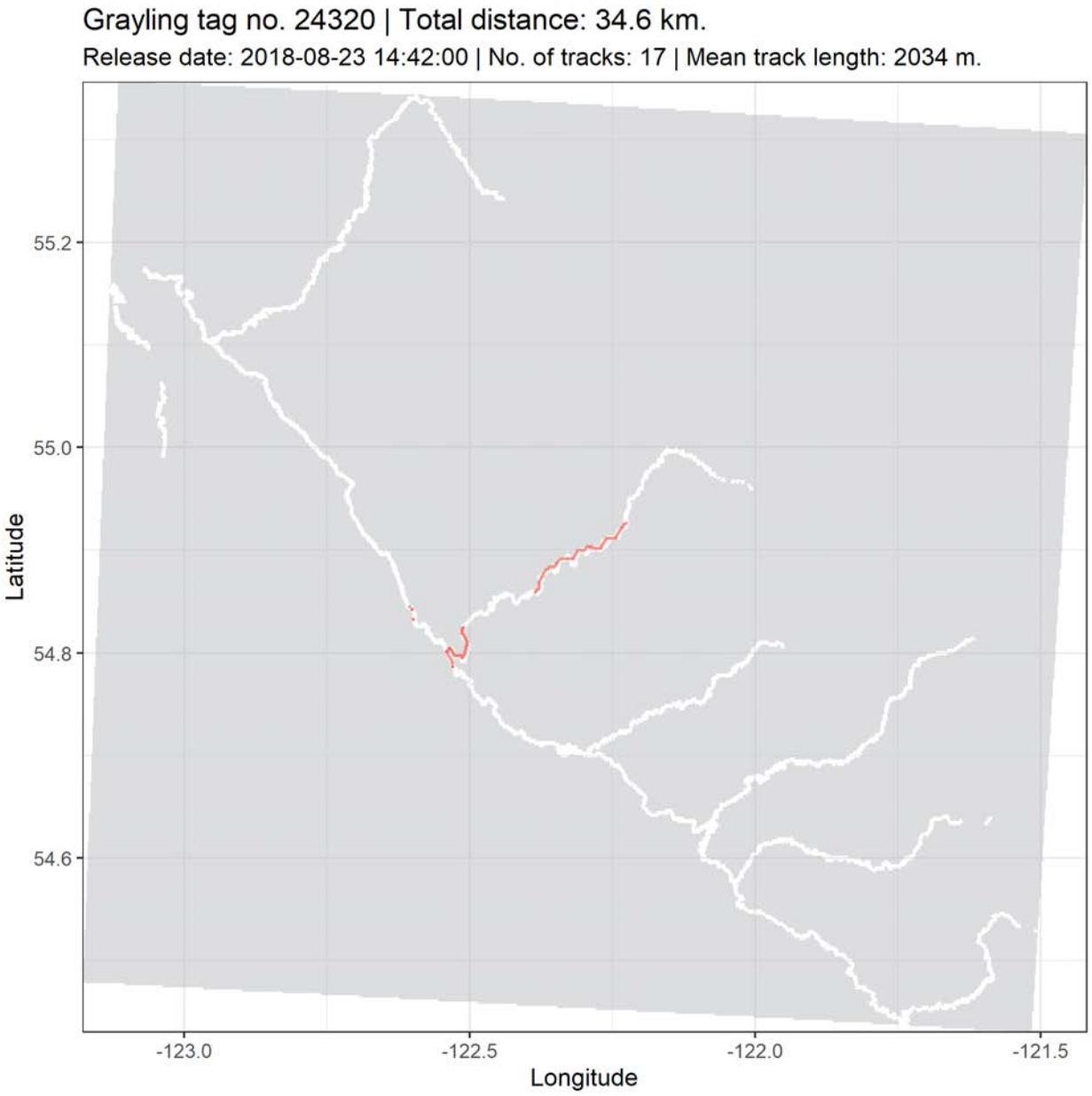
Grayling tag no. 24320 | Total distance: 34.6 km.
Release date: 2018-08-23 14:42:00 | No. of tracks: 17 | Mean track length: 2034 m.
55.2
55.0
54.8
54.6
Latitude
-123.0
-122.5
-122.0
-121.5
Longitude

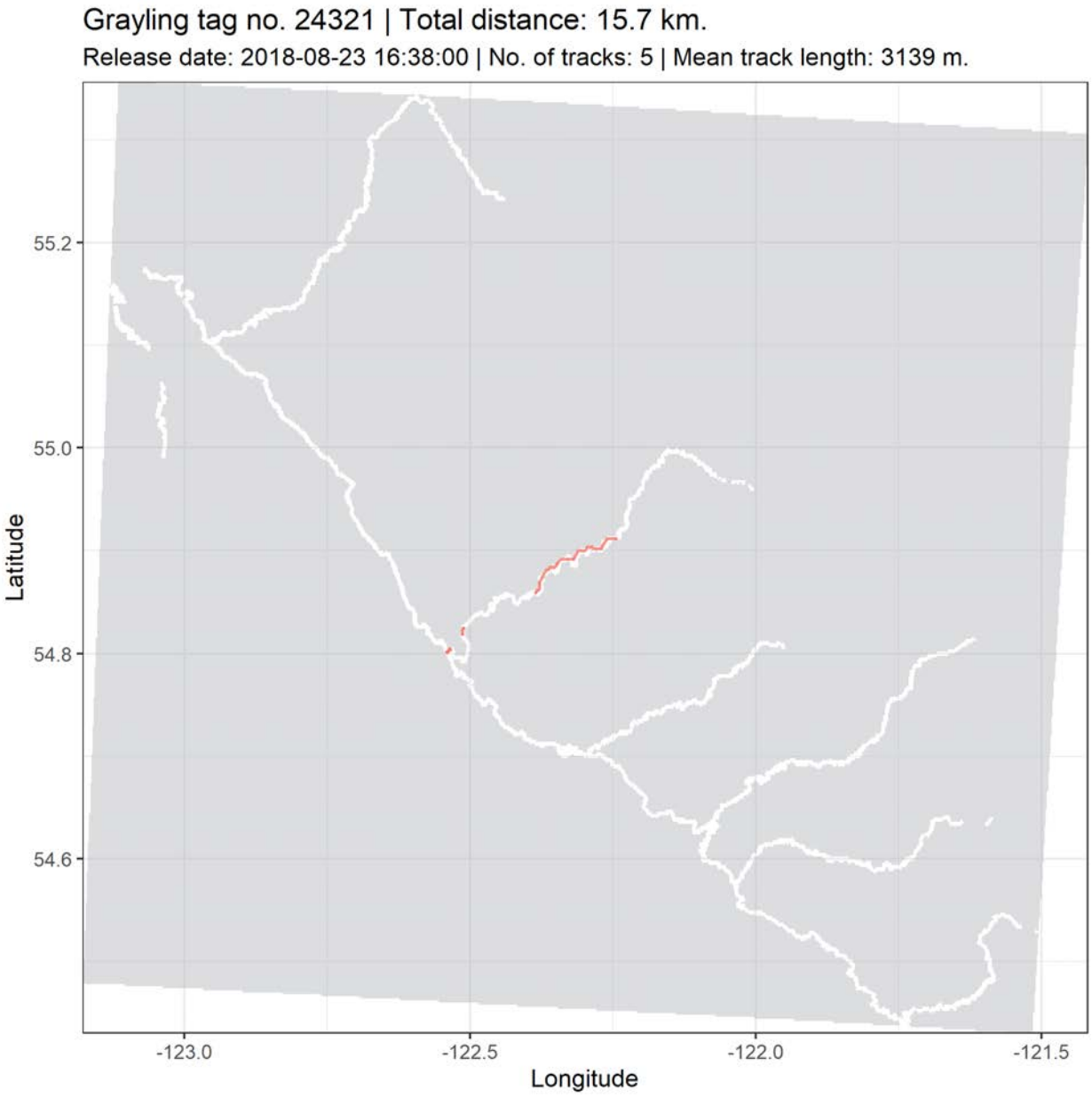
Grayling tag no. 24321 | Total distance: 15.7 km.
Release date: 2018-08-23 16:38:00 | No. of tracks: 5 | Mean track length: 3139 m.
55.2
55.0
54.8
54.6
Latitude
-123.0
-122.5
-122.0
-121.5
Longitude

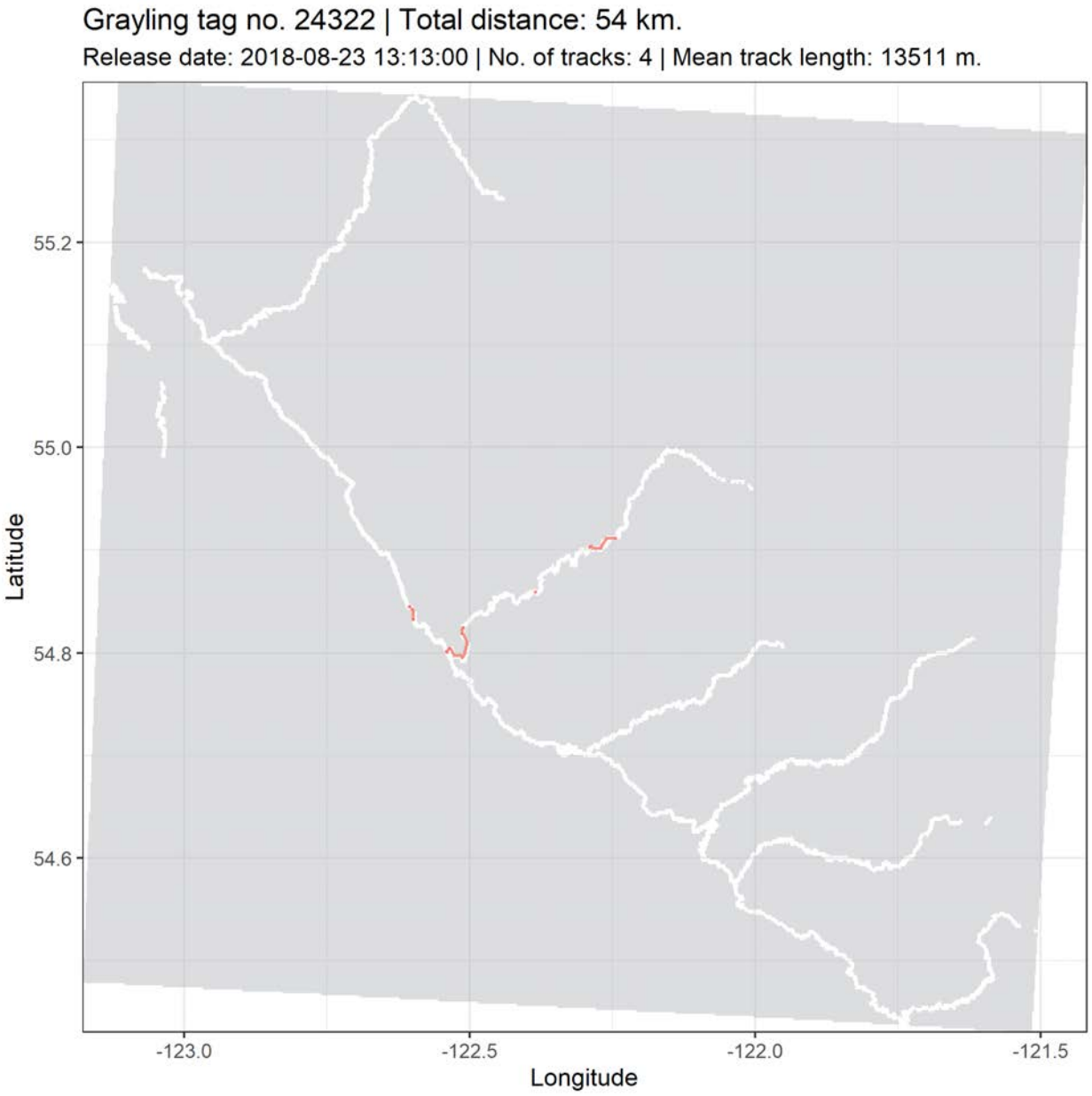
Grayling tag no. 24322 | Total distance: 54 km.
Release date: 2018-08-23 13:13:00 | No. of tracks: 4 | Mean track length: 13511 m.
55.2
55.0
54.8
54.6
Latitude
-123.0
-122.5
-122.0
-121.5
Longitude

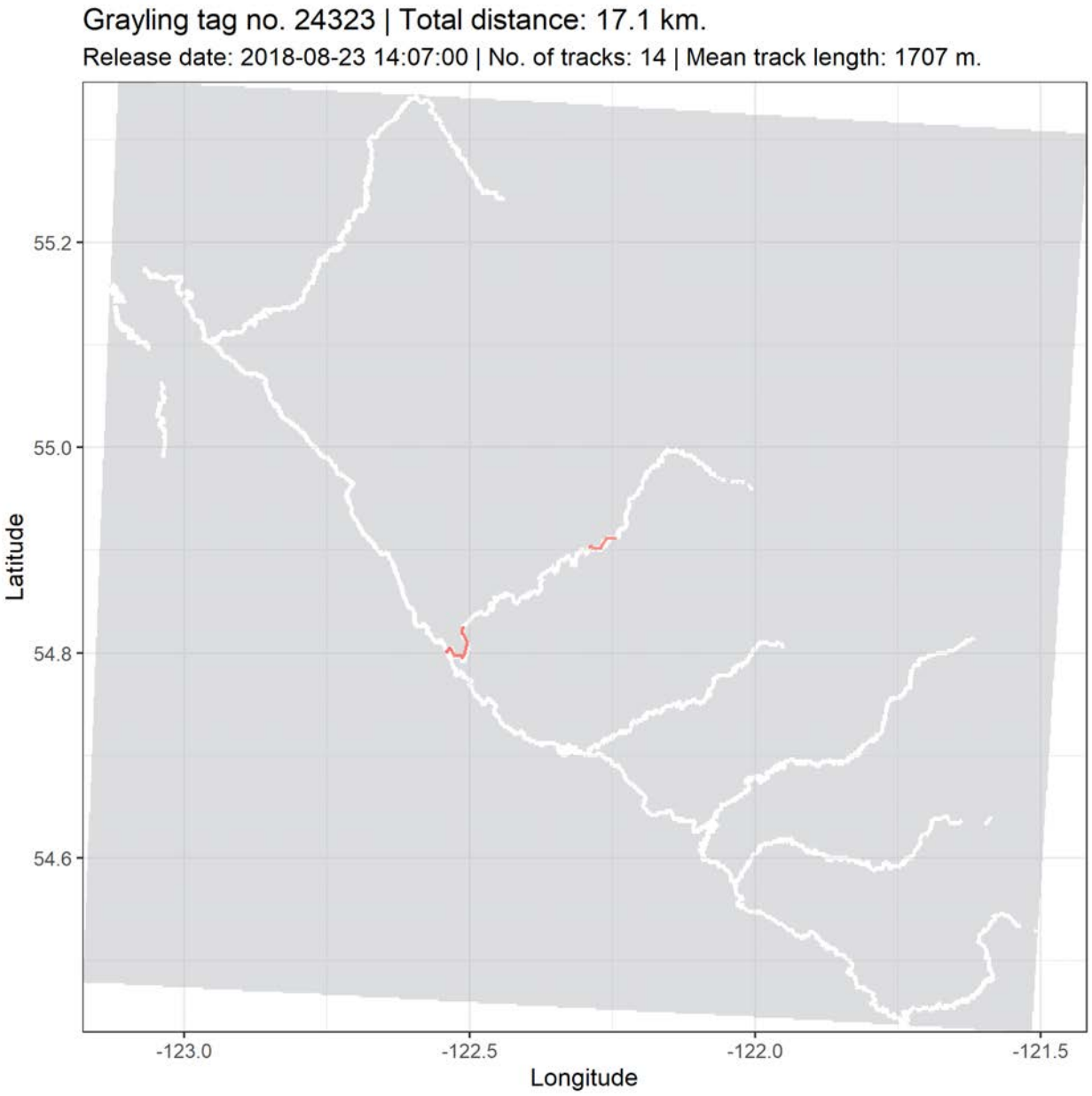
Grayling tag no. 24323 | Total distance: 17.1 km.
Release date: 2018-08-23 14:07:00 | No. of tracks: 14 | Mean track length: 1707 m.
55.2
55.0
54.8
54.6
Latitude
-123.0
-122.5
-122.0
-121.5
Longitude

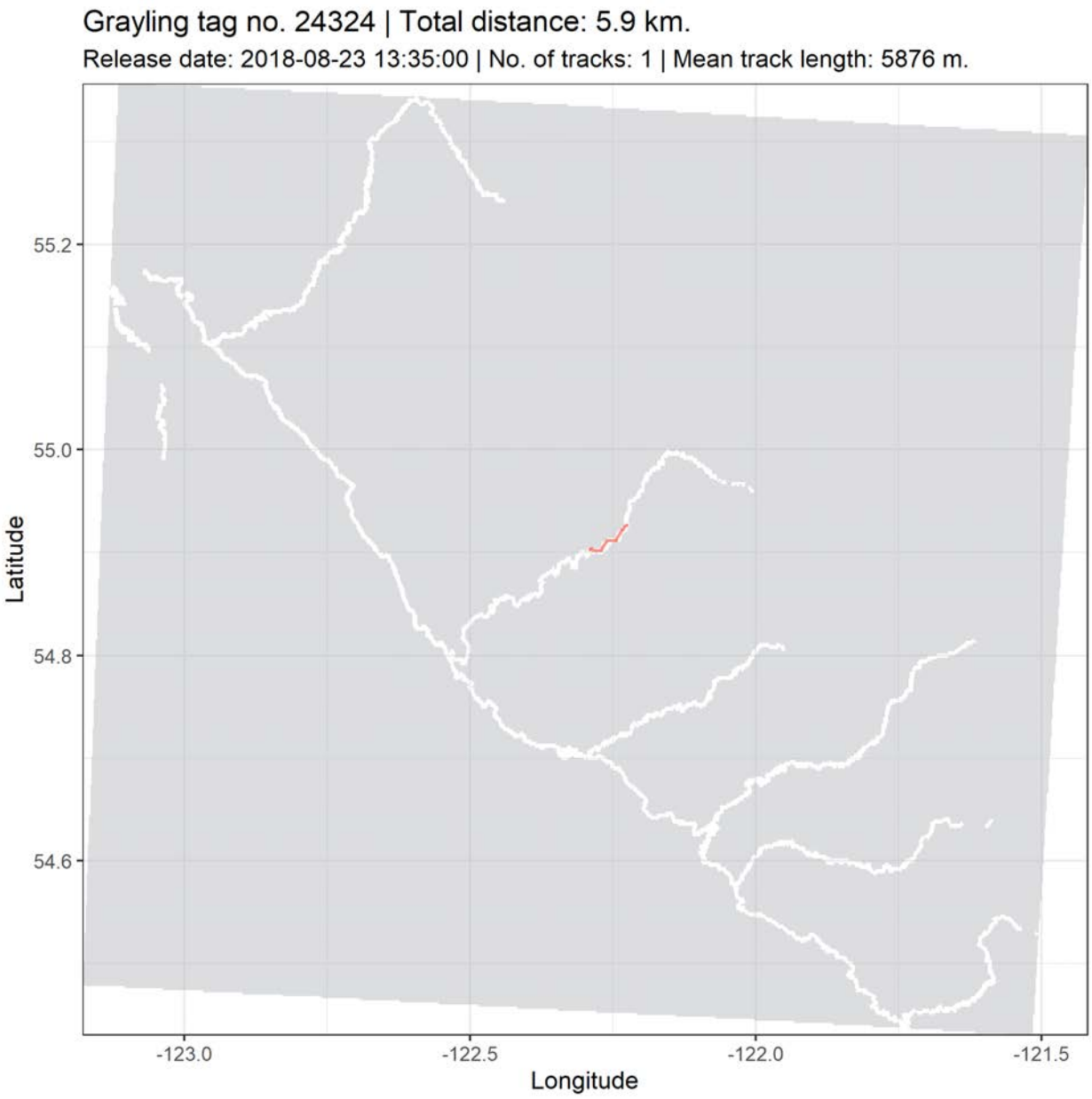
Grayling tag no. 24324 | Total distance: 5.9 km.
Release date: 2018-08-23 13:35:00 | No. of tracks: 1 | Mean track length: 5876 m.
55.2
55.0
54.8
54.6
Latitude
-123.0
-122.5
-122.0
-121.5
Longitude

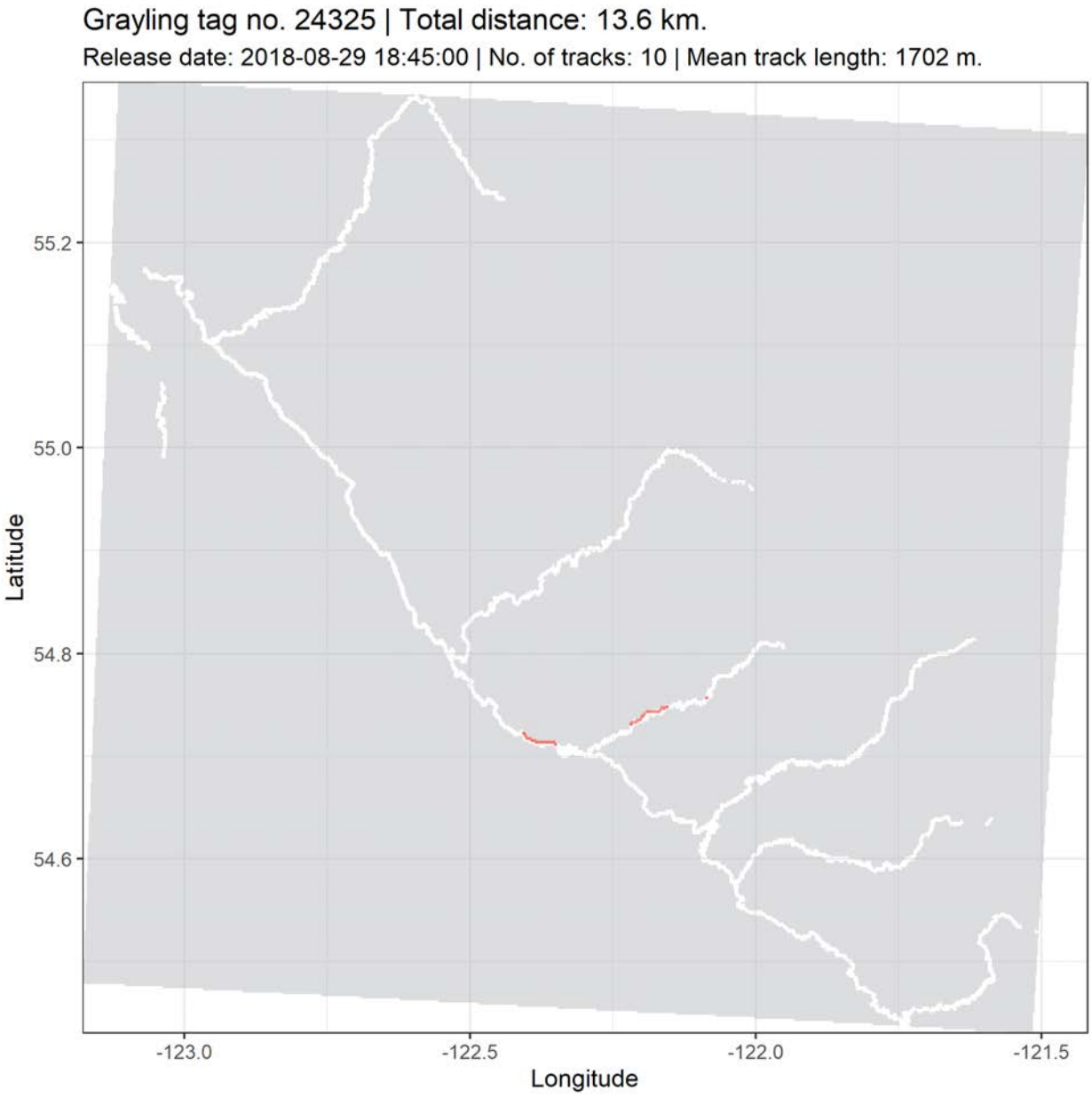
Grayling tag no. 24325 | Total distance: 13.6 km.
Release date: 2018-08-29 18:45:00 | No. of tracks: 10 | Mean track length: 1702 m.
55.2
55.0
54.8
54.6
Latitude
-123.0
-122.5
-122.0
-121.5
Longitude

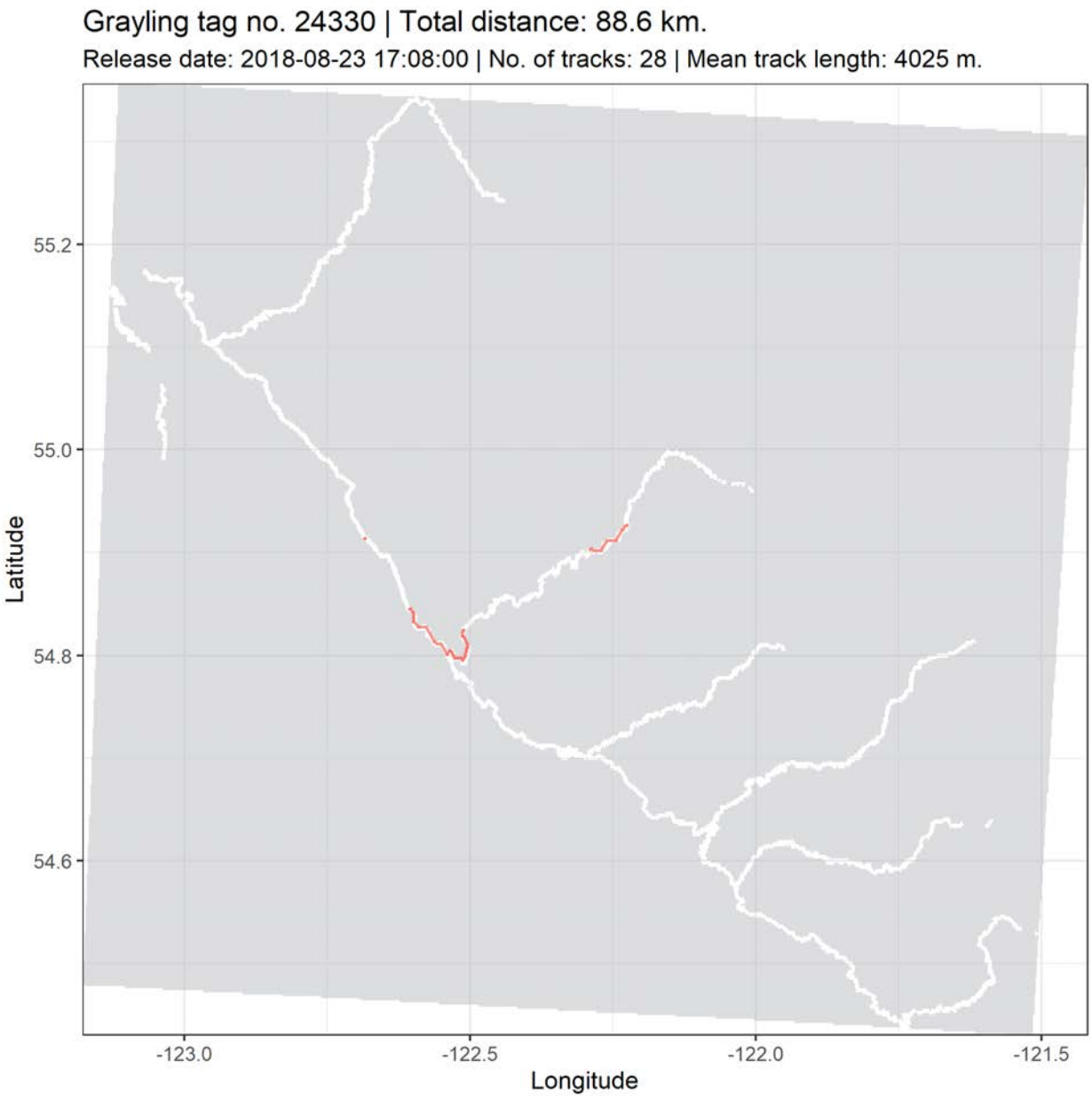
Grayling tag no. 24330 | Total distance: 88.6 km.
Release date: 2018-08-23 17:08:00 | No. of tracks: 28 | Mean track length: 4025 m.
55.2
55.0
54.8
54.6
Latitude
-123.0
-122.5
-122.0
-121.5
Longitude

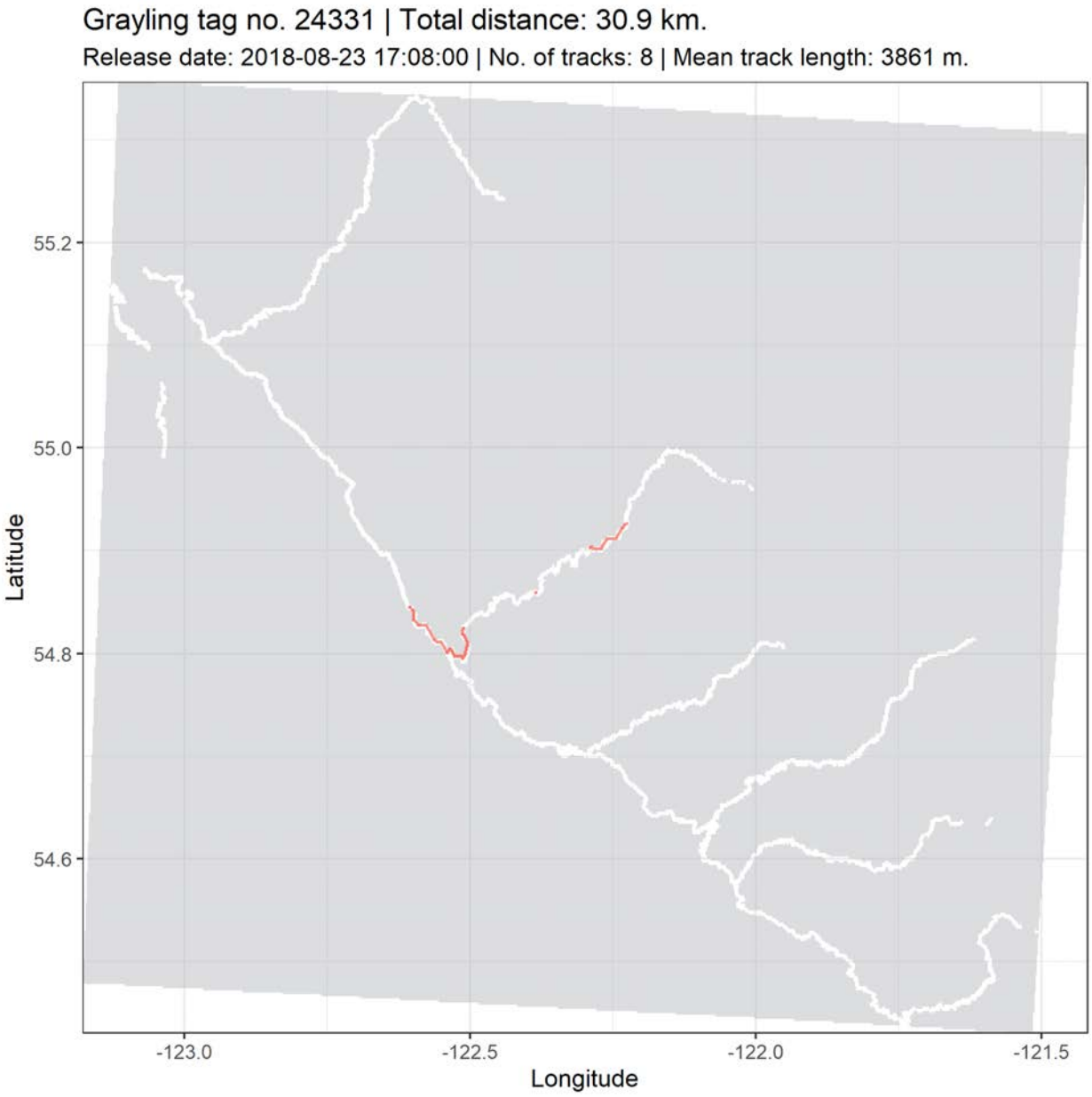
Grayling tag no. 24331 | Total distance: 30.9 km.
Release date: 2018-08-23 17:08:00 | No. of tracks: 8 | Mean track length: 3861 m.
55.2
55.0
54.8
54.6
Latitude
-123.0
-122.5
-122.0
-121.5
Longitude

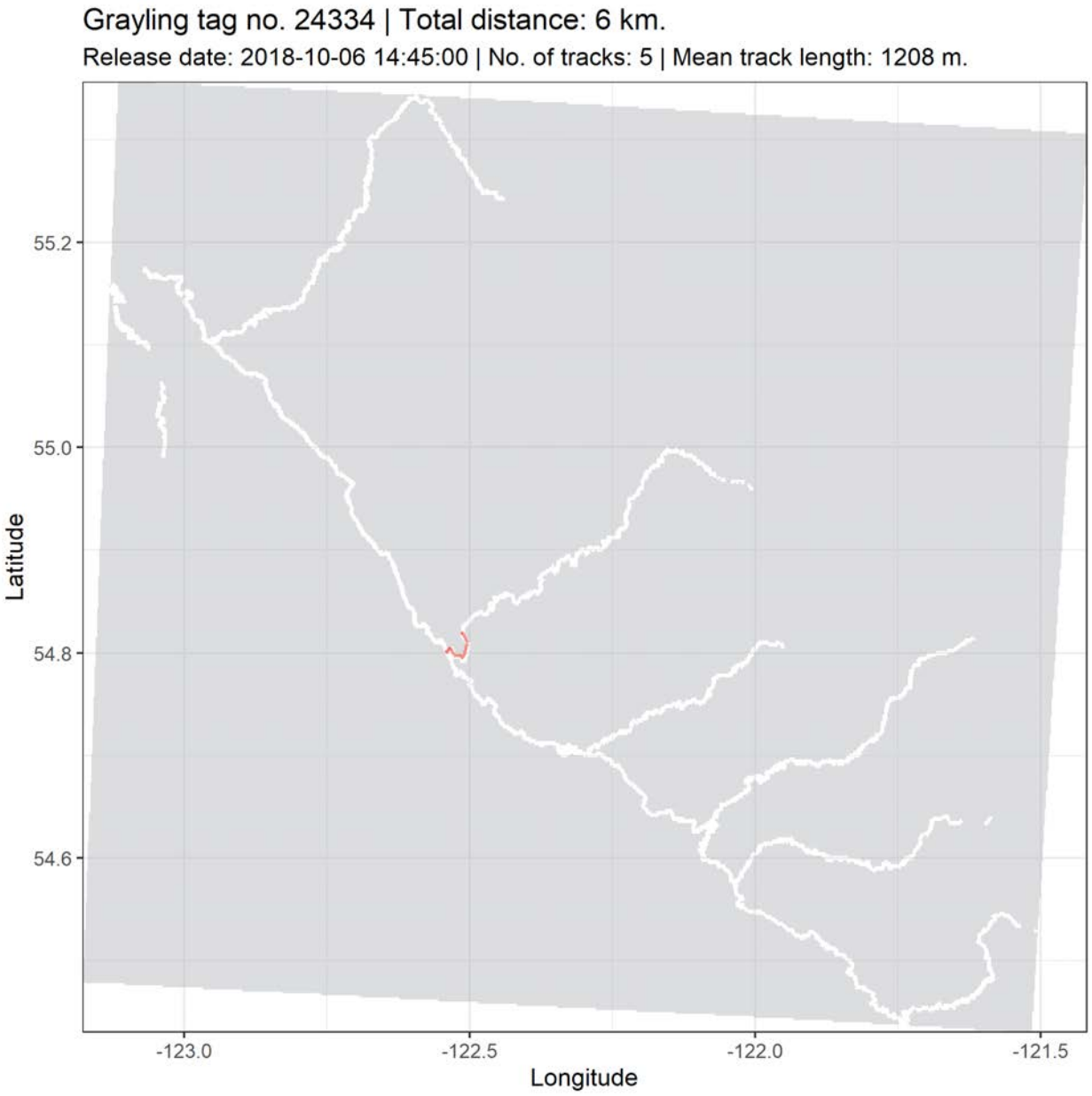
Grayling tag no. 24334 | Total distance: 6 km.
Release date: 2018-10-06 14:45:00 | No. of tracks: 5 | Mean track length: 1208 m.
55.2
55.0
54.8
54.6
Latitude
-123.0
-122.5
-122.0
-121.5
Longitude

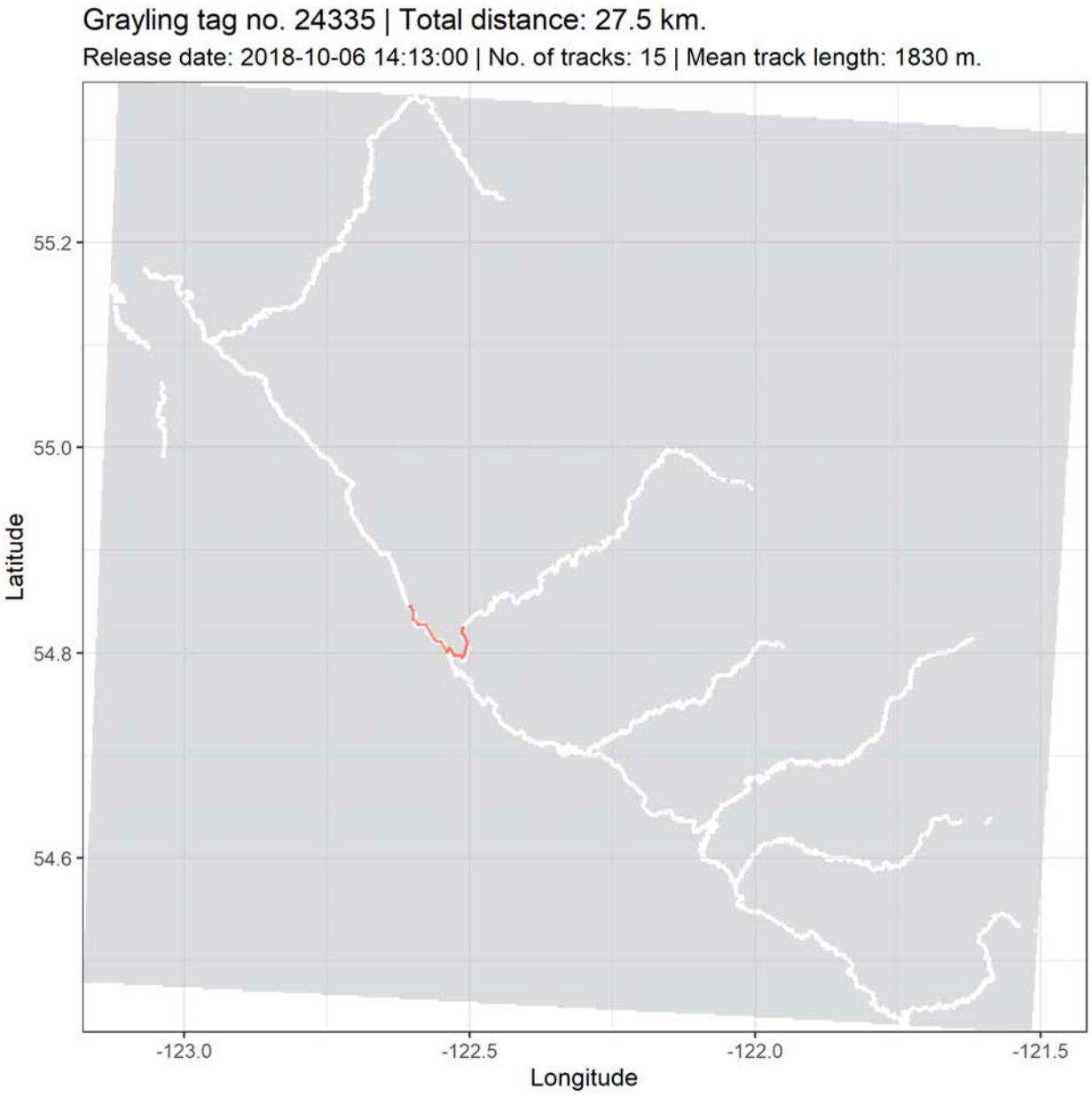
Grayling tag no. 24335 | Total distance: 27.5 km.
Release date: 2018-10-06 14:13:00 | No. of tracks: 15 | Mean track length: 1830 m.
55.2
55.0
54.8
54.6
Latitude
-123.0
-122.5
-122.0
-121.5
Longitude

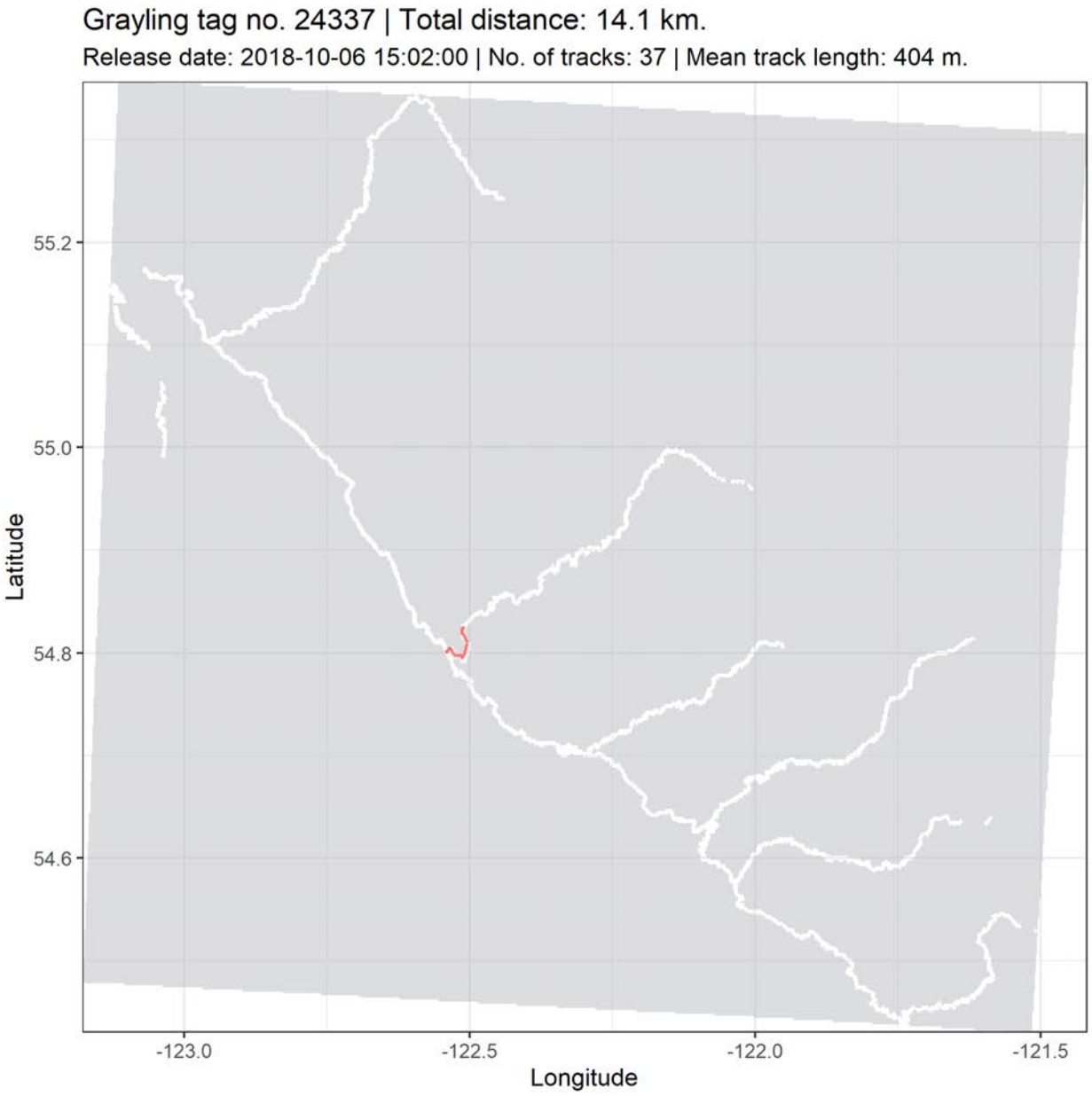
Grayling tag no. 24337 | Total distance: 14.1 km.
Release date: 2018-10-06 15:02:00 | No. of tracks: 37 | Mean track length: 404 m.
55.2
55.0
54.8
54.6
Latitude
-123.0
-122.5
-122.0
-121.5
Longitude

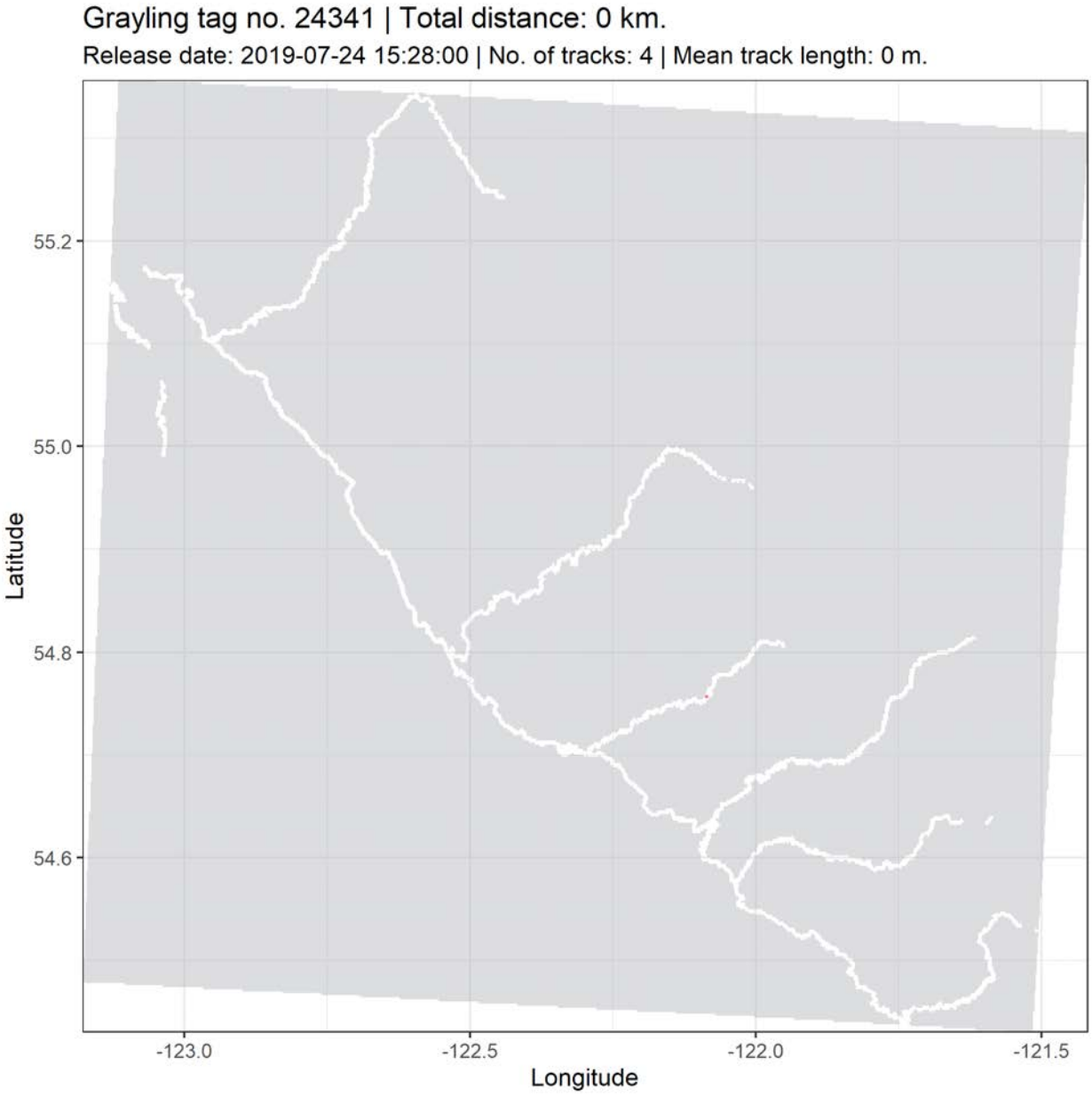
Grayling tag no. 24341 | Total distance: 0 km.
Release date: 2019-07-24 15:28:00 | No. of tracks: 4 | Mean track length: 0 m.
55.2
55.0
54.8
54.6
Latitude
-123.0
-122.5
-122.0
-121.5
Longitude

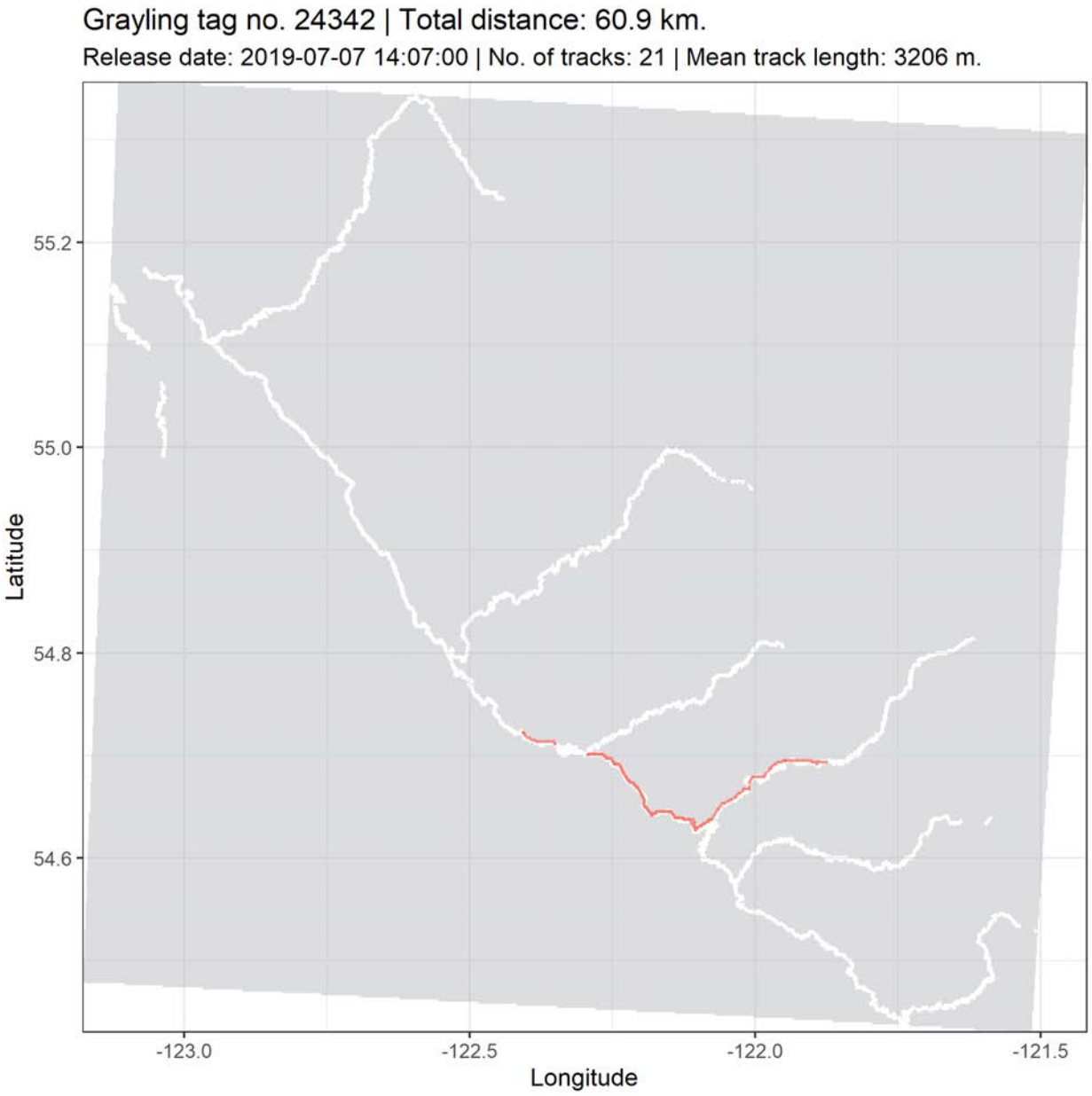
Grayling tag no. 24342 | Total distance: 60.9 km.
Release date: 2019-07-07 14:07:00 | No. of tracks: 21 | Mean track length: 3206 m.
55.2
55.0
54.8
54.6
Latitude
-123.0
-122.5
-122.0
-121.5
Longitude

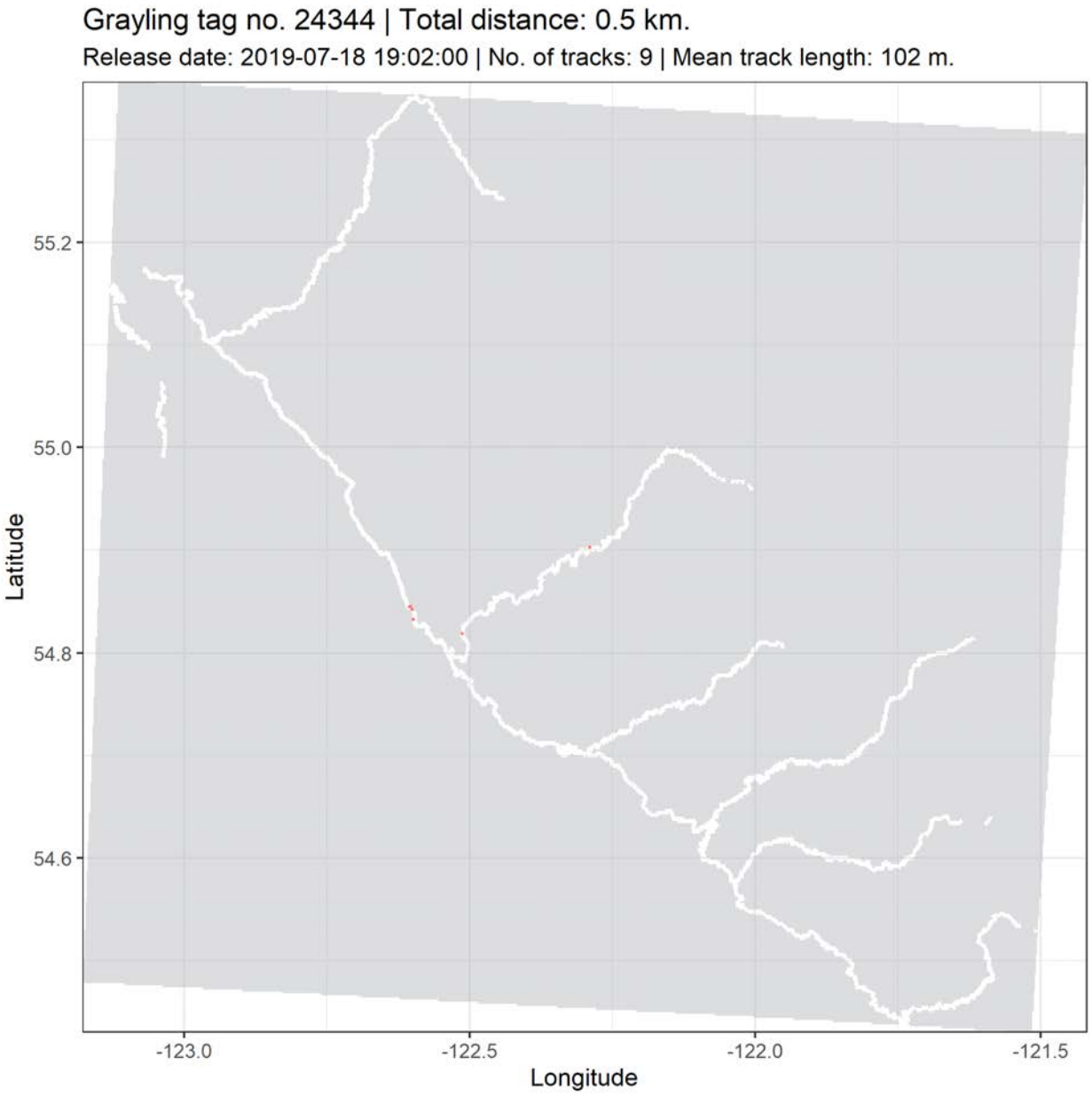
Grayling tag no. 24344 | Total distance: 0.5 km.
Release date: 2019-07-18 19:02:00 | No. of tracks: 9 | Mean track length: 102 m.
55.2
55.0
54.8
54.6
Latitude
-123.0
-122.5
-122.0
-121.5
Longitude

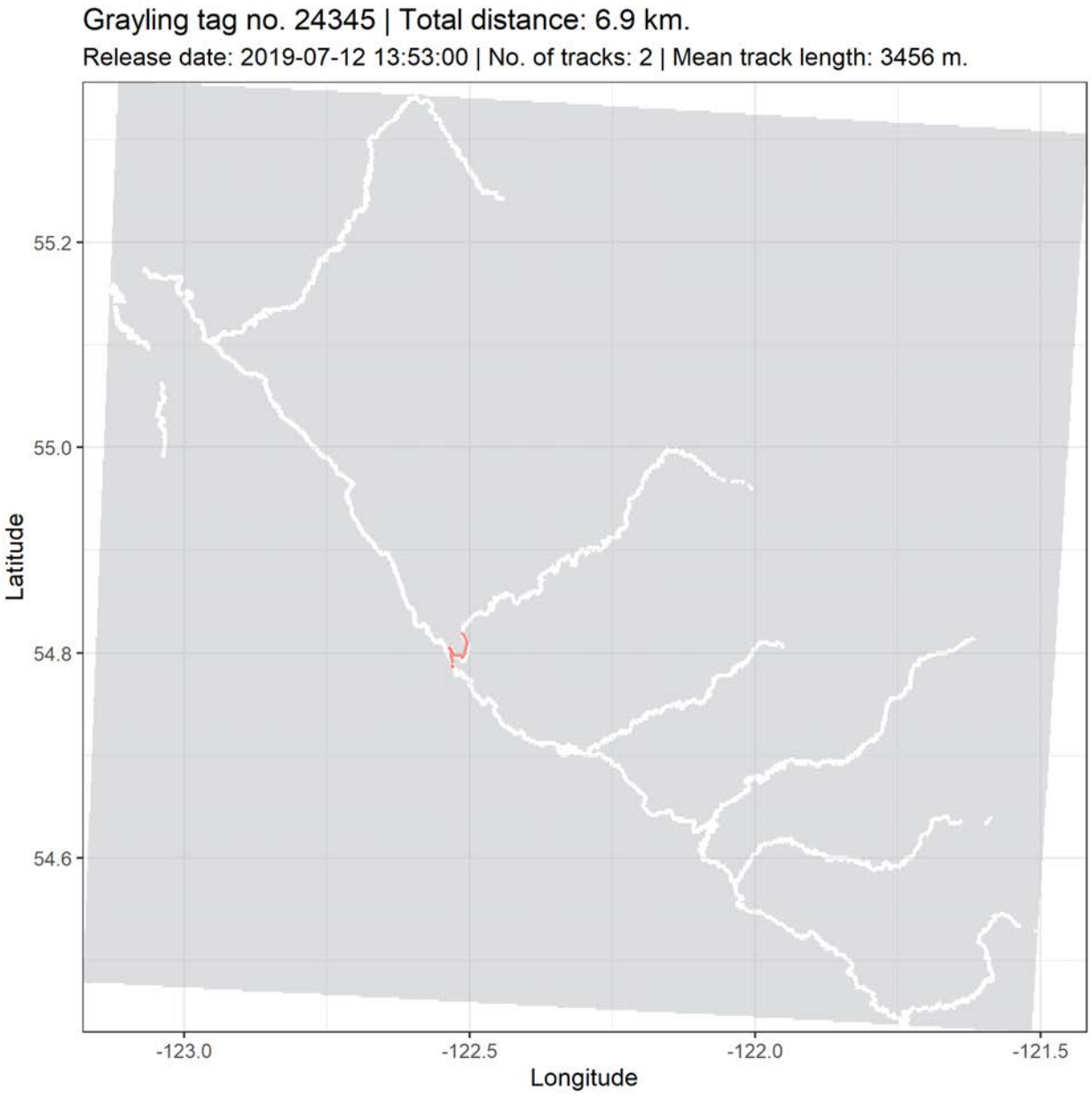
Grayling tag no. 24345 | Total distance: 6.9 km.
Release date: 2019-07-12 13:53:00 | No. of tracks: 2 | Mean track length: 3456 m.
55.2
55.0
54.8
54.6
Latitude
-123.0
-122.5
-122.0
-121.5
Longitude

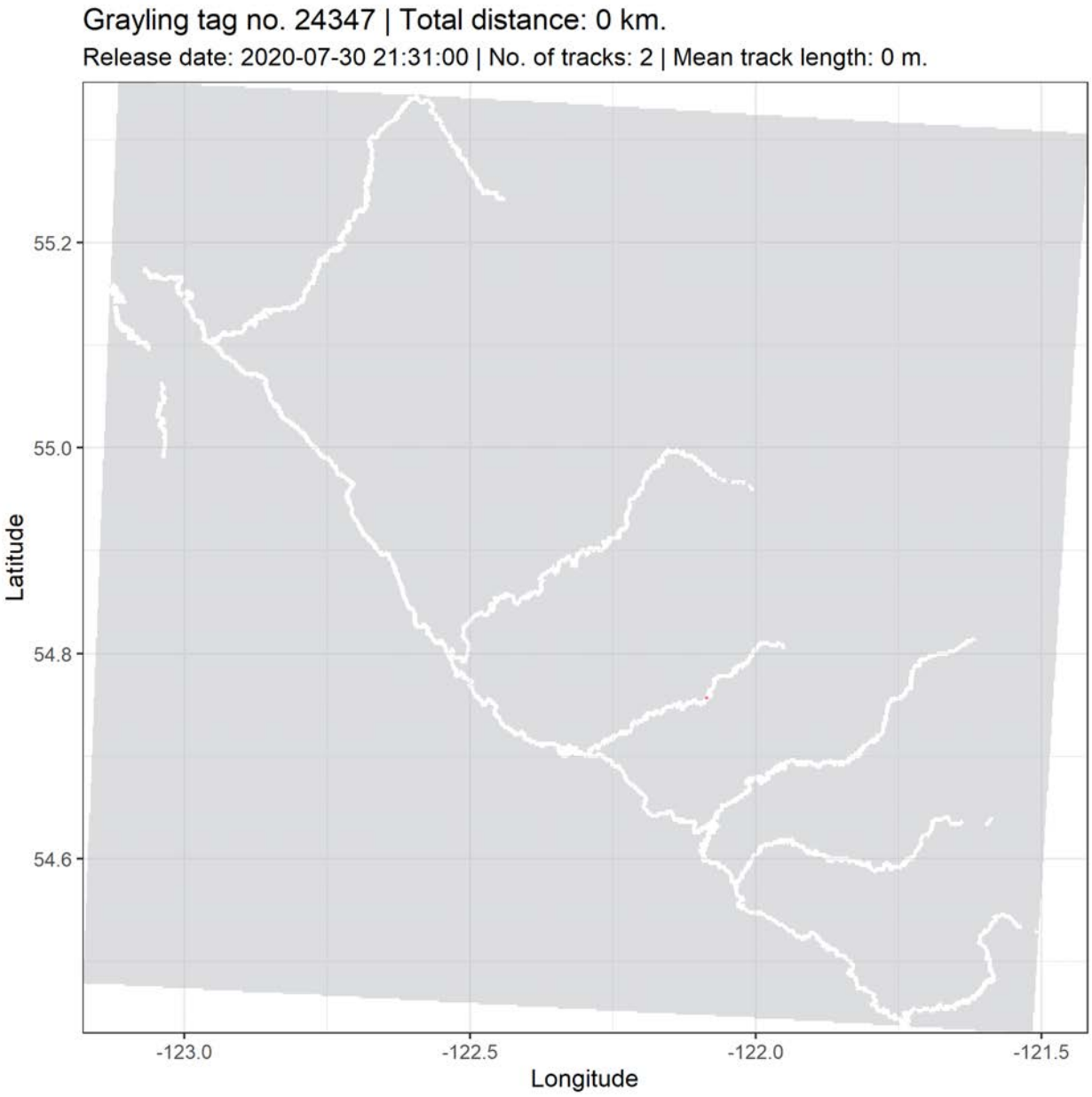
Grayling tag no. 24347 | Total distance: 0 km.
Release date: 2020-07-30 21:31:00 | No. of tracks: 2 | Mean track length: 0 m.
55.2
55.0
54.8
54.6
Latitude
-123.0
-122.5
-122.0
-121.5
Longitude

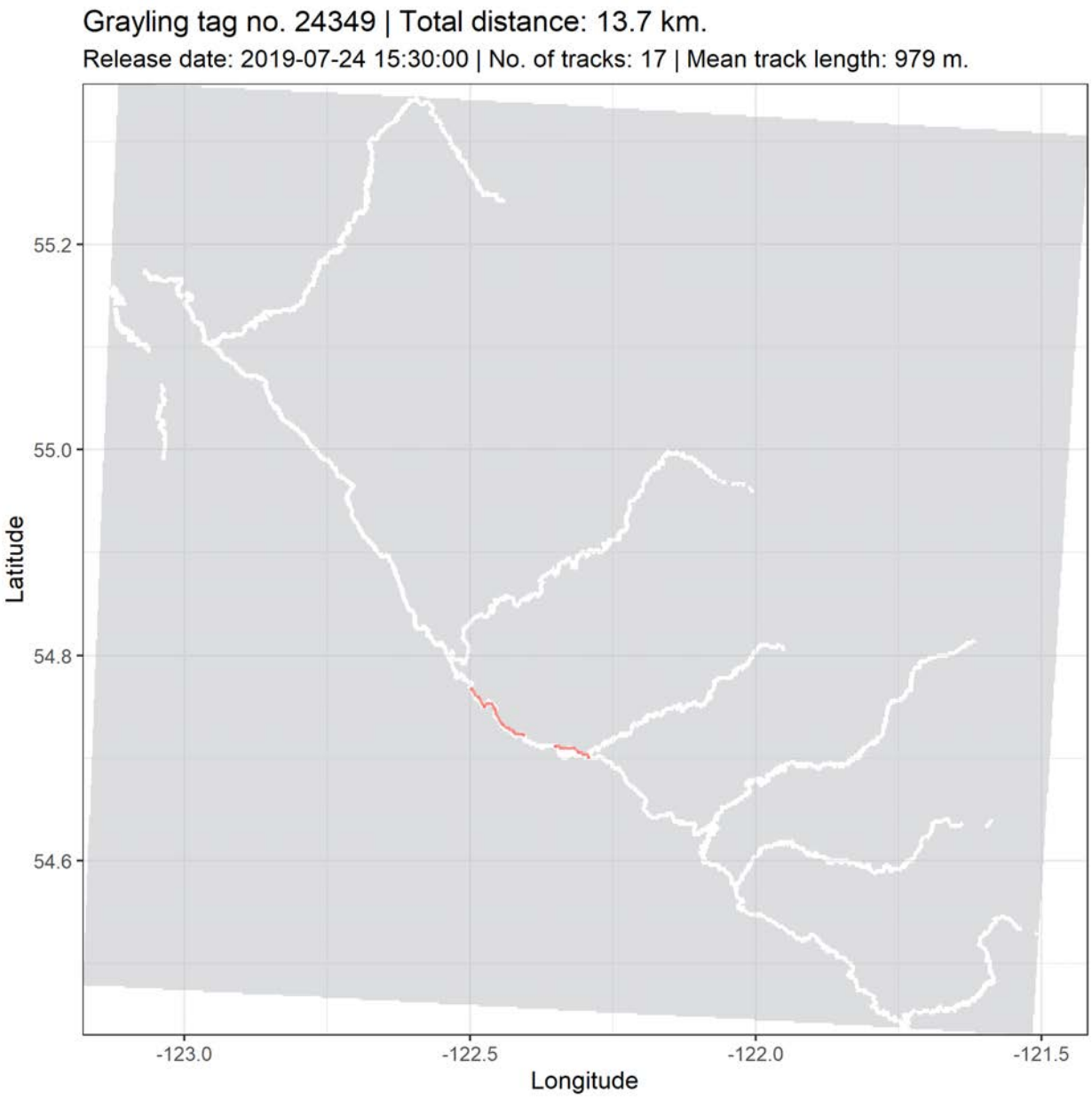
Grayling tag no. 24349 | Total distance: 13.7 km.
Release date: 2019-07-24 15:30:00 | No. of tracks: 17 | Mean track length: 979 m.
55.2
55.0
54.8
54.6
Latitude
-123.0
-122.5
-122.0
-121.5
Longitude

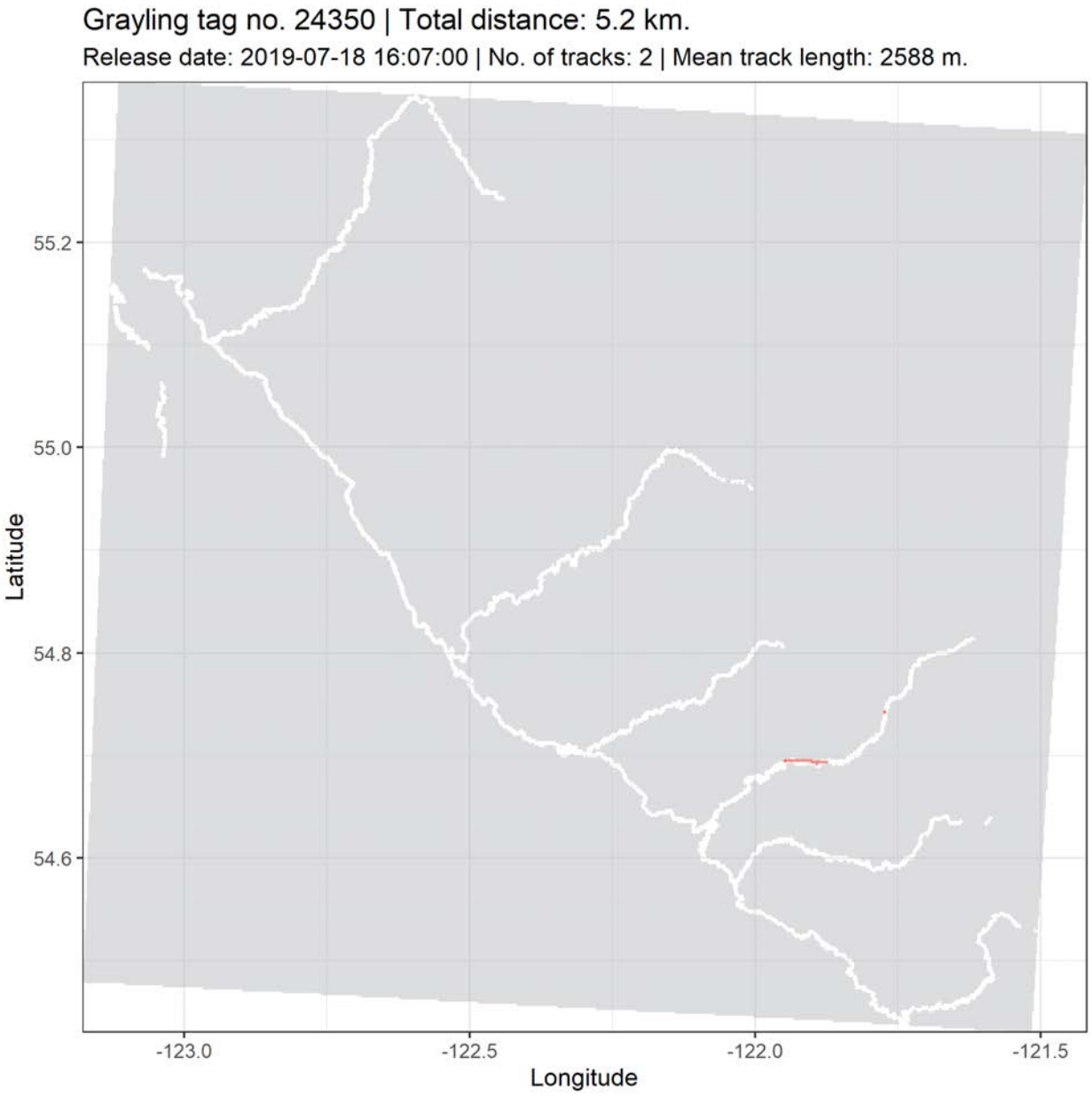
Grayling tag no. 24350 | Total distance: 5.2 km.
Release date: 2019-07-18 16:07:00 | No. of tracks: 2 | Mean track length: 2588 m.
55.2
55.0
54.8
54.6
Latitude
-123.0
-122.5
-122.0
-121.5
Longitude

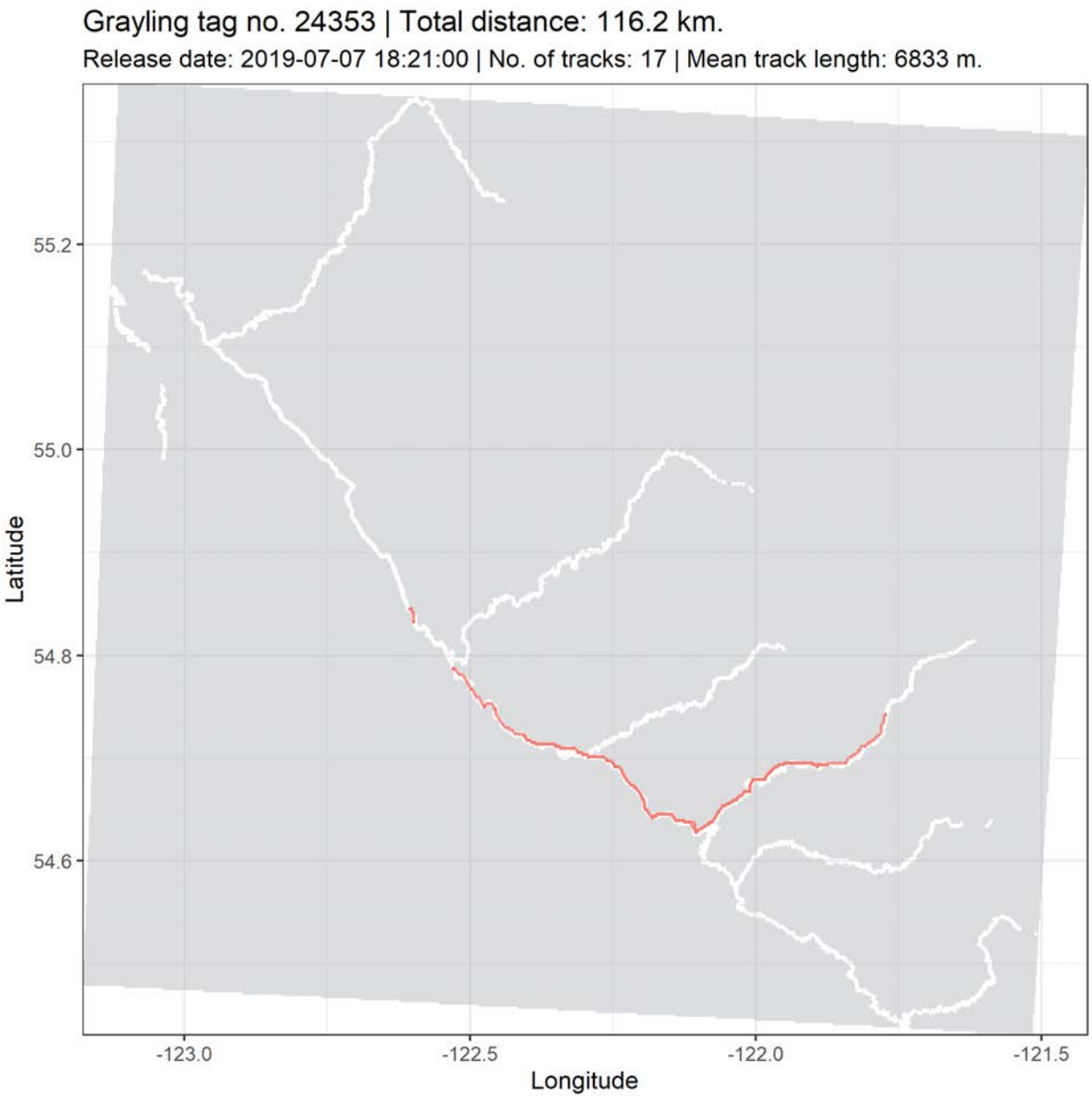
Grayling tag no. 24353 | Total distance: 116.2 km.
Release date: 2019-07-07 18:21:00 | No. of tracks: 17 | Mean track length: 6833 m.
55.2
55.0
54.8
54.6
Latitude
-123.0
-122.5
-122.0
-121.5
Longitude

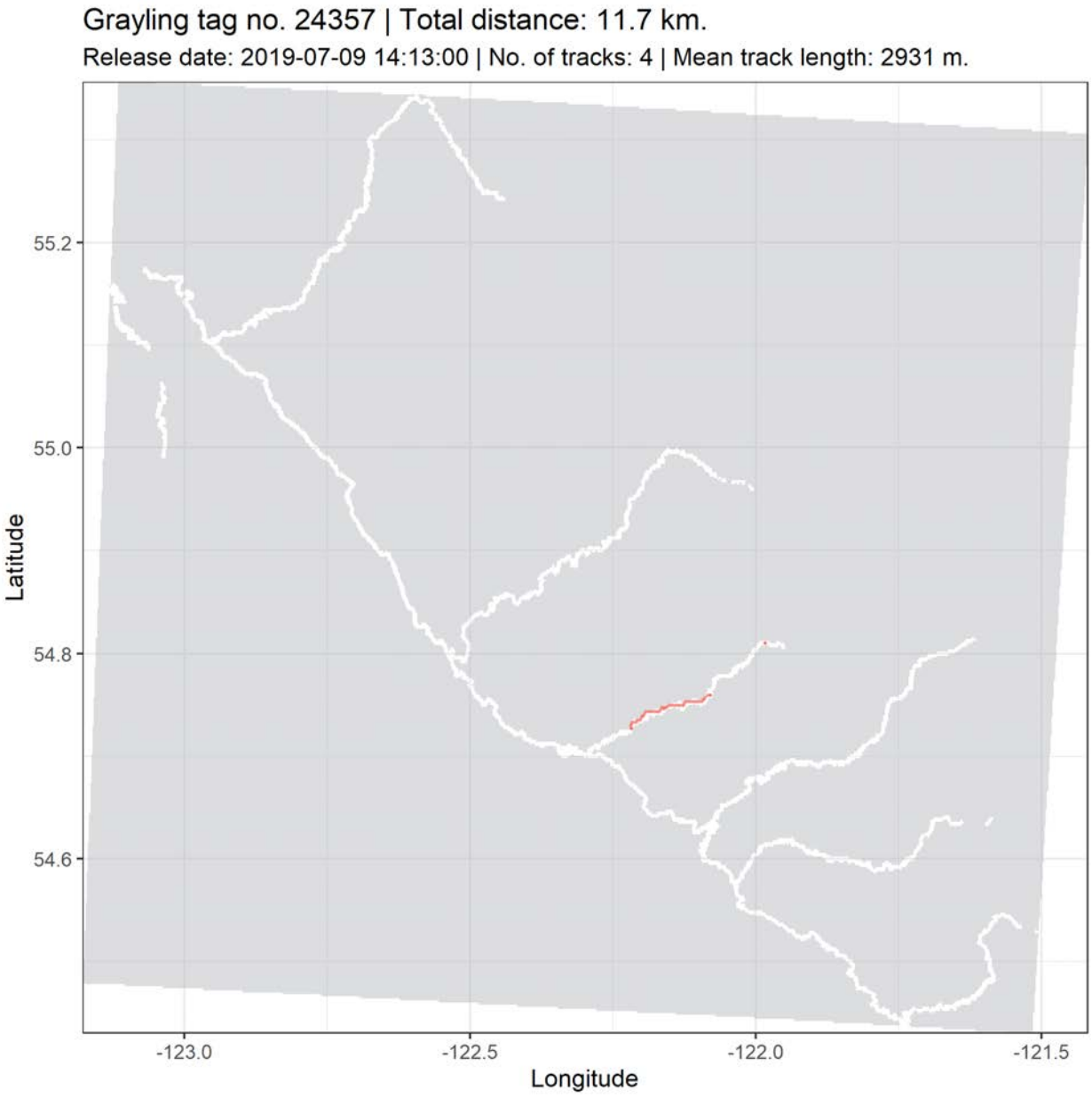
Grayling tag no. 24357 | Total distance: 11.7 km.
Release date: 2019-07-09 14:13:00 | No. of tracks: 4 | Mean track length: 2931 m.
55.2
55.0
54.8
54.6
Latitude
-123.0
-122.5
-122.0
-121.5
Longitude

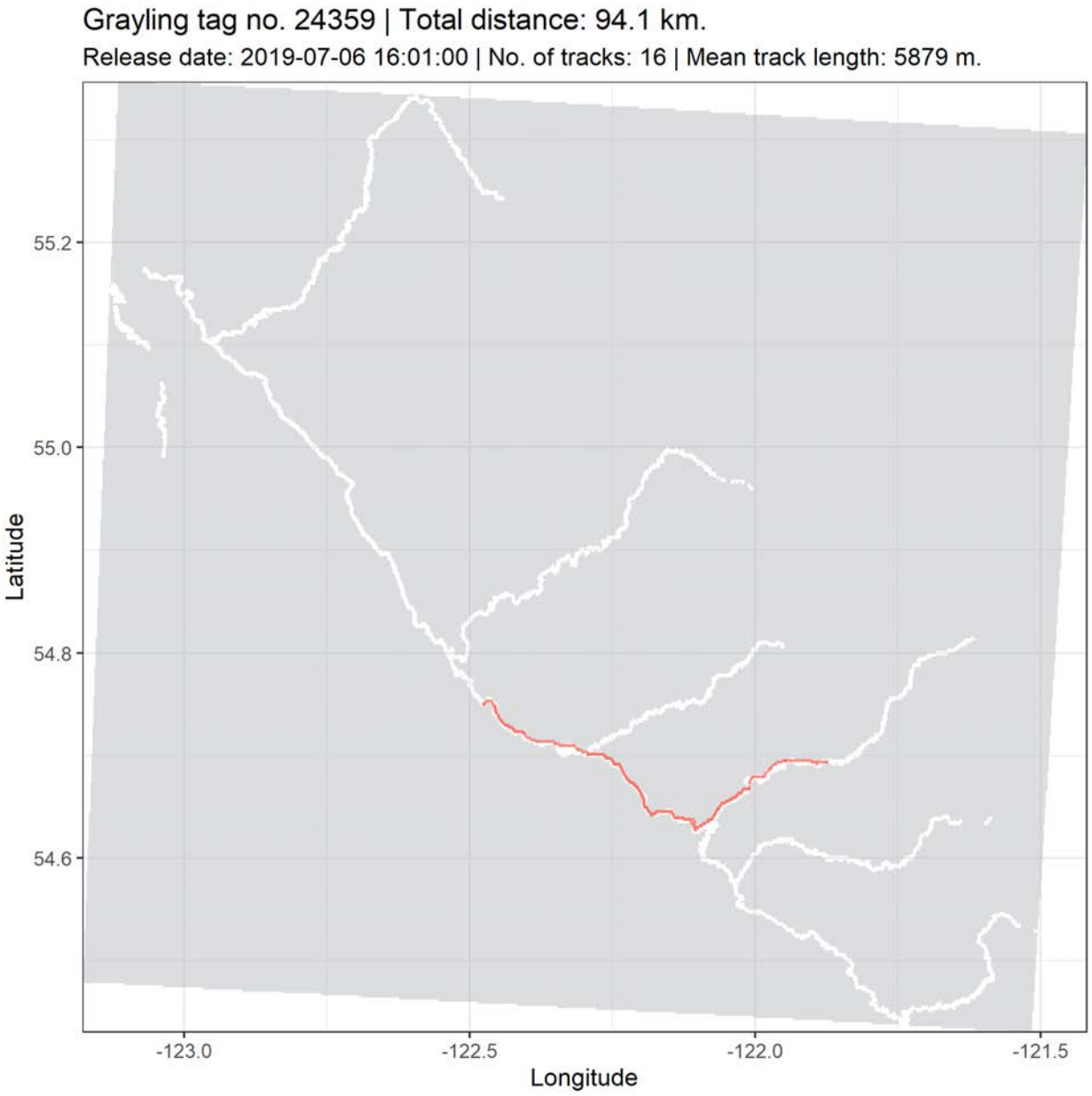
Grayling tag no. 24359 | Total distance: 94.1 km.
Release date: 2019-07-06 16:01:00 | No. of tracks: 16 | Mean track length: 5879 m.
55.2
55.0
54.8
54.6
Latitude
-123.0
-122.5
-122.0
-121.5
Longitude

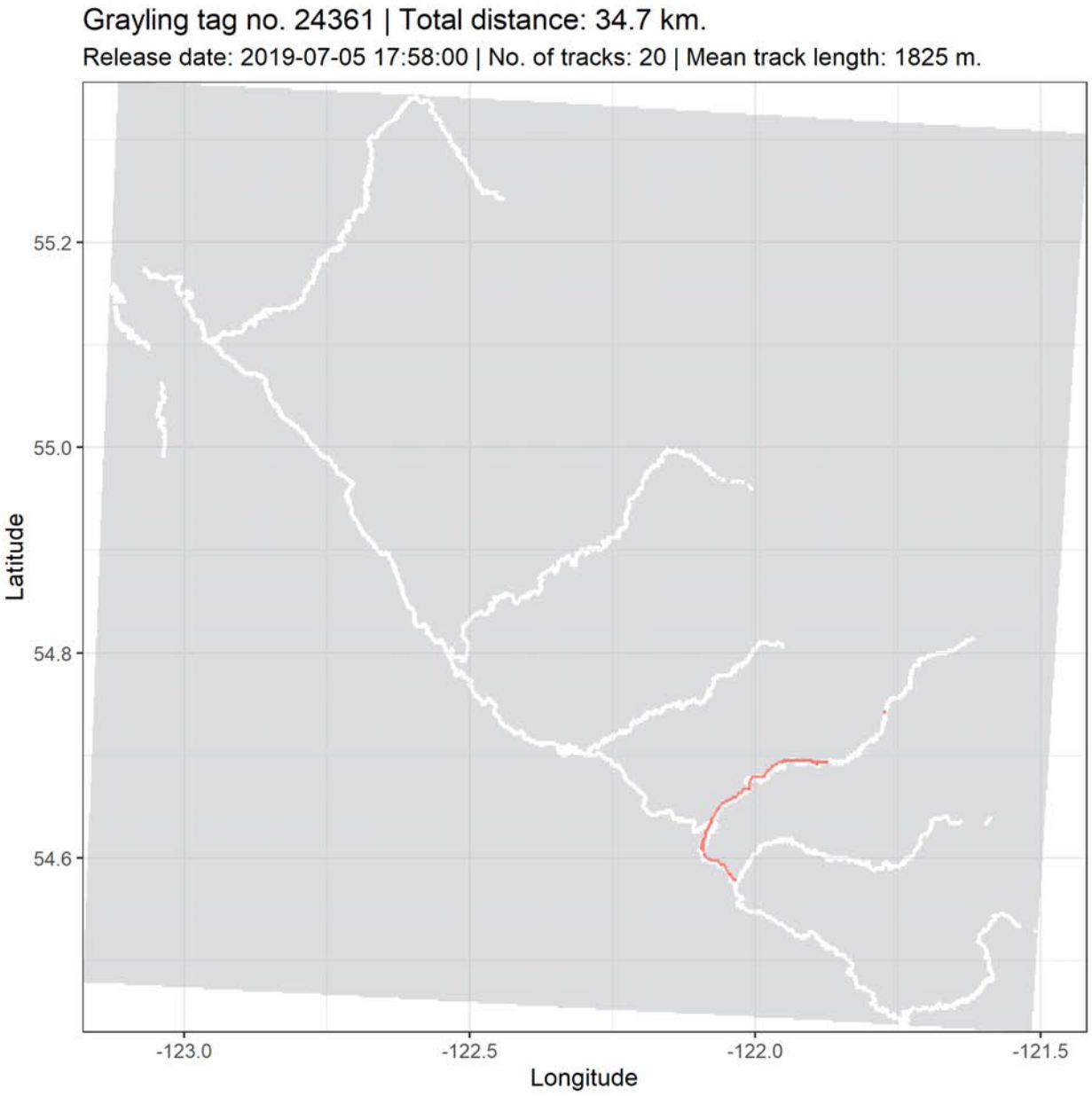
Grayling tag no. 24361 | Total distance: 34.7 km.
Release date: 2019-07-05 17:58:00 | No. of tracks: 20 | Mean track length: 1825 m.
55.2
55.0
54.8
54.6
Latitude
-123.0
-122.5
-122.0
-121.5
Longitude

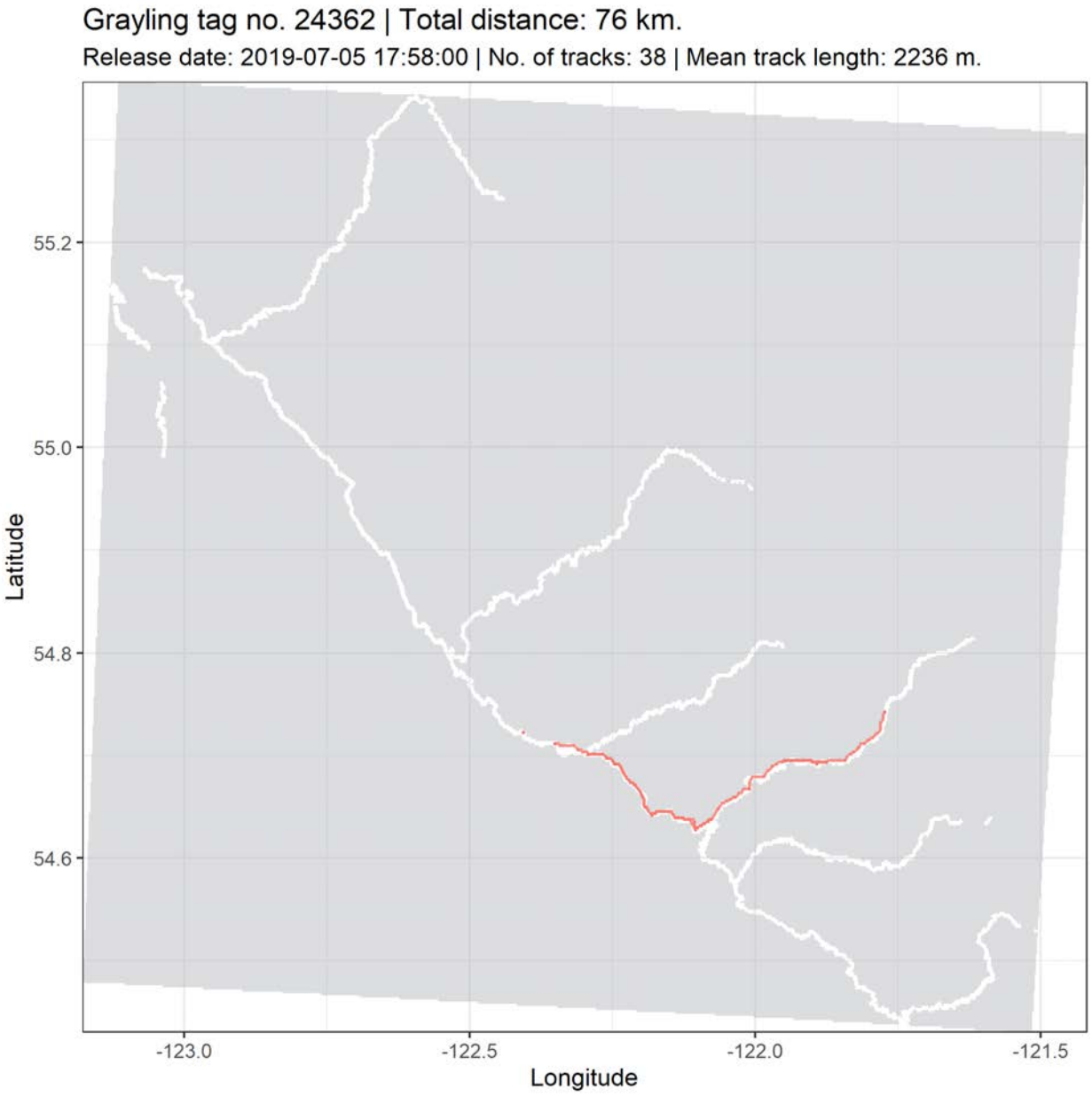
Grayling tag no. 24362 | Total distance: 76 km.
Release date: 2019-07-05 17:58:00 | No. of tracks: 38 | Mean track length: 2236 m.
55.2
55.0
54.8
54.6
Latitude
-123.0
-122.5
-122.0
-121.5
Longitude

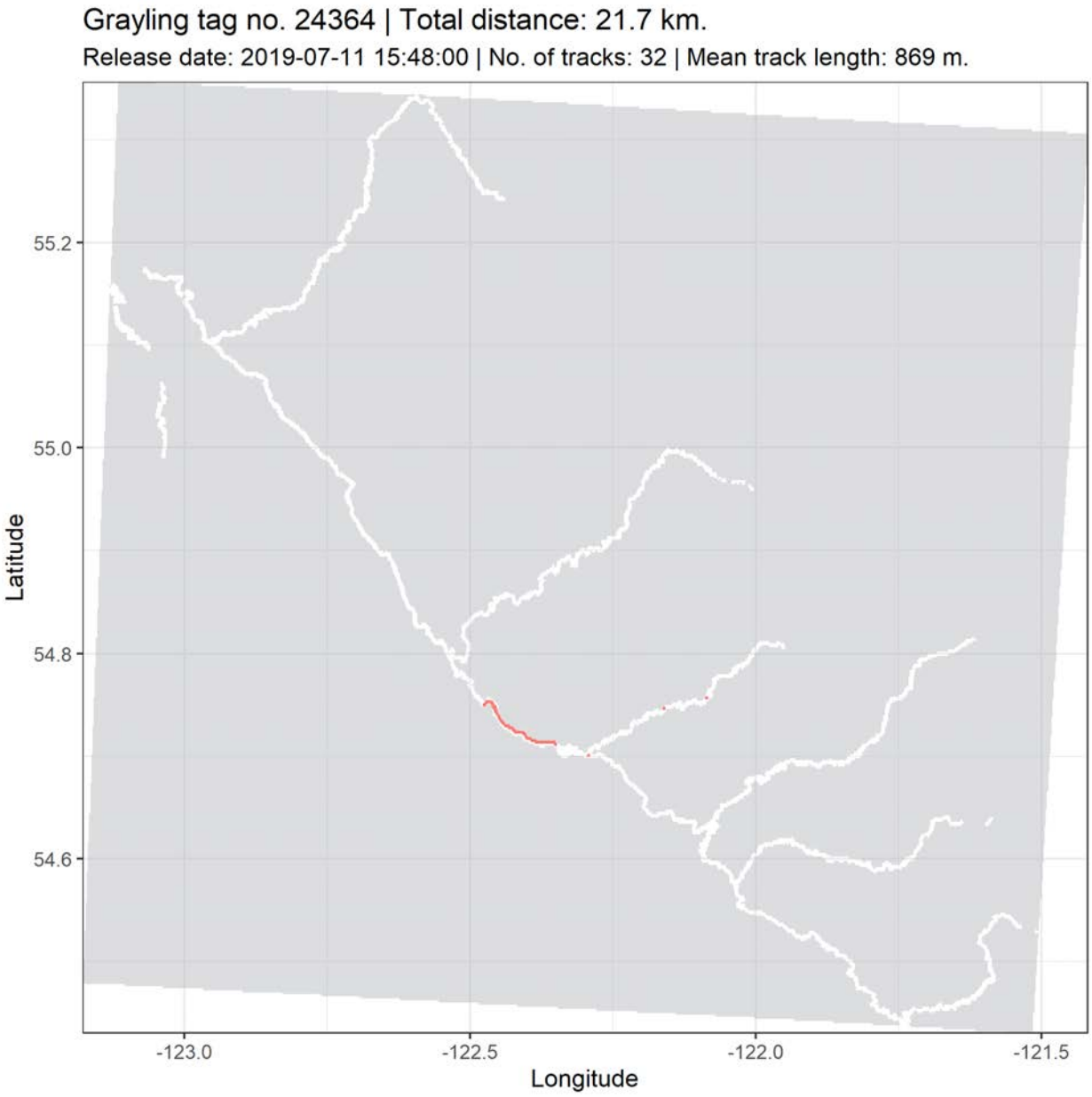
Grayling tag no. 24364 | Total distance: 21.7 km.
Release date: 2019-07-11 15:48:00 | No. of tracks: 32 | Mean track length: 869 m.
55.2
55.0
54.8
54.6
Latitude
-123.0
-122.5
-122.0
-121.5
Longitude

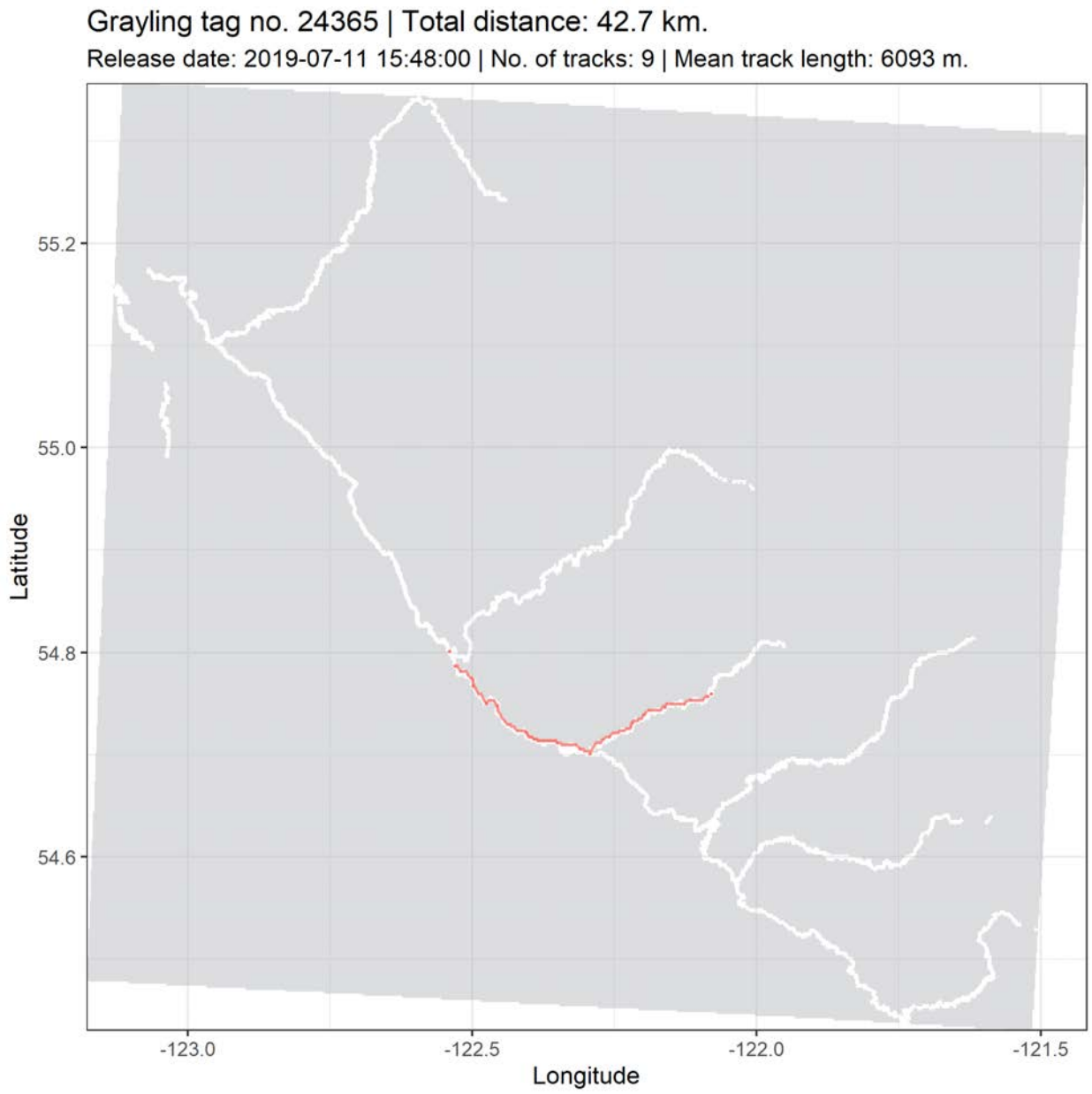
Grayling tag no. 24365 | Total distance: 42.7 km.
Release date: 2019-07-11 15:48:00 | No. of tracks: 9 | Mean track length: 6093 m.
55.2
55.0
54.8
54.6
Latitude
-123.0
-122.5
-122.0
-121.5
Longitude

.

**Appendix A.3 – Individual track histories – Bull trout**

These plots represent a visualization of the 'tracks' calculated in package *RSP* (Niella et al 2020). Each plot represents the track history of one individual since being tagged with an acoustic transmitter. Tracks represent movement events that last longer than 10 minutes but are capped at 24 hours. Plots with a large number of tracks but a small spatial extent indicate frequently overlapping of tracks. By default, this package assumes a 500 m detection range for acoustic receivers, which is being considered preliminary and will be refined in future analyses. Tags with limited movement histories have been filtered out.

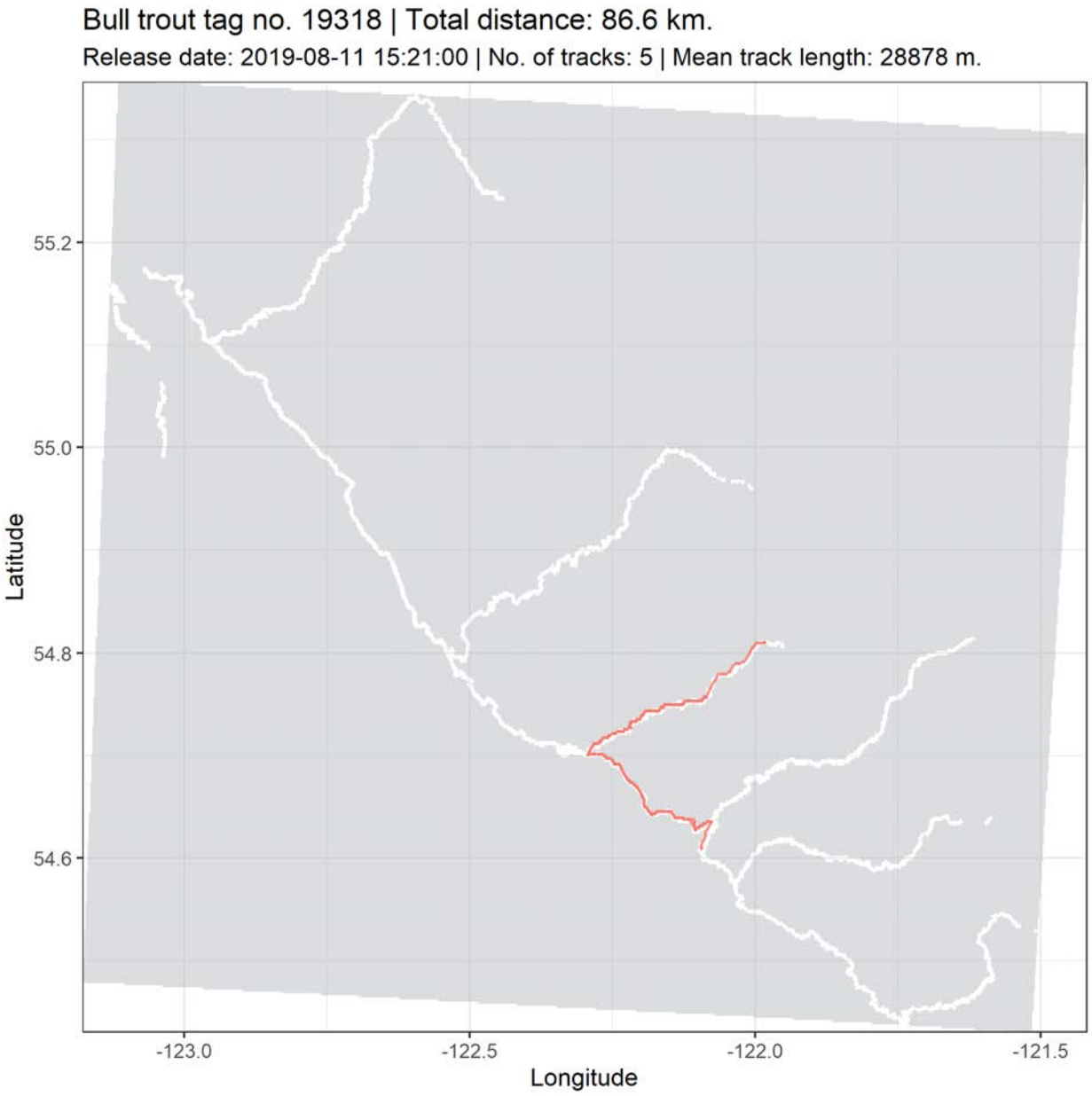
Bull trout tag no. 19318 | Total distance: 86.6 km.
Release date: 2019-08-11 15:21:00 | No. of tracks: 5 | Mean track length: 28878 m.
55.2
55.0
54.8
54.6
Latitude
-123.0
-122.5
-122.0
-121.5
Longitude

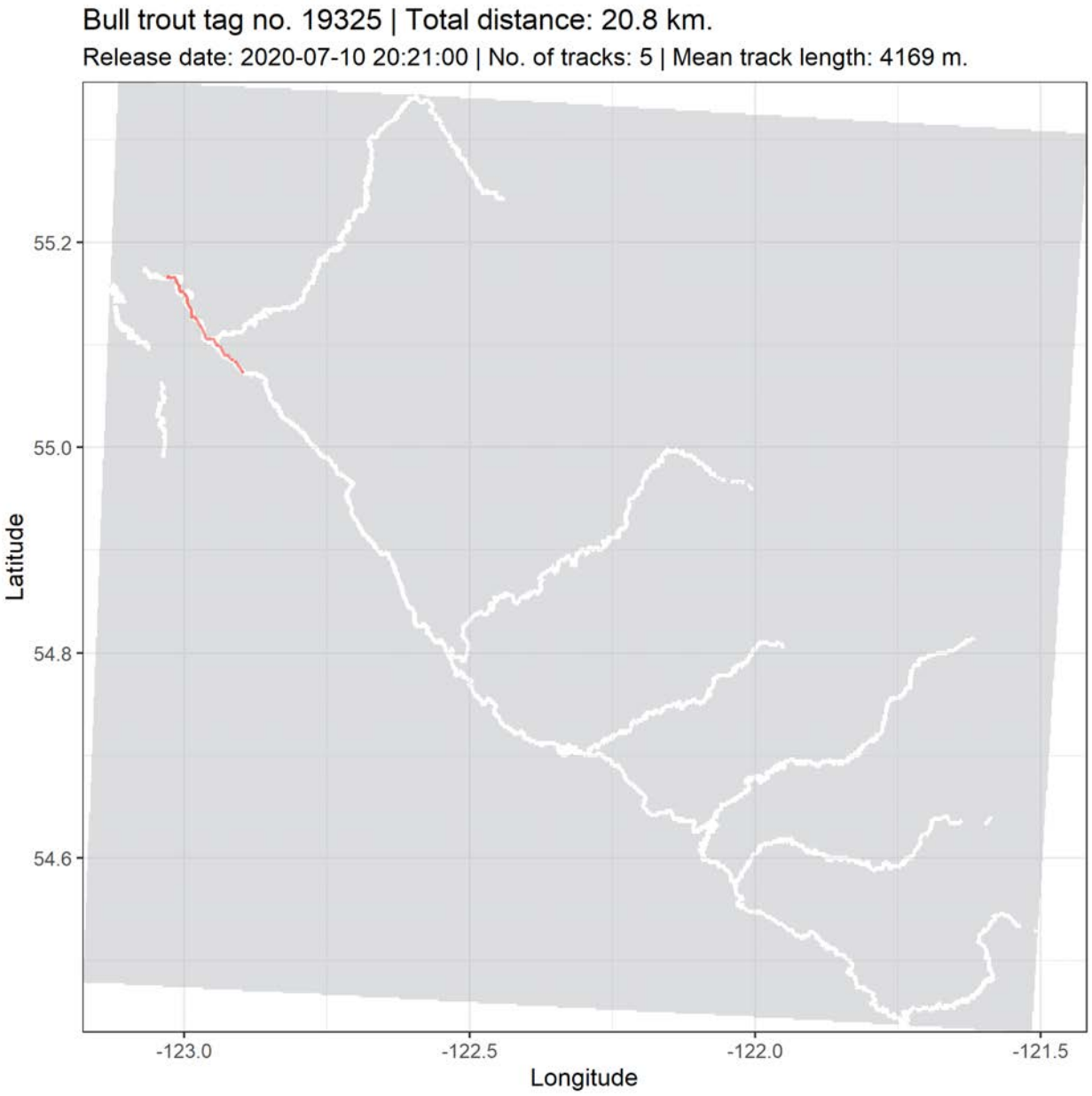
Bull trout tag no. 19325 | Total distance: 20.8 km.
Release date: 2020-07-10 20:21:00 | No. of tracks: 5 | Mean track length: 4169 m.
55.2
55.0
54.8
54.6
Latitude
-123.0
-122.5
-122.0
-121.5
Longitude

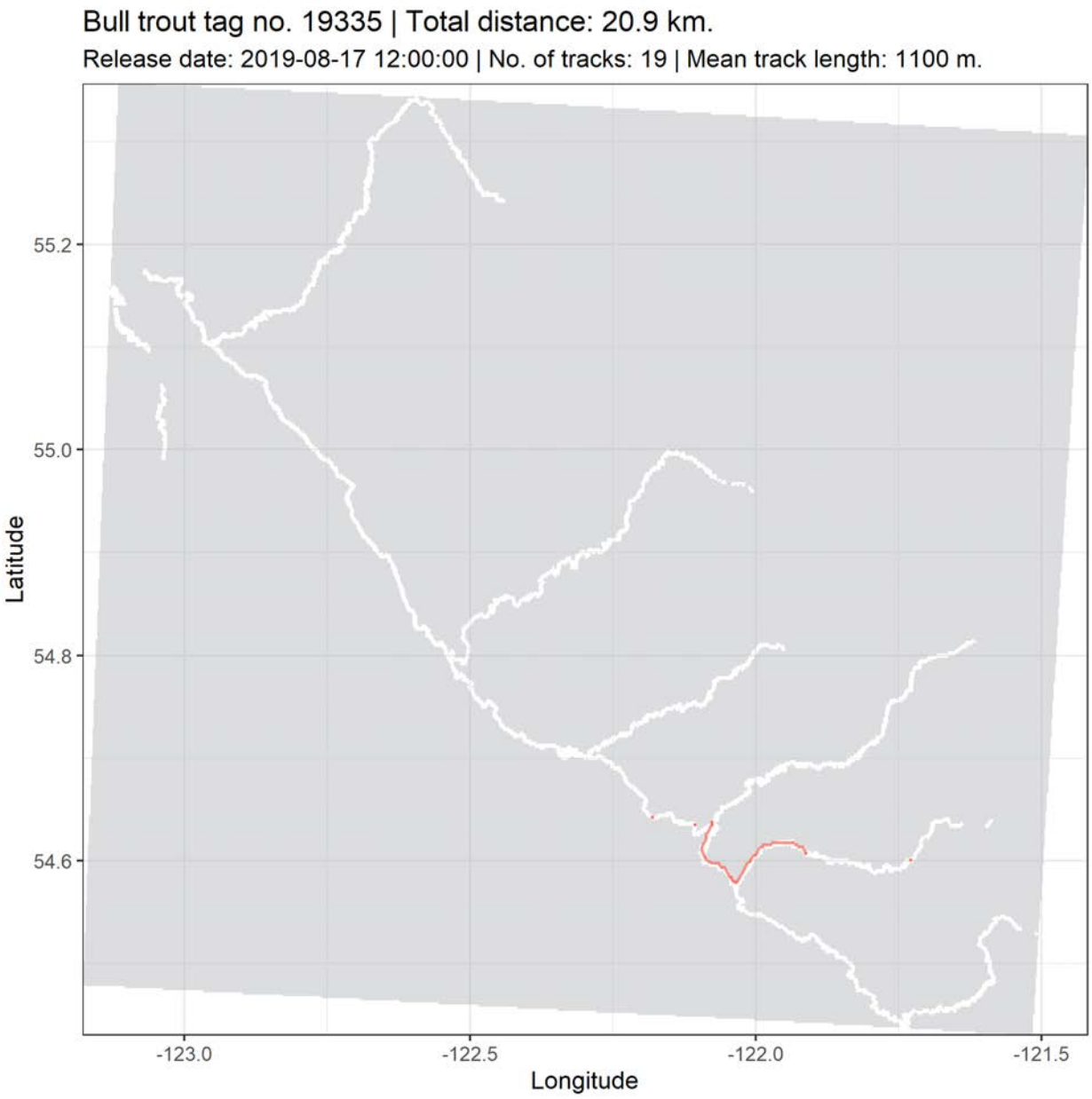
Bull trout tag no. 19335 | Total distance: 20.9 km.
Release date: 2019-08-17 12:00:00 | No. of tracks: 19 | Mean track length: 1100 m.
55.2
55.0
54.8
54.6
Latitude
-123.0
-122.5
-122.0
-121.5
Longitude

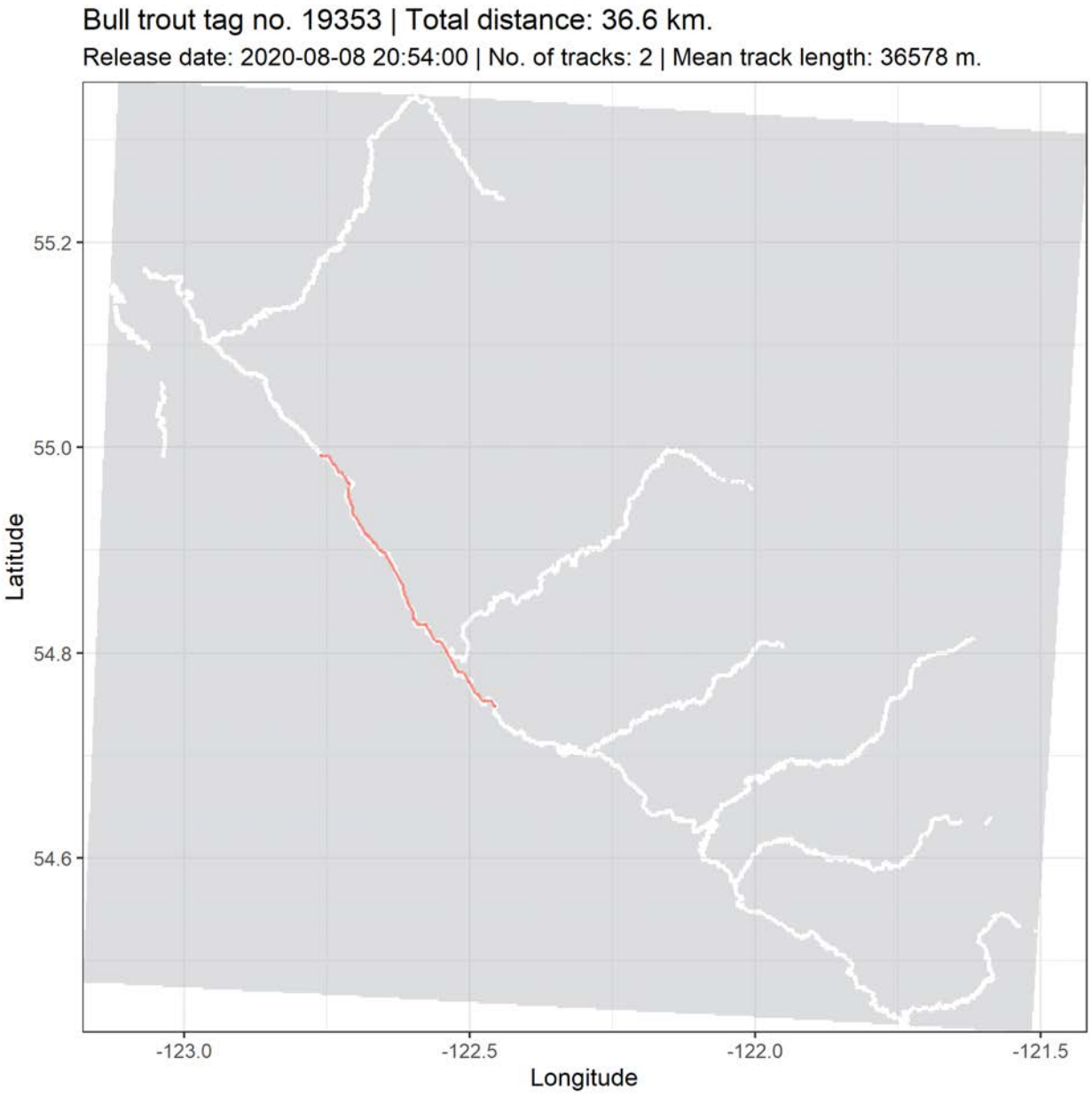
Bull trout tag no. 19353 | Total distance: 36.6 km.
Release date: 2020-08-08 20:54:00 | No. of tracks: 2 | Mean track length: 36578 m.
55.2
55.0
54.8
54.6
Latitude
-123.0
-122.5
-122.0
-121.5
Longitude

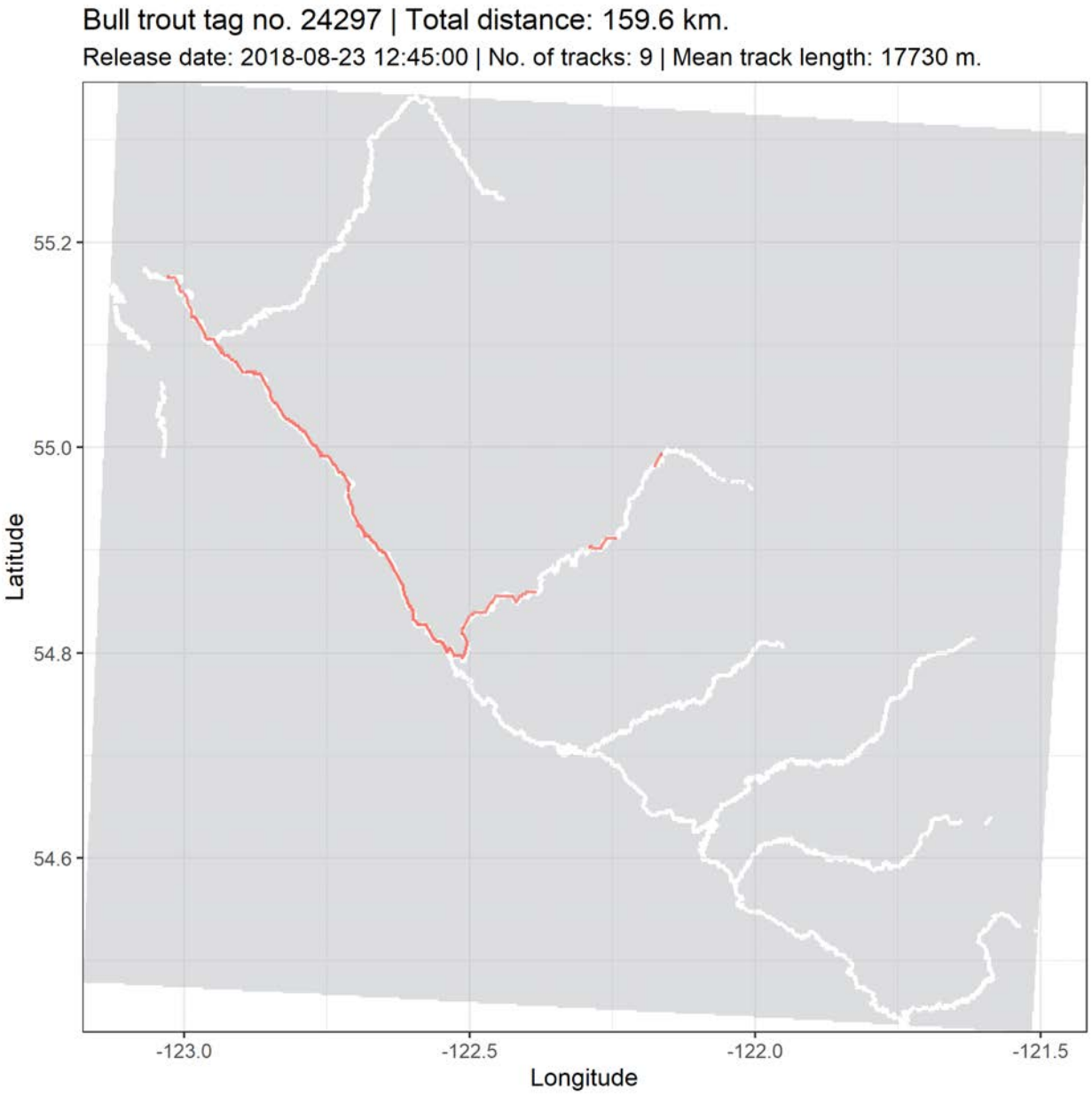
Bull trout tag no. 24297 | Total distance: 159.6 km.
Release date: 2018-08-23 12:45:00 | No. of tracks: 9 | Mean track length: 17730 m.
55.2
55.0
54.8
54.6
Latitude
-123.0
-122.5
-122.0
-121.5
Longitude

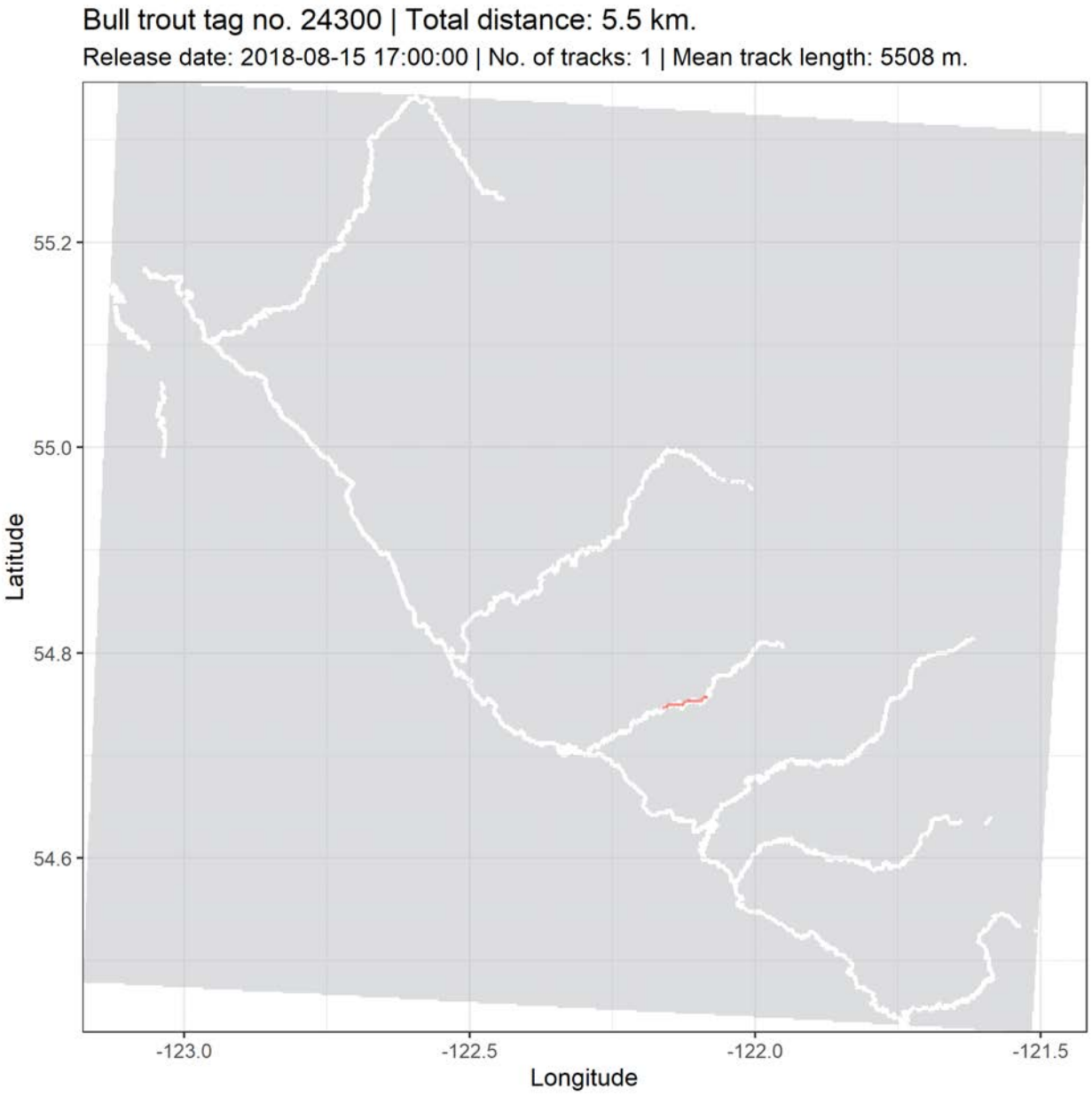
Bull trout tag no. 24300 | Total distance: 5.5 km.
Release date: 2018-08-15 17:00:00 | No. of tracks: 1 | Mean track length: 5508 m.
55.2
55.0
54.8
54.6
Latitude
-123.0
-122.5
-122.0
-121.5
Longitude

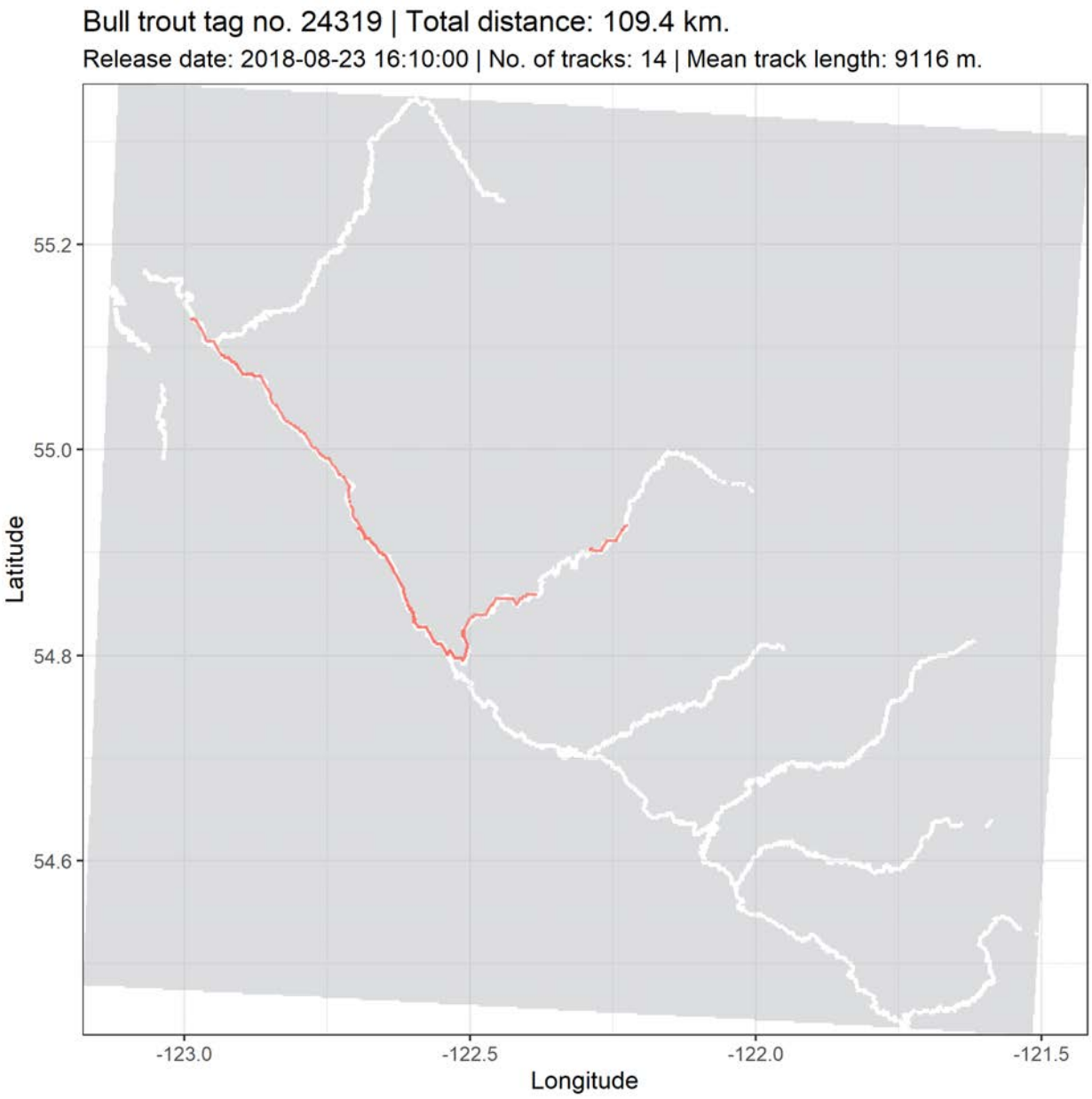
Bull trout tag no. 24319 | Total distance: 109.4 km.
Release date: 2018-08-23 16:10:00 | No. of tracks: 14 | Mean track length: 9116 m.
55.2
55.0
54.8
54.6
Latitude
-123.0
-122.5
-122.0
-121.5
Longitude

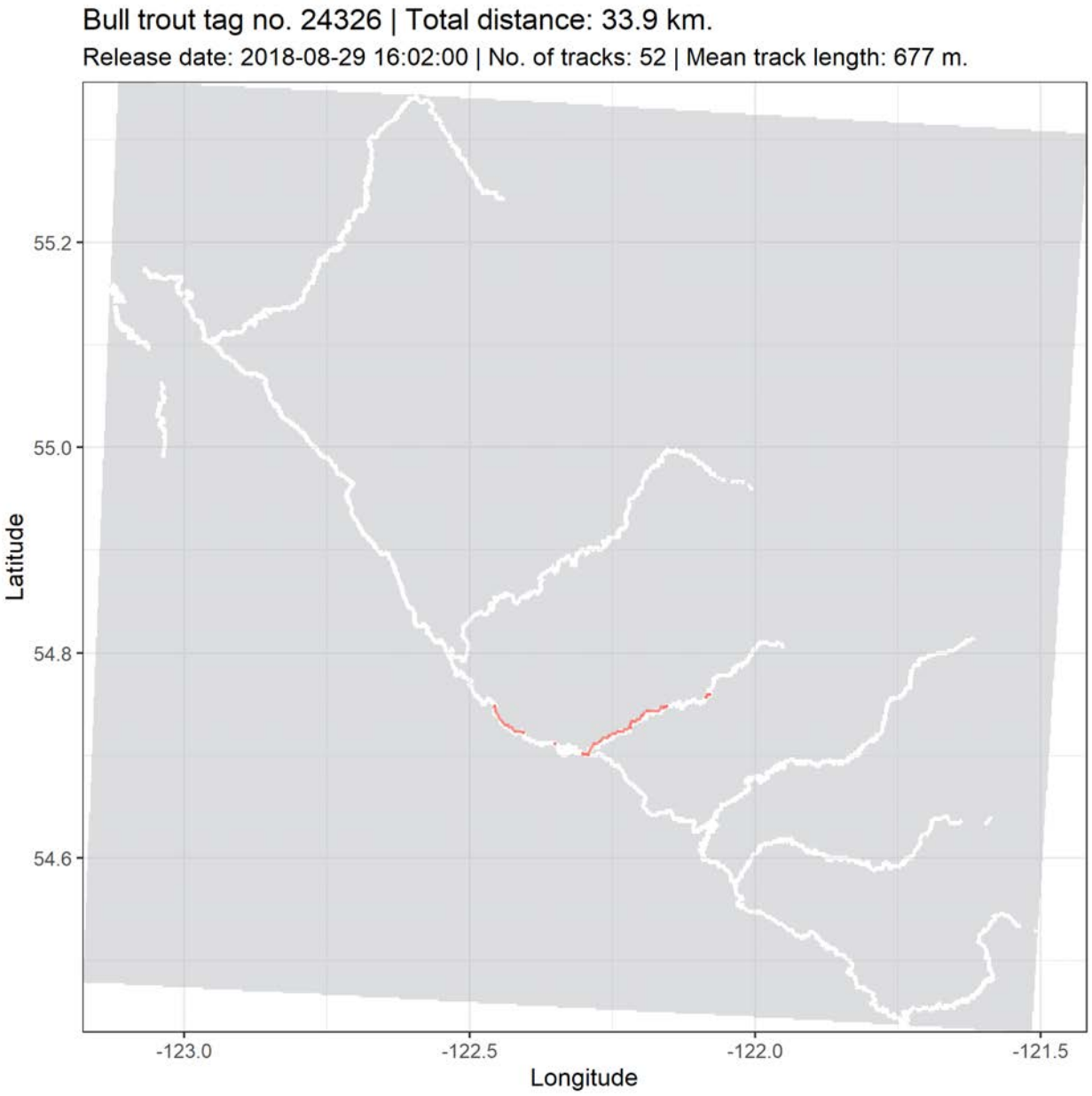
Bull trout tag no. 24326 | Total distance: 33.9 km.
Release date: 2018-08-29 16:02:00 | No. of tracks: 52 | Mean track length: 677 m.
55.2
55.0
54.8
54.6
Latitude
-123.0
-122.5
-122.0
-121.5
Longitude

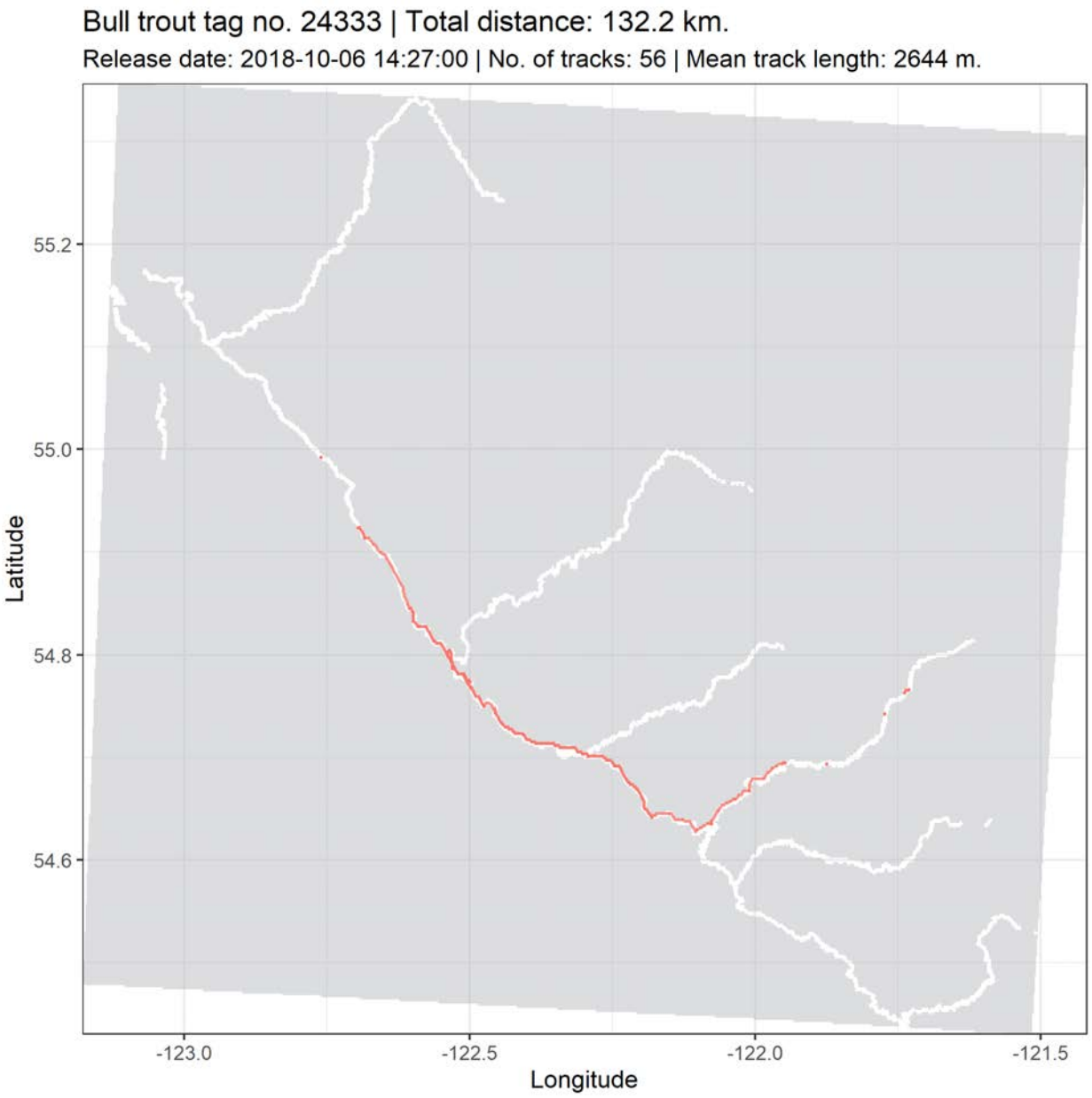
Bull trout tag no. 24333 | Total distance: 132.2 km.
Release date: 2018-10-06 14:27:00 | No. of tracks: 56 | Mean track length: 2644 m.
55.2
55.0
54.8
54.6
Latitude
-123.0
-122.5
-122.0
-121.5
Longitude

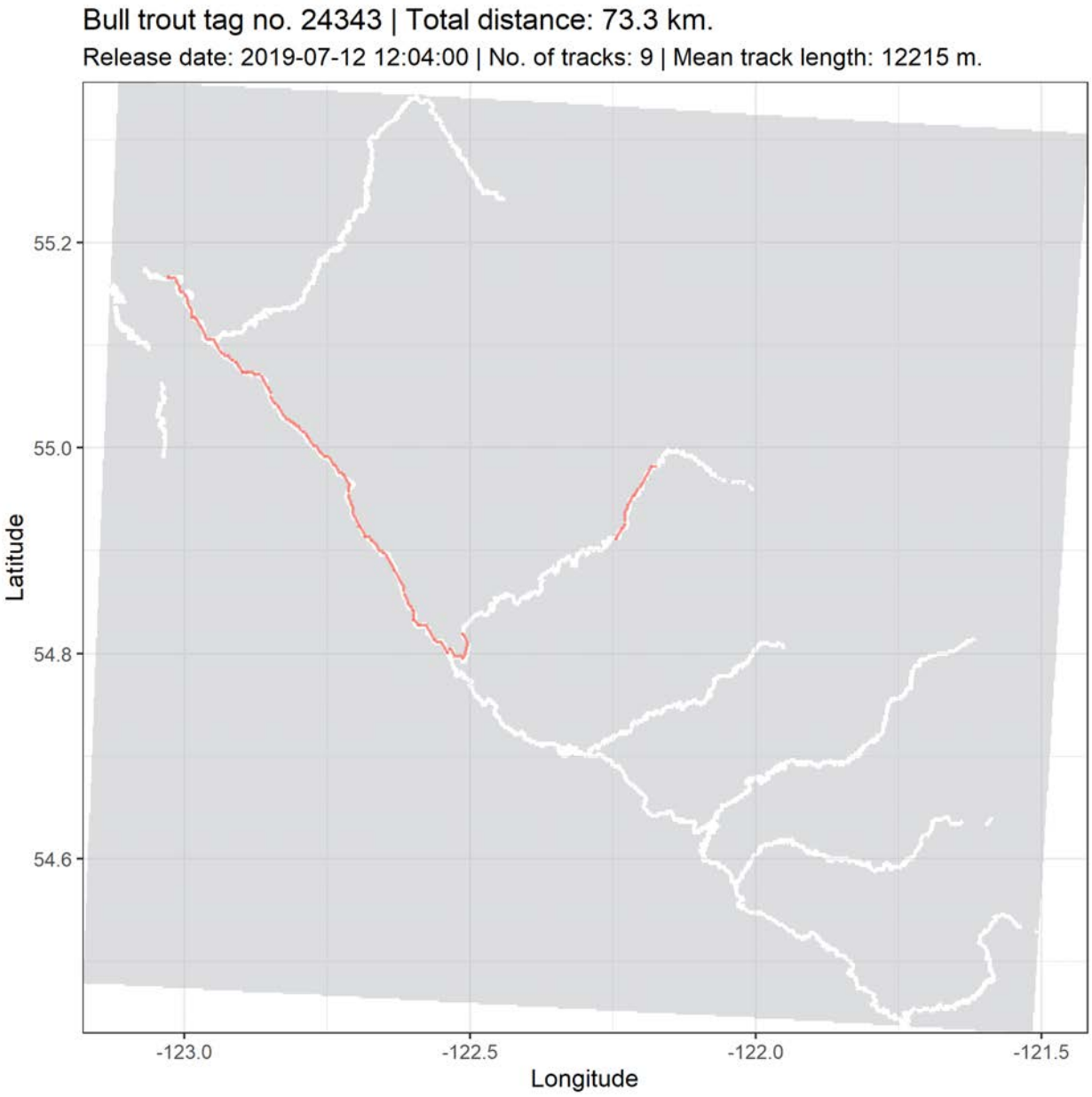
Bull trout tag no. 24343 | Total distance: 73.3 km.
Release date: 2019-07-12 12:04:00 | No. of tracks: 9 | Mean track length: 12215 m.
55.2
55.0
54.8
54.6
Latitude
-123.0
-122.5
-122.0
-121.5
Longitude

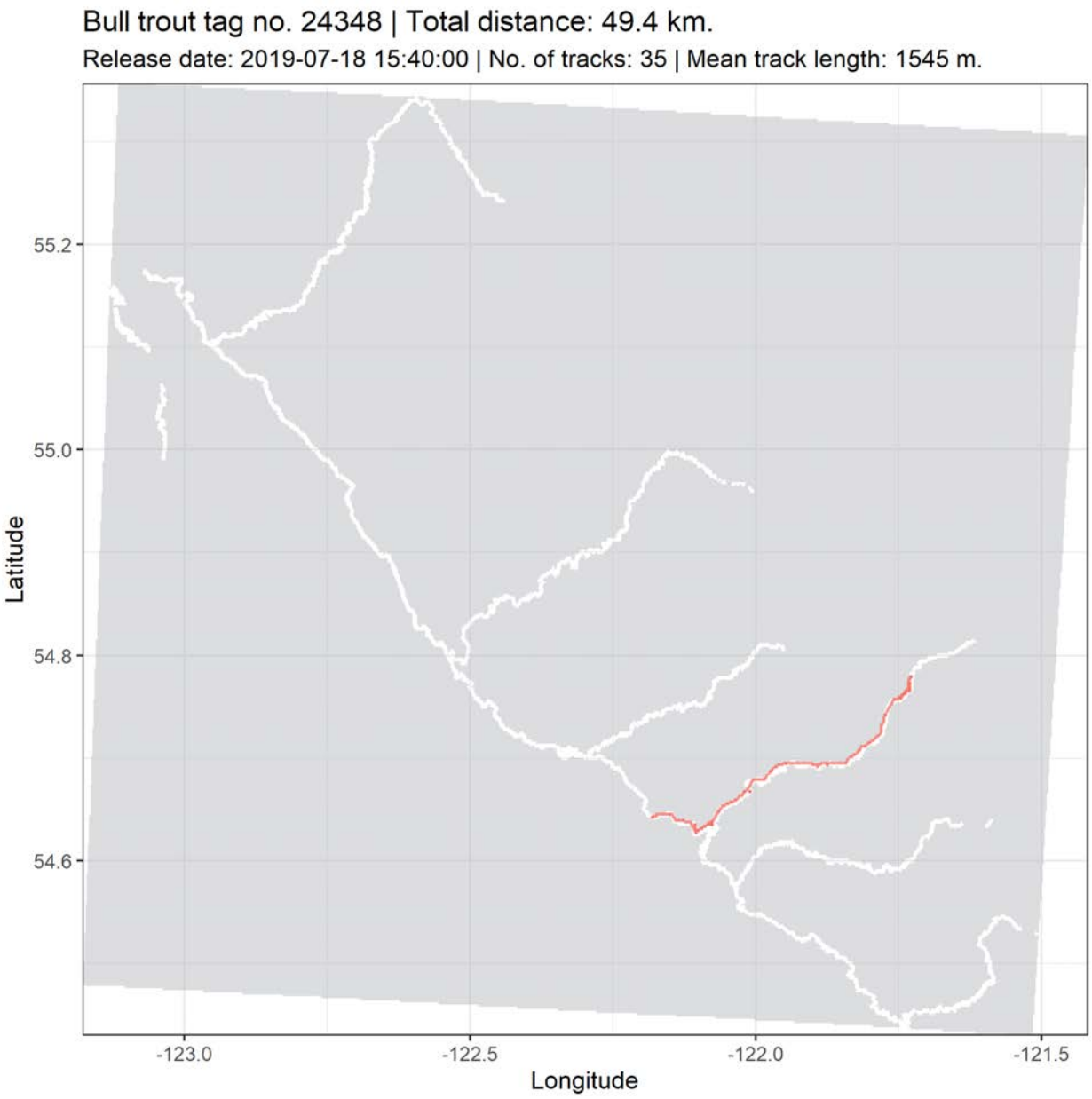
Bull trout tag no. 24348 | Total distance: 49.4 km.
Release date: 2019-07-18 15:40:00 | No. of tracks: 35 | Mean track length: 1545 m.
55.2
55.0
54.8
54.6
Latitude
-123.0
-122.5
-122.0
-121.5
Longitude

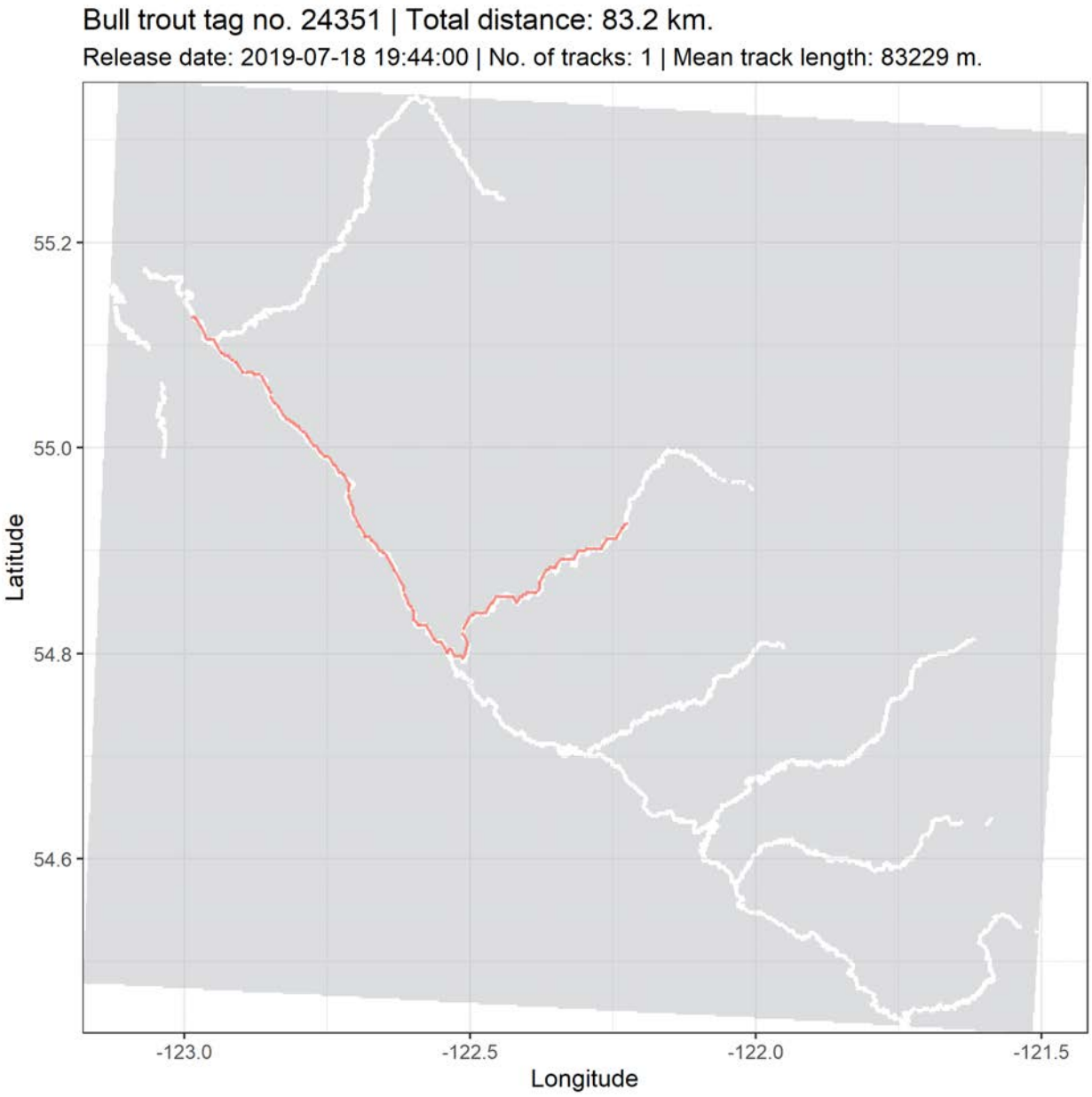
Bull trout tag no. 24351 | Total distance: 83.2 km.
Release date: 2019-07-18 19:44:00 | No. of tracks: 1 | Mean track length: 83229 m.
55.2
55.0
54.8
54.6
Latitude
-123.0
-122.5
-122.0
-121.5
Longitude

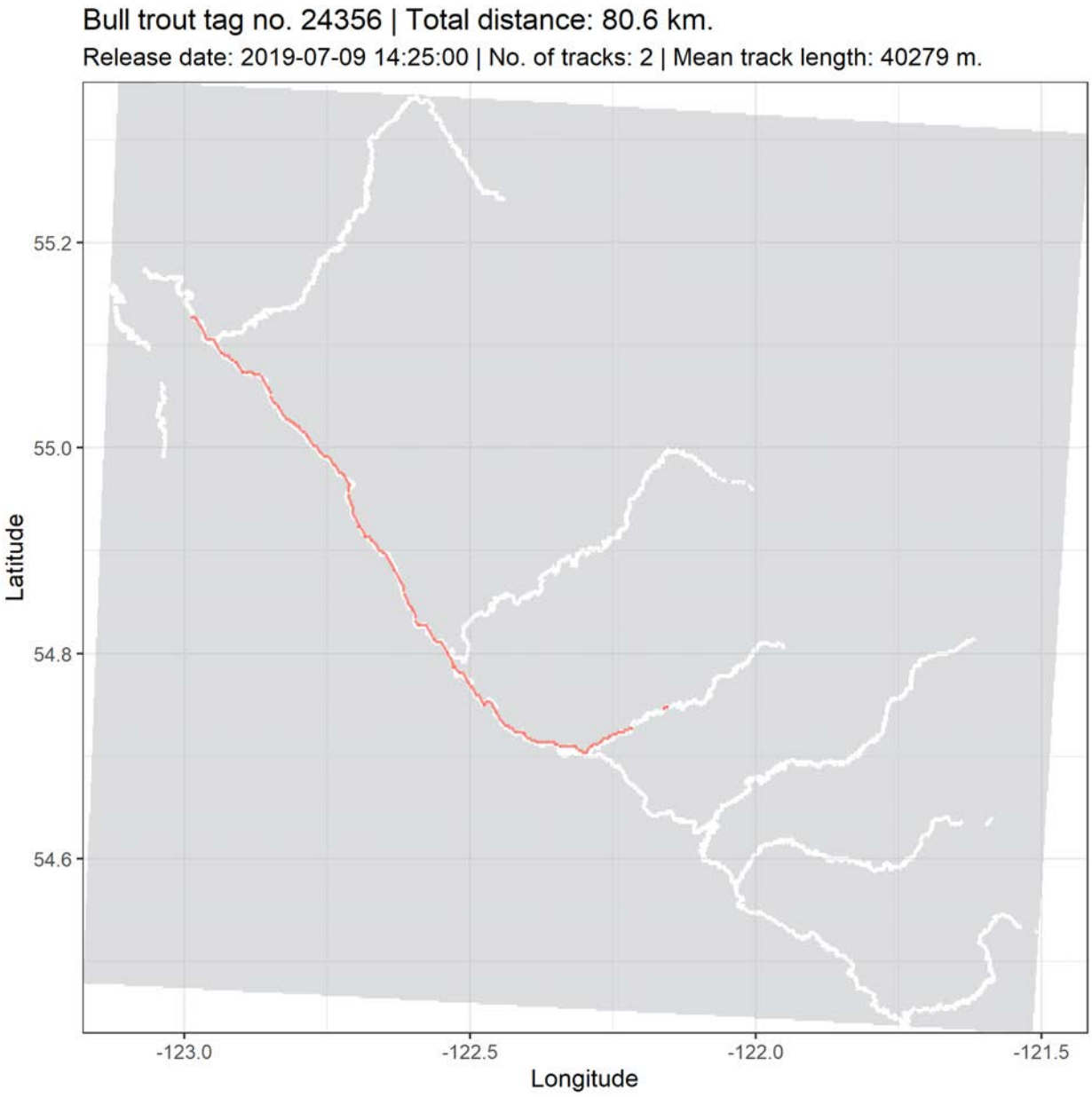
Bull trout tag no. 24356 | Total distance: 80.6 km.
Release date: 2019-07-09 14:25:00 | No. of tracks: 2 | Mean track length: 40279 m.
55.2
55.0
54.8
54.6
Latitude
-123.0
-122.5
-122.0
-121.5
Longitude

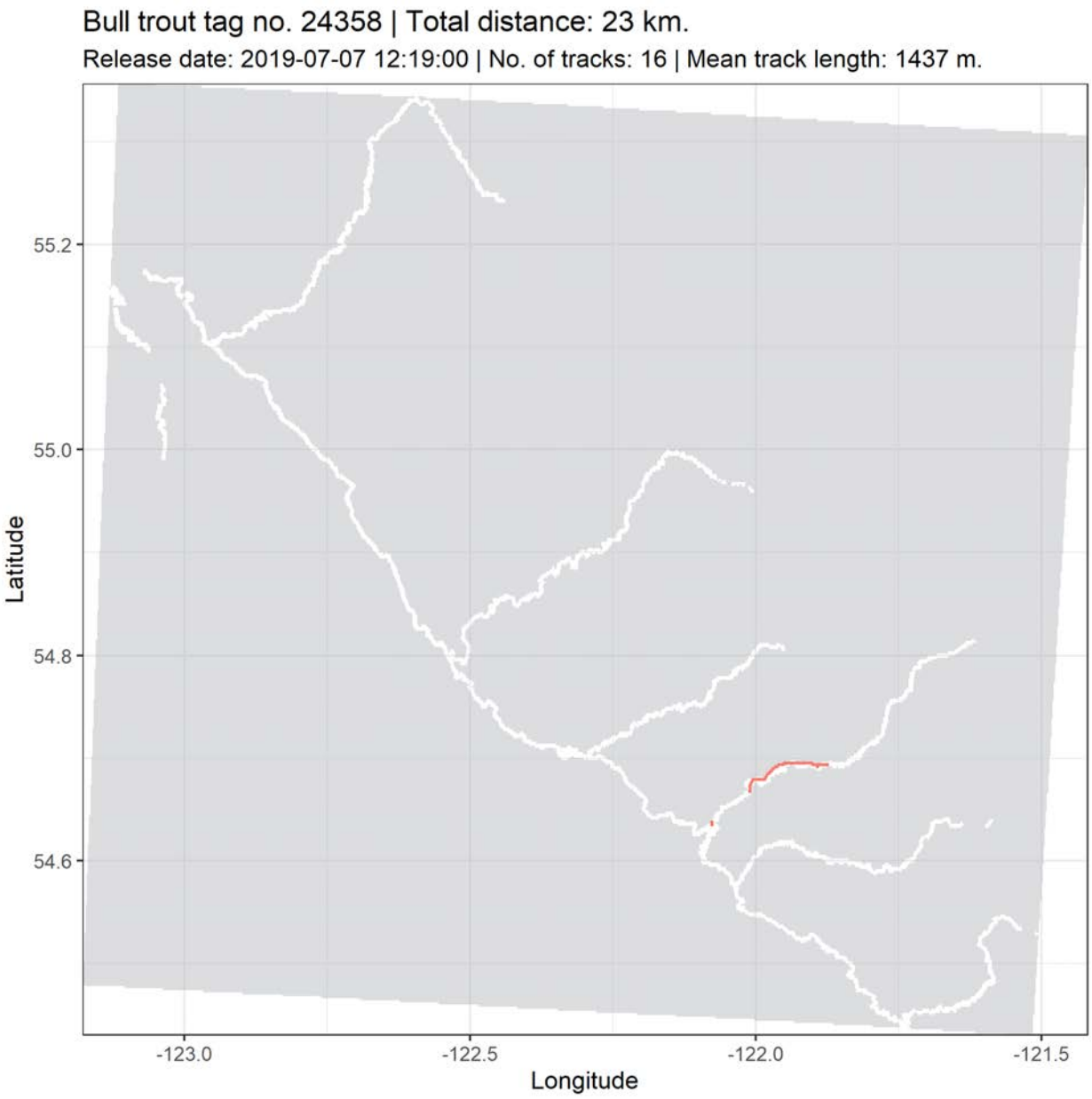
Bull trout tag no. 24358 | Total distance: 23 km.
Release date: 2019-07-07 12:19:00 | No. of tracks: 16 | Mean track length: 1437 m.
55.2
55.0
54.8
54.6
Latitude
-123.0
-122.5
-122.0
-121.5
Longitude

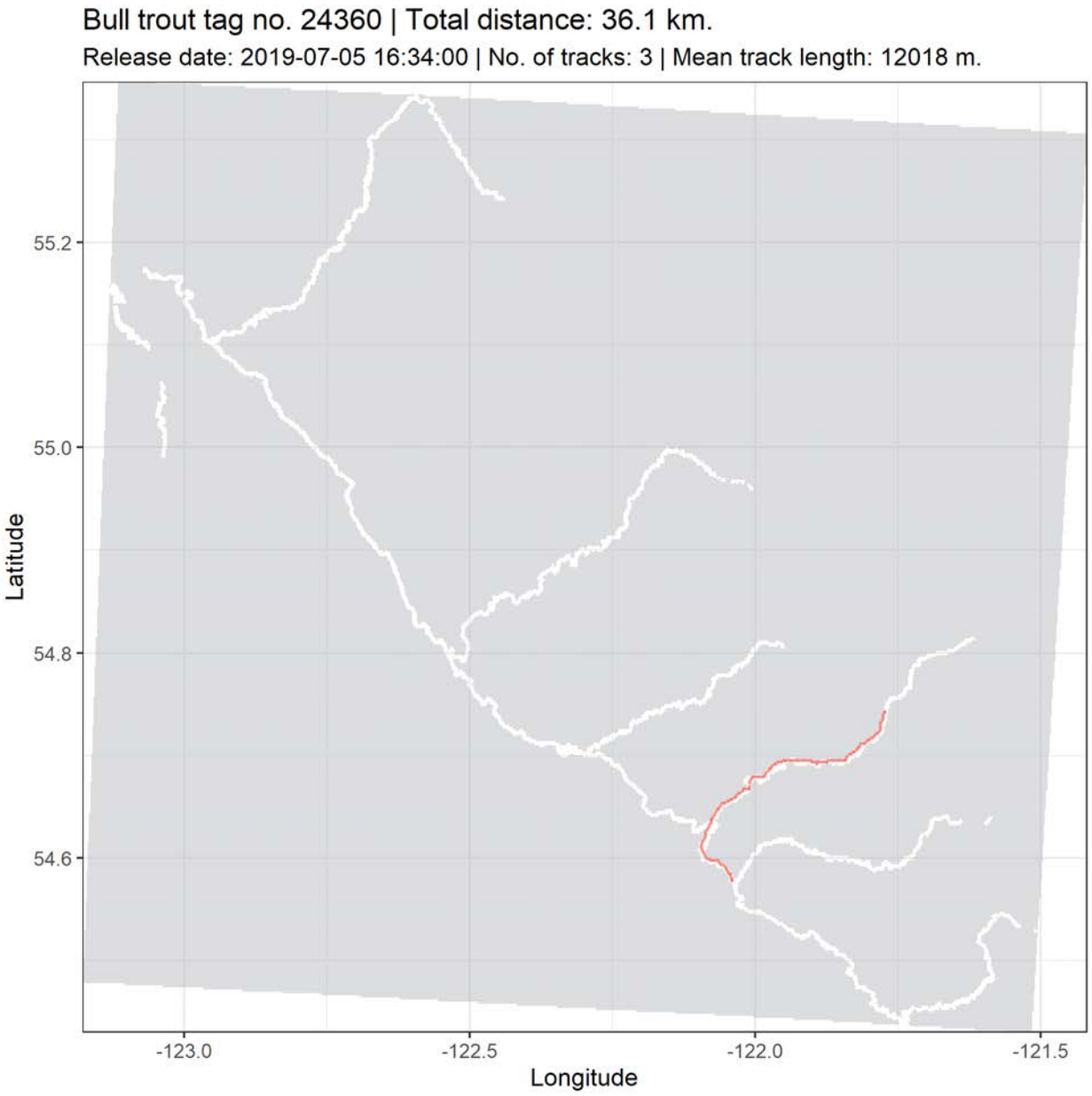
Bull trout tag no. 24360 | Total distance: 36.1 km.
Release date: 2019-07-05 16:34:00 | No. of tracks: 3 | Mean track length: 12018 m.
55.2
55.0
54.8
54.6
Latitude
-123.0
-122.5
-122.0
-121.5
Longitude

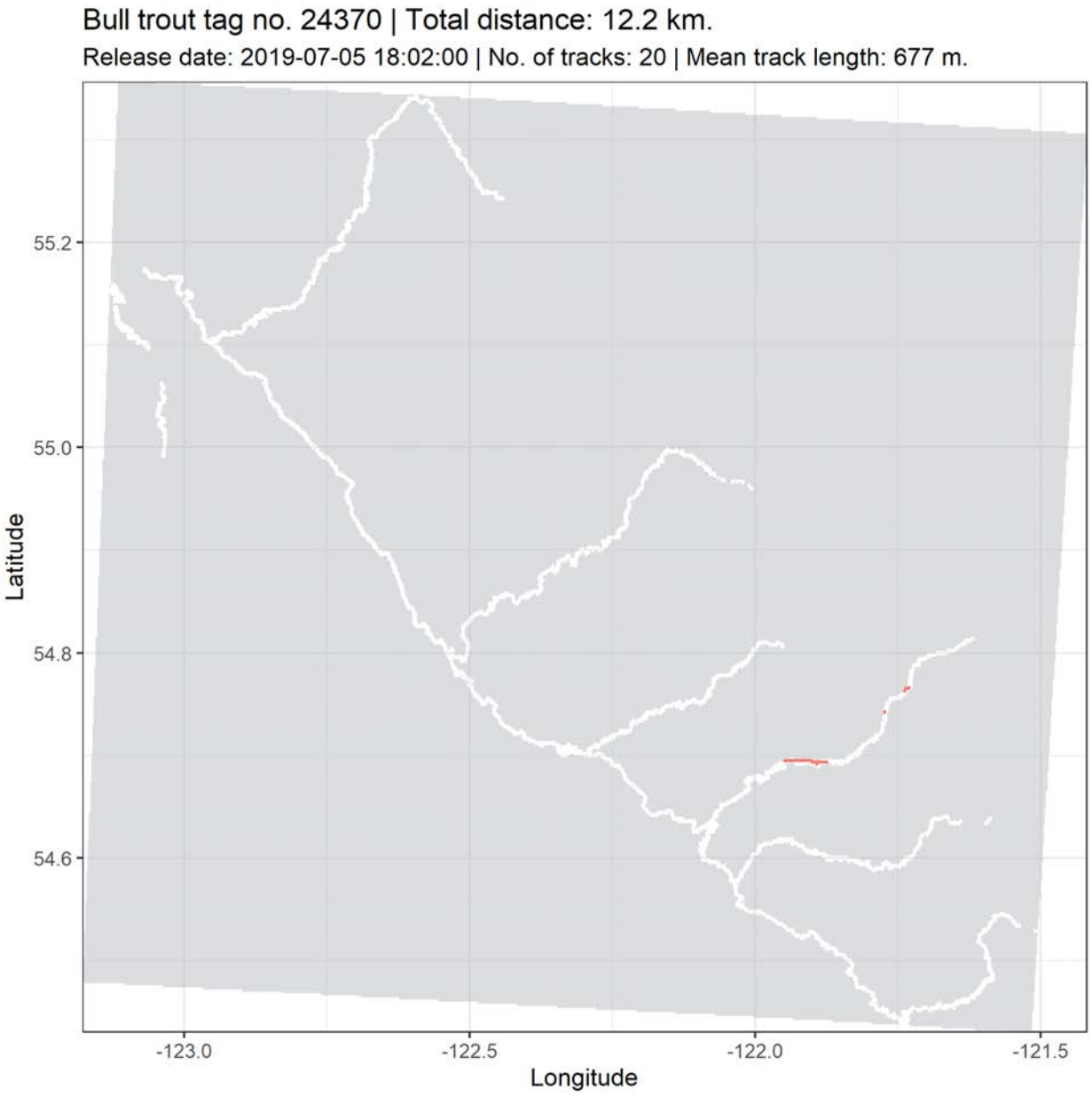
Bull trout tag no. 24370 | Total distance: 12.2 km.
Release date: 2019-07-05 18:02:00 | No. of tracks: 20 | Mean track length: 677 m.
55.2
55.0
54.8
54.6
Latitude
-123.0
-122.5
-122.0
-121.5
Longitude

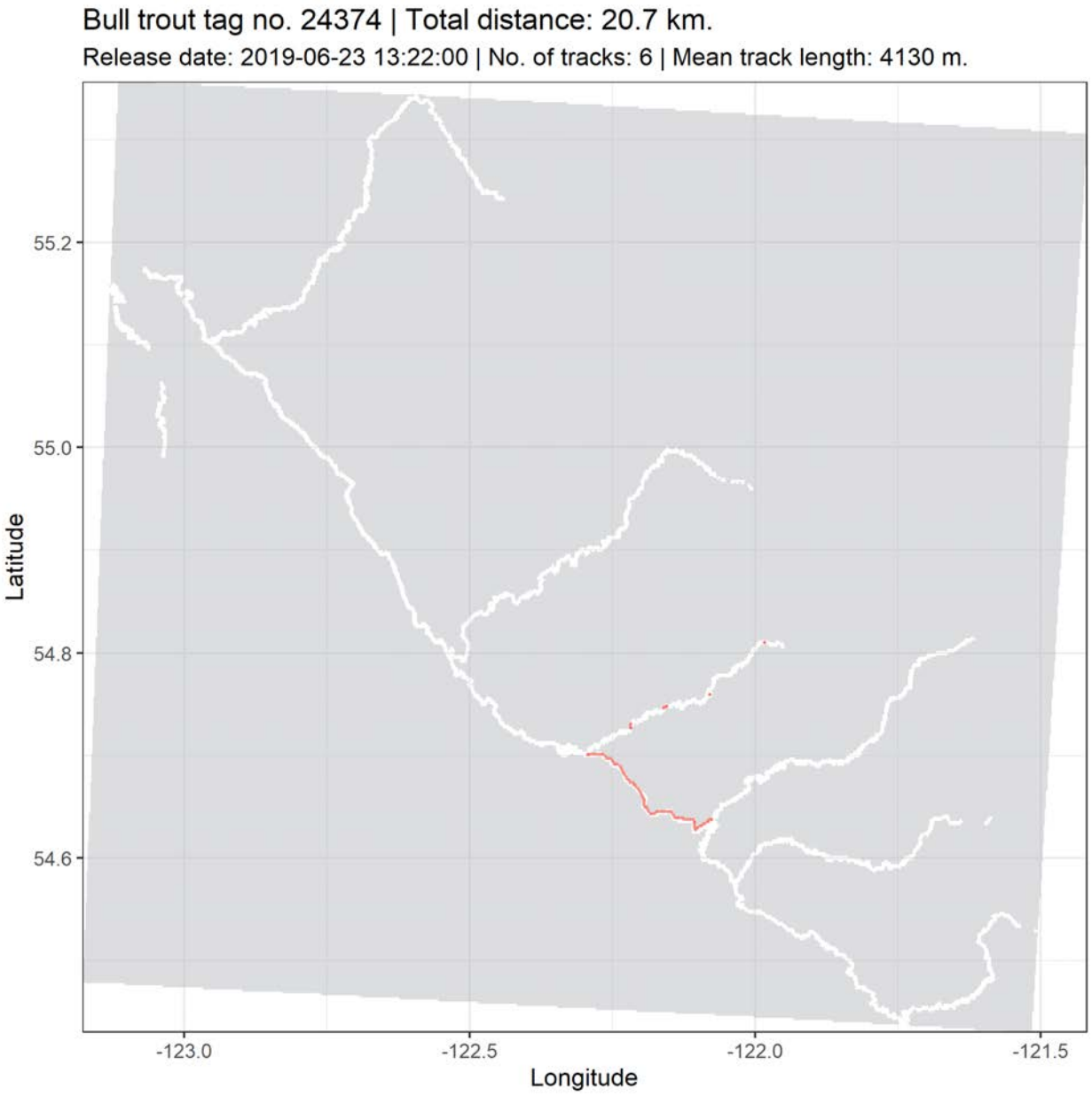
Bull trout tag no. 24374 | Total distance: 20.7 km.
Release date: 2019-06-23 13:22:00 | No. of tracks: 6 | Mean track length: 4130 m.
55.2
55.0
54.8
54.6
Latitude
-123.0
-122.5
-122.0
-121.5
Longitude

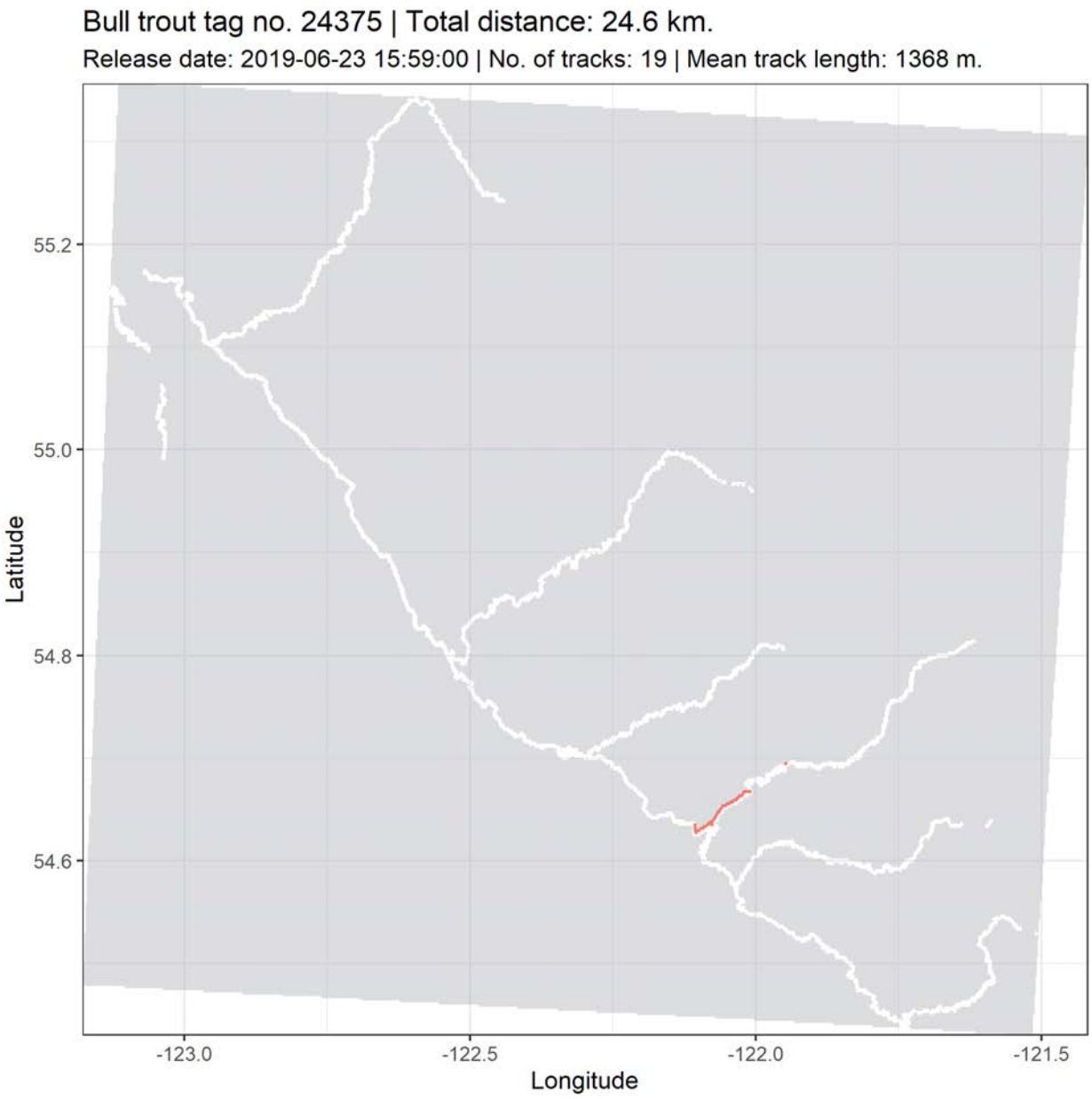
Bull trout tag no. 24375 | Total distance: 24.6 km.
Release date: 2019-06-23 15:59:00 | No. of tracks: 19 | Mean track length: 1368 m.
55.2
55.0
54.8
54.6
Latitude
-123.0
-122.5
-122.0
-121.5
Longitude

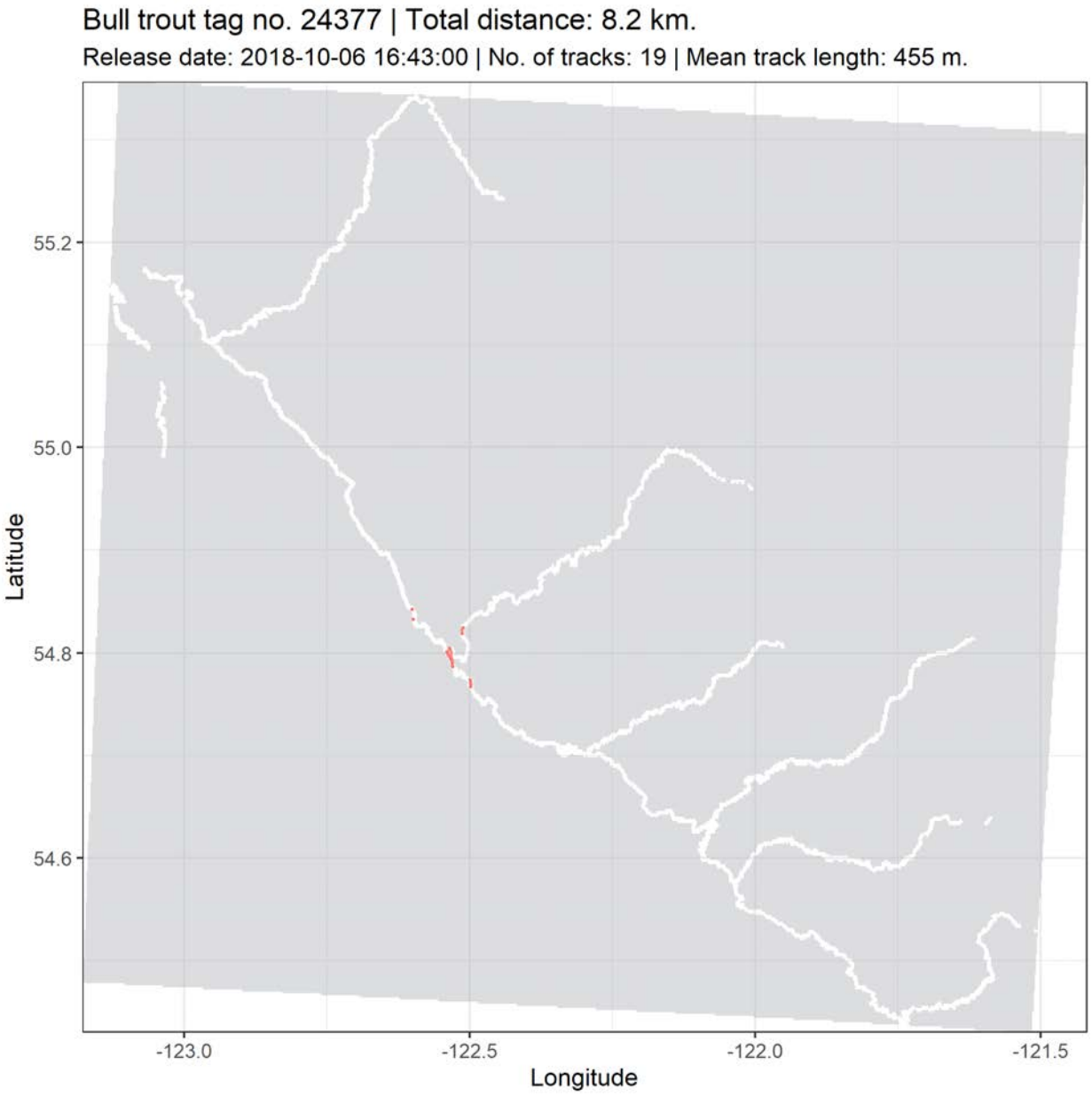
Bull trout tag no. 24377 | Total distance: 8.2 km.
Release date: 2018-10-06 16:43:00 | No. of tracks: 19 | Mean track length: 455 m.
55.2
55.0
54.8
54.6
Latitude
-123.0
-122.5
-122.0
-121.5
Longitude

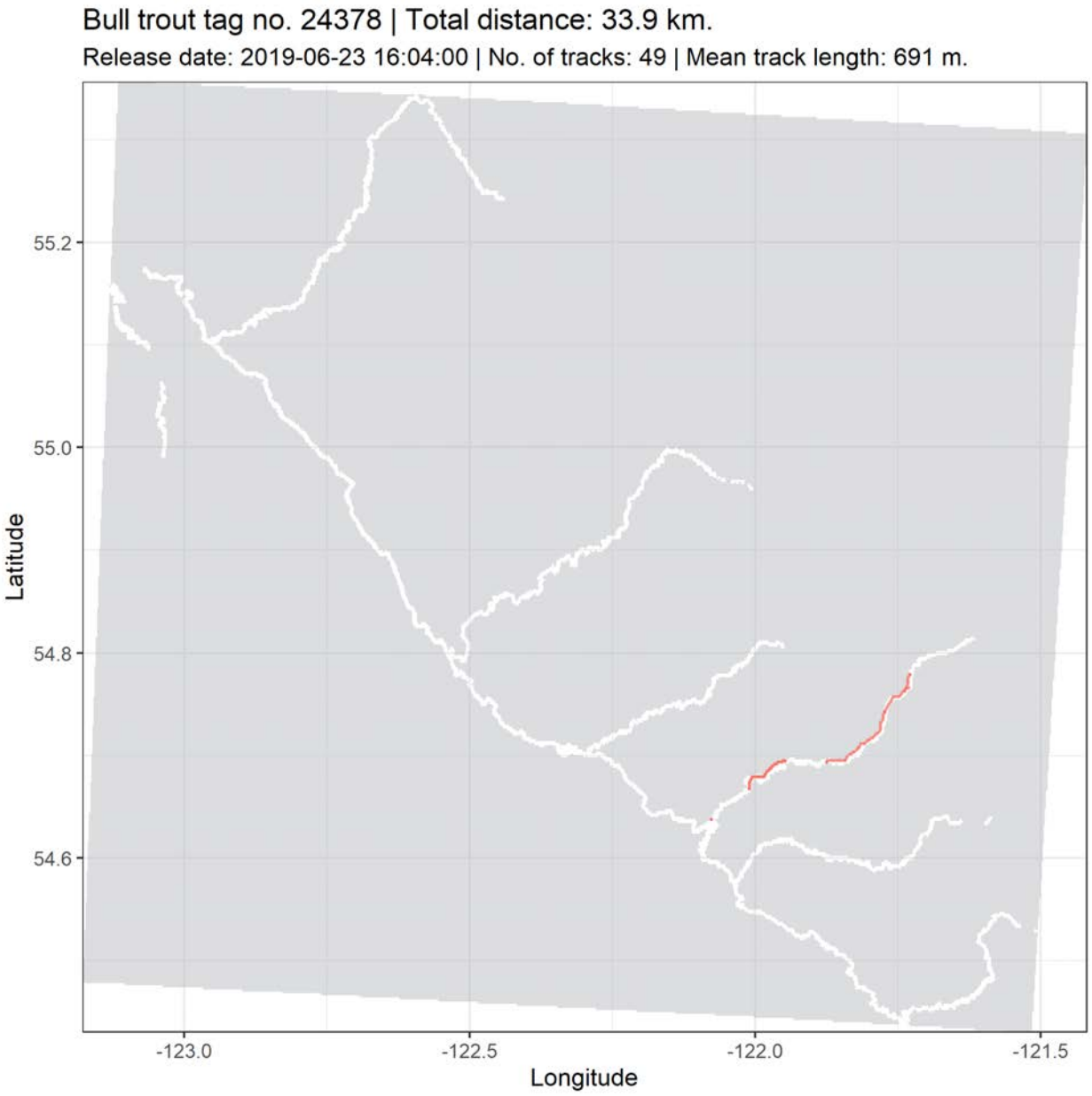
Bull trout tag no. 24378 | Total distance: 33.9 km.
Release date: 2019-06-23 16:04:00 | No. of tracks: 49 | Mean track length: 691 m.
55.2
55.0
54.8
54.6
Latitude
-123.0
-122.5
-122.0
-121.5
Longitude

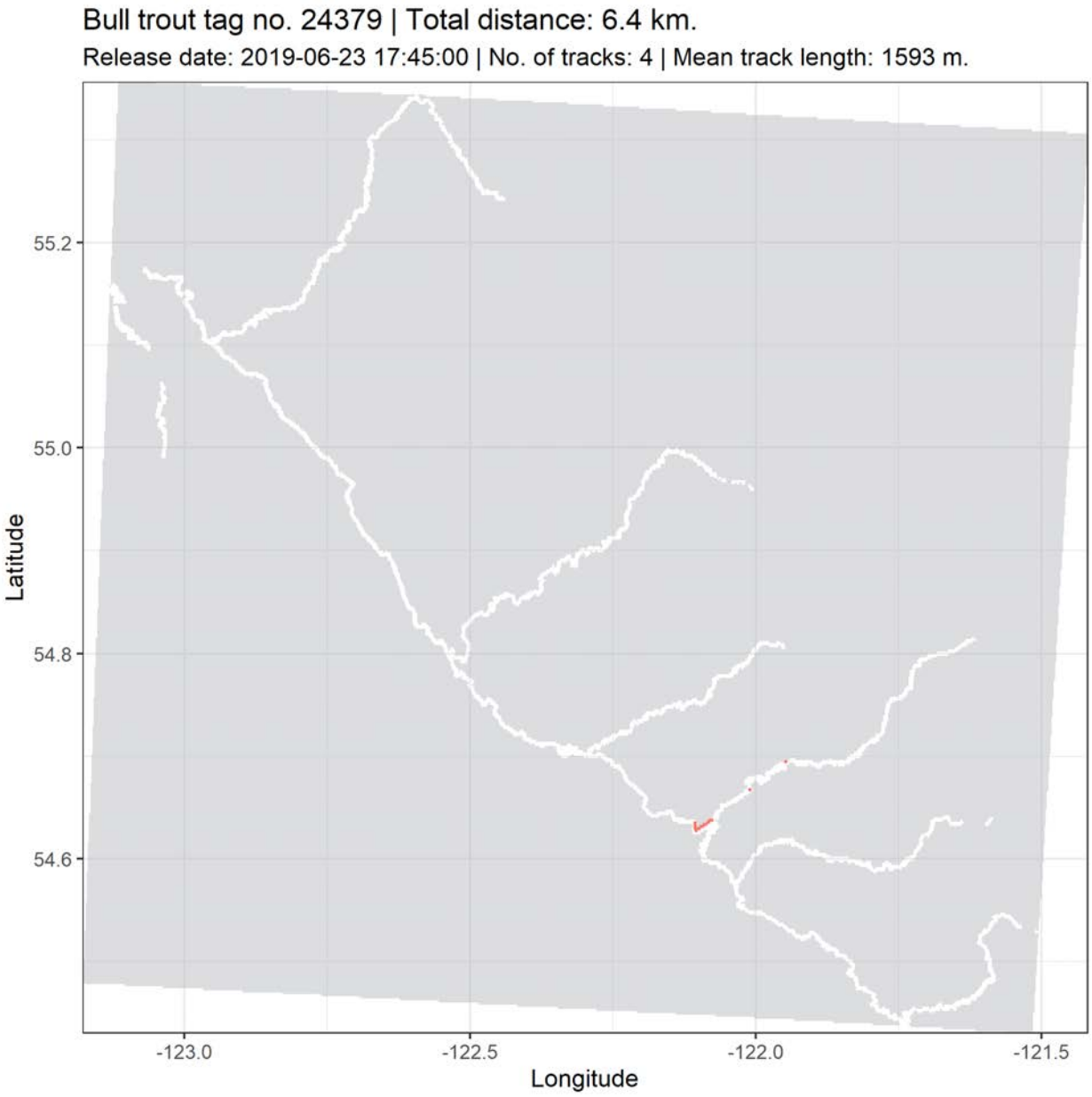
Bull trout tag no. 24379 | Total distance: 6.4 km.
Release date: 2019-06-23 17:45:00 | No. of tracks: 4 | Mean track length: 1593 m.
55.2
55.0
54.8
54.6
Latitude
-123.0
-122.5
-122.0
-121.5
Longitude

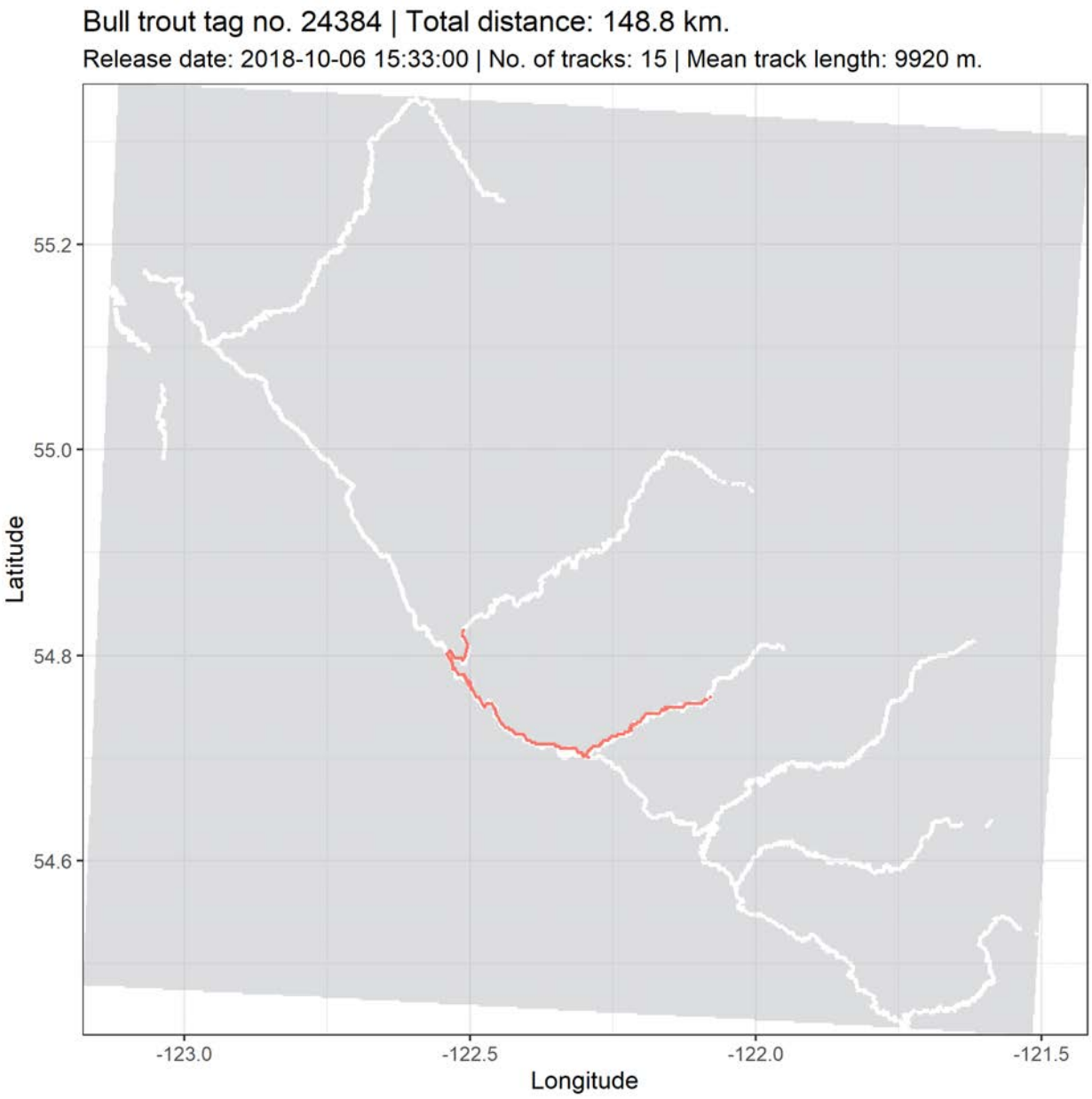
Bull trout tag no. 24384 | Total distance: 148.8 km.
Release date: 2018-10-06 15:33:00 | No. of tracks: 15 | Mean track length: 9920 m.
55.2
55.0
54.8
54.6
Latitude
-123.0
-122.5
-122.0
-121.5
Longitude

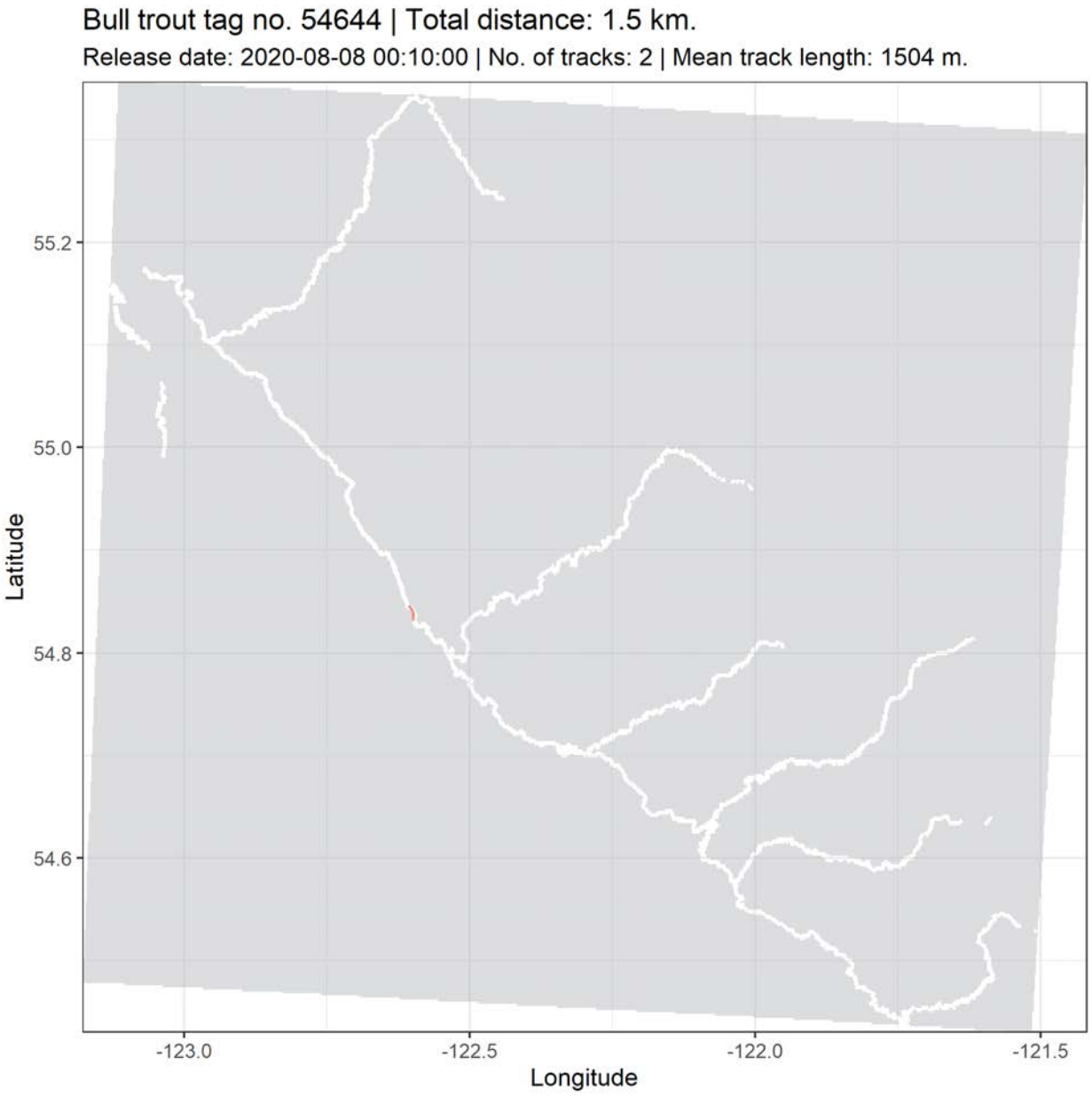
Bull trout tag no. 54644 | Total distance: 1.5 km.
Release date: 2020-08-08 00:10:00 | No. of tracks: 2 | Mean track length: 1504 m.
55.2
55.0
54.8
54.6
Latitude
-123.0
-122.5
-122.0
-121.5
Longitude

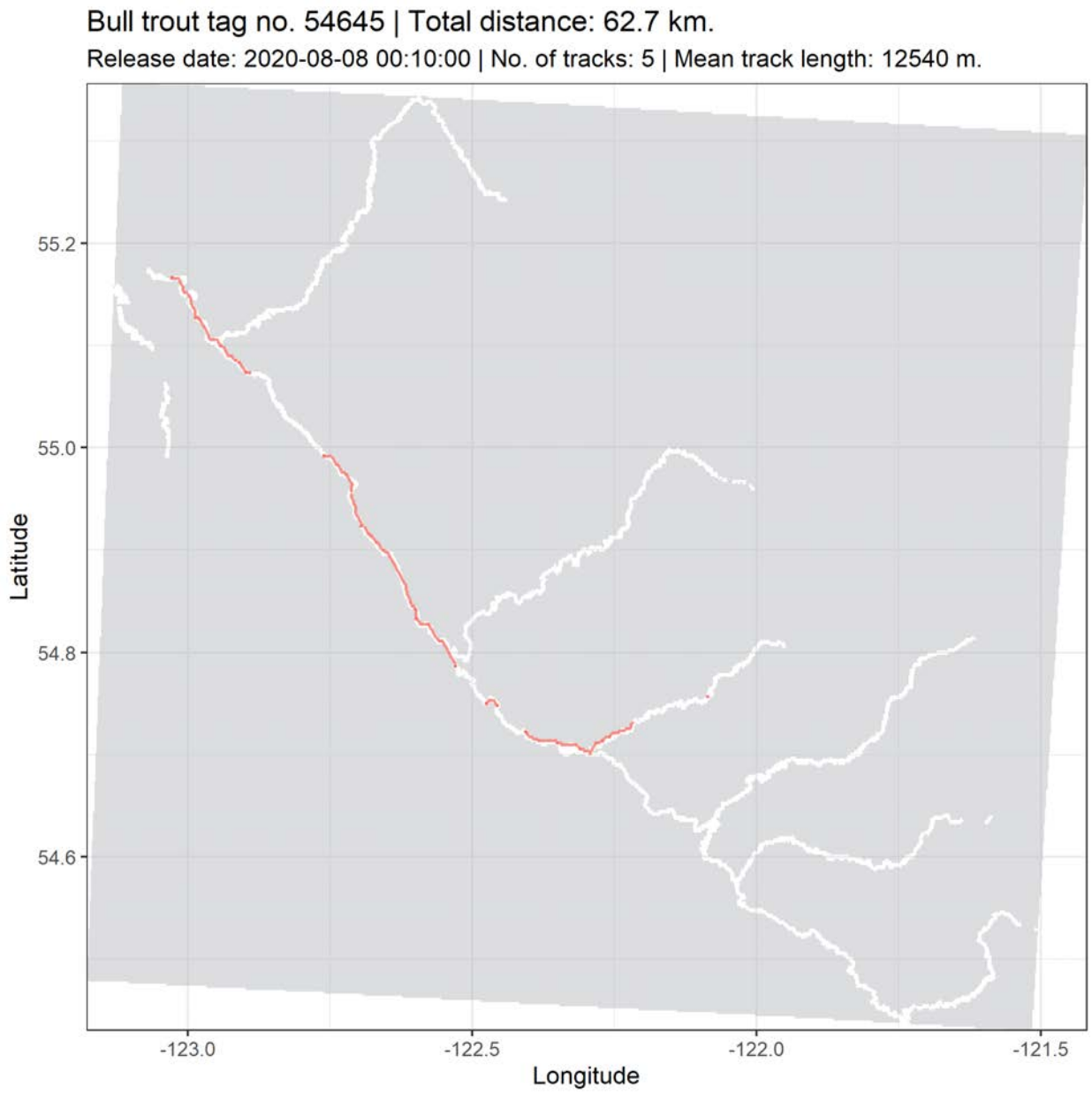
Bull trout tag no. 54645 | Total distance: 62.7 km.
Release date: 2020-08-08 00:10:00 | No. of tracks: 5 | Mean track length: 12540 m.
55.2
55.0
54.8
54.6
Latitude
-123.0
-122.5
-122.0
-121.5
Longitude

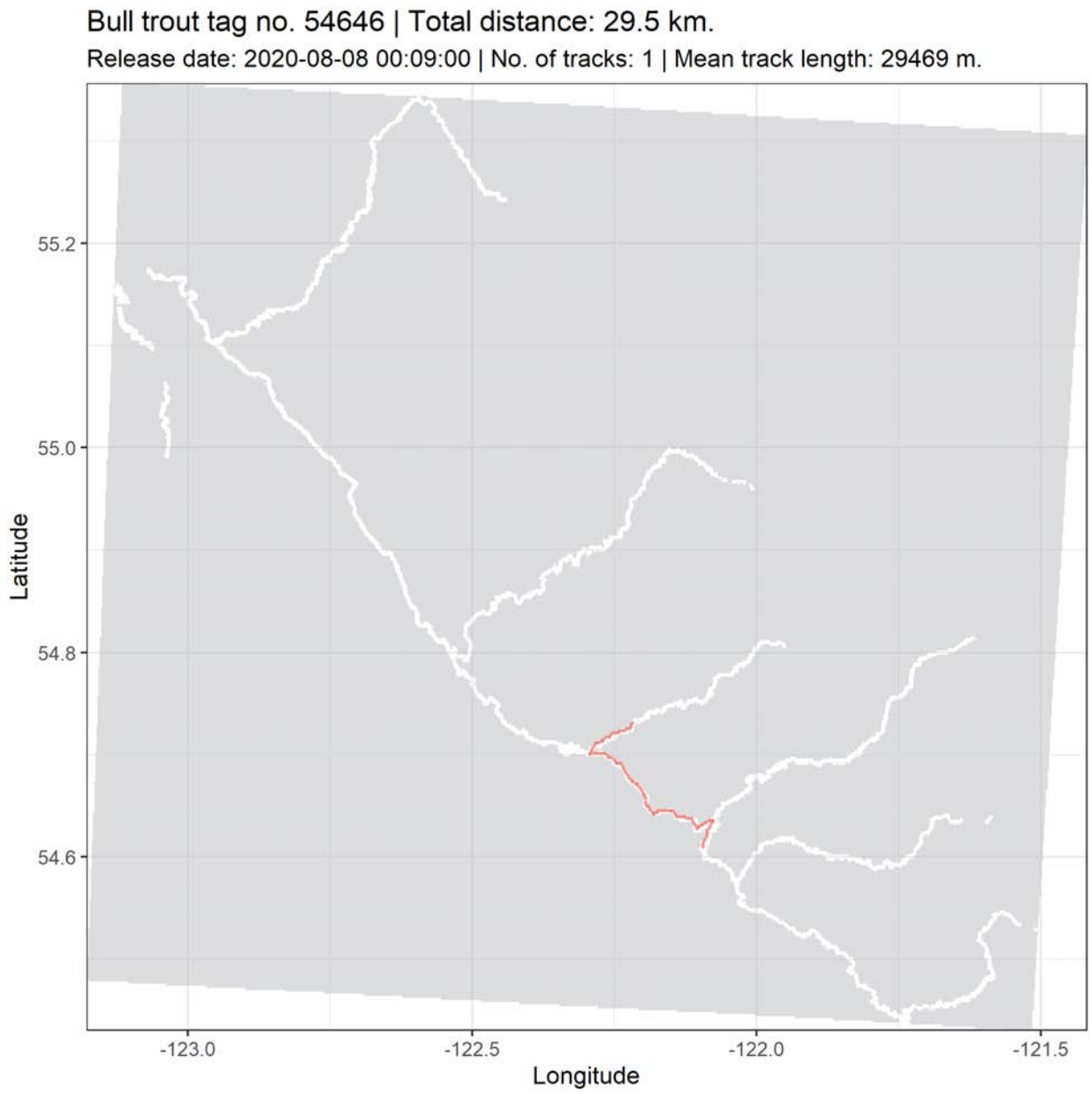
Bull trout tag no. 54646 | Total distance: 29.5 km.
Release date: 2020-08-08 00:09:00 | No. of tracks: 1 | Mean track length: 29469 m.
55.2
55.0
54.8
54.6
Latitude
-123.0
-122.5
-122.0
-121.5
Longitude

.

**Appendix A.4 – Species overlap by month**

These plots were generated by dynamic Brownian Bridge Movement Models in the package *RSP* (Niella et al. 2020). January – August 2020 have been plotted. September was omitted as it was the month most of the equipment downloads occurred and would represent a partial dataset.

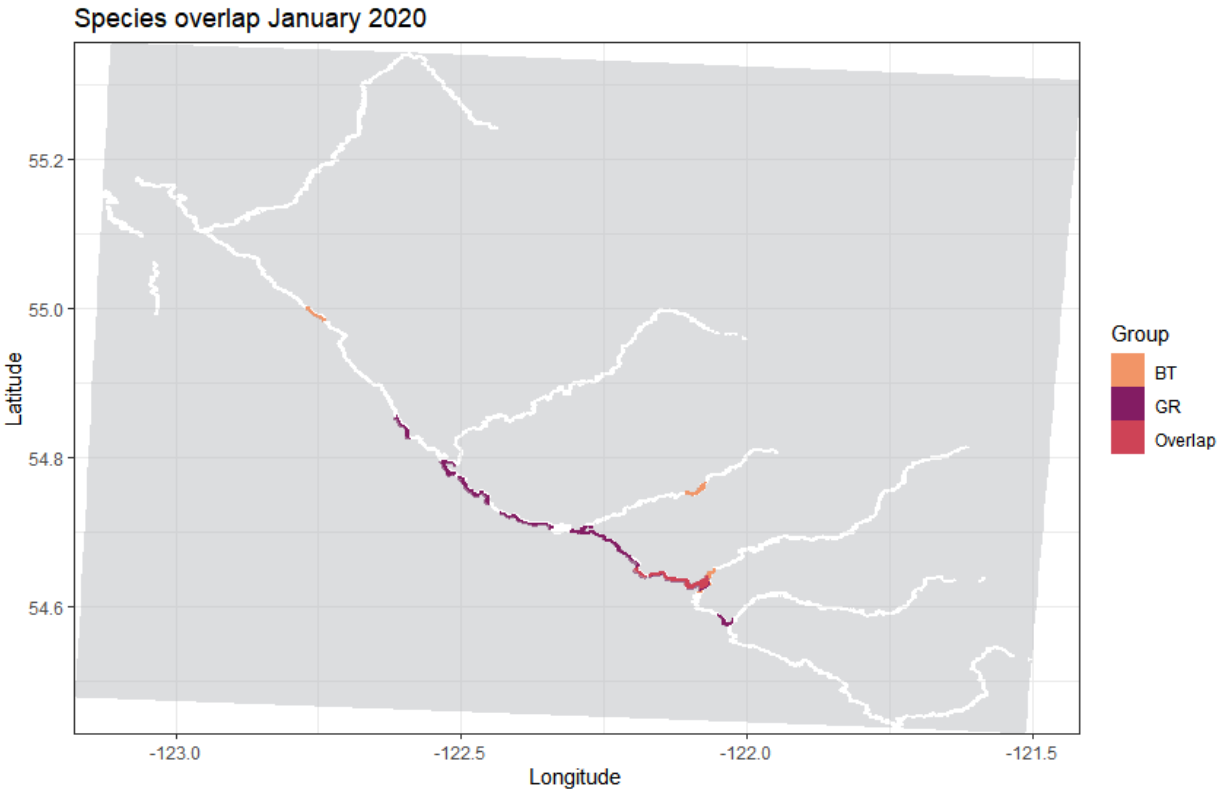
Species overlap January 2020
55.2
55.0
54.8
54.6
Latitude
-123.0
-122.5
-122.0
-121.5
Longitude
Group
BT
GR
Overlap

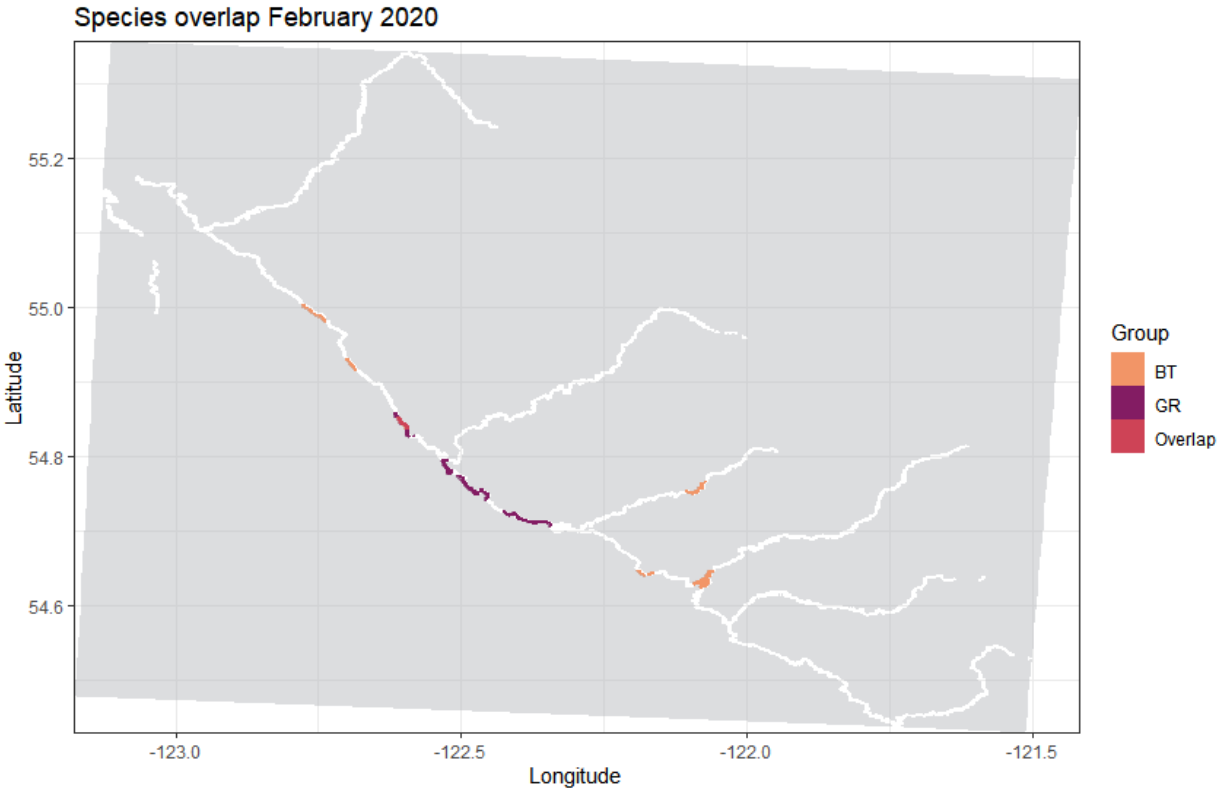
Species overlap February 2020
55.2
55.0
54.8
54.6
Latitude
-123.0
-122.5
-122.0
-121.5
Longitude
Group
BT
GR
Overlap

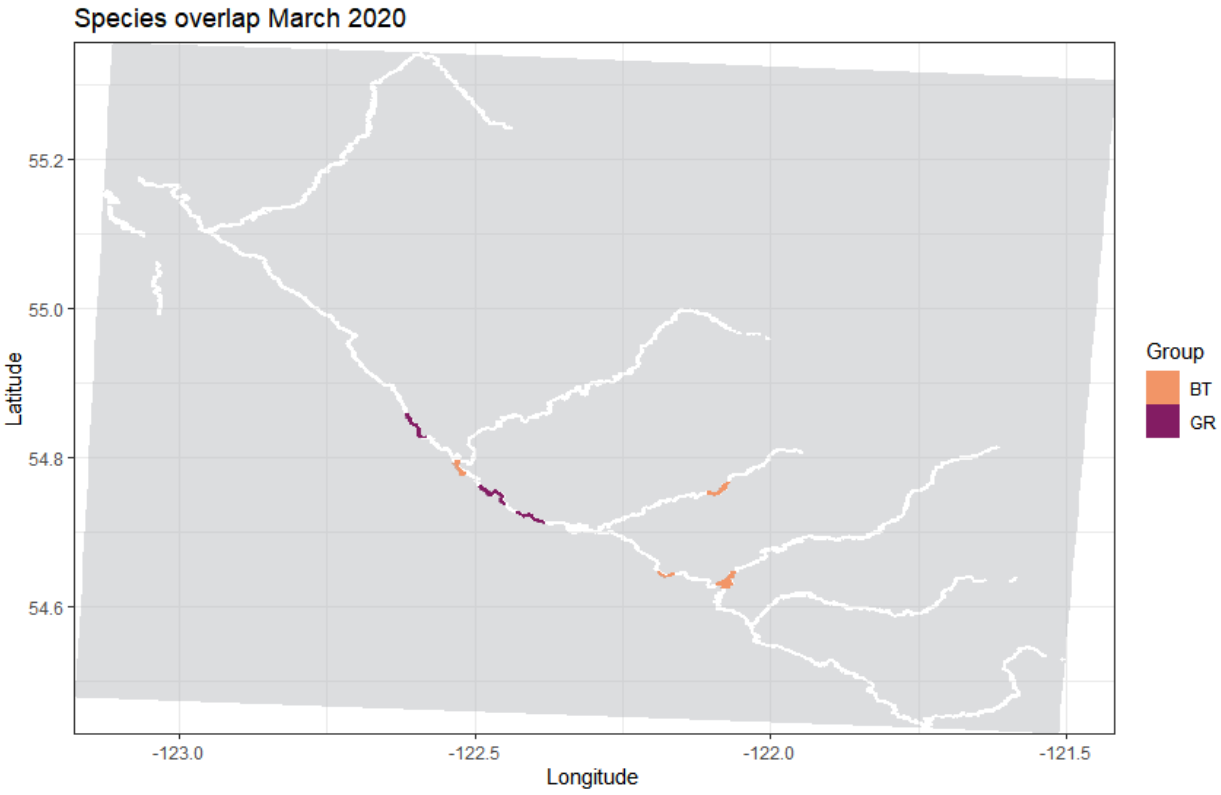
Species overlap March 2020
55.2
55.0
54.8
54.6
Latitude
-123.0
-122.5
-122.0
-121.5
Longitude
Group
BT
GR

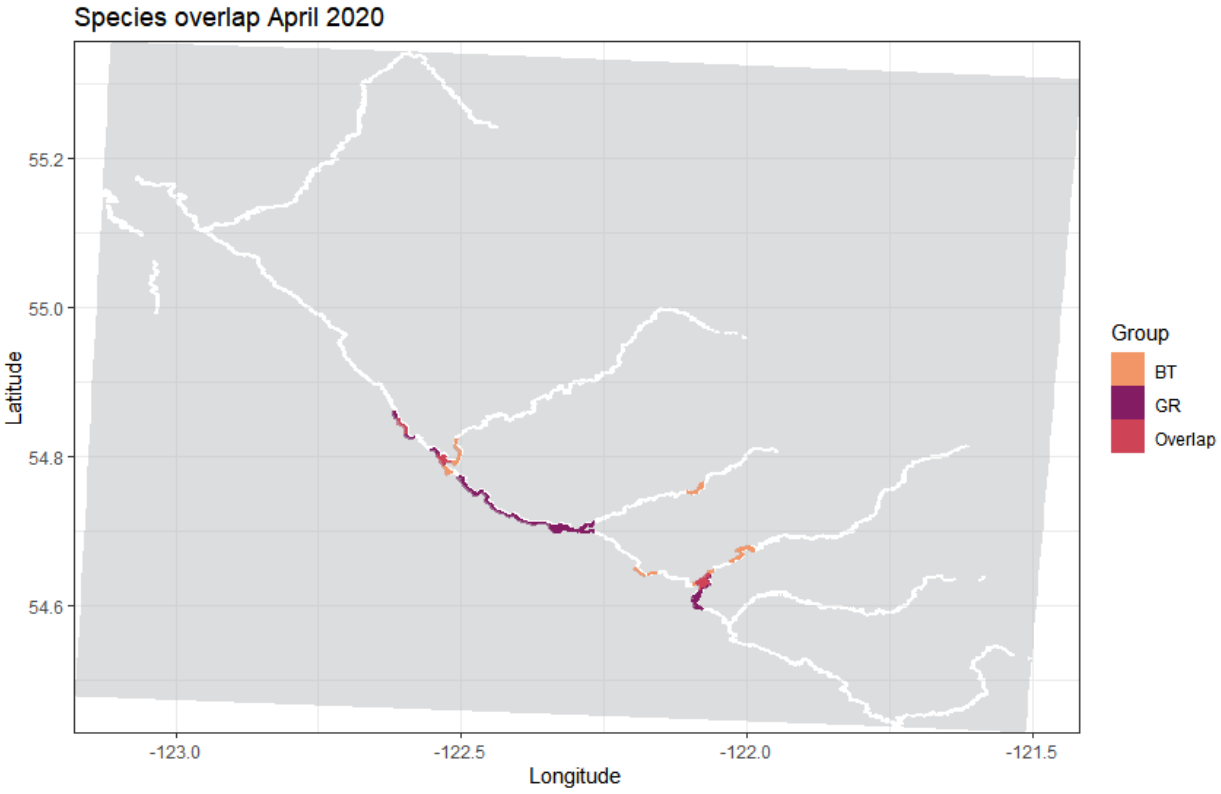
Species overlap April 2020
55.2
55.0
54.8
54.6
Latitude
-123.0
-122.5
-122.0
-121.5
Longitude
Group
BT
GR
Overlap

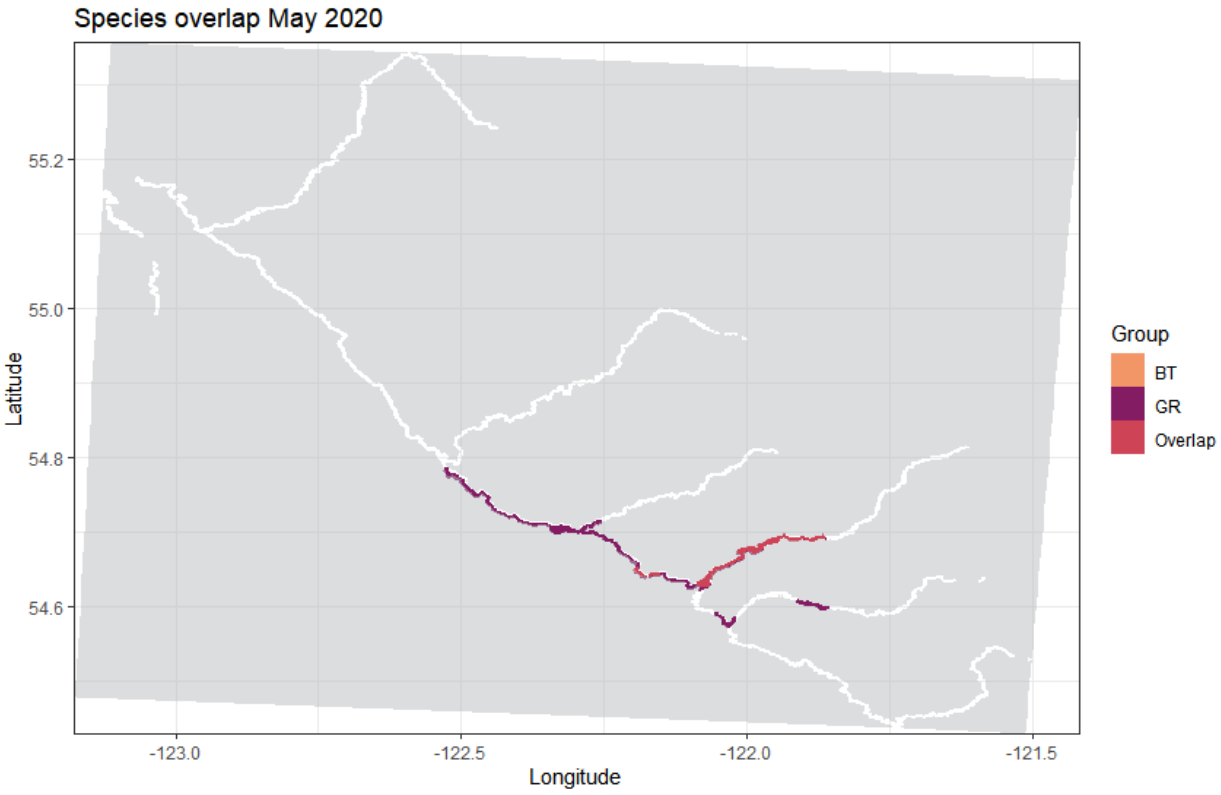
Species overlap May 2020
55.2
55.0
54.8
54.6
Latitude
-123.0
-122.5
-122.0
-121.5
Longitude
Group
BT
GR
Overlap

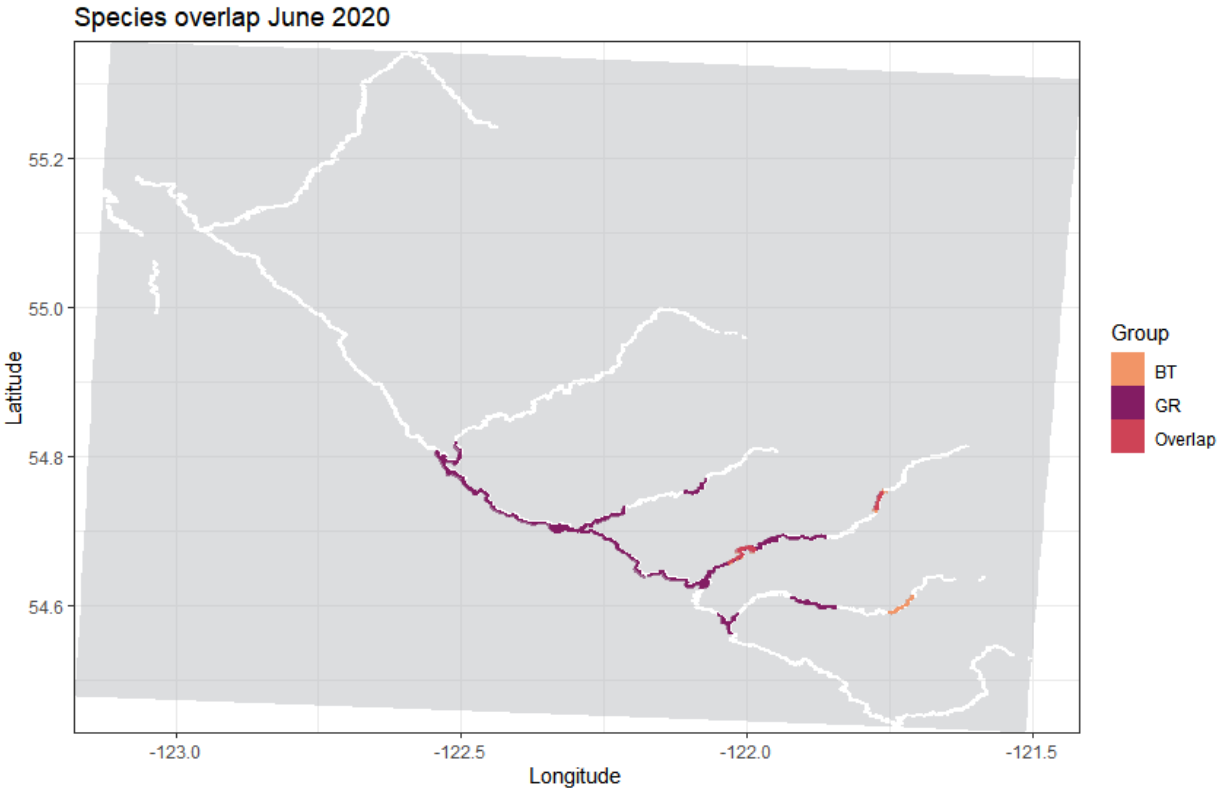
Species overlap June 2020
55.2
55.0
54.8
54.6
Latitude
-123.0
-122.5
-122.0
-121.5
Longitude
Group
BT
GR
Overlap

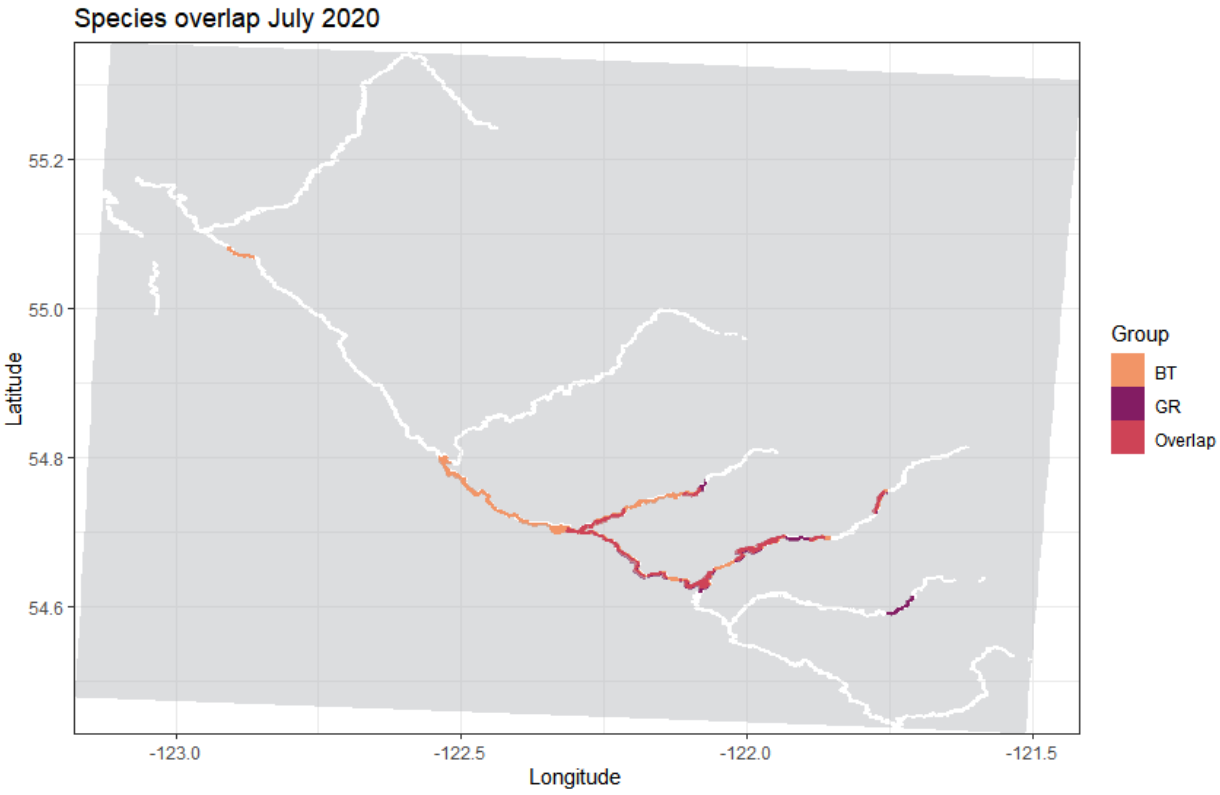
Species overlap July 2020
55.2
55.0
54.8
54.6
Latitude
-123.0
-122.5
-122.0
-121.5
Longitude
Group
BT
GR
Overlap

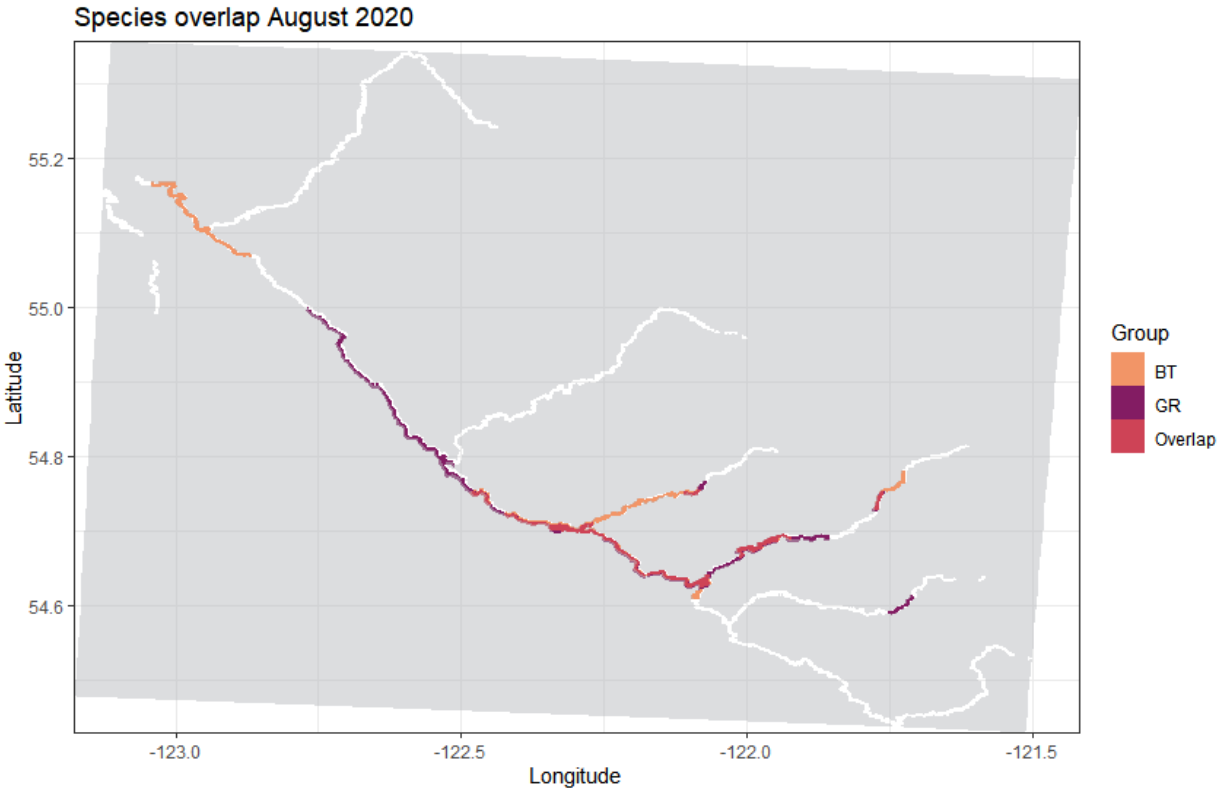
Species overlap August 2020
55.2
55.0
54.8
54.6
Latitude
-123.0
-122.5
-122.0
-121.5
Longitude
Group
BT
GR
Overlap

**Appendix A.5 – Arrival time plot**

These plots were generated by the package *actel* and uses the same dataset as the *RSP* analyses. Colours represent species and the height of the bar indicates the number of tags arriving in that river at that time. Peaks and valleys in the data can be seen offset with the Parsnip River and the tributaries, representing seasonal movements from the Parsnip mainstem into the tributaries. The plot for the Anzac River is active year-round, consistent with the findings from the overlap plots that the lowest reaches of the Anzac River are used as winter habitat.


Parsnip_River
Anzac_River
Table_River
Hominka_River
Missinka_River
n
2018-07
2019-01
2019-07
2020-01
2020-07
Group
Arctic grayling
Bull trout

**Appendix A.6 – Arctic grayling arrival times by sex**

These plots were generated for mid- and upper-tributary receivers as part of an exploratory analysis investigating sexual differences in Arctic grayling arrival times to the spawning grounds, characteristic of early-arriving males in Williston watershed Arctic grayling populations (Lashmar and Ptolemy 2002). Each plot represents a receiver site (receiver codes anzr – Anzac River, homr – Hominka River, misr – Missinka River, tblr – Table River; ## - Approximate river km of the receiver site, v – waypoint code indicating a receiver site). Information represented along the x-axis is informative only; it is not meant to represent a time axis as the overlap plots are generated by converting time series to radians. Coefficient of overlap and plot graphics are generated from package *overlap* (Ridout and Linkie 2009)

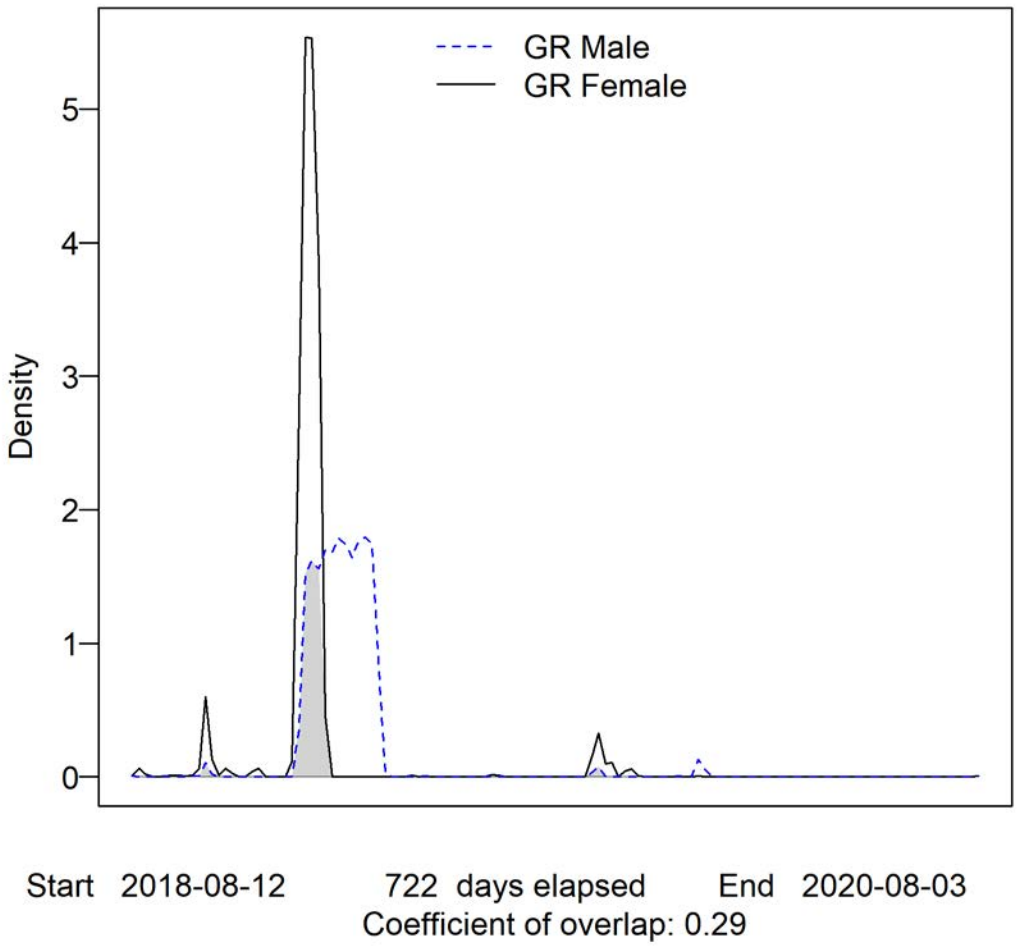
anzr07v
GR Male
GR Female
Density
0
1
2
3
4
5
Start 2018-08-12
722 days elapsed
End 2020-08-03
Coefficient of overlap: 0.29

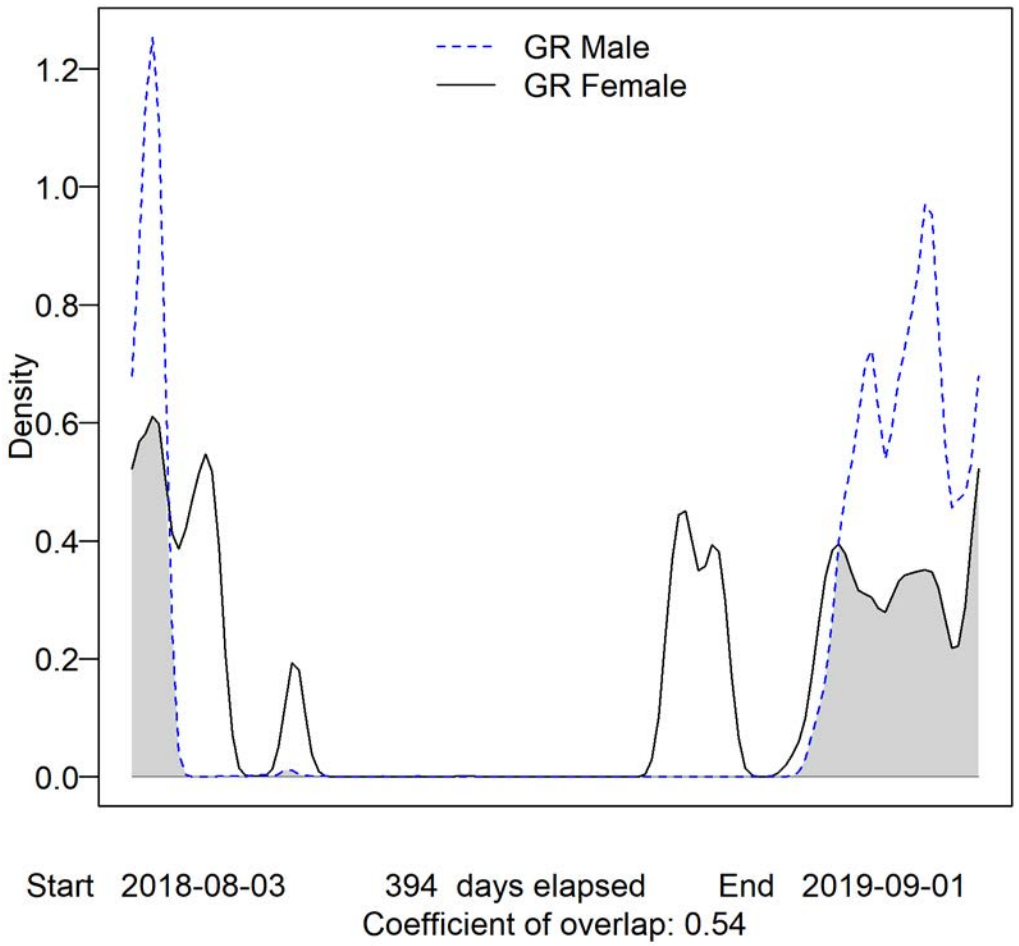
anzr08v
GR Male
GR Female
Density
1.2
1.0
0.8
0.6
0.4
0.2
0.0
Start 2018-08-03
394 days elapsed
End 2019-09-01
Coefficient of overlap: 0.54

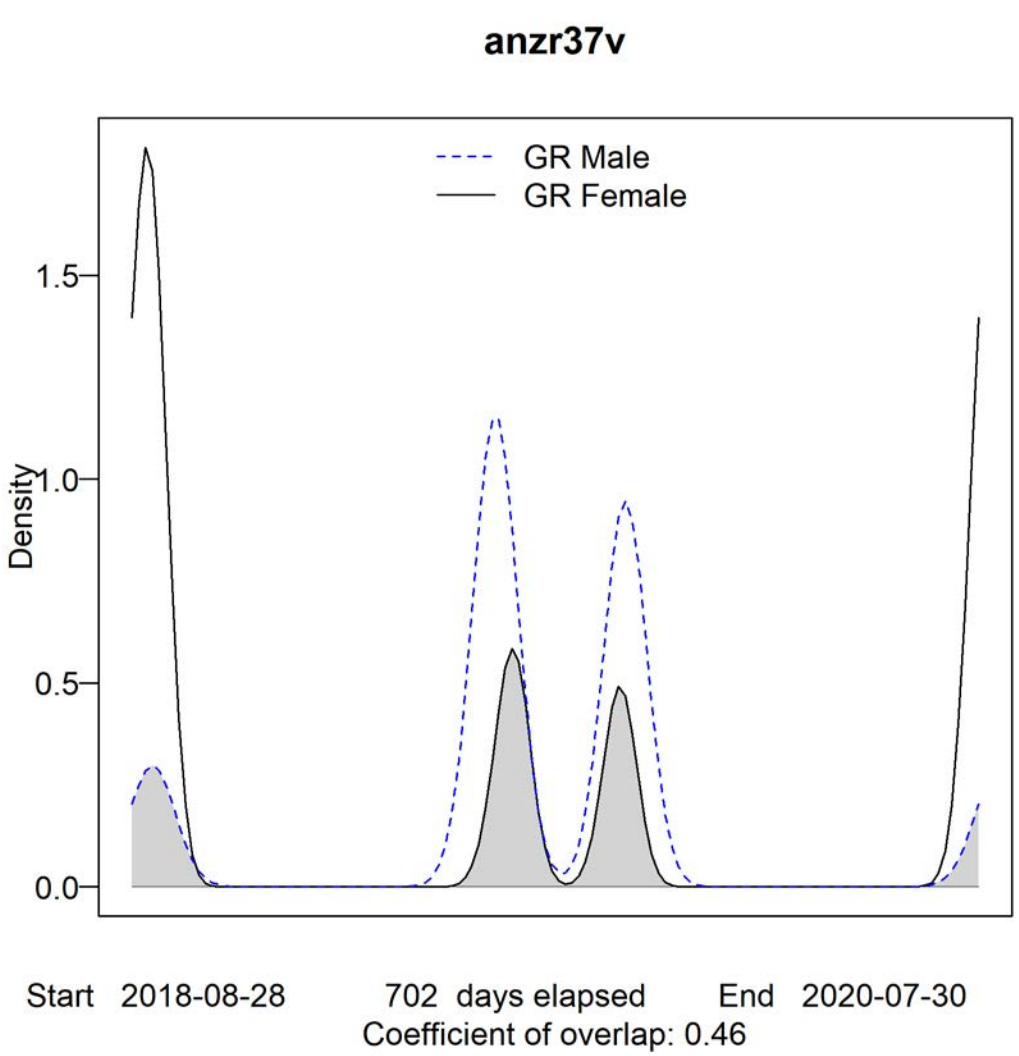
anzr37v
GR Male
GR Female
Density
1.5
1.0
0.5
0.0
Start 2018-08-28
702 days elapsed
End 2020-07-30
Coefficient of overlap: 0.46

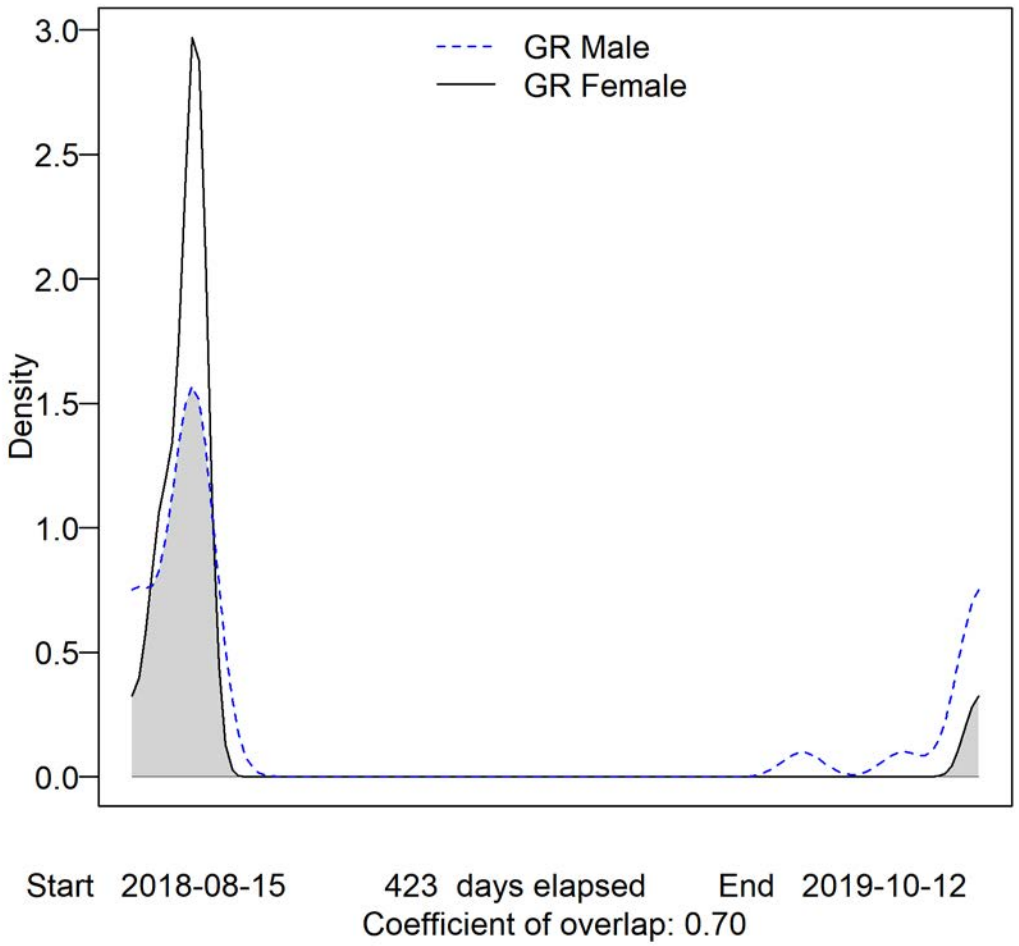
anzr42v
GR Male
GR Female
Density
3.0
2.5
2.0
1.5
1.0
0.5
0.0
Start 2018-08-15
423 days elapsed
End 2019-10-12
Coefficient of overlap: 0.70

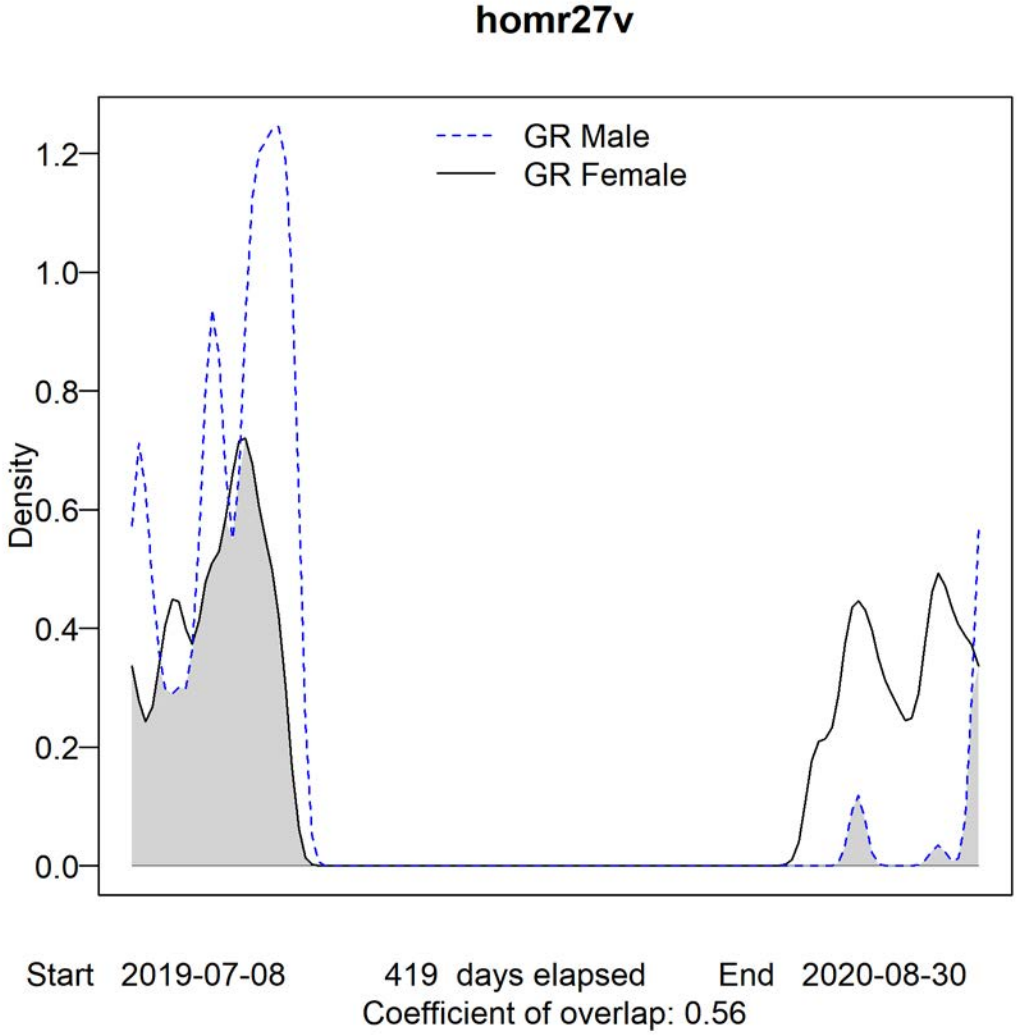
homr27v
GR Male
GR Female
Density
1.2
1.0
0.8
0.6
0.4
0.2
0.0
Start 2019-07-08
419 days elapsed
End 2020-08-30
Coefficient of overlap: 0.56

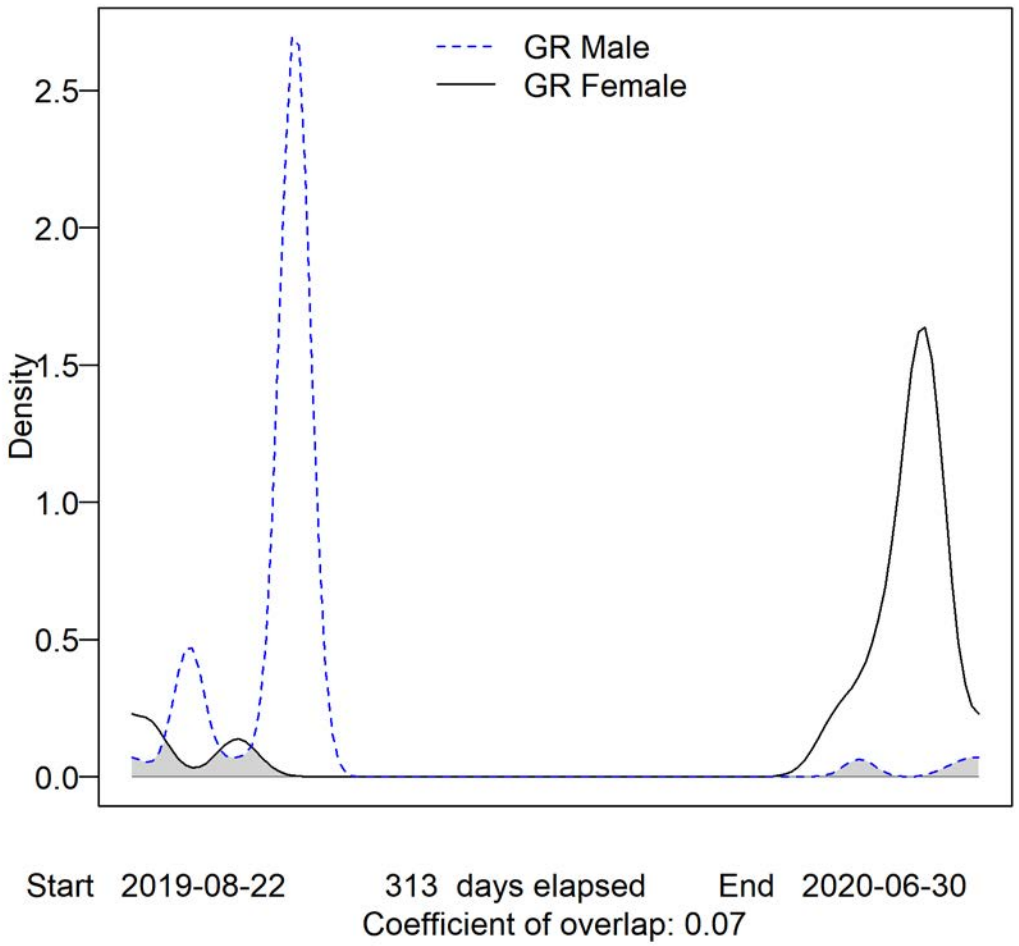
misr13v
GR Male
GR Female
Density
2.5
2.0
1.5
1.0
0.5
0.0
Start 2019-08-22
313 days elapsed
End 2020-06-30
Coefficient of overlap: 0.07

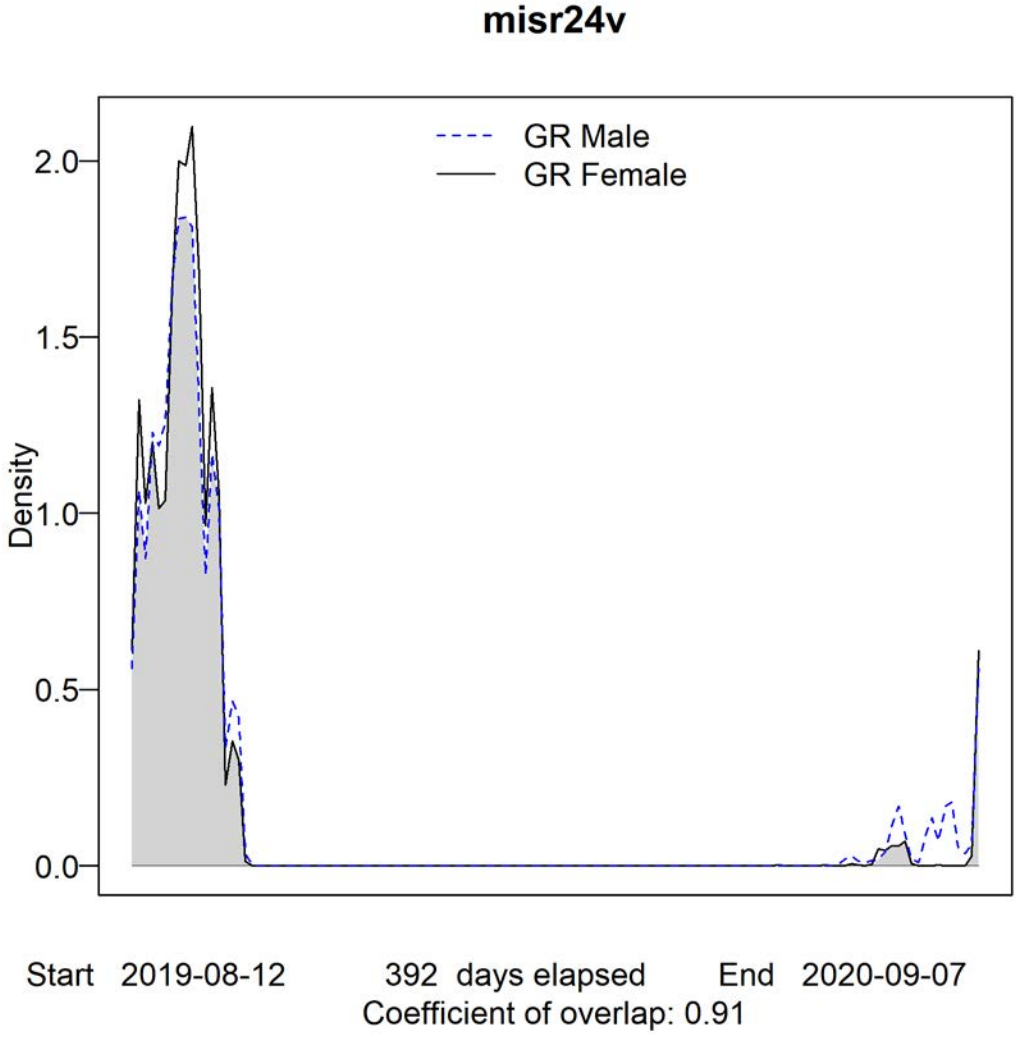
misr24v
GR Male
GR Female
Density
2.0
1.5
1.0
0.5
0.0
Start 2019-08-12
392 days elapsed
End 2020-09-07
Coefficient of overlap: 0.91

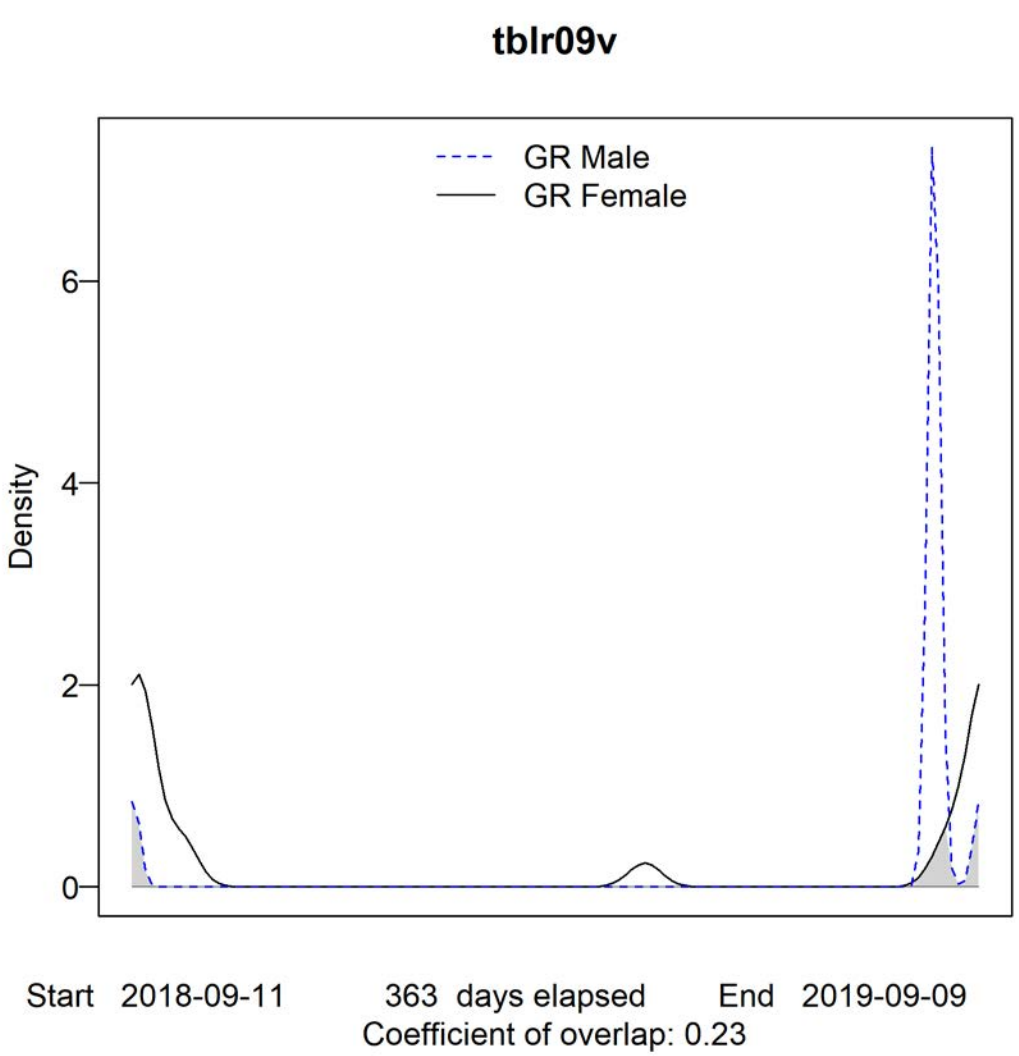
tblr09v
GR Male
GR Female
Density
6
4
2
0
Start 2018-09-11
363 days elapsed
End 2019-09-09
Coefficient of overlap: 0.23

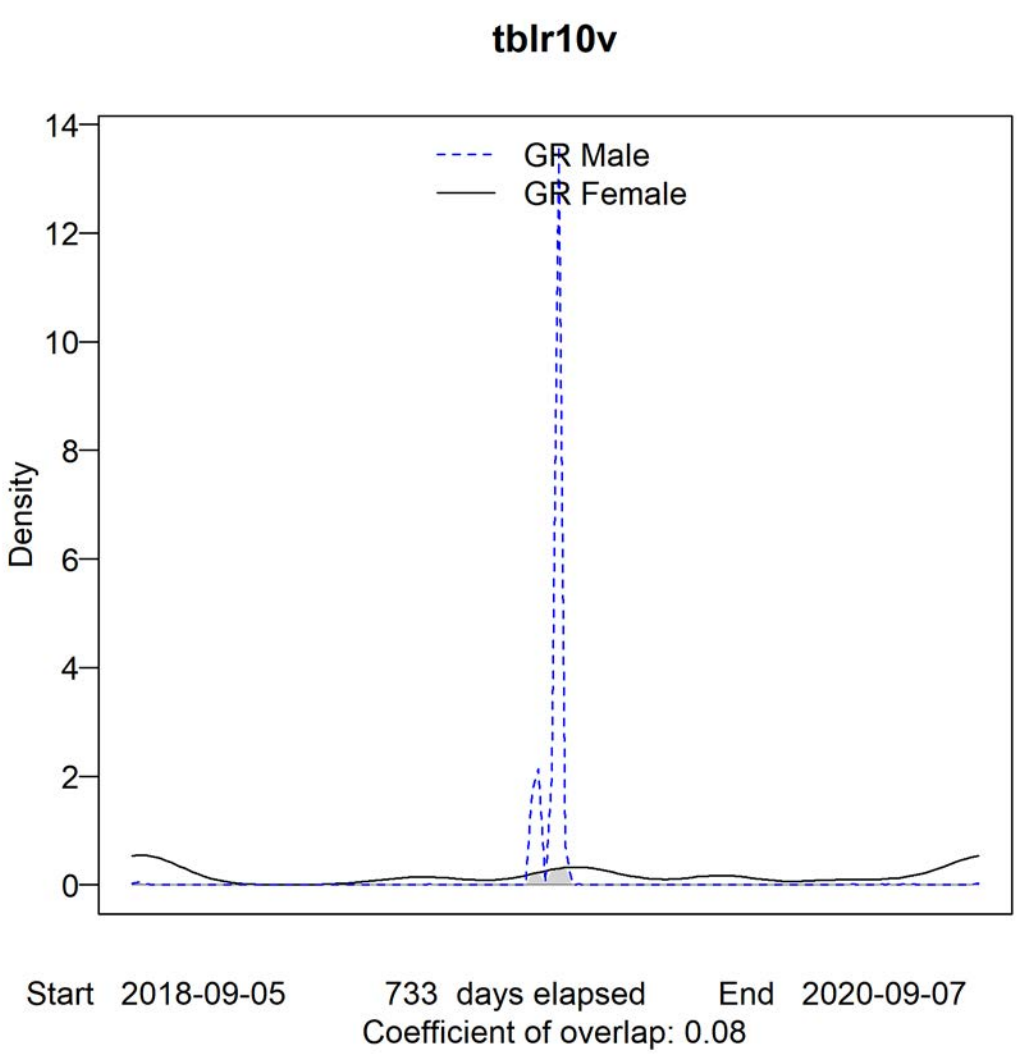
tblr10v
GR Male
GR Female
Density
14
12
10
8
6
4
2
0
Start 2018-09-05
733 days elapsed
End 2020-09-07
Coefficient of overlap: 0.08

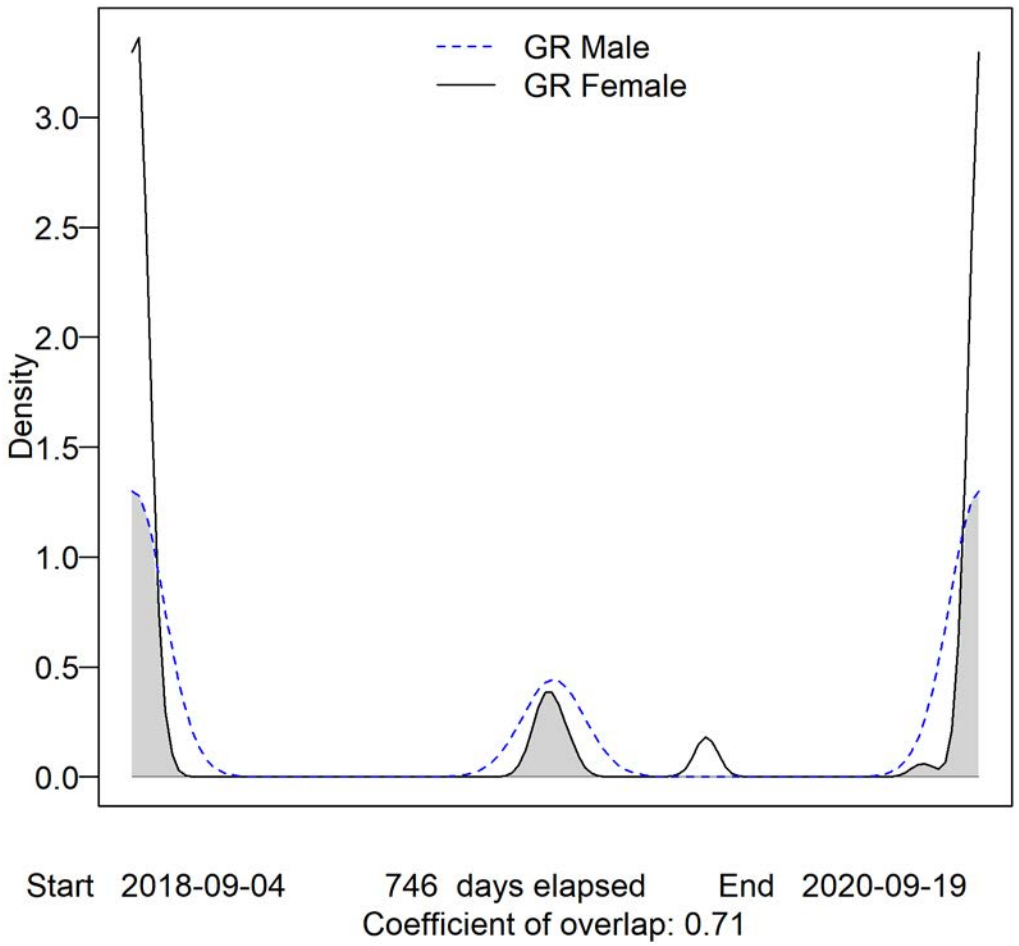
tblr15v
GR Male
GR Female
Density
3.0
2.5
2.0
1.5
1.0
0.5
0.0
Start 2018-09-04
746 days elapsed
End 2020-09-19
Coefficient of overlap: 0.71

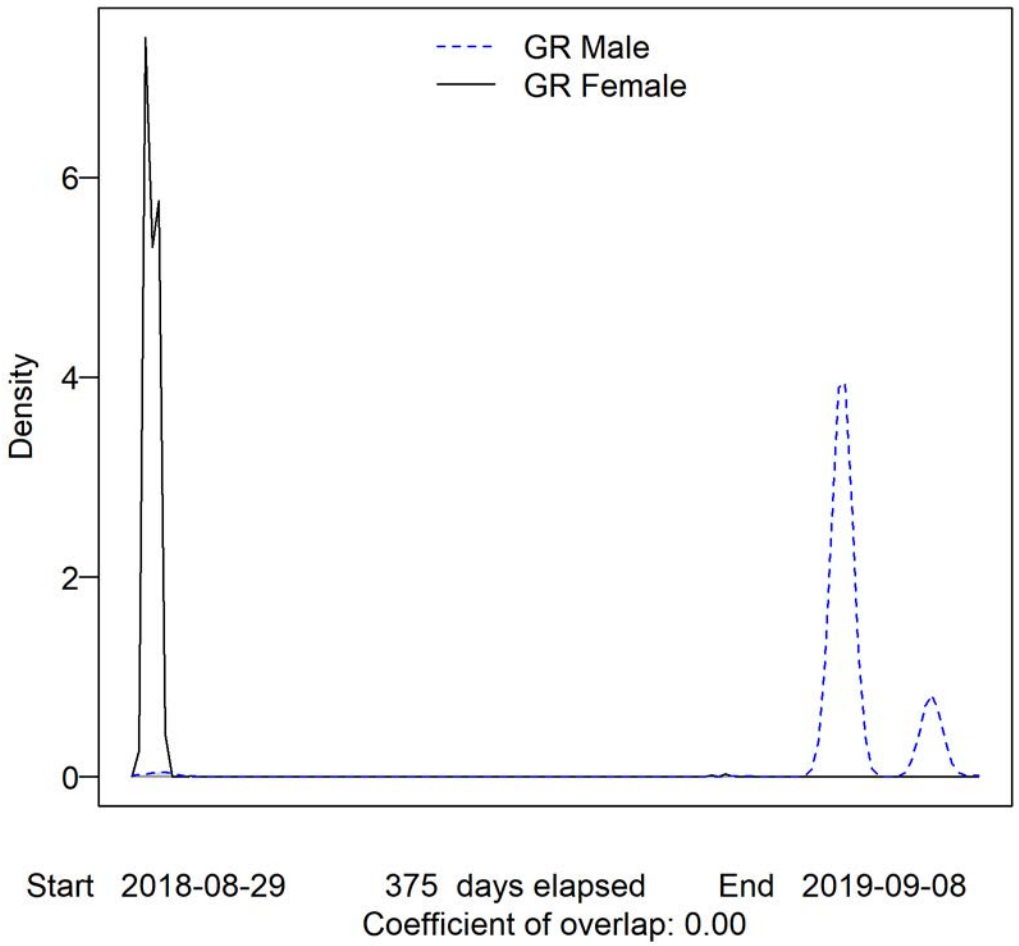
tblr16v
GR Male
GR Female
Density
6
4
2
0
Start 2018-08-29
375 days elapsed
End 2019-09-08
Coefficient of overlap: 0.00

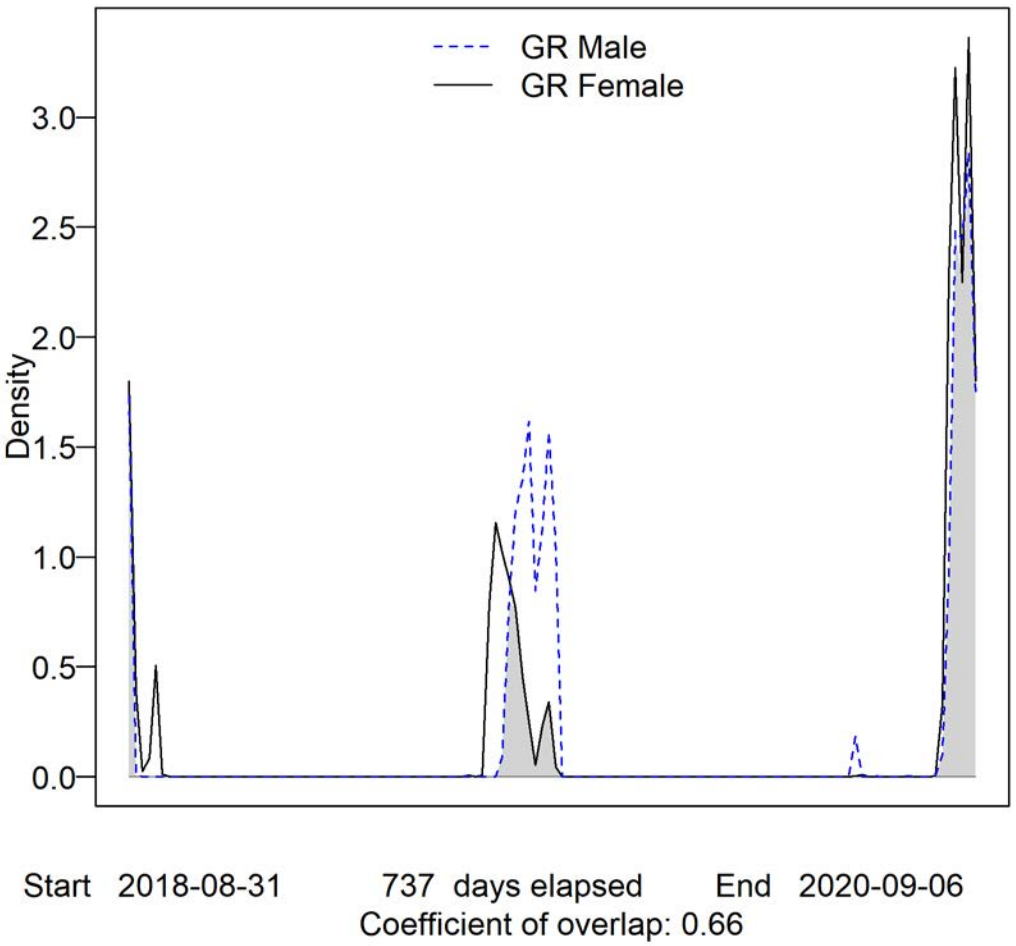
tblr23v
GR Male
GR Female
Density
3.0
2.5
2.0
1.5
1.0
0.5
0.0
Start 2018-08-31
737 days elapsed
End 2020-09-06
Coefficient of overlap: 0.66

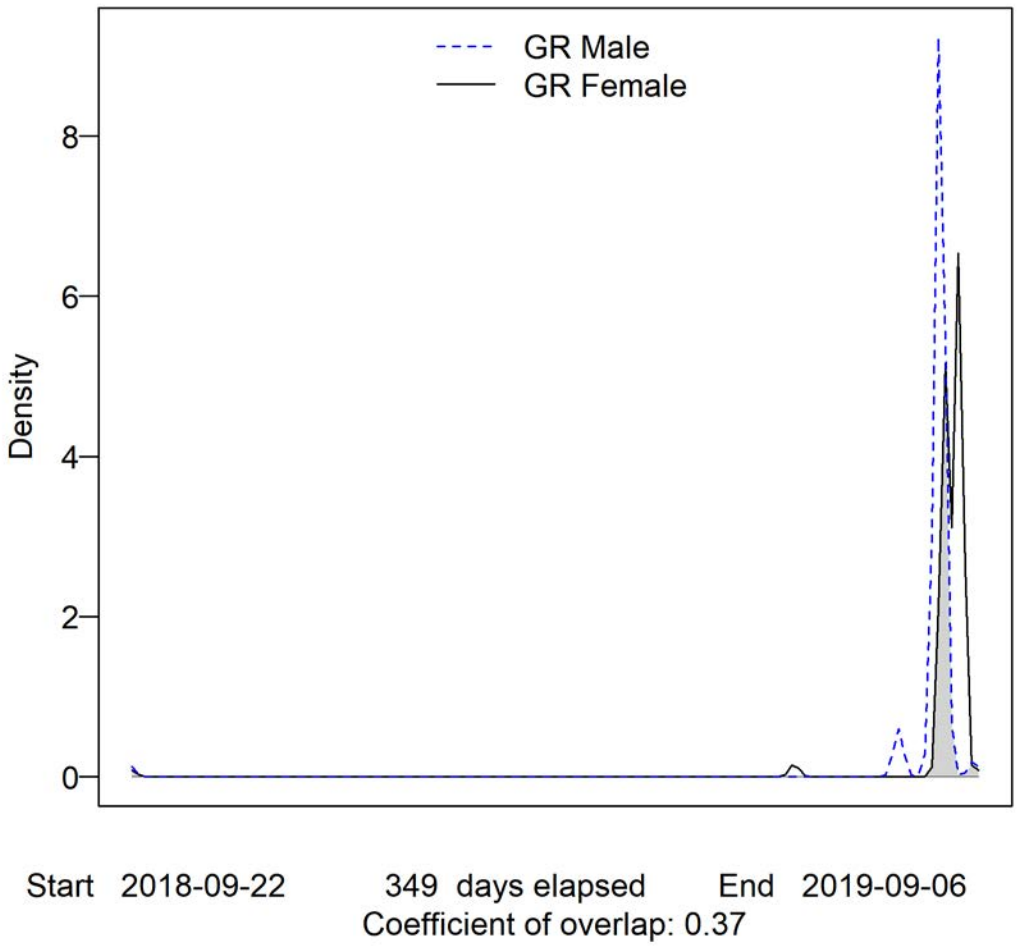
tblr24v
GR Male
GR Female
Density
0
2
4
6
8
Start 2018-09-22
349 days elapsed
End 2019-09-06
Coefficient of overlap: 0.37

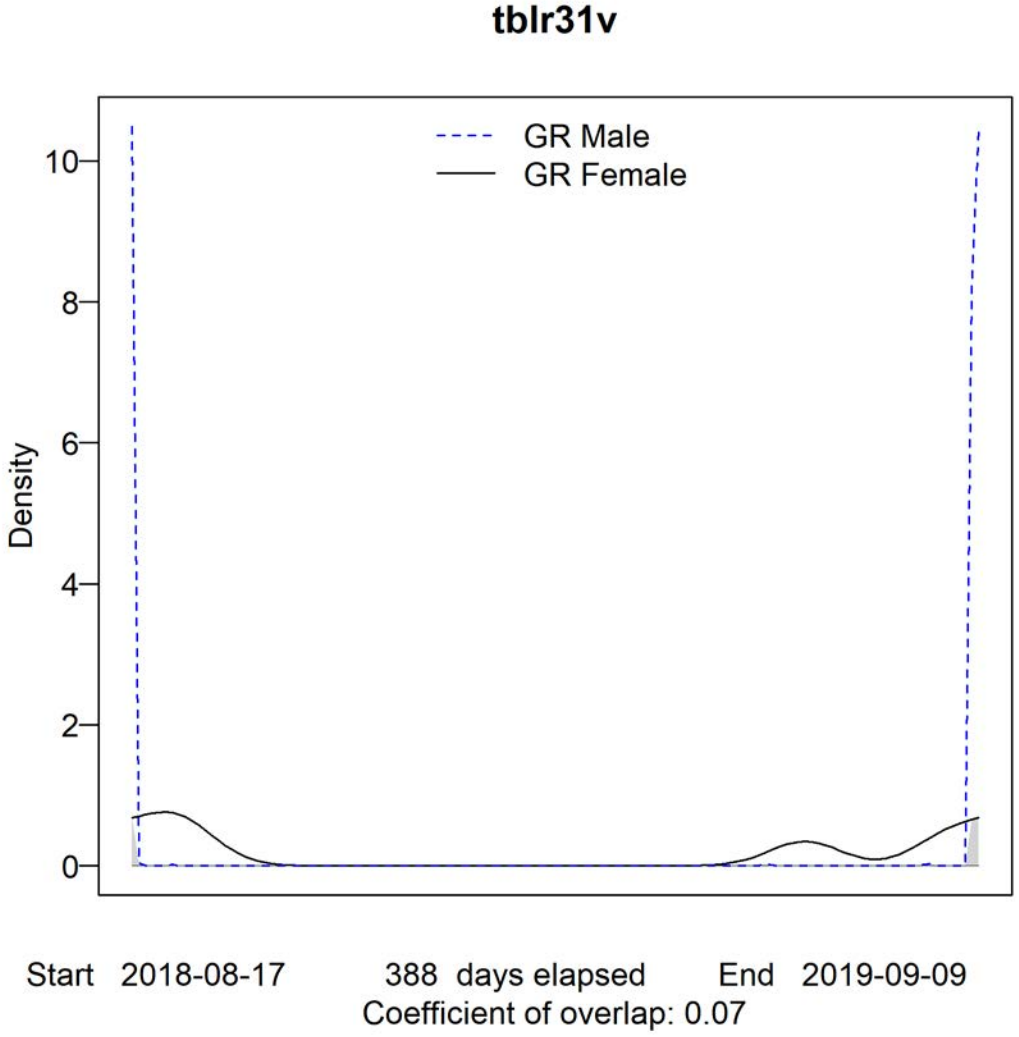
tblr31v
GR Male
GR Female
Density
10
8
6
4
2
0
Start 2018-08-17
388 days elapsed
End 2019-09-09
Coefficient of overlap: 0.07

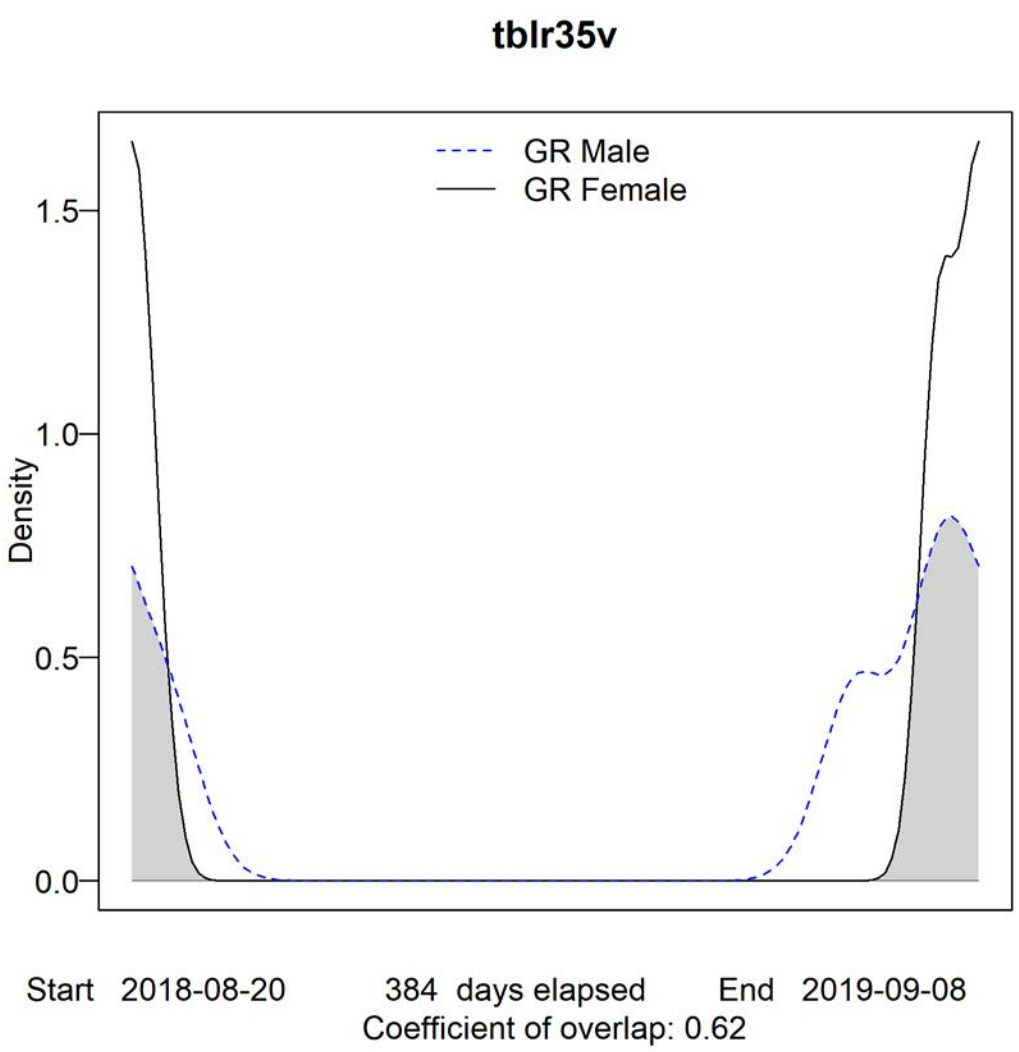
tblr35v
GR Male
GR Female
1.5
1.0
0.5
0.0
Density
Start 2018-08-20
384 days elapsed
End 2019-09-08
Coefficient of overlap: 0.62

.